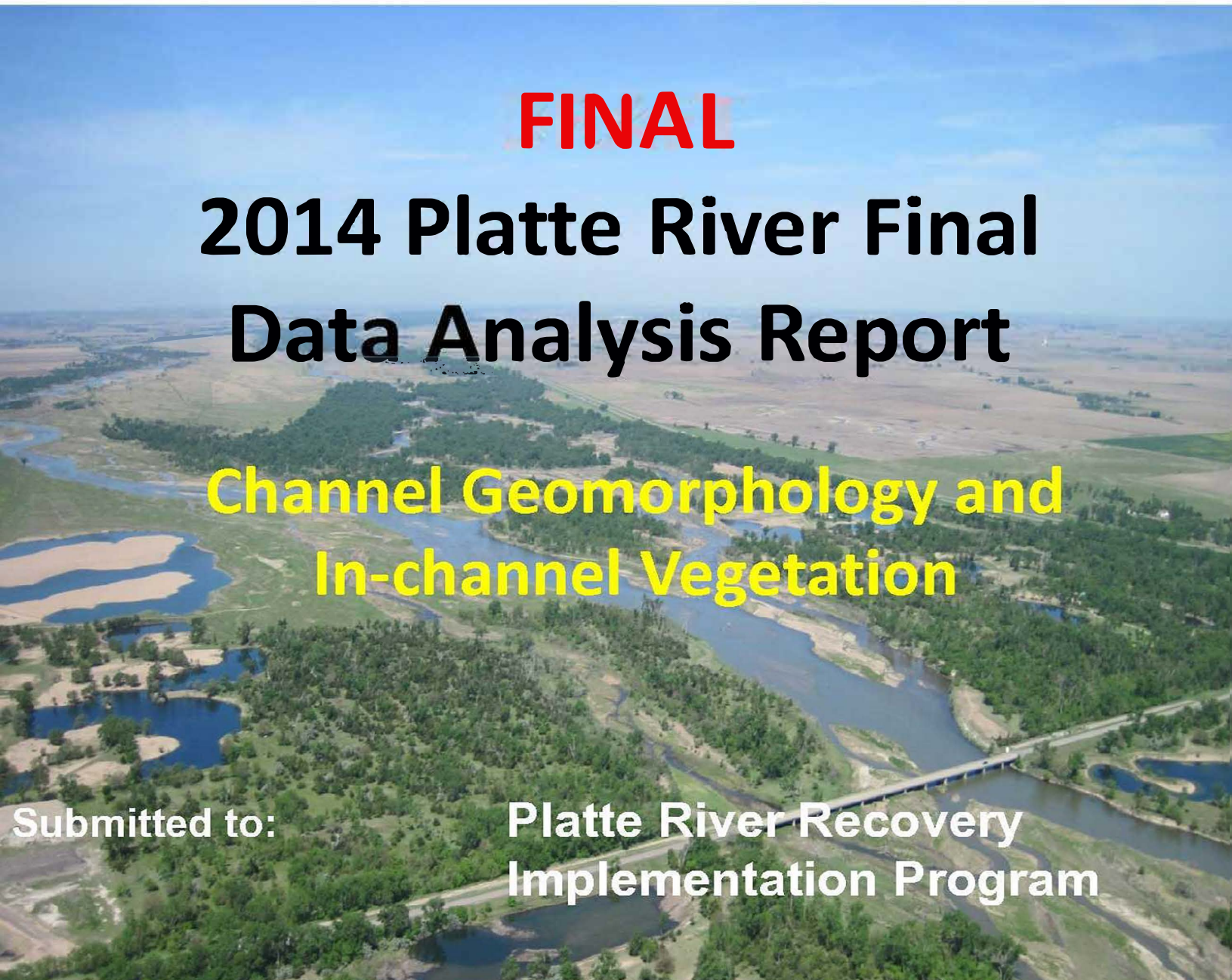


FINAL

2014 Platte River Final Data Analysis Report

**Channel Geomorphology and
In-channel Vegetation**



Submitted to:

**Platte River Recovery
Implementation Program**



Submitted by:

**3801 Automation Way, Suite 100
Fort Collins, CO 80525**



Channel Geomorphology and In-Channel Vegetation

2014 Final Data Analysis Report

PLATTE RIVER RECOVERY IMPLEMENTATION PROGRAM

Office of the Executive Director
4111 4th Avenue, Suite 6
Kearney, Nebraska 68845

December 22, 2015

Page intentionally left blank

TABLE OF CONTENTS

1	INTRODUCTION	1
1.1	Background.....	1
1.2	Scope of the Monitoring Program.....	1
1.2.1	Area of Interest	1
1.2.2	Anchor Points	3
1.2.3	Pure and Rotating Panel Points	3
1.2.4	Channel Geomorphology Monitoring.....	3
1.2.5	In-channel Vegetation Monitoring.....	4
1.2.6	Airborne Mapping of Topography (LiDAR)	5
1.3	Hypotheses and Performance Metrics	5
1.4	Big Questions	5
1.5	System-Scale Hypotheses	6
1.6	Priority Hypotheses.....	7
1.7	Performance Metrics.....	9
2	METHODS.....	11
2.1	Field Data Collection Methods	11
2.1.1	Landowner Contact.....	11
2.2	Topographic Ground Survey Methods.....	14
2.2.1	Survey Control.....	14
2.2.2	Geomorphic Transects.....	14
2.2.3	Unobstructed Channel Width	15
2.3	Vegetation Survey Methods	16
2.4	Sediment Sampling Methods	19
2.5	Data Analysis Methods	21
2.5.2	Performance Metrics.....	23
2.5.3	Trend Analysis	30
3	RESULTS	33
3.1	Hydrologic.....	33
3.1.1	Annual Peak Flow Event Discharge and Duration (DAP 5.1.1)	33
3.2	Hydraulic.....	40
3.2.1	Stage-Discharge Relationships (DAP 5.2.1)	40

3.3	Geomorphic	40
3.3.1	Braiding Index (DAP 5.3.1)	40
3.3.2	Total Channel Width (DAP 5.3.2)	45
3.3.3	Wetted Channel Width (DAP 5.3.3).....	49
3.3.4	Mean Channel Depth (DAP 5.3.4).....	53
3.3.5	Maximum Channel Depth (DAP 5.3.5)	53
3.3.6	Channel Width-to-Depth Ratio (DAP 5.3.6)	61
3.3.7	Channel Cross-sectional Area (DAP 5.3.6)	66
3.4	Vegetation	73
3.4.1	Green Line Elevation (GLE) (DAP 5.4.1).....	74
3.4.2	Total Unvegetated Channel Width (DAP 5.4.2)	81
3.4.3	Frequency of Occurrence by Species (DAP 5.4.3).....	85
3.4.4	Percent Cover by Species (DAP 5.4.4)	90
3.4.5	Areal Cover by Species (DAP 5.4.5)	96
3.4.6	Mean Elevation by Species (DAP 5.4.6)	101
3.4.7	Mean Vegetation Height (DAP 5.4.7)	104
3.5	Sediment	104
3.5.1	Bed-load versus Discharge Rating Curves (DAP 5.5.1)	104
3.5.2	Suspended Sediment Load versus Discharge Rating Curves (DAP 5.5.2).....	115
3.5.3	Bed-material Grain-size Distribution and Distribution Parameters (DAP 5.5.3)...	123
3.5.4	Bar Material Grain-size Distribution (DAP 5.5.4)	126
3.5.5	Bank Material Grain Size Distribution (DAP 5.5.5)	126
3.6	Whooping Crane Performance Metrics	128
3.6.1	Unobstructed Channel Width (DAP 5.6.1).....	128
3.6.2	Proportion of Channel Less Than Eight Inches Deep or Sand (DAP 5.6.2)	132
4	Hypothesis Testing and Trend Analysis	145
4.1	Flow #1	145
4.1.1	Sediment Balance Based on Transect Surveys	145
4.1.2	Sediment Balance Based on Sediment Load Rating Curves.....	153
4.1.3	Uncertainty in Sediment Balance Estimate	161
4.2	Flow #3	174
4.2.1.	Height of Green Line above 1,200-cfs Water Surface	178
4.2.2.	Green Line Elevation versus Stage at Annual Peak Discharge	178

4.2.3.	Green Line Elevation versus Stage at Germination Season Discharge	178
4.2.4.	Total Unvegetated Channel Width	178
4.2.5.	Total Unvegetated Channel Width versus Stage at Annual Peak Discharge	184
4.2.6.	Total Unvegetated Channel Width versus Stage at Mean Germination Season Discharge	184
4.2.7.	Total Unvegetated Channel Width versus Green Line Elevation	184
4.3	Flow #5	184
4.4	Mechanical #2	211
5	SUMMARY AND CONCLUSIONS	219
6	REFERENCES	227

LIST OF FIGURES

Figure 1.1.	Location map showing the project reach for the Channel Geomorphology and In-channel Vegetation Monitoring. Bed-load and suspended-sediment sampling bridge sites are shown as red circles.	2
Figure 1.2.	Clockwise from top left, illustrations of Priority Hypothesis Flow #1, Flow #3, and Flow #5.	8
Figure 1.3.	Illustration of Priority Hypothesis Sediment #1 (left) and Mechanical #2 (right). ...	9
Figure 2.1.	Mean daily flows at the USGS and NDNR stream gages between March 1 and September 30, 2014.....	12
Figure 2.2.	Mean daily flows at the USGS and NDNR stream gages between July 1 and August 15, 2014. Also show are the days on which each AP was surveyed.....	13
Figure 2.3.	Pipe dredge used to collect bed-material samples.	20
Figure 3.1.	Maximum mean daily discharge (Q_P) between January 1 of each year and the dates of the 2009 through 2014 monitoring surveys.....	34
Figure 3.2.	Duration of flows exceeding 5,000 cfs between January 1 of each year and the dates of the 2009 through 2014 monitoring surveys (DUR ₅₀₀₀).....	35
Figure 3.3.	Average mean daily discharge during the germination season (Q_{GER} ; June 1 – July 15) from 2009 through 2014.	36
Figure 3.4.	Average mean daily discharge during the spring whooping crane migration season (Q_{WC_Spring} ; March 21 – April 29) during 2009 through 2014.....	38
Figure 3.5.	Average mean daily discharge during the fall whooping crane migration season (Q_{WC_Fall} ; October 9 – November 10) during 2009 through 2014.....	39
Figure 3.6a.	Average braiding index at pure panel APs from 2009 through 2014.....	42
Figure 3.6b.	Average braiding index for the overall study reach, based on the pure panel AP data from 2009 through 2014. Whiskers represent ± 1 standard error on mean value.	43

Figure 3.6c.	Average braiding index by geomorphic reach, based on the pure panel AP data from 2009 through 2014. Also shown are Fotherby (2008) braiding indices. Whiskers represent ± 1 standard error on mean value.	44
Figure 3.7a.	Average total channel width at pure panel APs from 2009 through 2014.	46
Figure 3.7b.	Average total channel width for the overall study reach, based on the pure panel AP data from 2009 through 2014, omitting the J-2 return channel. Whiskers represent ± 1 standard error on mean value.	47
Figure 3.7c.	Average total channel width by reach, based on the pure panel AP data from 2009 through 2014. Whiskers represent ± 1 standard error on mean value. Also shown are valley confinement widths from Fotherby (2008). Note right-hand scale for this variable. Values above Fotherby (2008) line are ratio of valley confinement width to total channel width.	48
Figure 3.8a.	Average wetted width at 1,200 cfs at pure panel APs from 2009 through 2014.	50
Figure 3.8b.	Average wetted width at 1,200 cfs for the overall study reach, based on the pure panel AP data from 2009 through 2014. Whiskers represent ± 1 standard error on mean value.	51
Figure 3.8c.	Average wetted width at 1,200 cfs by geomorphic reach, based on the pure panel AP data from 2009 through 2014. Whiskers represent ± 1 standard error on mean value.	52
Figure 3.9a.	Mean channel (i.e., hydraulic) depth at 1,200 cfs at pure panel APs from 2009 through 2014.	54
Figure 3.9b.	Average mean channel (i.e., hydraulic) depth at 1,200 cfs for the overall study reach, based on the pure panel AP data from 2009 through 2014.	55
Figure 3.9c.	Average mean channel (i.e., hydraulic) depth at 1,200 cfs by geomorphic reach, based on the pure panel AP data from 2009 through 2014.	56
Figure 3.9d.	Surveyed cross-section profiles at AP15, transect four in 2011 and 2012. Note the removal of instream bars and the aggradation of the thalweg, which resulted in a wider, shallower channel.	57
Figure 3.10a.	Average maximum channel depth at 1,200 cfs at pure panel APs from 2009 through 2014.	58
Figure 3.10b.	Average maximum channel depth at 1,200 cfs for the overall study reach, based on the pure panel AP data from 2009 through 2014.	59
Figure 3.10c.	Average maximum channel depth at 1,200 cfs by geomorphic reach, based on the pure panel AP data from the 2009 through 2014 data.	60
Figure 3.11a.	Average width-to-depth (maximum depth) ratio at 1,200 cfs at pure panel APs from the 2009 through 2014 data.	62
Figure 3.11b.	Average width-to-depth (maximum depth) ratio at 1,200 cfs for the overall study reach, based on the pure panel AP data from 2009 through 2014.	63
Figure 3.11c.	Average width-to-depth (maximum depth) ratio at 1,200 cfs by geomorphic reach, based on the pure panel AP data from 2009 through 2014. Also shown are the width-to-depth ratios from Fotherby (2008).	64

Figure 3.11d. Average width-to-mean depth ratio at 1,200 cfs by geomorphic reach, based on the pure panel AP data from the 2009 to 2014 data. Also shown are the width-to-depth ratios from Fotherby (2008). Note: Fotherby (2008) does not report W/D for reach 1.....	65
Figure 3.12a. Year-to-year change in average cross-sectional area at pure panel APs from 2009 through 2014. Line connecting AP33 on the 2009 to 2010 series is dashed to show effect of mechanical bar removal. [Aggradation (+), Degradation (-)].....	67
Figure 3.12b. Year-to-year change in mean bed elevation at the pure panel APs from 2009 through 2014. Line connecting AP33 on the 2009 to 2010 series is dashed to show effect of mechanical bar removal. [Aggradation (+), Degradation (-)].....	68
Figure 3.12c. Year-to-year aggradation/degradation volumes in the overall study reach from 2009 through 2014. Quantity for 2009 to 2010 does not include changes at AP33 due to mechanical removal of a large mid-channel bar.....	69
Figure 3.12d. Year-to-year aggradation/degradation volumes in the overall study reach from 2009 through 2014. Quantity for Reach 3 during 2009 to 2010 does not include changes at AP33 due to mechanical removal of a large mid-channel bar.	70
Figure 3.13a. Aerial photographs showing the locations of the surveyed cross sections at AP33: (a) July 2009 (Discharge~310 cfs), (b) October 2010 (Discharge ~720 cfs).....	71
Figure 3.13b. Surveyed cross section profiles at AP33 (a) Downstream (XS7), (b) Upstream (XS1).....	72
Figure 3.14a. Difference between average GLE at pure panel APs in 2010 through 2014 from the initial survey in 2009.....	76
Figure 3.14b. Reach-wide average difference in GLE at Pure Panel APs from the 2009 GLE.....	77
Figure 3.14c. Average change in GLE from the 2009 survey, by geomorphic reach.....	78
Figure 3.15. Average difference between GLE and water-surface elevation associated with the maximum preceding discharge (Q_p) at pure panel APs from 2009 through 2014.....	79
Figure 3.16. Change in water-surface elevation from 2009 versus change in GLE from 2009: (a) preceding maximum discharge (Q_p ; DAP 5.1.1), (b) germination season discharge (Q_{GER} ; DAP 5.1.2), (c) maximum discharge during germination season	80
Figure 3.17a. Average unvegetated channel width at Pure Panel APs from 2009 through 2014.....	82
Figure 3.17b. Reach-wide average unvegetated channel width at pure panel APs from 2009 through 2014.....	83
Figure 3.17c. Average unvegetated channel width by geomorphic reach from 2009 through 2014.....	84

Figure 3.18.	Frequency of occurrence of the top-25 most commonly observed species in 2014, and any species of primary interest present below that threshold, 2009-2014. Results are organized by decreasing frequency according to the 2014 data.....	86
Figure 3.19.	Frequency of occurrence for the four species of primary interest for the 2009 through 2014 vegetation surveys.	87
Figure 3.20.	Mean frequency of occurrence of purple loosestrife (<i>Lythrum salicaria</i>) by geomorphic reach, 2009-2014.	88
Figure 3.21.	Mean frequency of occurrence of common reed (<i>Phragmites australis</i>) by geomorphic reach, 2009-2014.	89
Figure 3.22.	Mean frequency of occurrence of eastern cottonwood (<i>Populus deltoides</i>) by geomorphic reach, 2009-2014.	89
Figure 3.23.	Mean frequency occurrence of willow (<i>Salix sp.</i>) by geomorphic reach, 2009-2014.....	90
Figure 3.24.	Total surveyed area and area with measurable vegetation for each survey year, based on Daubenmire cover-class data.	91
Figure 3.25.	Percent cover of the top 25 most commonly observed species in 2014, and any species of primary interest present below that threshold, 2009 through 2014. Results are organized by decreasing frequency according to the 2014 data.....	92
Figure 3.26.	Percent cover of the species of primary interest from 2009 through 2014.	94
Figure 3.27.	Mean percentage of ground cover for Purple loosestrife (<i>Lythrum salicaria</i>), 2009 through 2014, by geomorphic reach.	95
Figure 3.28.	Mean percentage of ground cover for common reed (<i>Phragmites australis</i>), 2009 through 2014, by geomorphic reach.	95
Figure 3.29.	Mean percentage of ground cover for Eastern cottonwood (<i>Populus deltoides</i>), 2009 through 2014, by geomorphic reach.	96
Figure 3.30.	Mean percentage of ground cover for willow (<i>Salix sp.</i>), 2009 through 2014, by geomorphic reach.	96
Figure 3.31.	Areal cover of the top-25 most commonly observed species in 2014, and any species of primary interest present below that threshold, 2009-2014. Results are organized by decreasing frequency according to the 2014 findings.	97
Figure 3.32.	Areal cover of the four species of primary interest, 2009-2014.....	98
Figure 3.33.	Areal cover of purple loosestrife (<i>Lythrum salicaria</i>), 2009-2014 by geomorphic reach.	99
Figure 3.34.	Areal cover of common reed (<i>Phragmites australis</i>), 2009-2014 by geomorphic reach.	99
Figure 3.35.	Areal cover of Eastern cottonwood (<i>Populus deltoides</i>), 2009-2014 by geomorphic reach.	100
Figure 3.36.	Areal cover of willow (<i>Salix sp.</i>), 2009-2014 by geomorphic reach.....	100

Figure 3.37a. Mean elevation of the top 25 most commonly observed species in 2014, and any species of primary interest present below that threshold, 2010-2014, organized by decreasing frequency in 2014. Standard error bars (± 1) are included	102
Figure 3.37b. Mean elevation above the local 1,200-cfs water surface of the top 25 most commonly observed species in 2014, and any species of primary interest present below that threshold, 2010-2014, organized by decreasing frequency in 2014. Standard error bars (± 1) are included	103
Figure 3.37c. Mean height above the 1,200-cfs water surface of the four species of primary interest from 2009 through 2014. Standard error bars (± 1) are included	104
Figure 3.38. Bed-load transport rates measured at the Darr Bridge between 2009 and 2014. Also shown is the best-fit, power-function line through the data, the upper and lower 95-percent confidence bands on the best-fit line, and the MVUE bias corrected line.....	106
Figure 3.39. Bed-load transport rates measured at the Overton Bridge between 2009 and 2014. Also shown is the best-fit, power-function line through the data, the upper and lower 95-percent confidence bands on the best-fit line, and the MVUE bias corrected line.....	107
Figure 3.40. Bed-load transport rates measured at the Kearney Bridge between 2009 and 2014. Also shown is the best-fit, power-function line through the data, the upper and lower 95-percent confidence bands on the best-fit line, and the MVUE bias corrected line.....	108
Figure 3.41. Bed-load transport rates measured at the Shelton Bridge between 2009 and 2014. Also shown is the best-fit, power-function line through the data, the upper and lower 95-percent confidence bands on the best-fit line, and the MVUE bias corrected line.....	109
Figure 3.42. Bed-load transport rates measured at the Grand Island Bridge between 2009 and 2014. Also shown is the best-fit, power-function line through the data, the upper and lower 95-percent confidence bands on the best-fit line, and the MVUE bias corrected line.....	110
Figure 3.43. Power-function, best-fit lines for the measured bed- and suspended-sediment- transport rates at the five measurement sites.....	111
Figure 3.44. Average percentage of sand and gravel in the bed-load samples from the five primary measurement sites and the single sample collected at the Elm Creek Bridge. Embedded values represent number of samples at each site; whiskers represent ± 1 standard error about the mean.	112
Figure 3.45a. Particle size of bed-load samples from the five measurement sites, 2009- 2014: median (D_{50}).	113
Figure 3.45b. Particle size of bed-load samples from the five measurement sites, 2009- 2014: median (D_{84}).	114
Figure 3.46. Total suspended sediment concentrations from measurements taken since the start of the monitoring program in 2009.....	116

Figure 3.47. Average percentage of silt/clay and sand in the suspended sediment samples from the five primary measurement sites. Embedded values represent number of samples at each site; whiskers represent ± 1 standard error about the mean.	117
Figure 3.48. Suspended sand transport rates measured at the Darr Bridge between 2009 and 2014. Also shown is the best-fit, power-function line through the data, the upper and lower 95-percent confidence bands on the best-fit line, and the MVUE bias corrected line.	118
Figure 3.49. Suspended sand transport rates measured at the Overton Bridge between 2009 and 2014. Also shown is the best-fit, power-function line through the data, the upper and lower 95-percent confidence bands on the best-fit line, and the MVUE bias corrected line.	119
Figure 3.50. Suspended sand transport rates measured at the Kearney Bridge between 2009 and 2014. Also shown is the best-fit, power-function line through the data, the upper and lower 95-percent confidence bands on the best-fit line, and the MVUE bias corrected line.	120
Figure 3.51. Suspended sand transport rates measured at the Shelton Bridge between 2009 and 2014. Also shown is the best-fit, power-function line through the data, the upper and lower 95-percent confidence bands on the best-fit line, and the MVUE bias corrected line.	121
Figure 3.52. Suspended sand transport rates measured at the Grand Island (Highway 34/Highway2) Bridge between 2009 and 2014. Also shown is the best-fit, power-function line through the data, the upper and lower 95-percent confidence bands on the best-fit line, and the MVUE bias corrected line.	122
Figure 3.53. Average median (D_{50}) size of bed material samples collected at the APs during 2009 through 2014 monitoring surveys. Also shown are the D_{50} sizes of the samples collected by Reclamation in 1989.	124
Figure 3.54. Reach averaged median (D_{50}) particle size of samples collected for this monitoring program in 2009 through 2014, and by Reclamation in 1989. Whiskers represent reach-averaged D_{16} and D_{84}	125
Figure 3.55. Reach-averaged median (d_{50}) size of bar-material samples collected during 2009 through 2014 monitoring surveys.	127
Figure 3.56a. Average unobstructed channel width at pure panel APs from 2009 through 2014.	129
Figure 3.56b. Average unobstructed channel width for the overall study reach, based on the pure panel AP data from the 2009 through 2014. Whiskers represent ± 1 standard error on mean value.	130
Figure 3.56c. Average unobstructed channel width by reach, based on the pure panel AP data from 2009 through 2014. Whiskers represent ± 1 standard error on mean value. Note that the 2009 and 2010 values for Reach 2 include both AP35B and AP37B, while 2011-2014 include only AP35B. Average values for AP35B in 2009 and 2010 were 540 and 420 feet, respectively.	131
Figure 3.57a. Width of channel less than 8 inches deep (including exposed sandbars) at 2,400 cfs at the pure panel APs for each of the six monitoring surveys. Dashed black line is total channel width between bank stations.	133

Figure 3.57b. Overall reach-averaged width less than 8 inches deep (including exposed sandbars) at 2,400 cfs. Whiskers represent ± 1 standard error. Note: AP37B excluded from the average because data are available only for 2009 through 2010.....	134
Figure 3.57c. Average width less than 8 inches deep (including exposed sandbars) at 2,400 cfs by geomorphic reach. Whiskers represent ± 1 standard error. Note: AP37B excluded.	135
Figure 3.58a. Width of channel less than 8 inches deep (including exposed sandbars) during spring migration at the pure panel APs for each of the six monitoring years. Dashed black line is total channel width between bank stations.....	137
Figure 3.58b. Overall reach-averaged width less than 8 inches deep (including exposed sandbars) at the spring migration season. Whiskers represent ± 1 standard error. Note: AP37B excluded.....	138
Figure 3.58c. Average width less than 8 inches deep (including exposed sandbars) at the spring migration season by geomorphic reach. Whiskers represent ± 1 standard error. Note: AP37B excluded.....	139
Figure 3.59a. Width of channel less than 8 inches deep (including exposed sandbars) during all migration at the pure panel APs for each of the six monitoring years. Dashed black line is total channel width between bank stations.....	140
Figure 3.59b. Overall reach-averaged width less than 8 inches deep (including exposed sandbars) at the spring migration season. Whiskers represent ± 1 standard error. Note: AP37B excluded.....	141
Figure 3.59c. Average width less than 8 inches deep (including exposed sandbars) at the spring migration season by geomorphic reach. Whiskers represent ± 1 standard error. Note: AP37B excluded.....	142
Figure 3.60. Typical relationship between discharge and (a) width of the channel and (b) percentage of total active channel width with depth less than 8 inches, based on the three primary monitoring cross sections at AP17 and AP29.....	143
Figure 4.1. Vicinity map of the pilot sediment augmentation area showing the location of the Dyer Outfall and the five monitoring cross sections.	147
Figure 4.2a. Mean bed elevations at the Overton, based on USGS field measurement data collected during WY1987 through WY2014.....	149
Figure 4.4b. Mean bed elevations at the Overton, based on USGS field measurement data collected during WY2010 through WY2014 (same data as Figure 4.2a)...	150
Figure 4.5. Mean bed elevations at the Cottonwood Ranch Mid-Channel gage, based on USGS field measurement data collected during WY2001 through WY2014....	151
Figure 4.6. Mean bed elevations at the Kearney gage, based on USGS field measurement data collected during WY1982 through WY2014.	152
Figure 4.7. Mean bed elevations at the Grand Island gage, based on USGS field measurement data collected during WY1982 through WY2014.	154

Figure 4.8a.	Best-estimate of annual bed load passing the Darr, Overton, Kearney, Shelton and Grand Island measurement points during Survey Years (SY) 2010 through SY2014, based on integration of the bias-corrected bed-load rating curves over the survey year mean daily hydrograph. Whiskers are upper and lower 95-percent confidence limits from Monte Carlo simulation described in the next section.	155
Figure 4.6b.	Best-estimate of annual suspended sand load passing the Darr, Overton, Kearney, Shelton and Grand Island measurement points during Survey Years (SY) 2010 through SY2014, based on integration of the bias-corrected suspended sand rating curves over the survey year mean daily hydrograph. Whiskers are upper and lower 95-percent confidence limits from Monte Carlo simulation described in the next section.	156
Figure 4.6c.	Best-estimate of annual total sand/gravel load passing the Darr, Overton, Kearney, Shelton and Grand Island measurement points during Survey Years (SY) 2010 through SY2014, based on addition of the best estimates of bed load and suspended sand load. Whiskers are upper and lower 95-percent confidence limits from Monte Carlo simulation described in the next section; bar labels are percent bed load.	157
Figure 4.7.	Best-estimate of the annual sand transport balance between the five measurement locations from SY2010 through SY2014. Also shown are the 5-year averages from the rating curves and from the survey-based estimates.	158
Figure 4.8.	Estimated annual aggradation/degradation quantities from the pure panel AP survey data in the reaches encompassed by the five sediment-transport measurement sites. Also shown are the average annual aggradation/degradation quantities from both the surveys and the rating curves.	160
Figure 4.9.	(a) Suspended sand rating curves at Overton. Light grey lines are sample curves from the Monte Carlo simulation; (b) Distribution of estimated sediment loads at the mean (log) discharge of the measured data set from Monte Carlo simulation; (c) Distribution of the exponents on the Overton suspended sand load rating curve from the Monte Carlo simulation.	163
Figure 4.10.	Distribution of estimated annual suspended sand loads at Overton based on the 1,000 Monte Carlo trials for each of the five years covered by the monitoring surveys.	165
Figure 4.11.	Area used to test agreement between cross section-based volume estimates and estimates based on the complete LiDAR surface (~RM245.5, south channel at Jeffreys Island approximately midway between AP36 and AP37)...	167
Figure 4.12a.	Best-estimate of aggradation/degradation volumes based on the survey data (bars) and mean and upper and lower 95-percent confidence limits on the volumes predicted by the sediment rating curves (symbols) for 2010.....	168
Figure 4.12b.	Best-estimate of aggradation/degradation volumes based on the survey data (bars) and mean and upper and lower 95-percent confidence limits on the volumes predicted by the sediment rating curves (symbols) for 2011.....	168
Figure 4.12c.	Best-estimate of aggradation/degradation volumes based on the survey data (bars) and mean and upper and lower 95-percent confidence limits on the volumes predicted by the sediment rating curves (symbols) for 2012.....	169

Figure 4.12d. Best-estimate of aggradation/degradation volumes based on the survey data (bars) and mean and upper and lower 95-percent confidence limits on the volumes predicted by the sediment rating curves (symbols) for 2014.....	169
Figure 4.12e. Best-estimate of aggradation/degradation volumes based on the survey data (bars) and mean and upper and lower 95-percent confidence limits on the volumes predicted by the sediment rating curves (symbols) for 2014.....	170
Figure 4.13. Annual total runoff volume at the USGS Overton gage between WY1943 and WY2014. Also shown are the mean flows for the 48-year record used for the DOI (2006) model, the Tetra Tech (2010) model and the 5-year monitoring period.....	171
Figure 4.14. Estimated average annual total sand load passing the Overton, Kearney, and Grand Island gages during individual years from WY1984 through WY2014, based on integration of the respective rating curves over the USGS published mean daily flows. Also shown are the upper and lower 95-percent confidence limits from the Monte Carlo simulations.....	172
Figure 4.15. Average annual total sand load passing the Overton, Kearney, and Grand Island gages based on integration of the respective rating curves over the USGS published mean daily flows for the period from WY1984 through WY2014. Also shown are the median values and 5 th and 95 th percentiles from the Monte Carlo simulations.....	173
Figure 4.16a. Estimated annual sand transport balance between Overton, Kearney and Grand Island from WY1984 through WY2014.	175
Figure 4.16b. Estimated annual sand transport balance between Overton, Kearney and Grand Island from WY1984 through WY2014. Same as Figure 4.16a with confidence limits from Monte Carlo simulations.....	176
Figure 4.17. Mean and median annual sand transport balance between Overton, Kearney and Grand Island from WY1984 through WY2014. Also shown are the 5 th and 95 th percentile results from the Monte Carlo simulations.	177
Figure 4.18. Relationship between estimated mean sand balance and total flow volume in the Overton to Kearney and Kearney to Grand Island reaches.	177
Figure 4.19. Reach-wide average height of the GLE points above the 1,200-cfs water surface at the pure panel APs from 2009 through 2014.	179
Figure 4.20. Average height of the GLE above the 1,200 cfs water surface at the each of the pure panel APs during 2009 through 2014, and performance benchmark of +1.5 feet.....	180
Figure 4.21. Yearly change in GLE versus year-to-year difference in stage at maximum mean daily flow preceding each survey at the pure panel APs (Kendall's τ = 0.55, $p=<0.0001$).....	181
Figure 4.22. Yearly change in GLE versus year-to-year difference in stage at mean germination season discharge preceding each survey at the pure panel APs (Kendall's τ = 0.65, $p=<0.0001$).....	182
Figure 4.23. Yearly change in GLE versus year-to-year difference in stage at maximum germination season discharge preceding each survey at the pure panel APs (Kendall's τ = 0.60, $p=<0.0001$).....	183

Figure 4.24.	Yearly difference in total unvegetated channel width versus year-to-year difference in stage at maximum mean daily flow preceding each survey at the pure panel APs (Kendall's $\tau = 0.37$, $p=<0.0001$).....	185
Figure 4.25.	Yearly change in total unvegetated channel width versus year-to-year difference in stage at mean discharge during the germination season at the pure panel APs (Kendall's $\tau = 0.39$, $p=<0.0001$).....	186
Figure 4.26.	Yearly change in total unvegetated channel width versus year-to-year difference in GLE at the primary geomorphic transects of pure panel APs (Kendall's $\tau = 0.47$, $p=<0.0001$).....	187
Figure 4.27.	Average frequency of occurrence and percent cover for common reed (<i>Phragmites australis</i>) on a reach averaged basis observed during each of the six monitoring surveys.....	189
Figure 4.28.	Average percent cover of common reed (<i>Phragmites australis</i>) at the pure panel anchor points during the six monitoring periods.....	190
Figure 4.29.	Total runoff volume at Overton during four periods of the water year and the maximum mean daily discharge during the entire water year and between April 1 and August 1 (~time of monitoring surveys) from WY1990 through WY2014. Long-term average volume based on gage data from WY1941 through WY2014.....	191
Figure 4.30.	Cumulative distribution of inundation depths at the maximum discharge during the growing season for quadrats containing common reed during each of the five monitoring surveys.	193
Figure 4.31.	Depths and velocities from the Elm Creek 2-D model at a discharge of approximately 3,200 cfs: (a) Elm Creek Bridge to Kearney Diversion Structure, (b) downstream from Kearney Diversion Structure.....	194
Figure 4.32.	Incremental probability of plant removal for 1- and 2-year-old Cottonwood (1-year CW and 2-year CW), common reed (PHRAG) and reed canary grass (RCG) based on results from Pollen-Bankhead et al. (2011).....	195
Figure 4.33.	Typical lateral erosion and undercutting of the edge of a sand bar with common reed in the Elm Creek Complex.....	196
Figure 4.34.	Total precipitation during the period from April through July in each of the five monitoring years at five weather stations along the project reach. [Global Historical Climatology Network (GHCN) station numbers used as the data source follow the names].	197
Figure 4.35.	Growing degree days (GDD) above a baseline temperature of 86°F and average temperature at the Grand Island Station (GCHND Sta USW00014935) during the period from April through July during the monitoring period.	198
Figure 4.36.	Percentage of individual vegetation sampling quadrats sprayed at each of the pure panel APs prior to each sampling period. Spraying typically occurs in early-fall; thus, the spraying indicated for each year occurred during fall of the previous year.	201

Figure 4.37.	Percentage of all sampled quadrats sprayed at pure panel anchor points and number of pure panel APs receiving at least some spraying during the preceding fall of the indicated year. First number in each label is number of quadrats sprayed; second number is total number of sampled quadrats.....	202
Figure 4.38.	Change in percent cover of common reed versus percent of quadrats sprayed at pure panel APs with more than 3.5 percent average cover of common reed during the 2009 survey.....	208
Figure 4.39a	Change in percent cover of common reed versus growing degree days at pure panel APs with more than 3.5 percent average cover of common reed during the 2009 survey.....	209
Figure 4.39b-e.	Clockwise from top left, change in percent cover of common reed versus maximum inundation depth, duration of inundation, total precipitation during the growing season measured at Grand Island, and the 90 th percentile low flow during the growing season.	210
Figure 4.40.	Percent flow consolidation (i.e., percent of flow in the main flow path) at 8,000 cfs.....	213
Figure 4.41a.	Mean unvegetated channel width at sites with less than 85 percent flow consolidation and sites with 100-percent flow consolidation based on 2014 monitoring data.	214
Figure 4.41b.	Mean braiding index at sites with less than 85-percent flow consolidation and sites with 100-percent flow consolidation based on 2014 monitoring data.....	215
Figure 4.42.	Total unvegetated channel width versus braiding index (Kendall's $t = 0.19$, $p=0.004$).	216
Figure 4.43.	Total unvegetated channel width versus percent flow consolidation at 8,000 cfs (Kendall's $t = 0.18$, $p=0.012$).....	217
Figure 4.44.	Braiding index versus percent flow consolidation at 8,000 cfs (Kendall's $t = 0.24$, $p=0.002$).....	218
Figure 5.1.	Annual peak discharges at the USGS Overton, Kearney, and Grand Island gages (note that Kearney record started in 1982). Also shown by the black mark is the approximate WY2013 peak discharges prior to the September flood at the three locations.	220
Figure 5.2.	Flood frequency curves for the annual peak flows from WY1942 through WY2013 at the USGS Overton, Kearney (WY1982-WY2013, only), and Grand Island gages.....	221

LIST OF TABLES

Table 1.1.	Anchor point locations.....	4
Table 1.2.	PRRIP Big Questions relevant to the Geomorphology and Vegetation Monitoring Program (from PRRIP, 2012a).....	6
Table 1.3.	Performance metrics relevant to the Priority Hypotheses.....	9
Table 2.1.	Species grouped as genera.	17
Table 2.2.	Geomorphic reaches from Fotherby (2008).....	23
Channel Geomorphology and In-Channel Vegetation 2014 Final Data Analysis Report		

Table 2.3.	Performance metrics defined in the Channel Geomorphology and In-channel Vegetation Data Analysis Plan.....	24
Table 2.4.	Species considered in the analyses—the 25 most frequently observed species in 2014, and species of interest observed at lower frequencies.....	29
Table 2.5.	Summary of trend analysis specified in the Data Analysis Plan.....	32
Table 3.1.	Summary of vegetation survey sites (2009-2014).	73
Table 3.2.	Average green line elevations at pure panel APs observed during the six monitoring surveys.....	75
Table 3.3.	Summary of bed-load sediment discharge measurements taken since the start of the monitoring program in 2009. Also shown are the correlation coefficients (R^2) for best-fit, power-function regression lines through each of the data sets.	105
Table 3.4.	Summary of suspended sand load measurements taken since the start of the monitoring program in 2009. Also shown are the correlation coefficients (R^2) for best-fit, power-function regression lines through each of the data sets.	116
Table 4.1.	Summary of bed and suspended sand load regression equations and associated statistics.....	162
Table 4.2.	Probability of degradation when mean indicates degradation/aggradation when mean indicates aggradation.....	164
Table 4.3.	Anchor points at which at least some aerial spraying occurred during the indicated year.	200
Table 4.4.	Summary of PRRIP mechanical and other direct treatments at the APs for 2008 through 2013 other than aerial spraying.	203
Table 4.5.	Correlation (Spearman) and p-values for percent cover of common reed versus possible influencing variables.	206
Table 4.6.	Correlation (Spearman) and p-values for year-to-year change in percent cover of common reed versus possible influencing variables.	207
Table 4.7.	Correlation matrix for percent flow consolidation, average braiding index and average unvegetated channel width at all of the pure panel APs, and all pure panel APs, except AP9, AP21 and AP33.	212

LIST OF APPENDICES

- Appendix A.1: Mean Daily Flow-duration Curves for Germination Season
- Appendix A.2: Mean Daily Flow-duration Curves for Spring Whooping Crane
- Appendix A.3: Mean Daily Flow-duration Curves for Fall Whooping Crane
- Appendix B.1: Summary of Geomorphic and Selected Vegetation Metrics - 2009
- Appendix B.2: Summary of Geomorphic and Selected Vegetation Metrics - 2010
- Appendix B.3: Summary of Geomorphic and Selected Vegetation Metrics - 2011
- Appendix B.4: Summary of Geomorphic and Selected Vegetation Metrics - 2012
- Appendix B.5: Summary of Geomorphic and Selected Vegetation Metrics - 2013
- Appendix B.6: Summary of Geomorphic and Selected Vegetation Metrics - 2014
- Appendix C: Vegetation Data

LIST OF ACRONYMS AND ABBREVIATIONS

AMP	Adaptive Management Plan
AP	Anchor Point
cfs	Cubic Feet per Second
DAP	Data Analysis Plan
EA	Environmental Account
FAC	Facultative
FACU	Facultative Upland
FACW	Facultative Wetland
FSM	Flow, Sediment, and Mechanical
GDD	Growing Degree Days
GHCN	Global Historical Climate Network
GLE	Greenline Elevation
GPS	Global Positioning System
KDC	Kearney Diversion Channel
LiDAR	Light Detection and Ranging
NAD83	North American Datum of 1983
NAVD88	North American Vertical Datum of 1988
NDNR	Nebraska Department of Natural Resources
NWIS	National Water Information System
OBL	Obligate Wetland
PRRIP	Platte River Recovery Implementation Program
RM	River Mile
RP	Rotating Panel
SDHF	Short-duration High Flow
SMDF	Short-duration Medium Flow
SY	Survey Year (August 1 through July 31)
tpy	Tons per Year
USACE	United States Army Corps of Engineers
USGS	United States Geological Survey
VSZ	Vegetation Survey Zone
WY	Water Year

1 INTRODUCTION

1.1 Background

The Platte River Recovery Implementation Program (Program, aka PRRIP) was initiated on January 1, 2007, between Nebraska, Wyoming, Colorado, and the Department of the Interior to address endangered species concerns in the central and lower Platte River. Four “target” species are of primary concern to the Program: the whooping crane, piping plover, interior least tern, and pallid sturgeon. The intent of the Program is to rehabilitate habitat in the Platte River for these species by restoring a braided channel morphology with sand bars free of vegetation, increased channel widths and unobstructed views.

Because of the uncertainty in how the river will respond to management actions, the Program has developed several *Big Questions* and priority hypotheses related to the linkage between channel geomorphology, in-channel vegetation and habitat for the target species (PRRIP, 2006). To help answer these questions and test the hypotheses, a Channel Geomorphology and Vegetation Monitoring Program has been implemented to collect and analyze a suite of data over a multi-year time-frame with the following specific objectives:

- Document trends in channel geomorphology parameters throughout Central Platte River during the 13-year First Increment (2007-2019) of the Program, including shape, width, planform, aggradation/degradation trends, bed-material grain sizes, and sediment loads.
- Provide system-wide status in areal coverage and elevation range of in-channel seedlings and invasive vegetation to assist in implementing the Program’s Adaptive Management Plan (AMP) (PRRIP, 2012b) and use of water in the Environmental Account (EA), evaluate the extent of existing native and non-native invasive species infestations, and serve as a mechanism for identification of new invasive species populations before infestations become widespread.

A previous contractor team consisting of Ayres Associates and Olsson Associates implemented the Program’s monitoring protocol (PRRIP, 2010) during the first three years of the monitoring program, with the first year of the data collection occurring in 2009 (Ayres and Olsson, 2010, 2011 and 2012). The Program has also developed a draft Data Analysis Plan (PRRIP, 2012a).

Tetra Tech has continued to carry out the program beginning in 2012, including implementation of the Data Analysis Plan that was not included in the earlier contract. Results from the 2012 and 2013 data collection and the first two years of data analysis were presented in Tetra Tech (2013 and 2014). This report describes the data and results from Tetra Tech’s implementation of the sixth year of the monitoring program (2014) and the third year of implementation of the data analysis plan.

1.2 Scope of the Monitoring Program

1.2.1 Area of Interest

The area of interest for geomorphology and vegetation monitoring consists of channels within approximately 0.5 miles on either side of the centerline of the Platte River, beginning at the junction of U.S. Highway 283 and Interstate 80 near Lexington, Nebraska, and extending eastward to Chapman, Nebraska (approximately 100 miles) (**Figure 1.1**). Certain areas within this portion of the central Platte River have been prioritized for monitoring based on key priority hypotheses, ecological need, and Program actions undertaken during the First Increment.



Figure 1.1. Location map showing the project reach for the Channel Geomorphology and In-channel Vegetation Monitoring. Bed-load and suspended-sediment sampling bridge sites are shown as red circles.

1.2.2 Anchor Points

A systematic sample of locations along the river have been identified to serve as "anchors" for the data collection. These locations, referred to as anchor points (APs), are spaced at approximately 4,000-meter (2.5-mile) intervals along the centerline of the river, and each point has been labeled with a U.S. Army Corps of Engineers (USACE) River Mile (RM) (**Table 1.1**). The specific locations of some of the APs were selected to accommodate previously established cross sections within the historical database and to accommodate some land access issues; thus, the actual spacing can vary by up to 800 meters (0.5 miles) from the typical, 4,000-meter spacing. The basic geomorphic sampling unit consists of three transects spaced at approximately 150-meter intervals. The transects extend laterally across the historic flood plain and incorporate the current main channel, as well as all primary split-flow channels (i.e., those channels separated from the main channel by islands). Although the north channel (Reach 1) and south channel (Reach 2) of Jeffreys Island share the same AP number, these two channels are treated as separate reaches because the flows in the north channel are derived from the upstream river, while the flows in the south channel are almost entirely derived from flow releases from the J-2 Return.

1.2.3 Pure and Rotating Panel Points

The APs sampled each year under this protocol are components of a "pure panel" subset and a "rotating panel" subset. A panel is made up of a group of sampling sites that are always visited at the same time. Data collection is conducted at the pure panel sites (odd numbered sites in Table 1.1) every year, and the rotating panel sites have been divided into four groups that are visited once every four years on a rotating basis. As a result, 25 sample sites are surveyed each year (20 pure panels and 5 rotating panels). Each of the sites in the rotating panel series are to be surveyed three times in the First Increment. In accordance with the protocol, data were collected at all of the Pure Panel (i.e., odd-numbered) APs and at the five rotating APs that are designated as R2 (highlighted points in Table 1.1) during the 2014 field season. With this data set, the pure panel points have been sampled six times, the R2 rotating panel points have been sampled twice, and all other the rotating panel points have been sampled once. Per the Monitoring Protocol, the secondary channels at the Pure Panel points were not re-surveyed during the second through fourth year of the data collection. These channels were re-surveyed during 2013, and will not be re-surveyed again until 2017.

1.2.4 Channel Geomorphology Monitoring

The geomorphology portion of this monitoring program is designed to document trends in channel morphology across the entire study area throughout the First Increment (2007-2019). In addition, the data will document trends at specific sites or groups of sites within the overall study area. The monitoring is focused on measuring and tracking changes in river planform, river cross-sectional geometry (including bed elevation and channel width), longitudinal bed profile, streamflow, sediment loads, and bed, bar and bank material grain-size distributions. The monitoring data are collected through a combination of aerial photographs, airborne terrestrial LiDAR, topographic ground surveys, bed material sampling, ground photography, flow measurements at gaging stations, and sediment-transport measurements. The overall strategy is focused on a randomized scheme, but there is some sampling stratification (e.g., grain size) to reduce variability and improve future comparisons.

Table 1.1. Anchor point locations.

Anchor Point No.	Systematic Point at 4000 m (2.5 miles) (River Mile)	Closest Existing Cross Section	Recommended Anchor Point (River Mile)	Pure (P) or Rotating (R) Panel	Location
40	254	254.4	254.4	R1	Lexington
39	251.5 Bridge	250.5	250.8	P	Lexington bridge (Hwy 283)
38	249	249.5	249	R2	
37	246.5	246.5 N & 246.0 S	246.5 N & S	P	J2 Return - Jeffrey Island
36	244	244.0 N & S	244.0 N & S	R3	
35	241.5		241.5 N & S	P	
34	239	239.1	239.1	R4	D/S Overton bridge (Rd. 444)
33	236.5	237.3	236.4	P	Cottonwood Ranch transects
32	234	233.9	234.1 Main, N, S	R1	
31	231.5	231.5	231.5	P	U/S Elm Creek bridge (Hwy 183)
30	229	228.6	228.6	R2	D/S Kearney Diversion
29	226.5	226.4	226.4	P	
28	224 Bridge	224.3	224.3	R3	Odessa Rd. Bridge
27	221.5	222	221.9	P	
26	219	219.8	219	R4	
25	216.5		216.5	P	
24	214		214	R1	D/S Kearney bridge (Hwy 44)
23	211.5	210.6	211.5 Main & N1,N2	P	
22	209	208.4	208.4 Main & N1	R2	U/S 32 Rd. bridge (Hwy 10)
21	206.5	206.7 (no N)	206.7 Main & N1	P	
20	204	203.3 N&S	204.0 Main & N1	R3	
19	201.5	201.1 N maybe S	201.1 Main & N1	P	D/S Lowell Rd. bridge (Hwy 10C)
18	199	199.5	199.5	R4	
17	196.5	196.4	196.4	P	U/S Shelton Rd. bridge (Hwy 10D)
16	194	193.9	193.8	R1	
15	191.5	190.9	190.7	P	
14	189	189.3	189.3	R2	
13	186.5	187	186.7 Main & N1	P	D/S S. Nebraska Hwy 11 bridge
12	184	183.1	184.0 Main & N1	R3	
11	181.5	181.8 S	181.8 Main & N1	P	D/S S. Alda Rd. bridge
10	179	178.38 & 178.4 M & N	179.0 Main & N1,N2,N3	R4	
9	176.5	177.1	176.5 Main & N1,N2,N3	P	U/S SR 34/281 bridge (Doniphan)
8	174	174.6	174 Main & N1,N2,N3	R1	Grand Island
7	171.5	172.1 S & SM & N & NM	171.5 Main & N1,N2,N3	P	D/S I-80 bridge
6	169	168.7 N & S	169.1 Main & N1	R2	
5	166.5	166.9	166.9	P	D/S SR 34/Hwy 2 bridge
4	164	164.6	164	R3	
3	161.5	162.1	161.8	P	Phillips
2	159	158.7	158.7	R4	
1	156.5	157.3	156.6	P	D/S Bader Park Rd. br (Chapman)

1.2.5 In-channel Vegetation Monitoring

The vegetation monitoring portion of this program is designed to document the areal extent of species of interest within the Vegetation Survey Zone (VSZ) (as defined in the protocol) between the historic high banks. The APs have been identified to provide data collection locations that are consistent from year to year, and that are representative of the entire study area. The vegetation surveys are conducted in conjunction with the field component of the geomorphology monitoring (and at the same locations) so that the vegetation data points can be readily included in the topographic surveys.

Vegetation sampling is conducted within fixed-width (belt) transects that are centered on each of the APs, and extend across the VSZ that is generally defined as the area within the historic high banks. The width of each belt transect is approximately 300 meters (1,000 feet), extending for approximately 150 meters (500 feet) upstream and downstream of the AP. During the first four years of data collection, the overall belt transect consisted of seven, roughly parallel, vegetation transects spaced approximately 50 meters (165 feet) apart. The upstream, downstream and middle vegetation transects correspond to the three primary geomorphology transects.

Subsampling and statistical analyses of the large volume of data collected during the first four field seasons showed no significant difference ($p>0.05$ for all analysis) between vegetation data collected at all seven transects compared to five transects when Transects 2 and 6 are removed. Sampling two fewer transects per AP substantially increases the efficiency of the field component of this work, while retaining full comparability to vegetation data collected in prior years. As a result, the Monitoring Protocol has been modified to eliminate two transects (typically Transects 2 and 6, counting from the upstream end of each site).

Current vegetation species of interest include six woody species: narrow-leaf willow (*Salix exigua*), peach-leaf willow (*S. amygdaloidea*), eastern cottonwood (*Populus deltoides*), false indigo (*Amorpha fruticosa*), saltcedar (*Tamarix ramosissima*), and Russian olive (*Elaeagnus angustifolia*), as well as several herbaceous species, including purple loosestrife (*Lythrum salicaria*), common reed (*Phragmites australis*), rice cut grass (*Leersia oryzoides*), and river bulrush (*Bolboschoenus fluviatilis*). In addition, reed canary grass (*Phalaris arundinacea*) was also included because it is a vigorous competitor, is present in high densities in some areas, and it has a tendency to form dense rootmats and monocrop stands. Although the analysis focuses on these species of interest, it is important to note the in-channel monitoring documents all plant species encountered at each sample point.

1.2.6 Airborne Mapping of Topography (LiDAR)

Because of the characteristics of the vegetation on the historic overbanks and islands within the corridor between historic banks, ground surveys outside the active channel and mechanically modified areas would be very laborious and costly. As a result, contour base mapping has been developed from airborne terrestrial LiDAR data. Originally, airborne terrestrial LiDAR flights for mapping were to be flown at the beginning (baseline conditions) and end of the First Increment. Recognizing the high value of the LiDAR data, the Program changed these requirements and LiDAR data are now collected during the fall of each year in conjunction with Color InfraRed (CIR) photography. These data are used to develop topographic surfaces with ± 6 -inch vertical accuracy, sufficient for one-foot contour interval mapping of the area between the historic outer banks (approximately 1 mile in width).

1.3 Hypotheses and Performance Metrics

The AMP (PRRIP, 2006) for the 13-year, First Increment of the Program that extends from Program inception in 2007 through 2019, focuses on several critical scientific and technical uncertainties about the target species, physical processes, and the response of the target species to management actions. These uncertainties are captured in statements of broad hypotheses on pages 14-17 of the AMP and, as a means of better linking science learning to Program decision-making, those uncertainties comprise a set of “Big Questions” that provide a template for linking specific hypotheses and performance measures to management objectives and overall Program goals.

1.4 Big Questions

This monitoring program is focused on four specific Big Questions that relate directly to river morphology and in-channel vegetation (**Table 1.2**):

Big Question #1 – Will implementation of short-duration high flows (SDHF) produce suitable tern and plover riverine nesting habitat on an annual or near-annual basis?

Big Question #2 – Will implementation of SDHF produce and/or maintain suitable whooping crane riverine roosting habitat on an annual or near-annual basis?

Big Question #3 – Is sediment augmentation necessary for the creation and/or maintenance of suitable riverine tern, plover, and whooping crane habitat?

Big Question #4 – Are mechanical channel alterations (channel widening and flow consolidation) necessary for the creation and/or maintenance of suitable riverine tern, plover, and whooping crane habitat?

Table 1.2. PRRIP Big Questions relevant to the Geomorphology and Vegetation Monitoring Program (from PRRIP, 2012a).

PRRIP Big Questions = What we don't know but want to learn	Broad Hypothesis	Priority Hypotheses
Implementation – Program Management Actions and Habitat		
1. Will implementation of (SDHF) produce suitable tern and plover riverine nesting habitat on an annual or near-annual basis?	<i>PP-1a. Flows of 5,000 to 8,000 cfs magnitude in the habitat reach for a duration of three days at Overton on an annual or near-annual basis will build sandbars to an elevation suitable for least tern and piping plover habitat.</i>	Flow #1
2. Will implementation of SDHF produce and/or maintain suitable whooping crane riverine roosting habitat on an annual or near-annual basis?	<i>PP-1b. Flows of 5,000 to 8,000 cfs magnitude in the habitat reach for a duration of three days at Overton on an annual or near-annual basis will increase the average width of the vegetation-free channel.</i>	Flow #3, Flow #5
3. Is sediment augmentation necessary for the creation and/or maintenance of suitable riverine tern, plover, and whooping crane habitat?	<i>PP-2. Between Lexington and Chapman, eliminating the sediment imbalance of approximately 400,000 tons annually in eroding reaches will reduce net erosion of the river bed, increase the sustainability of a braided river, contribute to channel widening, shift the river over time to a relatively stable condition, and reduce the potential for degradation in the north channel of Jeffrey Island resulting from headcuts.</i>	Sediment #1
4. Are mechanical channel alterations (channel widening and flow consolidation) necessary for the creation and/or maintenance of suitable riverine tern, plover, and whooping crane habitat?	<i>PP-3. Designed mechanical alterations of the channel at select locations can accelerate changes towards braided channel conditions and desired river habitat.</i>	Mechanical #2

1.5 System-Scale Hypotheses

The above Big Questions are based on the following broad hypotheses that are directly related to river morphology and the influence of in-channel vegetation:

S-1: A combination of flow management, sediment management, and land management (i.e., Clear/Level/Pulse) will/will not generate detectable changes in the channel morphology of the Platte River on Program lands, and/or habitats for whooping crane, least tern, piping plover, pallid sturgeon, and other species of concern.

S-2: A combination of non-managed flows, sediment management, and land management (i.e., Clear/Level/Mechanical Maintenance) will/will not generate detectable changes in the channel morphology of the Platte River, and/or habitats for whooping crane, least tern, piping plover, pallid sturgeon, and other species of concern.

S-4: Program management actions will/will not be of sufficient scale and magnitude to cause detectable system wide changes in channel morphology and/or habitats for the target species.

PP-1: Flows of varying magnitude, duration, frequency and rate of change affect the morphology and habitat quality of the river, including:

- Flows of 5,000- to 8,000-cfs magnitude in the habitat reach for a duration of three days at Overton on an annual or near-annual basis will build sand bars to an elevation suitable for least tern and piping plover habitat;
- Flows of 5,000- to 8,000-cfs magnitude in the habitat reach for a duration of three days at Overton on an annual or near-annual basis will increase the average width of the vegetation free channel;
- Variations in flows of lesser magnitude will positively or negatively affect the sand bar habitat benefits for least terns and piping plovers.

PP-2: Between Lexington and Chapman, eliminating the sediment imbalance of approximately 400,000 tons annually in eroding reaches will:

- Reduce net erosion of the river bed;
- Increase the sustainability of a braided river;
- Contribute to channel widening;
- Shift the river over time to a relatively stable condition; and
- Reduce the potential for degradation in the north channel of Jeffrey Island.

1.6 Priority Hypotheses

The AMP (PRRIP, 2006) formalizes several detailed hypotheses that specifically address uncertainty in the underlying physical process relationships related to potential flow, sediment, and mechanical (FSM) actions. The Tier 1 physical process priority hypotheses related to potential FSM actions include (**Figure 1.2**):

Flow #1: Increasing the variation between river stage at peak (indexed by the $Q_{1.5}$ @ Overton) and average flows (1,200-cfs index flow), by increasing the stage of the $Q_{1.5}$ through Program flows, will increase the height of sandbars between Overton and Chapman by 30 to 50 percent from existing conditions, assuming balanced sediment budget.

Flow #3: Increasing $Q_{1.5}$ with Program flows will increase local boundary shear stress and frequency of inundation at the existing green line (elevation at which riparian vegetation can establish). These changes will increase riparian plant mortality along margins of the channel, raising the elevation of the green line, providing more exposed sandbar area and a wider, unvegetated main channel.

Flow #5: Increasing the magnitude and duration of the $Q_{1.5}$ will increase riparian plant mortality along the margins of the river. There will be different relations for different species. This will in turn lead to increasing channel width.

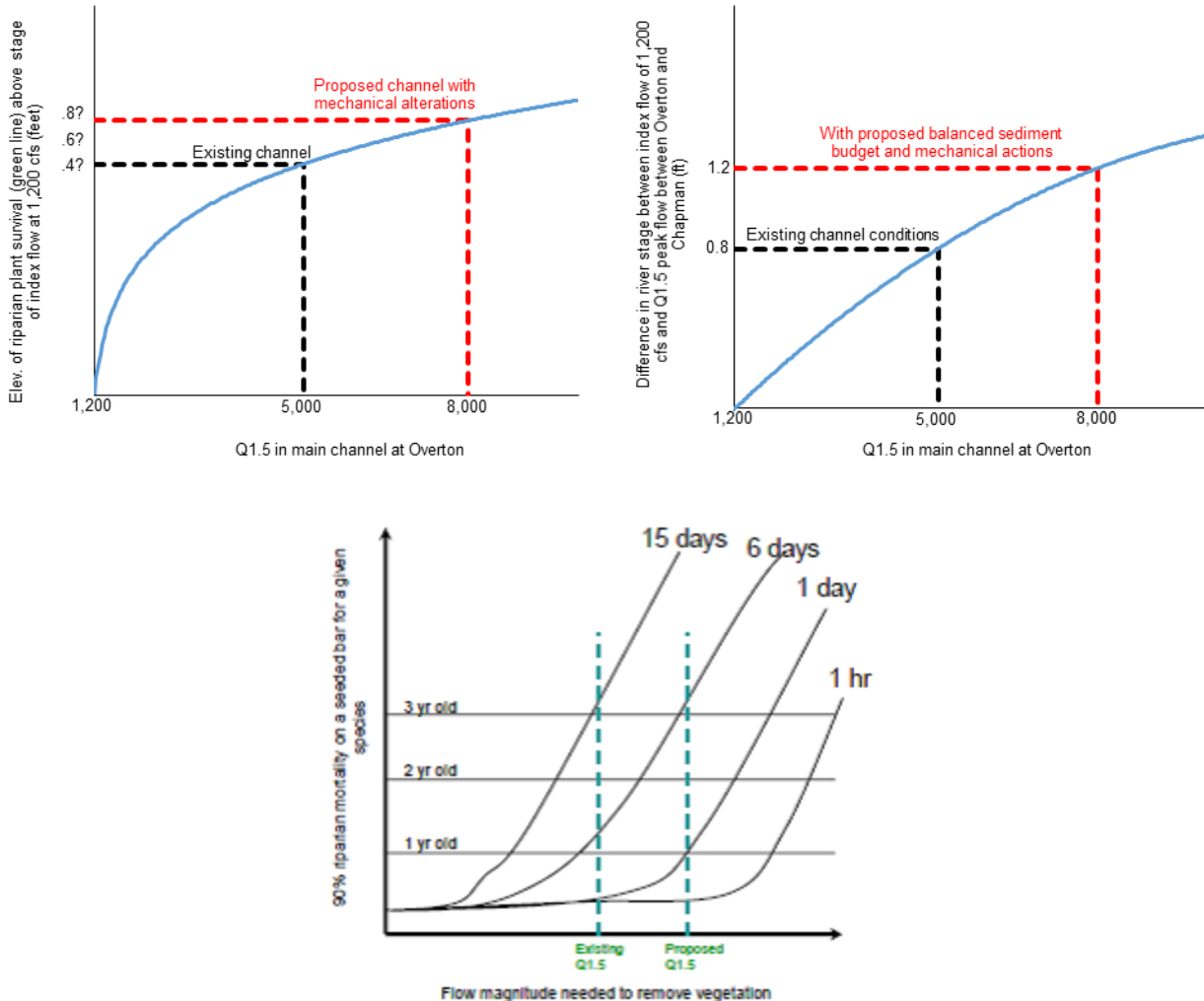


Figure 1.2. Clockwise from top left, illustrations of Priority Hypothesis Flow #1, Flow #3, and Flow #5.

Sediment #1: Average sediment augmentation near Overton of 185,000 tons/year under existing flow regime and 225,000 tons/year under GC proposed flow regime achieves a sediment balance to Kearney (**Figure 1.3**).

Mechanical #2: Increasing the Q1.5 in the main channel by consolidating 85 percent of the flow, and aided by Program flow and a sediment balance, flows will exceed stream power thresholds that will convert the main channel from meander morphology in anastomosed reaches to braided morphology with an average braiding index greater than 3 (Figure 1.3).

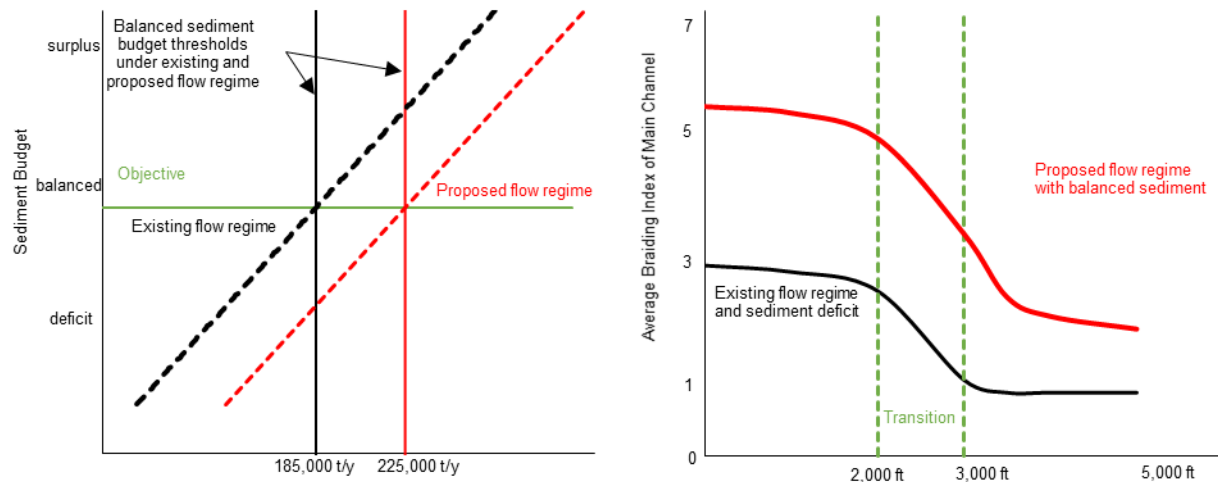


Figure 1.3. Illustration of Priority Hypothesis Sediment #1 (left) and Mechanical #2 (right).

1.7 Performance Metrics

The Program has identified a suite of performance metrics that are quantified using the data from the monitoring program, in conjunction with the available data from the various USGS stream gages and results from the Program's system-wide 1-D hydraulic model. Data and results from other Program activities, including the Elm Creek and Shoemaker Island FSM Experiments, the Pilot-scale Sediment Augmentation Project, and the Cottonwood Ranch Flow Consolidation project will also be considered, where appropriate, to supplement the data collected specifically for this monitoring program. Many of these performance metrics can be directly associated with the above-described priority hypotheses (Table 1.3).

Table 1.3. Performance metrics relevant to the Priority Hypotheses.

Hypothesis	Performance Metric(s)
Flow #1	<ul style="list-style-type: none"> • Stage-discharge relation
Flow #3	<ul style="list-style-type: none"> • Green line elevation • Vegetation percent cover • Unvegetated channel width • Channel stage-width relationship
Flow #5	<ul style="list-style-type: none"> • Vegetation species-specific elevation data • Vegetation species-specific areal coverage data • Stage-discharge relation • Green-line elevation
Sediment #1	<ul style="list-style-type: none"> • Sediment load • Bed and bar material grain-size distribution • Bank material grain-size distribution • Channel volume • Braiding index • Longitudinal profile
Mechanical #2	<ul style="list-style-type: none"> • Braiding index

Page Intentionally Left Blank

2 METHODS

The Program's Monitoring Protocol (PRRIP, 2010) and draft Data Analysis Protocol (PRRIP, 2012a) describe the methods that are to be used to collect and analyze the data from this program. A summary of the key elements of those protocols that were implemented from 2012 to 2014 are described in the following paragraphs. In assessing the following discussion, it is important to note that the Data Analysis Protocol is still in draft form; the specific methods and techniques for analyzing the data and relating the results to the Big Questions and Priority Hypotheses may evolve as additional data are obtained and the results are reviewed by the various entities involved in the Program.

2.1 Field Data Collection Methods

As discussed in Chapter 1, the field data being collected for this program fit into three general categories:

- Geomorphic data that describe the physical characteristics of the river, including dimension, planform, pattern, and boundary sediments.
- Vegetation data that describe the distribution, frequency, density and other relevant characteristics of the in-channel vegetation.
- Sediment-transport data to quantify the relationship between discharge and sediment-transport rates throughout the reach.

In accordance with the monitoring protocol, the 2014 geomorphology and vegetation data were collected during the period between July 8 and August 8. The total flow in the river was generally quite low during the survey period, ranging from a peak of than 688 cfs on July 8 at the USGS Kearney gage (USGS Gage No. 06770200), when AP15 was surveyed to a low of less than 40 cfs on July 29 (**Figures 2.1 and 2.2**). Maximum daily discharge at the Kearney gage was below 300 cfs from July 11 through August 7.

Field logistics required that the surveys were conducted in three separate trips. The first trip occurred from July 8 through July 12, and included AP14 to AP23. The second trip was conducted from July 21 to July 26, and included the anchor points upstream from AP23. The third trip took place from August 4 to August 8, and included the APs downstream from AP14.

Bed-load and suspended sediment-transport data were collected on June 16-18, near the peak of the spring runoff (Figure 2.1). Flows at Darr and Shelton were approximately 4,250 cfs, and 5,660 cfs¹, respectively. Flow at Overton peaked near 6,000 cfs during sampling, flow at Kearney was approximately 5,500 cfs, and flow at Grand Island was about 5,100 cfs. Flows throughout the year were unusually low, and the quantity and quality of existing sediment discharge measurements across the range of discharges observed throughout the spring, summer, and early fall did not require further sediment discharge measurements.

The following sections describe the specific field methods that were employed in implementing the monitoring protocol during the 2014 field season.

2.1.1 Landowner Contact

A protocol for obtaining landowner permission was established by the Program and the previous contractor before conducting the field survey work in Year 1 (2009). Program staff made the initial contact with the landowners and obtained written permission allowing access to their properties. Program staff also created a geodatabase that included landowner contact

¹There appeared to be an error in the reporting of flows by NDNR at Shelton. For a discussion of this, see Section 2.4.1.2.

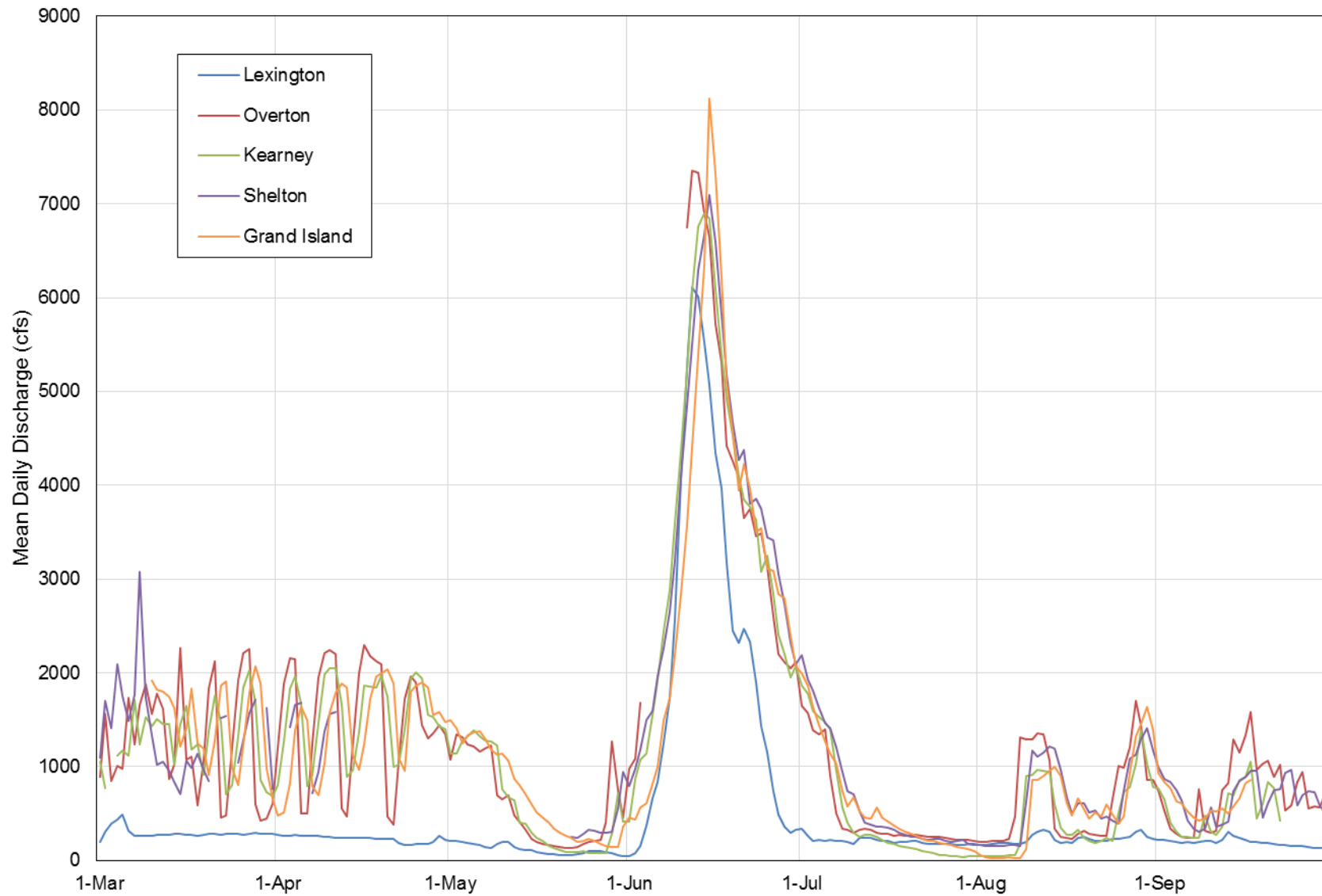


Figure 2.1. Mean daily flows at the USGS and NDNR stream gages between March 1 and September 30, 2014.

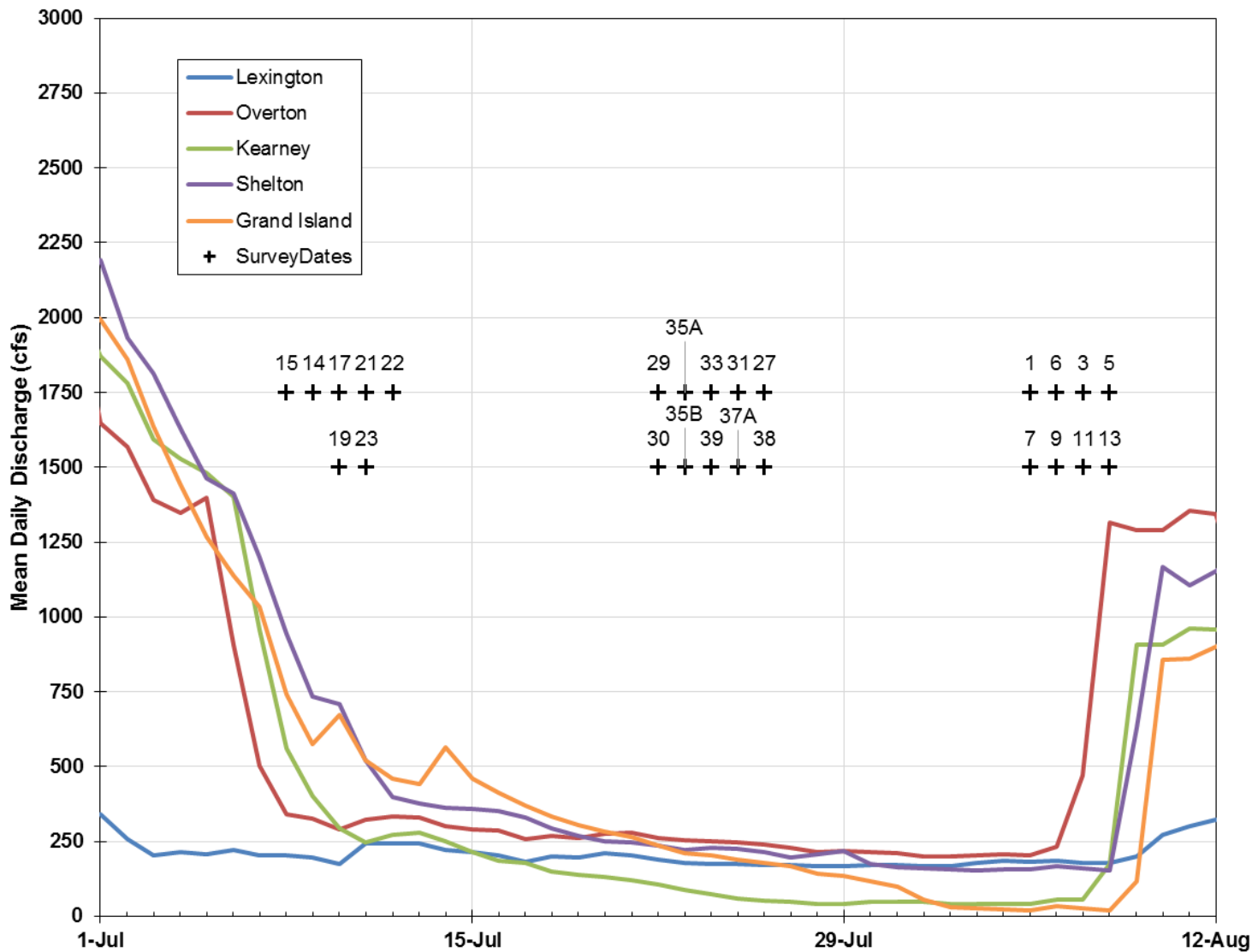


Figure 2.2. Mean daily flows at the USGS and NDNR stream gages between July 1 and August 15, 2014. Also shown are the days on which each AP was surveyed.

information for each AP. This database was updated during each of the subsequent years of the program. The signed permission forms and the updated geodatabase were provided to Tetra Tech prior to the start of the 2012 field work. A binder containing copies of the landowner permission forms was kept with the field crews in case questions or disputes arose while in the field. As landowner-program relationships are of paramount importance, Tetra Tech contacted the affected landowners by telephone before the start of each field effort in order to coordinate river access, maintain communication between landowners and the program, and notify landowners of work near their property.

In addition, significant coordination was conducted between the field crews and Program staff during the fieldwork to ensure that property access protocols were followed, to obtain updates on new landowner requirements, and to report problems with landowners or access. In this regard, it should be noted that Pure Panel AP37B was not surveyed between 2012 and 2014 because permission to access the property has been revoked by the property owner due to a dispute that arose during the 2011 data collection. Additionally, Pure Panel AP25 was not surveyed in 2013 or 2014 because the landowner on the south side of the river at this location revoked permission for access.

2.2 Topographic Ground Survey Methods

Ground surveys were conducted to obtain elevation profiles within the active channel (i.e., the accretion zone) at each of the 20 pure-panel and five rotating APs that were sampled during the 2014 field season. The surveys also included the horizontal and vertical location of all vegetation sample quadrats and bed and bar material samples.

2.2.1 Survey Control

The horizontal coordinates of all topographic survey points were referenced to the North American Datum of 1983 (NAD) and the elevations were referenced to the North American Vertical Datum of 1988 (NAVD88). The original primary control for the project was established by the previous contractor at approximately 12-mile intervals along the reach based on static GPS observations over an approximately 4-hour period at each point. Secondary control was subsequently established between the primary control points using RTK GPS. A more detailed description of the procedure for setting the primary and secondary control points can be found in Ayres and Olsson (2010, 2011 and 2012).

2.2.2 Geomorphic Transects

The topographic surveys of the geomorphology transects included only the portion of the cross sections where the ground had been inundated since the previous survey, and also included areas where the ground has been disturbed by discing, mowing, or grading, where natural processes have created significant topographic changes (i.e., channels and islands where sediment could have been deposited or eroded), and locations where new dikes or other river training structures have been placed or removed by landowners. The transect surveys included the channels, banks, and small islands within the accretion zone, but not the upland portions of the cross section beyond the potential bank erosion/deposition zone. As will be described below, data for these portions of the cross sections were obtained from the Program's LiDAR data. Per the monitoring protocol, ground surveys were also conducted on the secondary, split flow channels at the Pure Panel APs and the Year 2 Rotating Panel Points (R2) between Kearney and Grand Island.

The transects were surveyed using a Leica survey-grade global positioning system (GPS) per the requirements defined in the monitoring protocol. When each of the surveyed APs was originally established, transects were generally oriented perpendicular to the principal flow

direction and extended through all channels at the AP. In some instances where a single transect alignment would not remain perpendicular to the primary flow direction across all active channels, the transect was divided into an appropriate number of segments bounded by internal nodes that were also monumented in the field with a marker pin. The end-points of each cross section were monumented on both historic outer banks with a permanent metal marker (pin) set above the flood elevation and far enough from the active channel to avoid all but the most severe erosion effects.

The location of cross-section and transect marker pins, their monumentation, and the extent of the survey beyond the pins depended on accessibility and private property requirements and restrictions. The marker pins consist of approximately 18-inch long, 1/2-inch (#4) rebar, driven flush with the ground surface, and topped with an aluminum cap that is stamped with the AP and transect identification. The geographic coordinates and elevation of each marker pin were established with vertical and horizontal accuracies of 0.1 feet or less using standard survey techniques and criteria. In cases where previously established marker pins were lost, damaged, or displaced, a new marker pin was set at a suitable location prior to conducting the surveys.

In performing the surveys, a code was recorded in the GPS datalogger to identify the feature represented by each point to facilitate reduction and interpretation of the data. Typical features included:

- Top and toe of bank,
- Bed or ground elevation,
- Left and right edge of water of all channels,
- Water surface at exposed bars and islands,
- Edge of canopy of permanent woody vegetation >1.5 meters tall,
- Edge of vegetation (green line), and
- Other significant geomorphic features.

To ensure that the ground profile across each transect was adequately described, GPS readings were also taken at all significant breaks in slope. Where no obvious breaks in slope were present, GPS survey points were recorded at a maximum spacing of 15 meters (50 feet).

2.2.3 Unobstructed Channel Width

During the first four years of data collection, a key purpose of collecting the vegetation height data (described in the following section) was to facilitate analysis of the unobstructed channel width that is related to maximum sight distance for whooping cranes. In using these data to compute the sight distance metric, it became apparent that a direct measurement of the maximum distance between visual obstructions on each transect would simplify the analysis, improve the accuracy and reduce the uncertainty of the result. For this reason, the data collection protocol for this metric was changed in 2013 to direct measurement. This was accomplished at each of the surveyed transects, as follows:

1. When a substantial opening in vegetation that was greater than 1.5 m (4.9 feet) high occurred along the transect (e.g., bare sand and open water areas, grassy islands, etc.), the location of the edge of water at 2,400 cfs on one side of the opening was located using the RTK GPS, based on the modeled water-surface elevation for the transect.

2. A Simmons LRF 600 laser rangefinder, with magnification set at 4x and reported accuracy of ± 3 feet, was held at approximately 4.9 feet (1.5 m) above the ground and the distance to the next obstruction along the transect at that same height was measured and recorded.

When more than one opening occurred along the transect, a measurement was typically taken at each opening, and the largest of the measurements was used as the unobstructed channel width.

2.3 Vegetation Survey Methods

As discussed previously, during the first four years of monitoring, vegetation sampling was conducted at seven transects at each AP. Subsampling and statistical analyses of the large volume of data collected during these field seasons showed no significant difference ($p \leq 0.05$ for all analysis) between vegetation data collected at all seven transects compared to five transects when Transects 2 and 6 are removed. As a result, the Monitoring Protocol was modified in 2013 to eliminate two of transects (typically Transects 2 and 6, counting from the upstream end of each site) to increase the efficiency of the data collection.

The start and end points of the VSZ along the each transect were determined in the field by assessing local vegetation characteristics and topography. Areas identified as out of the active channel were not surveyed. These areas included any portion of each transect dominated by mature woody vegetation having greater than 25 percent tree canopy cover and/or areas that were located topographically above the active channel and dominated by upland vegetation. The first quadrat on each linear transect was sampled at the start of each VSZ. All subsequent quadrats along each linear transect were sampled at regular 15-meter intervals until the end of the VSZ was reached. Occasionally, more than one VSZ was identified on a single linear transect. In these cases, the start and end points of each VSZ were determined as described above. Areas along a transect identified as not within the VSZ were generally larger than 15 meters (50 feet) in width (i.e. upland vegetated islands).

The Daubenmire (1959) canopy coverage method was used to collect vegetation data within each quadrat. At each 15 meter increment along the VSZ, a 1 square-meter quadrat was placed on the ground. All plant species within the quadrat frame and present at greater than trace densities (i.e., >2 percent of the quadrat area) were identified, and their cover was documented using Daubenmire cover classes. Plant species were identified primarily using *The Flora of Nebraska* (Kaul et al., 2011), although other field guides were also referenced such as *Weeds of the Great Plains* (Stubbendieck et al., 2003) and *Grasses of Colorado* (Shaw, 2008). Plant taxonomy was based primarily on Kaul et al. (2011), but was standardized using the PLANTS Database (USDA-NRCS 2014) and the National Wetland Plant List (USACE, 2014).

An evaluation of the sampling methodology has shown that in many cases, analyzing data composed of individual species can obscure trends and patterns during analysis and lead to ineffective hypothesis testing. Additionally, earlier years of the study collected data largely to the genus level. To control for these two factors during analysis, related species within a genera have been grouped together as the genera if they share similar ecological niches (**Table 2.1**), as determined by their natural history and wetland indicator status (USACE, 2014). Although the discussion that follows refers frequently to “species”, the vegetation it is referring to may instead be a genus. The term “species” was retained for consistency with prior years, and is used loosely in this report. Species grouped under shared genera for analysis are as follows:

In previous annual reports, five species of primary interest: purple loosestrife (*Lythrum salicaria*), common reed (*Phragmites australis*), eastern cottonwood (*Populus deltoides*), willow (*Salix* sp.), and cattail (*Typha* sp.), were analyzed in greater detail than other species because of preliminary evidence suggesting their importance to this study. Because cattail has been

encountered relatively infrequently throughout this study, its importance to the Program has diminished, and it has not been evaluated in detail since 2012 (it continues to be identified in the field data, but is not analyzed in this report).

Table 2.1. Species grouped as genera.

Genus	Common Name
<i>Ambrosia</i> sp.	Ragweed species
<i>Ammannia</i> sp.	Redstem
<i>Artemisia</i> sp.	Artemisia species
<i>Bidens</i> sp.	Beggarticks species
<i>Chamaesyce</i> sp.	Sandmat
<i>Cyperus</i> sp.	Flatsedge
<i>Echinochloa</i> sp.	Barnyard grass species
<i>Eleocharis</i> sp.	Spikerush
<i>Euphorbia</i> sp.	Euphorbia species
<i>Hackelia</i> sp.	Hackelia species
<i>Helianthus</i> sp.	Sunflower
<i>Heterotheca</i> sp.	Heterotheca species
<i>Mentha</i> sp.	Mint species
<i>Polygonum</i> sp.	Polygonum species
<i>Potentilla</i> sp.	Cinquefoil
<i>Rorippa</i> sp.	Yellowcress
<i>Salix</i> sp.	Willow
<i>Schoenoplectus</i> sp.	Bullrush
<i>Solidago</i> sp.	Goldenrod
<i>Typha</i> sp.	Cat-tail
<i>Vernonia</i> sp.	Ironweed

Additional data collected at each quadrat included height of herbaceous and woody species, and vegetation community type. All quadrats with quantifiable vegetation cover (those with standing live vegetation) were photographed and archived. Specific data collected at each quadrat included the following:

- **Spatial data:** Horizontal coordinates and elevation of each quadrat (taken at the center point) were recorded with an RTK GPS on the same coordinate system used for the geomorphic data.
- **Plant species:** All plant species present within a quadrat frame at densities greater than 2 percent of the total quadrat area were recorded. Vegetation that was dead, standing, and identifiable was recorded as a plant species from 2009 through 2013 if it retained the same structure characteristics as analogous living vegetation. In order to more readily describe vegetation changes due to maintenance activities, dead, standing vegetation was recorded as *Percent Dead Organic Matter* beginning in 2014.
- **Daubenmire cover (percent) by species:** A measure of the degree to which above ground portions of plants cover the ground surface area. The potential presence of more than one vegetation layer in a quadrat allows total cover to exceed 100 percent in some cases, due to foliage overlap. Areal cover was quantified using the following *Daubenmire Cover* classes.

- Cover class 1: 2-5%
- Cover class 2: 6-25%
- Cover class 3: 26-50%
- Cover class 4: 51-75%
- Cover class 5: 76-95%
- Cover class 6: 96-100%

- **Areal cover (acres) by species:** Quantified by multiplying *Daubenmire Cover* (percent) by total area sampled for each plant species.
- **Herbaceous vegetation height:** A visual estimate of the actual maximum height of herbaceous vegetation in each quadrat was made. From 2009 through 2012, vegetation height was collected categorically using mean height classes, or directly as a mean height. Prior to the 2013 field survey, it was determined that actual maximum height values were more appropriate for hypothesis testing, and were collected starting in 2013. Maximum height data are generally suitable for comparison with data from prior years.
- **Woody vegetation height:** A visual estimate of the actual maximum height of woody vegetation in each quadrat. From 2009 through 2012, vegetation height was either collected categorically using mean height classes, or directly as an actual mean height value. Prior to the 2013 field survey, it was determined that actual maximum height values were more appropriate for hypothesis testing, and were collected starting in 2013. Maximum height data are generally suitable for comparison with data from prior years.
- **Percent dead organic matter:** The percent of each quadrat covered by dead organic matter, standing or downed. *Dead Organic Matter* was quantified from 2012 through 2013 as only downed organic matter (such as thatch, downed woody debris, etc.). Identifiable standing dead vegetation were quantified as living specimens under the *Plant Species* category. Beginning in 2014, dead standing vegetation was instead recorded as *Percent Dead Organic Matter* to more adequately describe vegetation changes from maintenance activities, particularly spraying. *Dead Organic Matter* was only quantified starting in 2012.
- **Percent bare ground:** The percent of each quadrat which is bare exposed ground with no organic matter of any kind, living or dead. *Bare ground* was only quantified after 2011.
- **Vegetation community:** The predominant vegetation community type was identified as best represented by the quadrat. Community types were based on *Terrestrial Ecological Systems and Natural Communities of Nebraska* (Rolfsmeier and Steinauer, 2010), although several that were quantified in the field were not officially recognized by this resource (due to the predominance of non-native species). Community types and/or habitat types identified during the 2012 and 2013 vegetation surveys are categorized by the following:
 - Eastern cottonwood – (peachleaf willow)/coyote willow woodland (Rolfsmeier and Steinauer, 2010),
 - Riparian dogwood – false indigo shrubland (Rolfsmeier and Steinauer, 2010),
 - Sandbar willow shrubland (Rolfsmeier and Steinauer, 2010),
 - Sandbar/mudflat (Rolfsmeier and Steinauer, 2010),
 - Russian olive sandbar,
 - Perennial sandbar (Rolfsmeier and Steinauer, 2010),

- Freshwater marsh (Rolfsmeier and Steinauer, 2010),
- Fallow agricultural land,
- Ruderal upland,
- Water, and
- Upland community,

All vegetation data were collected using either a Trimble Geo XT or XH datalogger. A data dictionary was developed specifically for this work and uploaded into the datalogger using Trimble GPS Pathfinder Office (version 5.30) software. During field sampling, each quadrat was uniquely identified by capturing the associated AP number, transect number, and quadrat number. All spatial data were collected using an RTK GPS roving unit at sub-inch accuracy.

Each AP was surveyed using two teams of two biologists. In general, each survey team was responsible for 2 to 3 transects at each AP, allowing the survey for each AP to be completed in one day, concurrent with the geomorphic surveys.

2.4 Sediment Sampling Methods

2.4.1.1 Bed and Bar Material

Up to 10 bulk bed-material samples and at least one composite bar-material sample were collected at each AP in accordance with the Monitoring Protocol. Typically, each transect was subdivided into three segments, and a representative bed-material sample was collected from each segment, insuring that one sample was taken from near the thalweg and the other two taken from the lowest elevation surface in other two segments. The 2012, 2013, and 2014 samples were analyzed in Tetra Tech's Fort Collins soils laboratory to determine the particle size gradations. Samples collected by the previous contractor in 2009, 2010 and 2011 were analyzed in a similar manner at a local soils laboratory. The samples were collected using a sampler constructed from a 4-inch diameter by 12-inch long PVC pipe, beveled at one end and covered with a 200-micron mesh at the other end (**Figure 2.3**). In collecting the samples, the sampler was pushed 4 to 6 inches deep at an angle into the bed of the channel at the sampling location. The resulting sample sizes for the 2014 data ranged from about 412 g to 3,600 g, and averaged about 740 g. Sample sizes in the earlier years were similar to the 2014 samples. Since the samples were often collected from below the water, the sampler was oriented with the opening facing upstream so that the water could drain from the sampler with minimal loss of the sample material. All bed samples collected from the main and secondary channels were transferred to individual sample bags that were labeled with the sampled AP, transect ID, sample number, and date, and the sample locations were determined using an RTK GPS roving unit.

Bar material samples were generally collected at the head of a high bar in the area with the coarsest material. Samples were taken at three different locations on the bar within relatively close proximity to each other to insure that the overall sample site was on the same geomorphic feature. The bar samples were collected with a shovel after noting and removing any armor or coarse lag material. This method results in an accurate estimation of the distribution of bed material mobilized and transported through the reach at flows in the range of the channel-forming discharge. An approximately equal volume of materials was collected at each of the three locations, and the material was placed in one or more sample bags that were labeled with the sampled AP, transect ID, sample number, and the date the sample was taken. The total weights of the bar samples in 2014 ranged from 496 to 3,420 g, and averaged about 830 g, and the range of sample sizes in previous years was similar. A single georeferenced survey point

was taken at the approximate center of the area encompassed by the three sites using one of the RTK GPS roving units.



Figure 2.3. Pipe dredge used to collect bed-material samples.

2.4.1.2 Bed-load and Depth-Integrated Suspended Sediment Sampling

The Monitoring Protocol specifies that bed-load and depth-integrated suspended-sediment sampling is to be conducted at the following five bridge locations during pre-defined flow ranges:

- Lexington (SH-L24A/Rd 755),
- Overton (SH-L24B/Rd 444),
- Kearney (SH-44/S. 2nd Ave.),
- Shelton (SH-L10D/Shelton Road), and
- Near Grand Island (US-34/Schimmer Drive).

Ideally, bed-load sampling would occur at the following flow ranges with the corresponding number of samples:

- 1,000 to 3,000 cfs – 3 samples.
- 3,000 to 5,000 cfs – 2 samples.
- >5,000 cfs – at least 1 sample, if such flows occur.

In addition, a single depth-integrated suspended sediment sample is to be collected at each location during the bed-load sampling in the greater than 5,000-cfs flow increment.

During 2014, flow in the Platte River was very low, and only one bed-load and suspended sediment sampling effort was undertaken. This effort occurred during June 16-18, 2014, near the peak of the spring runoff. According to Nebraska Department of Natural Resources gages (NDNR) at Darr/Lexington (NDNR 228400) and Shelton (NDNR 229300) flow was approximately 4,250 cfs during the sampling. Discharges at the USGS gages at Overton, Kearney and Grand Island were reported at approximately 6,000, 5,500 and 5,100 cfs, respectively. Suspended-sediment samples were collected in conjunction with each of the five bed-load samples. It is very likely that the flow reported by NDNR at Shelton is erroneous for the

date of the sediment sampling, as it is lower than both Kearney and Grand Island. To rectify this, the discharge at Shelton was obtained from the hydrologic routing analysis used for calculation of the hydrologic performance measures (for more information, refer to Section 2.5.2.1). The corrected flow was estimated to be approximately 5,660 cfs.

2.5 Data Analysis Methods

The basic data collected during the field program were evaluated in accordance with the draft Data Analysis Plan (PRRIP, 2012a).

2.5.1.1 Spatial and Temporal Scales

The Data Analysis Plan specifies that the data are to be evaluated at a range of spatial and temporal scales. The relevant *spatial* scales include the following:

- Transect—analyses to be summarized (i.e., mean and standard deviation) by transect. The draft Data Analysis Plan specifies that vegetation data are to be collected at seven transects that are spaced approximately 165 feet apart, and the geomorphic data are to be collected at three of these transects. This protocol was followed in 2009, 2010 and 2011. During 2012, geomorphic data were collected at all seven transects. As described elsewhere in this document, statistical analysis indicates that the information obtained from only five transects is essentially the same as is obtained from seven transects; thus, geomorphic and vegetation data were collected at five transects at each AP beginning with 2013, and the protocol was followed in 2014 and will be followed going forward.
- Anchor point—analyses to be summarized (mean and standard deviation) by anchor point: one summary for anchor point transects on the main channel, and a second summary for all side channel transects that occur at the anchor point. There are 40 anchor points spaced approximately 2.5 miles apart from Lexington to Chapman.
- Complex – analyses to be summarized for each of the following Platte River Recovery Implementation Program complexes: Plum Creek (AP35, AP36, AP37), Cottonwood Ranch (AP32, AP33), Elm Creek (AP29, AP30), Fort Kearney (AP22, AP23), and Shoemaker Island (AP12). Average and standard deviation will be reported for complex anchor points, and separately for non-complex anchor points.
- Bridge segment—analyses to be summarized (mean and standard deviation) by bridge segment: Lexington to Overton, Overton to Elm Creek, Elm Creek to Odessa, Odessa to Kearney, Kearney to Newark, Newark to Shelton, Shelton to Wood River, Wood River to Grand Island, and Grand Island to Chapman. The main channel will be summarized separately from the side channels.
- Geomorphic reach—reach-averaged results (mean and standard deviation) to be summarized by reach [based on reaches with consistent planform, as characterized in Fotherby (2008);

Reach	Description	River Miles	Main Channel Anchor Points	Side Channel Anchor Points
1	Lexington Bridge to Overton Bridge (including north channel of Jeffrey Island)	239.5-254.5	38 to 40; 37a, 36b, 35a	None

2	South channel of Jeffrey Island from J2 Return to Overton Bridge	239.5-247	37a, 36b, 35b	37b, 36a, 35b
3	Overton Bridge to Elm Creek Bridge	231-239.5	31, 32a, 33a, 34	32b-c, 33b-c
4	Elm Creek Bridge to Odessa Bridge	224-231	28-30	None
5	Odessa Bridge to Minden	208-231	22a, 22b, 23a, 24-27	23bS, 23bN
6	Minden to Gibbon Bridge	202-207	20a, 21a	20b, 21bS, 21bN
7	Gibbon Bridge to Wood River	187.5-202	14-18, 19a	19b
8	Wood River to Grand Island	173-187.5	8a, 9a, 10a, 11a, 12a, 13a	8b-c, 9bS, 9bN, 9c, 10b-c, 11b, 12b, 13b
9	Grand Island to Chapman	156.5-173	1-5, 6b, 7a	6a, 7bS, 7bN, 7c

- Table 2.2]. The main channel will be summarized separately from the side channels.
- System—analyses to be summarized (mean and standard deviation) for the overall study reach from Lexington to Chapman (i.e., all anchor points). The main channel will be summarized separately from the side channels.

The relevant *temporal* scales include the following:

- Annual—Main channel transect data at the 20 pure-panel anchor points that are monitored annually will be reduced and analyzed every year.
- Four-year (rotating panel and side channels)—Data for side channels at the pure-panel APs were initially collected in 2009, and data will be collected in these channels again every fourth year. The data from the rotating panel points will be reduced and summarized as part of the annual report for the year in which they were collected.
- First Increment—All data collected for this Program will be analyzed after the 2019 monitoring season to assess the change in each of the metrics over the course of the First Increment.

Reach	Description	River Miles	Main Channel Anchor Points	Side Channel Anchor Points
1	Lexington Bridge to Overton Bridge (including north channel of Jeffrey Island)	239.5-254.5	38 to 40; 37a, 36b, 35a	None
2	South channel of Jeffrey Island from J2 Return to Overton Bridge	239.5-247	37a, 36b, 35b	37b, 36a, 35b
3	Overton Bridge to Elm Creek Bridge	231-239.5	31, 32a, 33a, 34	32b-c, 33b-c
4	Elm Creek Bridge to Odessa Bridge	224-231	28-30	None

5	Odessa Bridge to Minden	208-231	22a, 22b, 23a, 24-27	23bS, 23bN
6	Minden to Gibbon Bridge	202-207	20a, 21a	20b, 21bS, 21bN
7	Gibbon Bridge to Wood River	187.5-202	14-18, 19a	19b
8	Wood River to Grand Island	173-187.5	8a, 9a, 10a, 11a, 12a, 13a	8b-c, 9bS, 9bN, 9c, 10b-c, 11b, 12b, 13b
9	Grand Island to Chapman	156.5-173	1-5, 6b, 7a	6a, 7bS, 7bN, 7c

Table 2.2. Geomorphic reaches from Fotherby (2008).

2.5.2 Performance Metrics

A suite of 35 individual performance metrics that can be quantified from the field data from this program and other available data sources have been identified for use in evaluating trends in channel morphology and in-channel vegetation for purposes of answering the Big Questions and testing the priority hypotheses (**Table 2.3**). As shown in the table, these metrics fall into six general categories: Hydrologic, Hydraulic, Geomorphic, Vegetation, Sediment, and Whooping Crane. A brief description of the data and methods that were used to quantify each of the metrics is provided in the following sections. Specific definitions and criteria are spelled out in more detail in the draft Data Analysis Protocol (PRRIP, 2012a).

Table 2.3. Performance metrics defined in the Channel Geomorphology and In-channel Vegetation Data Analysis Plan.

Variable/ Relationship	Monitoring Plan Section	Definition	Type	Reporting Scale	
				Temporal	Spatial
Hydrologic Performance Measures					
Q_P	5.1.1	Annual instantaneous peak discharge	Value	Annual	By Gage
DUR_{5000}	5.1.1	Duration of $Q > 5,000$ cfs	Value	Annual	By Gage
FDC_{Ger}	5.1.2	Flow duration curve for germination season (6/1-7/15)	Curve	Annual	By Gage
Q_{Ger}	5.1.2	Germination season discharge (Q_{Mean} 6/1-7/15)	Value	Annual	By Gage
Q_{WC_Spring}	5.1.3	Spring Whooping Crane migration discharge (Q_{mean} 3/21-4/29)	Mean Value	Annual	By Gage
Q_{WC_Fall}	5.1.3	Fall Whooping Crane migration discharge (Q_{mean} 10/9-11/10)	Mean Value	Annual	By Gage
FDC_{WC_Spring}	5.1.4	Spring Whooping Crane migration flow duration curve (3/21-4/29)	Curve	Annual	By Gage
FDC_{WC_Fall}	5.1.4	Fall Whooping Crane migration flow duration (10/9-11/10)	Curve	Annual	By Gage
Hydraulic Performance Measures					
Stg-Q	5.2.1	Stage-discharge rating curves for 500 cfs $\leq Q \leq 8,000$ cfs	Curve	Annual	AP Transect
Geomorphic Performance Measures					
BI	5.3.1	Braiding index	Value	By Survey ¹	Anchor Point and Subreach
W_T	5.3.2	Total channel width @ 1,200 cfs	Value	By Survey ¹	Transect and Anchor Point
$W_{T-Wetted}$	5.3.3	Wetted Channel Width (Total channel width (W_T)-Total width above 1,200-cfs WSEL)	Value	By Survey ¹	Transect and Anchor Point
D_H	5.3.4	Average channel depth (Cross sectional area @ 1,200 cfs / $W_{T-Wetted}$)	Value	By Survey ¹	Transect and Anchor Point
D_{Max}	5.3.5	Maximum channel depth (WSEL @ 1,200 cfs – Thalweg Elevation)	Value	By Survey ¹	Transect and Anchor Point

Variable/ Relationship	Monitoring Plan Section	Definition	Type	Reporting Scale	
				Temporal	Spatial
W/D	5.3.6	Wetted channel width ($W_{T\text{-Wetted}}$)/Maximum Channel Depth	Value	By Survey ¹	Transect and Anchor Point
ΔA_i	5.3.7	Change in cross sectional area @ 1,200 cfs from previous survey	Value	By Survey ¹	Transect and Anchor Point
ΔA_t	5.3.7	Change in cross sectional area @ 1,200 cfs from 2009 survey	Value	By Survey ¹	Transect and Anchor Point
LProf	5.3.8	Plot of longitudinal thalweg profile by ACOE River Mile (2009 and 2019, only)	Curve	2009, 2019	Reach
Vegetation Performance Measures					
GLE	5.4.1	Green line elevation (edge of 25% cover)	Value	By Survey ¹	Transect and Anchor Point
W_{Unveg}	5.4.2	Cumulative distance between pairs of GLE points within main channel, by transect	Value	By Survey ¹	Transect and Anchor Point
f_{species}	5.4.3	Frequency of occurrence for each species of interest and/or 25 most common species in current year	Value	By Survey ¹	Transect and Anchor Point
%Cover	5.4.4	Percent cover for each species of interest and/or 25 most common species in current year	Value	By Survey ¹	Transect and Anchor Point
AC_{Species}	5.4.5	Aerial cover occupied by each species of interest and/or 25 most common species in current year (Surface Area of AP X %Cover)	Value	By Survey ¹	Anchor Point
\bar{E}_{Species}	5.4.6	Mean elevation by species of interest and/or 25 most common species in current year	Value	By Survey ¹	Transect and Anchor Point
H_{species}	5.4.7	Mean vegetation height (not species specific)	Value	By Survey ¹	Transect and Anchor Point
Sediment Performance Measures					
$Q_{s\text{-bed}}-Q$	5.5.1	Bed-load versus discharge rating curve	Scatter Plot and Fitted Curve	Cumulative by sampling event	Five specified locations

Variable/ Relationship	Monitoring Plan Section	Definition	Type	Reporting Scale	
				Temporal	Spatial
Q_{s_susp-Q}	5.5.2	Suspended-sediment load versus discharge rating curve	Scatter Plot and Fitted Curve	Cumulative by sampling event	Five specified locations
GSD_{bed}	5.5.3	Bed material grain-size distribution curve of percent finer by weight	Curve	By Survey ¹	Transect and Anchor Point
GSD_{bar}	5.5.4	Bar material grain-size distribution curve of percent finer by weight	Curve	By Survey ¹	Transect and Anchor Point
GSD_{bank}	5.5.5	Bank material grain-size distribution curve of percent finer by weight	Curve	By Survey ¹	Transect and Anchor Point
$D_{50_bed, bar, bank}$	5.5.3-5	Median size of bed, bar and bank distributions	Value	By Survey ¹	Transect and Anchor Point
$D_{16_bed, bar, bank}$	5.5.3-5	16 th percentile size of bed, bar and bank distributions	Value	By Survey ¹	Transect and Anchor Point
$D_{84_bed, bar, bank}$	5.5.3-5	84 th percentile size of bed, bar and bank distributions	Value	By Survey ¹	Transect and Anchor Point
$G_{bed, bar, bank}$	5.5.3-5	Gradation coefficient for bed, bar and bank material samples ($G_i = D_{84}/D_{50} + D_{50}/D_{16}$)	Value	By Survey ¹	Transect and Anchor Point
Whooping Crane Performance Metrics					
W_{c_unobs}	5.6.1	Maximum distance in main channel between obstructions higher than 4.9 feet above 2,400 cfs WSEL	Value	By Survey ¹	Transect and Anchor Point
$W_{c_unobs_S}$	5.6.1	Maximum distance in main channel between obstructions higher than 4.9 feet above Q_{WC_Spring}	Value	By Survey ¹	Transect and Anchor Point
$W_{c_unobs_F}$	5.6.1	Maximum distance in main channel between obstructions higher than 4.9 feet above Q_{WC_Fall}	Value	By Survey ¹	Transect and Anchor Point
$W_{D<8_in}$	5.6.2	Maximum width in main channel with flow <8" deep, including exposed sandbars	Value	By Survey ¹	Transect and Anchor Point

¹Annual for Pure Panel Points/Every 4 years for rotating points

2.5.2.1 Hydrologic Performance Metrics

Data for eight hydrologic (or flow-related) performance metrics were derived primarily from the following gages that are maintained and operated by the U.S. Geological Survey (USGS) or NDNR:

- Platte River at Lexington (NDNR 228400)²,
- Platte River near Overton (USGS 06768000),
- Spring Creek near Overton (USGS 06768020),
- Buffalo Creek near Overton (USGS 06769000),
- Elm Creek near Elm Creek (USGS 06769525),
- Platte River near Kearney (USGS 06770200),
- Platte River near Shelton (NDNR 229300), and
- Platte River near Grand Island (USGS 06770500).

In the 2012 annual report, the Platte River near Odessa gage (NDNR 6770000) was also used; however, further evaluation of the data from that gage shows inconsistencies that make the data suspect for purposes of this study, particularly at high flows. For this reason, the Odessa gage is no longer being used in the analysis.

Data for the USGS gages were obtained from the National Water Information System (NWIS) website (<http://waterdata.usgs.gov/nwis>), and data for the NDNR gages were obtained from the NDNR real time gage index website (<http://data.dnr.nebraska.gov/RealTime/Gage/Index>). The specific values of the seven hydrologic performance metrics were computed by estimating a mean daily flow record for each AP using distance-weighted interpolation between each of the mainstem gages, adjusting gaged tributary inflows and ungaged losses or gains between the mainstem gages. The ungaged rate of gain or loss in each segment of the reach was estimated by taking the difference between the corresponding mean daily flows at the mainstem gages, subtracting the reported tributary inflows or adding the reported diversions (at the Kearney Canal Diversion), as appropriate, and dividing the remainder by the length of the segment.

The following specific clarifications to the DAP were employed in computing the hydrologic performance metrics:

- The annual peak flow event discharge (DAP 5.1.1; Q_P) was defined as the maximum mean daily discharge between January 1 and the date of the respective surveys during each year. The maximum mean daily flow is being used because instantaneous peak flow data are not available at all locations, and from a riverine process perspective, the mean daily discharge is a more meaningful value because it occurs for a sufficient duration to do work within the channel.
- DAP 5.1.2 defines the germination season discharge exceedance as *the frequency of flows within the April 1 to July 31 germination season*. Because a key use of this metric is to assess the effects of flow on cottonwood germination and persistence, the time-frame was modified to June 1 through July 15 to more closely correspond to the timing of cottonwood seed dispersal and germination. Although the duration of discharges is important, a specific, representative discharge during the germination season is also necessary to facilitate the

² In some cases, data from the Cozad gage (NDNR 6466500 for 1992 and later; USGS Gage No. 06766498 prior to 1992).

trend analyses. As a result, the representative germination season discharge (Q_{GER}) was defined as the mean discharge during the period.

2.5.2.2 Hydraulic Performance Metrics

The hydraulic performance metrics consist of stage versus discharge relationships at the transects that make up each of the APs. These relationships were developed by making multiple-profile runs with an updated version of the 1-D hydraulic model. The original model was based primarily on the 2009 LiDAR data and the transect survey data from the initial 2009 survey for this monitoring program, supplemented with other available survey data that had been collected in specific locations for other purposes. Certain of the geomorphic performance metrics from the 2012 and 2013 data appeared to be unreasonable, suggesting that the channel geometry had changed sufficiently since 2009 so that the relationships were no longer valid. At the time of the 2013 report, the model was being updated with the 2012 data LiDAR and survey data. Key metrics that relied on the model results were re-evaluated, and those changes have been incorporated into the results discussed in this document.

2.5.2.3 Geomorphic Performance Metrics

The geomorphic performance metrics include nine specific measures of channel geometry and form. Eight of the nine metrics were quantified for the original three years of data collected by the previous contractor and the 2012 and 2013 data collected by Tetra Tech for the 2013 annual report. The values of these eight metrics from the 2014 data analysis were added to the data sets for this report. Data for the 9th metric (longitudinal thalweg profile) were only collected in 2009 as part of the initial surveys, and these data will be collected again in 2019.

In quantifying the metrics, one relatively minor deviation from the draft Data Analysis Plan was employed. Total channel width is defined in the Plan as total channel width at 1,200 cfs, including non-wetted areas (e.g., exposed sand bars, and vegetated islands), but excluding ineffective flow areas. After evaluating the data in more detail, Tetra Tech recommended that the ineffective flow areas should be included in the width calculations, and Program staff agreed to the change (Jason Farnsworth, personal communication, March 2013).

2.5.2.4 Vegetation Performance Metrics

The vegetation performance metrics are quantified directly from the field data. Although over 170 individual species have been identified during the field surveys, the analysis considered only the 25 most frequently observed during the current sampling year, based on data collected in the main channel at the Pure Panel APs, and at APs 35b and 37b in Reach 2, due to their relationship with the J-2 Return (**Table 2.4**). In the case where species of interest (see Section 1.2.5) were uncommon and not within the 25 most frequently observed species, they were also included to maintain consistency with analyses from prior years. Data for the species not included in Table 2.3 (i.e., species that were not common or a species of interest) have been retained in the master dataset and are available for additional analysis.

Hypotheses testing and trend analyses were restricted to a select subset of four plant taxa: purple loosestrife, common reed, eastern cottonwood, and willow (*Salix exigua* and *S. amygdaloïdes* combined). These taxa were chosen because of their rapid growth rate and colonization of bars in the Platte River system and wide distribution. Other taxa were excluded from these analyses to streamline the statistical calculations that support hypothesis testing and trend analysis.

Table 2.4. Species considered in the analyses—the 25 most frequently observed species in 2014, and species of interest observed at lower frequencies.

Scientific Name	Common Name	Wetland Indicator Status ¹	Native (Y/N) ²
<i>Ambrosia</i> sp.	Ragweed	FACU	Yes
<i>Phalaris arundinacea</i>	Reed canary grass	FACU	Yes
<i>Xanthium strumarium</i>	Rough cockleburr	FAC	Yes
<i>Rumex crispus</i>	Curly dock	FAC	No
<i>Echinochloa</i> sp.	Barnyard grass	FACW	Yes
<i>Helianthus</i> sp.	Sunflower	FACU	Yes
<i>Lythrum salicaria</i>	Purple loosestrife	OBL	No
<i>Bidens</i> sp.	Bidens	FACW	Yes
<i>Populus deltoides</i>	Eastern cottonwood	FAC	Yes
<i>Conyza canadensis</i>	Horseweed	FACU	Yes
<i>Spartina pectinata</i>	Freshwater cord grass	FACU	Yes
<i>Carex emoryi</i>	Emory's sedge	OBL	Yes
<i>Phragmites australis</i>	Common reed	FACW	Yes
<i>Solidago</i> sp.	Goldenrod	FACU	Yes
<i>Eragrostis pectinacea</i>	Tufted lovegrass	FAC	Yes
<i>Cyperus odoratus</i>	Rusty flatsedge	FACW	Yes
<i>Leptochloa fusca</i>	Sprangletop	FACW	Yes
<i>Amorpha fruticosa</i>	False indigo-bush	FACW	Yes
<i>Salix exigua</i>	Narrow-leaf willow	FACW	Yes
<i>Bolboschoenus fluviatilis</i>	River bulrush	OBL	Yes
<i>Panicum capillare</i>	Common panic grass	FAC	Yes
<i>Polygonum lapathifolium</i>	Curlytop knotweed	OBL	Yes
<i>Cyperus squarrosus</i>	Bearded flatsedge	OBL	Yes
<i>Melilotus albus</i>	White sweetclover	FACU	No
<i>Leersia oryzoides</i>	Rice cut grass	OBL	Yes

¹ Source: North American Digital Flora: National Wetland Plant List (Lichvar and Kartesz 2012); Midwest Region; National Wetland Plants List (USACE 2013)

² Source: PLANTS Database (USDA-NRCS 2013)

Evaluation of the vegetation performance metrics provides at least three essential insights that facilitate understanding of the ecology of the study area and guide management actions, as follows:

1. Describes baseline conditions,
2. Provides a basis for tracking ecosystem changes through time, and
3. Provides a benchmark to measure response to experimental management actions.

Vegetation performance metrics for each survey year were partially examined in the annual reports from previous years of this monitoring program (Ayres and Olsson, 2010, 2011, 2012; Tetra Tech, 2013, 2014). The vegetation performance metrics presented in this report include a more comprehensive treatment of the previous data and incorporate data collected during the 2014 field season. The vegetation performance metrics provide insight into the most prevalent species at the sample sites (and by inference, the overall Central Platte River Reach), where they are distributed, and the ecological conditions that they collectively represent.

2.5.2.5 Sediment Performance Metrics

The sediment performance metrics fall into two general categories:

- Sediment-transport rates
- Bed-, bar- and bank-material particle size gradations

The sediment-transport data from the 2009, 2010 and 2011 data collection efforts have been reduced and plotted in the form of sediment discharge rating curves to support a variety of sediment-transport analyses, including the modeling that was conducted for the Sediment Augmentation Feasibility Study (Tetra Tech, 2010) and the Elm Creek FSM Experiment (Tetra Tech, 2012). These sediment discharge rating curves are updated each year with new measurements, such that the metric is cumulative. Performance metrics related to bed and bar material are calculated every field season. Bank material was collected in the first year of data collection, and will not be repeated until the final year of the first increment.

2.5.2.6 Whooping Crane Performance Metrics

The whooping crane performance metrics are intended to quantify the available sight distances and associated channel widths within the channel corridor. These metrics are based on a combination of direct measurements of unobstructed widths (2013 and 2014 data, only), vegetation height data (2009 through 2012) and hydraulic model results. The hydraulic model results were used to quantify the widths of the channel that consist of either bare sand or flow depths of less than 8 inches at a discharge of 2,400 cfs and at the whooping crane migration season discharges (i.e., average mean daily discharge during the period from March 21 through April 29 for the spring migration season and October 9 through November 11 for the fall migration season). As discussed in the 2012 annual report (Tetra Tech, 2013), there are at least two significant challenges in quantifying these metrics with 2009-2012 data:

1. Vegetation heights were not collected in a consistent manner across years; thus, interpretation of the data is confounded by differences in the data sets,
2. The data were collected in broad categories of vegetation heights which introduces significant uncertainty into the actual height of the vegetation.

2.5.3 Trend Analysis

For the 2012 annual report, a broad range of statistical comparisons were made across the 2009 through 2012 data sets to identify trends in the geomorphic, vegetation and sediment variables (**Table 2.5**). This resulted in a large number of analyses that are difficult to interpret in the context of Program priorities. To provide a more focused analysis, the Program directed that the trend analysis be restricted to the following priority hypotheses for the 2013 and 2014 reports:

1. Flow 1 – Perform a detailed analysis of changes in bed sediment volume within the main channel for each of the 6 years of available data, and evaluate the results in the context of the sediment balance along the study overall study reach. In presenting the analysis, address the amount of variability in sediment loads (and the resulting sediment balance) and the implications of this variability to drawing conclusions about whether each portion of the reach is in aggrading, degrading or in dynamic equilibrium.
2. Flow 3 – Determine the correlation between flow, green line elevation (GLE) and unvegetated width. As specified in the Data Analysis Plan, the edges of unvegetated segments along each transect are identified by the GLE points. In the 2012 annual report, the unvegetated width metric was defined as the length of the longest uninterrupted

segment between GLE points at each transect. For this analysis, the total unvegetated width, defined as the cumulative length of all unvegetated segments between GLE points within the main channel at each transect, was used. To remove the effects of river slope in the correlations, GLE values were normalized to the 1,200-cfs water surface (i.e., the difference between the GLE and the local 1,200-cfs water surface was used rather than the actual elevation). The following specific correlations will be evaluated using the metrics defined in this manner:

- a. GLE versus annual peak discharge (Q_p , Monitoring Plan Section 5.1.1), defined as the maximum mean daily discharge between January 1 and the date of the survey in each year.
- b. GLE versus germination season discharge (Q_{Ger} , Monitoring Plan Section 5.1.2), defined as the either the mean or median mean daily discharge between June 1 and July 15 (the primary season for establishment of cottonwood seedlings). For this analysis the correlations were performed using the both the mean and median discharges to assess which one provides the best correlation.
- c. Total unvegetated width (W_{unveg}) versus annual peak discharge (Q_{Ger}).
- d. Total unvegetated width (W_{unveg}) versus germination season discharge (Q_{Ger}).
- e. GLE versus total unvegetated width (W_{unveg}).

3. Flow 5 – Assess influence of spraying versus peak flows on phragmites distribution and frequency using vegetation plot data in conjunction with GIS-formatted records of annual spraying.
4. Mechanical 2 – Evaluate correlation between total unvegetated width (W_{unveg}), braiding index (BI) and percent consolidation at bankfull discharge.

Additional evaluations that were considered for the 2013 report, but were postponed and included in this annual report, include assessing the correlation between amount of lateral erosion into the primary banklines and large islands/bars, the braiding index and the annual peak discharge.

Table 2.5. Summary of trend analysis specified in the Data Analysis Plan.

Analysis Plan Section	Specified Analysis	Performance Metrics		Spatial Analysis Scale	
		Variable	Analysis Plan Section	Geomorphic Reach	System
6.1 Analyses for Broad Hypotheses S-1, S-2, and S-4					
6.1.1.1	Braiding Index Trend Analysis	BI	5.3.1	X	X
6.1.1.2	Aggradation/Degradation Trend Analysis	DA	5.3.7	X	X
6.1.1.3	Total Channel Width Trend Analysis	WT	5.3.2	X	X
6.1.1.4	Wetted Channel Width Trend Analysis	WT-Wetted	5.3.3	X	X
6.1.1.5	Unvegetated Channel Width Trend Analysis	WUnveg	5.4.2	X	X
6.1.1.6	Width-to-Depth Ratio Trend Analysis	W/D	5.3.6	X	X
6.2 Analyses for Broad Hypothesis PP-1					
6.2.1	Relationship between Annual Peak Flow and Unvegetated Channel Width	WUnveg, QP	5.4.2, 5.1.1	X	X
6.2.2	Relationship between Germination Season Discharge and Unvegetated Channel Width	WUnveg, QPGer	5.4.2, 5.1.2	X	X
6.3 Analyses for Broad Hypothesis PP-2					
6.3.1	Relationship between Sediment Augmentation and Channel Volume Change	DAi, VSedAug	5.3.7*	N/A	N/A
6.3.2	Relationship between Sediment Augmentation and Braiding Index	BI, VSedAug	5.3.7*	N/A	N/A
6.3.3	Relationship between Sediment Augmentation and Total Channel Width	WT, VSedAug	5.3.7*	N/A	N/A
6.3.4	Relationship between Sediment Augmentation and Width-to-Depth Ratio	W/D, VSedAug	5.3.7*	N/A	N/A
6.4 Analyses for Priority Hypothesis Flow 3					
6.4.1	Relationship between Annual Peak Flow and GLE	GLE, QP	5.4.1, 5.1.1	X	X
6.4.2	Relationship between GLE and 1,200cfs WSEL	GLE, WSEL ₁₂₀₀	5.4.1, 5.2.1	X	X
6.4.3	Relationship between GLE and Unvegetated Channel Width	GLE, WUnveg	5.4.1, 5.4.2	X	X
6.5 Analyses for Priority Hypothesis Flow 5					
6.5.1	Relationship between annual peak flow and mean vegetation elevation by species	Ē _{species} , QP	5.4.6, 5.1.1	X	X
6.5.2	Relationship between germination season discharge and mean vegetation elevation by species	Ē _{species} , QPGer	5.4.6, 5.1.2	X	X
6.6 Analyses for Priority Hypothesis Sediment 1					
6.6.1	Relationship between Sediment Augmentation and trends in bed and bar grain size distribution	Di, VSedAug	5.5.3, 5.5.5*	N/A	N/A
6.7 Analyses for Priority Hypothesis WC-X					
6.7.1	Analysis of Wetted Widths across a Range of Discharges	WT-Wetted	5.6.2	X	X
6.7.2	Analysis of Portion of Channel with flow depth <8in. at a range of discharges	WD<8_in	5.6.2	X	X
6.8 Analyses for Vegetative Species of Interest					
6.8.1	Frequency of Occurrence Trend Analysis	f _{species}	5.4.3	X	X
6.8.2	Percent Cover Trend Analysis	% Cover	5.4.4	X	X
6.8.3	Aerial Coverage Trend Analysis	ACSpecies	5.4.5	X	X

* Sediment augmentation volume developed from sediment augmentation monitoring records.

3 RESULTS

The performance metrics for the 2009 through 2013 data were quantified using the procedures described in Chapter 2. As noted, the specific definition of some of the metrics has changed from the earlier definitions to better represent the intent of the analysis. Associated adjustments to the values were made for all of the years of data. The hydrologic, geomorphic and selected vegetation metrics are summarized in **Appendices A, B and C**, respectively.

3.1 Hydrologic

To facilitate quantification of the suite of hydrologic performance measures, a record of mean daily flows from October 1, 2008, through the date of the last 2014 monitoring survey was compiled for all of the USGS and NDNR mainstem and tributary gages within the reach (Figure 1.1). These flow records were then used to estimate an equivalent record for each of the APs by distance-weighted interpolation between the measured mainstem flows, taking into account measured tributary inflows and diversions, as described in Chapter 2. Flow-duration curves at the mainstem gages for each the flow-duration related metrics are provided in Appendix A.

3.1.1 Annual Peak Flow Event Discharge and Duration (DAP 5.1.1)

The maximum mean daily flows between January 1 and the surveys (Q_P) during 2009, 2012 and 2013 were in the range of 1,500 to 2,000 cfs upstream from Overton and the confluence of the North and South Channels at Jeffreys Island, and 3,000 to 4,000 cfs downstream from that point (**Figure 3.1**). The flows were much higher in 2010, 2011, and 2014, generally ranging from 7,000 to 8,500 cfs in 2010, from 7,200 cfs to over 10,000 cfs in 2011, and from 6,000 to 8,000 cfs in 2014. In these high-flow years, the maximum mean daily discharge tended to increase in the downstream direction. Maximum mean daily flows from the J-2 Return into the South Channel at Jeffreys Island (Geomorphic Reach 2) were in the range of 1,800 to 2,000 cfs during all six years.

The maximum mean daily discharge did not exceed 5,000 cfs (DUR_{5000}) at any location in the reach prior to the 2009, 2012, and 2013 surveys, and it occurred for six days upstream from Overton and for 15 to 17 days downstream from Overton, with a slight increase in the downstream direction in 2010 (**Figure 3.2**). During the sustained high-flow period in 2011, the discharge exceeded 5,000 cfs for about 50 days upstream from Overton, 70 to 80 days between Overton and the Kearney Diversion Canal (KDC) Return, and about 80 days downstream from that point. During 2014, the maximum mean daily discharge exceeded 5,000 cfs for at least four days throughout the entire reach, with a maximum duration of eight days (at 14 APs).

3.1.1.1 Germination Season Discharge (DAP 5.1.2)

The mean discharge during the germination season (Q_{GER} , defined as June 1 through July 15 for purposes of this study) was considerably higher during 2014 than during the previous two years. In 2014, Q_{GER} ranged from 1,500 to 2,300 cfs upstream from Overton, and it was consistently near 2,700 cfs at every AP downstream from Overton. By comparison, in 2013, mean germination season flows ranged from 400 to 550 cfs upstream from Overton, and were relatively constant in the range of 1,000 to 1,200 cfs downstream from Overton (**Figure 3.3**). Germination season flows were similarly low in 2012, ranging from 100 to 180 cfs upstream from Overton, relatively constant at about 270 cfs between Overton and the Kearney Diversion, decreasing between the Kearney Diversion and the KDC Return, and then increasing back to the 260- to 320-cfs range.

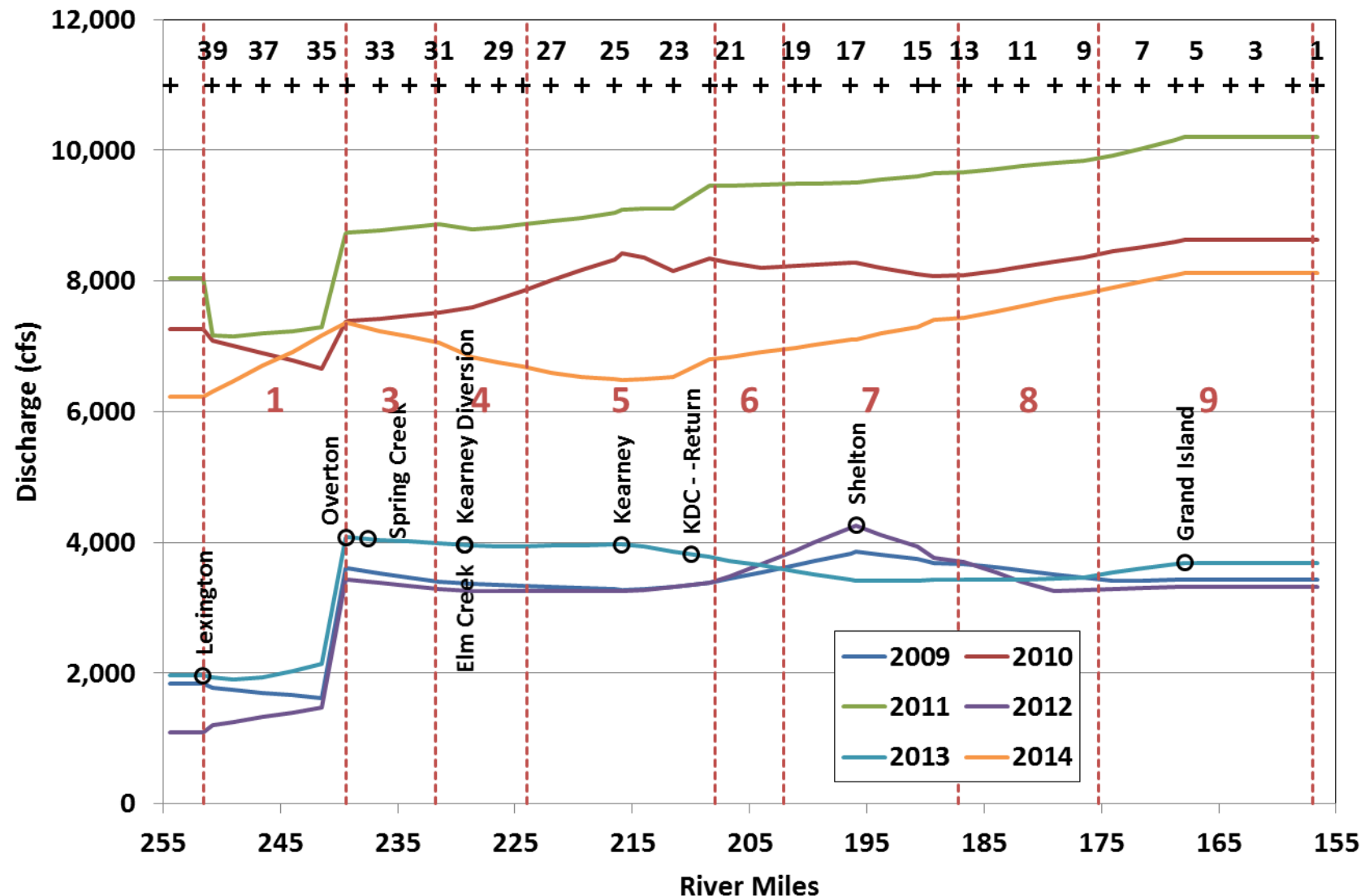


Figure 3.1. Maximum mean daily discharge (Q_p) between January 1 of each year and the dates of the 2009 through 2014 monitoring surveys.

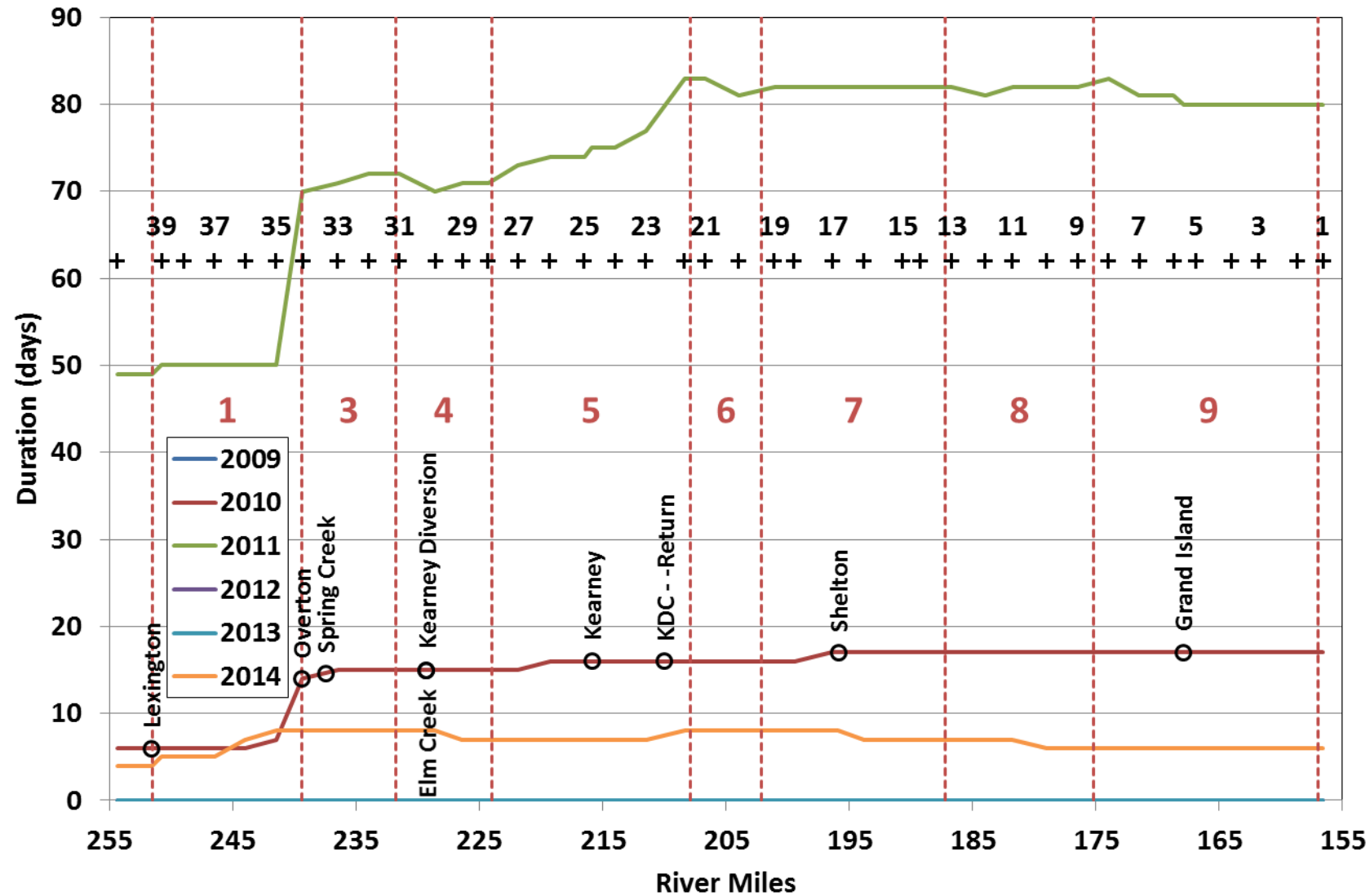


Figure 3.2. Duration of flows exceeding 5,000 cfs between January 1 of each year and the dates of the 2009 through 2014 monitoring surveys (DUR₅₀₀₀).

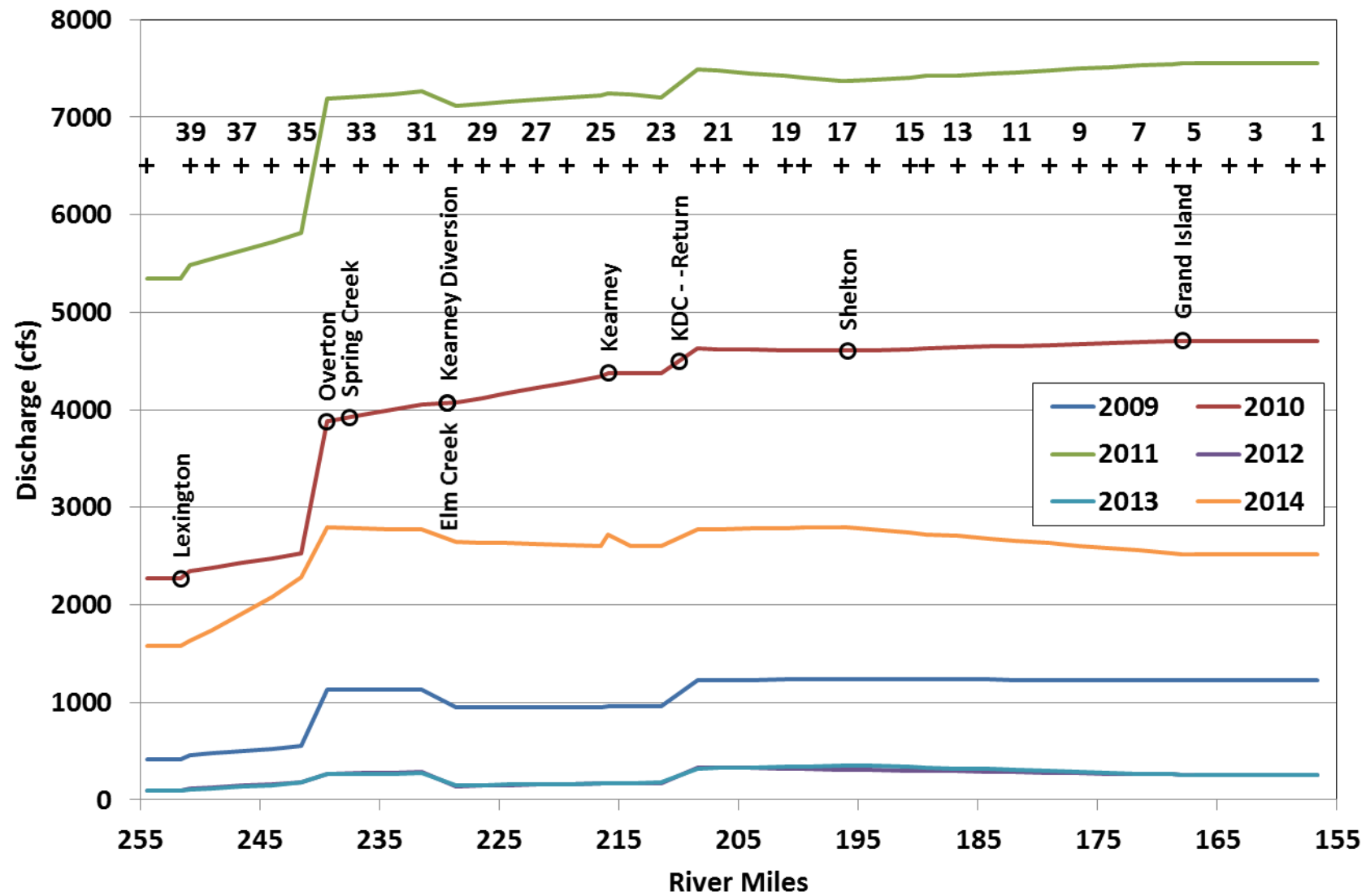


Figure 3.3. Average mean daily discharge during the germination season (Q_{GER} ; June 1 – July 15) from 2009 through 2014.

Germination season flows were highest in 2010 and 2011. In 2010, the germination season flows ranged from 2,300 to 2,400 cfs upstream from Overton, 3,900 to 4,700 cfs between Overton and the KDC Return, and were relatively constant at about 4,700 cfs downstream from that point. In 2011, Q_{GER} was between 5,300 and 5,800 cfs upstream from Overton, and was as high as 7,600 cfs downstream from Overton.

3.1.1.2 Spring and Fall Whooping Crane Migration Season Discharge (DAP 5.1.3)

Discharge at the APs during the 2014 spring whooping crane migration season was very similar to discharges which occurred during the same time frame in 2009, 2010, 2012, and 2013 (**Figure 3.4**). The mean discharge during the spring whooping crane migration season (Q_{WC_Spring} ; March 21 to April 29) at Lexington was slightly lower than in 2014 than during the four other low-water years, and steadily increased downstream, reaching a discharge of about 1,400 cfs at Overton. For comparison, Q_{WC_Spring} was about 1,200 cfs at Overton in 2009, and about 1,700 cfs in 2012. Spring germination discharge remained in the same general range as the other four low flow years, never rising above 1,500 cfs, and never sinking below 1,250 cfs. Discharges were much higher in 2011, in the range of 2,000 to 2,100 cfs upstream from Overton, and steadily increasing from 3,600 to 4,300 cfs downstream.

With the exception of 2012, 2014 was the driest year for fall whooping crane migration discharge since the program's inception. The mean discharge during the 2014 fall whooping crane migration season (Q_{WC_Fall} ; October 9 to November 10) ranged from 200 to 500 cfs upstream of Overton, and steadily increased from Overton to the KDC, where it plateaued near 850 cfs (**Figure 3.5**). In 2012, Q_{WC_Fall} peaked near 500 cfs at Overton, and decreased in the downstream direction. 2009, 2010, and 2013 were similar to each other, with flows generally near 500 cfs upstream from Overton, and between 1,500 and 2,000 cfs downstream from Overton. Consistent with the other discharge metrics, the fall whooping crane migration discharge was much higher throughout the reach in 2011, ranging from 1,200 cfs to nearly 1,500 cfs upstream from Overton, and from about 3,200 to 3,700 cfs downstream from Overton, with a general trend of increasing discharge in the downstream direction. Due to lingering effects of the September 2013 flood, the 2013 flows were much higher than in 2012, ranging from 250 to 800 cfs upstream from Overton, and from 1,750 to 1,800 cfs downstream from Overton.

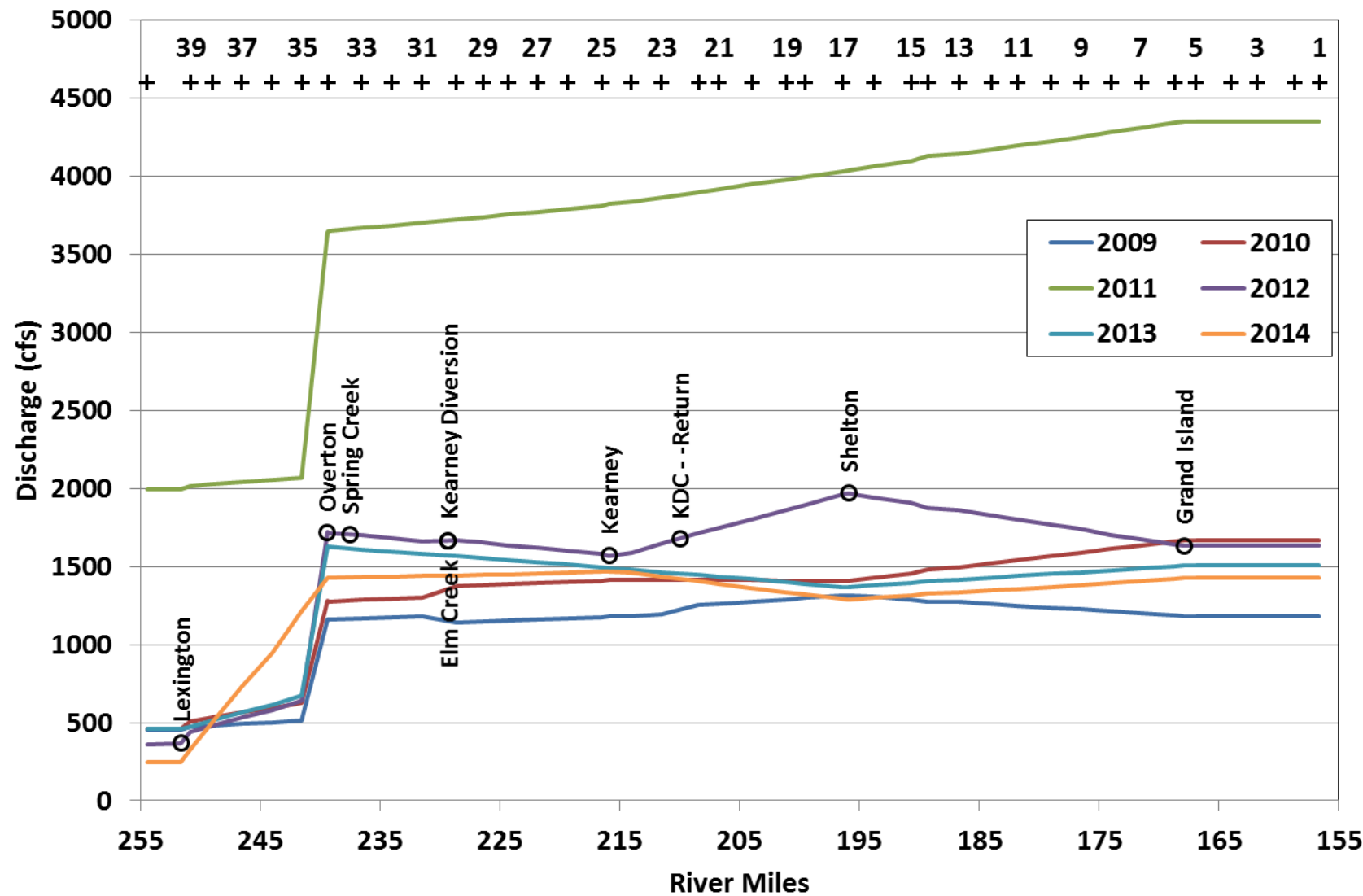


Figure 3.4. Average mean daily discharge during the spring whooping crane migration season (Q_{wc_Spring} ; March 21 – April 29) during 2009 through 2014.

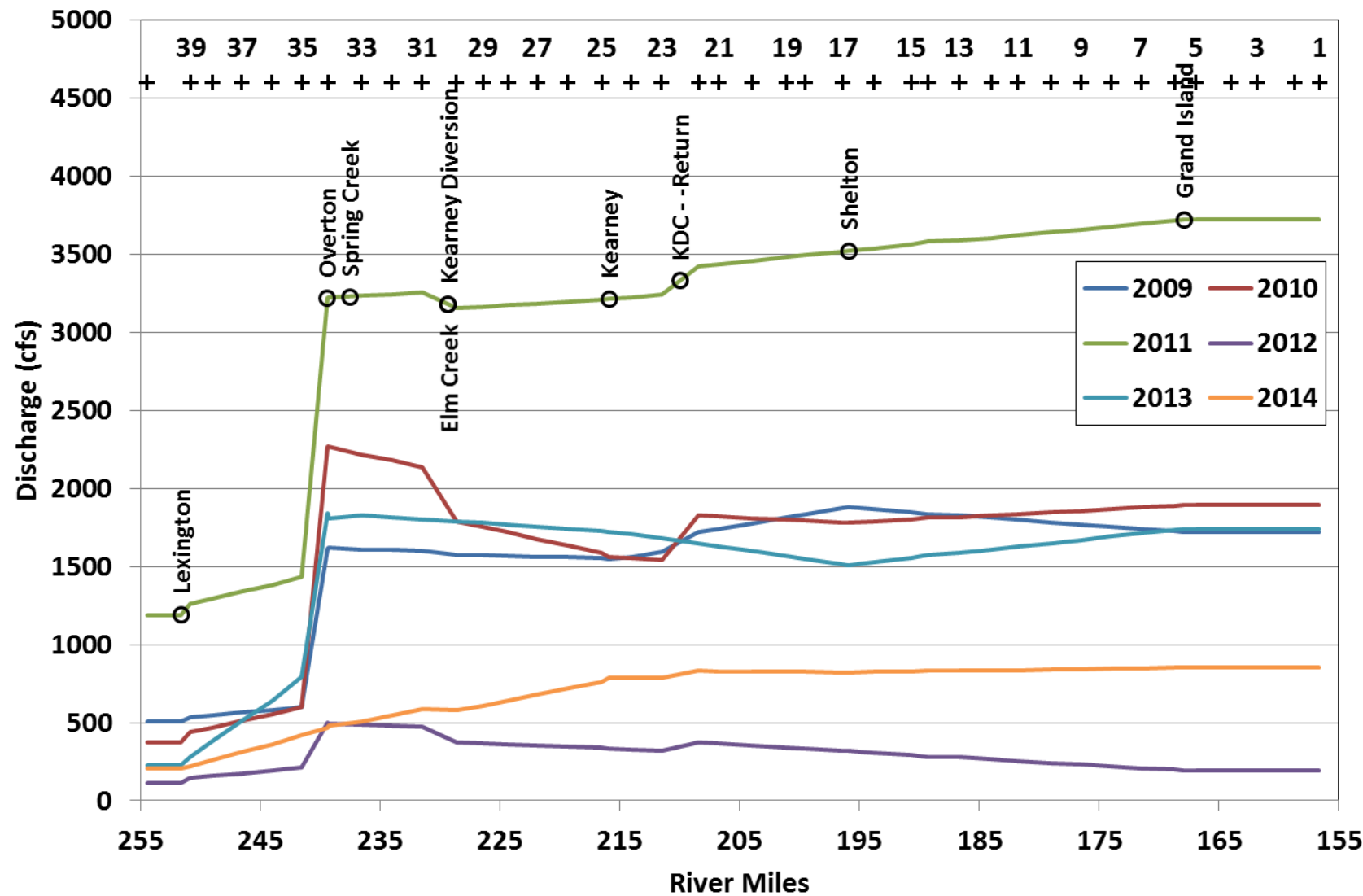


Figure 3.5. Average mean daily discharge during the fall whooping crane migration season (Q_{WC_Fall} ; October 9 – November 10) during 2009 through 2014.

3.2 Hydraulic

3.2.1 Stage-Discharge Relationships (DAP 5.2.1)

The PRRIP 1-D hydraulic model that is based primarily on the 2012 LiDAR and survey data was used to define stage-discharge relationships for transects at each of the APs for the 2012 through 2014 surveys. The previously developed model that was based primarily 2009 topography was used when analyzing the 2009 through 2011 monitoring data. The applicable rating curves can be obtained from the HEC-RAS model output files.

3.3 Geomorphic

A suite of six geomorphic metrics are defined in the DAP to describe various aspects of the channel planform and cross sectional geometry (Table 2.2):

- Braiding Index (DAP 5.3.1) – Average number of wetted channels crossed by each transect at a given AP at a 1,200 cfs reference flow,
- Total Channel Width (DAP 5.3.2) – Total width, including non-wetted areas (e.g., exposed sand bars) at a 1,200 cfs reference flow,
- Wetted Channel Width (DAP 5.3.3) – Cumulative width of individual wetted channels at a 1,200 cfs reference flow,
- Mean Channel Depth (DAP 5.3.4) – Average water depth (hydraulic depth) at a 1,200 cfs reference flow,
- Maximum Channel Depth (DAP 5.3.5) – Maximum depth (i.e., depth at thalweg) at 1,200 cfs reference flow, and
- Channel Width-to-Depth Ratio (DAP 5.3.6) – Ratio of wetted channel width to maximum channel depth at a 1,200 cfs reference flow.

The values of these metrics were initially quantified at the transect scale using the survey data and the predicted water-surface elevations from the existing HEC-RAS model³ that was primarily based on the 2009 LiDAR data (Appendix B). As discussed in the 2012 and 2013 reports, the values of several of the metrics showed significantly more year-to-year variability than anticipated. As a result, the 1-D model was updated with 2012 LiDAR data and the affected metrics for 2012 and 2013 were reevaluated and included in this report, along with the 2014 survey data.

Appendix B includes the results for both the Pure Panel and Rotating APs; however, the discussion below focuses on the Pure Panel AP results because the bulk of the Rotating APs have only been sampled once (the R2 APs were sampled for the second time in 2014). Average values for the various scales being considered in the analysis (i.e., AP, geomorphic reach, system-wide) were then developed from the individual transect results.

3.3.1 Braiding Index (DAP 5.3.1)

Based on the initial, 2009 survey data, the average braiding index at the Pure Panel APs ranged from about 1.3 (AP37) to 7.3 (AP1) (Figure 3.6a). The overall range was similar in subsequent

³As discussed in the 2012 annual report, the stage-discharge rating curves in much of the reach appear to have shifted significantly since creation of the original model, mostly as a result of the 2011 high flows. The HEC-RAS model was updated with 2012 LiDAR. There does not appear to be a significant error induced by the severe flooding which occurred during the September 2013 flooding that would affect the analysis of the 2014 survey data. It remains to be seen whether the flooding during the summer of 2015 will cause significant stage-discharge shifts that will require a further update to the HEC-RAS model.

years, with maximum values exceeding 8 at AP1 and AP17 in 2010, at AP19 in 2013, and at AP21 in 2014. Relatively large changes occurred at several of the APs over the period of the surveys, particularly AP1, AP15, AP17, AP21 and AP35. At AP1, the transects at the upstream and downstream limits of the site had several small channels that were inundated by only a small amount at the estimated 1,200-cfs water-surface in 2009, 2010 and 2011, and these channels either disappeared or the slight year-to-year change in water-surface elevation required to achieve reasonable in-channel velocities inundated the bars that separated several of these channels in 2012 and 2013. Similar year-to-year variability occurred at AP15, AP17 and AP21, although activities at the Rowe Sanctuary likely also affected AP21. Based on these results, it appears that the braiding index is very sensitive to small changes in water-surface elevation, especially when it is referenced to the 1,200-cfs water-surface that barely inundates many of the low-elevation, in-channel bars.

The reach-wide average braiding index showed some variation throughout the survey period, although it remained between 4.1 and 4.7 (**Figure 3.6b**)⁴. The lowest average value occurred in 2012, but the difference from the other years is not statistically significant. Geomorphic Reach 6 (Minden to Gibbon) consistently had the highest braiding index, followed by Reaches 4 (Elm Creek to Odessa) and 7 (Gibbon to Wood River) (**Figure 3.6c**). Reach 9 (Grand Island to Chapman) also had relatively high braiding indices. The braiding index for Reach 6 is derived from only AP21 that, as noted above, is located at the Rowe Sanctuary and has a very high braiding index. Rotating AP20 that was surveyed only in 2011 had a braiding index of 4.7, and AP22 that was surveyed in 2010 and 2014 had braiding indices of 3.0 and 4.0, suggesting that AP21 may not be representative of the remainder of Reach 6. Reaches 1, 2 and 8 (Lexington to Overton, south channel at Jeffreys Island, and Wood River to Grand Island, respectively) consistently had the lowest braiding index, although Reach 8 has become progressively more braided during the first increment.

Fotherby (2008) states that “*a reach of river was ...labeled as having a fully braided river pattern if the main channel had a braiding index of 3 or more throughout the reach.*” In her analysis, however, she categorized reaches with main channel braiding index (defined as the average number of channels) less than 2.5 as wandering or meandering, 2.5 to 3.5 as braided and greater than 3.5 as anastomosed (See Fotherby, 2008, Section 4.1). The currently defined PRRIP subreaches were classified by Fotherby (2008) (Table 2.2) as follows⁵:

- Reach 1 – Wandering
- Reach 2 – Meandering
- Reach 3 (*Reach 3A*) – Anastomosed with some braiding
- Reach 4 (*Reach 3B*) – Braided
- Reach 5 – Anastomosed with some braiding (*Reach 3C*); anastomosed (*Reach 3D*)
- Reach 6 (*Reach 4A*) – Braided
- Reach 7 (*Reach 4B*) - Anastomosed with some braiding
- Reach 8 - Anastomosed with some braiding (*Reach 4C*); braided (*Reach 4D*)
- Reach 9 (*Reach 5*) – Alternating braided and anastomosed.

⁴Because APs 25 and 37 were not surveyed in all years, it was assumed that the values of the geomorphic variables during the non-surveyed years remained the same as the last surveyed year for purposes of developing the geomorphic and overall reach averages to avoid bias resulting from simply eliminating these values.

⁵Fotherby (2008) reach designations in *italics*, where different from current definition

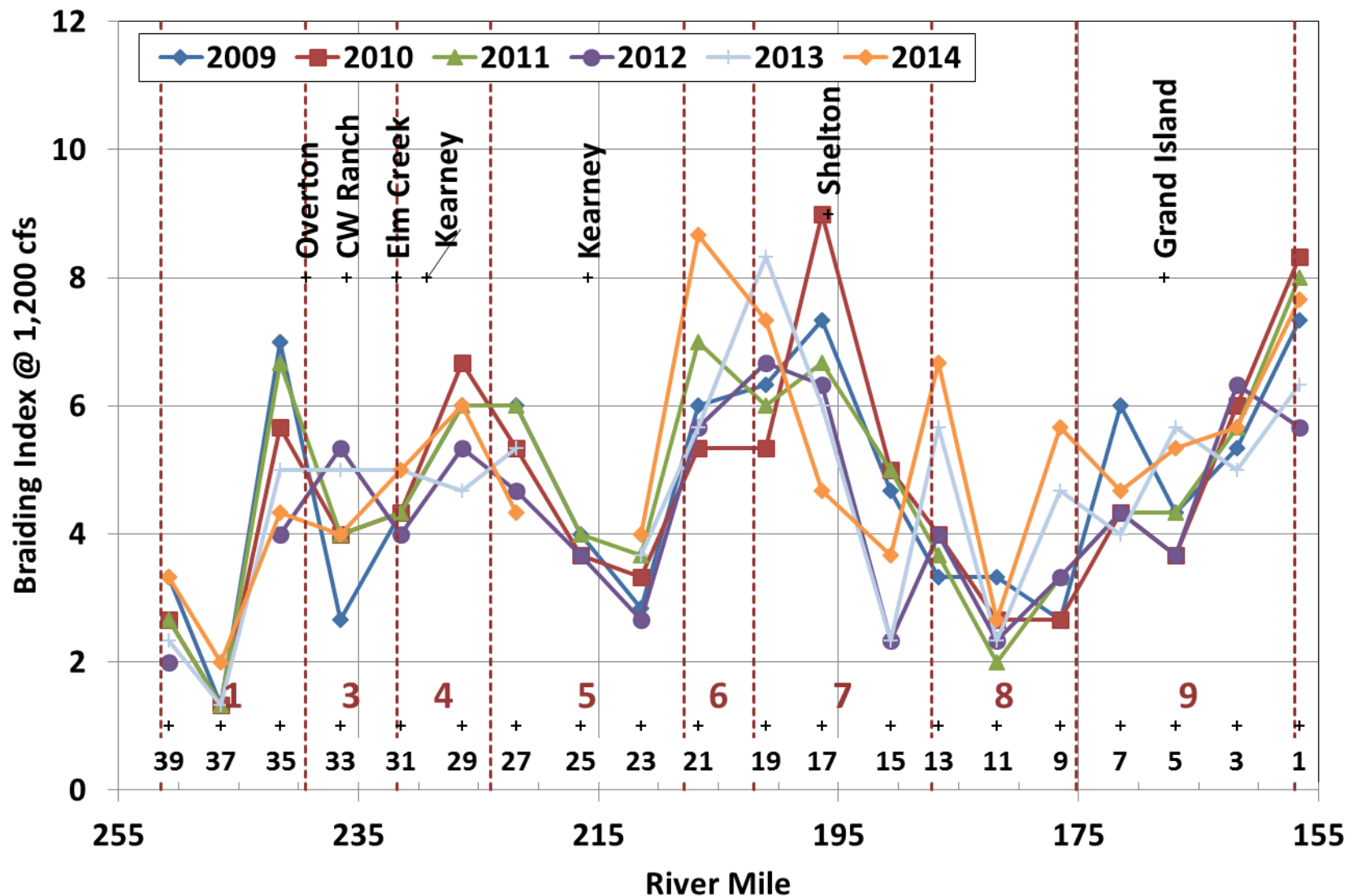


Figure 3.6a. Average braiding index at pure panel APs from 2009 through 2014.

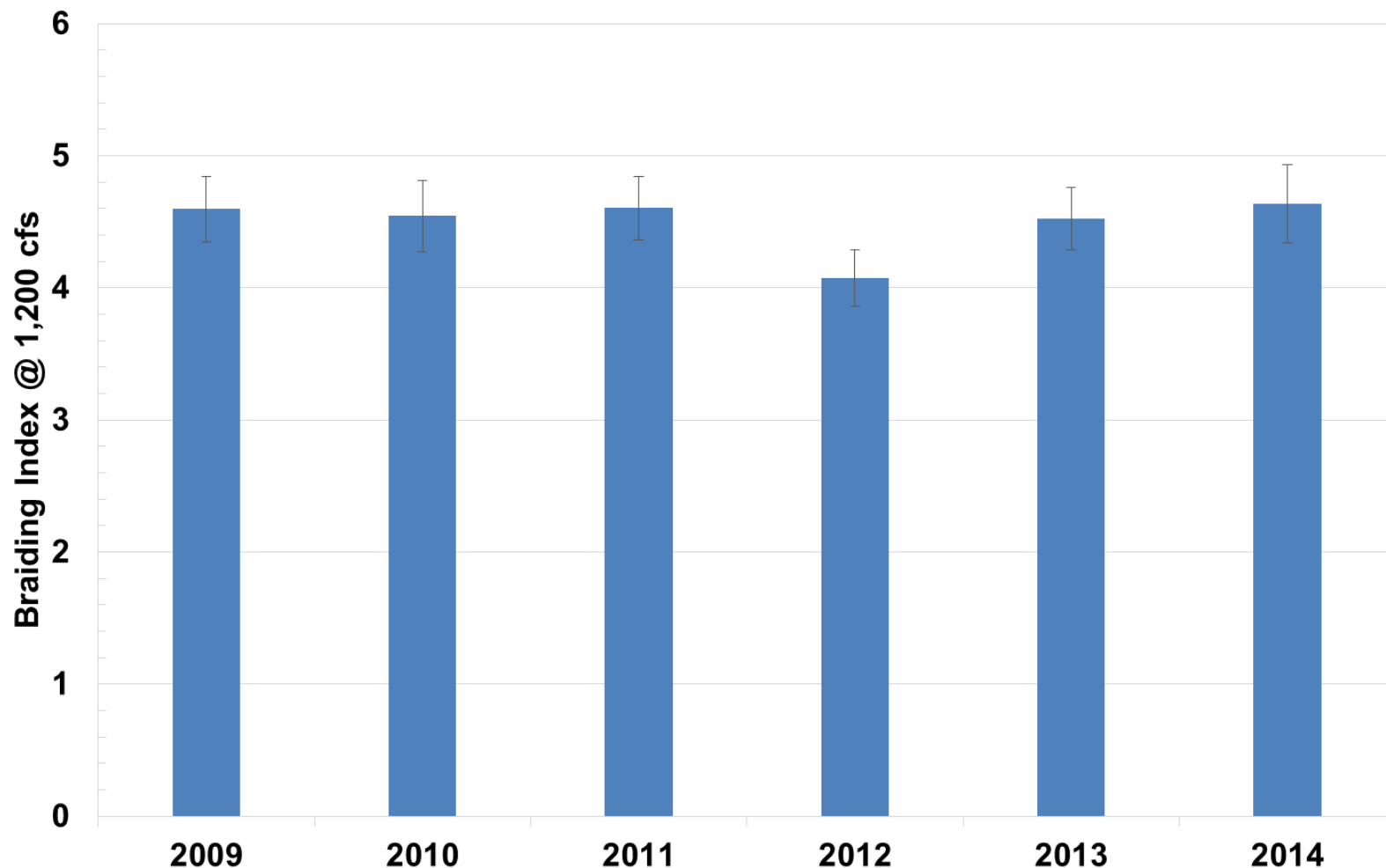


Figure 3.6b. Average braiding index for the overall study reach, based on the pure panel AP data from 2009 through 2014. Whiskers represent ± 1 standard error on mean value.

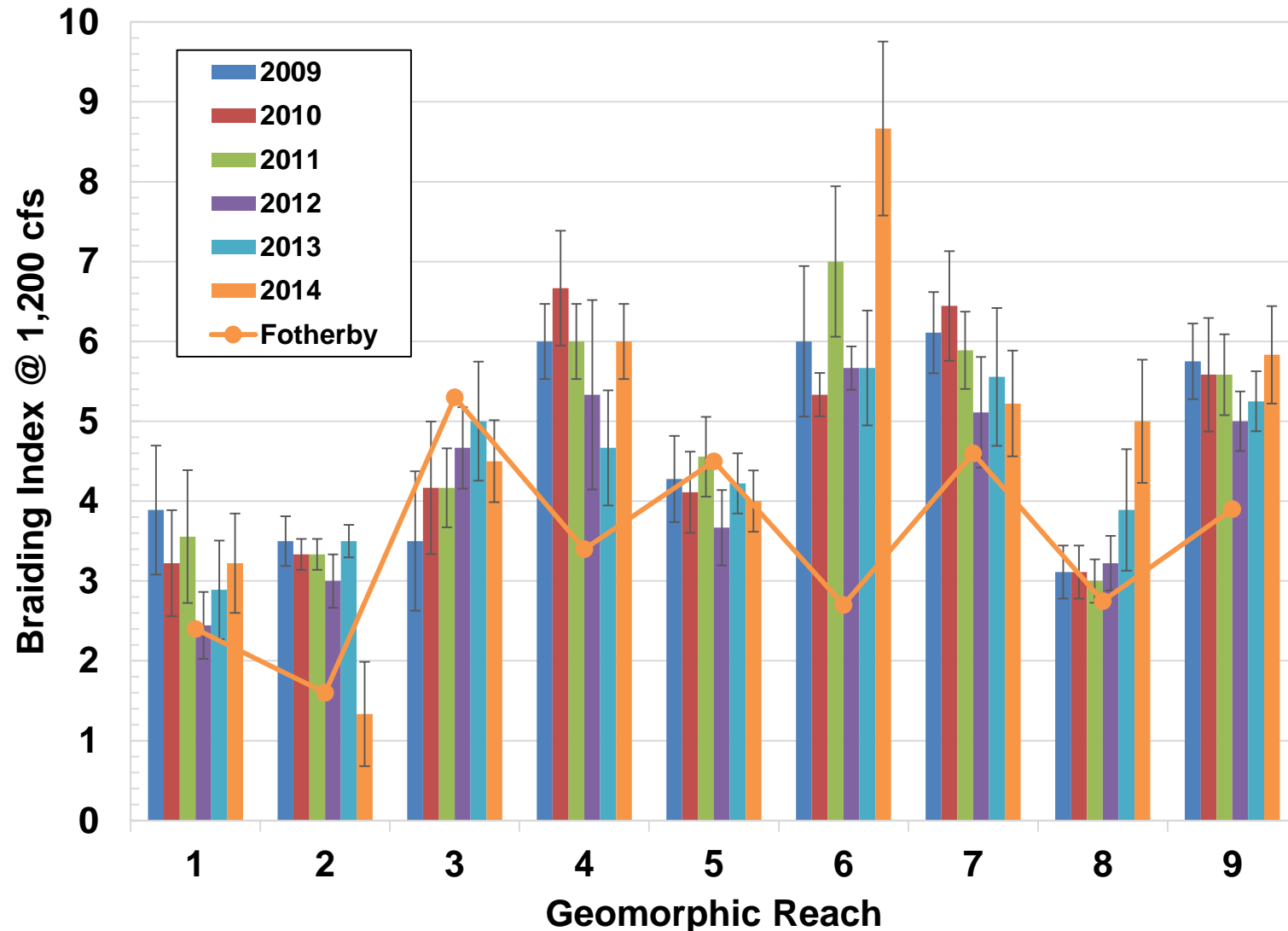


Figure 3.6c. Average braiding index by geomorphic reach, based on the pure panel AP data from 2009 through 2014. Also shown are Fotherby (2008) braiding indices. Whiskers represent ±1 standard error on mean value.

Fotherby's (2008) braiding indices were developed by counting the number of individual channels evident in the 1998 color-infrared (CIR) photography that was taken when the discharge along the reach varied from about 450 cfs at Overton to 1,030 cfs at Grand Island (Friesen et al., 2000). The braiding indices for Reaches 1 and 2 developed for this study (reference discharge of 1,200 cfs) are considerably higher than those from Fotherby (2008) [average of 4.5 and 3.0 over the six surveys for this study versus 2.4 and 1.6 from Fotherby (2008), respectively]. Fotherby's (2008) braiding indices for Reaches 3 and 5 were similar to those found in this study, although for Reach 3, Fotherby's index was higher than most of the field surveys. Fotherby's (2008) braiding indices for the remaining reaches were considerably lower than those obtained for this study, with Reach 6 having the greatest difference [average of 6.4 over the six surveys for this study versus 2.7 from Fotherby (2008)]. Differences in methodology, however, likely account for at least some of the differences, and activities associated with Program and partner activities that include channel grading, discing and herbicide spraying to eliminate noxious weeds (primarily phragmites), and tree and riparian vegetation clearing to promote channel widening also contribute the differences. As noted above, this is especially true for Reach 6, where the value for this study is based on conditions at AP21 at the Rowe Sanctuary where the channel has been manipulated extensively over the last +/-5 years to improve habitat.

Based on Fotherby's (2008) classification system and the average values for this study, none of the reach would be classified in the meandering or wandering categories, only Reach 2 would be solidly in the braided category, Reach 8 would be borderline between braided and anastomosed and the remainder would be in the anastomosed category. Although some portions of the reach are certainly anastomosed, as evidenced by the presence of one or more relatively persistent, secondary channels, all of the pure panel APs, with the possible exception of APs 35, 37 and 39, exhibit at least some degree of braiding.

3.3.2 Total Channel Width (DAP 5.3.2)

The total channel width at 1,200 cfs generally increases in the downstream direction for all data sets, with the widths ranging from slightly more than 200 feet at AP37 (north channel at Jeffreys Island) to nearly 1,800 feet at AP1 (**Figure 3.7a**). This metric changed very little at most APs over the 6-year monitoring period. Along with AP 37, the APs with the narrowest total channel width include AP23, AP25, AP31, and AP39. The widest, in addition to AP1, include AP17, AP21, AP27, AP29, AP33, and AP35. In spite of the general downstream-increasing trend, the total channel width tends to alternate between wide and narrow segments along the overall reach. The very large total channel width at AP1 is somewhat deceptive because this part of the reach is highly anastomosed, with roughly one-third of the width occupied by large islands with mature woody vegetation. Similar conditions occur at AP17 near Shelton, and AP27 between Kearney and the KDS, although the proportion of total width occupied by vegetated islands is less extreme than at AP1. The wide channels at AP21 and AP33 most likely result from restoration activities at the Rowe Sanctuary and Cottonwood Ranch, respectively.

The average total channel width for the overall reach has remained relatively consistent since 2009 (**Figure 3.7b**). There is, however, considerable variability among the geomorphic reaches, with Reach 2, at the upstream end of the overall monitoring reach, having the narrowest average width (450 to 550 feet during 2009 through 2013, and narrowing to about 320 feet in 2014), and Subreach 6 (Minden to Gibbon) the widest (about 1,250 feet) (**Figure 3.7c**). The year-to-year variability within the reaches is also relatively small with the exception of Reach 2. Due to access issues only one pure panel anchor point (AP35) has been surveyed in Reach 2 since 2011; thus, drawing firm conclusions about the representativeness of these changes to the overall South Channel at Jeffreys Island is tenuous.

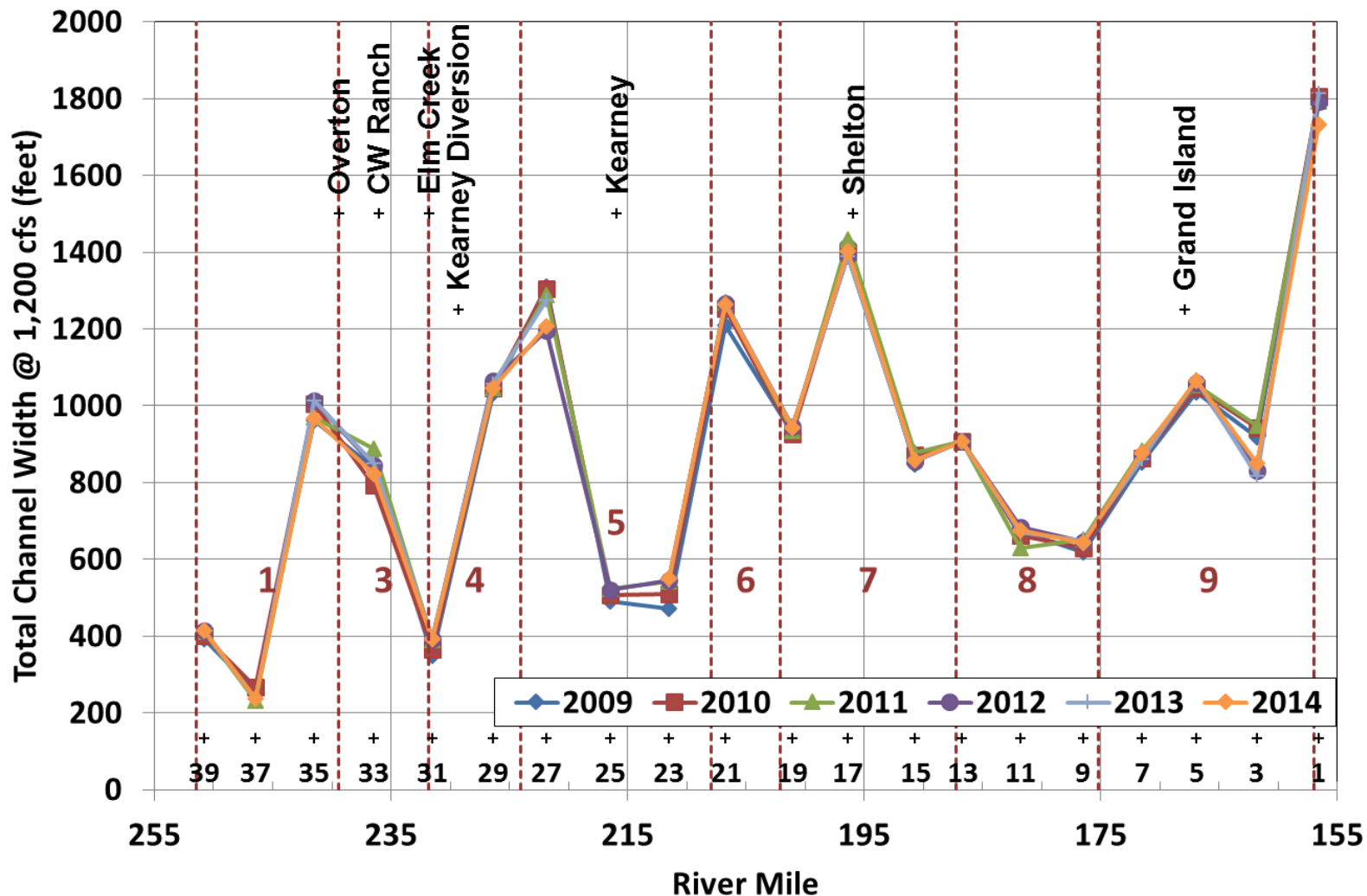


Figure 3.7a. Average total channel width at pure panel APs from 2009 through 2014.

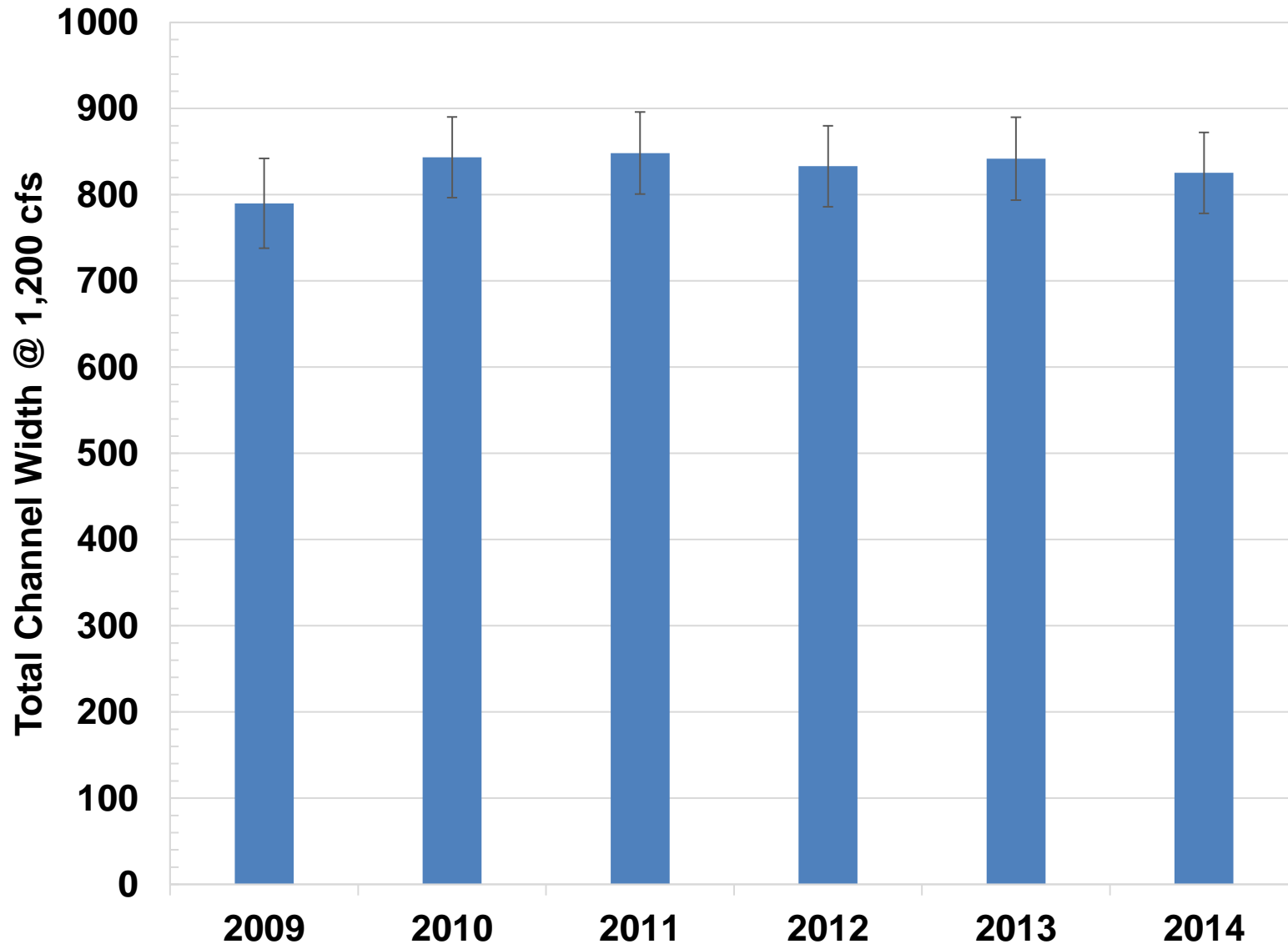


Figure 3.7b. Average total channel width for the overall study reach, based on the pure panel AP data from 2009 through 2014, omitting the J-2 return channel. Whiskers represent ± 1 standard error on mean value.

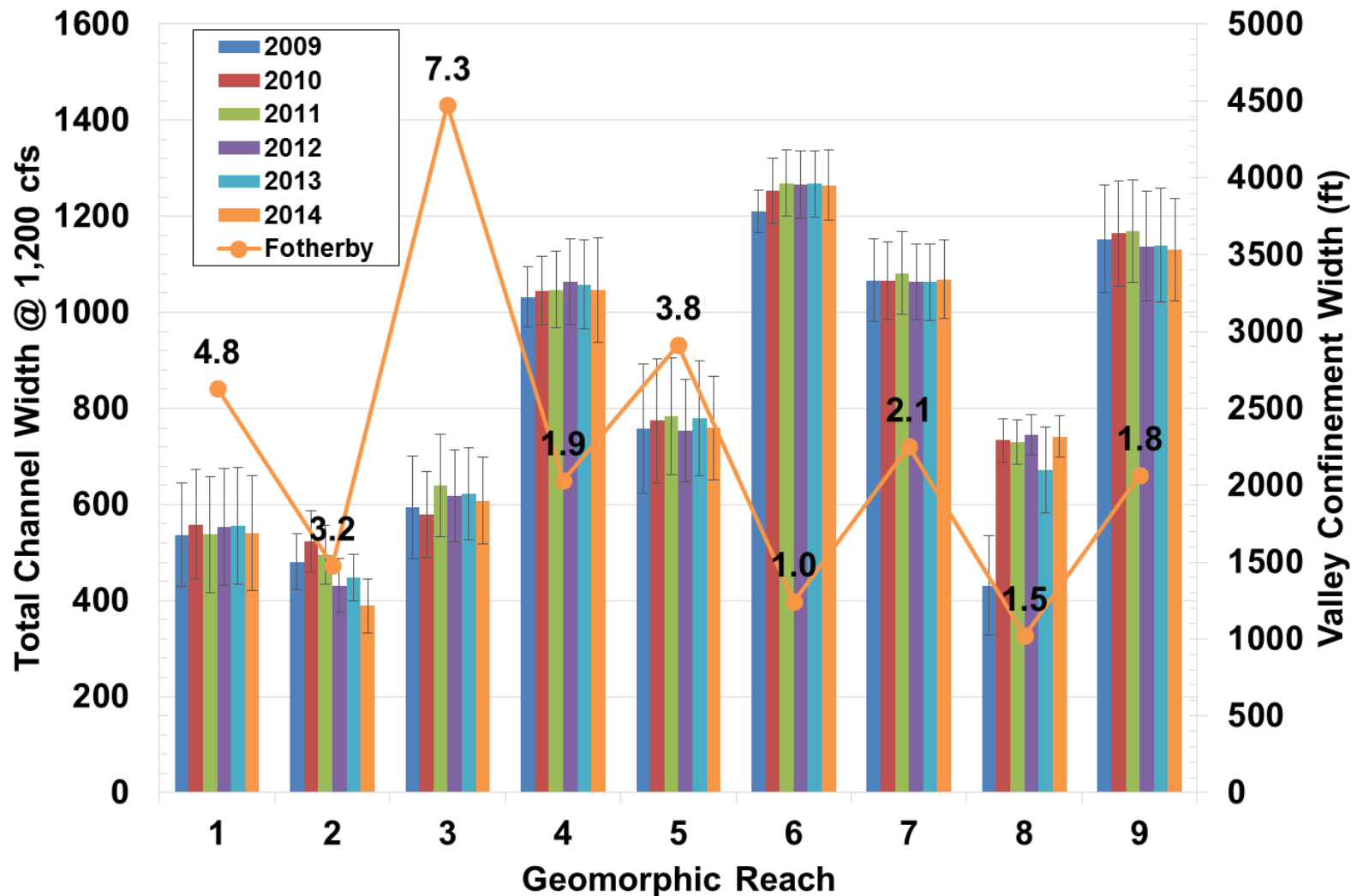


Figure 3.7c. Average total channel width by reach, based on the pure panel AP data from 2009 through 2014. Whiskers represent ± 1 standard error on mean value. Also shown are valley confinement widths from Fotherby (2008). **Note right-hand scale for this variable.** Values above Fotherby (2008) line are ratio of valley confinement width to total channel width.

Fotherby (2008) concluded that valley confinement associated with both the natural geology of the reach and human influences is the primary driver of channel form in essentially the entire portion of the study reach downstream from Overton, while sediment size and transport capacity are the primary drivers upstream from Overton. With the exception of Reach 6, where Fotherby's (2008) valley confinement width is about the same as the total channel width and Reach 8, where it is about 50 percent larger, the confinement widths through the reach are significantly larger than the total channel width (Figure 3.7c). The margin between the valley confinement feature and the total channel width in Reaches 6 and 8 may be sufficiently small to have a direct influence on the channel pattern, however, this is probably not the case in other portions of the reach. It is particularly interesting to note that AP21, where Fotherby's (2008) valley confinement width is essentially the same as the total channel width, is one of the most braided of all of the Pure Panel APs.

3.3.3 Wetted Channel Width (DAP 5.3.3)

The wetted channel width at 1,200 cfs ranged from about 200 feet (AP37, 2011 and 2014) to over 1,000 feet (AP21, 2013) (Figure 3.8a). Similar to total channel width, wetted width generally increases in the downstream direction. The wetted widths at AP7, AP23, AP31, AP35, AP37 and AP39 are narrower than the typical widths in other parts of the reach (generally in the 200- to 300-foot range). Unlike total channel width, the wetted width changed substantially at many of the APs over the 6-year monitoring period as the channels and macro-scale bedforms and bars changed shape.

The reach-wide average wetted width increased by a modest (but not statistically significant) amount from about 450 in 2009 to about 500 feet in 2012, and then declined back to about 430 feet in 2014 (Figure 3.8b). Similar to the total width, there is considerable variability among the geomorphic reaches, with Reaches 1 and 2 having the narrowest average wetted widths (~300 feet and ~280 feet, respectively, averaged across all years), and Subreach 6 (Minden to Gibbon) the widest [690 feet (2009) to 1,000 feet (2013)] (Figure 3.8c). The year-to-year variability in wetted width is generally greater in most reaches than the total width, again due to changes in shape of the macro-scale bedforms and bars.

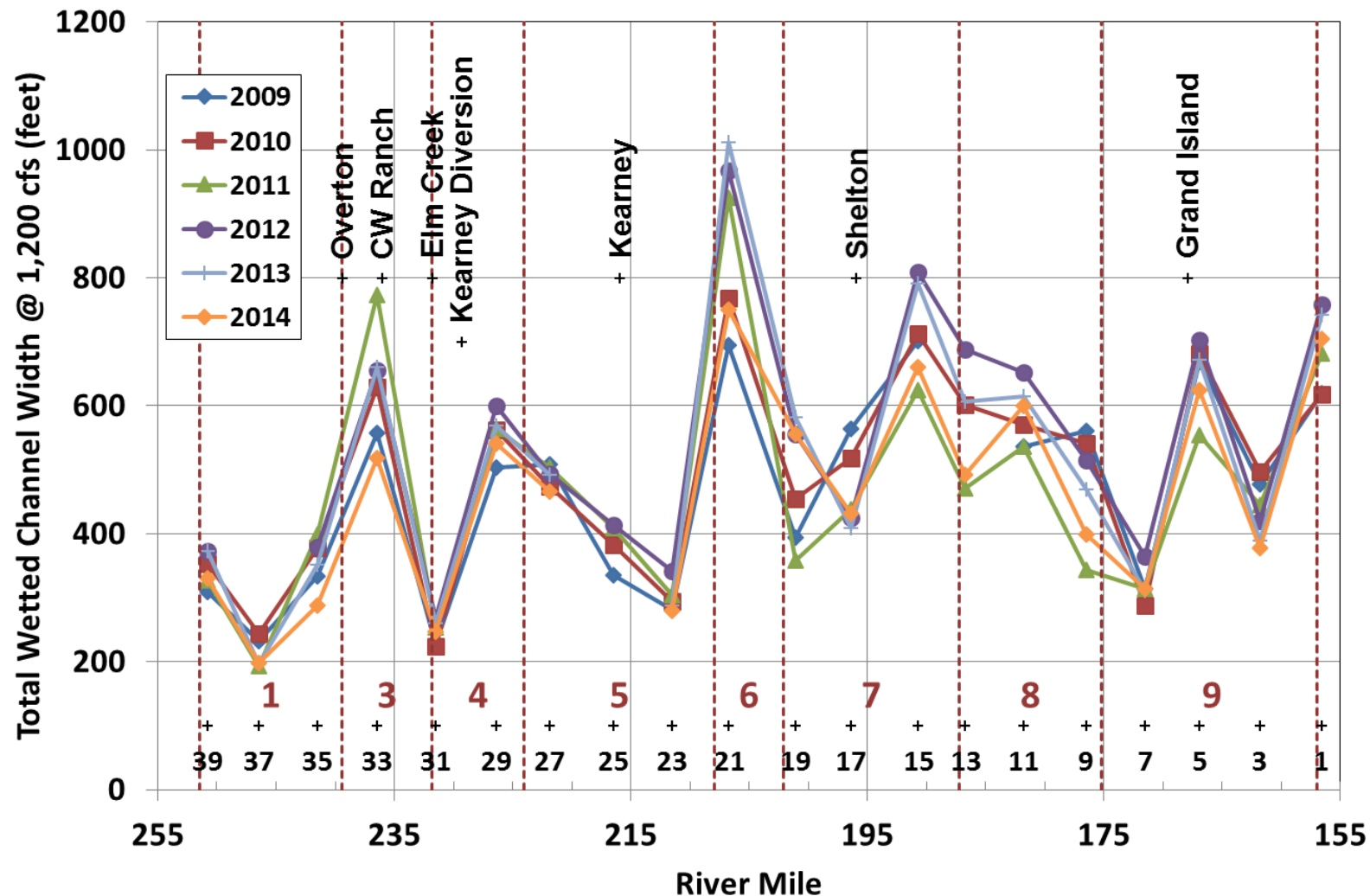


Figure 3.8a. Average wetted width at 1,200 cfs at pure panel APs from 2009 through 2014.

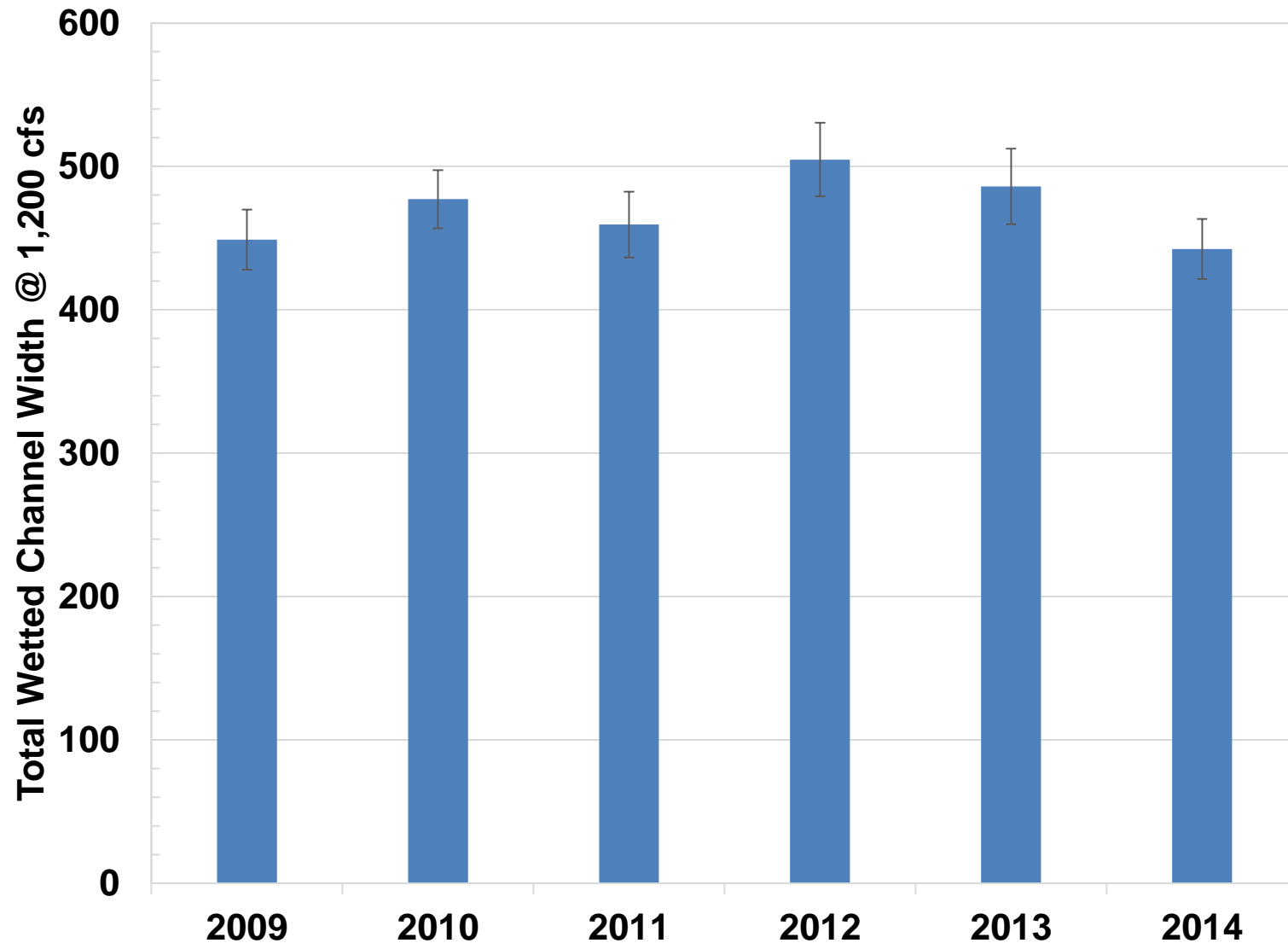


Figure 3.8b. Average wetted width at 1,200 cfs for the overall study reach, based on the pure panel AP data from 2009 through 2014. Whiskers represent ± 1 standard error on mean value.

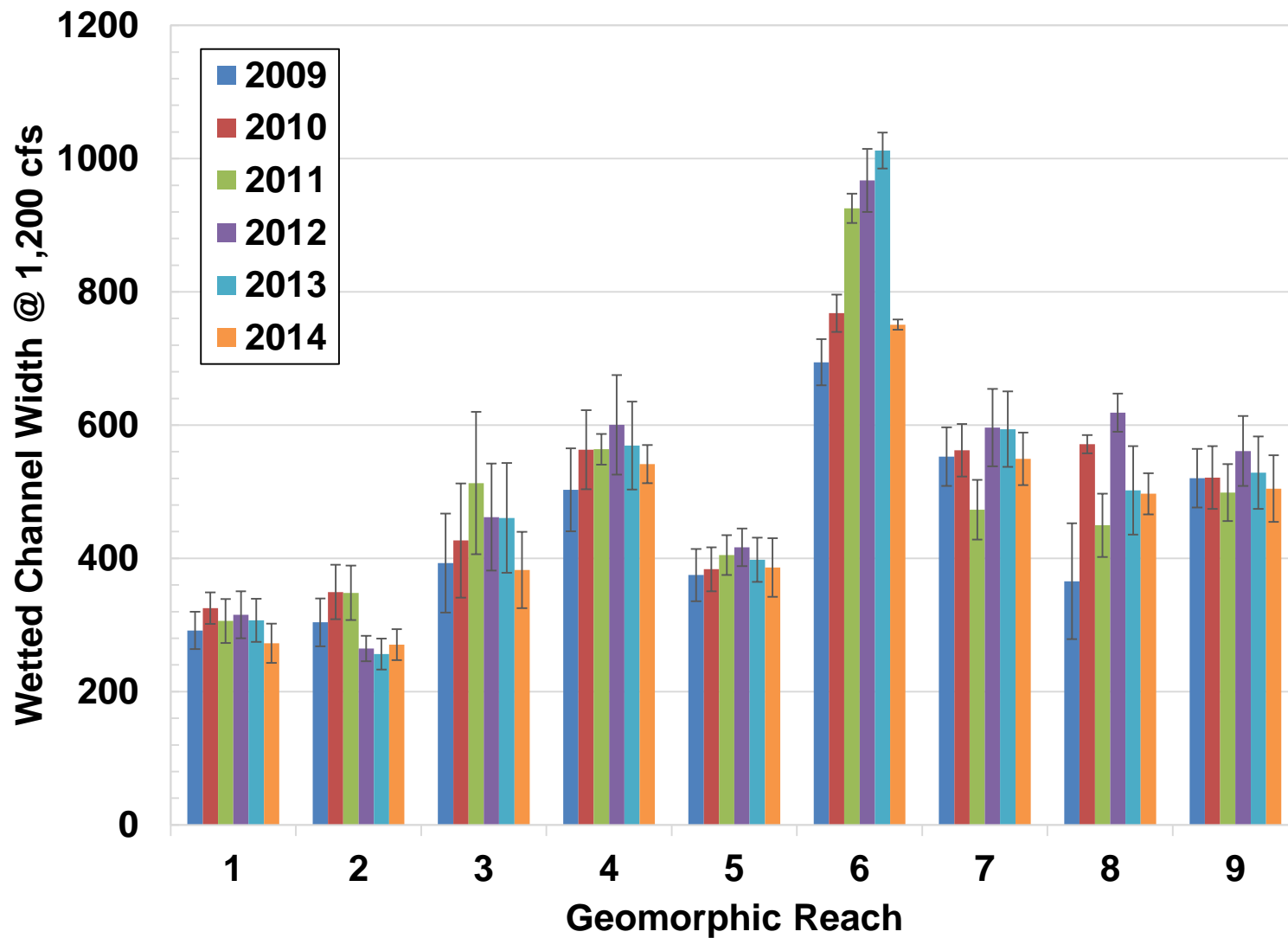


Figure 3.8c. Average wetted width at 1,200 cfs by geomorphic reach, based on the pure panel AP data from 2009 through 2014. Whiskers represent ± 1 standard error on mean value.

3.3.4 Mean Channel Depth (DAP 5.3.4)

In 2009, mean channel depth along the mainstem (i.e., not considering the south channel at Jefferys Island) at 1,200 cfs ranged from about 0.7 feet (AP9) to 2.0 feet (AP37A), with a general trend of decreasing depth in the downstream direction (**Figure 3.9a**). Mean channel depth at AP37B, in the south channel, was approximately 2.3 feet. Mean channel depths in subsequent years followed a similar pattern, but varying by up to 1 foot from year to year.

The mean channel depth over the entire study reach averaged about 1.3 feet in 2009, increasing to nearly 1.5 feet in 2011, and then decreasing back to about 1.1 feet in 2012 and 2013 (**Figure 3.9b**). The 2014 data show a small rebound to about 1.3 feet. The differences between 2009, 2010 and 2011 are not statically significant (based on the Kruskal-Wallis test, $p=0.125$), nor are the differences between 2012, 2013 and 2014 ($p=0.202$). However, the differences between these two groups of years is statistically significant ($p<0.0001$).

Geomorphic Reach 2 (south channel at Jeffreys Island) consistently had the largest mean depth through the first six years of data collection, followed by Reaches 1 and 3 (**Figure 3.9c**). Reaches 6 and 8 typically exhibit the smallest mean depth. These depths tend to be inversely proportional to the wetted channel width.

Some of the differences in depth between years are attributable to changes in the stage-discharge rating curve at the individual transects. There appears to have been a systematic shift in channel geometry as a result of the 2011 high flows that tended to reduce the topographic variability of the channel, widening the wetted channel at 1,200 cfs and decreasing the mean depth (see Section 3.3.3). As a result downstream from Overton (Reaches 3 to 9), the mean depth in 2012 was significantly reduced compared to 2011. A typical example occurred at AP15, Transect 4, where the wetted width increased from about 500 feet to over 780 feet due to general flattening of the bed across the river (**Figure 3.9d**).

3.3.5 Maximum Channel Depth (DAP 5.3.5)

The relative magnitudes and trends in the maximum channel depth (i.e., the thalweg depth) at 1,200 cfs are very similar to those for the mean channel depth, but as expected, the individual magnitudes are 2.5 to 3 times greater (**Figure 3.10a**). Thalweg depths from the 2014 survey data are within the range of values of the previous five surveys. Maximum channel depth tends to decrease in the downstream direction, although trends are somewhat obscured by scatter in the data. Such scatter is to be expected because thalweg depth is more heavily influenced by local controls and scour processes than mean channel depth which provides a better analytical point for reach-scale processes.

The reach-wide average maximum depth increased from about 3.0 feet in 2009 to about 3.9 feet in 2011, and then declined back to about 2.5 feet in 2012 and 2013. The 2014 data show an increase back to approximately 3.2 feet (**Figure 3.10b**). Consistent with the mean channel depth, the average maximum depth in the geomorphic subreaches generally declines in the downstream direction, with the highest values occurring in Reach 2 and the lowest values occurring in Reaches 6 (AP21) and 8 (**Figure 3.10c**). Similar to trends observed with mean channel depth, there is a noticeable decrease in maximum channel depth between the 2011 and 2012 datasets, most likely due to processes similar to the illustration of Figure 3.9d. The pronounced increase in maximum channel depth between 2013 and 2014 may have been caused by scour during the September 2013 flood.

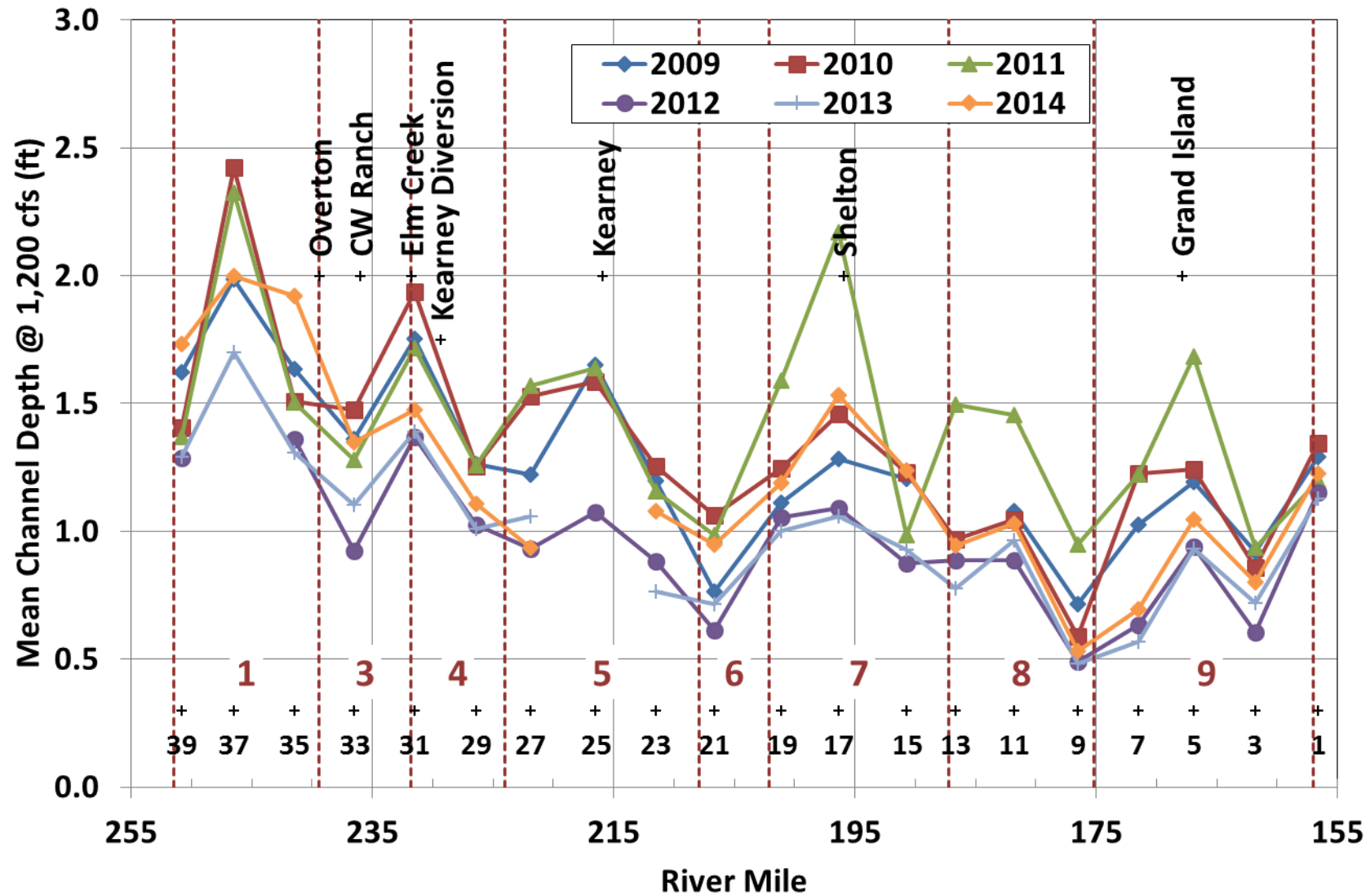


Figure 3.9a. Mean channel (i.e., hydraulic) depth at 1,200 cfs at pure panel APs from 2009 through 2014.

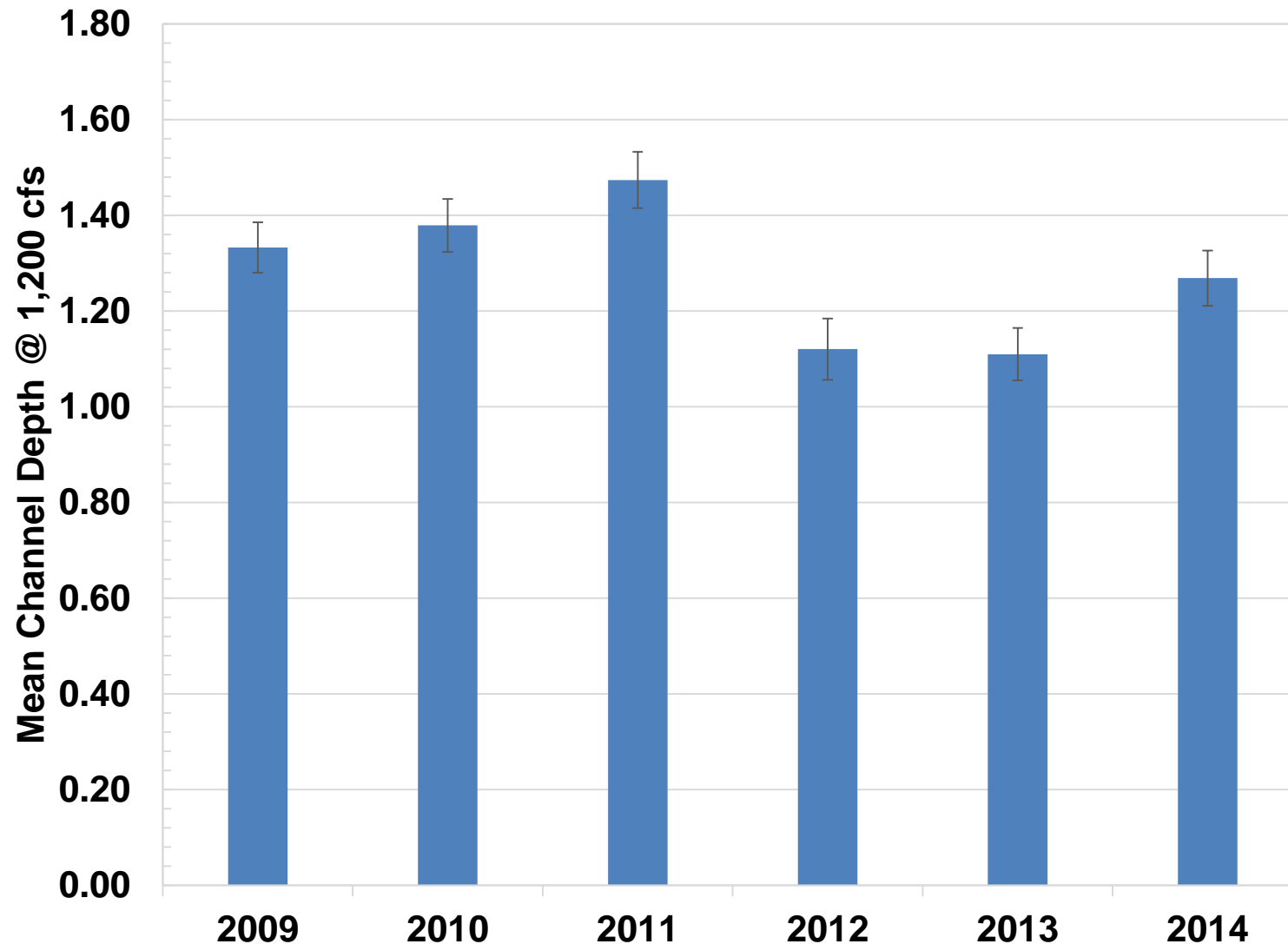


Figure 3.9b. Average mean channel (i.e., hydraulic) depth at 1,200 cfs for the overall study reach, based on the pure panel AP data from 2009 through 2014.

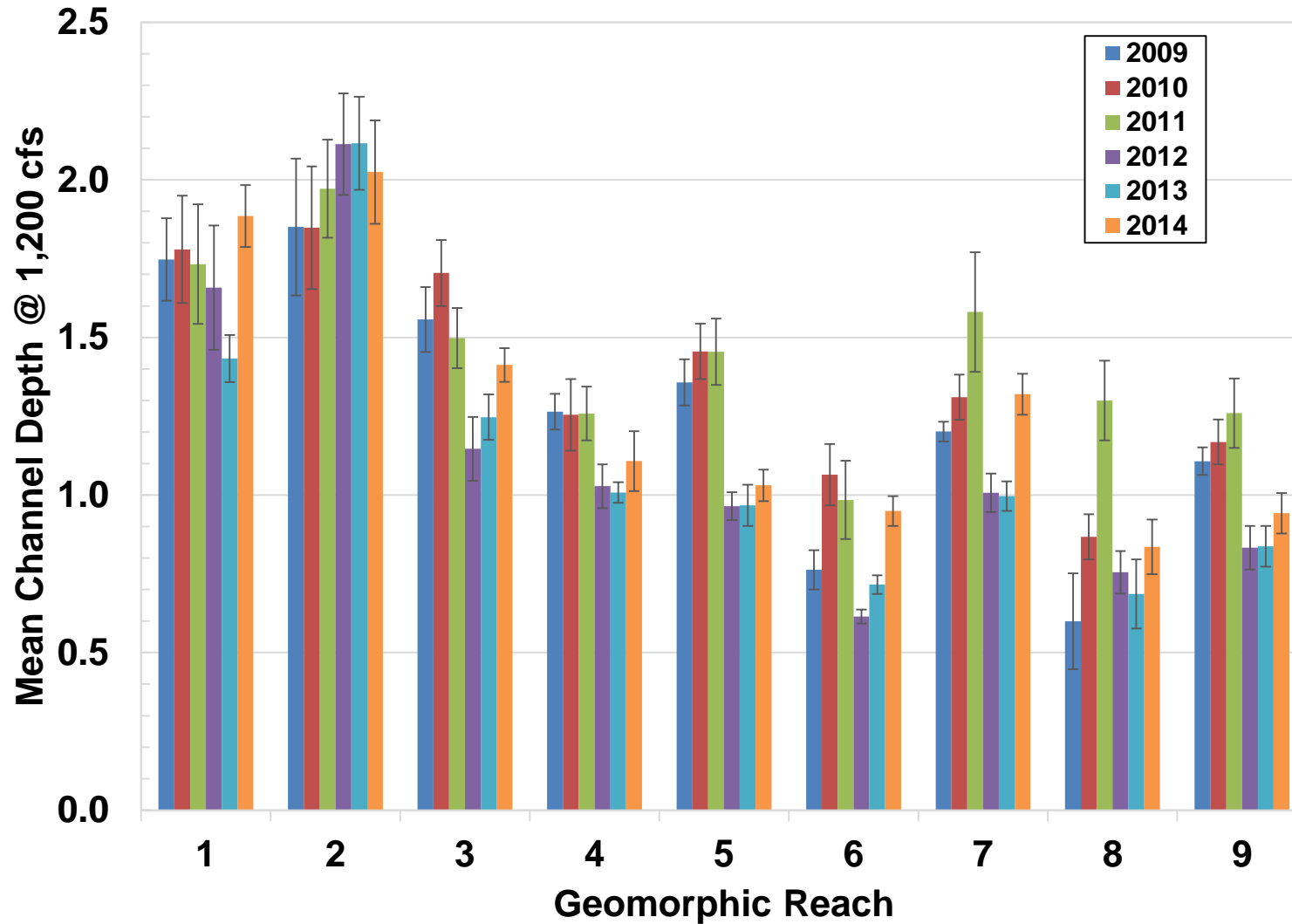


Figure 3.9c. Average mean channel (i.e., hydraulic) depth at 1,200 cfs by geomorphic reach, based on the pure panel AP data from 2009 through 2014.

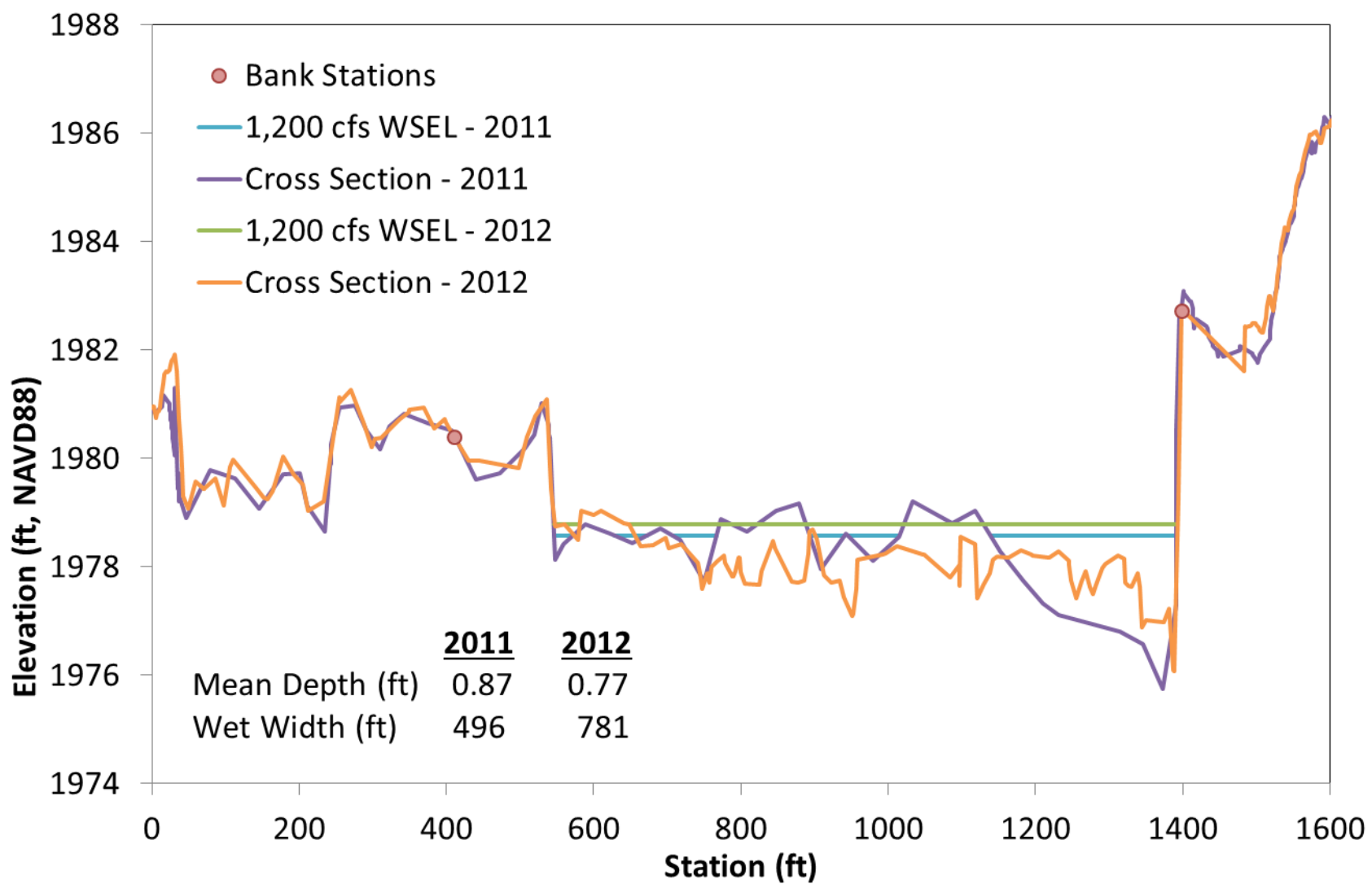


Figure 3.9d. Surveyed cross-section profiles at AP15, transect four in 2011 and 2012. Note the removal of instream bars and the aggradation of the thalweg, which resulted in a wider, shallower channel.

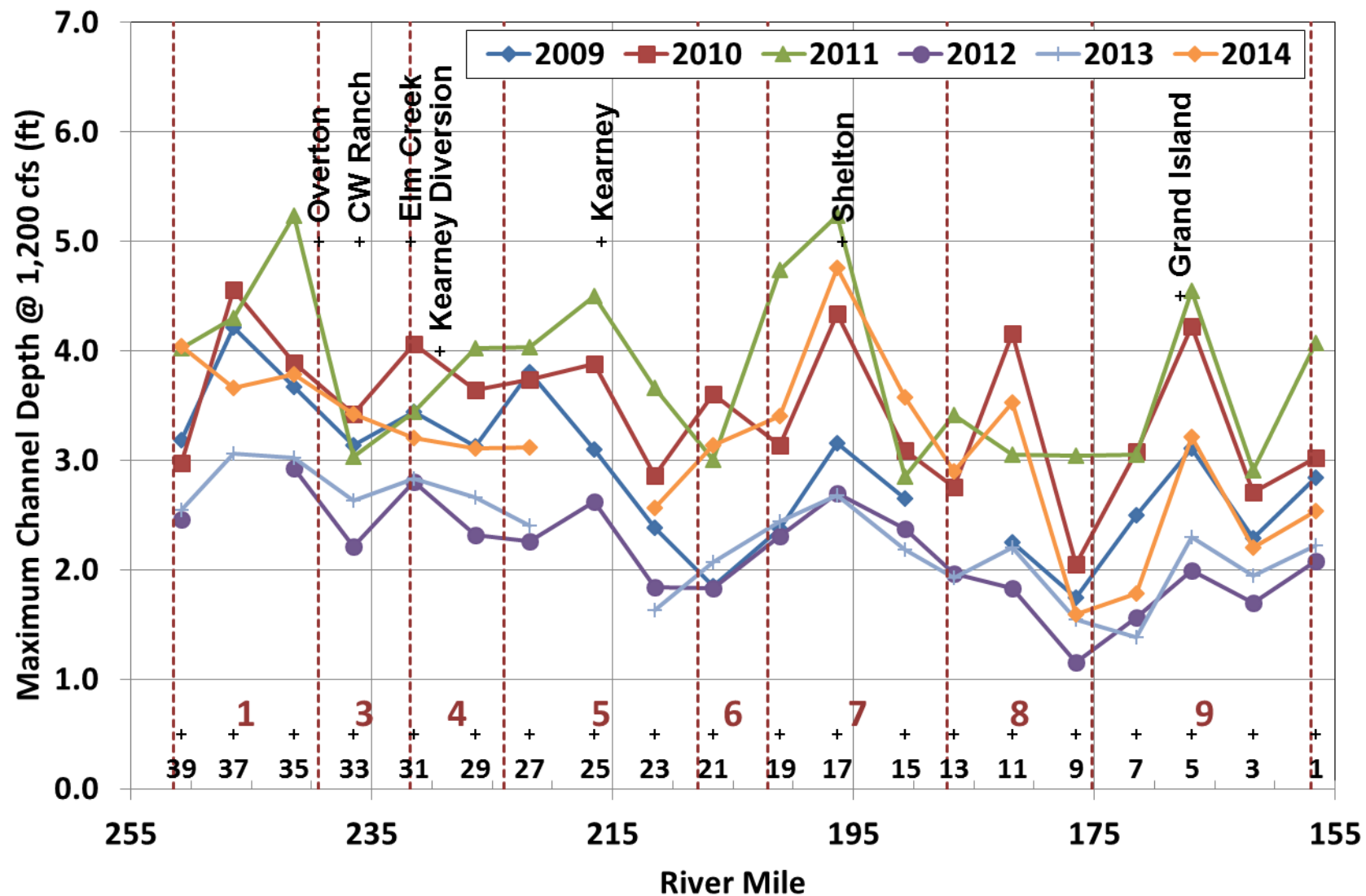


Figure 3.10a. Average maximum channel depth at 1,200 cfs at pure panel APs from 2009 through 2014.

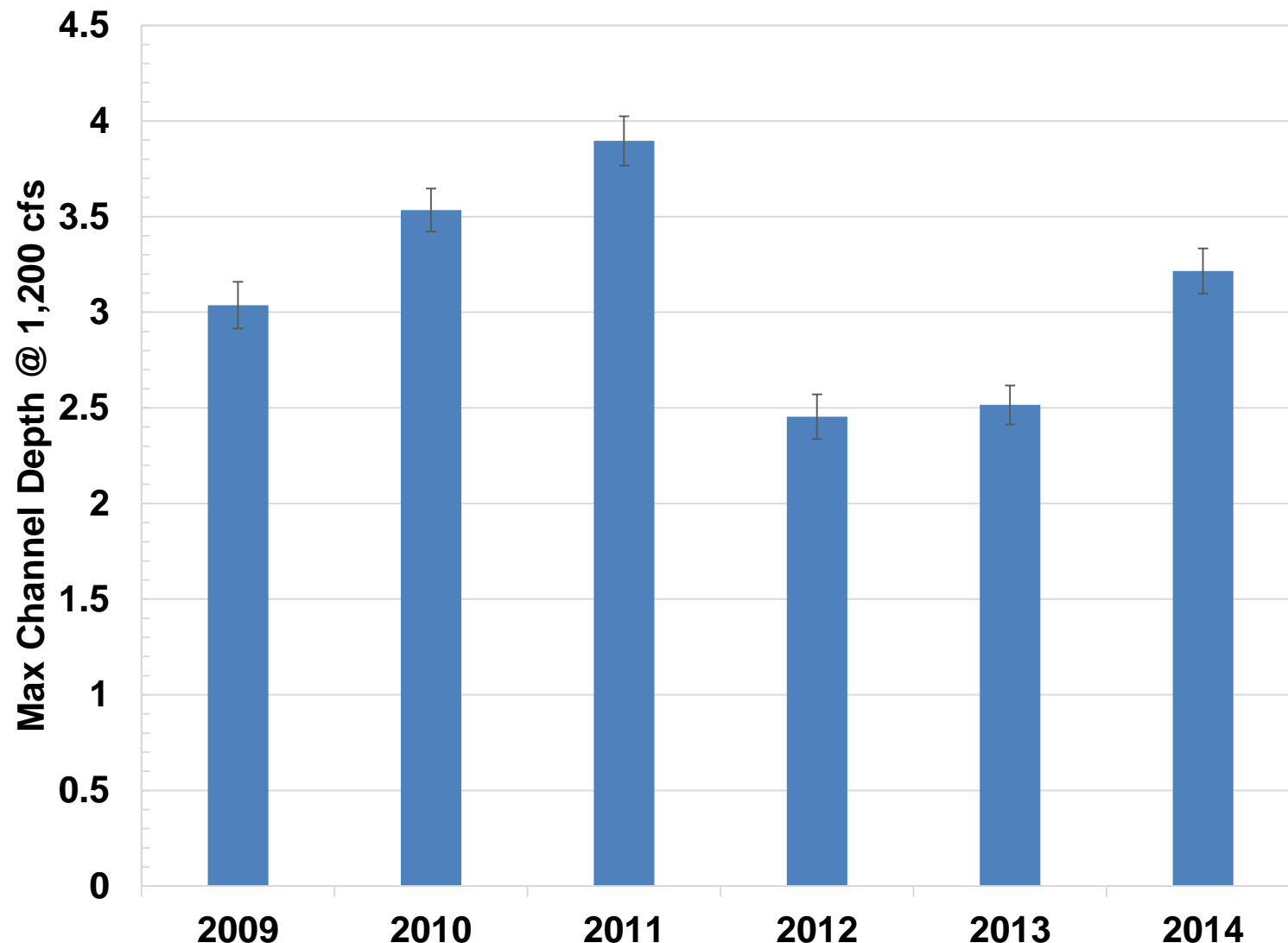


Figure 3.10b. Average maximum channel depth at 1,200 cfs for the overall study reach, based on the pure panel AP data from 2009 through 2014.

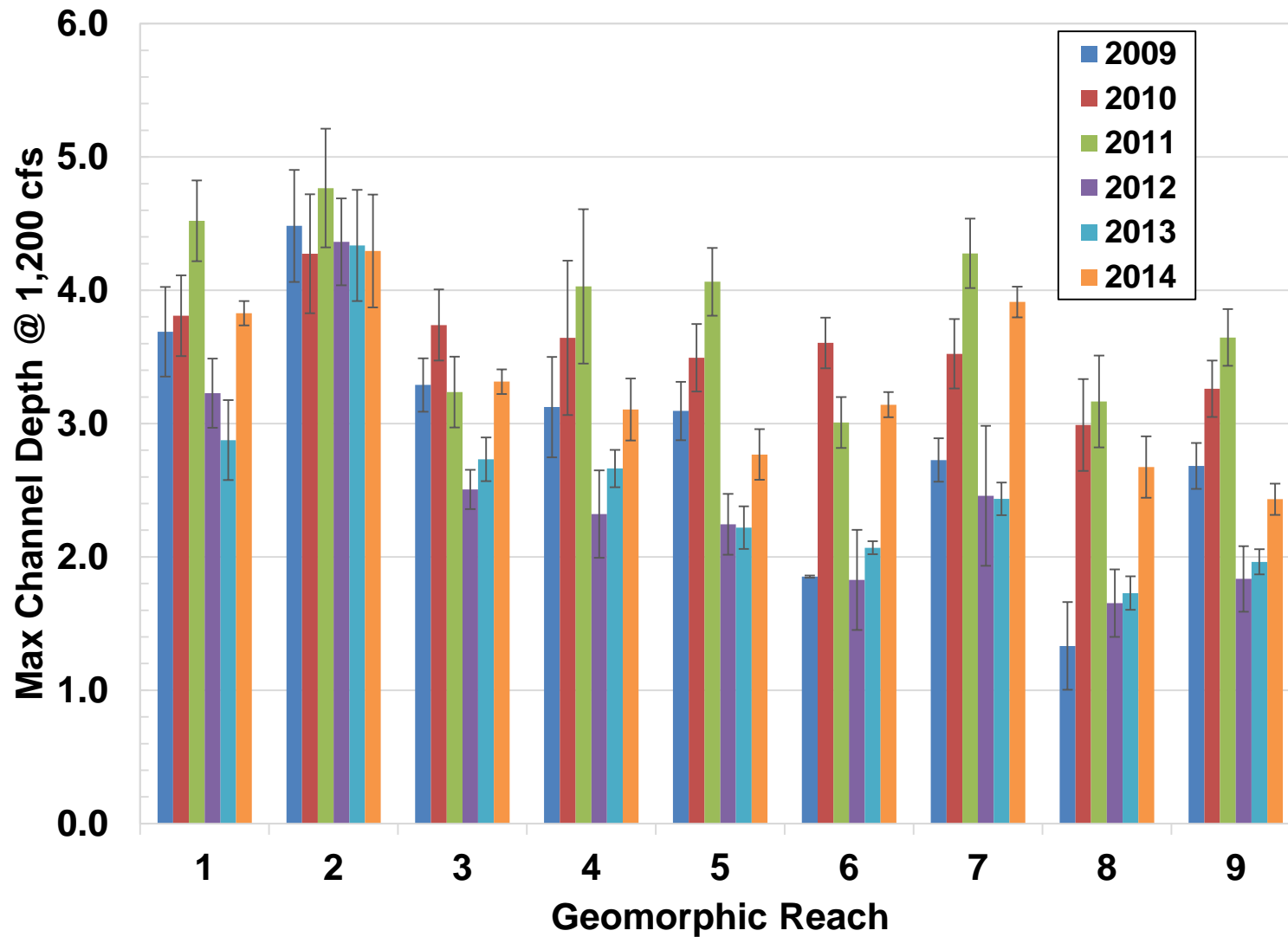


Figure 3.10c. Average maximum channel depth at 1,200 cfs by geomorphic reach, based on the pure panel AP data from the 2009 through 2014 data.

3.3.6 Channel Width-to-Depth Ratio (DAP 5.3.6)

The average width-to-depth⁶ ratio at 1,200 cfs at the pure panel APs ranges from about 50 (AP37A, 2011) to over 500 (AP21, 2012), with a general trend of increasing values in the downstream direction (**Figure 3.11a**). In 2011 and 2012, AP21 had the highest width-to-depth ratios observed in the entire program reach. Several APs in the downstream part of the reach (AP1, 5, 9, 11, 13 and 15) also had relatively high width-to-depth ratios in 2012. Most of the APs experienced a substantial decline in width-to-depth ratios from 2013 to 2014.

For the overall reach, the average width-to-depth ratio declined from about 170 in 2009 to 130 in 2011 (**Figure 3.11b**). Between the 2011 and 2012 surveys, the ratio increased to over 240, and it then declined back to about 215 in 2013 and 150 in 2014. This trend is consistent with the trends in channel width and depth discussed above, in which the topographic variability across many of the cross sections tended to decrease as the individual braid channels filled in and the sand bars flattened during the 2011 high flows (see Figure 3.9d). The average width-to-depth ratios for the geomorphic reaches follow the same general trend as the individual AP averages, with Reach 2 having the smallest values and Reach 6 (again, as represented by AP21) having the largest values (**Figure 3.11c**). The ratios for the three downstream reaches (Reaches 7, 8 and 9) are generally larger than Reaches 3, 4 and 5.

Fotherby (2008) computed width-to-depth ratios using results from the hydraulic model discussed by Murphy et al. (2006) at a discharge of 2,000 cfs. Her calculations differ from those specified in the DAP, and reported above, in that she used the mean depth rather than the maximum (thalweg) depth and she used a higher discharge, both of which tend to make the ratios larger. The width-to-depth ratios obtained from the data from this monitoring program using the mean depth (and a discharge of 1,200 cfs) are, however, reasonably consistent with Fotherby's (2008) values, except in Reach 6, where the current data indicate much larger ratios (**Figure 3.11d**). This difference is most likely due to mechanical activities in the channel at the Rowe Sanctuary.

⁶Maximum channel depth was used to quantify this metric, per the DAP.

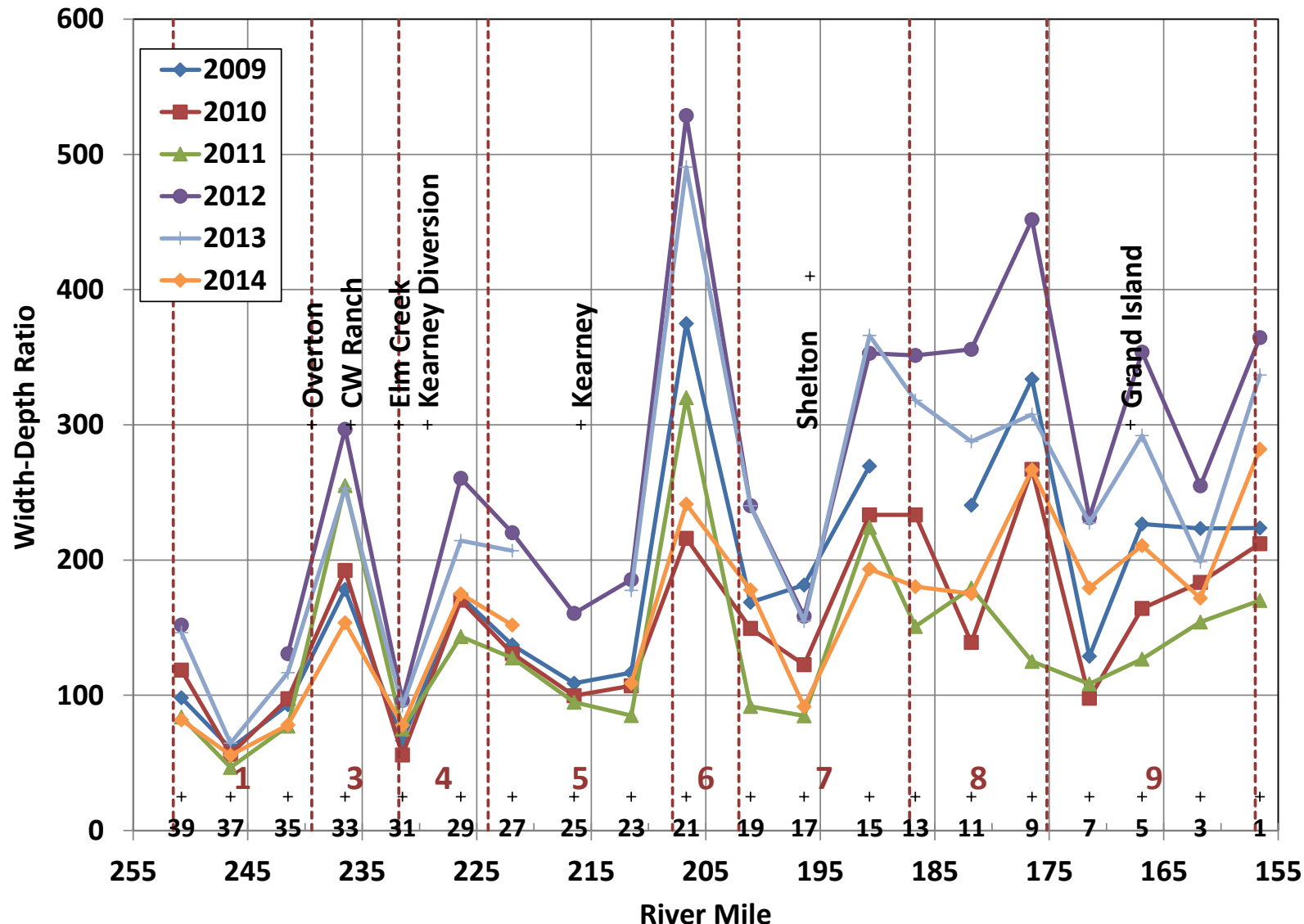


Figure 3.11a. Average width-to-depth (maximum depth) ratio at 1,200 cfs at pure panel APs from the 2009 through 2014 data.

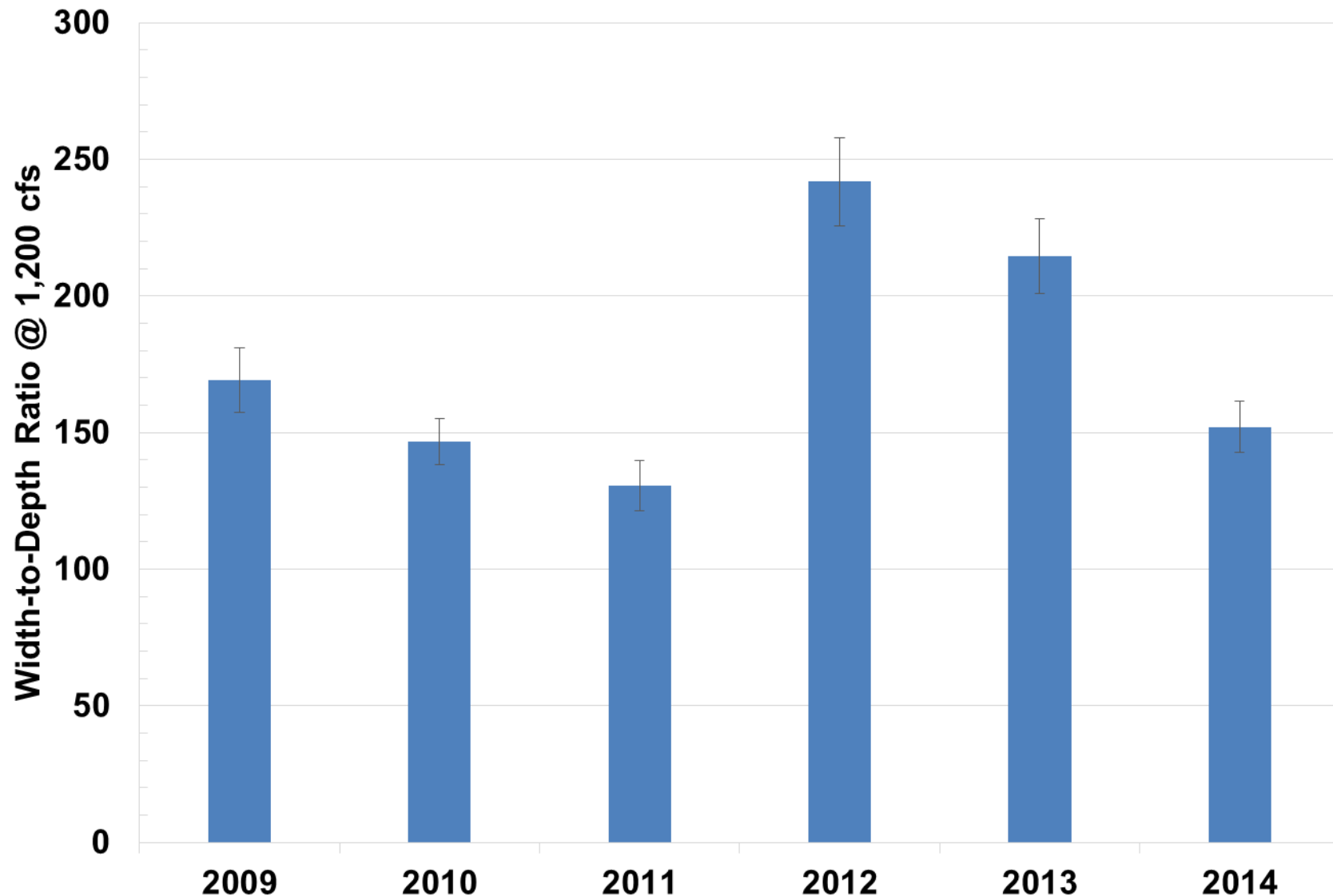


Figure 3.11b. Average width-to-depth (maximum depth) ratio at 1,200 cfs for the overall study reach, based on the pure panel AP data from 2009 through 2014.

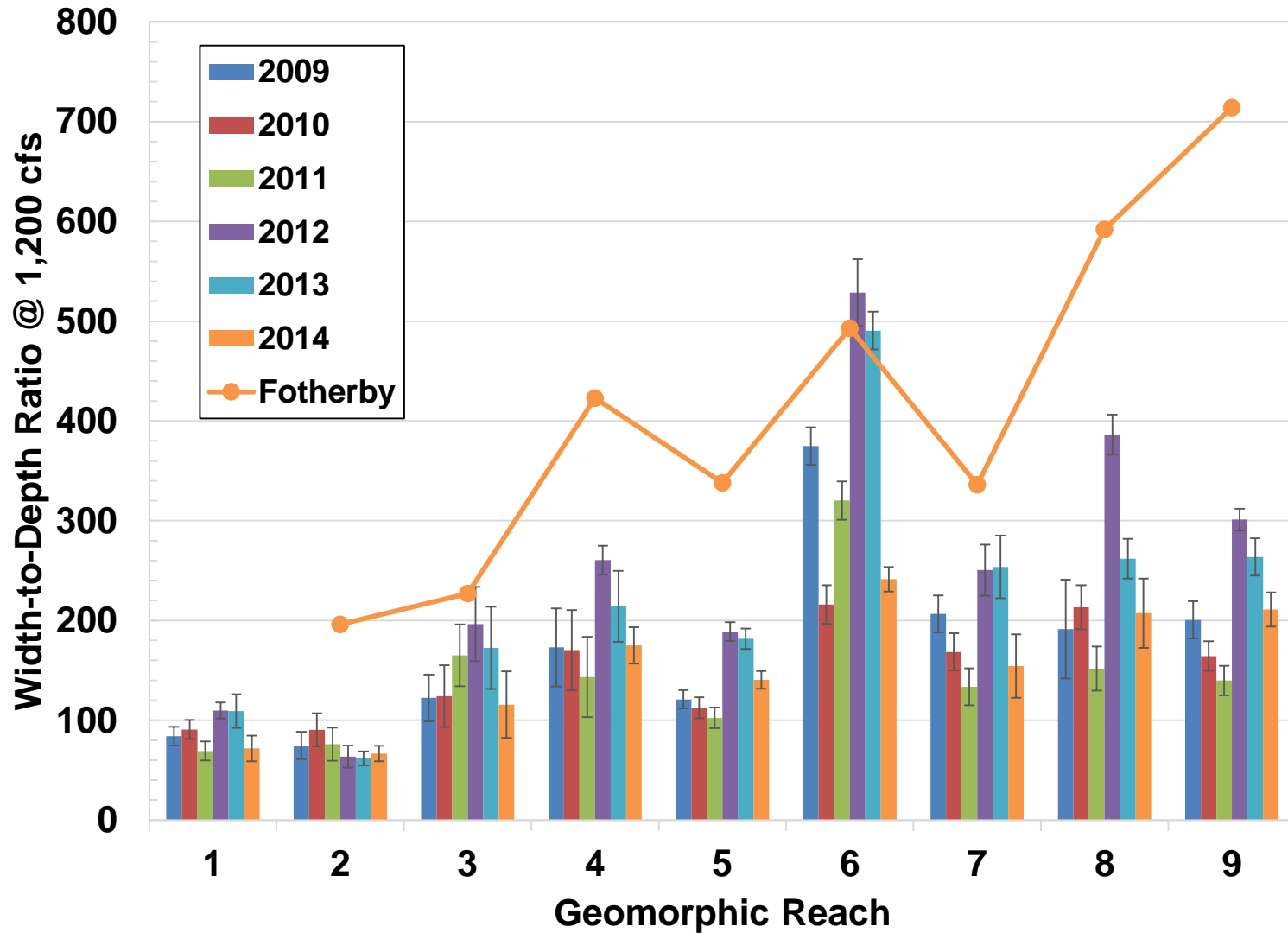


Figure 3.11c. Average width-to-depth (maximum depth) ratio at 1,200 cfs by geomorphic reach, based on the pure panel AP data from 2009 through 2014. Also shown are the width-to-depth ratios from Fotherby (2008).
Note: Fotherby (2008) did not report W/D for Reach 1.

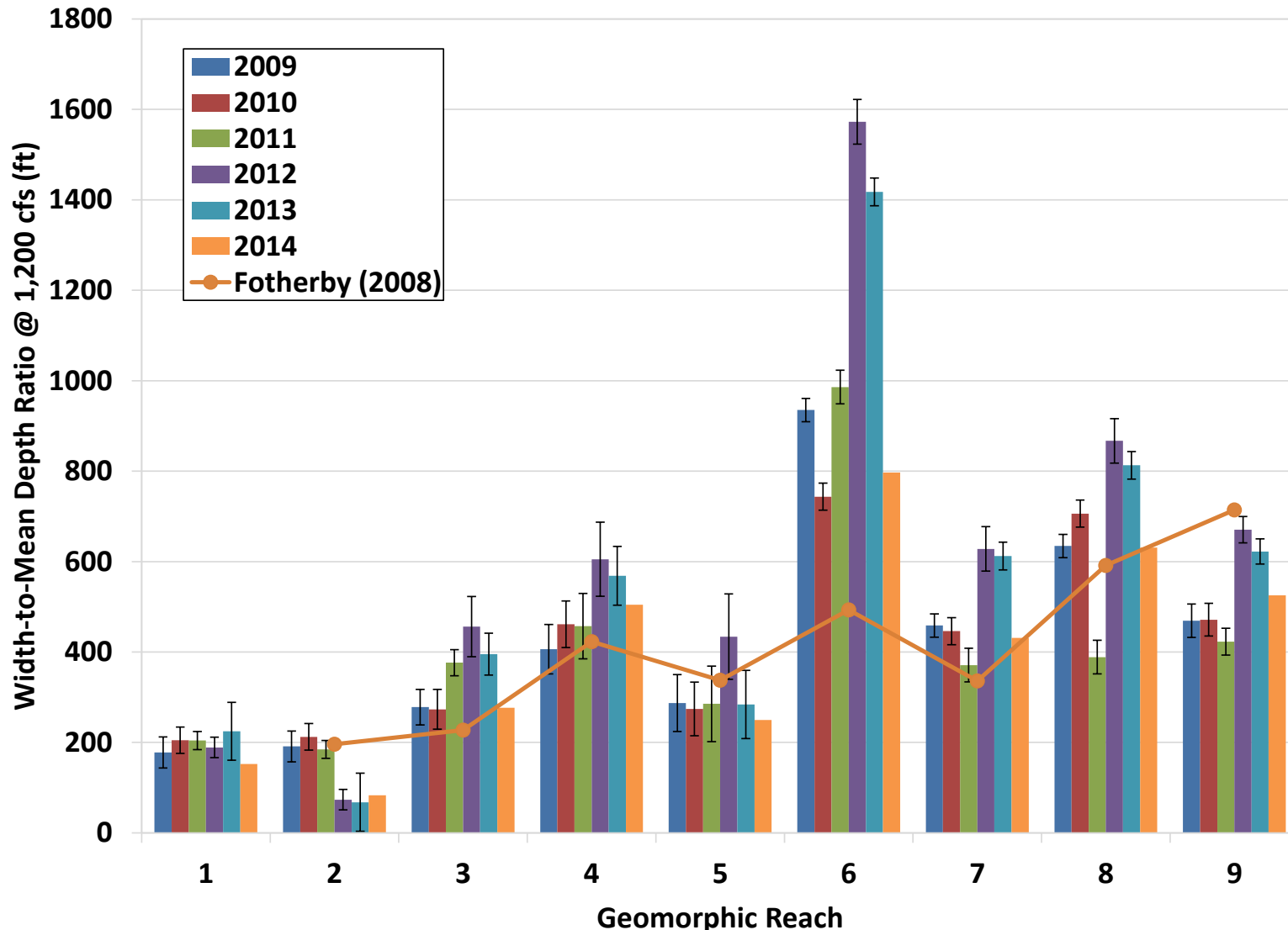


Figure 3.11d. Average width-to-mean depth ratio at 1,200 cfs by geomorphic reach, based on the pure panel AP data from the 2009 to 2013 data. Also shown are the width-to-depth ratios from Fotherby (2008).

Note: Fotherby (2008) does not report W/D for reach 1.

3.3.7 Channel Cross-sectional Area (DAP 5.3.6)

The cross-sectional area data at the individual APs indicates that the overall reach was generally degradational from AP19 upstream and in-balance to slightly aggradational downstream from AP19 between 2009 and 2010 (**Figure 3.12a through 3.12c**)⁷. Between the 2010 and 2011 surveys, most of the reach downstream from AP 37 was in-balance or slightly degradational. Significant aggradation occurred between the 2011 and 2012 surveys, primarily in the middle portion of the reach between Shelton and Kearney. Between the 2012 and 2013 surveys, the reach upstream from AP15 was approximately in balance, with AP15, AP19, AP21, and AP27 degrading and the other APs aggrading by a small amount. All APs downstream from AP 15 with the exception of AP1 aggraded during this period. Between 2013 and 2014, the overall reach was very nearly in balance. The changes in cross-sectional area represent changes in average bed elevation at the cross sections in the range of ± 0.5 feet (**Figure 3.12b**).

The overall aggradation/degradation quantities over the five-year monitoring period were estimated based on the assumption that the changes at the APs are representative of the changes in the intervening reaches of the river. The 2009 to 2010 changes at AP33 were excluded from the analysis because this calculation is intended to provide information about the overall sediment-transport balance in the reach, and the changes at AP33 result from mechanical grading rather than differences in sediment-transport rates. Not considering the changes at AP33, the overall study reach degraded by about 2.4M tons between 2009 and 2010 and an additional 1.2M tons between 2010 and 2011 (Figure 3.12c). The reach then aggraded by about 5.6M tons between 2011 and 2012, and an additional approximately 1.6M tons between 2012 and 2013. From 2013 to 2014, the reach degraded by about 0.5M tons; thus, the overall reach experienced net aggradation of about 3.1M tons over the five years encompassed by the surveys.

On a geomorphic reach basis, the bulk of the degradation volume between 2009 and 2010 occurred in Reaches 4, 5, and 6 (from Elm Creek to Gibbon), with substantial degradation also occurring in Reaches 1 and 2 (Lexington to Overton, including the J-2 return (**Figure 3.12d**)). Modest aggradation occurred during this period in Reaches 7, 8 and 9 (downstream from Gibbon). Reach 1 aggraded during all three years from 2010 through 2013, and then experienced about 80,000 tons of degradation between 2013 and 2014, resulting in net aggradation of about 540,000 tons (or about 107,000 tpy) over the five year monitoring period. The changes in Reach 2 (South Channel at Jeffreys Island) are represented by AP35. This reach appears to have been slightly degradational in all years since 2009, except for 2012 to 2013, with net degradation of 340,000 tons (or about 70,000 tpy) during the survey period. The small amount of aggradation during 2012 to 2013 is probably associated with a slight backwater condition caused by the sand pile that was created by the pilot sediment augmentation project just downstream. Reach 3 (Overton to Elm Creek Bridge) was essentially in balance between the 2009 and 2010 surveys, degraded from 2010 to 2011 and 2012 to 2013, and aggraded from 2011 to 2012 and 2013 to 2014. This resulted in net degradation of about 90,000 tons (or about 18,000 tpy) over the period. After degrading by about 400,000 tons during the first year, Reach 4 was aggradational in the subsequent three years, and degradational during the final survey year, resulting in a net gain of nearly 550,000 tons (about 109,000 tpy) since 2009.

⁷Note that the indicated degradation at AP33 between the 2009 and 2010 surveys resulted from mechanical removal of a large, vegetated mid-channel bar; the loss of sediment volume does not reflect a general sediment imbalance in the reach (**Figure 3.13a**). The most upstream cross section at AP33 also widened by about 135 feet during this period between 2009 and 2011 (**Figure 3.13b**), due primarily to deflection of the flow around the graded material and into the banks. The material from the bar was graded directly into the channel where most, if not all, was entrained and carried downstream.

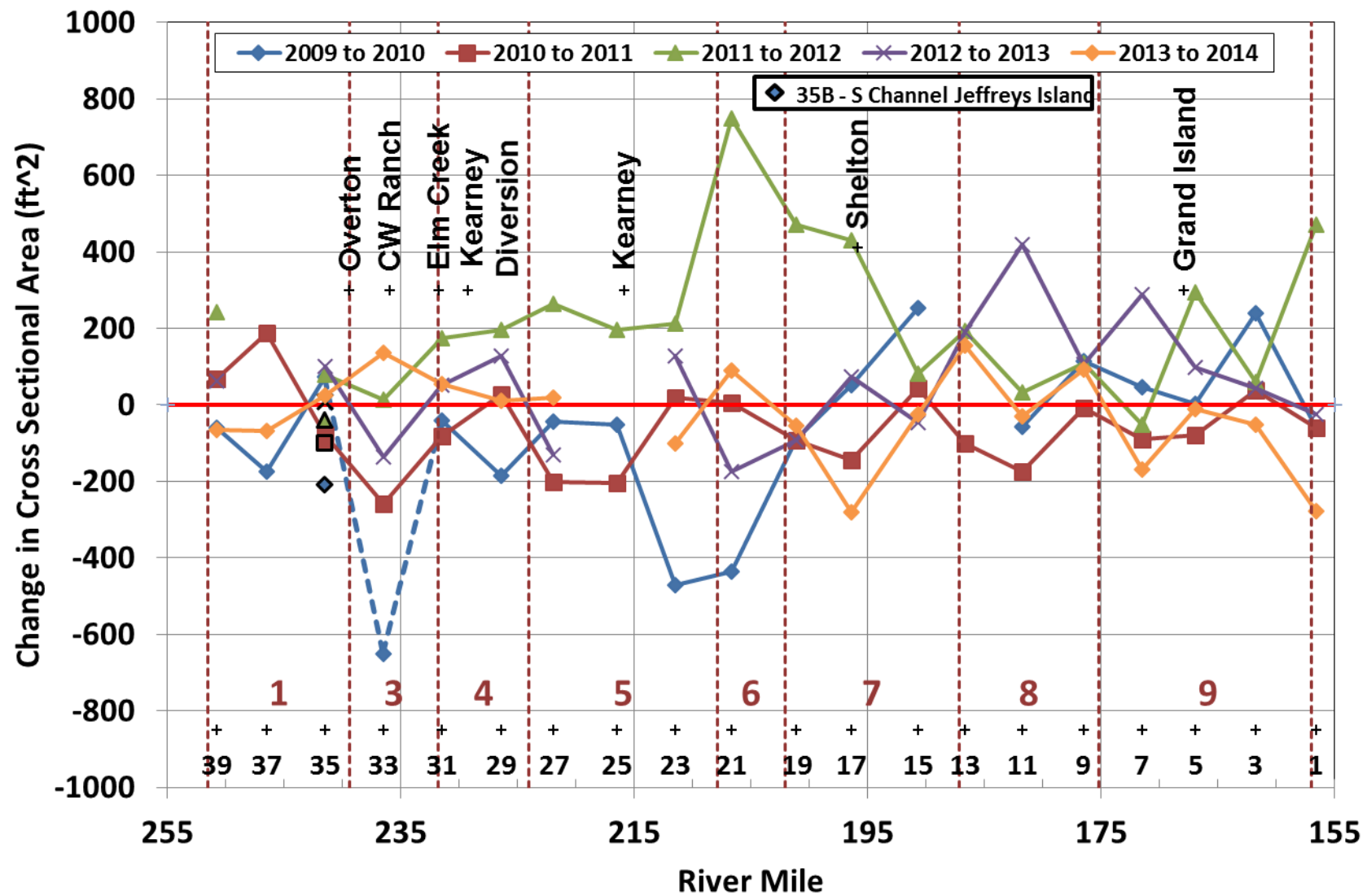


Figure 3.12a. Year-to-year change in average cross-sectional area at pure panel APs from 2009 through 2014. Line connecting AP33 on the 2009 to 2010 series is dashed to show effect of mechanical bar removal. [Aggradation (+), Degradation (-)]

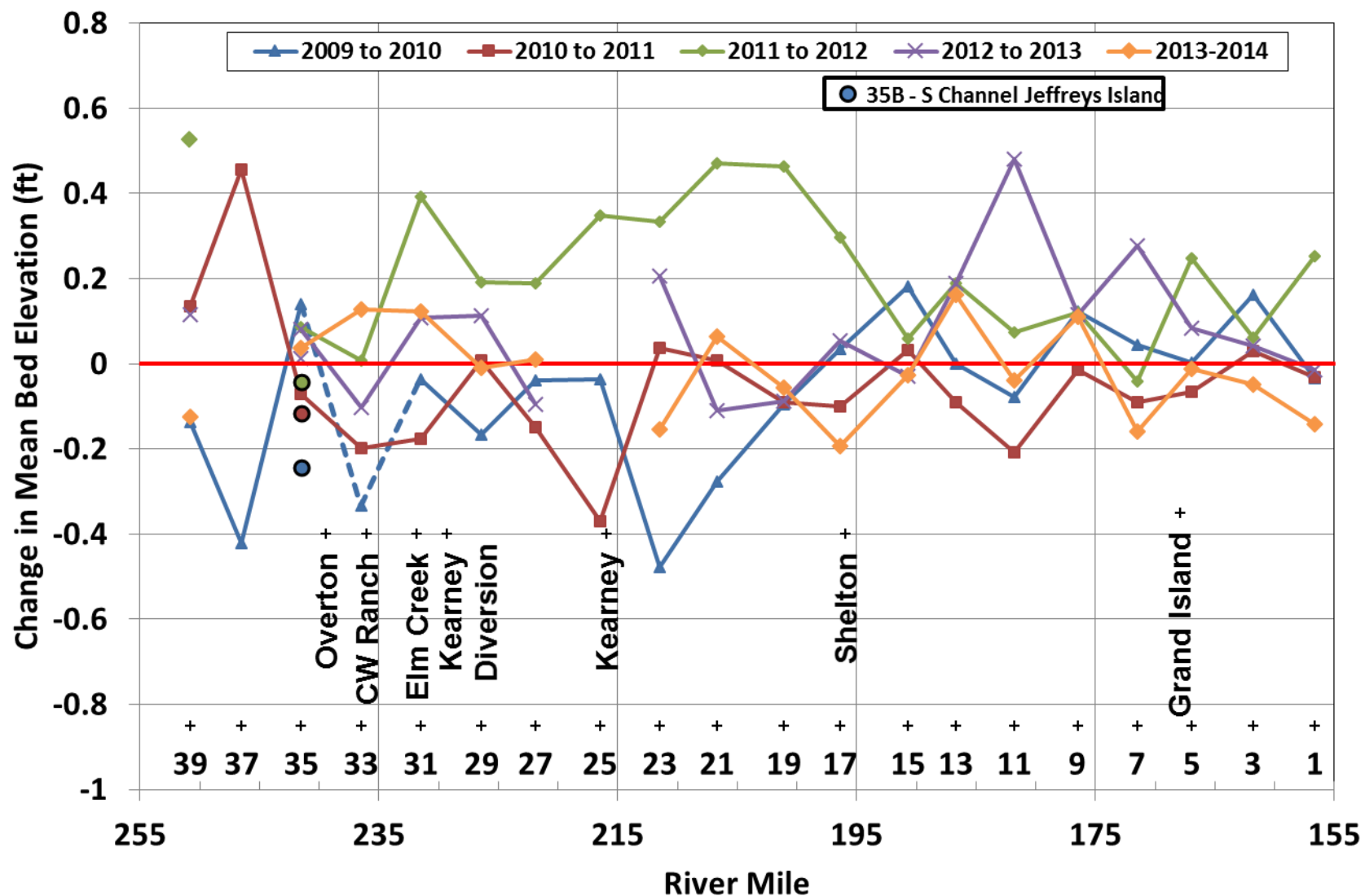


Figure 3.12b. Year-to-year change in mean bed elevation at the pure panel APs from 2009 through 2014. Line connecting AP33 on the 2009 to 2010 series is dashed to show effect of mechanical bar removal. [Aggradation (+), Degradation (-)]

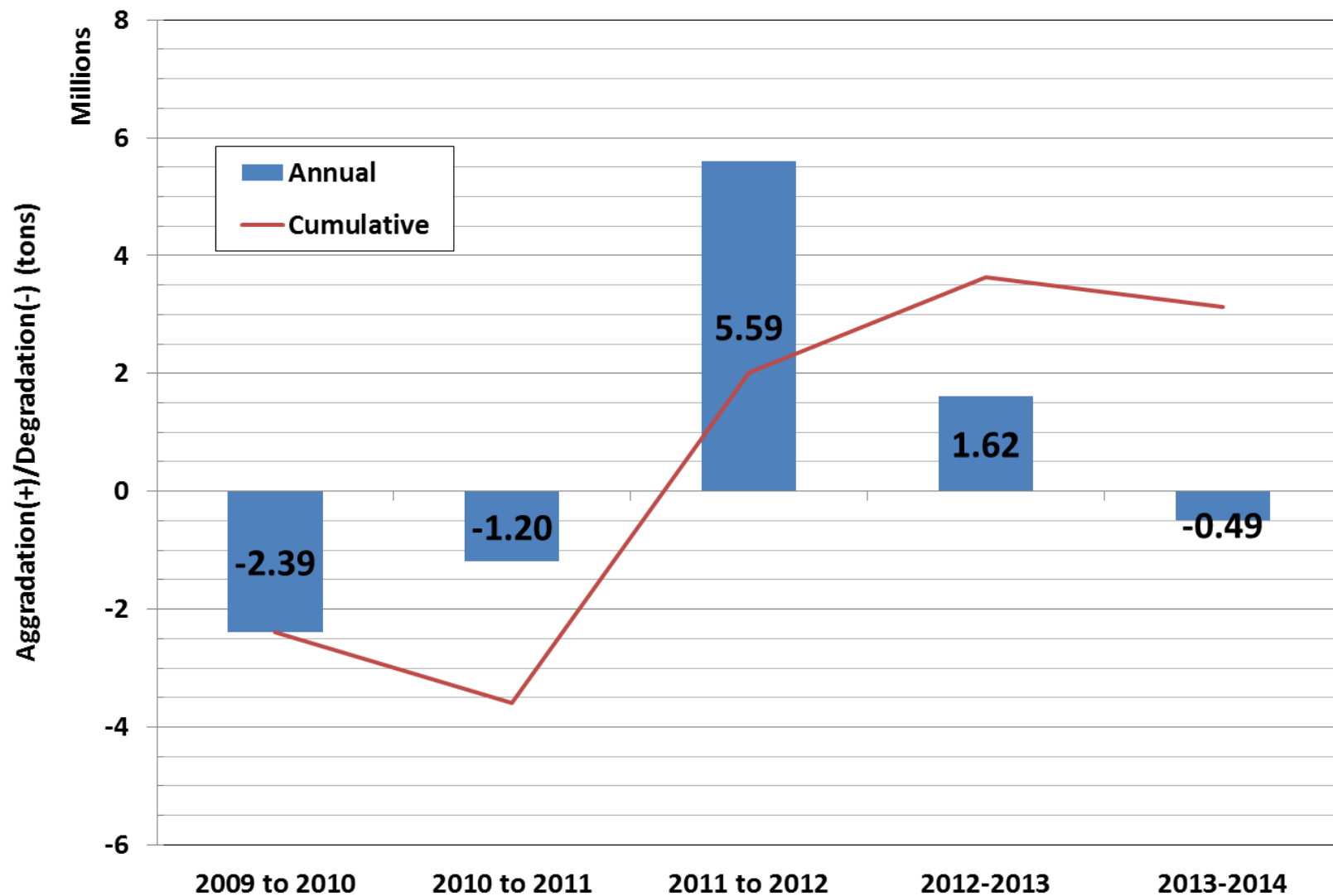


Figure 3.12c. Year-to-year aggradation/degradation volumes in the overall study reach from 2009 through 2014. Quantity for 2009 to 2010 does not include changes at AP33 due to mechanical removal of a large mid-channel bar.

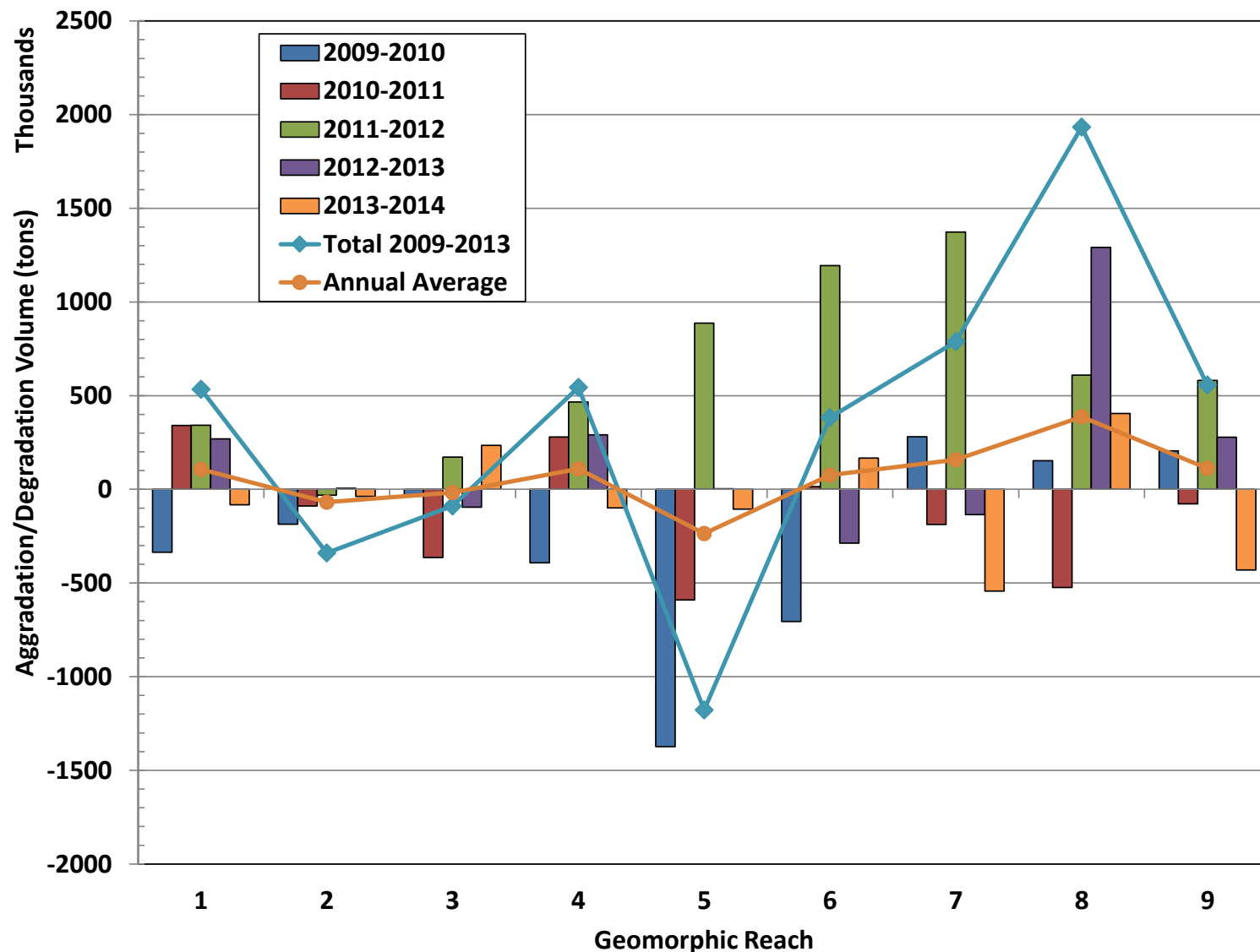


Figure 3.12d. Year-to-year aggradation/degradation volumes in the overall study reach from 2009 through 2014. Quantity for Reach 3 during 2009 to 2010 does not include changes at AP33 due to mechanical removal of a large mid-channel bar.

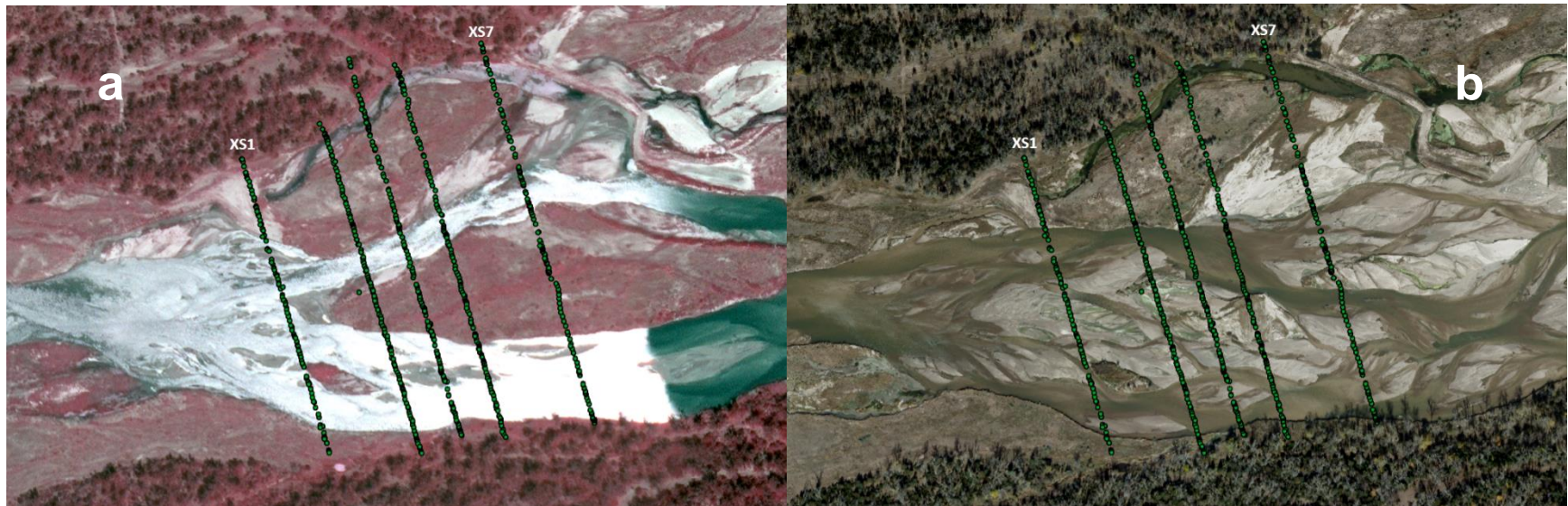


Figure 3.13a. Aerial photographs showing the locations of the surveyed cross sections at AP33: (a) July 2009 (Discharge~310 cfs), (b) October 2010 (Discharge~720 cfs).

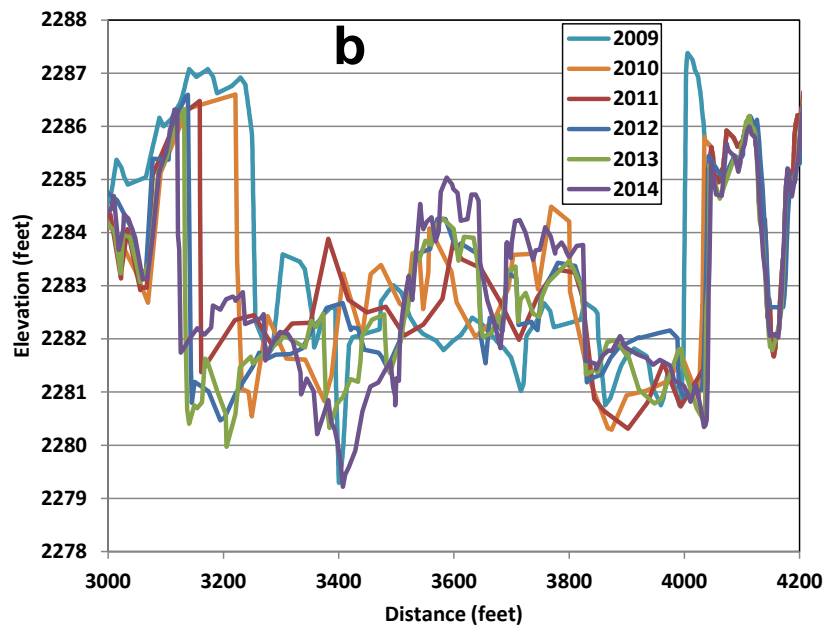
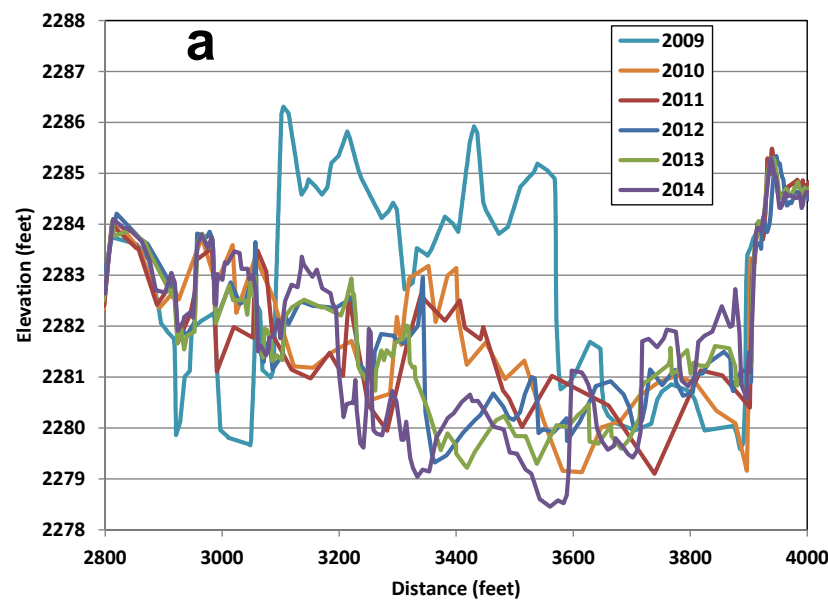


Figure 3.13b. Surveyed cross section profiles at AP33 (a) Downstream (XS7), (b) Upstream (XS1).

Reaches 5 and 6 (Odessa to Mindon and Minden to Gibbon, respectively) both degraded between 2009 and 2010, and Reach 5 continued to degrade while Reach 6 was approximately in balance between 2010 and 2011. Both reaches aggraded significantly from 2011 to 2012. The changes during 2012 through 2014 were less significant than the earlier years. Over the 5 year period of the surveys, Reach 5 degraded by a total of 1.2M tons (or about 240,000 tpy) and Reach 6 aggraded by about 380,000 tons (or about 80,000 tpy). Reaches 7 through 9 (Gibbon to Wood River, Wood River to Grand Island, and Grand Island to Chapman, respectively) were all net aggradational over the 5-year period, with about 790,000 tons (~160,000 tpy) of aggradation in Reach 7, 1.9M tons (~390,000 tpy) in Reach 8 and 560,000 tons (~110,000 tpy) in Reach 9.

3.4 Vegetation

The vegetation monitoring surveys have produced large datasets (**Table 3.1**) that provide the basis for a broad range of analyses. In 2009, a total of 4,496 quadrats were sampled along 308 individual transects at 27⁸ APs (from 41 independent survey sites including primary and secondary channels at most APs); with 3,119 quadrats and 154 transects from pure panel APs. Only species of inquiry for that year were quantified; totaling 26 individual species. In 2010, 5,469 quadrats (approximately 1,000 more than in 2009) were sampled at 26 APs and 29 independent sites, along 210 transects. Unlike 2009, all specimens encountered in quadrats were documented, totaling 125 separate species, and this protocol was followed in subsequent years. In 2011, 5,447 quadrats (4,342 at pure panel APs) and 102 separate species were documented. The 2012 survey totaled 4,401 quadrats (2,987 at pure panel APs) and 125 species at 25 APs and 27 total survey sites. In 2013, secondary channels were surveyed for the second time (2009 being the first), and the monitoring protocol was modified to surveying only 5 transects per AP. That year, a total of 3,174 quadrats at 41 independent sites, located along 220 transects were sampled, and 179 species were identified; a third of which (64) were encountered no more than twice. In 2014, a total of 2,978 quadrats at 28 independent sites, located along 140 transects were sampled, and 149 species were identified; of which less than a third (31) were encountered no more than twice.

Table 3.1. Summary of vegetation survey sites (2009-2014).

Year	Anchor Points	Sites	No. of Transects		No. of Quadrats		No. of Individual Species
			Pure Panel	Total	Pure Panel	Total	
2009 [†]	27	41	154	308	3,119	4,496	26
2010	26	29	154	210	4,210	5,469	125
2011	27	29	147	189	4,342	5,447	102
2012	25	27	140	189	2,987	4,401	125
2013 ^{†‡}	25	41	105	220	2,157	3,174	179
2014 [‡]	24	28	120	140	2,259	2,978	149

[†] Includes Secondary channels surveyed once every four years

[‡] Only 5 transects sampled at each AP

⁸ APs 35A, 36B and 37A are in the North Channel at Jeffreys Island and 35B, 36A and 37B are in the South Channel. All 6 of these sites are considered to be primary APs for purposes of the analysis because the flows are derived from different sources (upstream main channel for the former; J-2 Return for the latter) and because they represent different geomorphic reaches.

3.4.1 Green Line Elevation (GLE) (DAP 5.4.1)

The green line elevations (GLEs) varied by an average of about 2 feet throughout the 6 years of survey data, with the highest elevations recorded during 2011 when long-duration, high flows were present in the reach and the lowest elevations occurring during the very low-flow conditions in 2013 (Table 3.2; Figure 3.14a). In 2010, the GLEs averaged about 1.0 feet higher than in 2009, increasing to an average of about 1.9 feet higher in 2011, and then decreasing back to only about 0.3 feet higher, on average, in 2012. In 2013, the GLE averaged about 0.2 feet lower than in 2009, and the 2014 GLEs averaged approximately 0.9 feet higher than in 2009 (Figure 3.14b). As expected from the AP averages and the overall monitoring reach averages, the averages for the geomorphic reaches were also relatively consistent within each of the years, particularly in 2010, 2011, and 2014 when the high flows shifted the greenline vertically throughout the entire reach (Figure 3.14c).

During 2009, 2010 and 2011, the GLEs were consistently in the range of 1 to 2 feet below the water surface associated with the maximum preceding discharge (Q_p ; DAP 5.1.1) (Figure 3.15), with generally greater differences upstream from the Kearney Diversion and downstream from Grand Island. During the low-flow years in 2012 and 2013, the GLE tended to be above the preceding maximum water-surface elevation. The 2014 data exhibits a similar trend to the first three years of data, but with a somewhat greater difference at most APs (typically 2 feet to 4 feet upstream from the KDS and 1 foot to 2 feet downstream from the KDS).

With some notable exceptions, differences in GLE from the initial survey in 2009 during each of the subsequent years were relatively consistent throughout the reach (Figure 3.14a), suggesting that the GLE is responsive to the hydrologic conditions in any particular year. The data also suggests that the GLE is responsive to the relative change in stage associated with the preceding flows that is a function of both the discharge and the hydraulic geometry relationship at the cross sections, especially during high-flow years. Three different measures of the preceding discharge were considered in quantifying these observations: (1) preceding maximum discharge (Q_p ; DAP 5.1.1), (2) germination season discharge (Q_{GER} ; DAP 5.1.2), and (3) maximum discharge during the germination season. Spearman correlation analysis shows that the correlation between change in GLE from 2009 and the difference in maximum preceding stage from 2009 is significant for the two highest-flow years (2010 and 2011), but not significant for the other years (Figure 3.16a). Linear regression on the two metrics produces a similar result, with 2010 and 2011 exhibiting the highest R^2 values. Correlation between the change in mean germination season stage and change in GLE is statistically significant for all years except for 2012 (Figures 3.16b and 3.16c). Once again, linear regression shows a similar result; the R^2 value for 2012 is considerably lower than the values for the other four datasets. Correlation between maximum germination season discharge and change in GLE from 2009 reveals a similar result, except the 2014 correlation is no longer statistically significant. When only the difference in discharge is used rather than the difference in stage, the correlations are considerably lower, verifying the importance of the hydraulic geometry relationships (i.e., narrower cross sections at which the stage changes more rapidly with discharge tend to have larger differences in GLE during the high-flow years than those with relatively flat stage-discharge rating curves).

Table 3.2. Average green line elevations at pure panel APs observed during the six monitoring surveys.

Anchor Point	River Mile	Green line Elevation (ft)					
		2009	2010	2011	2012	2013	2014
39	250.8	2372.6	2374.5	2375.1	2373.6	2373.5	2373.9
37	246.5	2347.5	2348.5	2349.2	†	2347.2	2347.9
35	241.5	2315.1	2316.6	2317.7	2315.5	2314.4	2315.9
33	236.5	2281.8	2282.8	2283.2	2282.4	2281.1	2282.5
31	231.5	2249.5	2250.6	2251.4	2249.6	2249.3	2250.1
29	226.4	2215.2	2216.2	2217.1	2215.9	2214.8	2216.2
27	221.9	2184.3	2185.8	2186.5	2184.5	2184.1	2185.5
25	216.5	2148.4	2149.7	2150.3	2148.3	†	†
23	211.5	2114.0	2115.0	2115.9	2114.1	2114.2	2115.4
21	206.7	2083.7	2085.6	2084.2	2083.9	2083.6	2084.3
19	201.1	2047.3	2048.2	2048.9	2047.5	2047.3	2048.6
17	196.4	2016.0	2017.1	2018.2	2016.1	2015.8	2017.2
15	190.7	1978.1	1979.2	1980.2	1978.1	1978.2	1979.5
13	186.7	†	1953.8	1954.5	1952.4	1952.7	†
11	181.8	1921.8	1922.8	1923.3	1921.6	1921.9	1922.1
9	176.5	1888.9	1889.7	1890.0	1889.5	1888.6	1889.6
7	171.5	1856.6	1857.5	1858.3	1856.6	1855.8	1856.9
5	166.9	1828.3	1829.0	1829.8	1827.9	1827.8	1828.6
3	161.8	1792.1	1793.1	1793.6	1792.0	1791.1	1792.6
1	156.6	1762.0	1762.7	1763.5	1761.7	1761.3	1762.4

†No data collected at this AP for the indicated year.

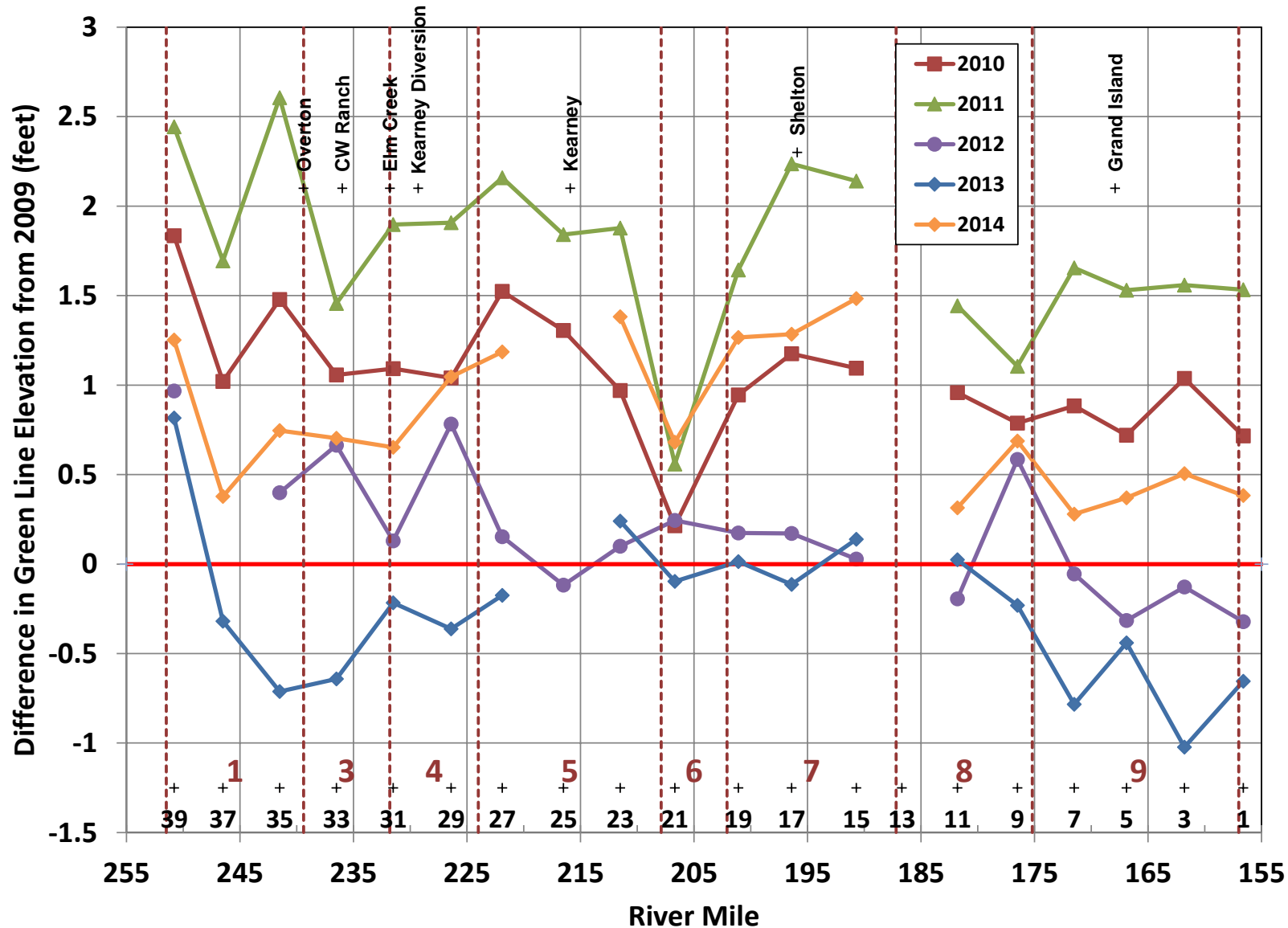


Figure 3.14a. Difference between average GLE at pure panel APs in 2010 through 2014 from the initial survey in 2009.

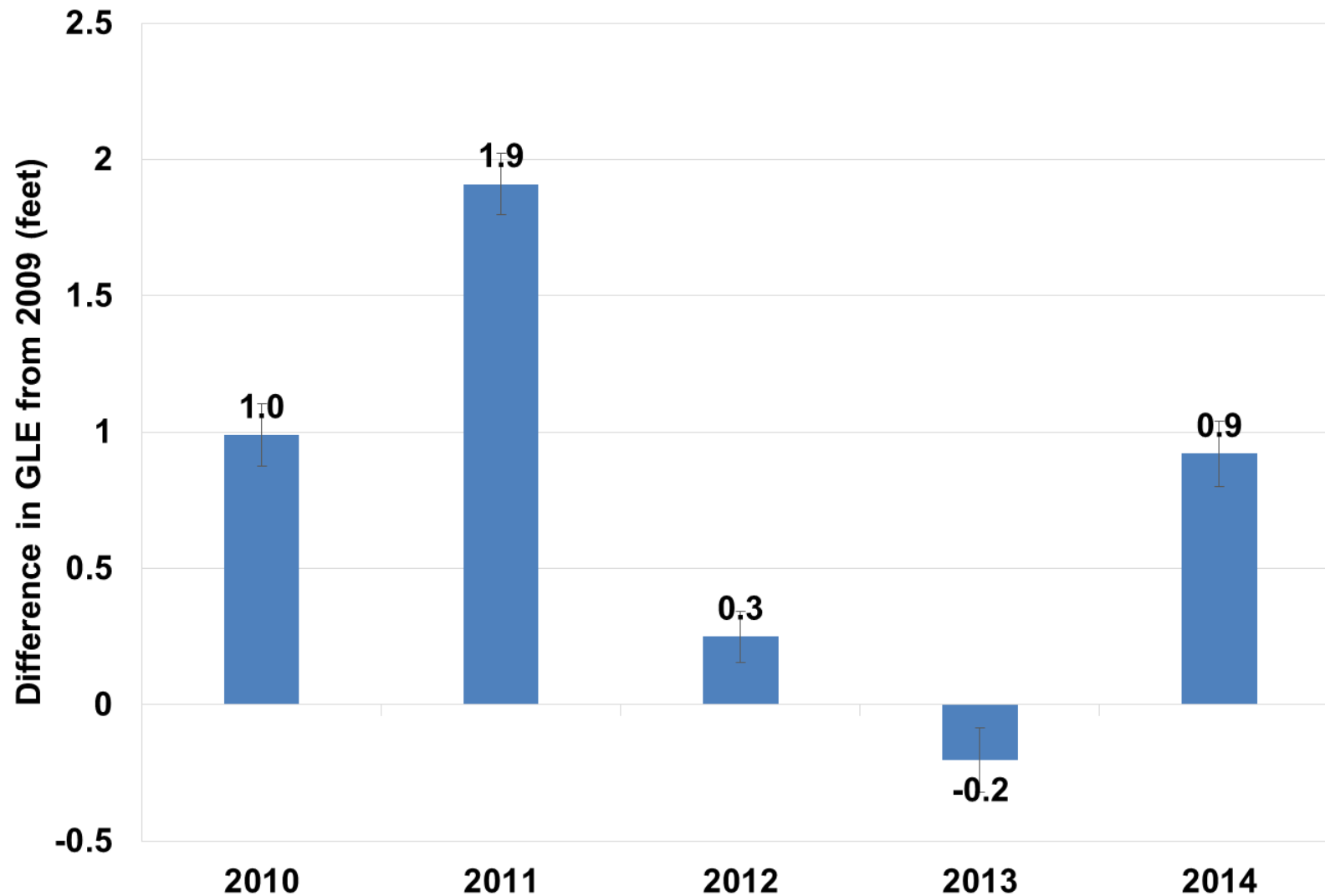


Figure 3.14b. Reach-wide average difference in GLE at Pure Panel APs from the 2009 GLE.

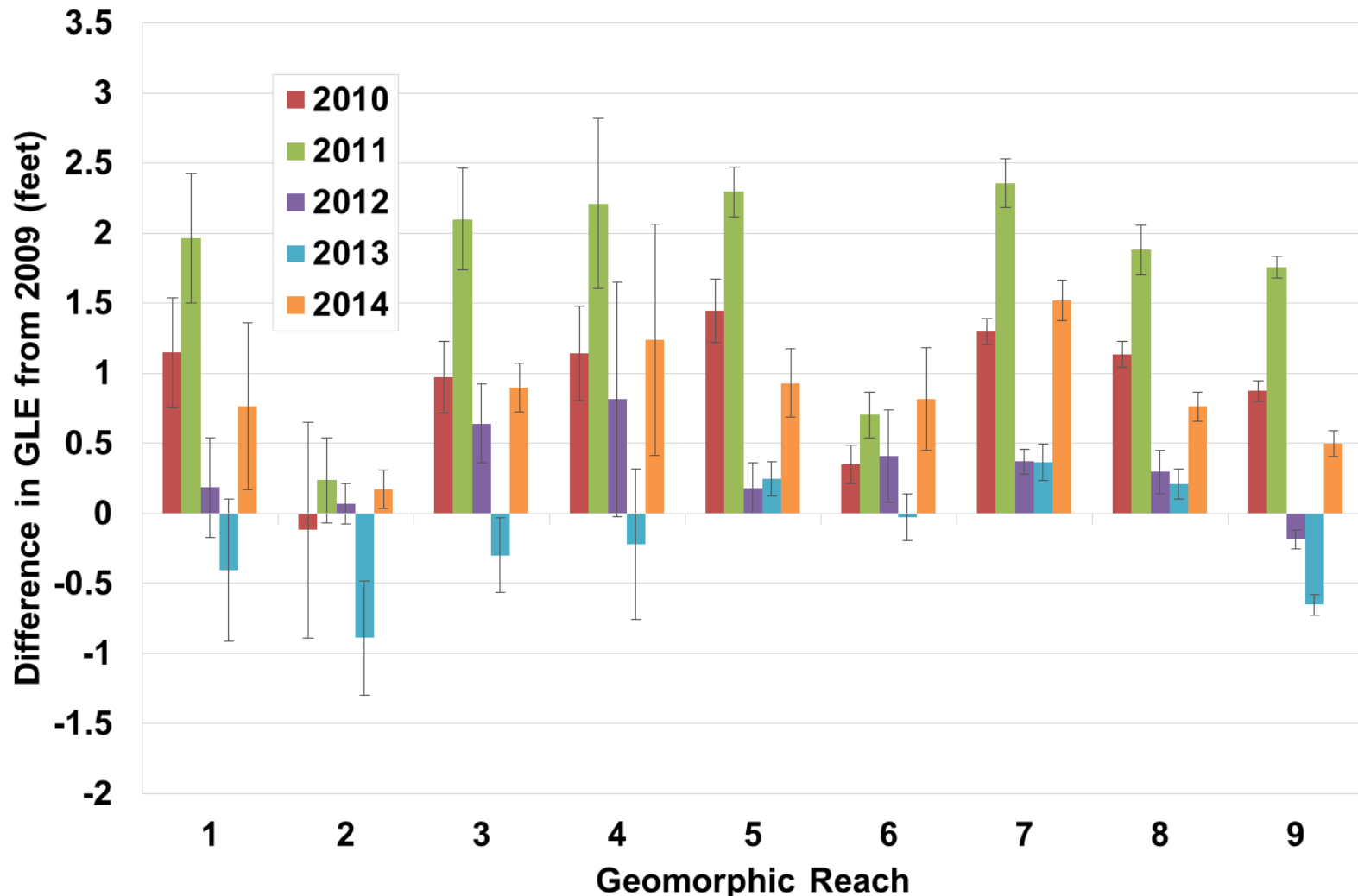


Figure 3.14c. Average change in GLE from the 2009 survey, by geomorphic reach.

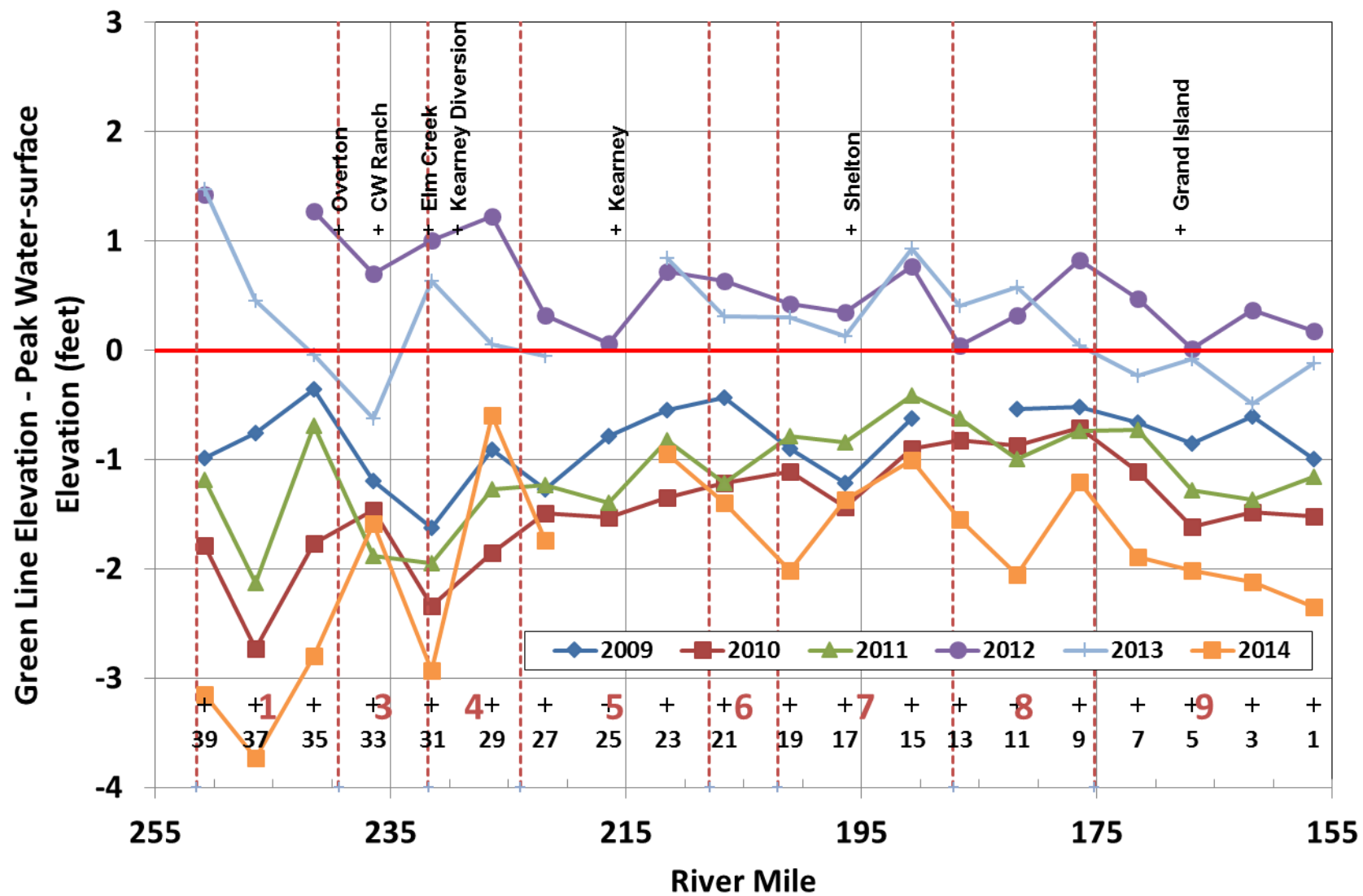


Figure 3.15. Average difference between GLE and water-surface elevation associated with the maximum preceding discharge (Q_P) at pure panel APs from 2009 through 2014.

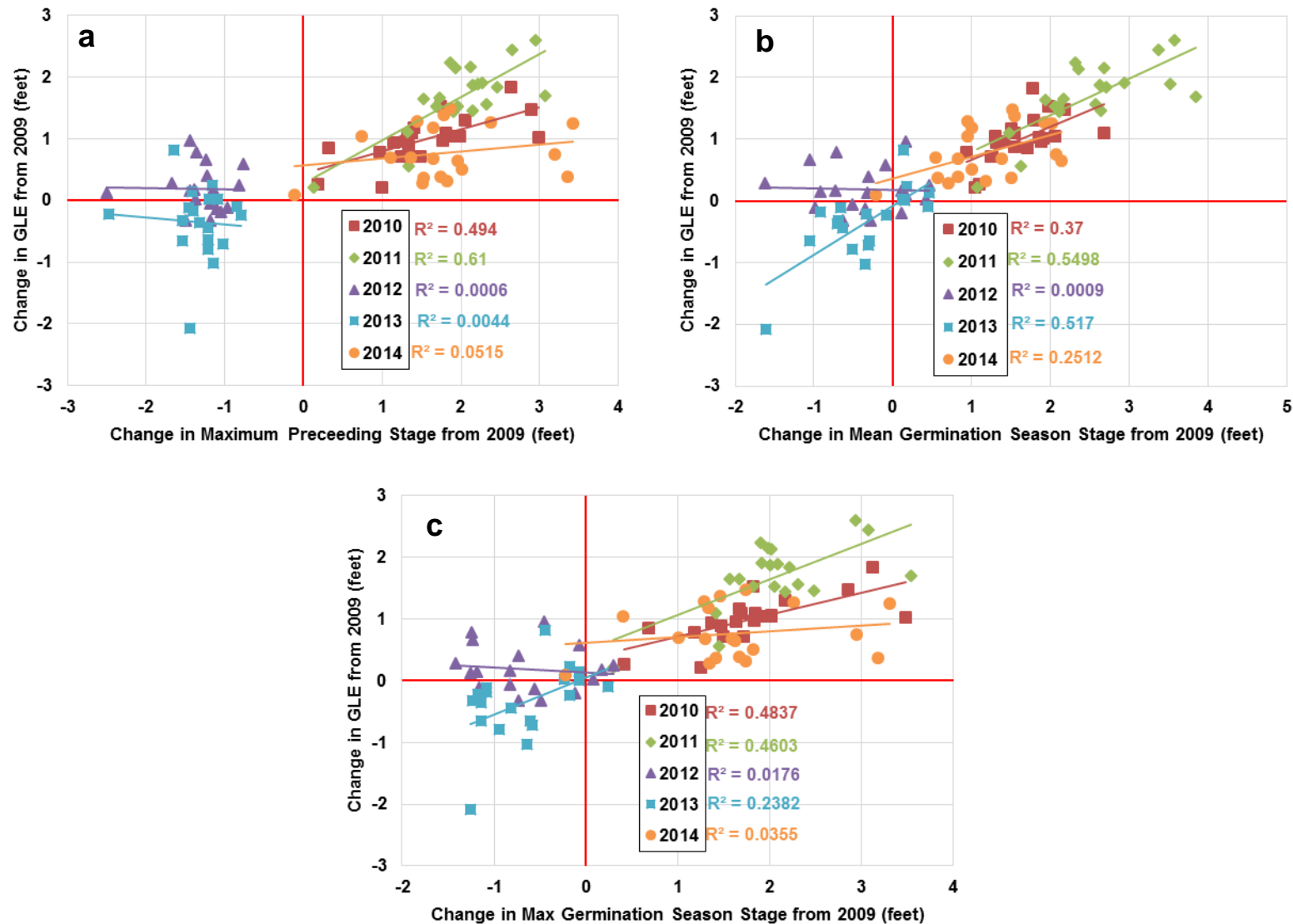


Figure 3.16. Change in water-surface elevation from 2009 versus change in GLE from 2009: (a) preceding maximum discharge (Q_p ; DAP 5.1.1), (b) germination season discharge (Q_{GER} ; DAP 5.1.2), (c) maximum discharge during germination season.

3.4.2 Total Unvegetated Channel Width (DAP 5.4.2)

The draft DAP defines unvegetated channel width (W_{Unveg}) as the *maximum width between vegetation within the channel and/or the channel banks*, and specifies that it is to be quantified by calculating *the distance between each pair of GLE points that bound the unvegetated channel segment*. After evaluating the first four years of data, it was determined that the total unvegetated width (sum of all unvegetated lengths across each transect) would better represent the original intent of this metric. The widths were determined by overlaying the surveyed GLE points over the applicable aerial photography and physically measuring the unvegetated distance between pairs of points using GIS software. This resulted in a shapefile and summary table with georeferenced points that define the ends of each unvegetated segment and the associated widths. For a variety of reasons, a suitable GLE point was not measured on one side of the unvegetated zone in every location. These reasons included the presence of rock or other bank protection or a raw vertical bank where vegetation could not establish at an elevation comparable to the other GLE points at the site. In these cases, the aerial photography, adjacent survey data, and in some cases, ground photographs were used to identify an appropriate location for the missing GLE points. The measurements for the 2009, 2010 and 2011 data were initially made by Program staff, and Tetra Tech staff made the measurements for the 2012 through 2014 data. Tetra Tech also checked the 2009, 2010, and 2011 measurements to insure consistency with the approach used for the later data.

The resulting measurements indicate that the unvegetated width varied considerably throughout the reach and from year-to-year. The narrowest unvegetated widths typically occurred at AP7, AP23, AP31 and AP35 through AP39, and the widest occurred at AP15, AP21 (Rowe Sanctuary), AP29 and AP33 (Cottonwood Ranch) (**Figure 3.17a**). The reach-wide average unvegetated width for the Pure Panel APs increased from about 430 feet in 2009 to 630 feet in 2011 (**Figure 3.17b**). The average width decreased substantially between 2011 and 2013 to only 300 feet, due to vegetation encroachment during these low-flow years. The 2014 widths increased to more than 520 feet due to the higher flows during the early summer. Geomorphic Reach 6 had the widest average width during all six years, followed by Reaches 4, 7, and 9 (**Figure 3.17c**). The year-to-year variability within the geomorphic reaches is similar to the reach-wide average.

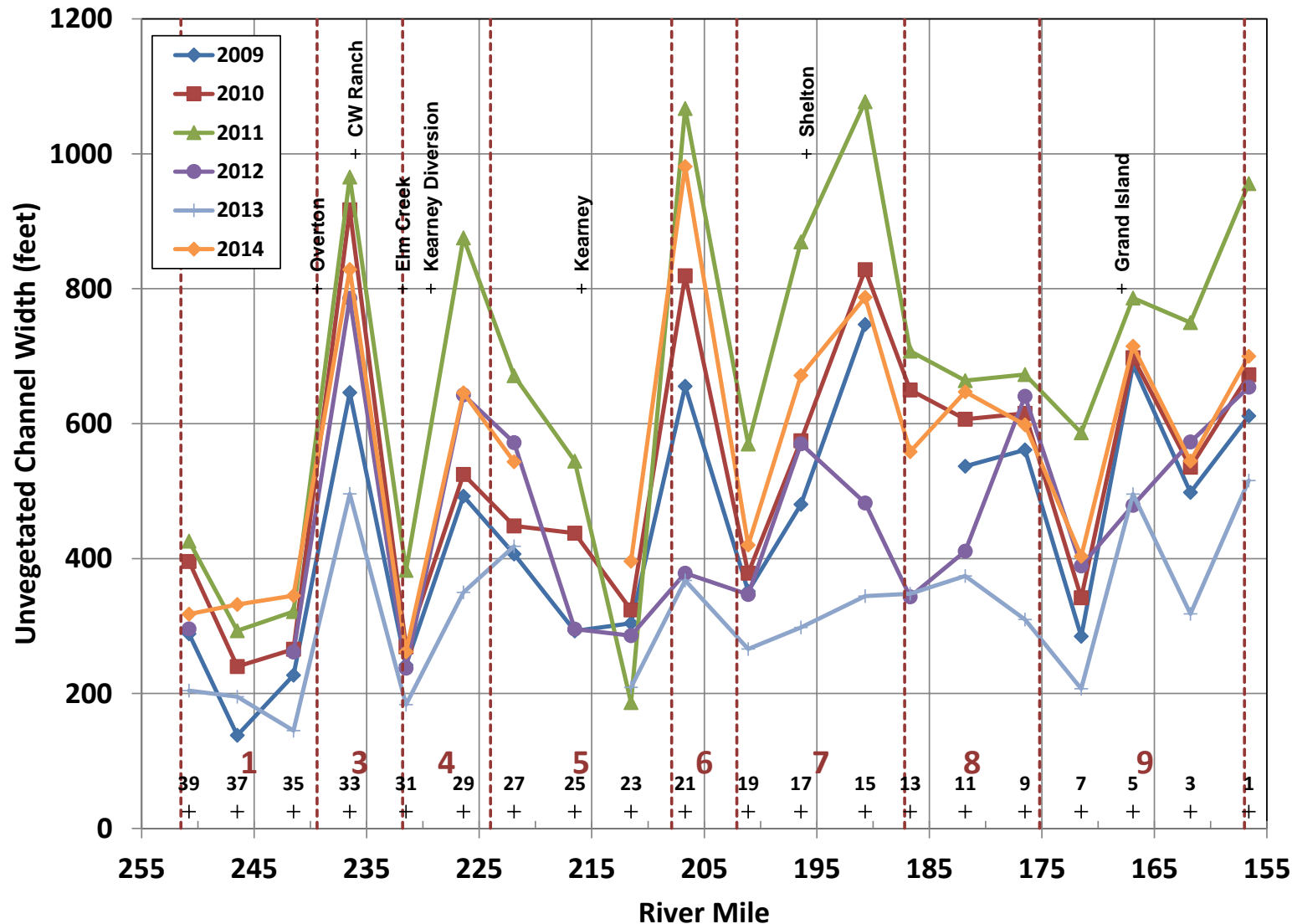


Figure 3.17a. Average unvegetated channel width at Pure Panel APs from 2009 through 2014.

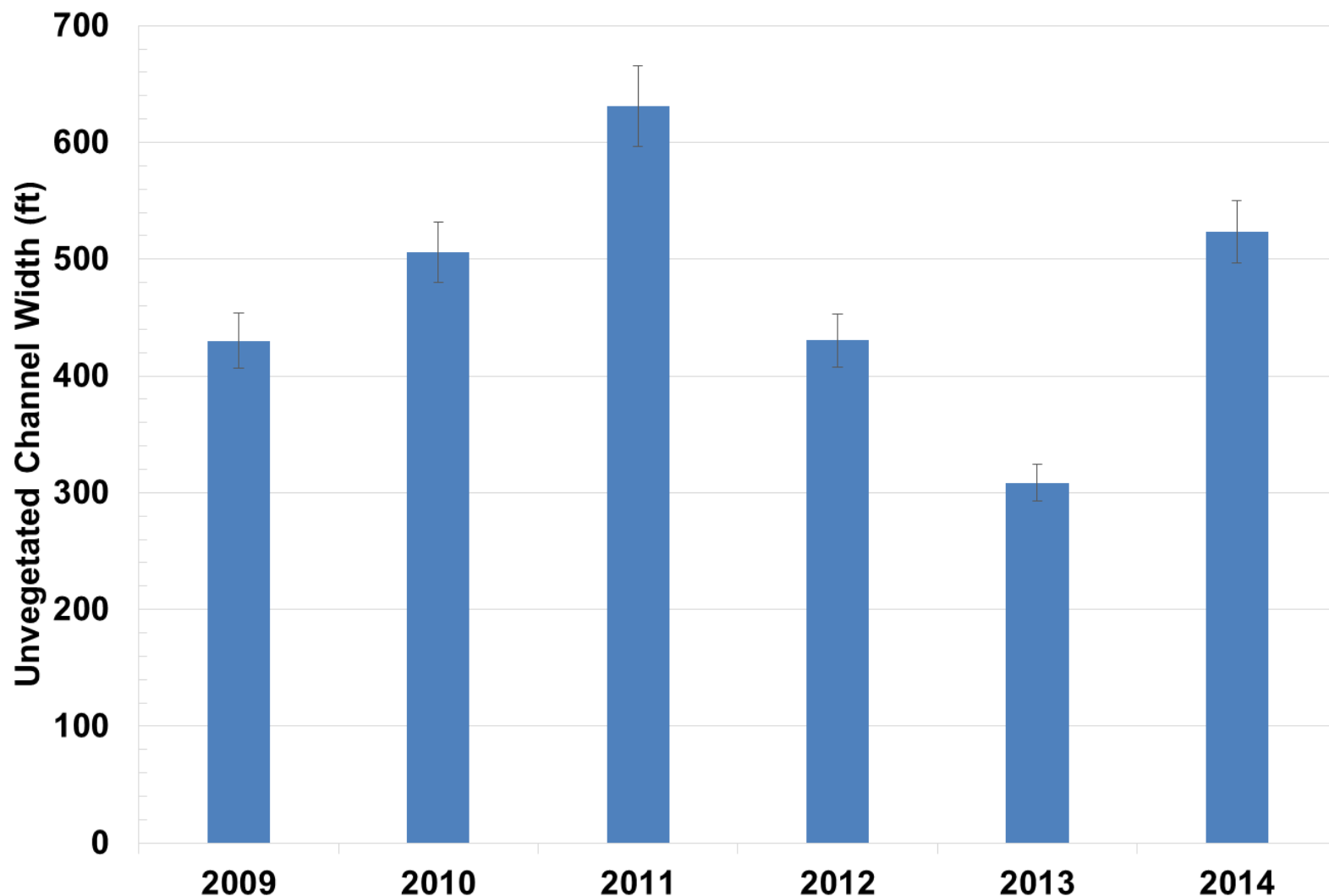


Figure 3.17b. Reach-wide average unvegetated channel width at pure panel APs from 2009 through 2014.

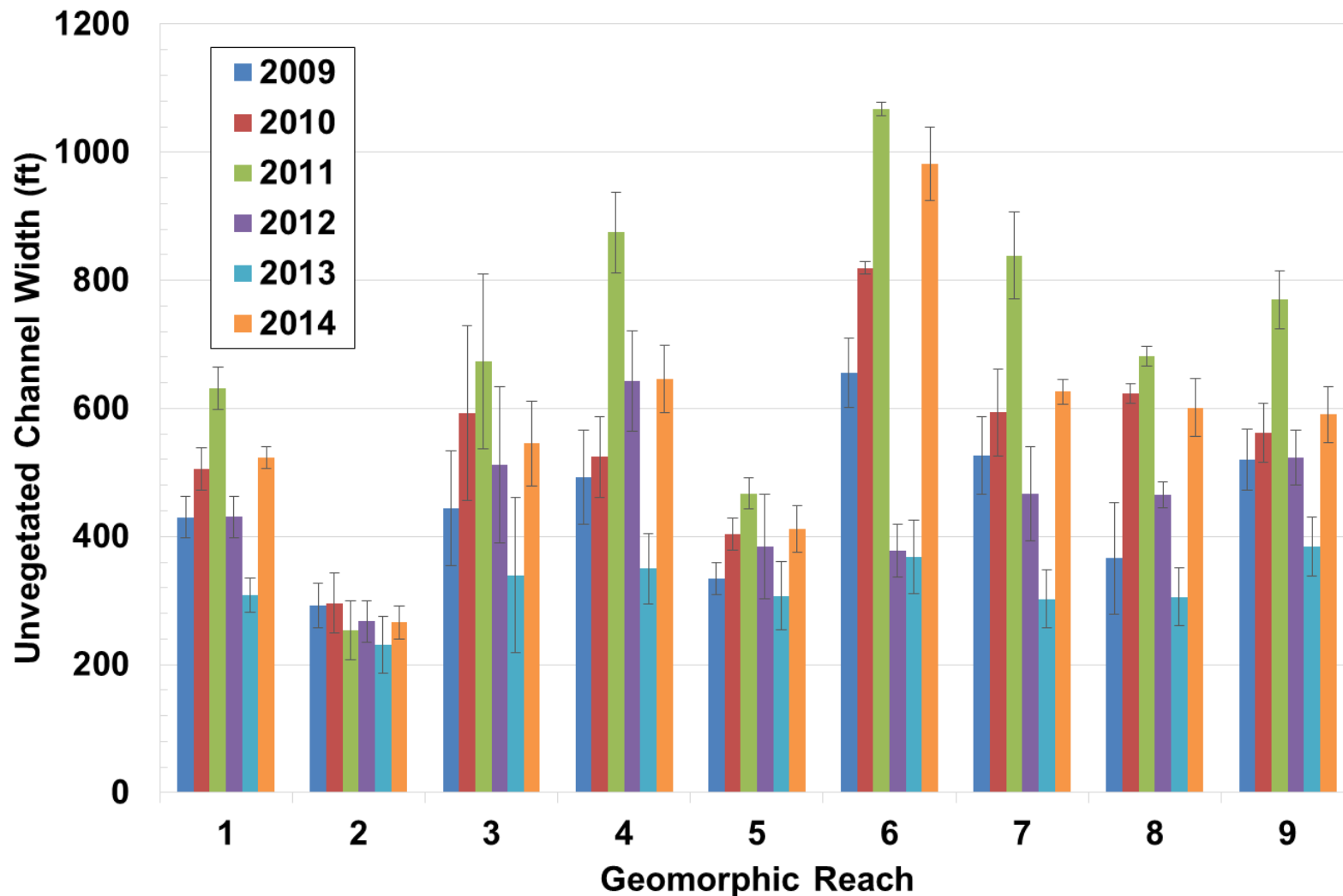


Figure 3.17c. Average unvegetated channel width by geomorphic reach from 2009 through 2014.

3.4.3 Frequency of Occurrence by Species (DAP 5.4.3)

Based on the frequency of occurrence analysis, ragweed (*Ambrosia* sp.) was the most common taxa encountered in the reach during the initial survey in 2009 (28 percent of all quadrats), followed by rough cocklebur (*Xanthium strumarium*) (21 percent), purple loosestrife (20 percent), common reed (20 percent), and reed canary grass (*Phalaris arundinacea*) (15.5 percent) (Figure 3.18). The moderately high-flow years of 2010 and 2011 resulted in more hydrophilic species becoming more frequent. The most frequently occurring species in 2010 was flatsedge (*Cyperus* sp.) (52 percent), common reed (25 percent), beggar's tick (*Bidens* sp.) (22 percent), rice cut grass (*Leersia oryzoides*) (21 percent), and reed canary grass (20 percent). Flatsedge again was the most frequently observed species in 2011 (37 percent) followed by reed canary grass (29 percent), common reed (20 percent), purple loosestrife (15 percent), and beggar's tick (14 percent). During the post-flood, but dry 2012 survey year, the most common species were flatsedge (51 percent), sprangletop (*Leptochloa fusca*) (16.6 percent), Eastern cottonwood (16.3 percent), ragweed (16.3 percent), and barnyard grass (*Echinochloa* sp.) (12.4 percent). In 2013, when flows were also low, annual ragweed (35 percent) returned as the most frequent species and flatsedge (33 percent) was nearly as common. These were followed by sprangletop (22 percent), rough cocklebur (16.6 percent), and reed canary grass (15 percent). The 2014 survey year mostly maintained the same pattern as 2013, with ragweed being the most common taxa (29 percent), followed by reed canary grass (16.5 percent), rough cocklebur (15 percent), flatsedge (13 percent), and dock (12.6 percent). Interestingly, sprangletop was much less common with a frequency of 4.3 percent in 2014.

In total, twelve species have been ranked in the top five most common species observed in any one year. Of those, eight maintained their top five ranking for more than one year, while four only occurred once. Patterns across years include taxa such as flatsedge and reed canary grass being consistently very common (in the top five in five out of six survey years), whereas species such as Eastern cottonwood, barnyard grass, rice cut grass, and curly dock have been infrequently common (each in the top five in only one of six survey years). Other species that have been common in some years range between these extremes. Eastern cottonwood is the only woody species that occurred at high frequencies, although during the single year that it qualified (2012), its densities were driven by a large recruitment of seedlings onto bare ground in the active channel or on bars that had been inundated during the 2011 high flows, and not by the presence of older, established individuals. (Note that sampling does not occur in areas with >25-percent canopy cover, as would be strongly associated with older cottonwoods; thus, high frequencies are unlikely to be seen for older, mature life stages). All twelve taxa would be considered pioneers and/or invasives, and with the exception of ragweed, all have wetland indicator classifications of Facultative (FAC) or wetter, which means they generally occur more than 50% of the time in wetlands. These characteristics strongly suggest that these species respond favorably to disturbance in a wet habitat, and often are the first to colonize an area after a disturbance. Other, more long-term ecological factors would be responsible for determining whether these pioneering species would continue to persist across years.

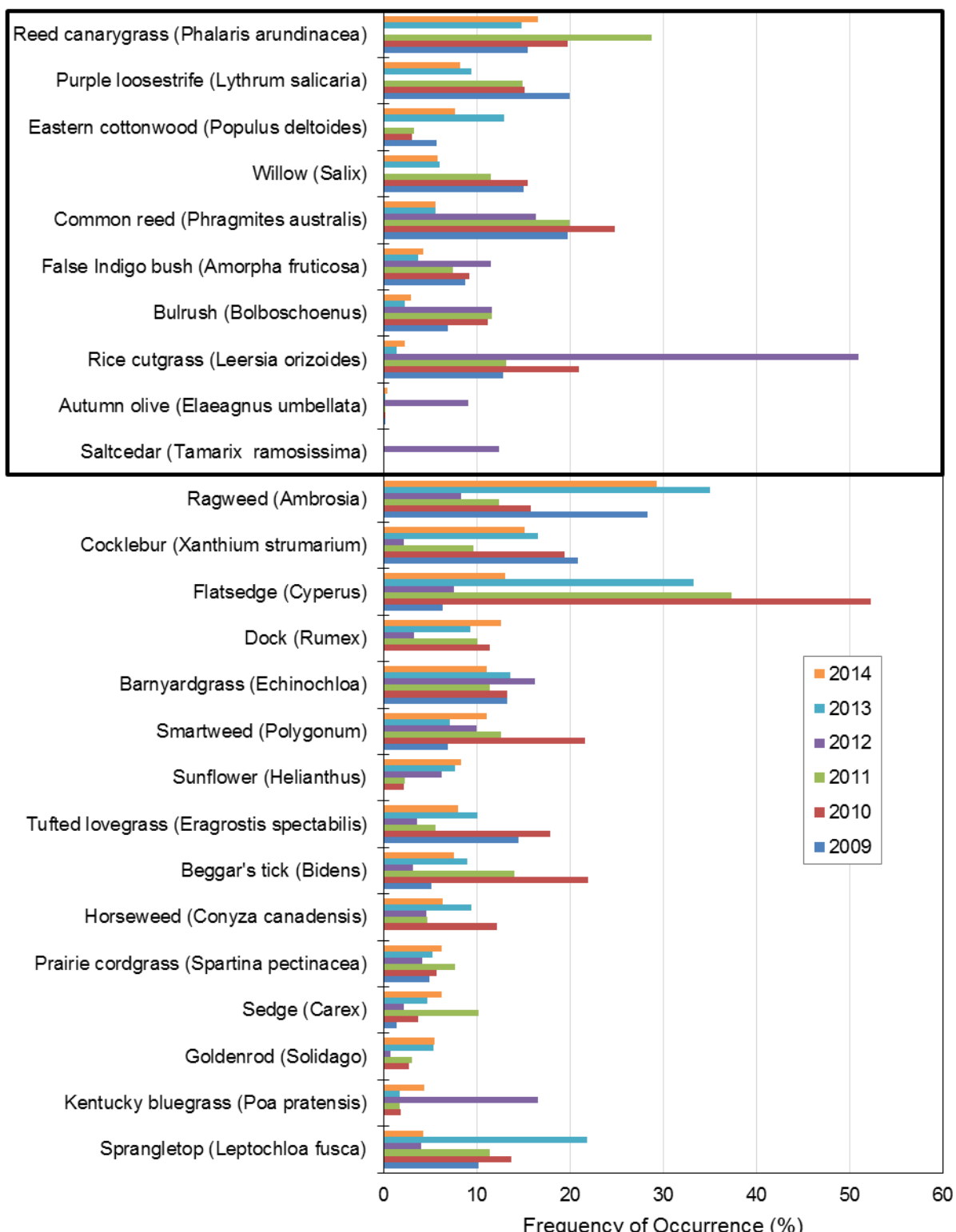


Figure 3.18. Frequency of occurrence of the top-25 most commonly observed species in 2014, and any species of primary interest present below that threshold, 2009-2014. Results are organized by decreasing frequency according to the 2014 data.

Frequencies of the four species of primary interest ranged widely between years. The frequency of purple loosestrife in the overall study reach declined by around one-half between 2009 and 2014 (it had a frequency of 20 percent in 2009, 15 percent in 2010, 15 percent in 2011, 7.6 percent in 2012, 9.4 percent in 2013, and 8.3 percent in 2014) (Figure 3.19); however, that decline was not consistent, potentially due to the new areas available for colonization in 2012. Both common reed and willows had similar patterns. The frequency of common reed declined from 2009 to the present by around two-thirds (19.7 percent in 2009, 24.8 percent in 2010, 20 percent in 2011, 4.2 percent in 2012, 5.6 percent in 2013, and 5.6 percent in 2014), and the frequency of willow declined from 2009 to the present by over two-thirds (15 percent in 2009, 15.5 percent in 2010, 11.5 percent in 2011, 4.6 percent in 2012, 6 percent in 2013, and 5.8 percent in 2014). Eastern cottonwood had a relatively unique pattern—although it declined from 2009 to 2011 (5.7 percent in 2009, 3 percent in 2010, and 3.3 percent in 2011), its frequency increased markedly in 2012 (16.3 percent) and has since remained higher than during the first three years (12.9 percent in 2013 and 7.7 percent in 2014); likely due to the new areas available for colonization in 2012.

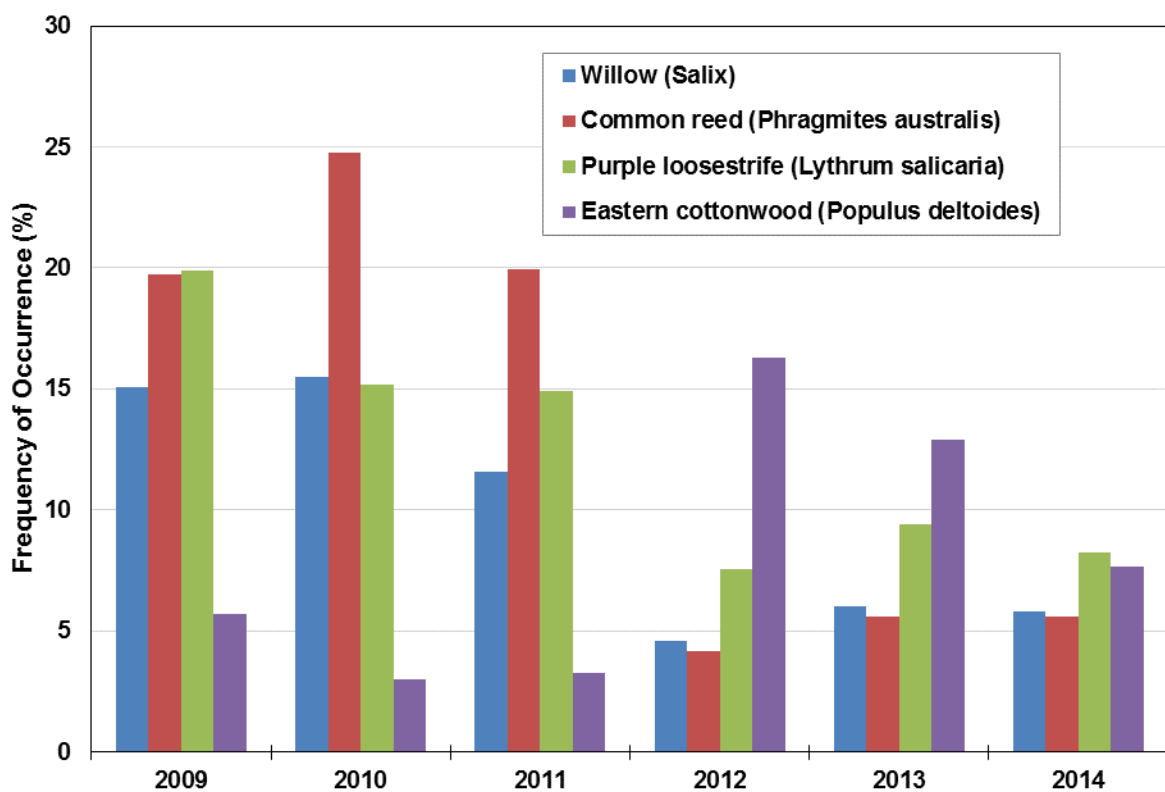


Figure 3.19. Frequency of occurrence for the four species of primary interest for the 2009 through 2014 vegetation surveys.

The high flows in 2011, followed by very low flows in 2012 appear to be associated with the shift in vegetation pattern observed between those years—prior to 2012, all species declined in frequency, whereas from 2012 to 2014, both increases and decreases in frequency occurred. One clear pattern is the substantial increase in Eastern cottonwood frequency in 2012. As discussed above, the Eastern cottonwood is well adapted to invade disturbed wet areas through effectively propagating numerous seeds each spring. In contrast, willow, purple loosestrife, and common reed propagate both by seed and by runners/rhizomes or fragments that may not have

distributed so widely. The steady decline in Eastern cottonwood frequency from 2012 to 2014 may indicate low survival of seedlings in the continued dry conditions.

The distribution of the species of primary interest along the study reach was assessed based on the average frequency of occurrence within each of the nine geomorphic reaches. In general, purple loosestrife (*Lythrum salicaria*) has consistently been most prevalent in the downstream half of the study reach (Geomorphic Reaches 6 through 9), although in 2009, it was also present in relatively high frequencies (>7.5 percent) in Reaches 1 (Figure 3.20). With the exception of Reach 6 in 2010, the frequency of purple loosestrife generally declined in all geomorphic reaches after 2009, but remained relatively abundant in Reaches 6 through 9 in 2013. In 2014, purple loosestrife remained above 7 percent relative frequency for Reaches 6 through 9, with the highest frequency in Reach 7 (14 percent).

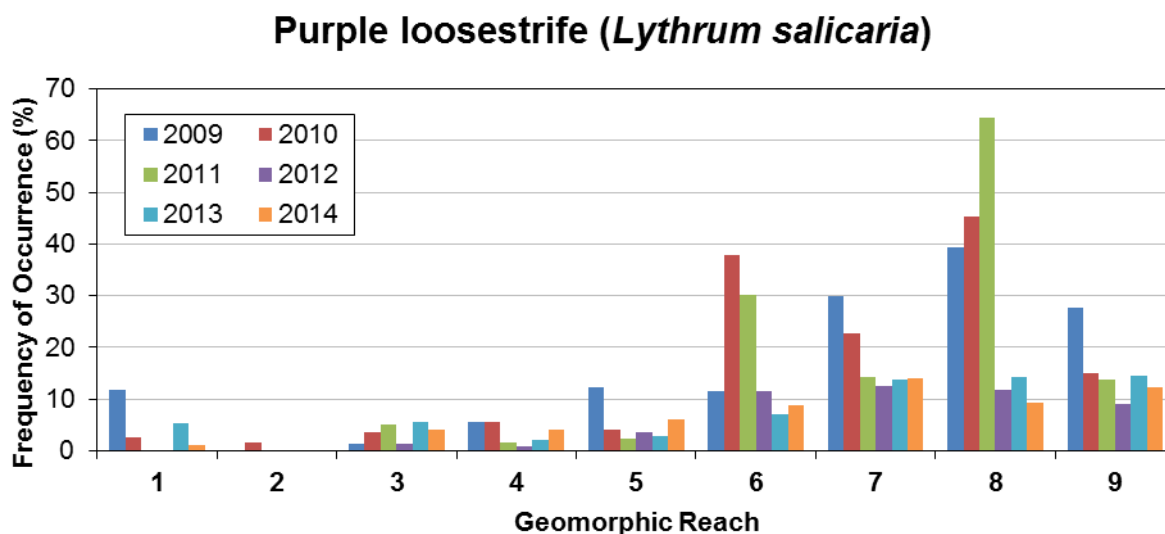


Figure 3.20. Mean frequency of occurrence of purple loosestrife (*Lythrum salicaria*) by geomorphic reach, 2009-2014.

In 2009, common reed (*Phragmites australis*) was most prevalent in the middle reaches (Reaches 4 and 5) as well as at the downstream end of the survey area (Reaches 7 and 9) (Figure 3.21). A large amount of common reed was also present in Reach 1 at the upstream end of the study reach. The frequency remained relatively high in those reaches in 2010 and then decreased from 2011 through 2014, sometimes substantially. Exceptions were Reaches 1 and 7, which saw substantial increases in common reed in 2013; although the frequency was still well below the levels in 2009 and 2010. In 2014, common reed was most frequent in Reach 9 (9%), Reach 5 (9%), and Reach 1 (6%) but still remained well below 2009/2010 levels. Overall, prevalence of common reed has drastically decreased since 2009.

Common reed (*Phragmites australis*)

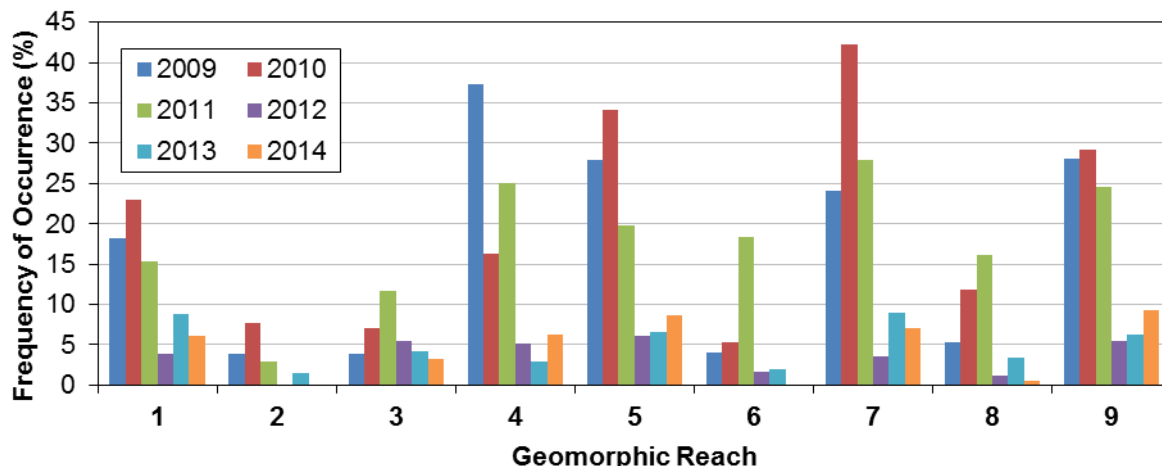


Figure 3.21. Mean frequency of occurrence of common reed (*Phragmites australis*) by geomorphic reach, 2009-2014.

Eastern cottonwood (*Populus deltoides*) was present at relatively low frequencies throughout the entire study reach in 2009, with slightly increased frequency downstream (11% and 10% in Reaches 8 and 9, respectively) (Figure 3.22). The frequency of cottonwood generally declined throughout the survey area in 2010, with Reaches 2 and 3 being exceptions, where it increased from trace levels to 5% and 8% respectively. Eastern cottonwood continued to show a general decline in 2011 in most reaches, except in Reach 2 where the frequency increased to about 10%. A very large increase occurred in most reaches in 2012. Reach 1 increased to 28%, 23% in Reach 3, and 21% in reach 7, and 18% to 14% in Reaches 4, 8, and 9. No cottonwoods were documented in Reach 2 in 2012 or 2013. In 2013, the frequency of cottonwood declined in Reaches 1, 3, and 5 and remained relatively unchanged in the remaining reaches. In 2014, cottonwoods decreased in all reaches except 5, remaining the highest in Reach 1 and 5 (19% and 12.5%, respectively). Large decreases in frequency of Eastern cottonwood occurred in Reaches 4, 7, 8, and 9 in 2014.

Eastern cottonwood (*Populus deltoides*)

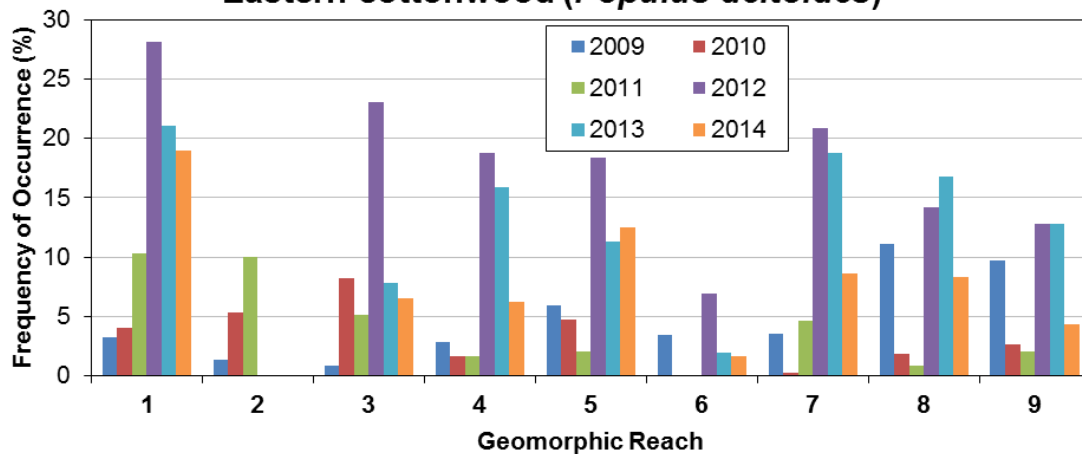


Figure 3.22. Mean frequency of occurrence of eastern cottonwood (*Populus deltoides*) by geomorphic reach, 2009-2014.

Willow (*salix sp.*) was present throughout the study reach in 2009, with the highest frequency occurring in Reach 4 (51 percent), followed by Reach 5 (22 percent), and Reach 2 (22 percent) (Figure 3.23.). Other reaches where willow was present at frequencies greater than 5% include Reaches 1, 2, 8, and 9. A substantial reduction in the frequency of willow occurred between 2009 and 2010 in Reaches 4 and 9, and moderate increases in Reaches 5 and 7. From 2011 through 2013, the frequency of willow generally declined throughout the survey area. Exceptions to this general trend occurred in Reach 1, where its frequency increased to 8.7 percent in 2012 and 17.5 percent in 2013, as well as in Reach 6, where its frequency increased to 8.6 percent in 2012 and 7.6 percent in 2013. In 2014, large changes in willow frequency occurred only in Reach 1 where it decreased to 12 percent, a reduction of 5 percent from the prior year. The other reaches either generally showed a slight decline (Reach 2, 5, 6, 8, and 9) or slight increase (Reach 3, 4, and 7).

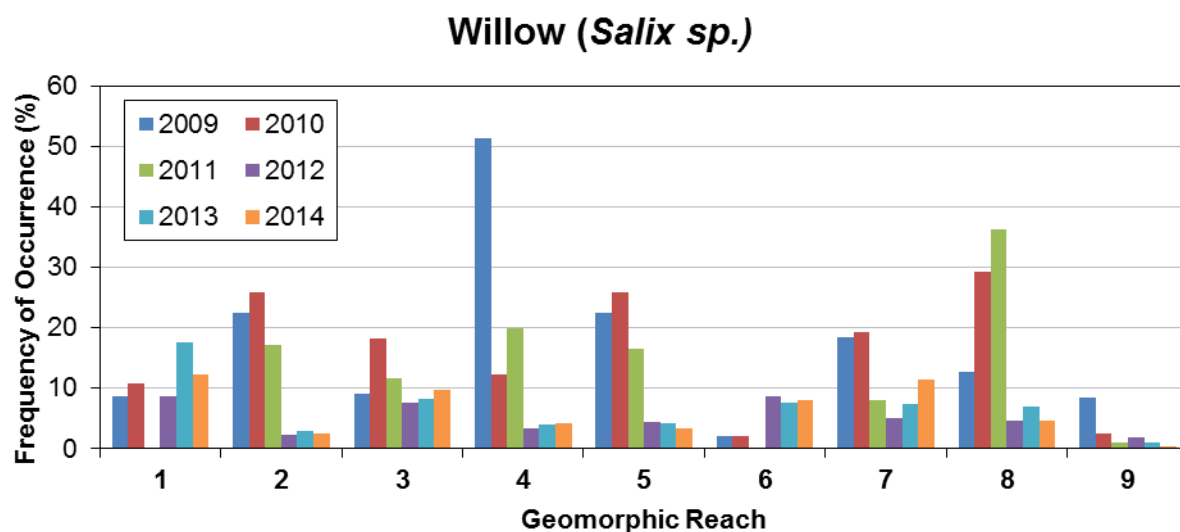


Figure 3.23. Mean frequency occurrence of willow (*Salix sp.*) by geomorphic reach, 2009-2014.

3.4.4 Percent Cover by Species (DAP 5.4.4)

The total area encompassed by the belt transects used for the vegetation surveys ranged from 491 acres in 2014, to 590 acres in 2010 (Figure 3.24). The Daubenmire data indicates that 55 percent (317 acres) and 47 percent (277 acres) of the survey area had measurable vegetation⁹ in 2009 and 2010, respectively, but declined substantially to only about 29 percent (168 acres) in 2011 when flows were high. The area with measurable vegetation then increased to about 65 percent (361 acres) in 2012 and 73 percent (360 acres) in 2013; both very dry years. In 2014, the area of measurable vegetation decreased to 55 percent (270 acres). Collectively, these trends correspond well with trends in GLE and unvegetated channel width.

⁹Unvegetated areas are defined as either bare ground, dead organic matter, or open water.

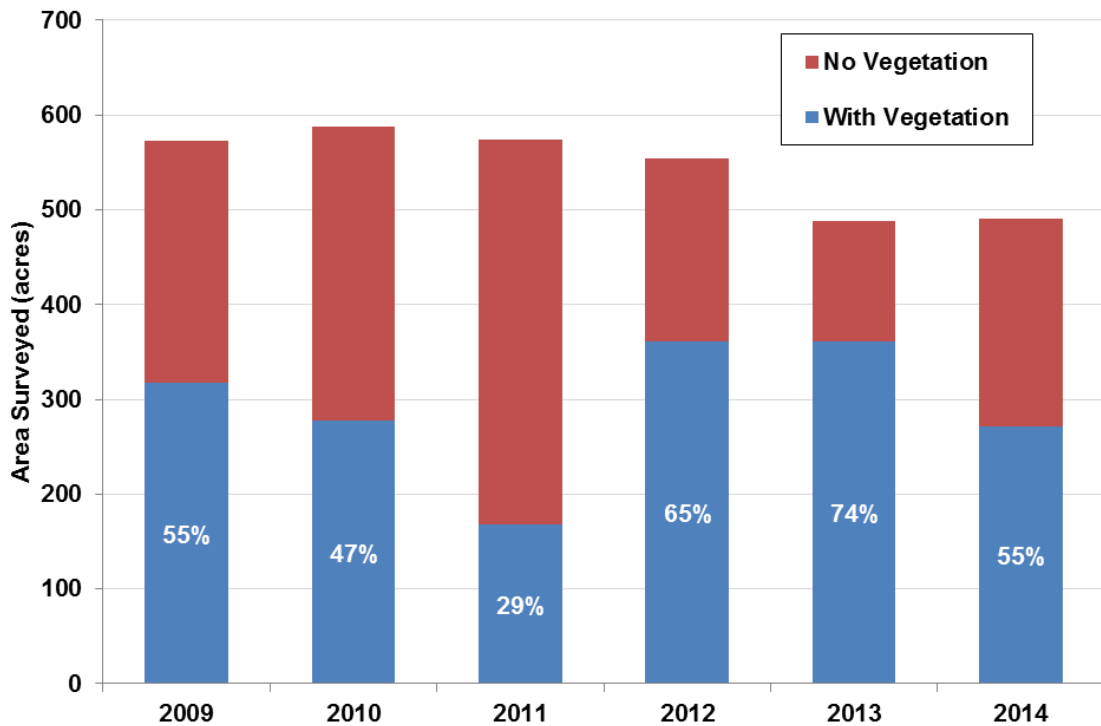


Figure 3.24. Total surveyed area and area with measurable vegetation for each survey year, based on Daubenmire cover-class data.

Using Daubenmire Cover data, in 2009, the percent cover for each species ranged from effectively 0 to 8.7 percent across all sampled main channel quadrats at pure panel APs. The ranges were similar in subsequent years (0 to 11.8 percent in 2010, 0 to 16.2 percent in 2011, 0 to 4.3 percent in 2012, 0 to 7.5 percent in 2013, and 0 to 9.0 percent in 2014) (Figure 3.25). This data indicates that no one species accounted for more than about 16-percent cover of the survey area for any year.

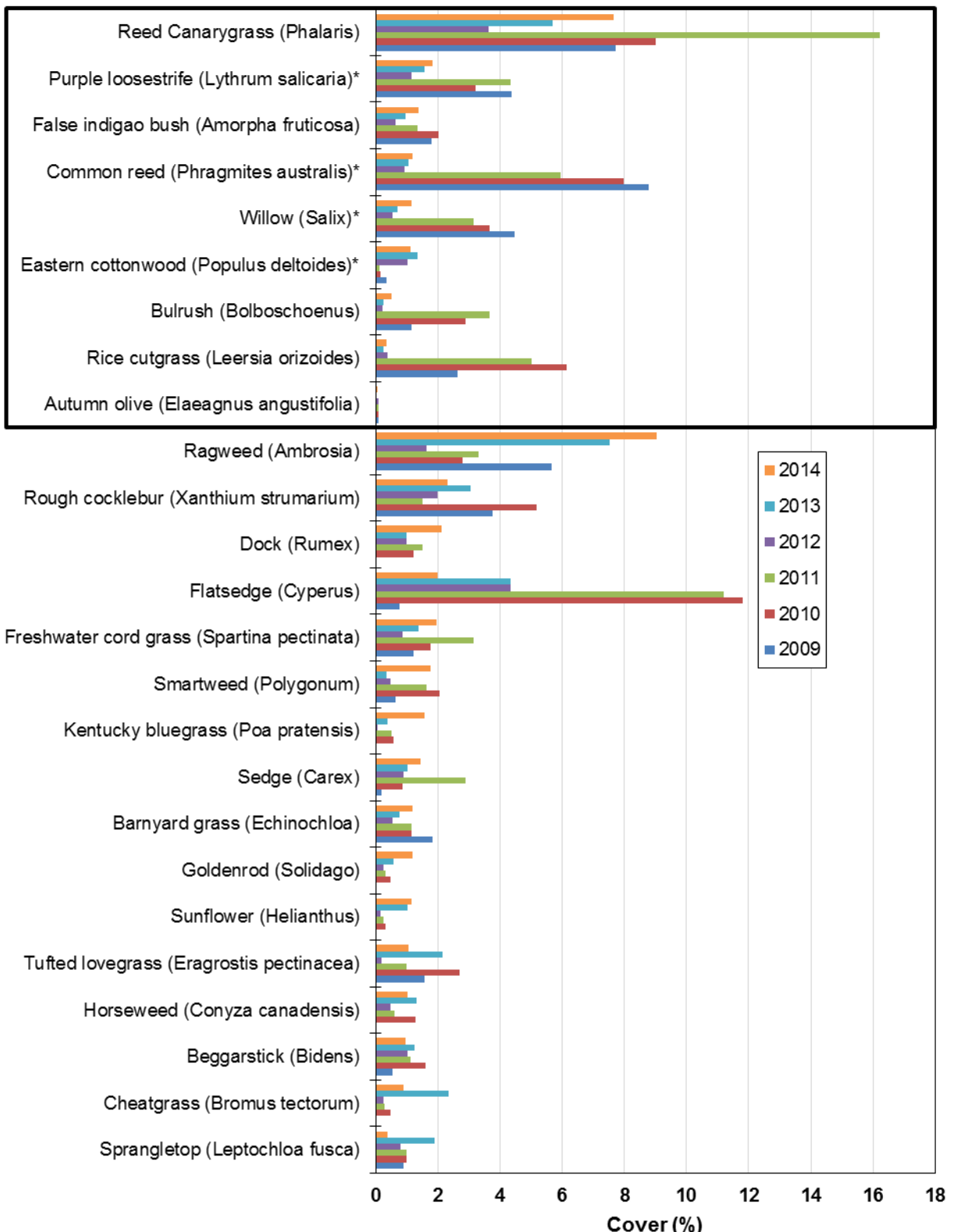


Figure 3.25. Percent cover of the top 25 most commonly observed species in 2014, and any species of primary interest present below that threshold, 2009 through 2014. Results are organized by decreasing frequency according to the 2014 data.

In assessing these results, it is important to understand that cover was sampled as a percentage category based on the area of each sample quadrat, and each species was quantified separately. As a result, some areas can be counted more than once where overlap among species occurs. For example, if a quadrat is full of only live plants and only two species are present and occupy different strata, their total cover could be greater than 100 percent if the areas occupied by each overlap. This correctly reflects the ecological process in place along the Platte River by capturing the regular occurrences of neighboring plants with intermingled canopies.

Common reed was the species with the greatest percent cover in 2009 (8.7 percent), followed by reed canary grass (7.7 percent), ragweed (5.7 percent), willow (4.5 percent), and purple loosestrife (4.4 percent). The percent cover of common reed declined substantially after 2009, but remained in the top two in terms of percent cover in 2010 and 2011 (8 and 6 percent, respectively), then continued to decline to relatively low levels in 2012, 2013, and 2014 (0.9, 1.1, and 1.2 percent, respectively). Reed canary grass remained in the top two across all years, and had the highest cover of any species in 2010 and 2011. (9 and 16 percent, respectively), but decreased in cover to 3.6 percent in 2012, 5.7 percent in 2013, and 7.7 percent in 2014 (ragweed had the greatest cover that year at 9 percent). Other species with substantial cover in 2010 included flatsedges (11.8 percent), rice cut grass (6.1 percent), and rough cocklebur (5.2 percent). Rice cut grass and purple loosestrife also had substantial cover in 2011 (5 and 4.3 percent, respectively), as did river bulrush (3.7 percent). In 2012, relatively high cover species included rough cocklebur (1.9 percent), flatsedges (4.3 percent), and purple loosestrife (1.1 percent). In 2013, species with relatively high cover included rough cocklebur (3.1 percent) and flatsedges (4.3 percent). For 2014, cover of rough cocklebur increased to 3.1 percent, and flatsedges remained the same. In general, species with the highest percent cover also had high frequencies of occurrence, although some higher frequency species had lesser cover as they primarily occurred as seedlings.

In general, the year-to-year patterns noted in frequency of occurrence are also present for percent cover. Willow, purple loosestrife and common reed generally showed significant decline in percent cover in 2012, and then either moderately increased (purple loosestrife) or leveled-out (common reed) (**Figure 3.26**). Eastern cottonwood showed an initial decline during the first three years and then a slight increase in percent cover from 2012 to 2013, only to decline slightly again in 2014. Percent cover, however, does not reflect the large increase in frequency seen in Eastern cottonwood in 2012, indicating that although this species was observed in many quadrats, its total canopy was small as it occurred primarily as seedlings that did not occupy much space.

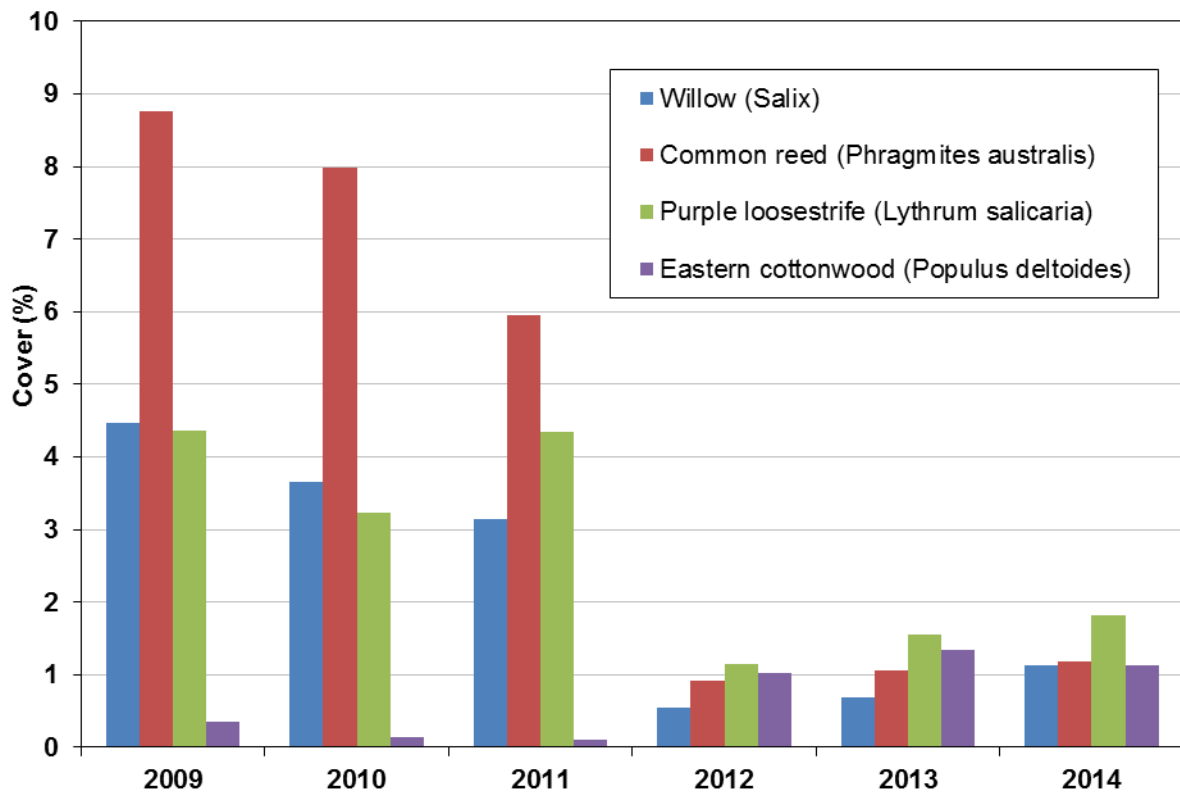


Figure 3.26. Percent cover of the species of primary interest from 2009 through 2014.

The spatial patterns of percent cover for the four species of primary interest are also similar to those identified in frequency of occurrence. Purple loosestrife has been observed covering a greater amount of area in Reaches 6 through 9 throughout the first increment. Ground cover percentage of purple loosestrife has fell immensely after 2011 in Reaches 6, 7 and 8. (Figure 3.27). Common reed was most common in the downstream reaches at the beginning of the first increment, but has been substantially reduced throughout the entire program reach (Figure 3.28). Eastern cottonwood was found at low frequencies during the first three years of surveys. There was a large colonization by 2012, with populations remaining high in 2013 and 2014, although in 2014 there was a noticeable decline in frequency (Figure 3.29). Willow was observed at its highest proliferation in 2009 in Reach 4 (16 percent), but has not been observed exceeding 3 percent in any reach since 2011 (Figure 3.30).

Purple loosestrife (*Lythrum salicaria*)

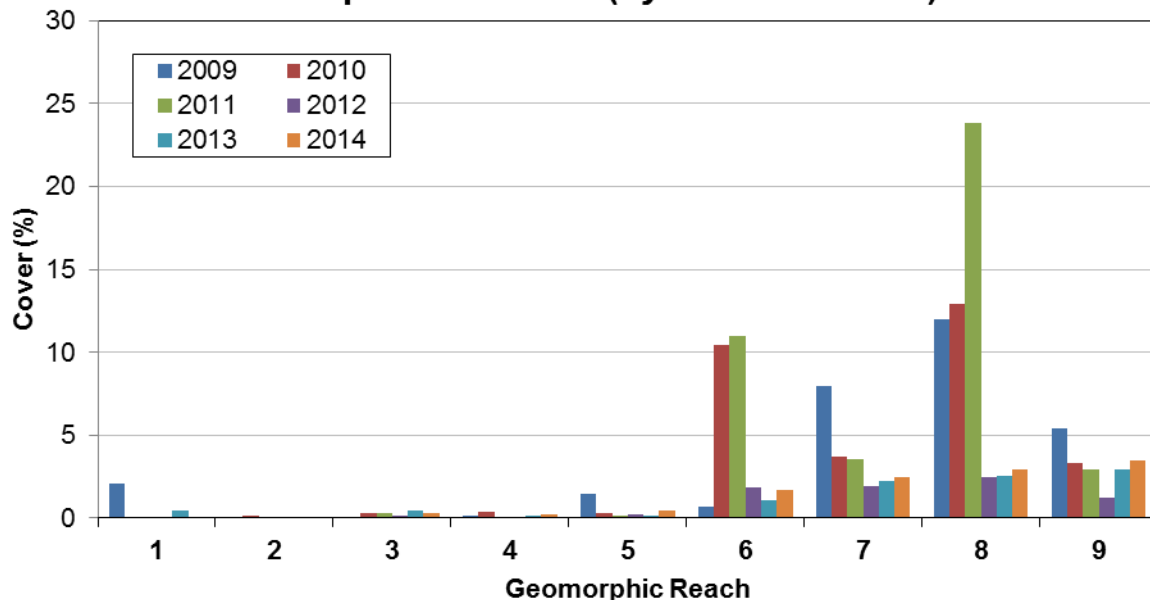


Figure 3.27. Mean percentage of ground cover for Purple loosestrife (*Lythrum salicaria*), 2009 through 2014, by geomorphic reach.

Common reed (*Phragmites australis*)

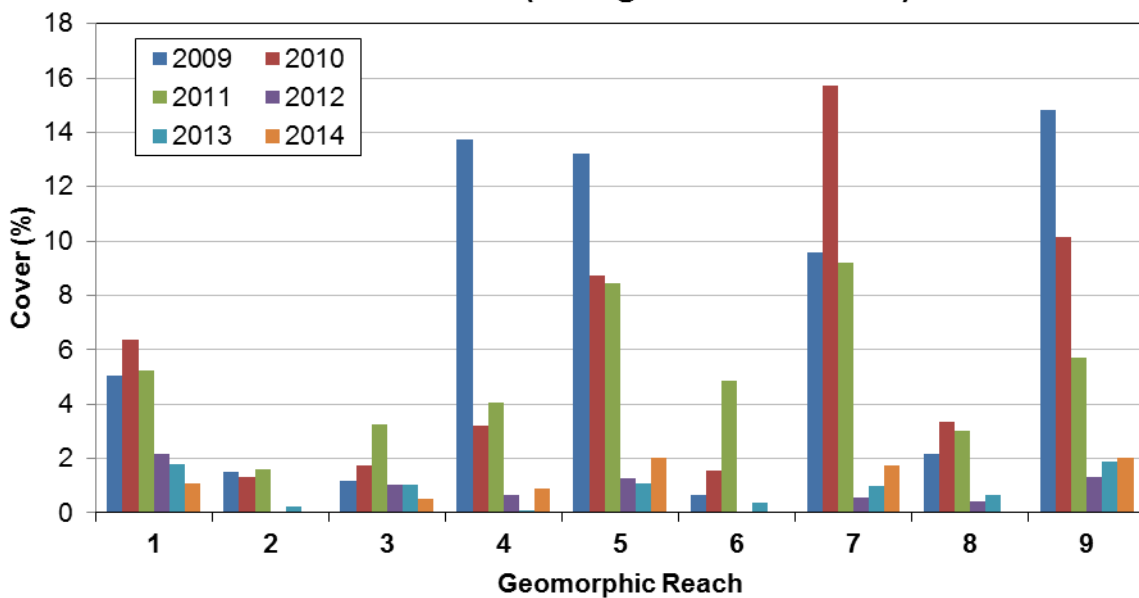


Figure 3.28. Mean percentage of ground cover for common reed (*Phragmites australis*), 2009 through 2014, by geomorphic reach.

Eastern cottonwood (*Populus deltoides*)

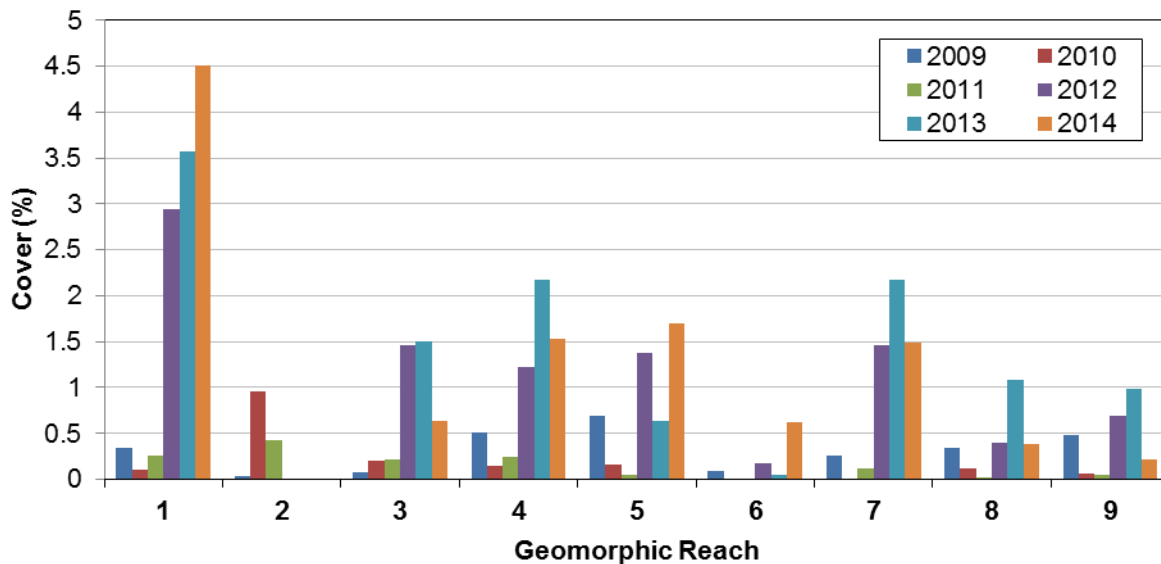


Figure 3.29. Mean percentage of ground cover for Eastern cottonwood (*Populus deltoides*), 2009 through 2014, by geomorphic reach.

Willow (*Salix sp.*)

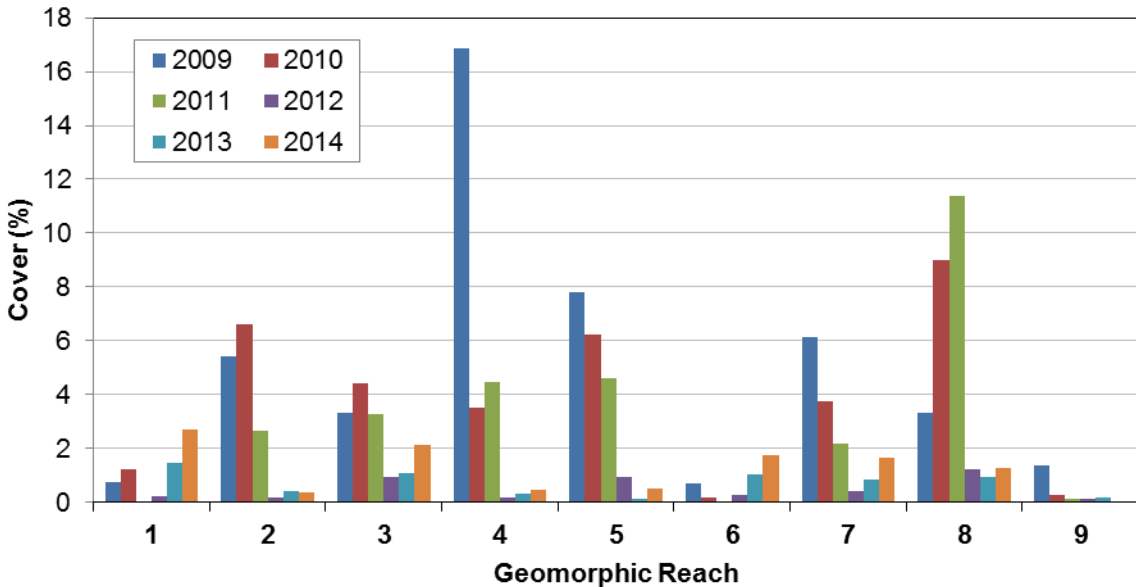


Figure 3.30. Mean percentage of ground cover for willow (*Salix sp.*), 2009 through 2014, by geomorphic reach.

3.4.5 Areal Cover by Species (DAP 5.4.5)

Because areal cover is the mathematical product of the percent cover and the sample area, with a few exceptions, all trends and patterns identified for percent cover also apply to areal cover (Figure 3.31). The only major exception was in 2011 where common reed had a relatively high percent cover but low areal cover. Similar but less extreme patterns also occurred for willow and purple loosestrife. These slightly uncoupled findings may result from patches of these species

Channel Geomorphology
and In-Channel Vegetation
2014 Final Data Analysis Report

that result in higher percent cover in some reaches that skew the average percent cover, but as they only occur in fewer locations, their areal cover is less.

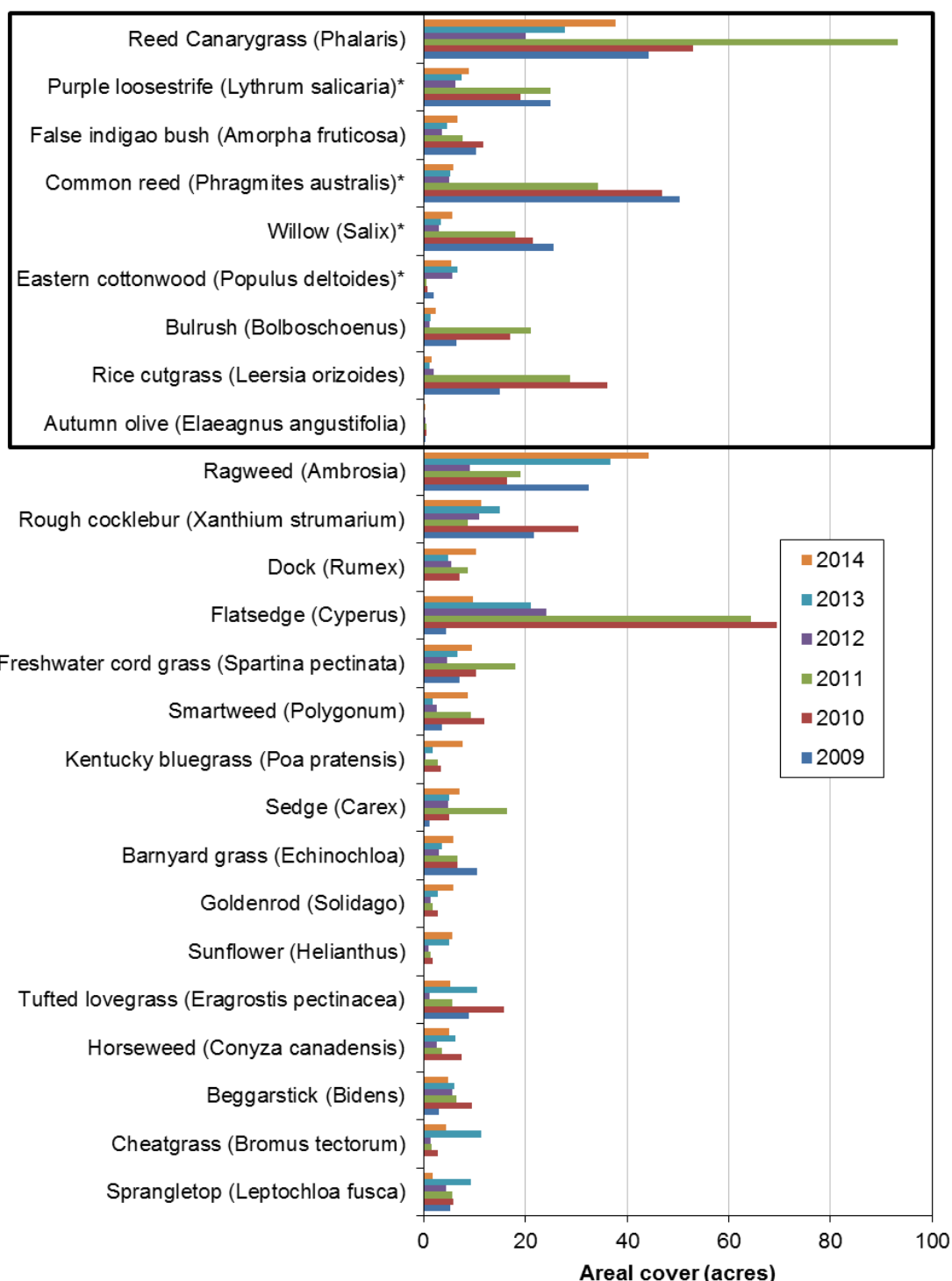


Figure 3.31. Areal cover of the top-25 most commonly observed species in 2014, and any species of primary interest present below that threshold, 2009-2014. Results are organized by decreasing frequency according to the 2014 findings.

Of the four species of primary interest, purple loosestrife declined from about 25 acres in 2009 to 19 acres in 2010, increased to 25 acres in 2011, and decreased to 6.3 acres in 2012, and then increased back to about 7.6 acres and 8.9 acres in 2013 and 2014, respectively (**Figure 3.32**). The total cover of common reed declined from 50 acres in 2009 to 47 acres in 2010, 34 acres in 2011, and remained relatively steady at 5.0, 5.2, and 5.8 acres in 2012, 2013, and 2014. Eastern cottonwood was present in very small quantities in the first three years (2 acres in 2009, 0.9 acres in 2010, and 0.6 acres in 2011), but increased to about 5.6 acres in 2012 and 6.6 acres in 2013, with a slight decline in 2014 to 5.5 acres. The aerial cover of willow declined through the period from about 26 acres in 2009 to 22 acres in 2010, 18 acres in 2011, and 3 acres in 2012, and then increased back to about 3.4 acres in 2013, and increased again to 5.6 acres in 2014.

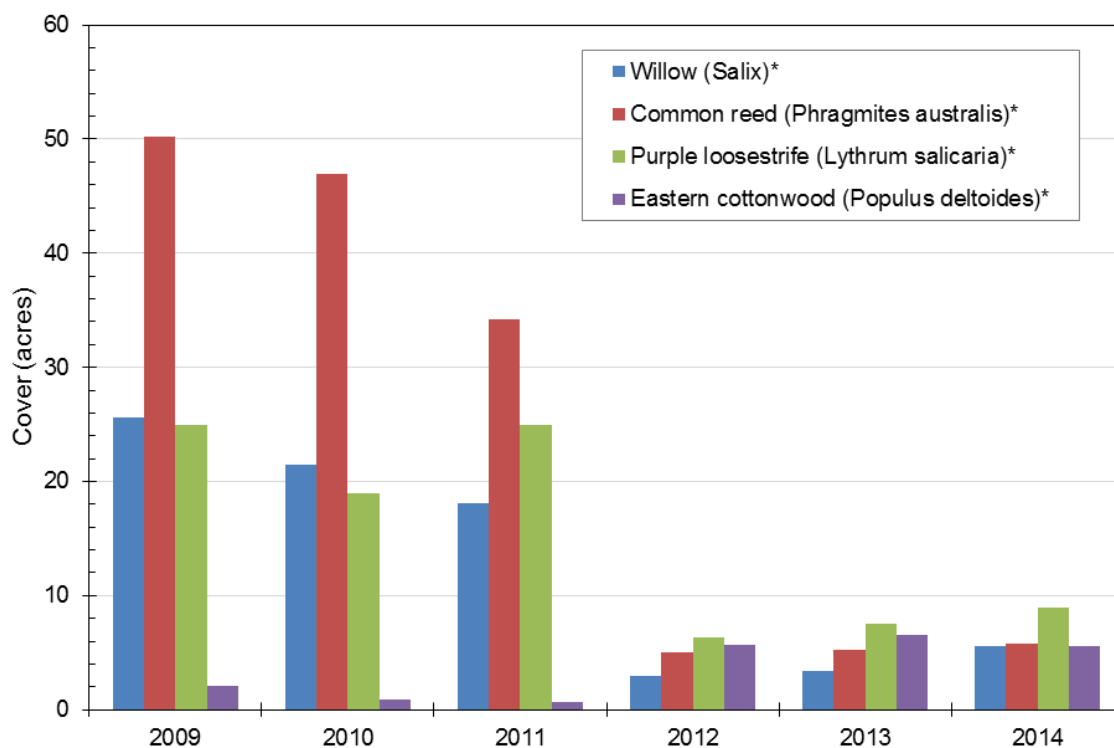


Figure 3.32. Areal cover of the four species of primary interest, 2009-2014.

As with percent cover, the spatial patterns of areal cover of the four species of primary interest are very similar to the frequency of occurrence. Based on the 2014 data, most purple loosestrife was located in Reaches 7, 8, and 9, at the downstream end of the program reach (**Figure 3.33**). Common reed is relatively evenly distributed throughout the study reach, with the largest areal cover occurring in Reach 9 (**Figure 3.34**). Eastern cottonwood has been observed throughout the program reach with the greatest areal cover occurring in Reaches 1, 5, and 7 (**Figure 3.35**). Willow occurs throughout the study reach with the greatest cover occurring in Reaches 3, 7, and 8 (**Figure 3.36**).

Purple loosestrife (*Lythrum salicaria*)

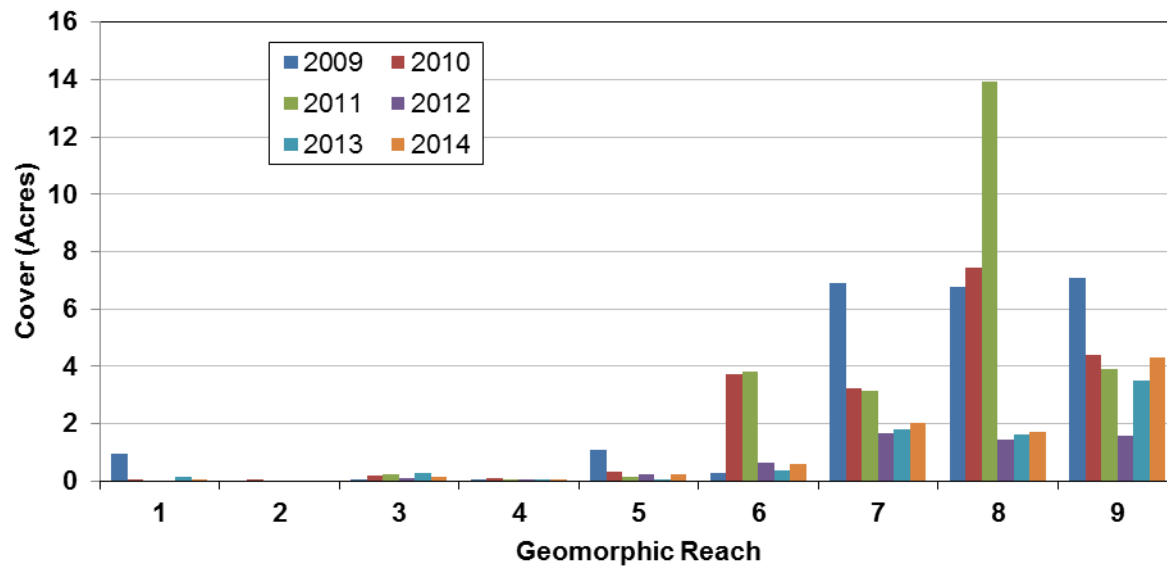


Figure 3.33. Areal cover of purple loosestrife (*Lythrum salicaria*), 2009-2014 by geomorphic reach.

Common reed (*Phragmites australis*)

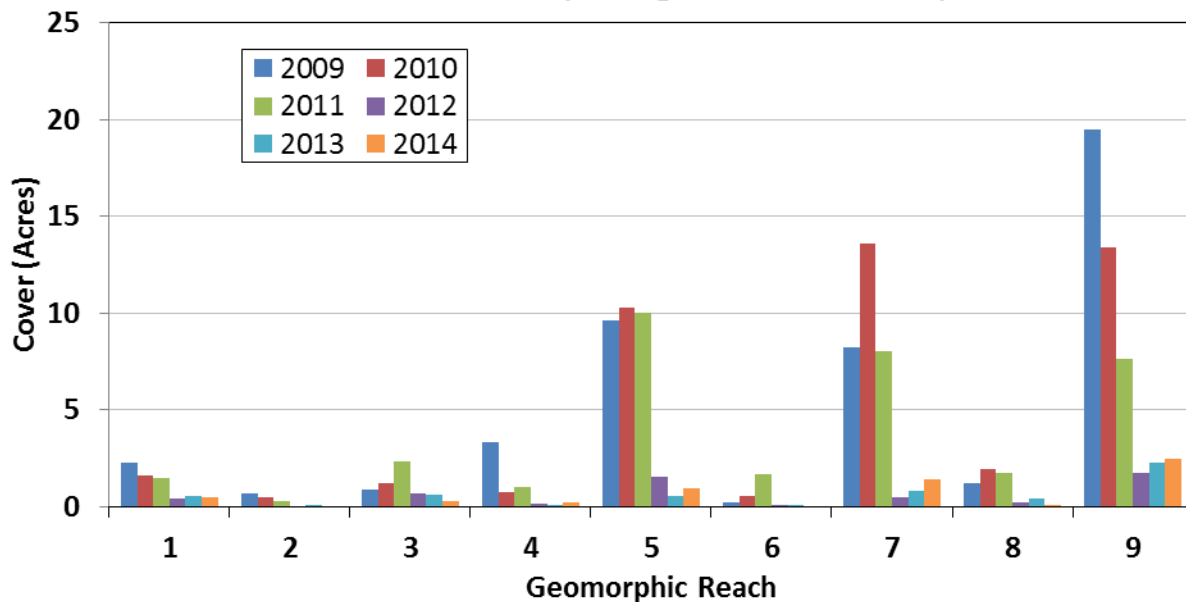


Figure 3.34. Areal cover of common reed (*Phragmites australis*), 2009-2014 by geomorphic reach.

Eastern cottonwood (*Populus deltoides*)

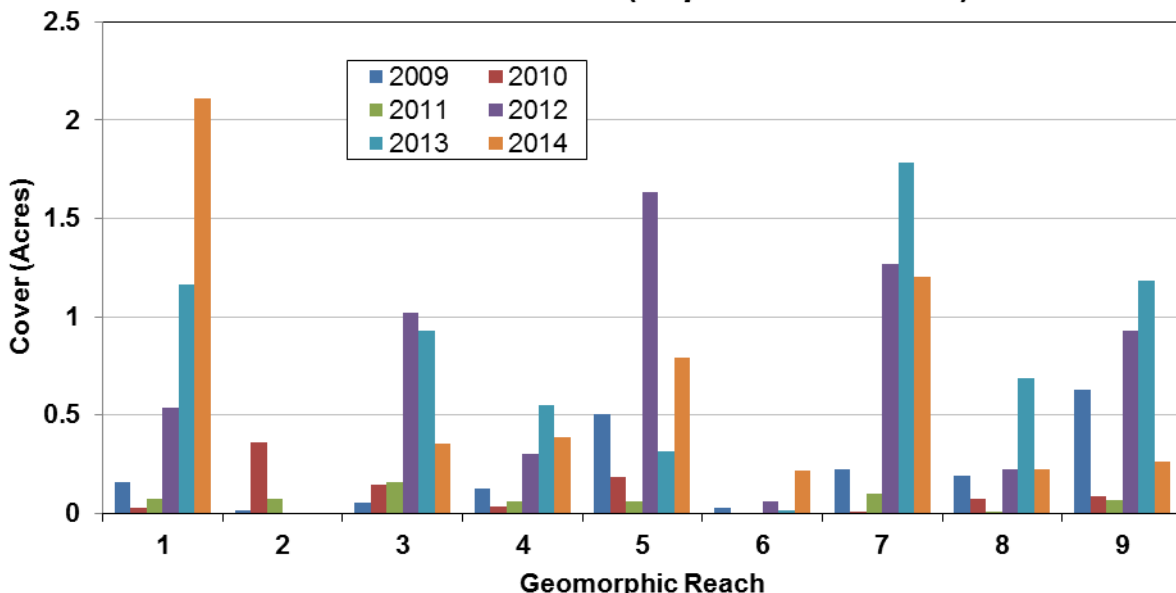


Figure 3.35. Areal cover of Eastern cottonwood (*Populus deltoides*), 2009-2014 by geomorphic reach.

Willow (*Salix sp.*)

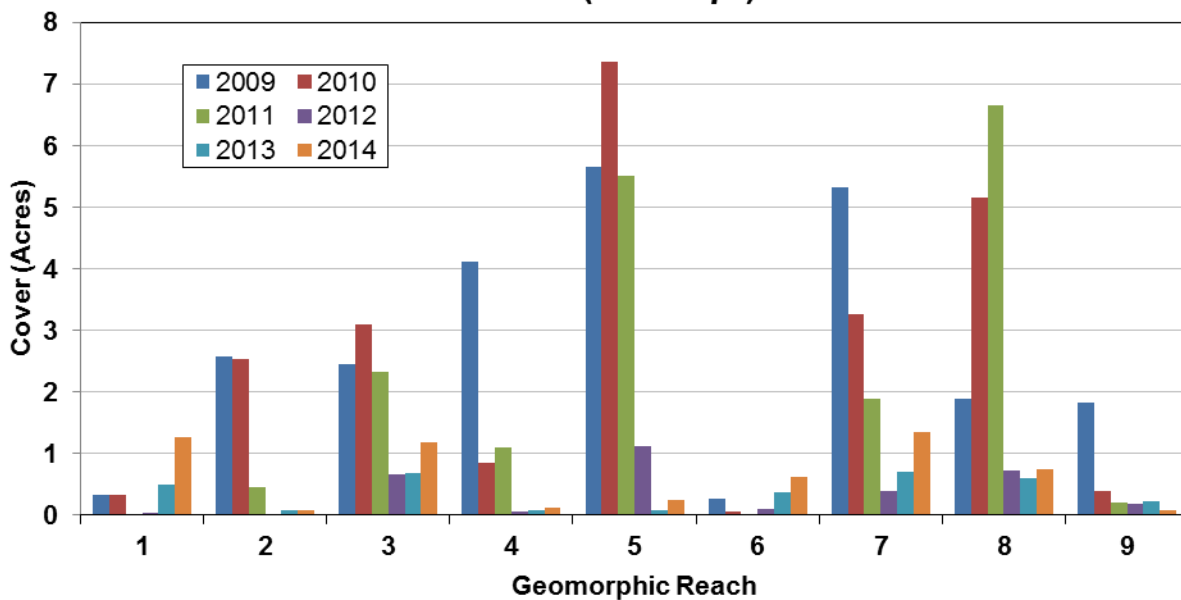


Figure 3.36. Areal cover of willow (*Salix sp.*), 2009-2014 by geomorphic reach.

During 2011, the survey area was inundated with a long-duration, high-flow event, which likely reduced vegetation and increased the extent of bare ground. In 2012, the vegetated area doubled (Figure 3.34), suggesting that newly established bare ground became available for plant establishment during the subsequent dry spring and summer, and was quickly colonized. The frequency of occurrence of both Eastern cottonwood and willow increased much more in 2012 and 2013 than their cover values, indicating the establishment of new stands of young

plants. The high-flow event in the fall of 2013 likely influenced vegetation in a similar fashion, however, both cottonwood and willow occurrences declined from the previous year. That year, seedling establishment on newly disturbed bare ground was likely constrained by the relatively wet 2014 growing season, in which flows may have continued to disturb areas where germination had occurred. It is, therefore, likely that large recruitment events of riparian, seed-dispersed species such as Eastern cottonwood require a disturbance event prior to the growing season, followed by low enough flows during the growing season to allow establishment. (Like most riparian seedlings, those of Eastern cottonwood require ample soil moisture to prevent desiccation, but cannot be submerged for extended periods). The natural distribution of cottonwood age classes indicates periodic episodes of colonization followed by many years with much reduced colonization.

3.4.6 Mean Elevation by Species (DAP 5.4.6)

Mean elevation of each of the species of primary interest and other commonly occurring species were evaluated by averaging the elevations of all quadrats in which each species was observed, and also by evaluating the average height relative to the local 1,200-cfs water-surface. The average elevation of each species is controlled by both the elevation profile of the river, and the local effects of flows and other factors. The differences in elevation between the APs is generally greater than the elevation range within each individual AP; thus, the raw averages are indicative of the most common locations of the species along the reach, while the height relative to the local 1,200 cfs is indicative of the effects of flow and other local factors.

The data indicate that Russian olive (*Elaeagnus angustifolia*) and salt cedar (*Tamarix ramosissima*) generally grows at the highest elevations; however, they were infrequently encountered (salt cedar was only observed once) and only occurred in a few reaches. Because of the limited number of observations of these species, this pattern may not be particularly meaningful. Commonly occurring species found at relatively high mean elevations included Eastern cottonwood (in 2011 and 2014), sunflower (*Helianthus* sp., 2011), cheatgrass (*Bromus tectorum*, 2012), common panic grass (*Panicum capillare*, 2014), white sweet clover (*Melilotus albus*, 2011), and tufted lovegrass (*Eragrostis pectinacea*, 2011) (**Figure 3.37a**). With two exceptions, these species have wetland indicator status of either Facultative-Upland (FACU) or Not Listed (NL), indicating species typically found in upland habitats. Tufted lovegrass and common panic grass are both Facultative (FAC) species, which are generally found equally in upland and wetland habitats.

None of the species of interest were in the top five highest elevation zones relative to the local 1,200-cfs water surface (**Figure 3.37b**). The species that grew at the lowest relative elevation in 2014 was rice cutgrass (*Leersia oryzoides*). The four species of primary interest tended to grow at among the lowest elevations of the sampled species, and thus, likely have more influence on the green line elevation and sandbar habitats. The average relative elevation of all four of these species increased from 2009 through the high-flow year in 2011, and then declined substantially in the dry years of 2012 and 2013, with an apparent increase in 2014 (**Figure 3.37c**).

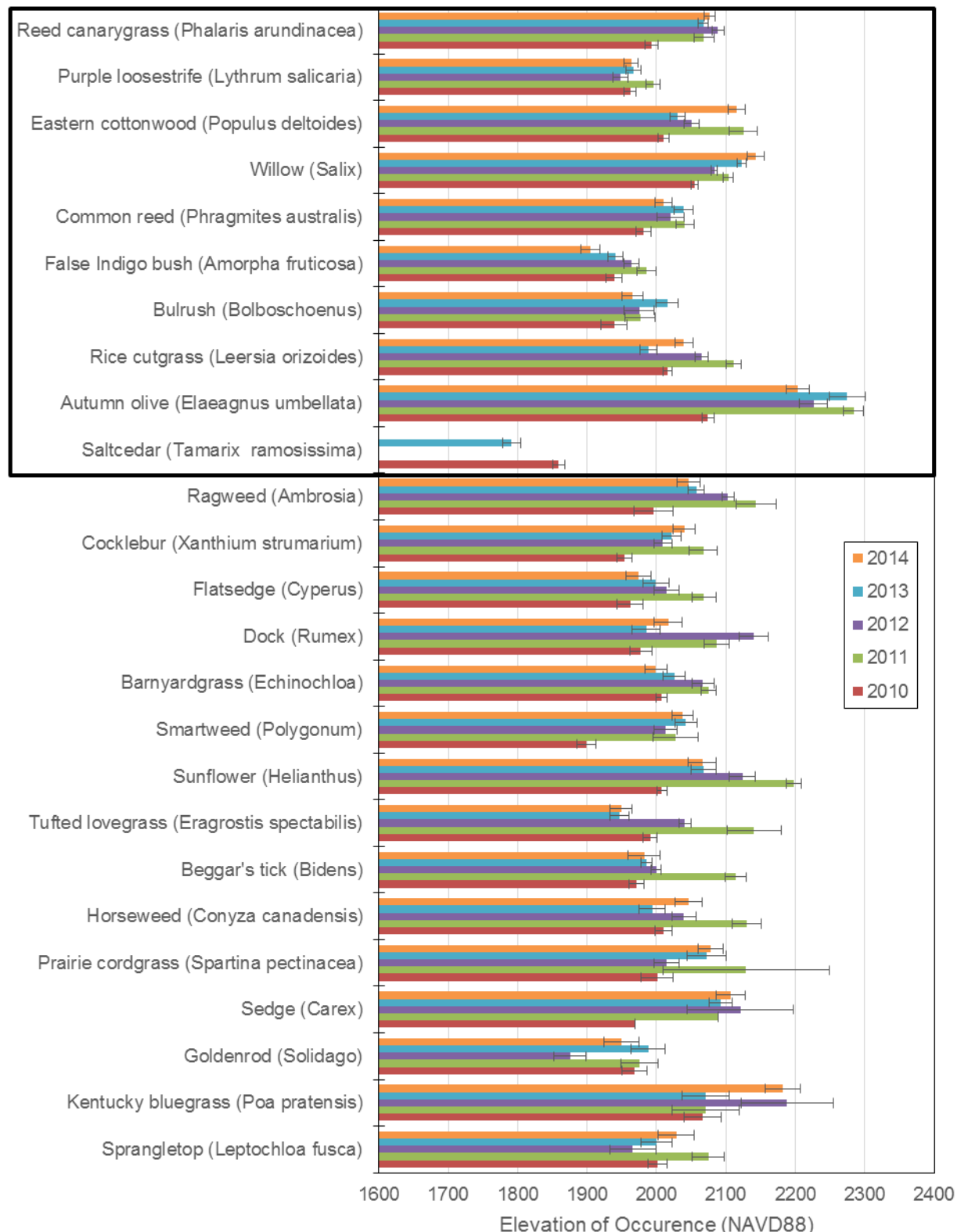


Figure 3.37a. Mean elevation of the top 25 most commonly observed species in 2014, and any species of primary interest present below that threshold, 2010-2014, organized by decreasing frequency in 2014. Standard error bars (± 1) are included.

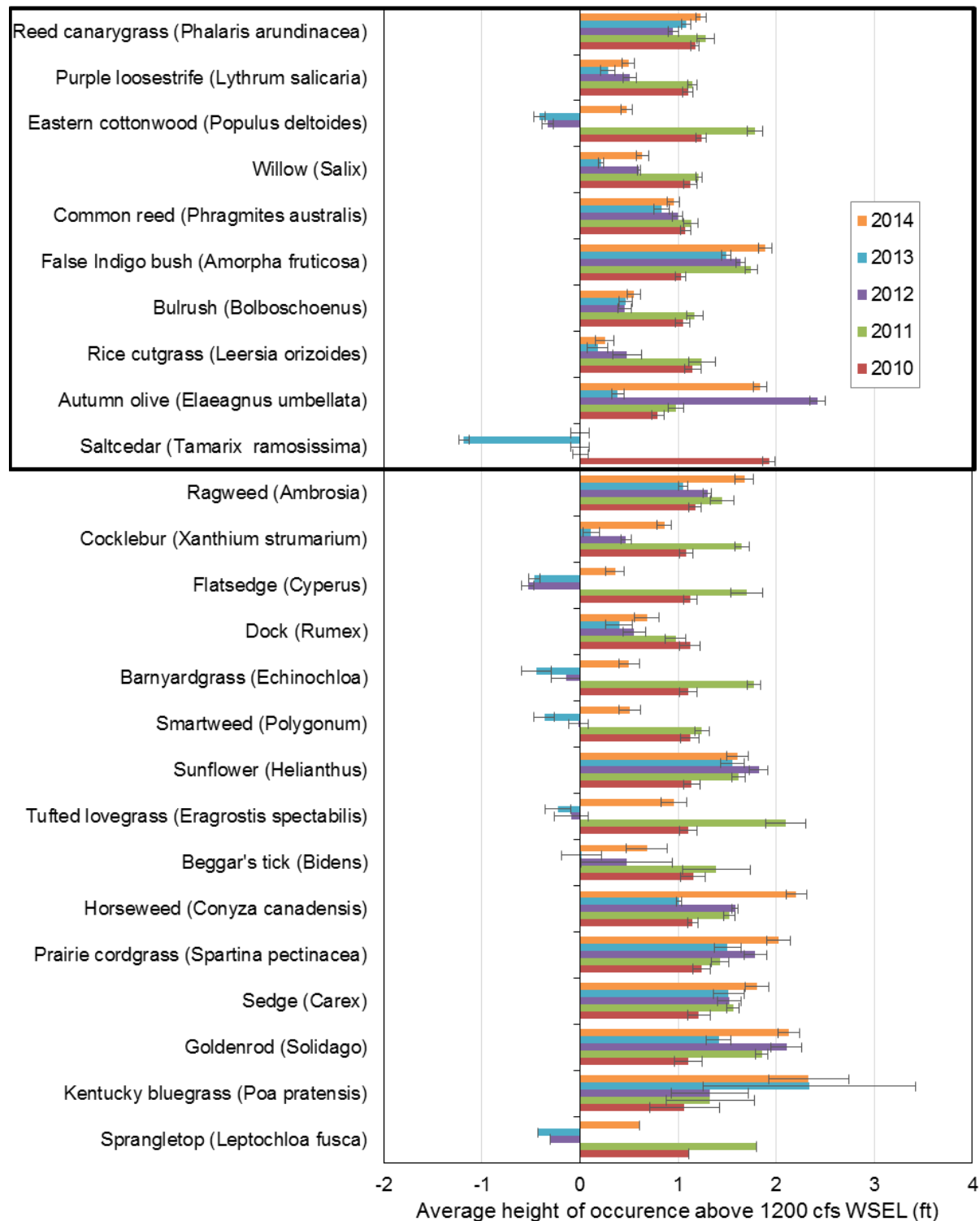


Figure 3.37b. Mean elevation above the local 1,200-cfs water surface of the top 25 most commonly observed species in 2014, and any species of primary interest present below that threshold, 2010-2014, organized by decreasing frequency in 2014. Standard error bars (± 1) are included.

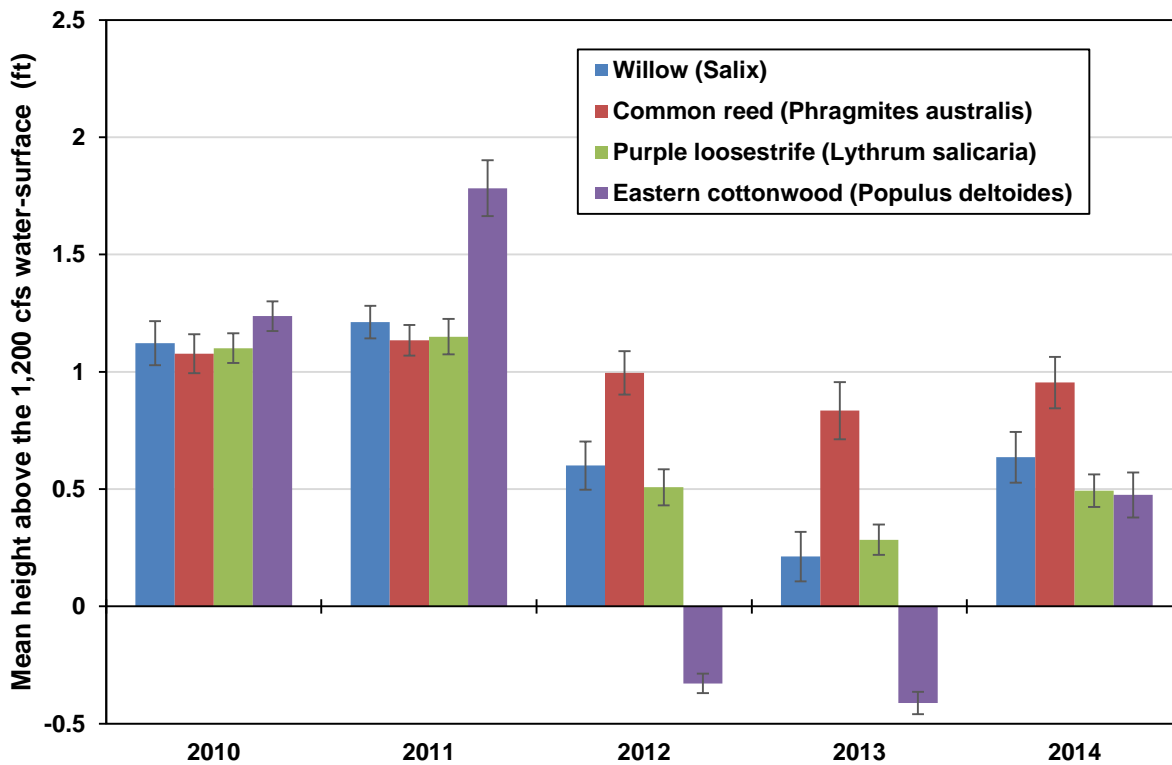


Figure 3.37c. Mean height above the 1,200-cfs water surface of the four species of primary interest from 2009 through 2014. Standard error bars (± 1) are included.

3.4.7 Mean Vegetation Height (DAP 5.4.7)

Mean vegetation height was included among the original metrics to facilitate calculating estimates of unobstructed sight distance. As described above, methods for sampling vegetation height has varied since the program's inception. In 2009, 2010, and 2012, the data were collected categorically as a mean value, whereas in 2011, data were collected as a combination of actual mean heights and categorical mean heights. In 2013 and 2014 the method was modified to document actual maximum heights only. Regardless of sample year, all heights were collected as average values across all woody or herbaceous species in each quadrat, and were not collected directly for each species. As noted elsewhere in this report, unobstructed sight distances were measured directly in the field using a laser rangefinder beginning in 2013. Consequently, the value of this metric for estimating unobstructed sight distance has been substantially reduced for years after 2012. Mean vegetation height data continue to be collected for this study to maintain consistency, and allow for comparisons between all years of the study, if such analysis becomes necessary. See discussion in Section 3.6.1 regarding Unobstructed Channel Width for a complete analysis and discussion.

3.5 Sediment

3.5.1 Bed-load versus Discharge Rating Curves (DAP 5.5.1)

To-date, a total of 55 bed-load sediment samples have been collected for this monitoring program at the five designated bridge sites: Darr (State Hwy L-24A), Overton (State Hwy 24B), Kearney (State Hwy 44), Shelton (State Hwy 10D), and Grand Island (US-34). One additional bed-load sample has been collected at the Elm Creek Bridge (US-183). Sampling flows have been as low as 920 cfs, and ranged up to nearly 12,000 cfs during the September 2013 flood

(Table 3.3) As of 2014, nine (9) samples have been collected at Darr, with 12 samples each at Overton, Kearney, and Shelton and 11 samples at Grand Island.

Typical of sediment-transport data, the sampled loads have exhibited high variability but show sufficiently strong trends to allow development of reasonable bed-load transport rating curves (**Figures 3.38** through **3.42**). The best-fit, power-function curves were developed using least-squares, linear regression on the logarithms of the measured bed loads and corresponding discharges, a well-accepted procedure in sediment-transport analysis (Runkel, et al, 2004; Shen and Julien, 1993). Correlation coefficients (R^2) for the best-fit relationships range from 0.44 (Overton) to 0.78 (Darr). The curves indicate that the bed-load transport rates are reasonably consistent through the reach, although Overton generally has the lowest rates, and Darr has the highest rates at discharges exceeding about 1,000 cfs (**Figure 3.43**).

The samples contained 69- to 84-percent sand and 16- to 32-percent gravel, on average, with the Grand Island samples being the finest (84 percent sand) and the Overton samples being the coarsest (31 percent gravel) (**Figure 3.44**). In general, the percentage of sand in the samples tends to increase in the downstream direction. Most of the coarser fraction of the samples was in the very fine to fine gravel size range (i.e., 2 to 8 mm), with a few containing small amounts of medium gravel (8 to 16 mm). Although there is significant scatter in the data, both the median (D_{50}) size and the D_{84} size of the samples at all sites except Kearney tended to increase with increasing discharge (**Figures 3.45a** and **3.45b**). The contrary trend at Kearney is an artifact of the 11,500 cfs sample that was collected during the September 2013 flood. If this sample is eliminated from the data set, the trend is consistent with the other sites.

As will be discussed in a later section of this report, the rating curves were developed to provide a means of estimating the quantity of sediment carried past each of the measurement locations over specific periods of time. Because the regressions are performed in logarithmic space, simply transforming the results back to linear space provides an unbiased estimate of the median value of the loads, but not the mean value that is most important to the analysis (Hirsch et al., 1993; Ferguson 1986; Thomas 1985; Walling 1977). Several methods for correcting for this bias have been proposed in the literature, including the *smearing estimate* (Duan, 1983) and the Maintenance of Variance Unbiased Estimator (*MVUE*) method (Cohn and Gilroy, 1991). The *smearing estimate* results in a constant percentage adjustment to all of the estimated loads, regardless of the distribution of the underlying data, while the *MVUE* method provides an adjustment for each load based on the statistical distribution of the data. USGS (1992) recommends the *MVUE* method, and this method was, therefore, selected for use in this study. The rating curves that reflect the *MVUE* adjustments are shown by the blue lines in Figures 3.38 through 3.42.

Table 3.3. Summary of bed-load sediment discharge measurements taken since the start of the monitoring program in 2009. Also shown are the correlation coefficients (R^2) for best-fit, power-function regression lines through each of the data sets.

Sample Location	Discharge Range (cfs)			Total Samples	R^2
	1,000-3,000	3,000-5,000	>5,000		
Darr	5	2	2	9	0.78
Overton	3	6	3	12	0.44
Elm Creek	0	0	1	1	N/A
Kearney	4	5	3	12	0.47
Shelton	4	6	2	12	0.56
Grand Island	3	4	3	10	0.64
Total Samples	19	23	14	56	

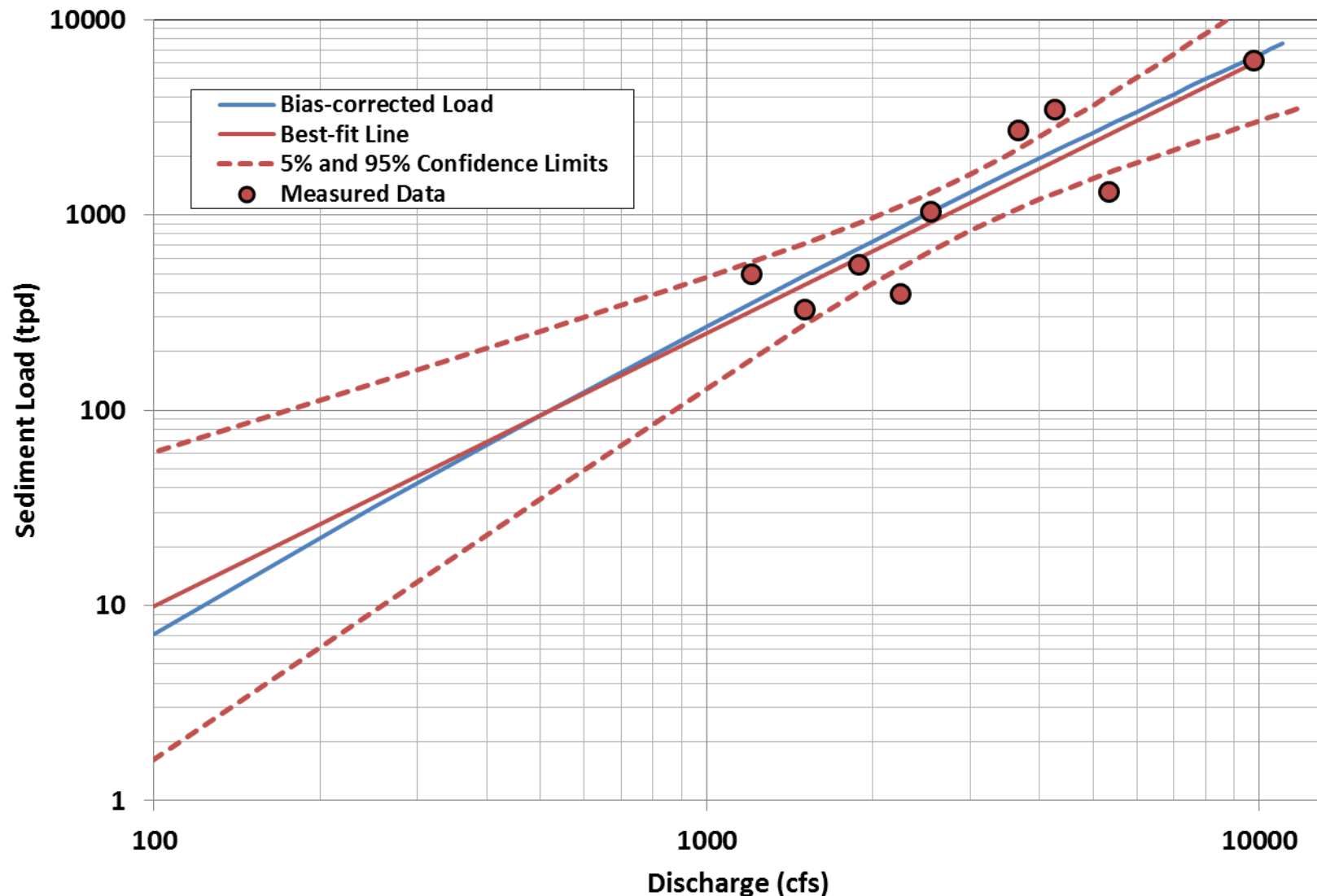


Figure 3.38. Bed-load transport rates measured at the Darr Bridge between 2009 and 2014. Also shown is the best-fit, power-function line through the data, the upper and lower 95-percent confidence bands on the best-fit line, and the MVUE bias corrected line.

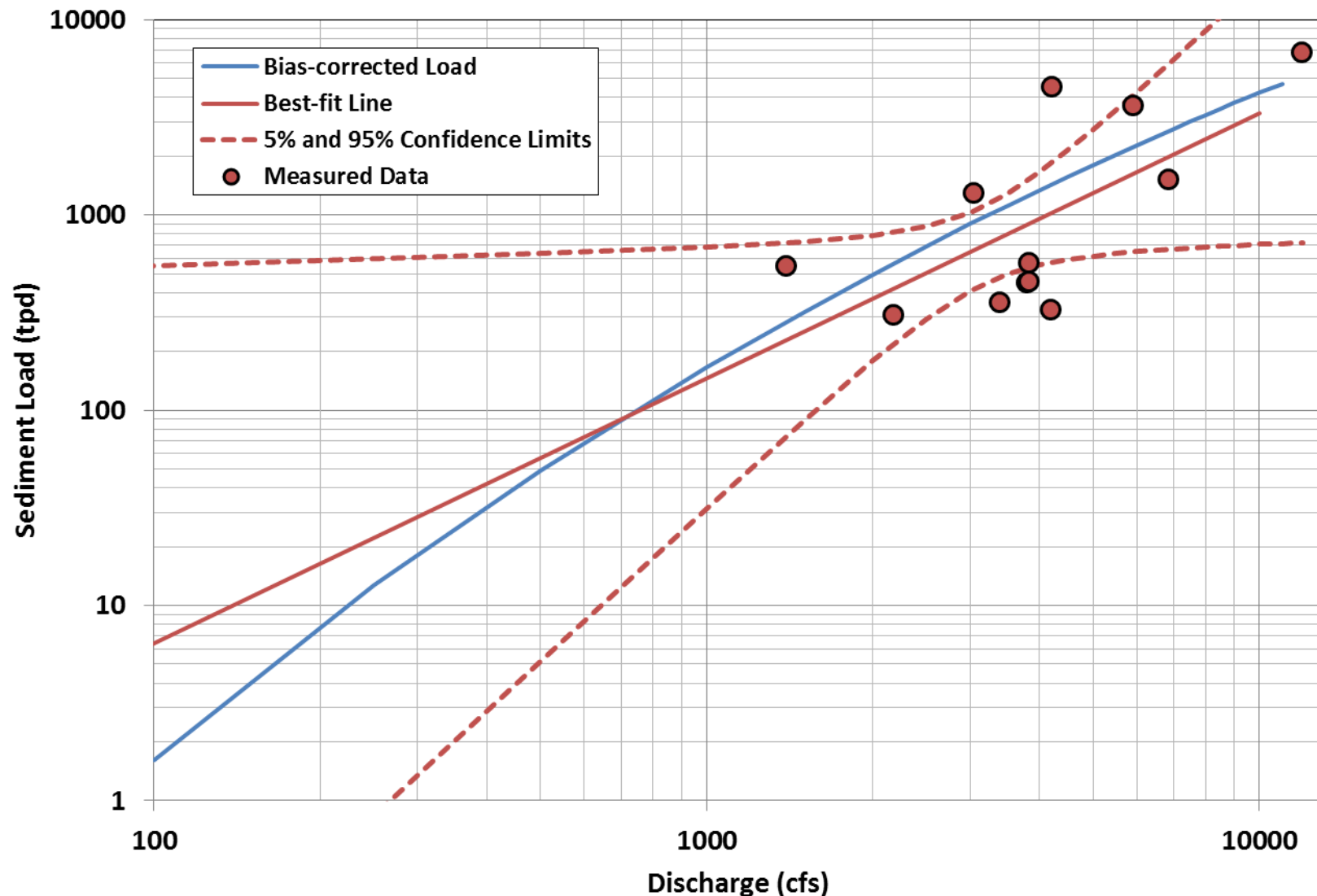


Figure 3.39. Bed-load transport rates measured at the Overton Bridge between 2009 and 2014. Also shown is the best-fit, power-function line through the data, the upper and lower 95-percent confidence bands on the best-fit line, and the MVUE bias corrected line.

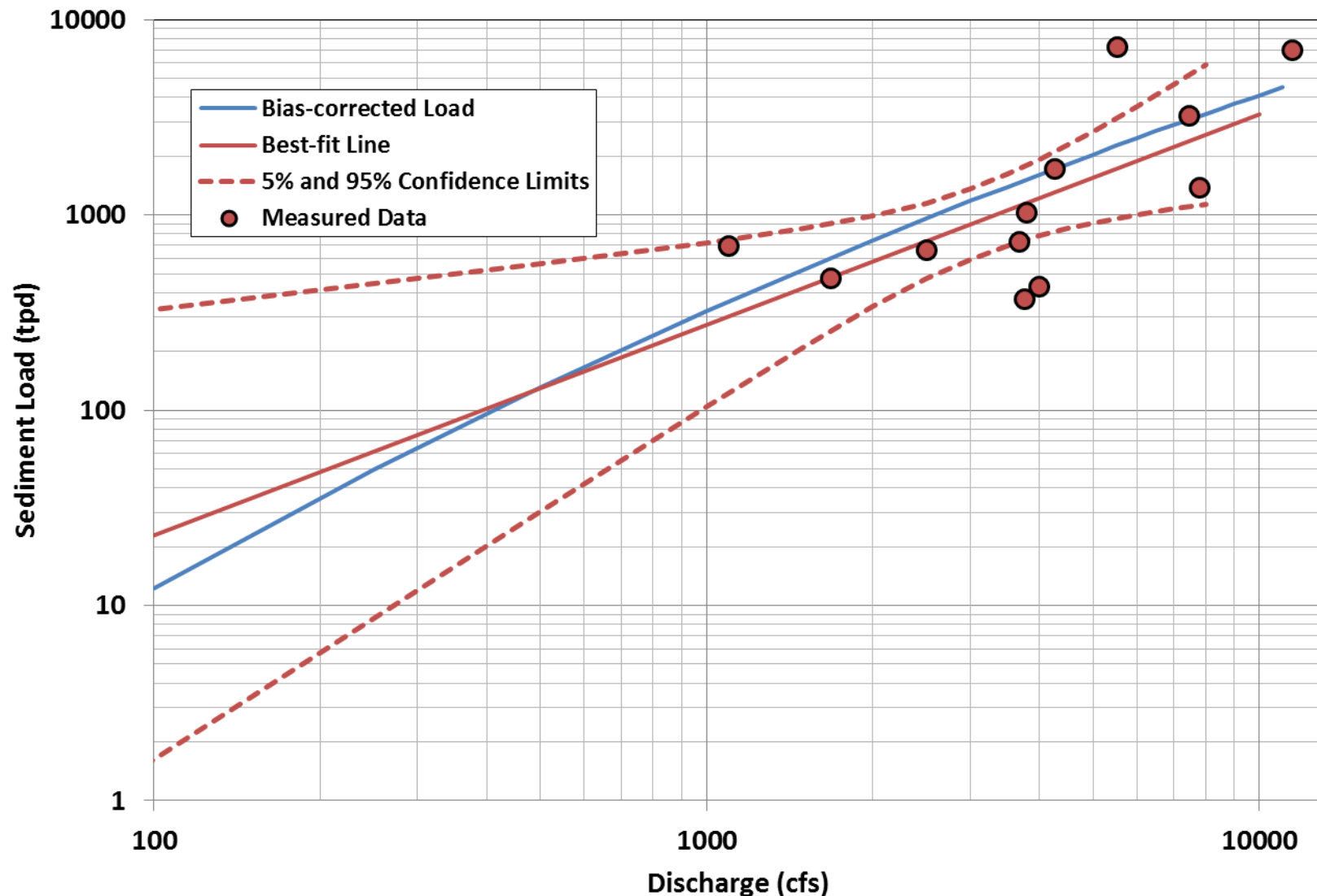


Figure 3.40. Bed-load transport rates measured at the Kearney Bridge between 2009 and 2014. Also shown is the best-fit, power-function line through the data, the upper and lower 95-percent confidence bands on the best-fit line, and the MVUE bias corrected line.

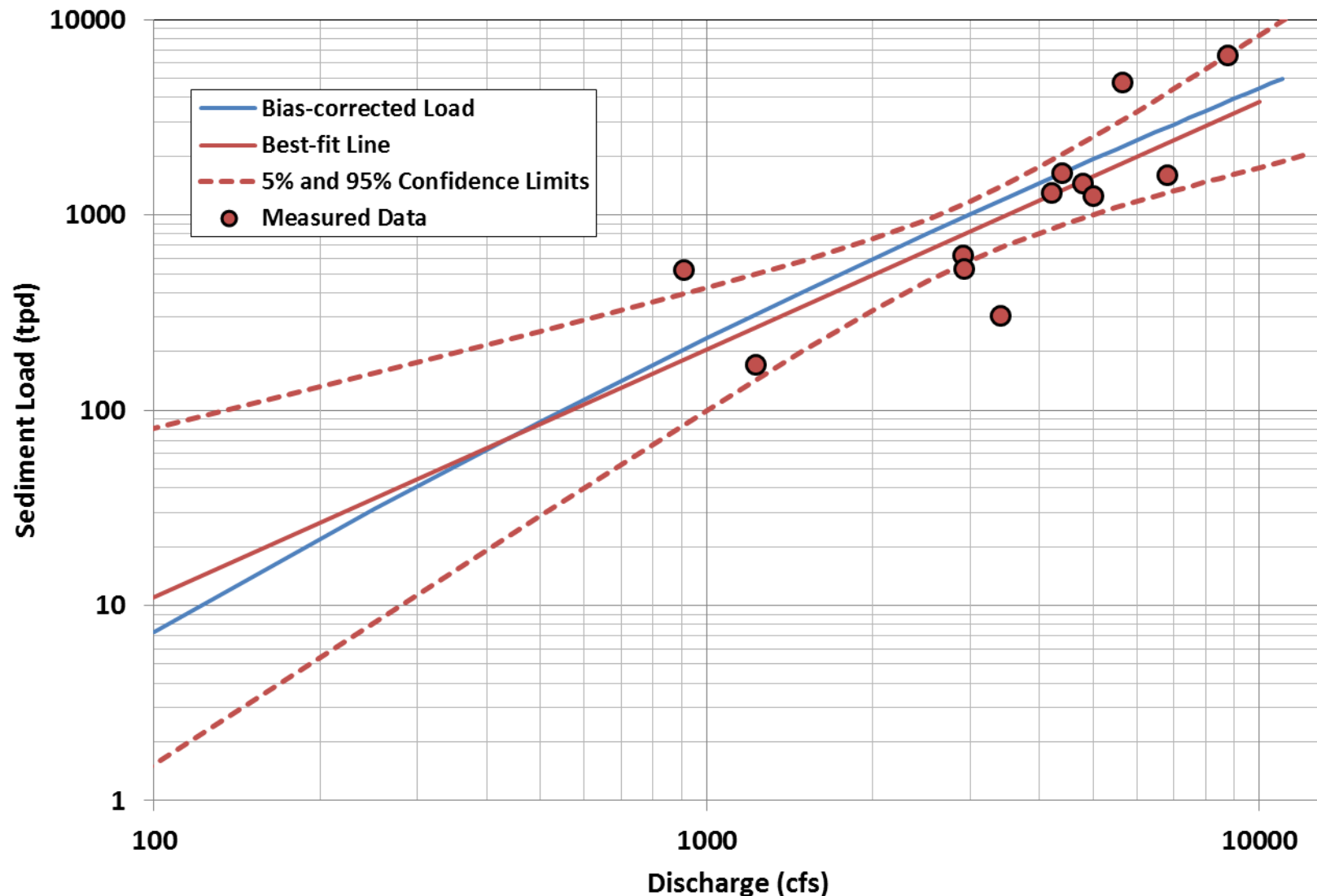


Figure 3.41. Bed-load transport rates measured at the Shelton Bridge between 2009 and 2014. Also shown is the best-fit, power-function line through the data, the upper and lower 95-percent confidence bands on the best-fit line, and the MVUE bias corrected line.

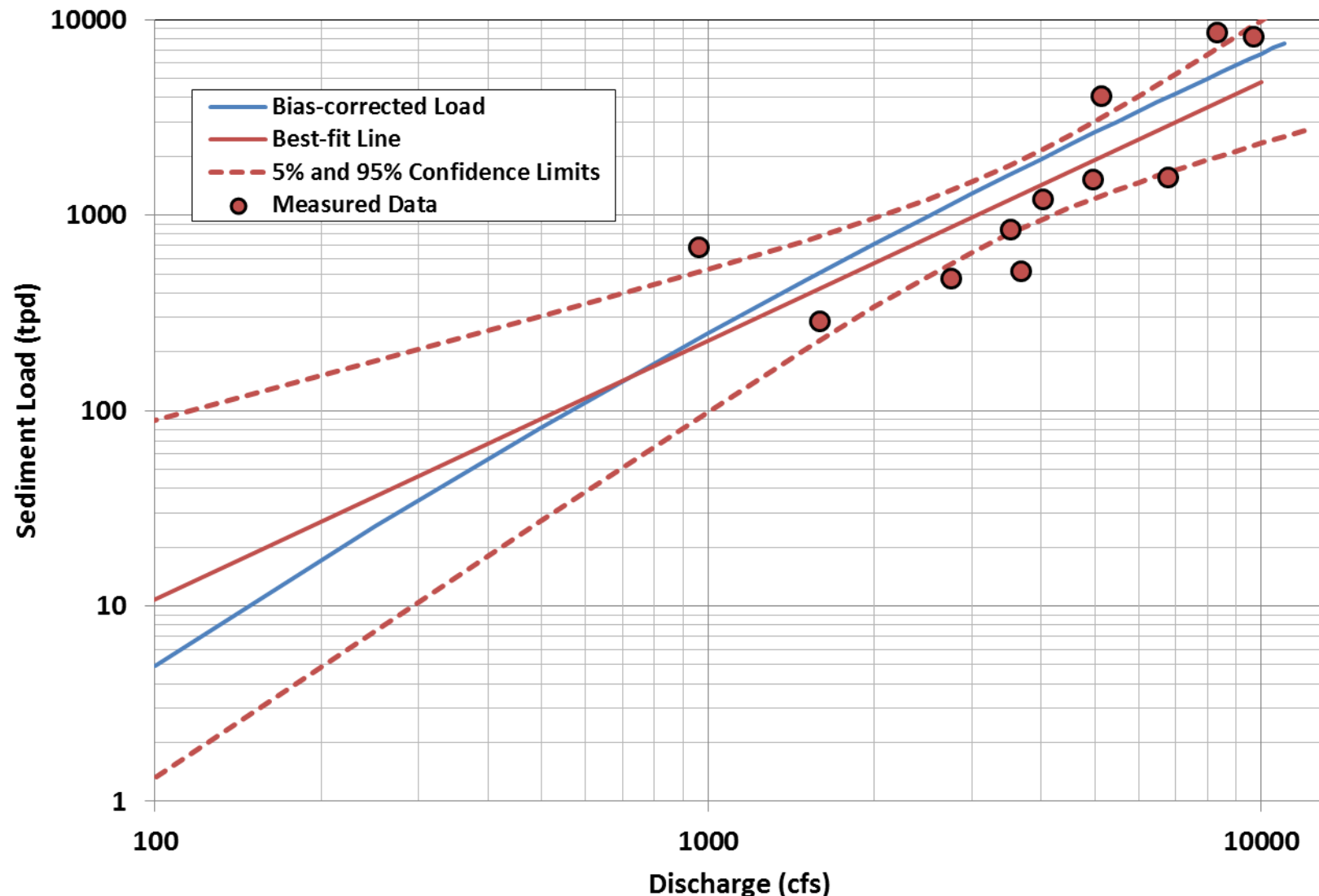


Figure 3.42. Bed-load transport rates measured at the Grand Island Bridge between 2009 and 2014. Also shown is the best-fit, power-function line through the data, the upper and lower 95-percent confidence bands on the best-fit line, and the MVUE bias corrected line.

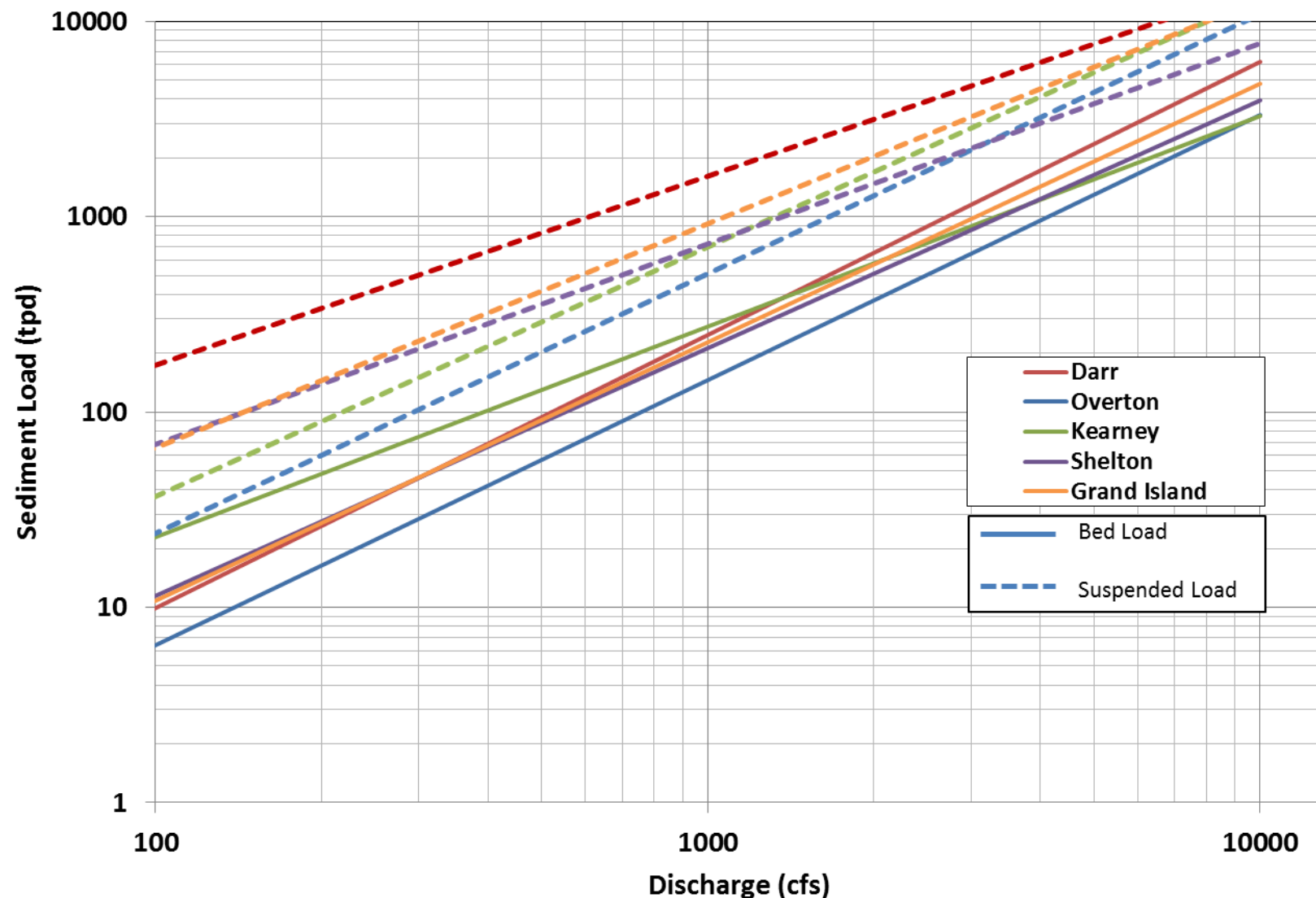


Figure 3.43. Power-function, best-fit lines for the measured bed- and suspended-sediment-transport rates at the five measurement sites.

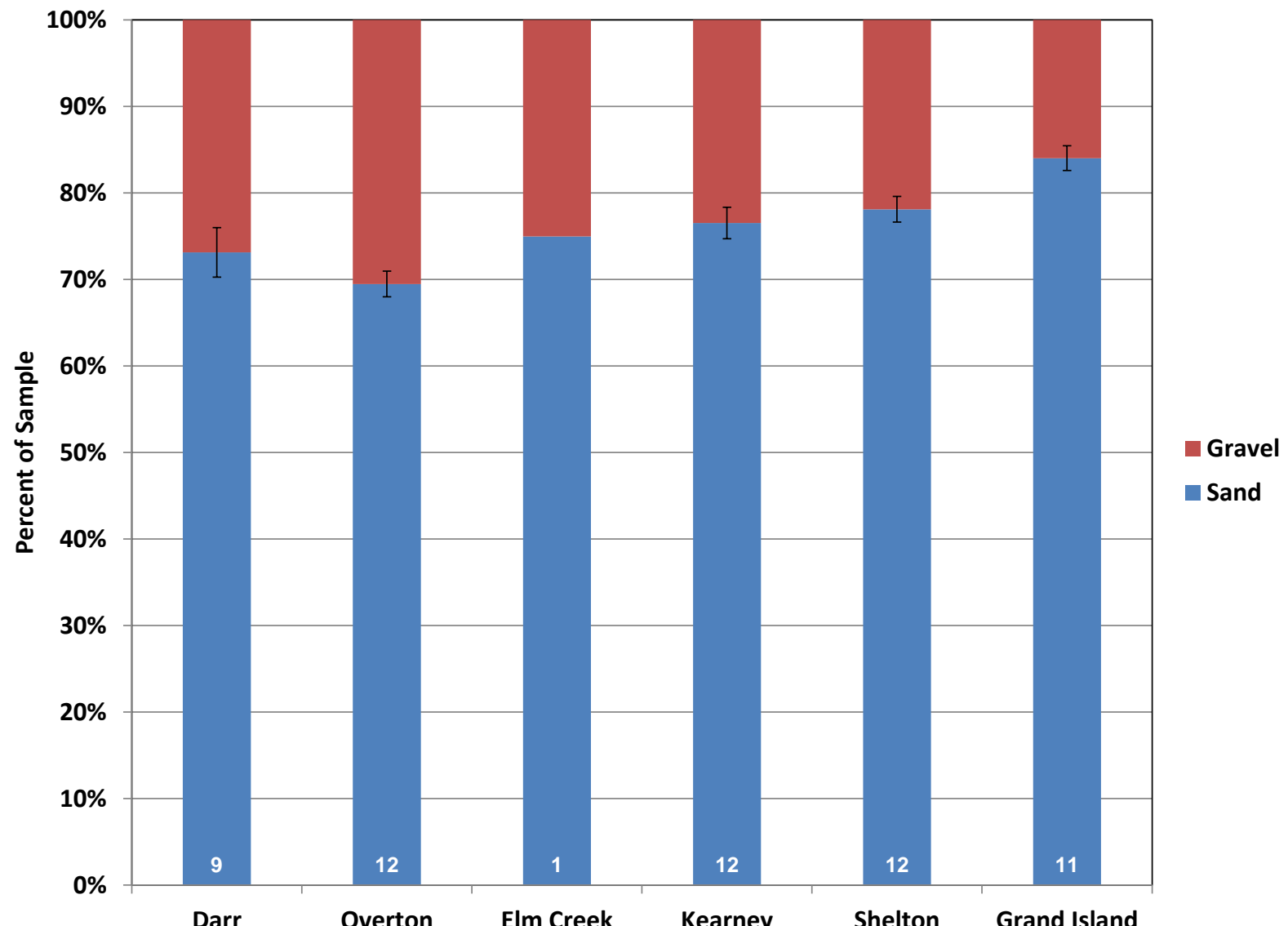


Figure 3.44. Average percentage of sand and gravel in the bed-load samples from the five primary measurement sites and the single sample collected at the Elm Creek Bridge. Embedded values represent number of samples at each site; whiskers represent ± 1 standard error about the mean.

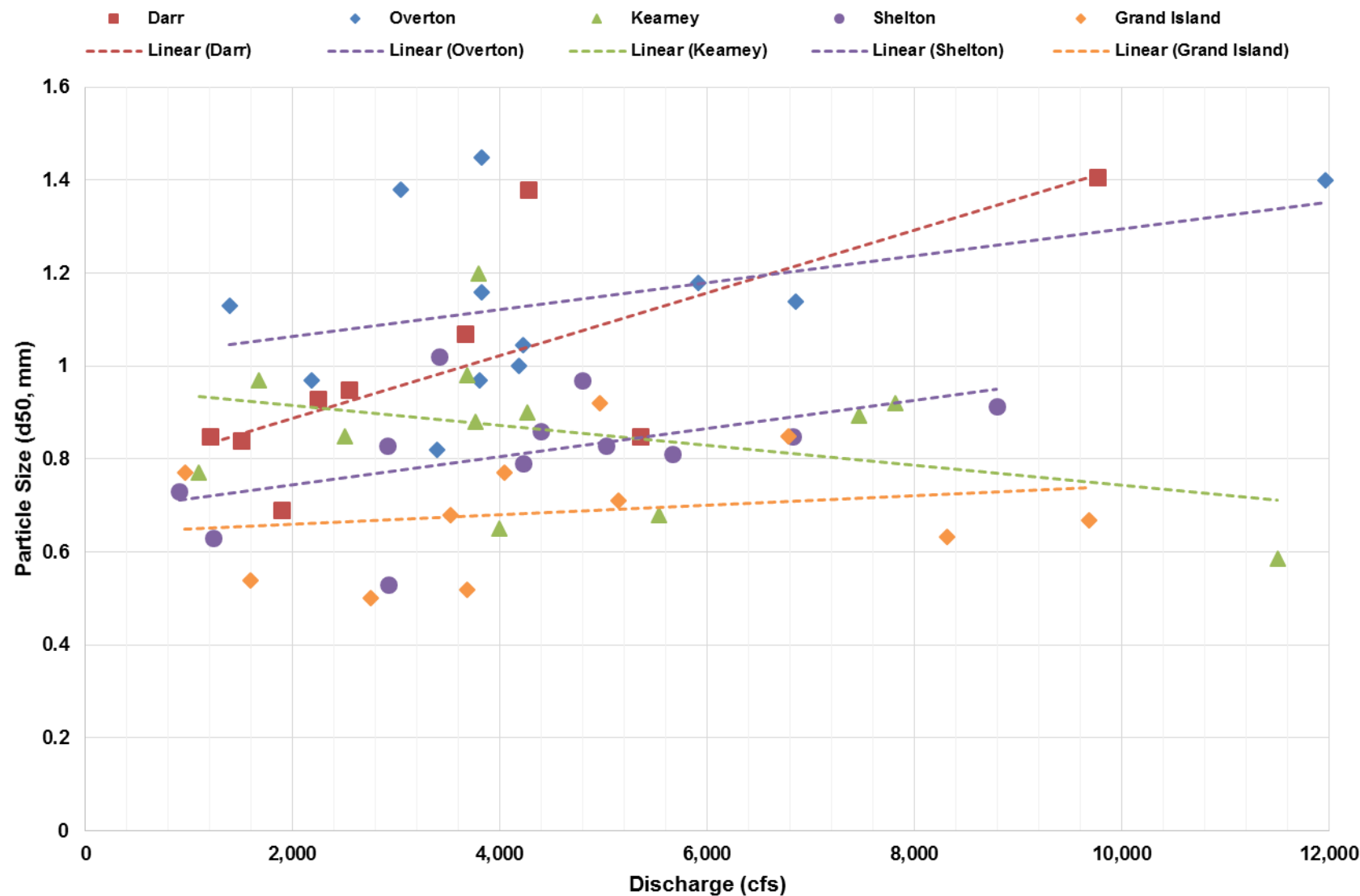


Figure 3.45a. Particle size of bed-load samples from the five measurement sites, 2009-2014: median (D₅₀).

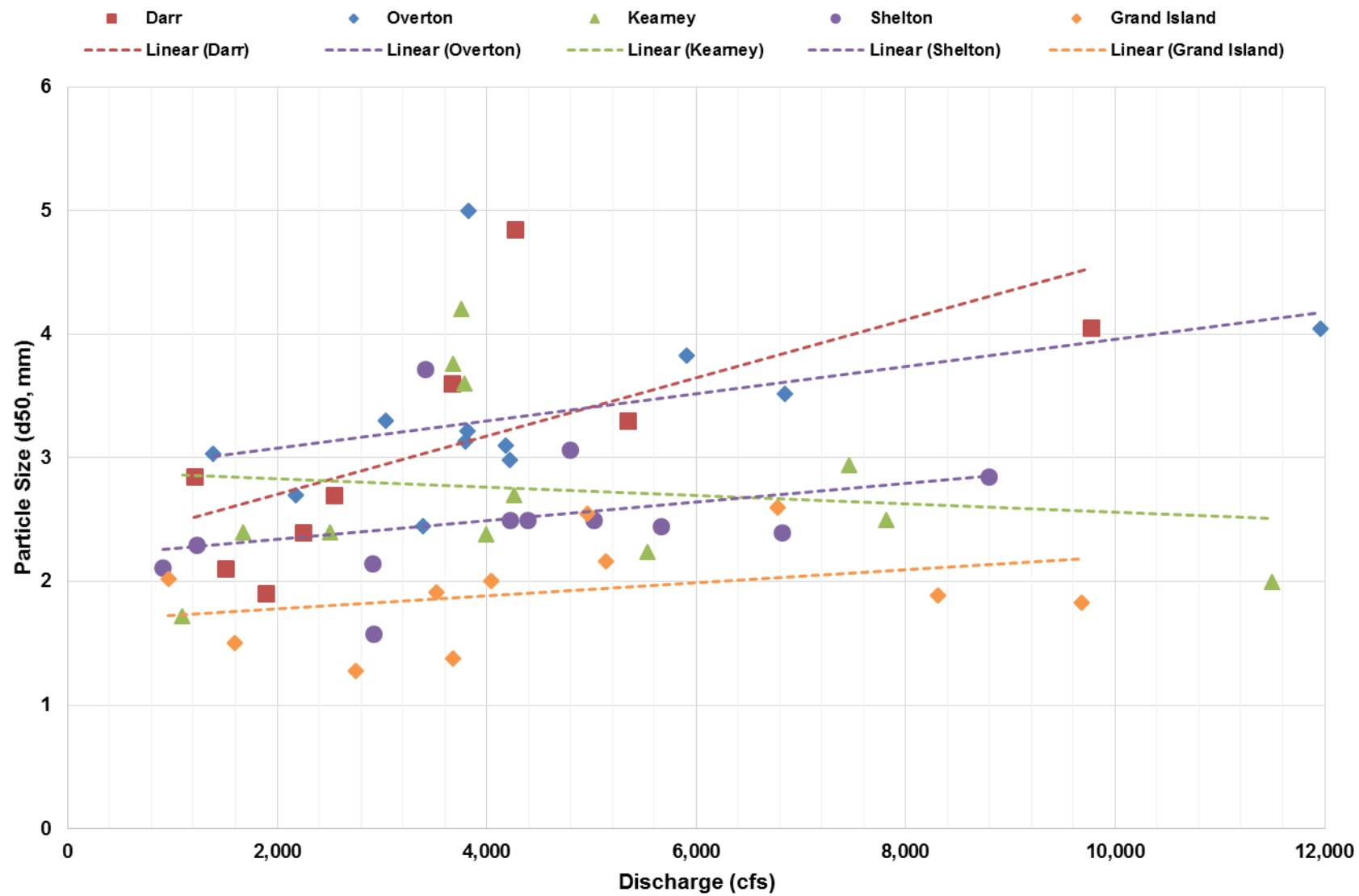


Figure 3.45b. Particle size of bed-load samples from the five measurement sites, 2009-2014: median (D_{84}).

3.5.2 Suspended Sediment Load versus Discharge Rating Curves (DAP 5.5.2)

A total of 62 suspended sediment samples have been collected at the five designated bridge sites at flows ranging above 12,000 cfs (**Table 3.4**) An additional sample was collected at the Elm Creek Bridge during the September 2013 flood, and single samples were collected at Lexington (US-283) in 2009 and at Gibbon (State Hwy 10C) in 2011. For purposes of the analysis, the Lexington sample was included in the Darr data set. The total suspended sediment concentrations (i.e., silt/clay and sand) ranged from about 125 ppm to 1,700 ppm. Due to the significant scatter in the data, the correlation between suspended sediment concentration and discharge is not statistically significant at any of the sites (**Figure 3.46**).

The samples contained 57-percent to 81-percent silt/clay and 19- to 43-percent sand, on average, with Overton samples having the most sand (~81 percent) and the Shelton samples having the least (~57 percent) (**Figure 3.47**). There is essentially no correlation between the median size of the material in these samples and discharge. In general, the percentage of silt/clay in the samples tended to increase in the downstream direction to Shelton, and Grand Island having sand content similar to Kearney.

To facilitate analysis of the sediment-transport balance that will be described in Section 4.1, the sand fraction of the samples was separated from the silt/clay fraction and suspended sand load rating curves were developed from the resulting sand-load data sets (**Figures 3.48** through **3.52**). With the exception of the Shelton site, all of the suspended sediment loads were considered in the regression analysis. At Shelton, the sand load for the sample that was collected on September 26, 2013, on the rising limb of the flood hydrograph appears to unreasonably low. The residual for this sample when it is included in the regression has a Z-score of -1.99, confirming that it is, in fact, an outlier. Review of the field notes and discussions with the field crew revealed nothing that would suggest that conditions during the sampling were different from previous sampling efforts. As will be discussed Section 4.1.3, inclusion of this data point results in a rating curve that appears to predict unreasonably low total sand transport volumes at the Shelton site compared to the up- and downstream sites. As a result, the data point was not considered in the analysis.

Correlation coefficients (R^2) for the above relationships range from 0.72 (Overton) to 0.86 (Shelton), similar to those of the bed-load rating curves. For purposes of estimating annual sediment loads, bias-correct lines were also developed using the MVUE method described in the previous section. The curves indicate that the suspended sand loads vary considerably through the reach, with Darr being 3 to 5 times higher than at the other sites at flows in the range of 500 cfs, decreasing to 2 to 3 times higher in the range of 5,000 cfs (Figure 3.48). A substantial amount of the sand in these samples is less than 1 mm (i.e., fine, medium and coarse sand), with relatively minor amounts of very coarse sand (1 – 2 mm).

Table 3.4. Summary of suspended sand load measurements taken since the start of the monitoring program in 2009. Also shown are the correlation coefficients (R^2) for best-fit, power-function regression lines through each of the data sets.

Sample Location	Discharge Range (cfs)			Total Samples	R^2
	1,000-3,000	3,000-5,000	>5,000		
Darr/Lexington	6	2	3	11	0.75
Overton	5	5	4	14	0.72
Elm Creek	0	0	1	1	N/A
Kearney	6	2	4	12	0.77
Gibbon	0	0	1	1	N/A
Shelton	6	3	3	12	0.86
Grand Island	5	3	5	13	0.76
Total Samples	28	15	20	64	

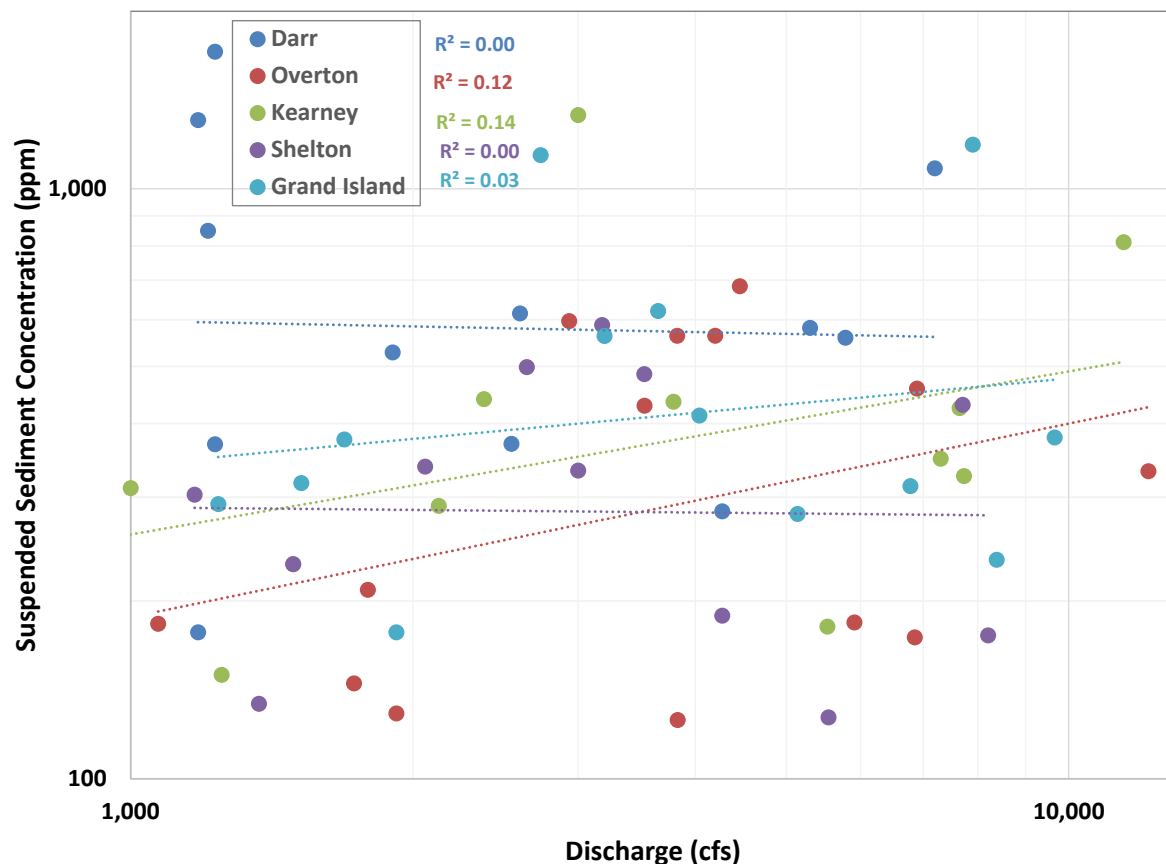


Figure 3.46. Total suspended sediment concentrations from measurements taken since the start of the monitoring program in 2009.

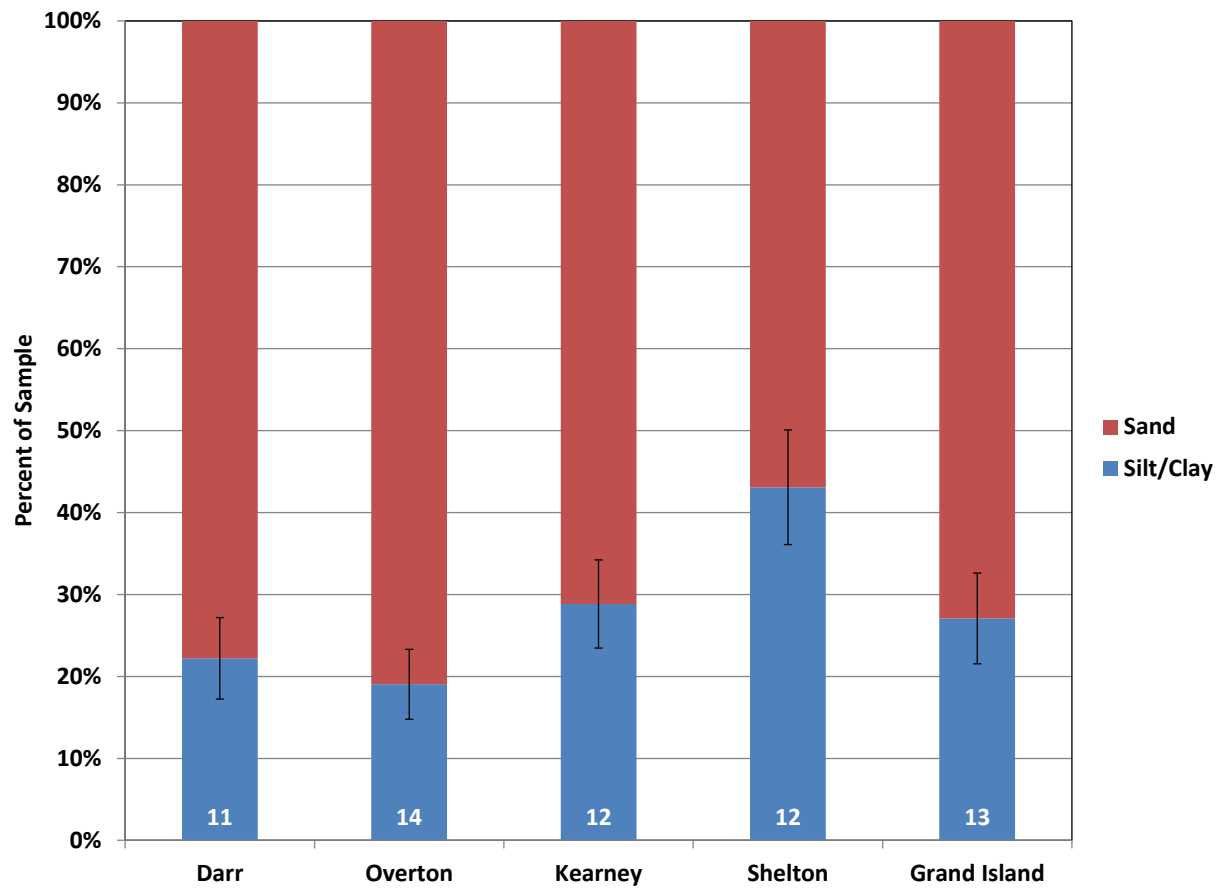


Figure 3.47. Average percentage of silt/clay and sand in the suspended sediment samples from the five primary measurement sites. Embedded values represent number of samples at each site; whiskers represent ± 1 standard error about the mean.

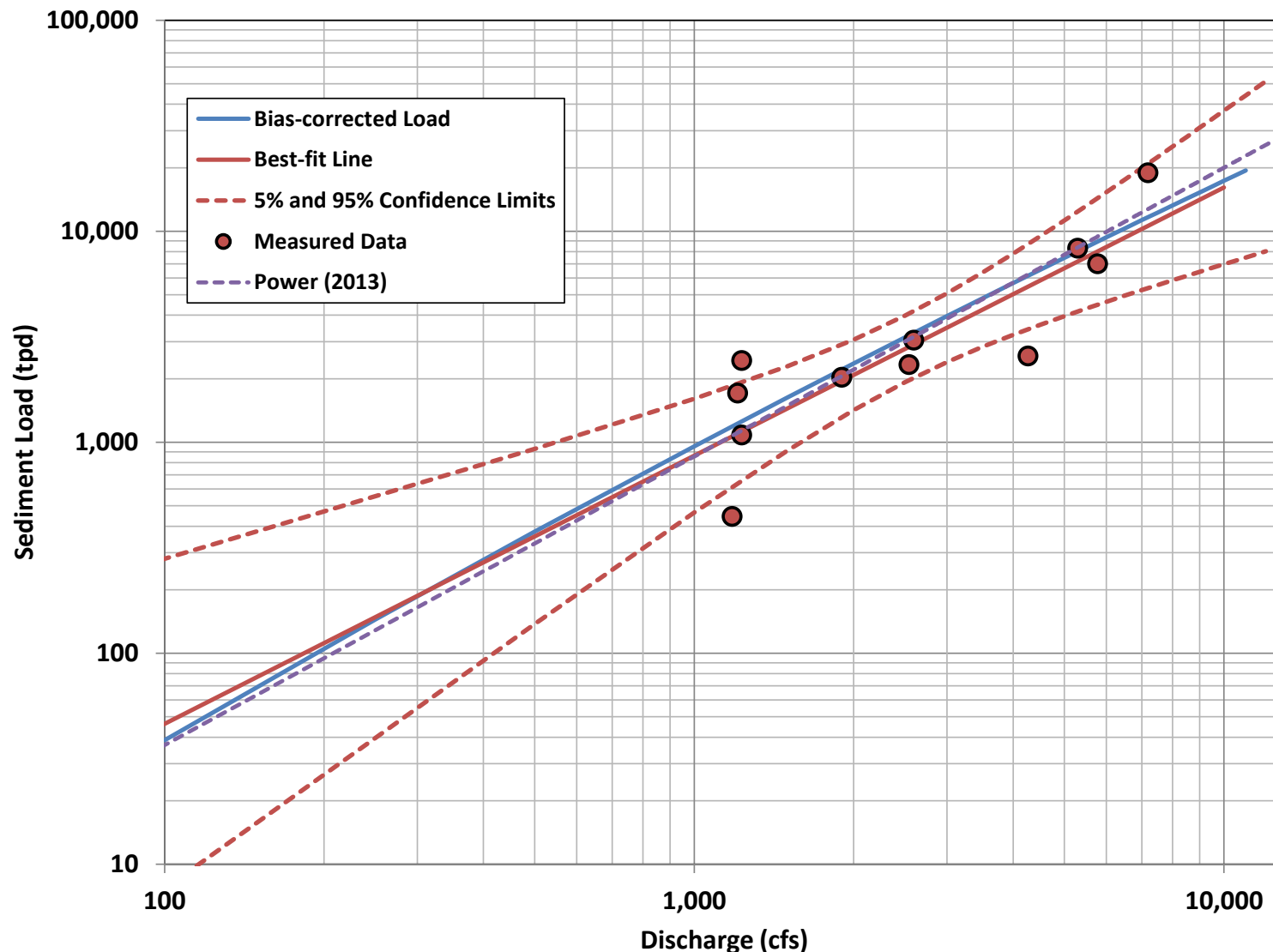


Figure 3.48. Suspended sand transport rates measured at the Darr Bridge between 2009 and 2014. Also shown is the best-fit, power-function line through the data, the upper and lower 95-percent confidence bands on the best-fit line, and the MVUE bias corrected line.

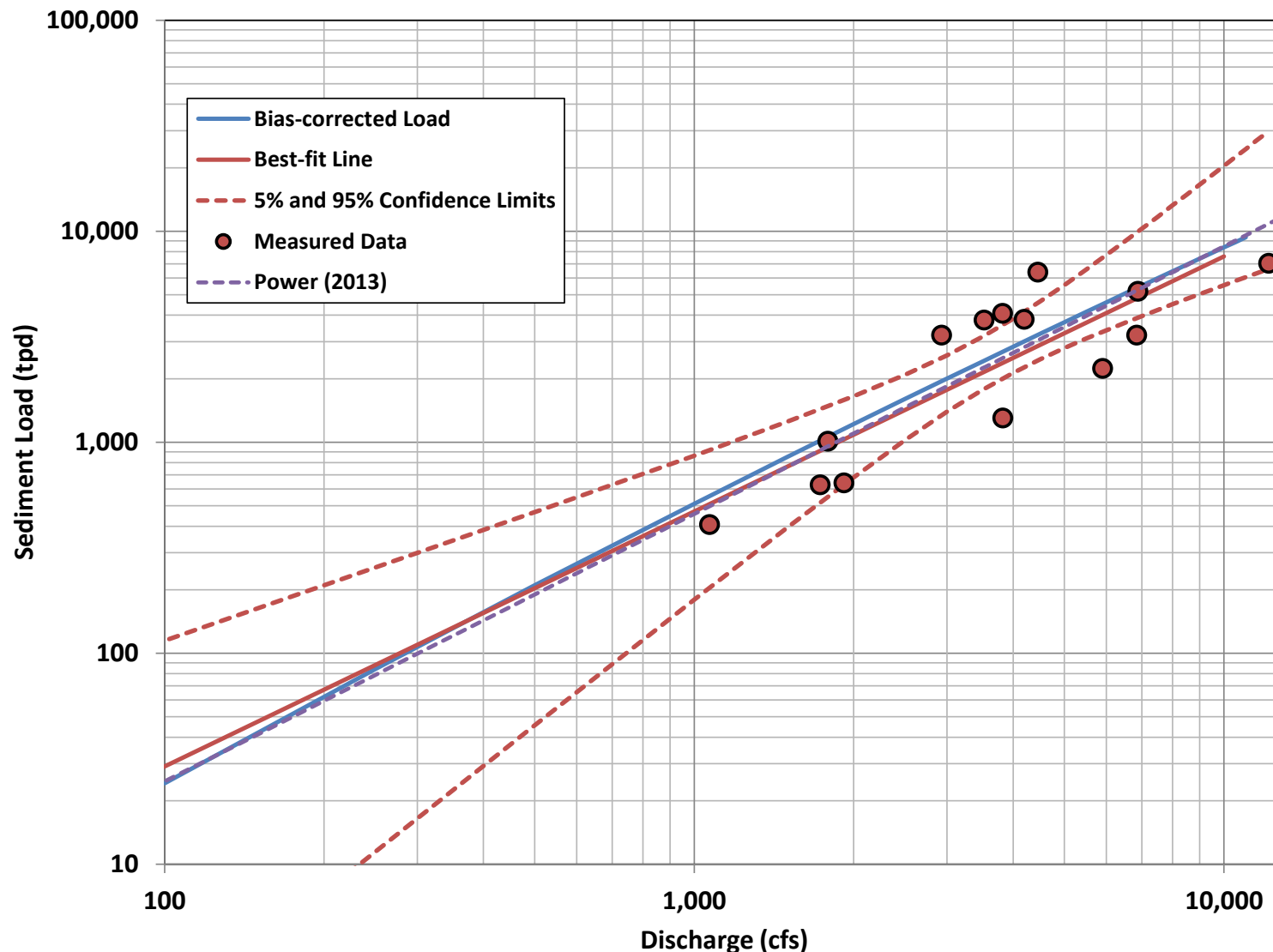


Figure 3.49. Suspended sand transport rates measured at the Overton Bridge between 2009 and 2014. Also shown is the best-fit, power-function line through the data, the upper and lower 95-percent confidence bands on the best-fit line, and the MVUE bias corrected line.

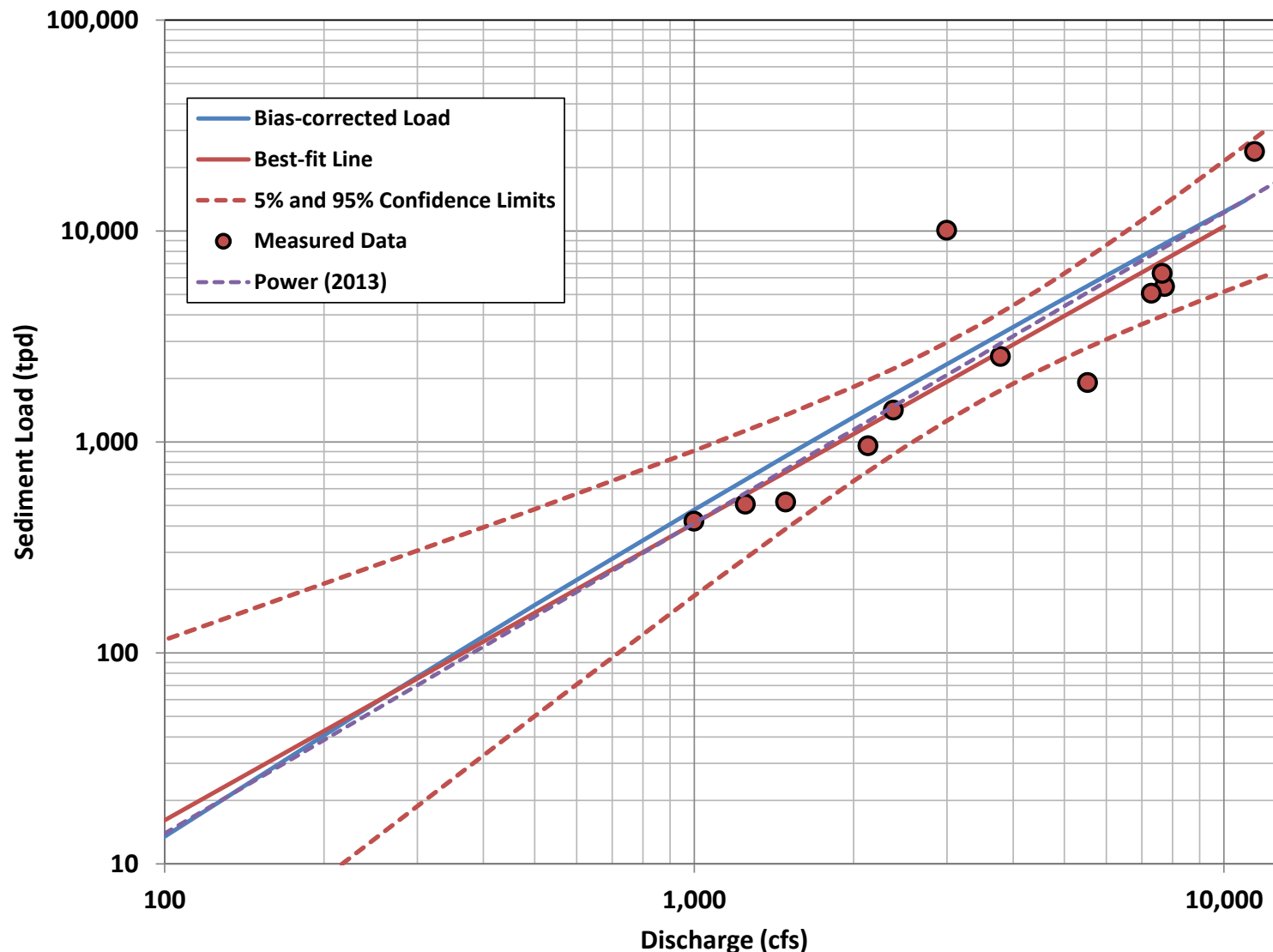


Figure 3.50. Suspended sand transport rates measured at the Kearney Bridge between 2009 and 2014. Also shown is the best-fit, power-function line through the data, the upper and lower 95-percent confidence bands on the best-fit line, and the MVUE bias corrected line.

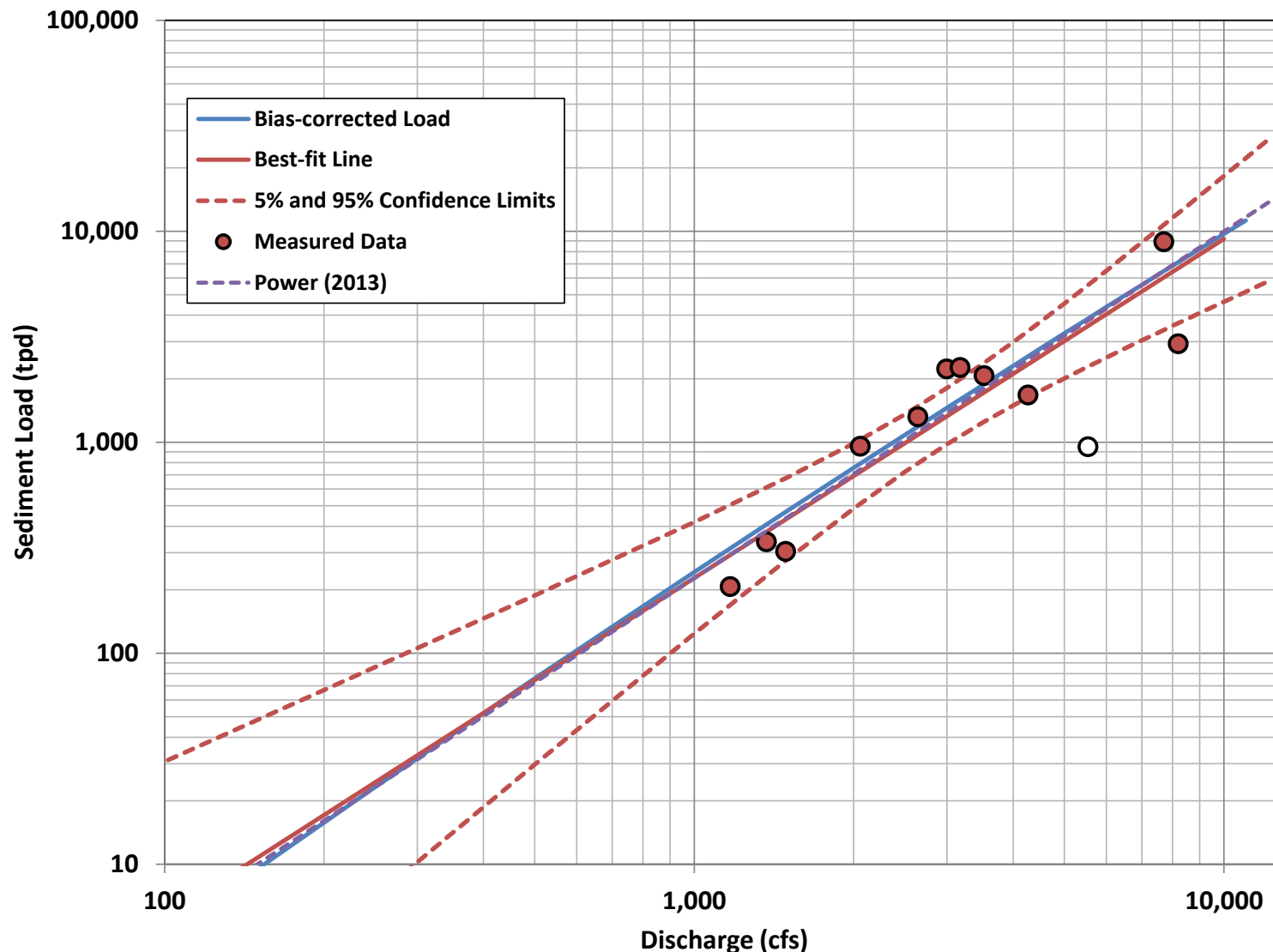


Figure 3.51. Suspended sand transport rates measured at the Shelton Bridge between 2009 and 2014. Also shown is the best-fit, power-function line through the data, the upper and lower 95-percent confidence bands on the best-fit line, and the MVUE bias corrected line.

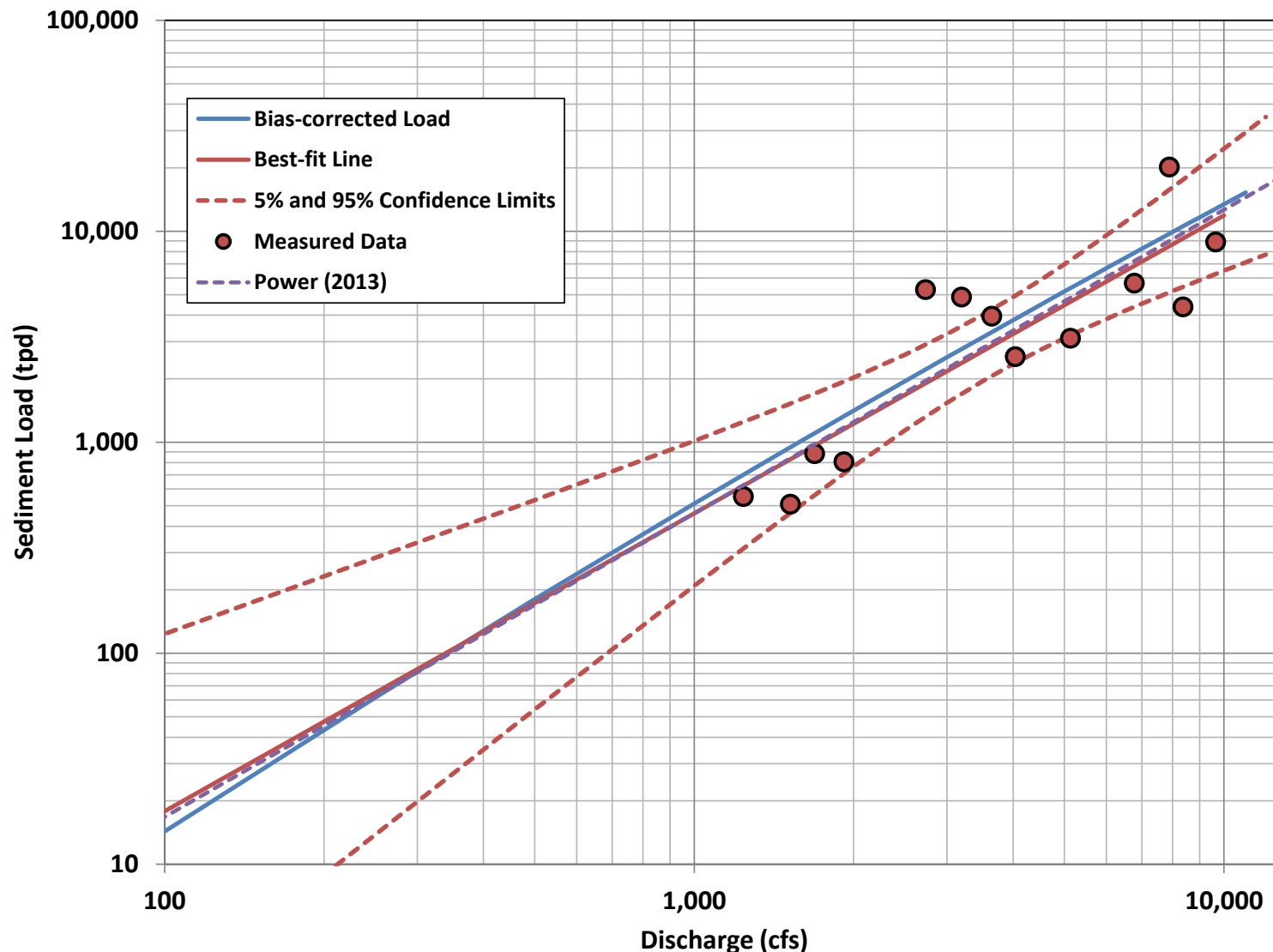


Figure 3.52. Suspended sand transport rates measured at the Grand Island (Highway 34/Highway2) Bridge between 2009 and 2014. Also shown is the best-fit, power-function line through the data, the upper and lower 95-percent confidence bands on the best-fit line, and the MVUE bias corrected line.

3.5.3 Bed-material Grain-size Distribution and Distribution Parameters (DAP 5.5.3)

The total number of bed material samples collected during each of the 6 years of monitoring that have been completed, to-date, ranged from 230 (2012) to 260 (2009). These sample sets included 9 to 10 samples at the surveyed APs and a single sample at each of the five bridges at which bed-load measurements are being made (except for 2012, when no sample was collected at the Darr Bridge). For purposes of evaluating trends in the typical bed material sizes along the reach, the samples at each of the APs were averaged to provide a representative bed-material gradation (**Figure 3.53**). The resulting median (D_{50}) bed-material size generally consisted of very coarse sand (1 to 2 mm) in the upstream part of the reach, decreasing to coarse sand (0.5 to 1 mm) in the downstream part of the reach. Linear regression of the D_{50} versus distance along the reach (excluding Reach 2, J-2 Return Channel) indicates that the trend of decreasing grain size in the downstream direction is statistically significant in all years except 2012. The 2012 trend is not statistically significant primarily because of the relatively fine gradation of the samples at AP35 and AP39. A sample set collected by the Bureau of Reclamation in 1989 showed similar trends, although the median grain size was typically finer than those collected as part of this monitoring program. Samples collected in 2014 are consistent with previous years throughout the entire program reach.

The reach-averaged D_{50} of the 1989 Reclamation samples was 0.72 mm, and the average D_{84} and D_{16} was 0.34 and 2.35 mm, respectively (**Figure 3.54**). The 2009 bed-material samples were considerably coarser, with average D_{50} of about 1.2 mm and D_{84} and D_{16} of 0.77 and 4.3 mm, respectively. The data showed a general finer trend from 2010 to 2012, when reach-averaged D_{50} was 0.72 mm and the D_{84} and D_{16} were 2.44 and 0.39 mm, respectively. The samples became coarser in 2013 and 2014, with the d_{50} increasing to 1.0 mm, with D_{16} and D_{84} of 0.36 and 3.84 mm, respectively. Based on the non-parametric Kruskal-Wallis test, the difference between the 2012 average and all of the other years except 2013 was statistically significant at the 90-percent confidence level, and the difference between 2009 and 2013 was also statistically significant. The differences between all other pairs of years were not statistically significant.

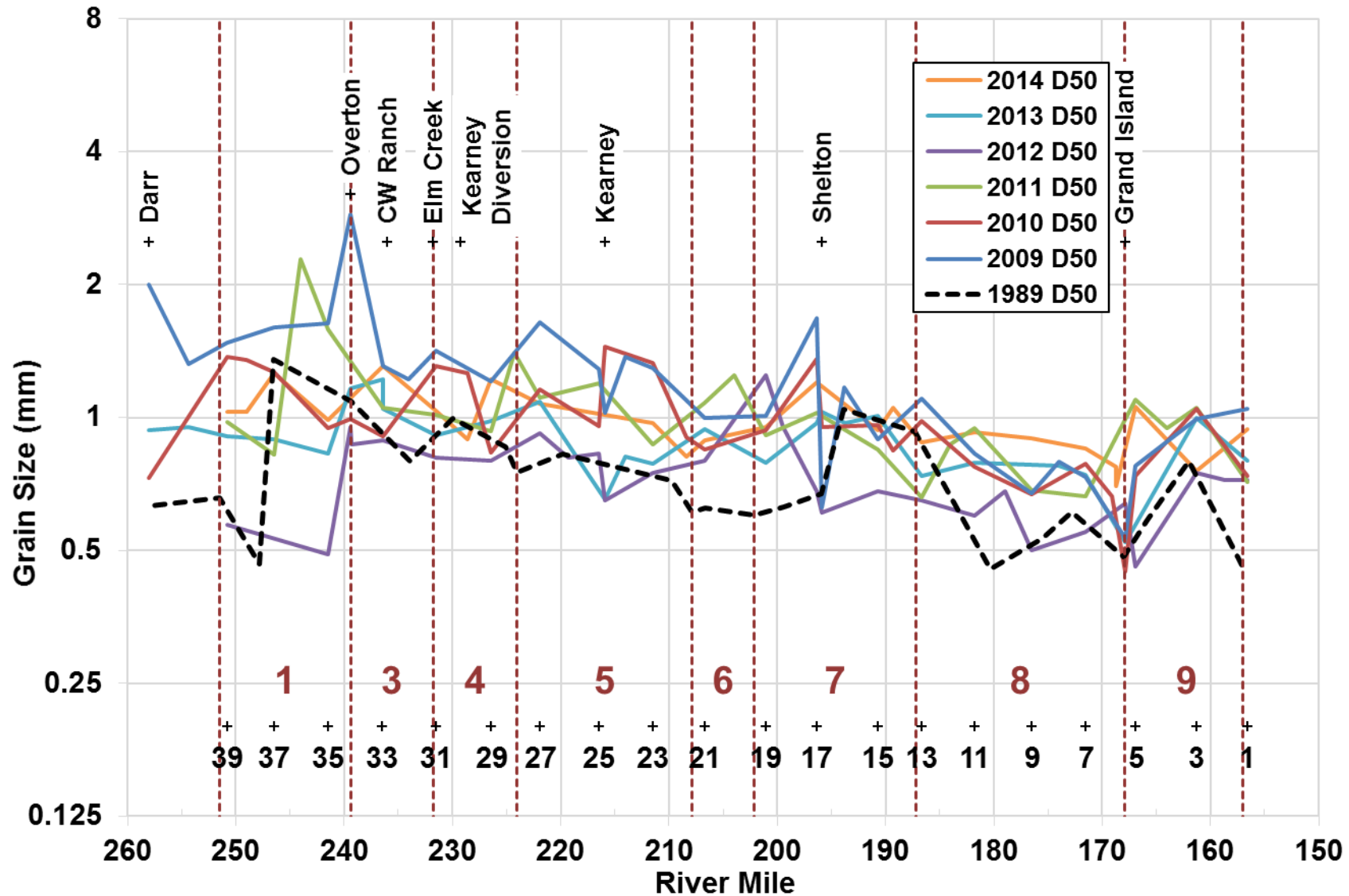


Figure 3.53. Average median (D₅₀) size of bed material samples collected at the APs during 2009 through 2014 monitoring surveys. Also shown are the D₅₀ sizes of the samples collected by Reclamation in 1989.

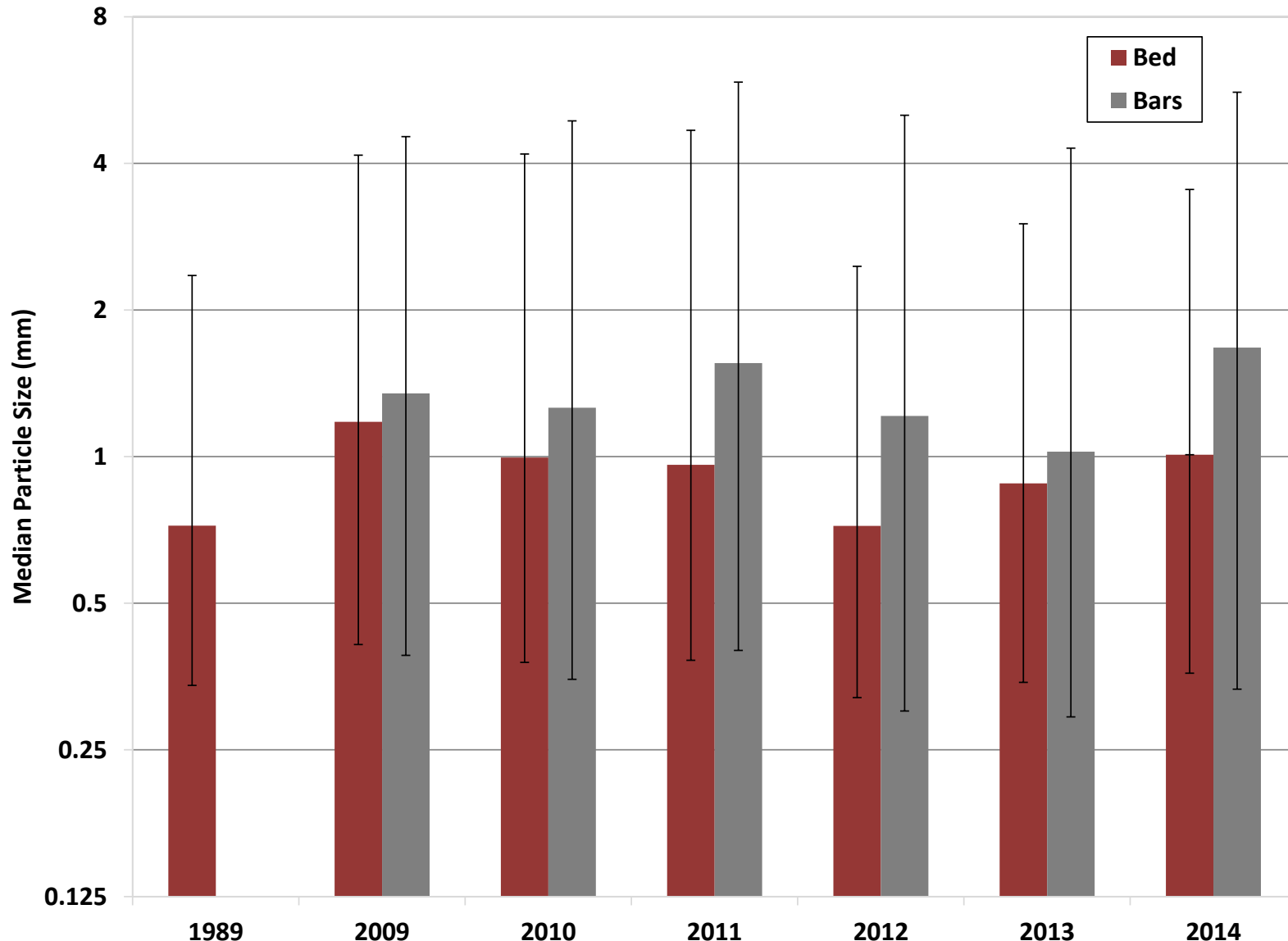


Figure 3.54. Reach averaged median (D_{50}) particle size of samples collected for this monitoring program in 2009 through 2014, and by Reclamation in 1989. Whiskers represent reach-averaged D_{16} and D_{84} .

3.5.4 Bar Material Grain-size Distribution (DAP 5.5.4)

The gradations of the bar material samples were generally coarser and more highly variable than the bed material samples (**Figure 3.55**). The D_{50} of these samples varied from medium sand (0.25-0.5 mm) to fine gravel (4 to 8 mm). Visual inspection of the plot indicates a general fining trend in the downstream direction, however, the variability along the reach is sufficiently high that this trend is not statistically significant. The reach-averaged D_{50} increased from 1.35 mm in 2009 to 1.56 mm in 2011, and then declined to about 1.0 mm in 2014 (Figure 3.54). The reach-averaged D_{16} and D_{84} were similar to the bed material samples, with the D_{16} ranging from 0.3 mm (2013) to 0.4 mm (2011) and the D_{84} ranging from 3.8 mm (2013) to 5.9 mm (2011). Again, due to the relatively high variability in the sample gradations, the differences in year-to-year D_{50} values are not statistically significant.

3.5.5 Bank Material Grain Size Distribution (DAP 5.5.5)

Bank material samples are specified in the scope of work to be collected during the first and last year of the first increment. Therefore, no bank-material samples have been taken since 2009. Results from the 2009 samples are summarized in Ayres and Olsson (2010).

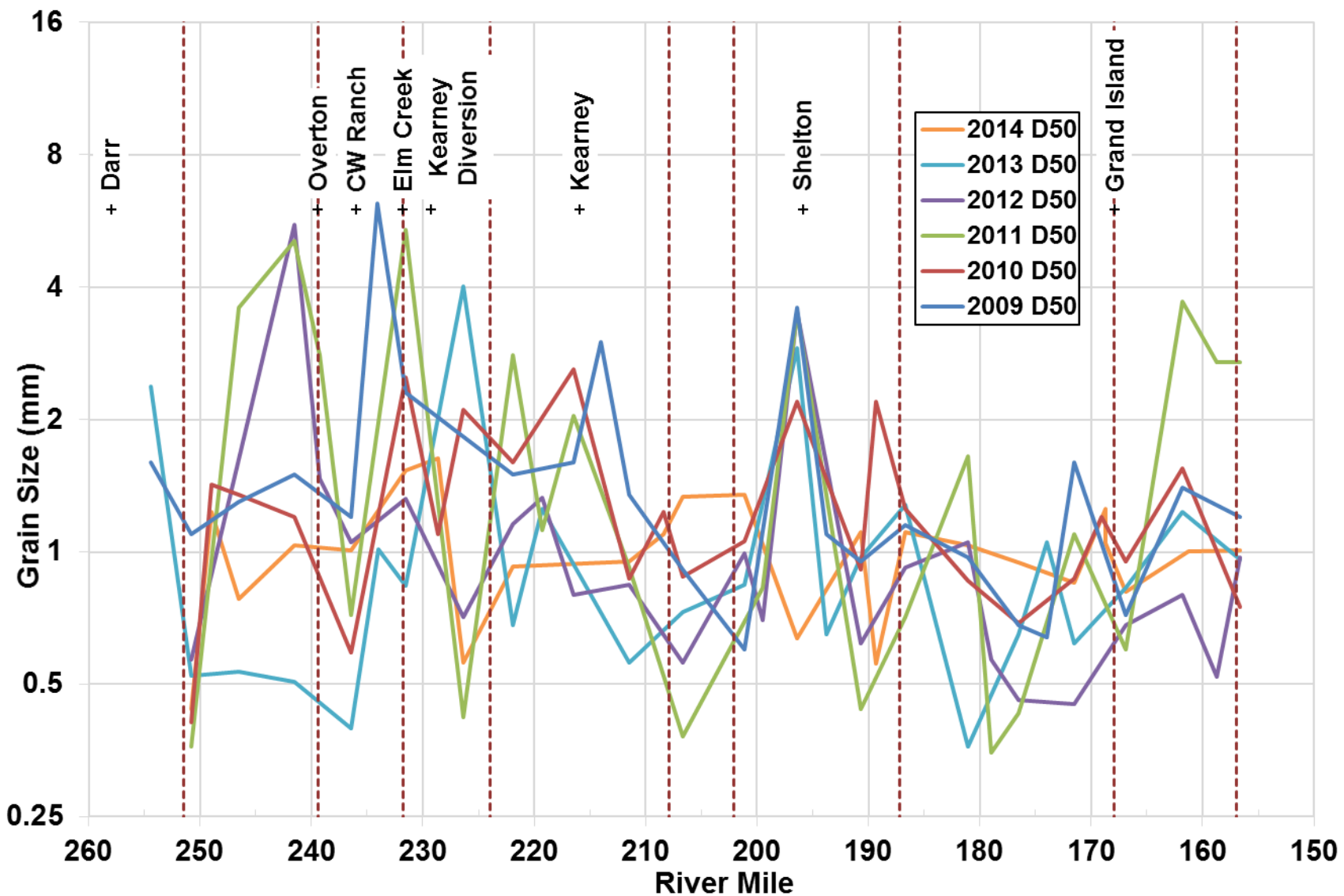


Figure 3.55. Reach-averaged median (d_{50}) size of bar-material samples collected during 2009 through 2014 monitoring surveys.

3.6 Whooping Crane Performance Metrics

3.6.1 Unobstructed Channel Width (DAP 5.6.1)

Unobstructed channel widths were determined based on the assumption that vegetation higher than 4.9 feet above a reference elevation would obstruct the line-of-sight for migrating whooping cranes. During the 2009 through 2012 surveys, vegetation heights were recorded in the field data in the following height classes:

- **Woody species:**
 - W1: 0-59 inches (<1.5 meters)
 - W2: 60-120 inches (1.5-3 meters)
- **Herbaceous species:**
 - H1: 0-12 inches (<0.3 meters)
 - H2: 13-59 inches (0.3 to 1.5 meters)
 - H3: 60-84 inches (1.5-2.1 meters)

For purposes of estimating unobstructed channel widths, the vegetation height for each quadrat was assumed to be the mid-point of the height class of the highest woody or herbaceous species that occurred in the quadrat. The elevation of the top of the vegetation was then estimated by adding the estimated height to the surveyed elevation in the center of the quadrat. The unobstructed width at each transect was then determined to be the longest distance between quadrats with top-of-vegetation elevation more than 4.9 feet above the reference elevation. Per the DAP, these distances were determined for three different reference elevations: (1) the water-surface elevation at 2,400 cfs, (2) the water-surface elevation corresponding to the median discharge during the spring migration season, and (3) the water-surface elevation for the median discharge during the fall migration season. As discussed in the methods section (Section 2.5.2.6), because of the uncertainty introduced by the height-class data, the data collection procedure was modified in 2013 to directly measure the unobstructed channel width using a laser range finder.

The average unobstructed channel widths at the pure panel APs ranged from about 140 feet (AP37A, 2012) to about 1,350 feet (AP33, 2010) (**Figure 3.56a**). With the exception of AP21 and AP33 that are relatively wide compared to the other APs, visual inspection of the data indicates a general trend of increasing width in the downstream direction. Because of the variability in the data, however, this trend is not statistically significant. Except for 2012, when the unobstructed width was only about 230 feet based on the height class data, AP33 typically had among the largest widths, ranging from about 1,350 feet in both 2009 and 2010 to about 900 feet in 2013. AP21 was also relatively wide compared to the other APs, with widths ranging from 690 feet (2013) to 1,300 feet (2011). The direct measurements in 2013 and 2014 produced unobstructed widths that are generally similar to those from the previous years.

The reach-wide average unobstructed channel widths were relatively consistent during the first 3 years of the monitoring surveys, ranging from 625 feet in 2009 to 670 feet in 2010 and 720 feet in 2011 (**Figure 3.56b**). The 2012 data indicate a significant reduction as vegetation encroachment reduced the average unobstructed width to only 425 feet. The direct measurements in 2013 indicate an increase in width to about 520 feet, with a further increase in 2014 to 560 feet. Since climatic and hydrologic conditions during 2012 and 2013 were similar, the difference in average width between these two years may result more from differences in

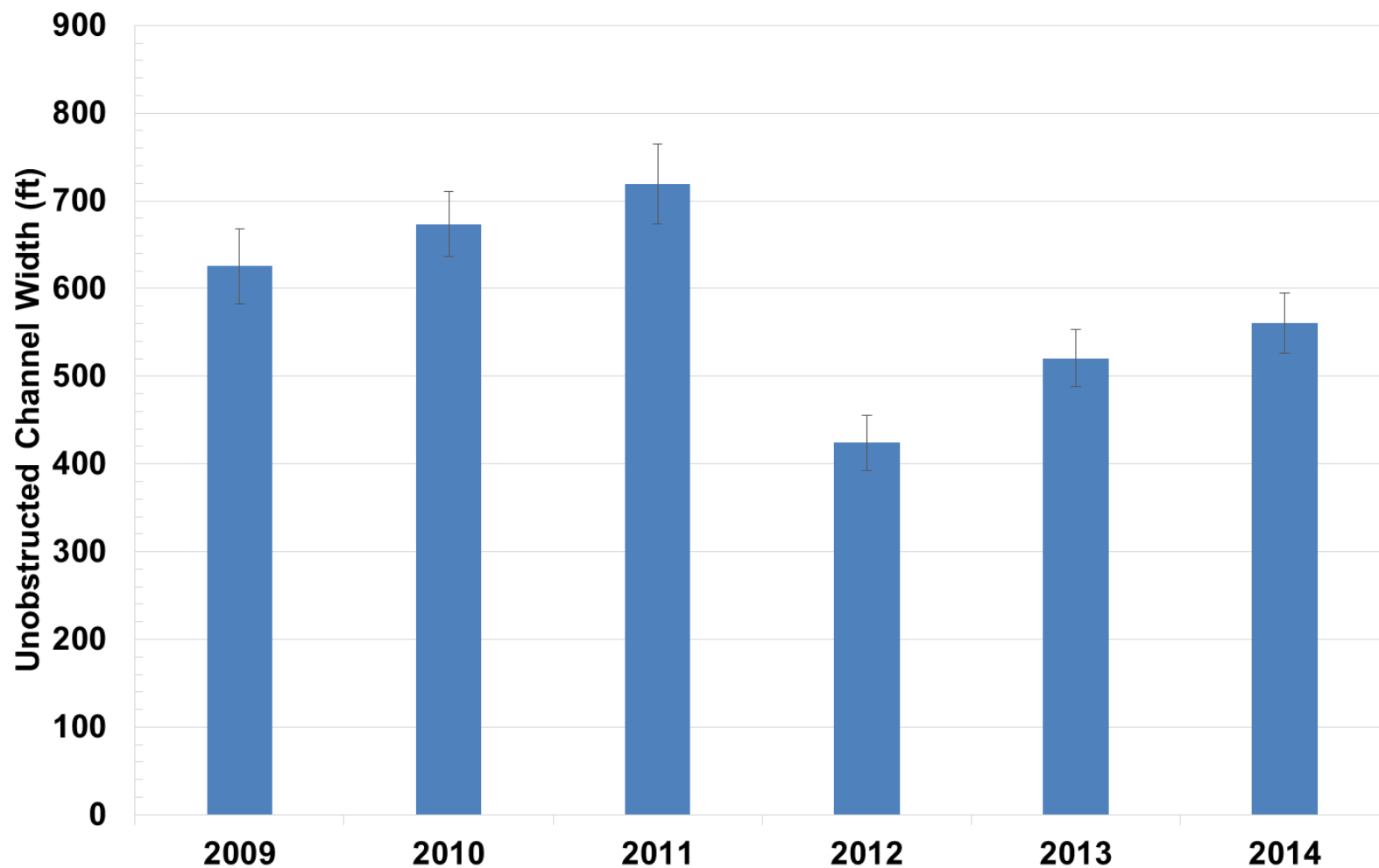


Figure 3.56a. Average unobstructed channel width at pure panel APs from 2009 through 2014.

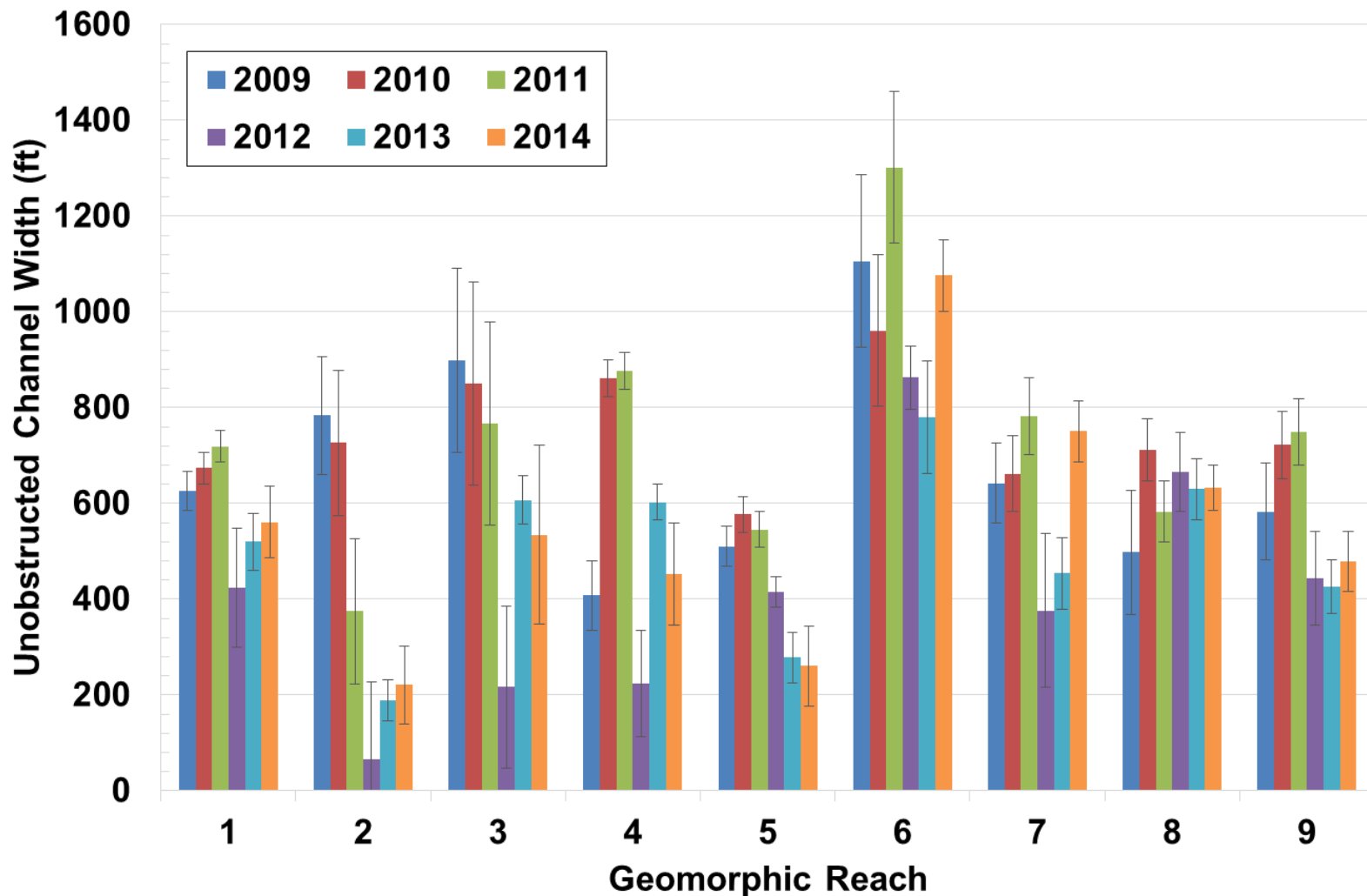


Figure 3.56b. Average unobstructed channel width for the overall study reach, based on the pure panel AP data from the 2009 through 2014. Whiskers represent ±1 standard error on mean value.

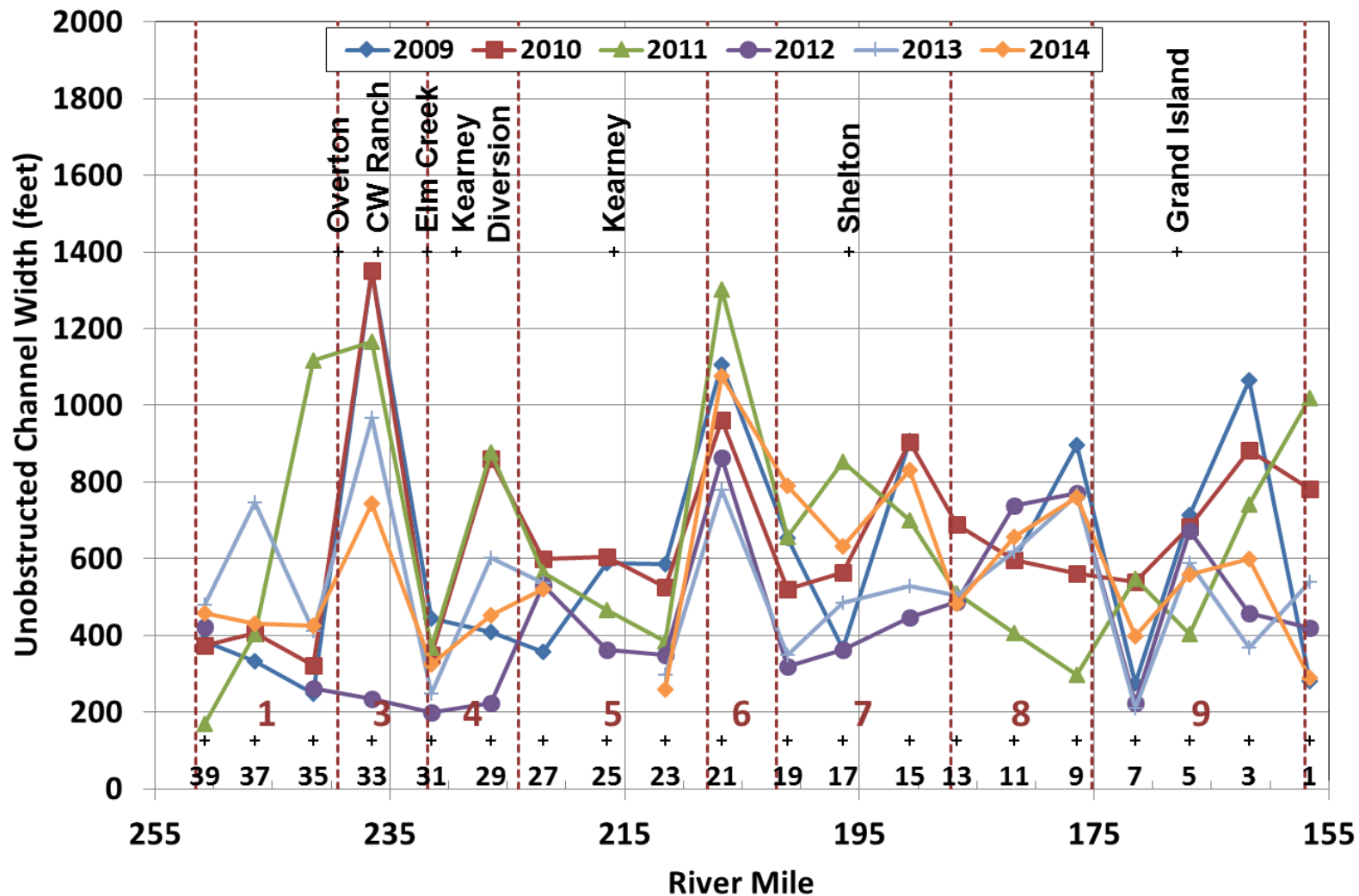


Figure 3.56c. Average unobstructed channel width by reach, based on the pure panel AP data from 2009 through 2014. Whiskers represent ± 1 standard error on mean value. Note that the 2009 and 2010 values for Reach 2 include both AP35B and AP37B, while 2011-2013 include only AP35B. Average values for AP35B in 2009 and 2010 were 540 and 420 feet, respectively.

measurement technique than actual, on-the-ground changes. The data indicate that Geomorphic Reaches 6 and 3 typically had the largest unobstructed width considering all six surveys (**Figure 3.56c**).

3.6.2 Proportion of Channel Less Than Eight Inches Deep or Sand (DAP 5.6.2)

The channel width inundated to a depth of 8 inches or less, including both vegetated and unvegetated, exposed sand bars¹⁰, was evaluated for three different target discharges: (1) 2,400 cfs (2) the median discharge during the spring whooping crane migration season and (3) the median discharge during the fall whooping crane migration season. As discussed in Section 3.1.1.2, the spring discharge in the portion of the reach downstream from Overton was in the range of 1,000 cfs to 2,000 cfs during 2009, 2010, 2012 and 2013, and varied from about 3,600 cfs to 4,400 cfs in 2011. In 2014, the spring discharge was approximately 1,400 cfs downstream from Overton (Figure 3.4). The fall discharge downstream from Overton generally ranged between about 1,500 cfs and 2,000 cfs during 2009, 2010 and 2013, was much lower (less than 500 cfs) in 2012 and ranged from about 3,200 cfs to 3,700 cfs in 2011. In 2014, it was approximately 850 cfs (Figure 3.5).

The widths less than 8 inches deep at 2,400 cfs were less than 200 feet at AP31, 37A (north channel at Jeffreys Island) and AP39 during all six years, and they ranged from 200 feet to 250 feet during all years at AP11 and AP25 (**Figure 3.57a**). Other pure panel APs with relatively small widths less than 8 inches deep include AP9, AP13, AP15, AP23 and AP33. Pure panel APs with relatively large widths less than 8 inches deep at 2,400 cfs (i.e., typically greater than 600 feet) include AP1, AP3, AP7, AP17, AP19, AP21, AP27, and AP35. AP1 had the largest width, generally in the range of 1,200 feet.

The reach-wide average width less than 8 inches deep at 2,400 cfs ranged from about 520 feet in 2009 to 530 feet in 2011, and then decreased to about 475 feet in 2012 (**Figure 3.57b**). Increases were observed in both 2013 and 2014, with the average unobstructed width greater than 550 feet in 2014. Because of the relatively high variability of the basic data, none of these differences are statistically significant at the 90-percent confidence level based on the Kruskall-Wallace test. Ignoring Reach 2, Geomorphic Reaches 3 and 8 generally had the smallest width less than 8 inches deep, averaging 240 feet and 310 feet respectively. (**Figure 3.57c**). It should be noted, however, that the 2009 data for Reach 8 is biased low because AP13 was not included, as it was moved for subsequent surveys. Reaches 6 (710 feet) and 9 (790 feet) typically had the widest average width less than 8 inches deep.

¹⁰The draft DAP indicates that this is the maximum **contiguous** width. Based on discussions with Jason Farnsworth, it was determined that this metric should be the total width with less than 8 inches of depth within the active channel in order to meet the intent of the metric. The widths from this analysis represent the total width of all areas within the active channel with less than 8 inches of depth, including vegetated and unvegetated sand bars.

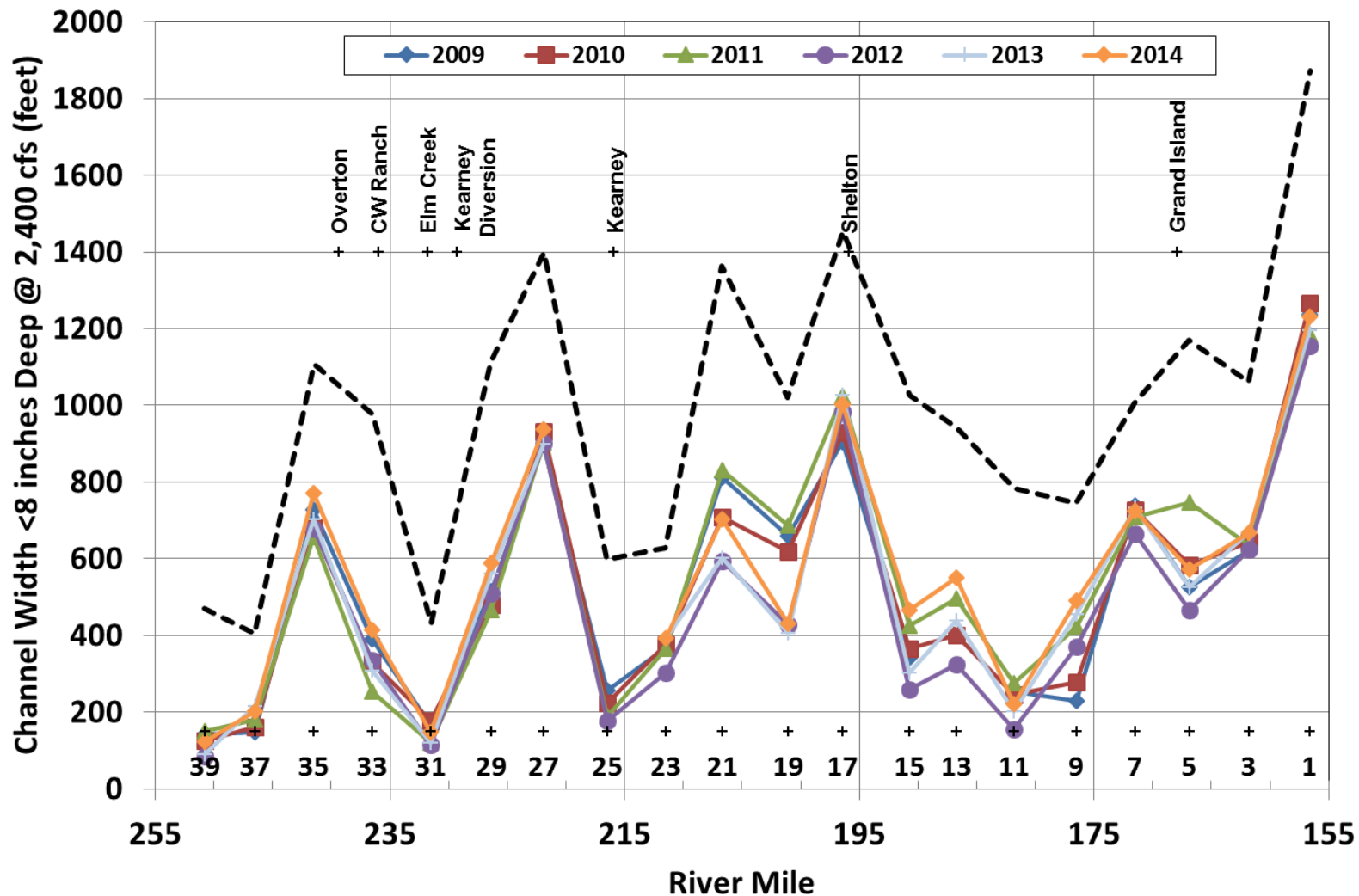


Figure 3.57a. Width of channel less than 8 inches deep (including exposed sandbars) at 2,400 cfs at the pure panel APs for each of the six monitoring surveys. Dashed black line is total channel width between bank stations.

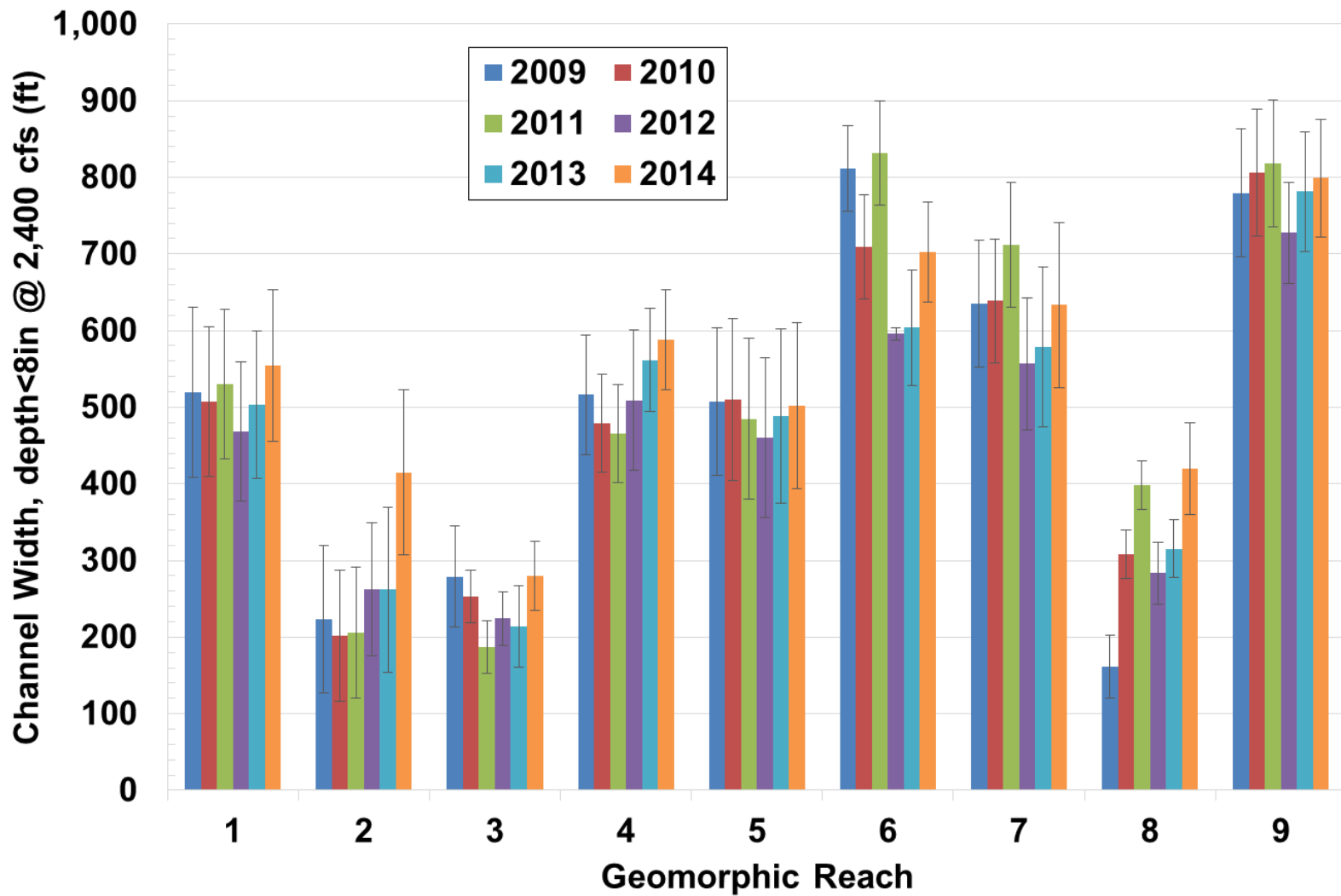


Figure 3.57b. Overall reach-averaged width less than 8 inches deep (including exposed sandbars) at 2,400 cfs. Whiskers represent ± 1 standard error. Note: AP37B excluded from the average because data are available only for 2009 through 2010.

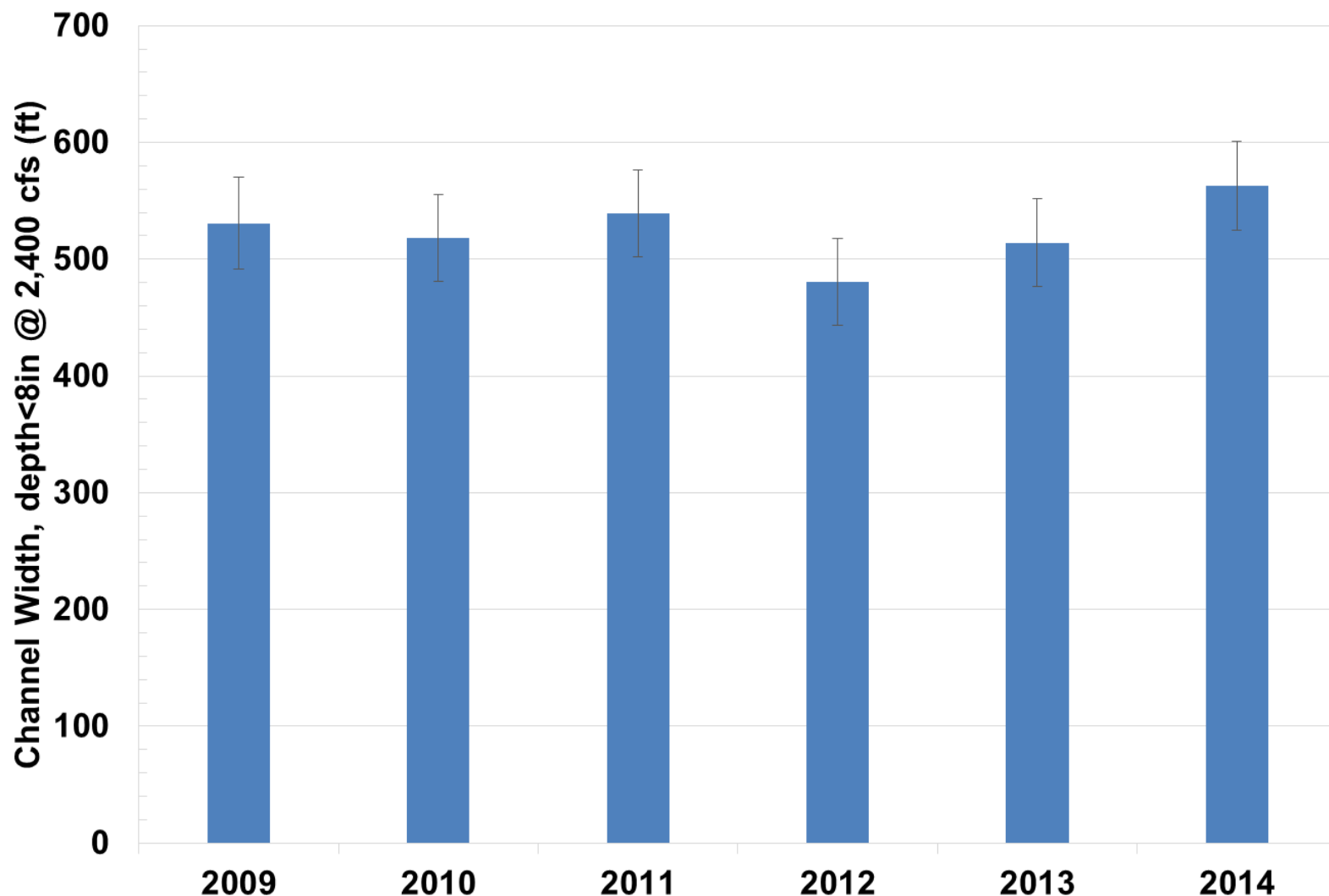


Figure 3.57c. Average width less than 8 inches deep (including exposed sandbars) at 2,400 cfs by geomorphic reach. Whiskers represent ± 1 standard error. Note: AP37B excluded.

The spatial distribution of widths with depth less than 8 inches for the spring and fall whooping crane migration season discharges are similar to the patterns for 2,400 cfs, however, the year-to-year differences are greater because of the year-to-year differences in the target discharge (**Figures 3.58a** and **3.59a**). The data also indicate that nearly the entire channel was inundated to a depth less than 8-inches during both spring and fall migration period in 2014.

The reach-wide average for the spring whooping crane migration season discharge was about 710 feet in 2009. High flows in 2011 caused the metric to decrease to 420 feet. The greatest width inundated to a depth of less than 8-inches was about 960 feet (2014) (**Figure 3.58b**). The reach-wide average for the fall whooping crane migration season discharge was about 640 feet in 2009. During the high flow year of 2011, the metric decreased to about 470 feet, and it increased substantially to about 900 feet in 2012 and 970 feet in 2014 (**Figure 3.59b**). The only year in which the metric was significantly different between the spring and fall periods was 2012, most likely due to the tendency for reduced topographic complexity in the channel, as discussed above.

The spatial pattern of average width among the geomorphic reaches for the spring and fall discharges is essentially the same as the width at 2,400 cfs, and the year-to-year variability follows the same temporal pattern and the reach-wide averages (**Figure 3.58c** and **Figure 3.59c**).

As expected, the monitoring data indicate that both the actual width and the portion of the active channel with flow depth less than 8 inches tend to decrease with increasing discharge (**Figure 3.60**). The average widths at 2,400 cfs at the pure panel APs represent 20 percent to 75 percent of the bank-to-bank channel width, with an overall average of about 50 percent for all five years. The average widths at the pure panel APs using the spring migration season discharge represent 15 percent to over 90 percent of the bank-to-bank width, with the reach-wide average ranging from 41 percent (2011) to 74 percent (2009). For the fall migration season discharge, the average widths at the APs represent about 20 percent (2011) to essentially 100 percent of the bank-to-bank channel width, with the reach-wide average ranging from 47 percent (2011) to 93 percent (2012). The 2012 and 2014 values are very high because of the relatively high migration season discharge.

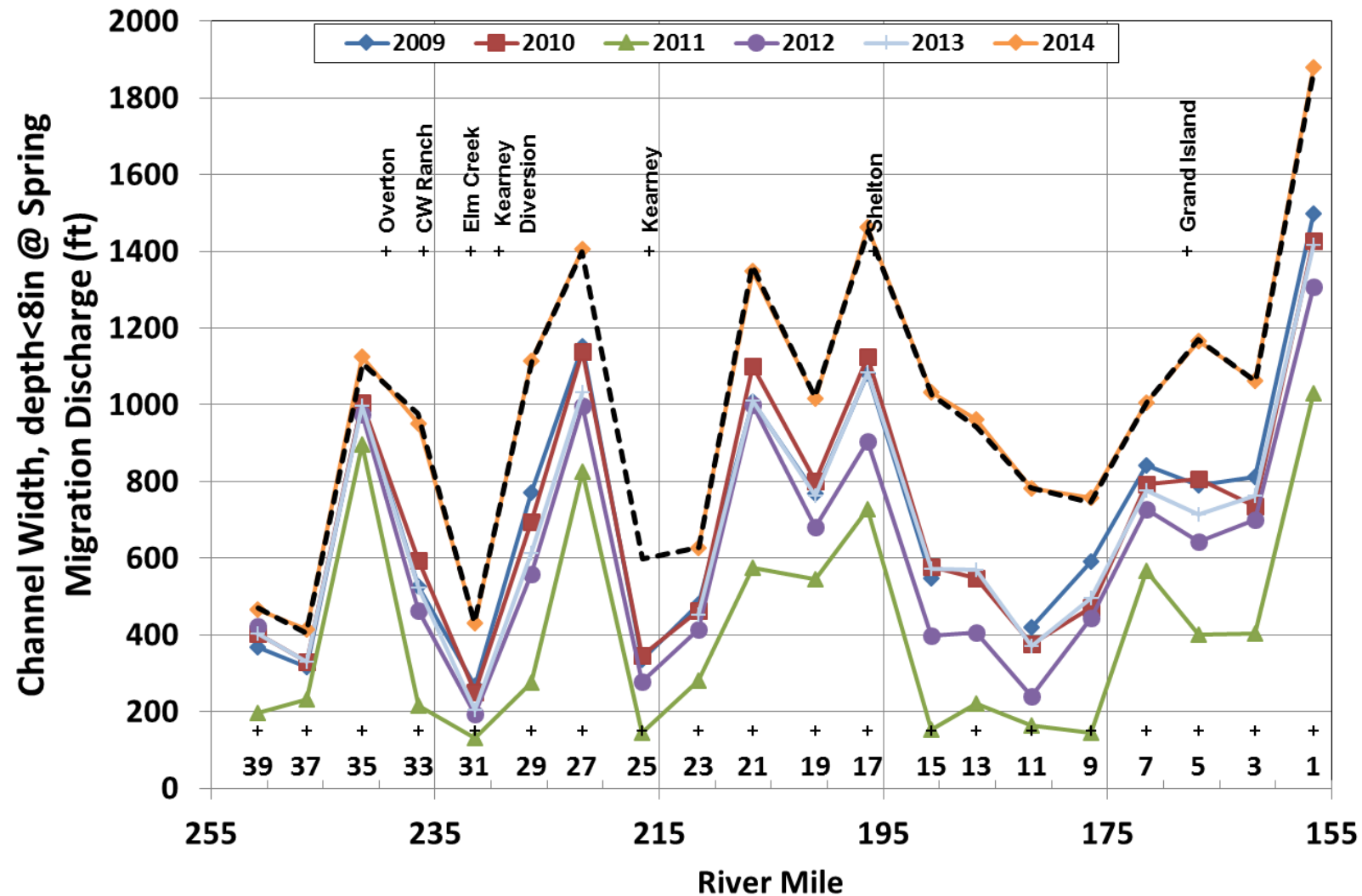


Figure 3.58a. Width of channel less than 8 inches deep (including exposed sandbars) during spring migration at the pure panel APs for each of the six monitoring years. Dashed black line is total channel width between bank stations.

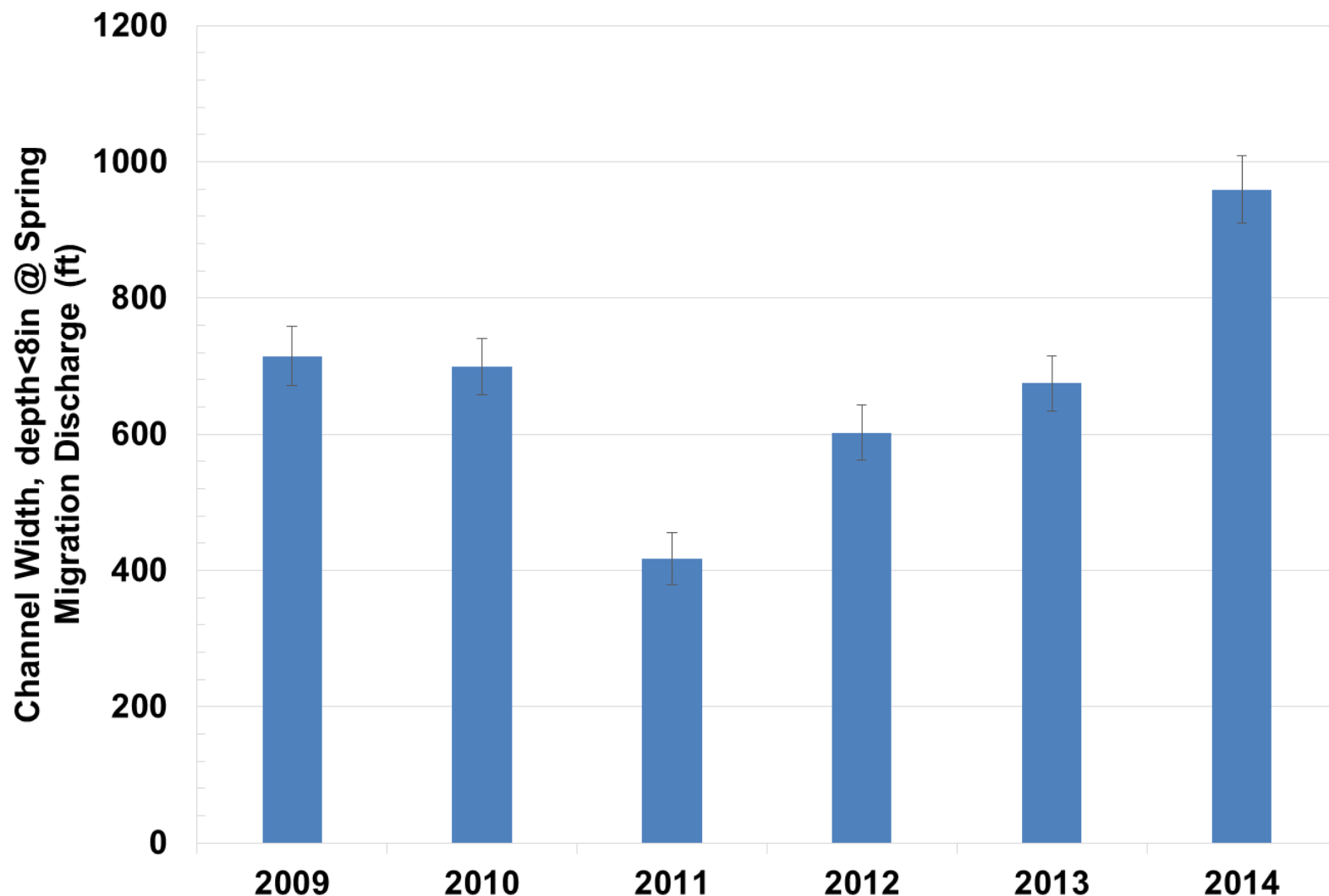


Figure 3.58b. Overall reach-averaged width less than 8 inches deep (including exposed sandbars) at the spring migration season. Whiskers represent ± 1 standard error. Note: AP37B excluded.

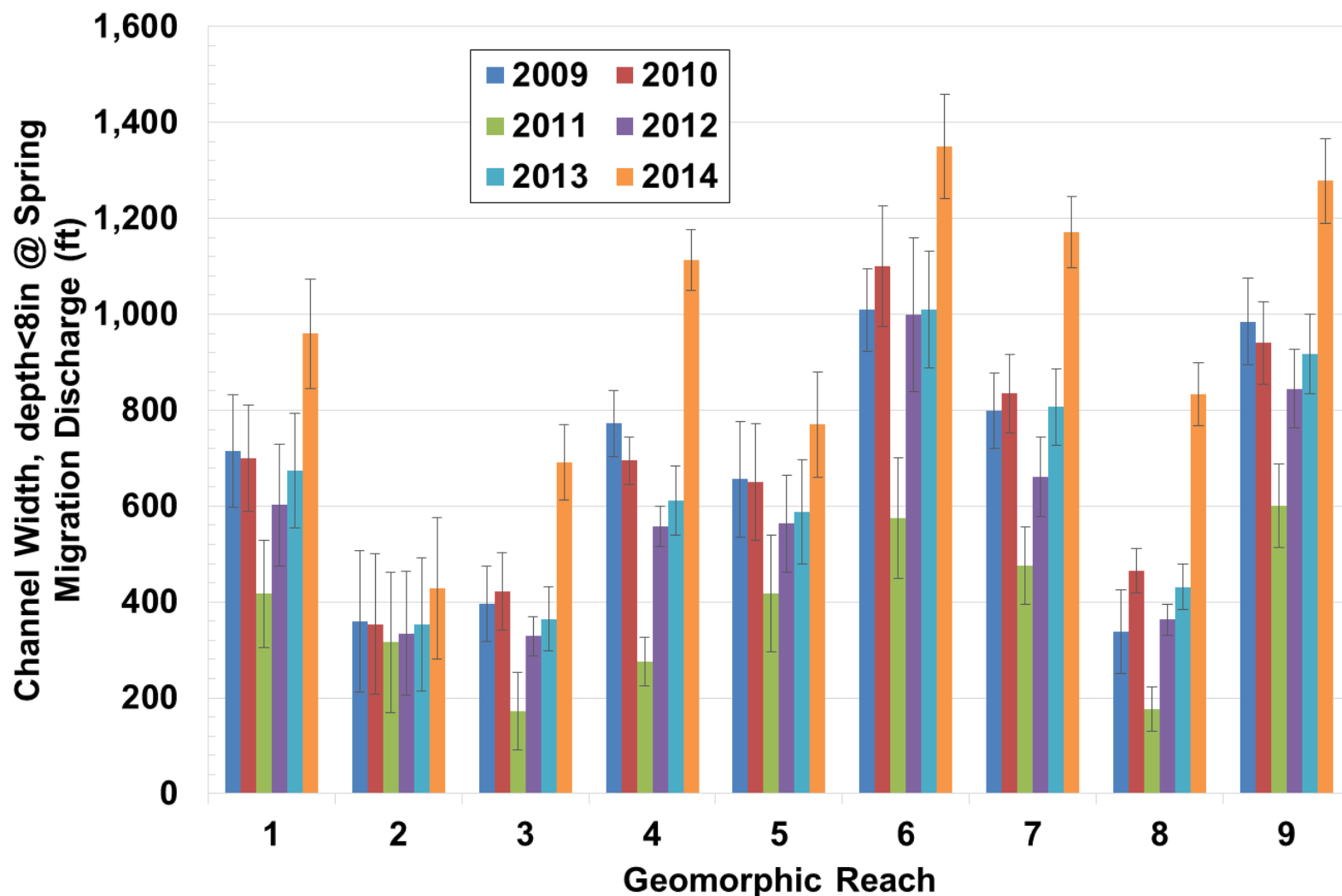


Figure 3.58c. Average width less than 8 inches deep (including exposed sandbars) at the spring migration season by geomorphic reach. Whiskers represent ± 1 standard error. Note: AP37B excluded.

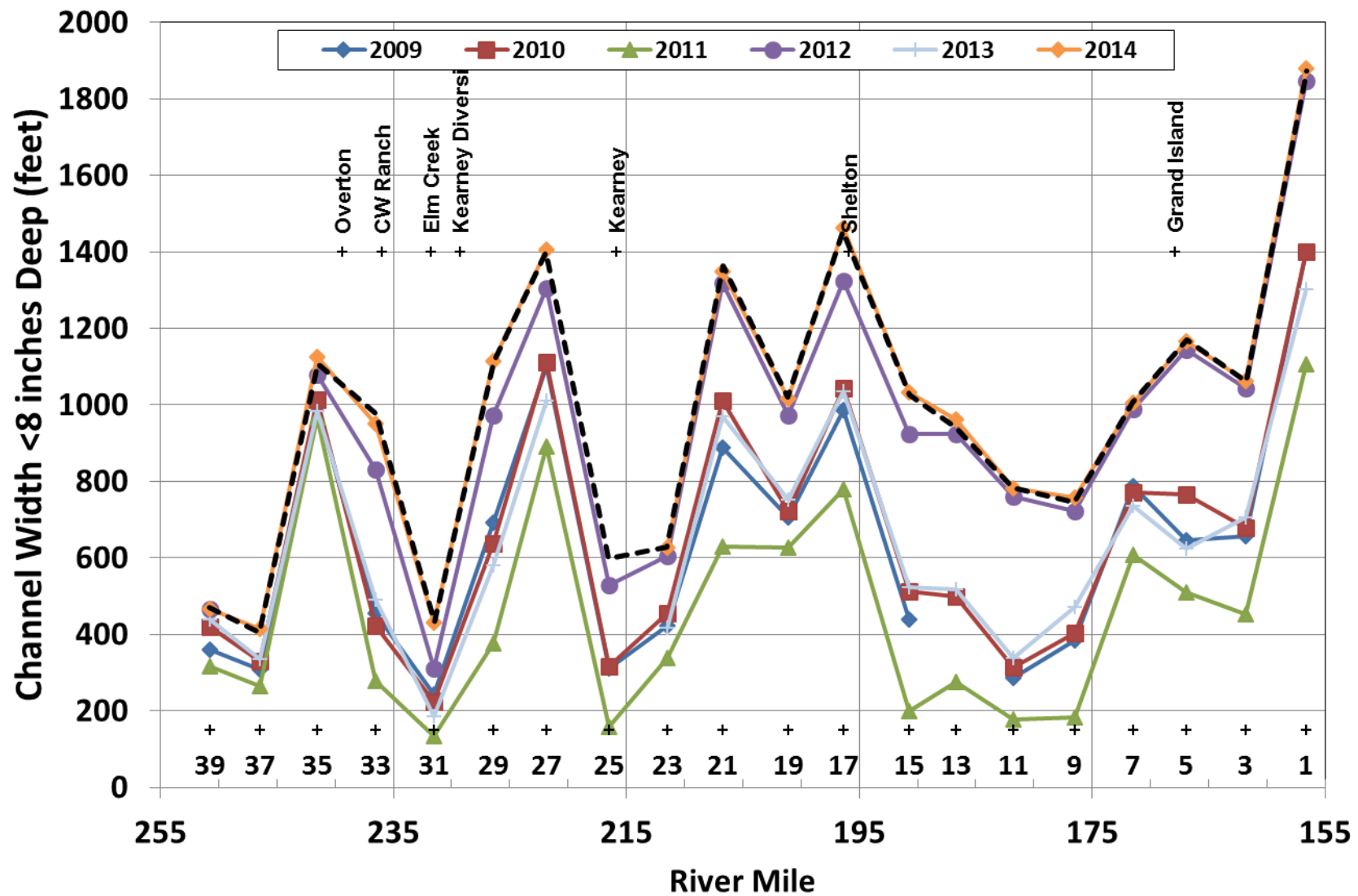


Figure 3.59a. Width of channel less than 8 inches deep (including exposed sandbars) during all migration at the pure panel APs for each of the six monitoring years. Dashed black line is total channel width between bank stations.

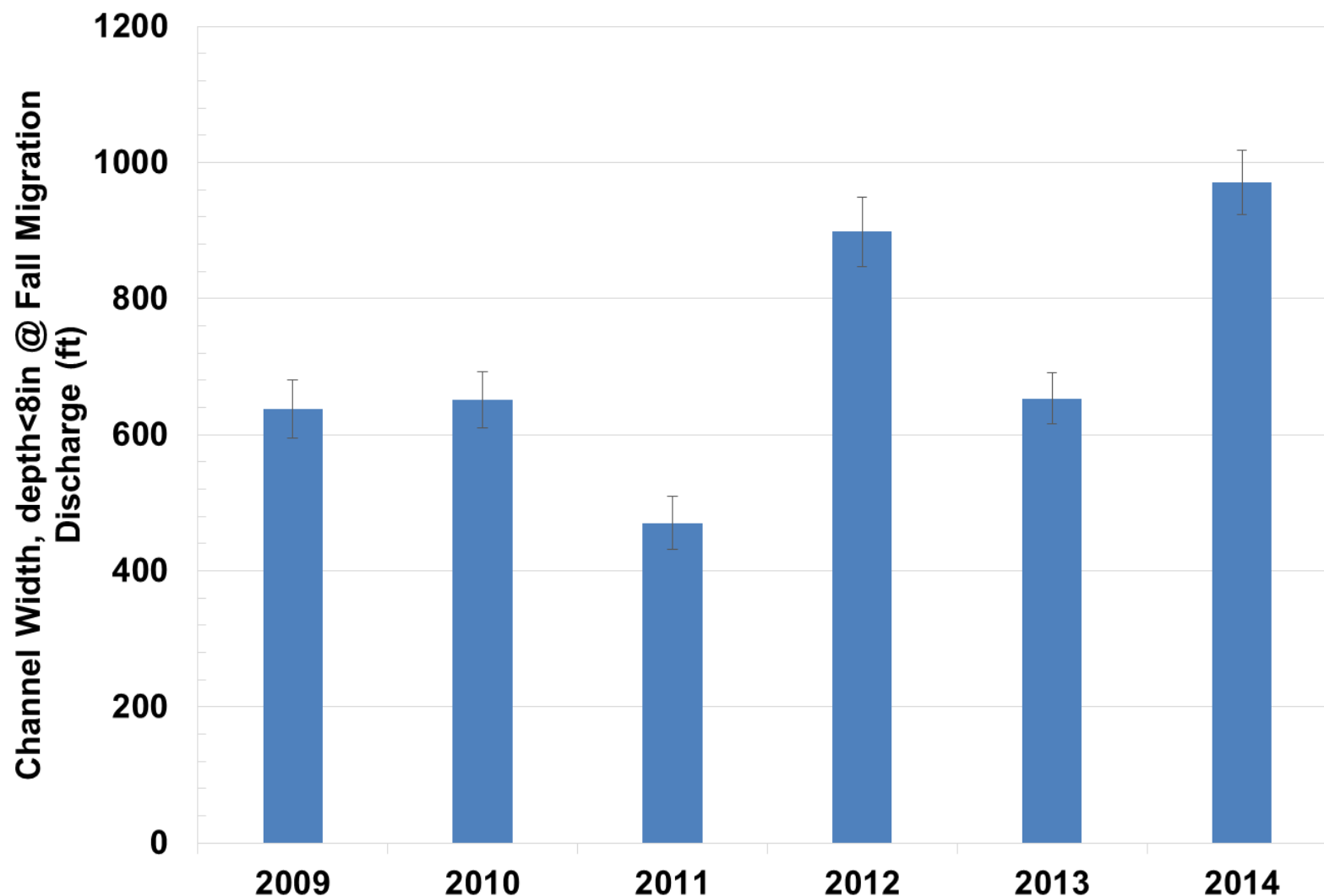


Figure 3.59b. Overall reach-averaged width less than 8 inches deep (including exposed sandbars) at the spring migration season. Whiskers represent ± 1 standard error. Note: AP37B excluded.

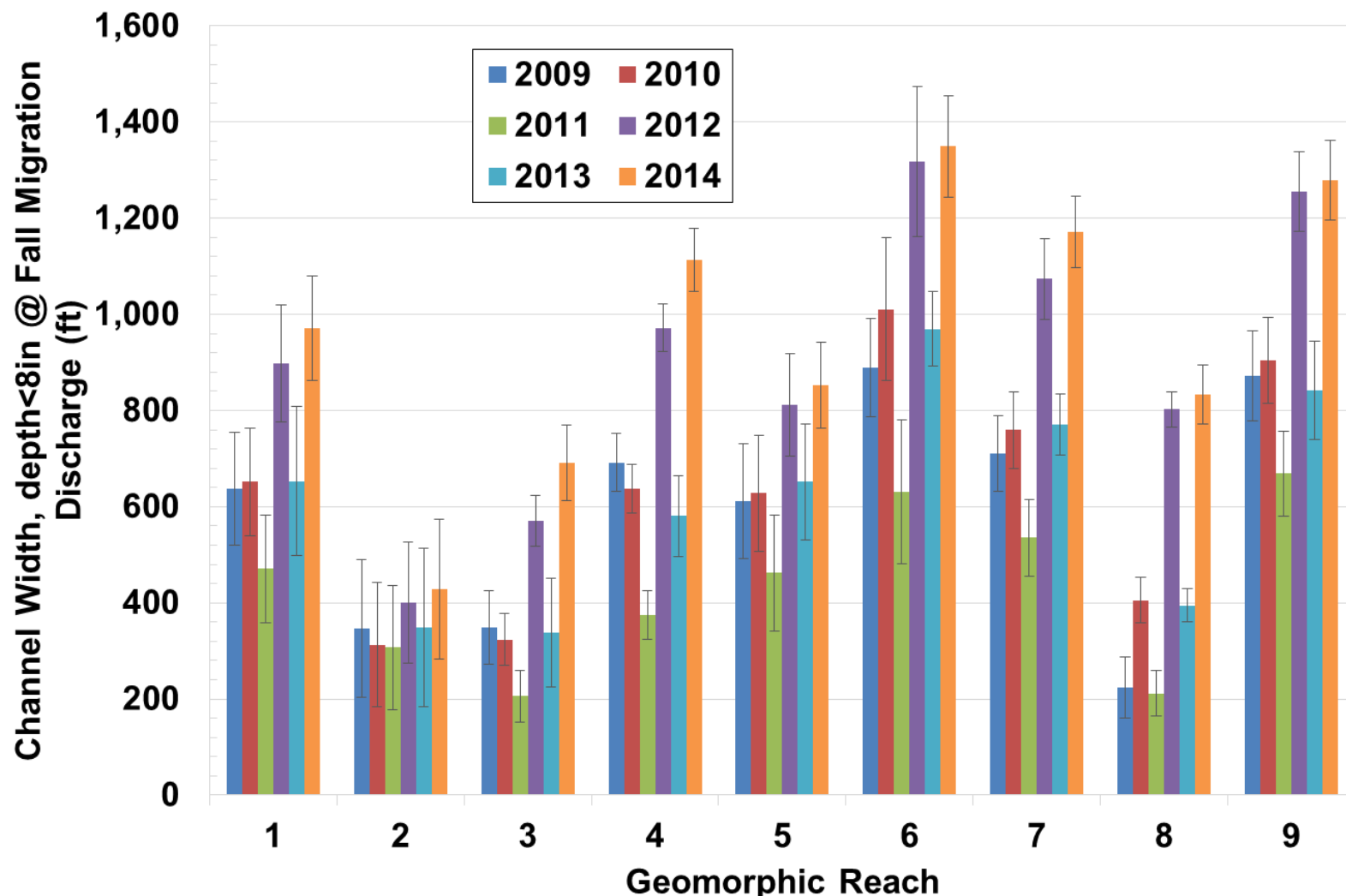


Figure 3.59c. Average width less than 8 inches deep (including exposed sandbars) at the spring migration season by geomorphic reach. Whiskers represent ±1 standard error. Note: AP37B excluded.

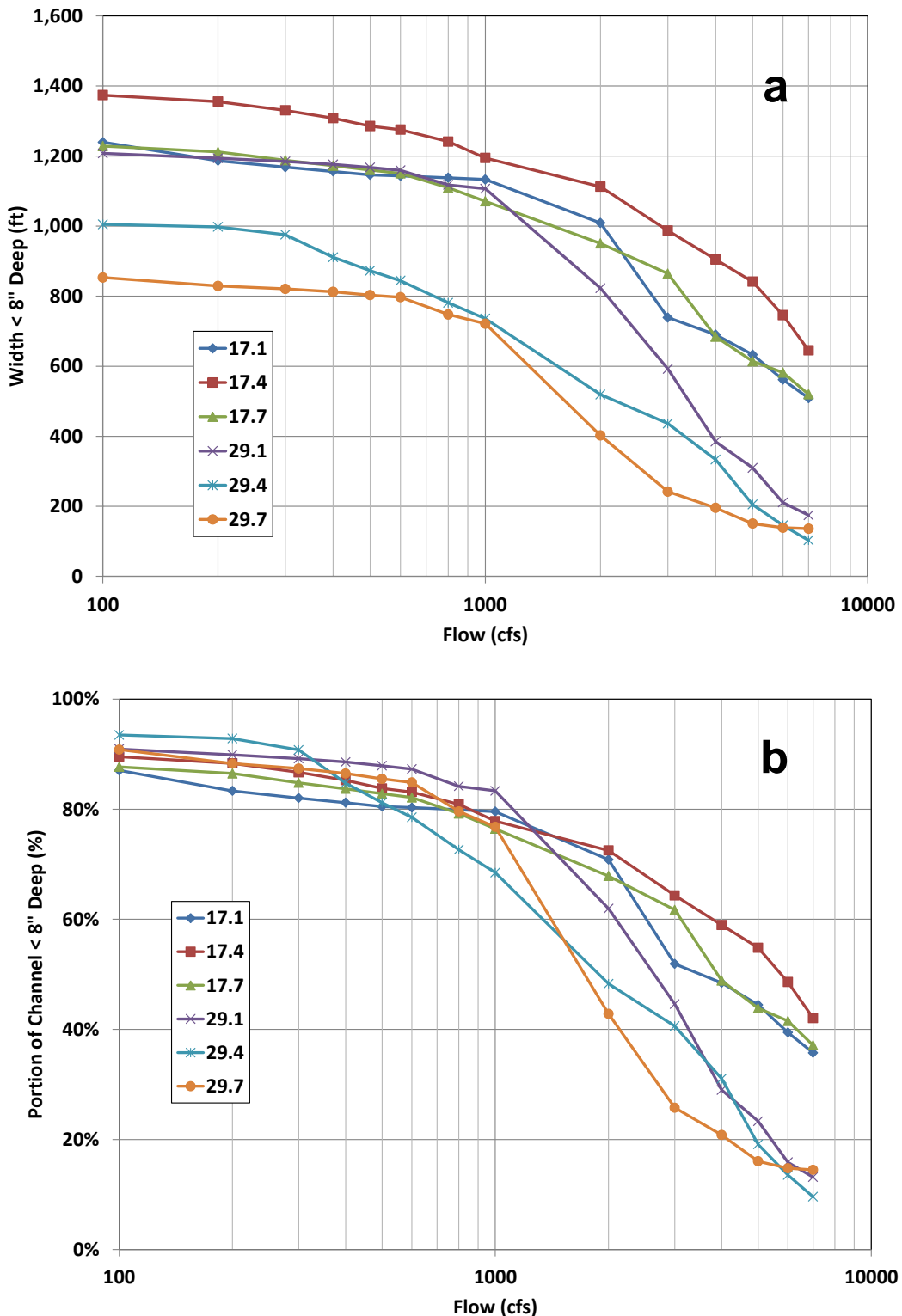


Figure 3.60. Typical relationship between discharge and (a) width of the channel and (b) percentage of total active channel width with depth less than 8 inches, based on the three primary monitoring cross sections at AP17 and AP29.

Page Intentionally Left Blank

4 HYPOTHESIS TESTING AND TREND ANALYSIS

As noted in Section 2.5.3, a broad range of statistical comparisons were made across the 2009 through 2012 data sets for the 2012 annual report to identify trends in the geomorphic, vegetation and sediment variables (Table 2.5). This resulted in a large number of analyses that are difficult to interpret in the context of Program priorities. To provide a more focused analysis, the Program directed that the analysis for the 2013 annual report be restricted to specific aspects of the following four hypotheses:

1. Flow #1
2. Flow #3
3. Flow #5
4. Mechanical #2

Similar to the 2013 annual report, the 2014 report focuses on these four hypotheses. The analysis is presented in the following sections.

4.1 Flow #1

Increasing the variation between river stage at peak (indexed by the Q_{1.5} @ Overton) and average flows (1,200-cfs index flow), by increasing the stage of the Q_{1.5} through Program flows, will increase the height of sandbars between Overton and Chapman by 30 to 50 percent from existing conditions, assuming balanced sediment budget.

Evaluation of the validity of this hypothesis hinges on an understanding of the relative sediment balance along the reach. Two primary sources of data are available to assess the sediment balance: (1) year-to-year changes in bed sediment volume, based on repeat surveys of the three geomorphic transects at the pure panel APs (Section 3.3.7), and the resulting changes over the 5-year period encompassed by the surveys at the rotating panel APs, and (2) comparison of the annual sediment loads passing each of the five measurement sites, obtained by integrating the sediment load rating curves over the applicable flow records (Sections 3.5.1 and 3.5.2).

4.1.1 Sediment Balance Based on Transect Surveys

As discussed in Section 3.3.7, extrapolation of the volume changes from the transect surveys at the pure panel APs over the intervening, unsurveyed reaches indicates that the overall reach between Lexington and Chapman degraded by about 2.4M tons during Survey Year (SY)¹¹ 2010, about 1.2M tons during SY2011, and then aggraded by about 5.6M tons during SY2012 and an additional 1.6M tons during SY2013. During SY2014, the reach degraded by about 0.5M tons (Figure 3.12c). This resulted in estimated net aggradation in the overall reach of about 3.1M tons over the 5-year period encompassed by the surveys, or about 630,000 tons per year.

The monitoring data also indicate that Geomorphic Reach 1 (Lexington to Overton Bridge, including the north channel at Jeffreys Island) degraded by about 336,000 tons during SY2010, and then aggraded by 341,000 tons in each of the two succeeding years, followed by additional aggradation of about 270,000 tons in SY2013 and degradation of 83,000 tons in the SY2014,

¹¹The transect surveys and other detailed field data during all years were generally collected between mid-July and late-August. To simplify the discussion and to facilitate comparison of the aggradation/degradation trends based on the surveys with those based on the sediment load rating curves, Survey Years are defined as the period between August 1 of the previous year and July 31 of the current year [e.g., Survey Year (SY) 2010 refers to the period from August 1, 2009 through July 31, 2010].

resulting in net **aggradation** over the 5-year period of about 535,000 tons, or an average of about 170,000 tons/year (Figure 3.12d).

Based on the repeat surveys at AP35B, Reach 2 (south channel at Jeffreys Island, where essentially all of the flow is derived from the J-2 Return) degraded by about 187,000 tons during SY2010, and it also degraded during SY2011, SY2012, and SY2014 (~89,000, ~32,000 and ~38,000 tons, respectively). Considering the approximately 5,500 tons of aggradation during SY2013, the reach experienced net **degradation** over the 5-year period of approximately 340,000 tons, or about 68,000 tpy.

Two pure panel APs (AP35B and AP37B) are located in Reach 2. Because permission to access AP37B was revoked by the landowner prior to the 2011 surveys, the aggradation/degradation quantities are based only on the repeat surveys at AP35B to insure consistency in the estimates across all years. (The 2009 and 2010 data indicate that AP37B degraded by about 16,000 tons during the first year of the monitoring program, while AP35B degraded by only about 10,000 tons; thus, the estimates based on only AP35B may be on the low side for this reach). AP35B is located about 2 miles upstream from the Overton Bridge and about 1 mile upstream from the outfall at the Dyer Property where 82,000 tons of sand was pumped and mechanically graded into the river between September 2012 and June 2013 as part of the Program's Pilot Sediment Augmentation Project (The Flatwater Group et al., 2014). A monitoring cross section on the return channel about 1,200 feet upstream from the Dyer outfall (XS-1, **Figure 4.1**) showed little net change between the pre- and post-augmentation surveys in August 2012 and August 2013; thus, the augmentation does not appear to have affected aggradation/degradation patterns in the majority of Reach 2 upstream from the outfall. Surveys at the other Pilot Study monitoring sections indicate that about 26,000 tons of sediment accumulated between the outfall and XS-5 between August 2012 and August 2013. Since the pumped sediment was mechanically graded into the river, it is assumed that the remaining 56,000 tons of augmented sediment were transported downstream past the pilot-augmentation monitoring area.

Based on the surveys at AP31, Reach 3 (Overton Bridge to Elm Creek Bridge) degraded by about 36,000 tons during SY2010. As noted above, AP33 was excluded from the SY2010 calculation because a large mid-channel bar was mechanically graded into the channel in Fall 2009; thus, the changes would not reflect trends in the overall sediment-transport balance in the reach. Based on both AP31 and AP33, Reach 3 degraded by an additional 363,000 tons during SY2011 and 95,000 tons during SY2013. Considering the approximately 171,000 tons of aggradation during SY2012 and 234,000 tons of aggradation during SY2014, this reach appears to have experienced net **degradation** of about 89,000 tons over the five-year monitoring period, or an average of about 18,000 tons/year. Other mechanical grading activities added about 200,000 tons of sediment into the main river channel during the 4-year monitoring period [50,000 tons each in 2010 and 2011, and 100,000 tons during SY2013 (Jason Farnsworth, personal communication, 2014; The Flatwater Group et al., 2014)]. About 130,000 tons of sediment were also graded into the channel during the 5-year period prior to the start of this monitoring program.

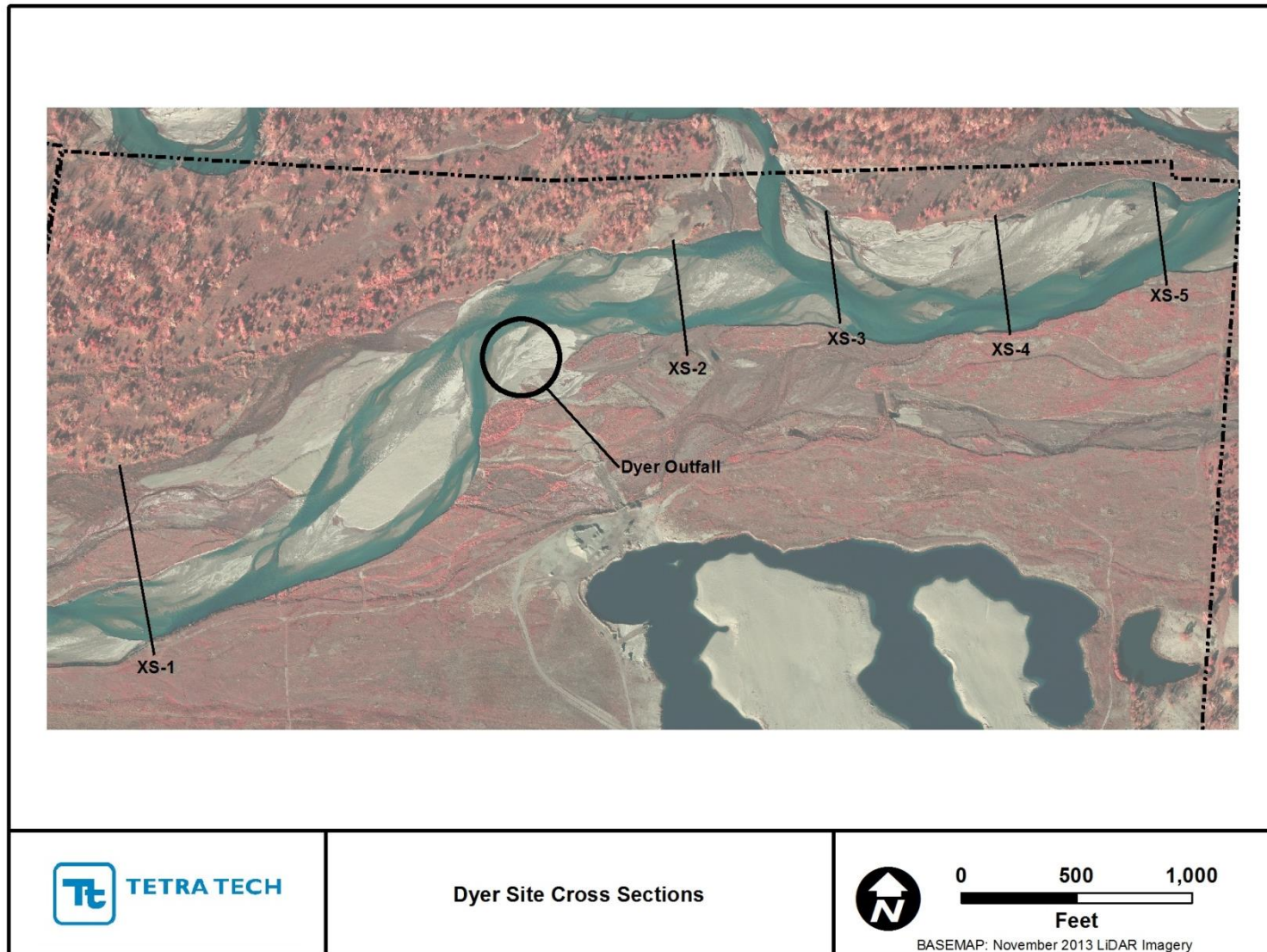


Figure 4.1. Vicinity map of the pilot sediment augmentation area showing the location of the Dyer Outfall and the five monitoring cross sections.

Long-term measurements by the USGS at the Overton gage that is located at the boundary between Reaches 1, 2 and 3 indicate that the channel steadily degraded by a total of about 3.5 feet between 1987 and 2010, area aggraded back by about 0.5 in 2011, and has been relatively stable or slightly aggrading since early-2012 (**Figures 4.2a** and **4.2b**). Comparison of the data collected at rotating panel point AP34 (immediately downstream from the Overton Bridge) for this monitoring program in July 2012 with surveys conducted at the same transects for the Pilot Sediment Augmentation Study in December 2012 showed a modest degradational tendency. Similar measurements at the USGS Cottonwood Ranch Mid-Channel Gage, that is located about 3 miles upstream from the Elm Creek Bridge, indicate that this location degraded by about 1 foot between WY2001 and WY2007, aggraded by about 1.5 feet between WY2007 and early-WY2012, and has remained relatively stable since 2012 (**Figure 4.3**). These trends are qualitatively similar to the trends indicated by the anchor point surveys, in which Reach 3 degraded between SY2009 and SY2011, and aggraded in SY2012 and SY2014, with relatively modest degradation in 2013 (Figure 3.12d).

Based on the surveys at AP29, Reach 4 (Elm Creek to Odessa) degraded by about 392,000 tons during SY2010 surveys, and then aggraded in 2011, 2012 and 2013 (279,000, 466,000 and 291,000 tons, respectively). In 2014, this reach degraded by about 100,000 tons, resulting in net aggradation over the 5-year period of about 545,000 tons or about 109,000 tpy. AP29 is located about midway between the Kearney Canal Diversion Structure (KDS) and the Odessa Bridge. Repeat surveys at 13 cross sections between the KDS and AP29 for the Elm Creek Adaptive Management Experiment indicate that this part of the reach aggraded by about 3,300 tons between April 2011 and August 2013, a rate considerably lower than is indicated by the monitoring data at AP29 (Tetra Tech, 2014). The Elm Creek data also indicate that the portion of the reach between the Elm Creek Bridge and the KDS degraded by about 57,000 tons during the 27-month period encompassed by the surveys, with about 22,000 tons of degradation between April 2011 and August 2011, about 9,000 tons of aggradation between August 2011 and August 2012, and the remaining 43,000 tons of degradation between August 2012 and August 2013. The downstream portion of the Elm Creek Reach degraded by about 17,000 tons between August 2011 and August 2012, and then aggraded back by about the same amount between August 2012 and August 2013. The modest amount of aggradation in the downstream portion of the reach occurred during Summer 2011. These results suggest that basing the aggradation/ degradation trends for Reach 4 solely on the surveys at AP29 may not accurately represent the amount of change that is actually occurring in the overall reach.

Reach 5 (Odessa to Minden), which includes pure panel AP23, AP25 and AP27, degraded by about 1.37M tons during SY2010 surveys and an additional 590,000 tons during SY2011. The reach then aggraded by about 888,000 tons during SY2012, with very little change (~3,000 tons of aggradation) during SY2013. Degradation of about 105,000 tons in SY2014 resulted in net degradation over the 5-year period of about 1.18M tons, or about 236,000 tons/year. USGS gage measurement data indicate that the cross section at the Kearney gage, which is located in the middle of the reach, aggraded by 0.5 to 0.75 feet between 1982 and 1986, remained relatively stable until 2002, and then degraded by about one foot between 2002 and 2005 (**Figure 4.4**). Based on the low-flow measurements, the mean bed elevation appears to have been relatively stable to slightly degrading since 2005.

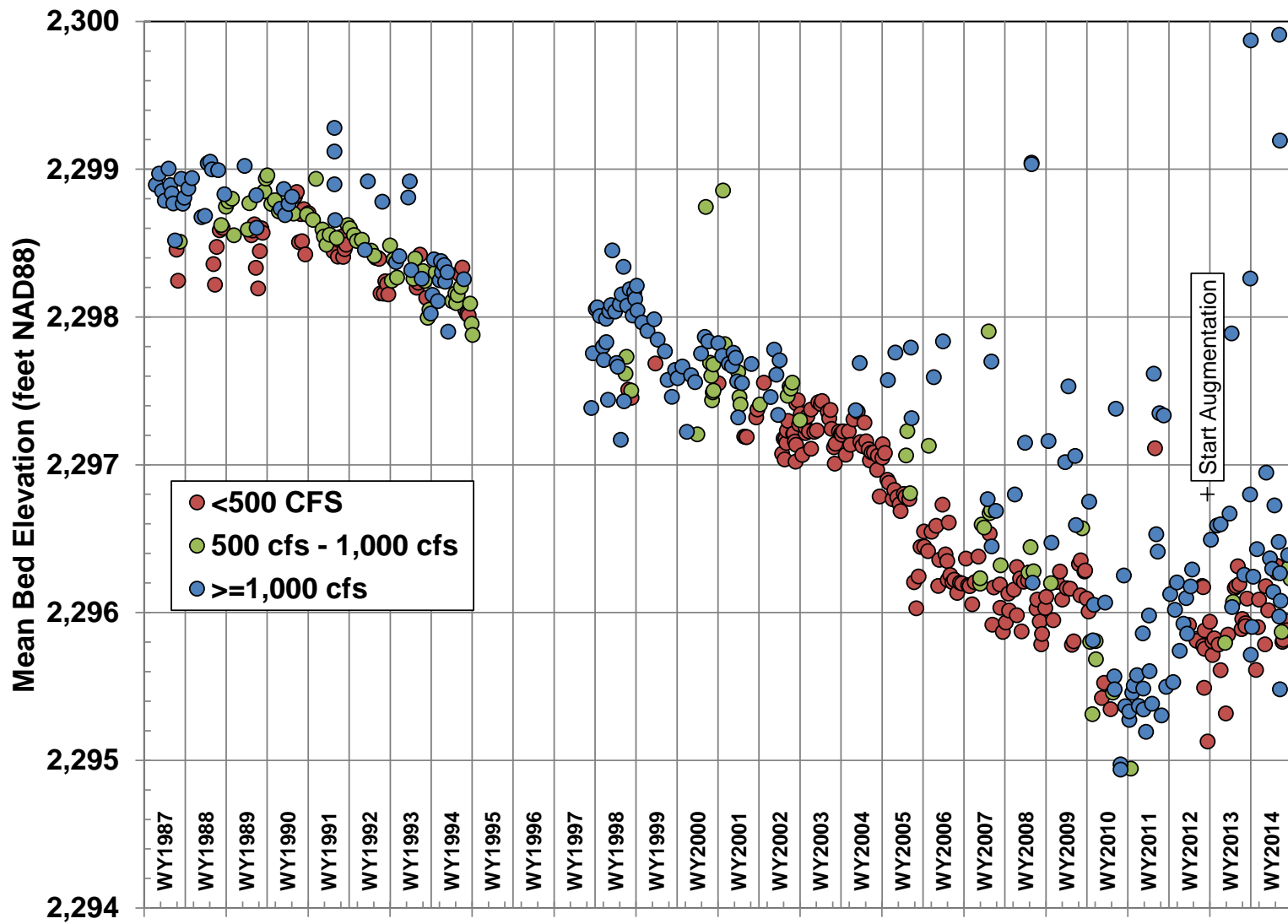


Figure 4.2a. Mean bed elevations at the Overton, based on USGS field measurement data collected during WY1987 through WY2014.

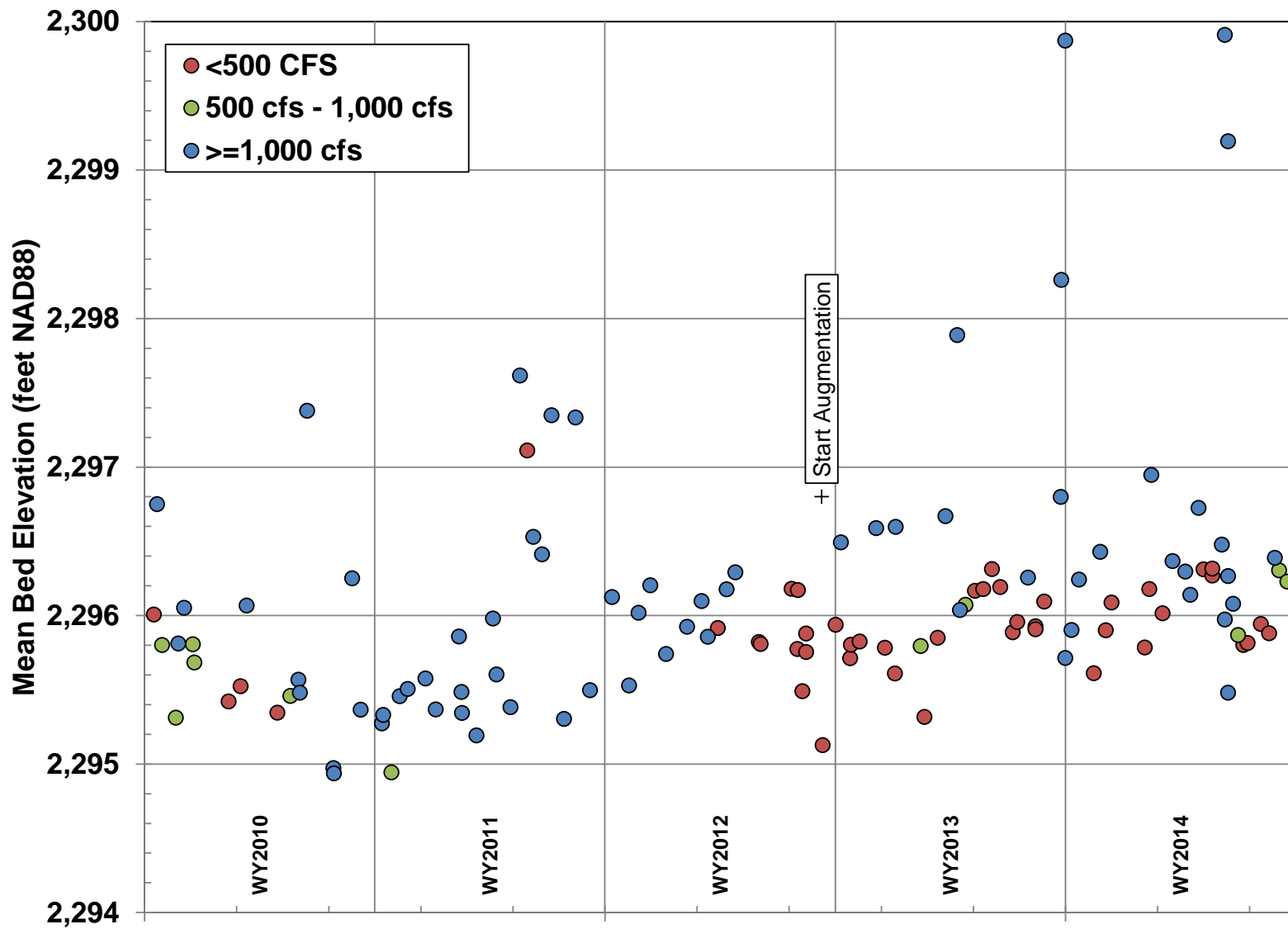


Figure 4.2b. Mean bed elevations at the Overton, based on USGS field measurement data collected during WY2010 through WY2014 (same data as Figure 4.2a).

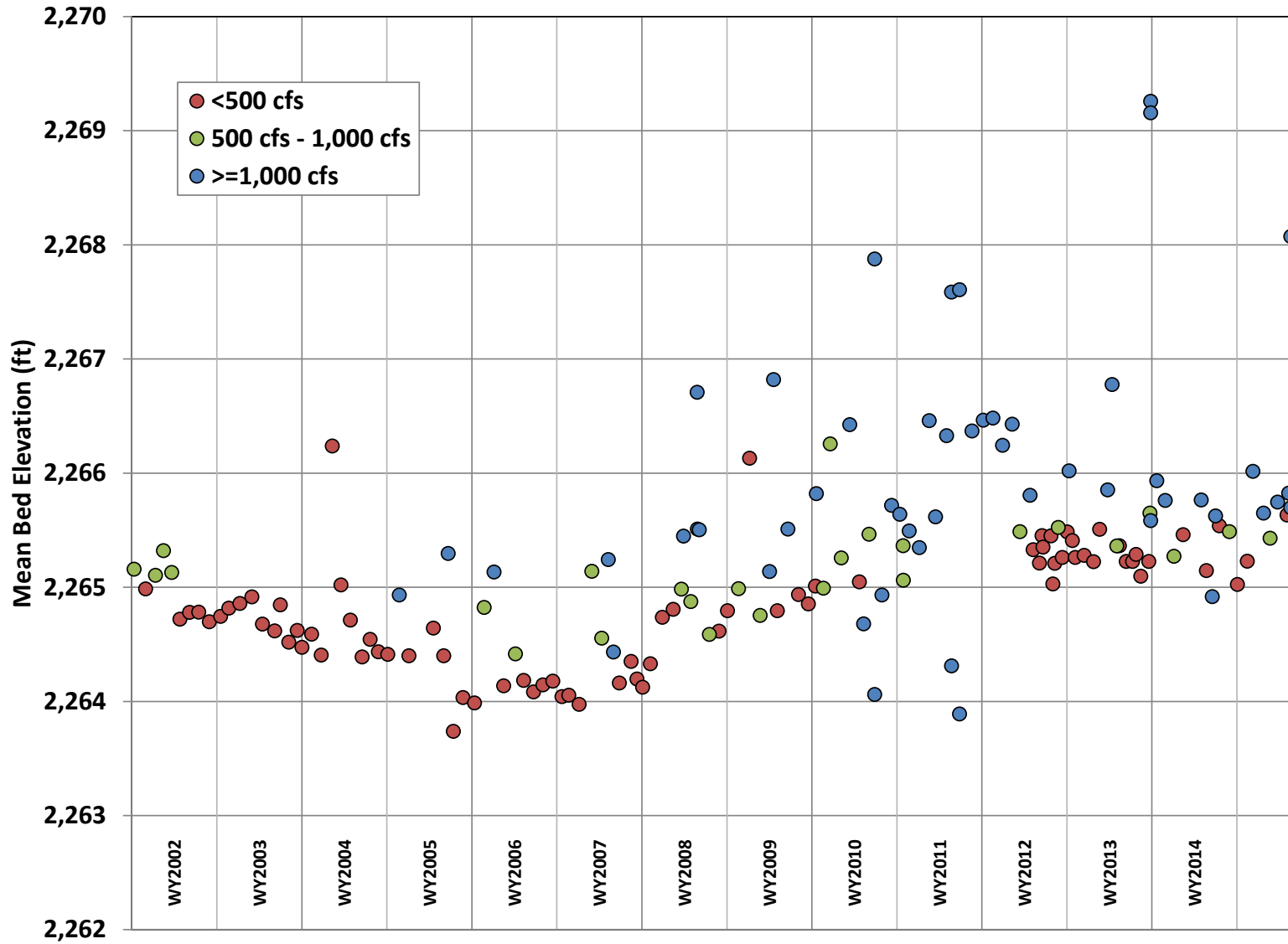


Figure 4.3. Mean bed elevations at the Cottonwood Ranch Mid-Channel gage, based on USGS field measurement data collected during WY2001 through WY2014.

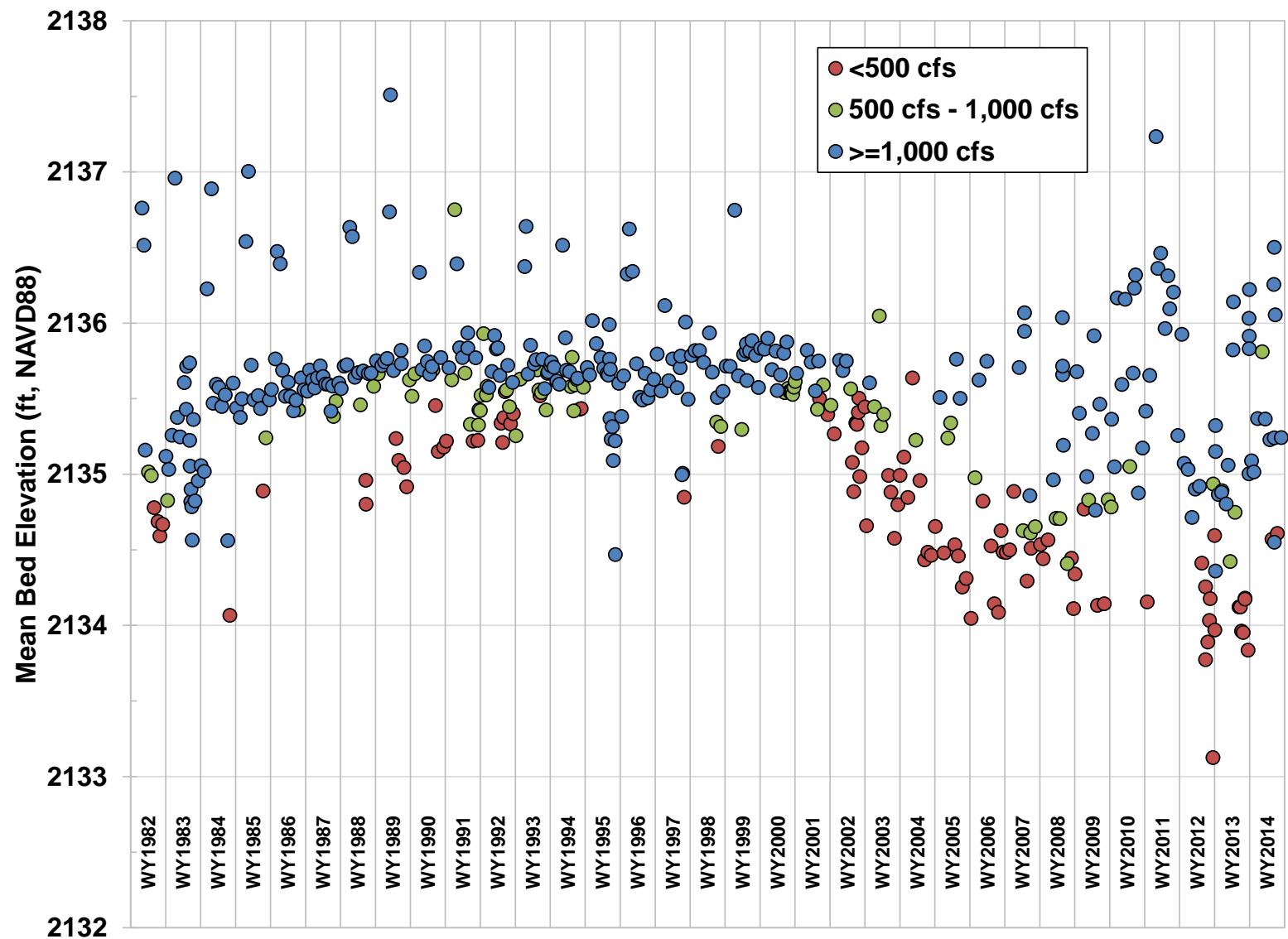


Figure 4.4. Mean bed elevations at the Kearney gage, based on USGS field measurement data collected during WY1982 through WY2014.

Based on the surveys at AP21, near the Rowe Sanctuary, Reach 6 aggraded by 383,000 tons over the 5-year period, or an average of about 77,000 tons/year. The year-to-year changes, however, varied significantly from 706,000 tons of degradation during SY2010 to 1.2M tons of aggradation during SY2012.

The temporal patterns of aggradation and degradation were similar in Reaches 7, 8 and 9 during the first three years, with cumulative aggradation of about 639,000 tons during SY2010, degradation of 789,000 tons during SY2011, and aggradation of 2.56M tons during SY2012. In SY2013, Reach 7 degraded by 135,000 tons, while Reaches 8 and 9 aggraded by a combined 1.57M tons. In SY2014, Reaches 7 and 9 degraded by a combined total of 973,000 tons while Reach 8 aggraded by 405,000 tons. Over the 5-year period, all three reaches experienced net aggradation (788,000 tons in Reach 7, 1.93M tons in Reach 8, and 557,000 tons in Reach 9), a combined annual aggradation rate of about 660,000 tpy. USGS measurement data indicate that the cross section at the Grand Island gage, which is located at the boundary between Reaches 8 and 9, may have degraded by about 0.5 feet between the early-1980s and 2006, but has not shown a systematic aggradation/degradation trend since that time (**Figure 4.5**).

4.1.2 Sediment Balance Based on Sediment Load Rating Curves

The sediment balance during the five years encompassed by the surveys was estimated from the sand load rating curves discussed in Sections 3.5.1 and 3.5.2 by integrating the MVUE bias-corrected curves over the respective mean daily flow records and comparing the resulting loads between stations. The integrations were performed using flow data for the Survey Years that extend from August 1 of the previous year to July 31 of the current year to facilitate comparison of the sediment balance based on the rating curves with the aggradation/degradation estimates from the transect surveys.

Because the rating curves for the bed and suspended loads were developed separately using data points that do not necessarily represent the same time and discharge, the total load cannot be calculated by simply adding corresponding data points. In addition, the scatter in the data and resulting confidence bands on the two sets of curves are quite different; thus, quantification of the uncertainty associated with each part of the load, as discussed in the next section, requires separate treatment of the data sets. The bed- and suspended sand-load curves were, therefore, integrated separately and the resulting volumes were combined to estimate the total load of sand and coarser material. These volumes represent the “best-estimate” of the bed, suspended sand, and total sand/gravel load at each site (**Figures 4.6a through 4.6c**). The results indicate that the total sand load generally increased in the downstream direction during SY2010, SY2011, SY2012 and SY2014, but decreased downstream from Overton during SY2013, when the flows were generally very low¹².

Based on these results, the total sand load passing Overton exceeded the load passing Darr by a total of about 891,000 tons over the five year period (~178,000 tpy, on average) (**Figure 4.7**). Considering the 82,000 tons of sediment that was pumped and graded into the south channel at Jeffreys Island about one mile upstream from the Overton Bridge between September 2012 and June 2013 for the Pilot Sediment Augmentation Project and assuming that the sediment input from J-2 Return flows is negligible, this indicates that the segment of the study reach between the Darr Bridge and Overton (including the south channel at Jeffreys Island) degraded by about 809,000 tons over the 5-year period, or an average of about 162,000 tpy. The bulk of the deficit (~349,000 tons) occurred during SY2012.

¹² A short-duration medium flow (SDMF) release with peak discharge of 4,090 cfs and discharge exceeding 3,800 cfs for about 54 hours at the Overton gage, was, however, made in early April 2013.

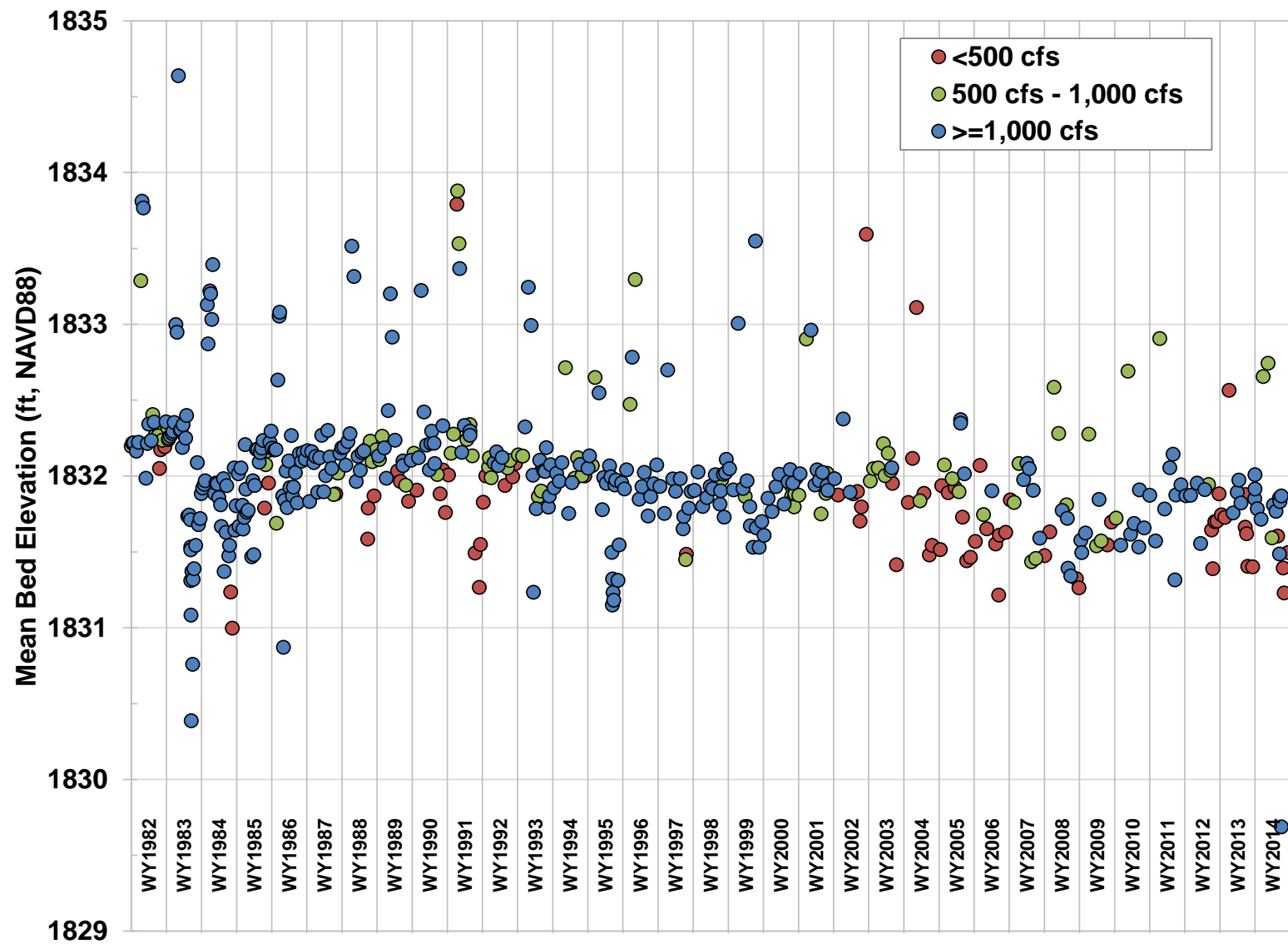


Figure 4.5. Mean bed elevations at the Grand Island gage, based on USGS field measurement data collected during WY1982 through WY2014.

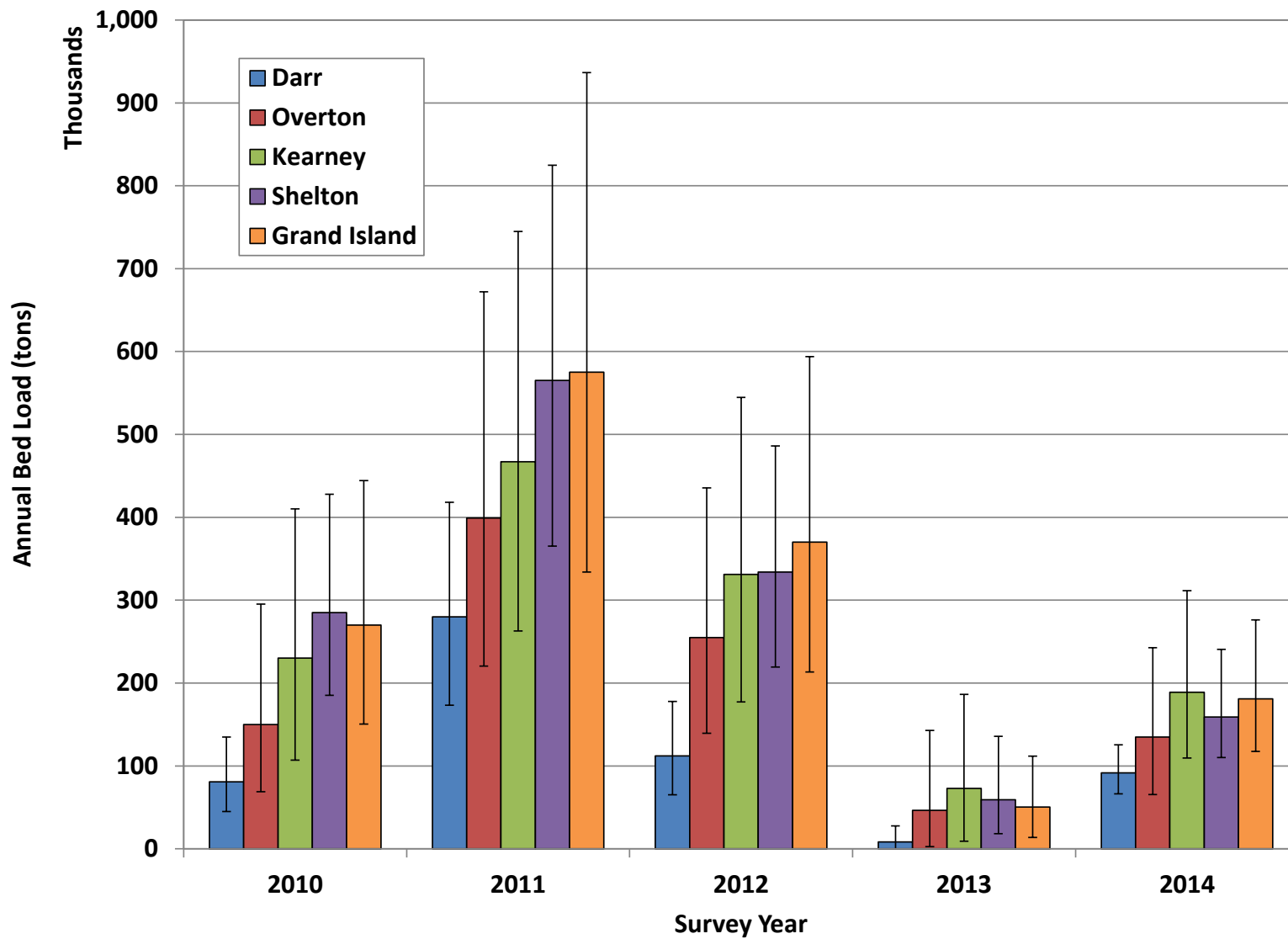


Figure 4.6a. Best-estimate of annual bed load passing the Darr, Overton, Kearney, Shelton and Grand Island measurement points during Survey Years (SY) 2010 through SY2014, based on integration of the bias-corrected bed-load rating curves over the survey year mean daily hydrograph. Whiskers are upper and lower 95-percent confidence limits from Monte Carlo simulation described in the next section.

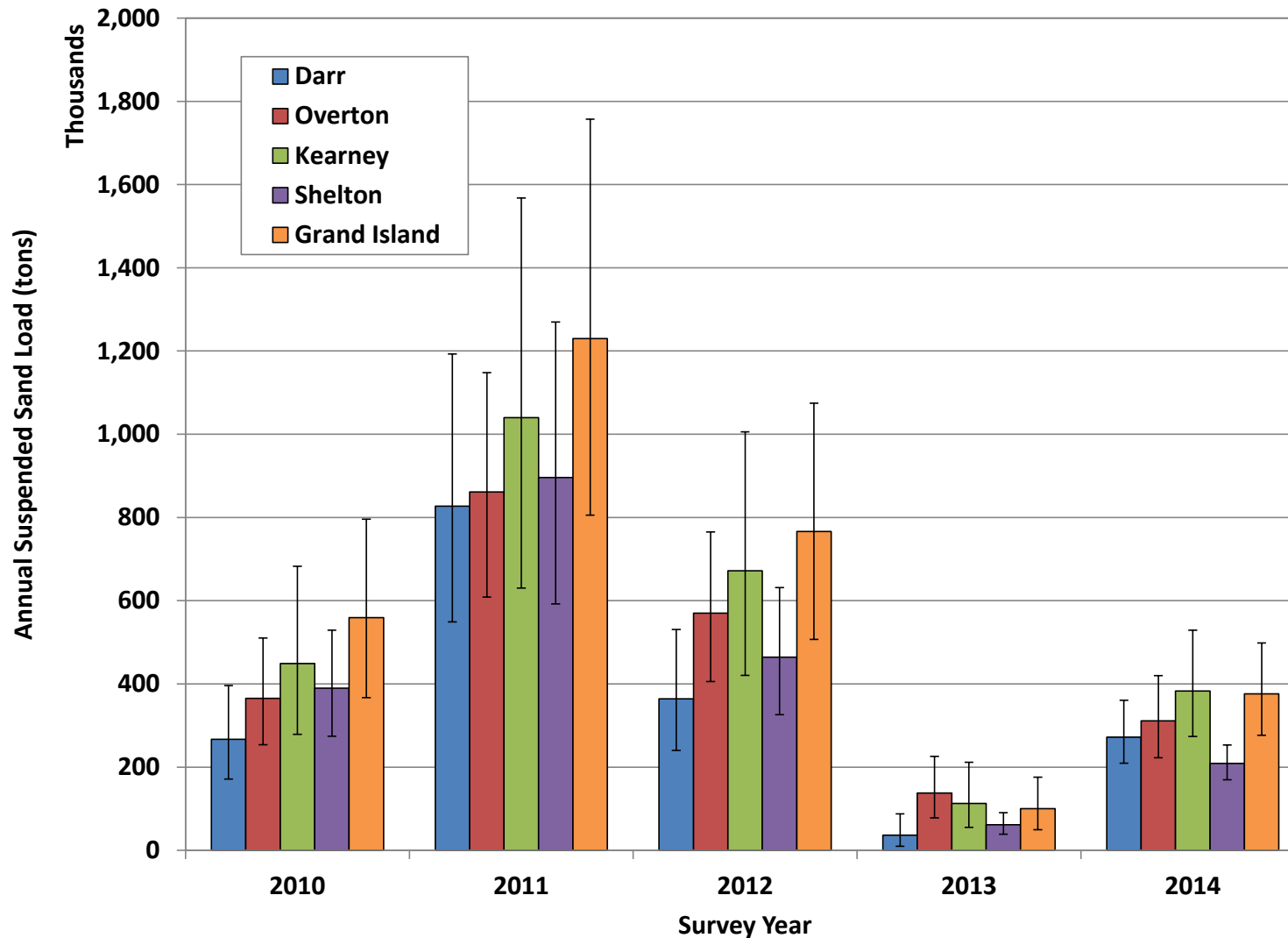


Figure 4.6b. Best-estimate of annual suspended sand load passing the Darr, Overton, Kearney, Shelton and Grand Island measurement points during Survey Years (SY) 2010 through SY2014, based on integration of the bias-corrected suspended sand rating curves over the survey year mean daily hydrograph. Whiskers are upper and lower 95-percent confidence limits from Monte Carlo simulation described in the next section.

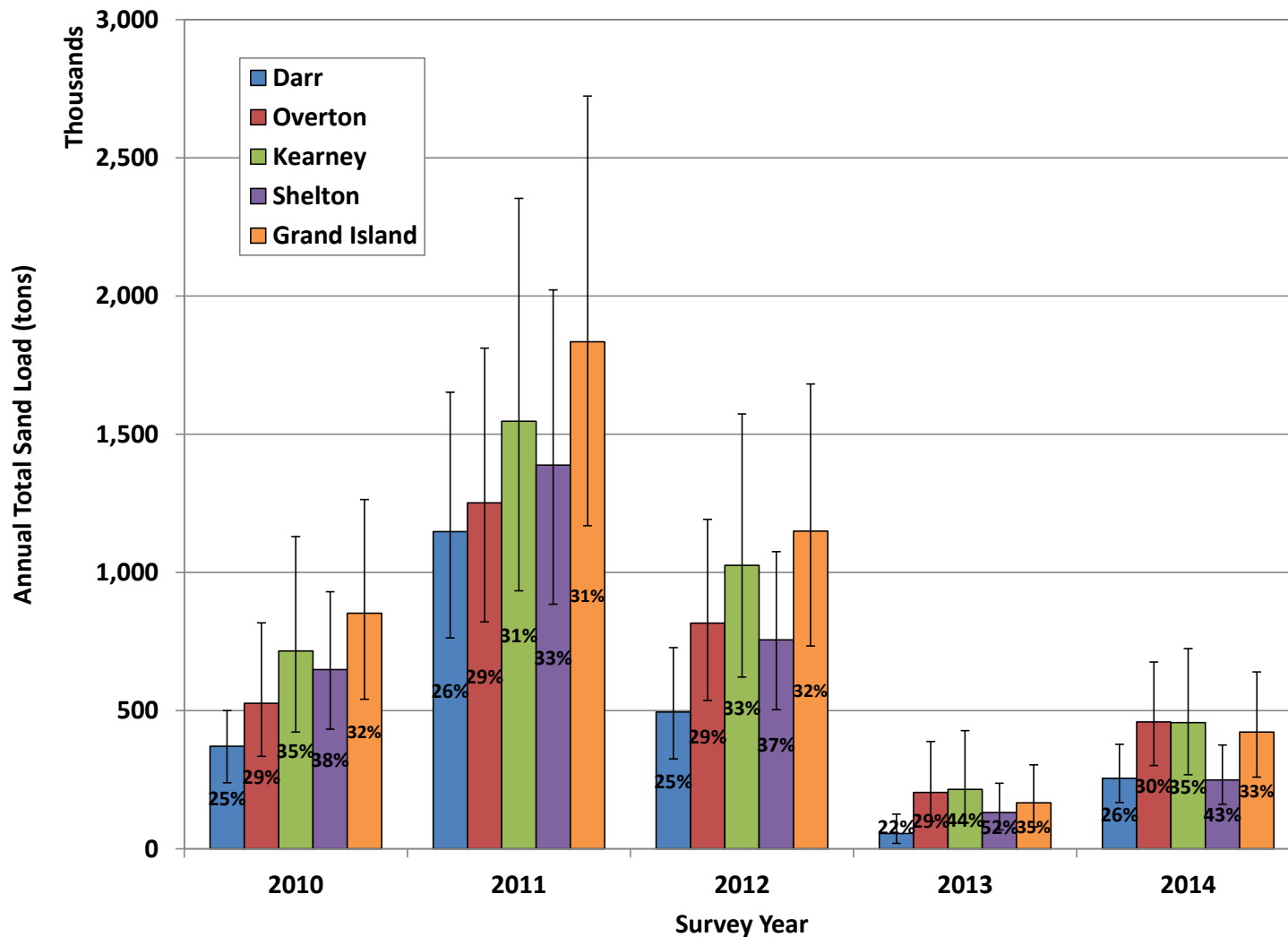


Figure 4.6c. Best-estimate of annual total sand/gravel load passing the Darr, Overton, Kearney, Shelton and Grand Island measurement points during Survey Years (SY) 2010 through SY2014, based on addition of the best estimates of bed-load and suspended sand load. Whiskers are upper and lower 95-percent confidence limits from Monte Carlo simulation described in the next section; bar labels are percent bed load.

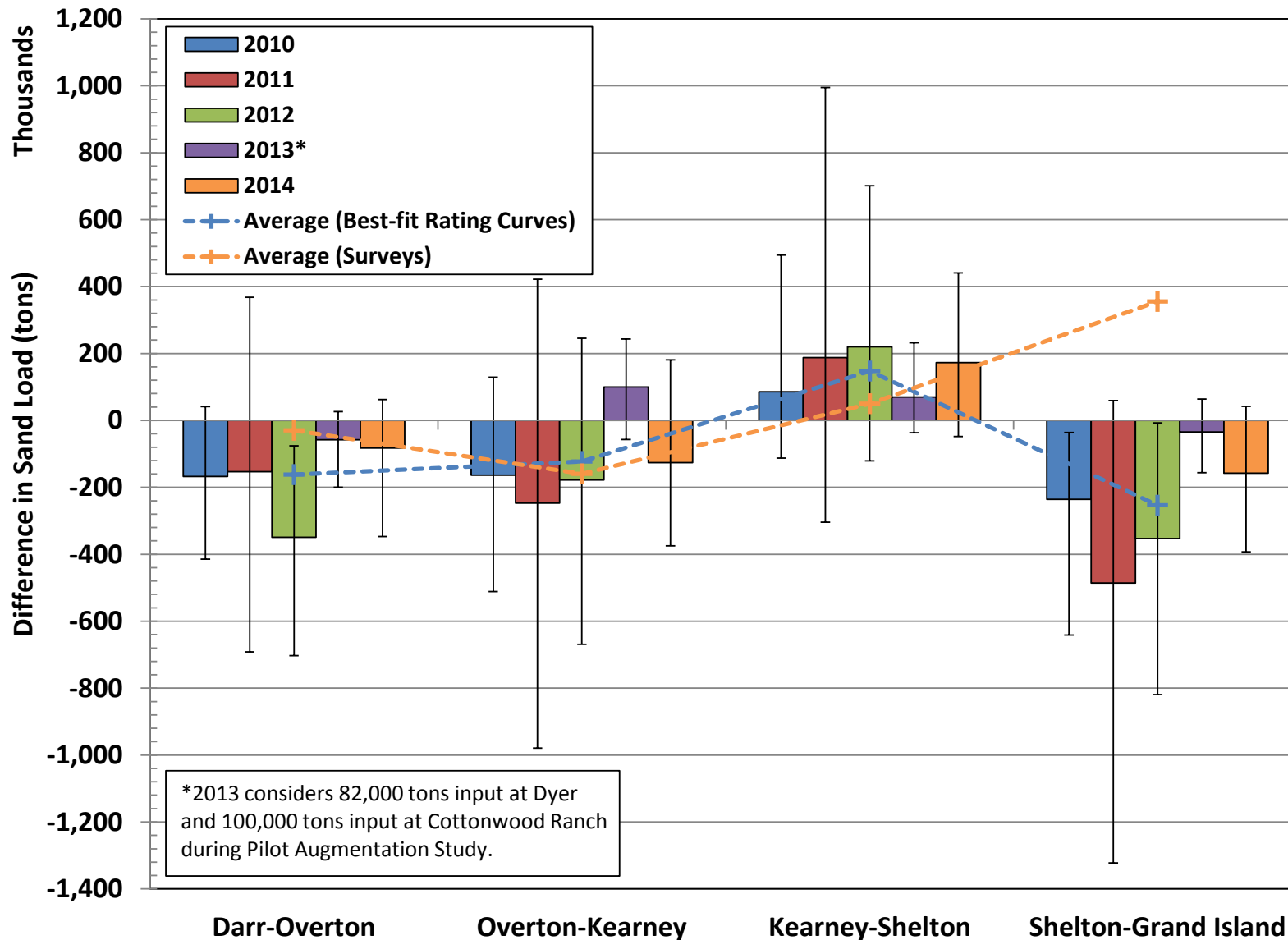


Figure 4.7. Best-estimate of the annual sand transport balance between the five measurement locations from SY2010 through SY2014. Also shown are the 5-year averages from the rating curves and from the survey-based estimates.

The total sand load passing Kearney exceeded the load at Overton by about 717,000 tons over the 5-year period (~143,000 tpy, on average). As noted above, approximately 50,000 tons of sediment were graded into the river at Cottonwood Ranch, just downstream from AP31 during SY 2010 and SY2011, and 100,000 tons of sediment were graded into the channel at this location between September 2012 and April 2013 as part of the Pilot Sediment Augmentation project. Assuming that none of the graded material would have been available for transport in the river in the absence of the grading, this additional input indicates that the reach between Overton and Kearney degraded by about 567,000 tons over the 5-year period, or about 113,000 tpy.

The total sand load passing Kearney exceeded the load passing Shelton by about 525,000 tons over the 5-year period, or an average of about 105,000 tpy. Most of the excess sediment occurred during SY2012 and SY2014, which combined for a surplus of nearly 409,000 tons (about 78 percent of the total). The bias-corrected rating curves also indicate that the reach between Shelton and Grand Island degraded by a total of about 1.05M tons (211,000 tpy) over the five-year period covered by the surveys. Nearly 682,000 tons of this degradation occurred during SY2011 and SY2012.

Some of the apparent sediment deficit in the overall reach indicated by these results may be attributed to unquantified tributary input, although it is unlikely that tributary input is sufficient to substantively change the overall result. DOI et al. (2006) estimated that the total tributary input between Overton and Wood River (~8 river miles downstream from Shelton) was about 105,000 tpy over the 48-year period from 1947 through 1990, or 11 percent to 18 percent of the estimated loads in the river. It is not clear from the DOI et al. (2006) report whether these loads include silts and clays, as well as the sand load, but the context in which it was presented implies that it does not include the silts and clays. The incremental contributing drainage area between Overton and Grand Island is only about 1,320 mi², about 2.5 percent of the approximately 52,000 mi² total drainage area. Based on the relatively small incremental drainage area and the conditions at the mouths of the significant tributaries that include Plum Creek (south bank tributary to south channel at Jeffreys Island), Spring Creek (north bank tributary just downstream from Overton Bridge), Buffalo and Elm Creek (north bank tributary just upstream from the KDS), and North Dry Creek [south bank tributary just upstream from Kearney (Highway 44) Bridge], sand loading from the tributaries to the Platte River mainstem is likely much smaller than the DOI et al. (2006) estimate and negligible compared to the typical loads in the river.

The average net change over the 5-year period based on the bias-correct rating curves is similar to the estimates from the monitoring surveys in the two middle reaches (Overton-Kearney and Kearney-Shelton, but quite different in the other two reaches (Figures 4.7 and 4.8). The surveys indicate that the reach between Darr and Overton was roughly in balance to slightly degradational (net degradation of ~30,000 tpy), with degradation during SY2010, SY2011, and SY2014 and aggradation in SY2012 and SY2013. The rating curves indicate that the reach degraded during all five years by an average of about 178,000 tons/year.

Both data sets indicate that the reach between Overton and Kearney was net degradational over the 5-year period, with an average deficit of about 143,000 tpy based on the rating curves and 160,000 tpy based on the anchor point surveys. However, the surveys indicated significant degradation during SY2010, SY2011, and SY2013, and aggradation SY2012 and SY2014 in amounts that are substantially higher on a year-to-year basis than indicated by the rating curves. The rating curve method predicted degradation during all five years.

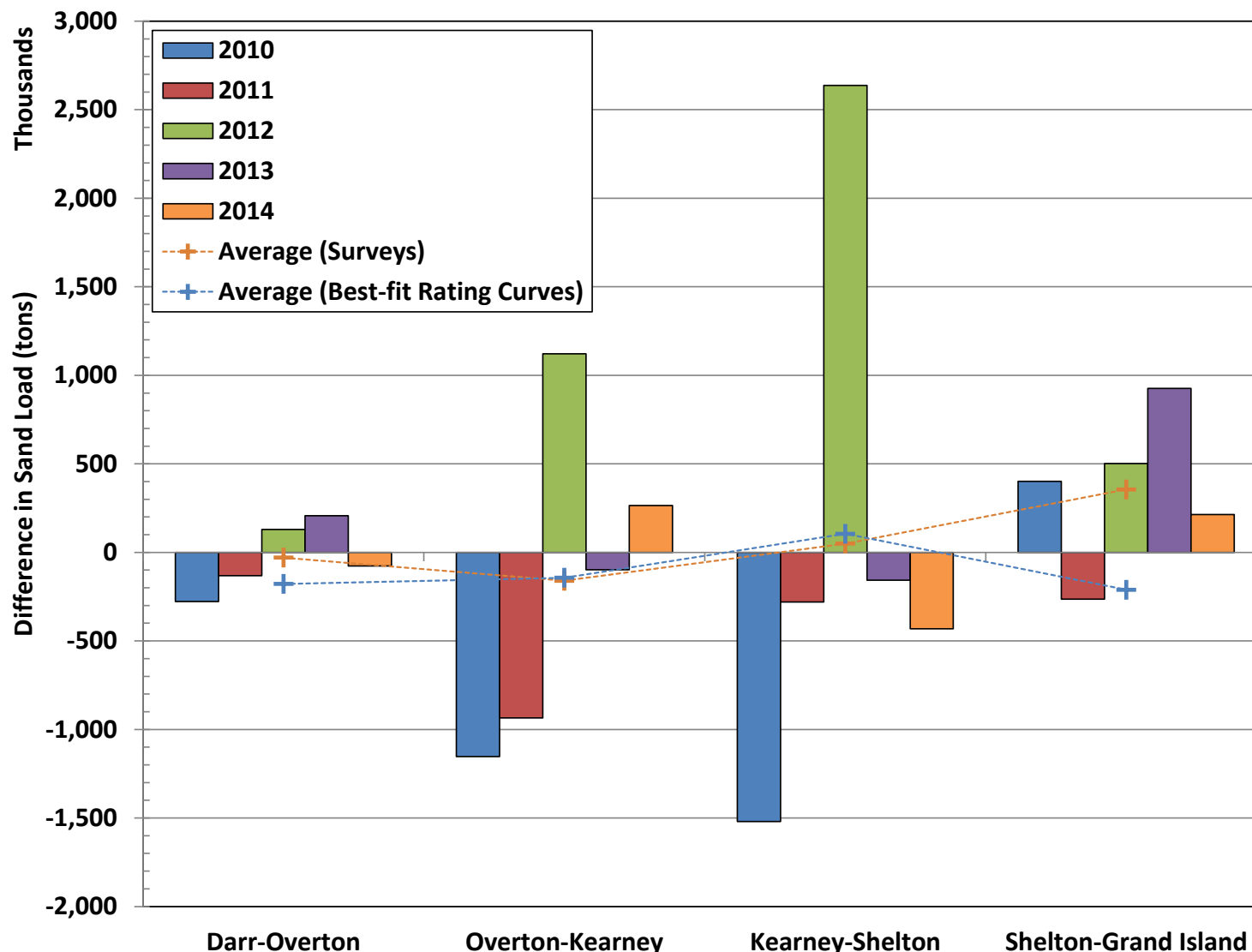


Figure 4.8. Estimated annual aggradation/degradation quantities from the pure panel AP survey data in the reaches encompassed by the five sediment-transport measurement sites. Also shown are the average annual aggradation/degradation quantities from both the surveys and the rating curves.

Both methods indicate net aggradation over the period between Kearney and Shelton (105,000 tpy based on the surveys and 50,000 tpy based on the rating curves), although degradation occurred during four of the years based on the surveys and aggradation occurred during all years based on the rating curves. The results from the two methods are very different downstream Shelton. The rating curves indicate degradation of about 211,000 tpy over the 5-year period, while the anchor point surveys indicate about 356,000 tpy of aggradation. Based on the surveys, aggradation occurred in all years except SY2011, while degradation occurred in all five years based on the rating curves.

4.1.3 Uncertainty in Sediment Balance Estimate

There is considerable uncertainty in the sediment balance estimates for both of the above sets of data. The survey-based estimates rely on data at only three transects that are spaced about 500 feet apart in each approximately 5-mile length of the river. Each transect represents the cross-section profile along only a single line across the river; thus, uncertainty is introduced into the result because the surveyed lines may not accurately reflect the changes that occur in the intervening approximately 500 feet of the river. In addition, the cumulative length encompassed by the three cross sections at each AP represents only about 4 percent of the total length that is being characterized by the AP, and there is uncertainty as to how well the aggradation/degradation response at the AP represents the response in the longer, unsurveyed portions of the reach. Uncertainty in the elevations of the individual survey points also contributes to uncertainty, although this appears to be a very minor factor compared to the other sources of uncertainty. The rating curve-based sediment balance is also subject to relatively large uncertainty because of the inherently high variability in the data used to develop the rating curves. These sources of uncertainty were quantified, to the extent possible with the available data, to help understand the implications to the Program's ability to draw valid conclusions about whether each portion of the reach is aggrading, degrading or in dynamic equilibrium.

The uncertainty in the rating curve-based estimates was quantified by performing Monte Carlo simulations of the annual loads based on the uncertainty bands on each rating curve. The simulations were performed by generating 1,000 estimates of the annual loads for each site assuming that the variability in the logarithm of the individual, estimated loads at the mean of the logarithms of the discharges in each data set follows a normal distribution with mean equal to the load estimated from the rating curve and upper and lower 95-percent confidence limits equal to the corresponding confidence limits on the regression equation at the mean discharge (**Table 4.1**). It was also assumed that the slope of the regression line varies about the best-estimate slope based on a normal distribution parameterized by the standard deviation of the slope term from the regression analysis. The difference in annual sediment load between the sites was then calculated for each of the 1,000 sets of annual loads, and the resulting data set was used to assess the variability in the estimated aggradation/degradation volumes.

The above assumptions are illustrated using the suspended sand curves at the Overton site in **Figure 4.9**. The best-estimate sediment load at the back-transformed log mean discharge of the data set (2,517 cfs) is 2,213 tons per day (tpd), and the upper and lower 95-percent confidence limits on the regression line at this discharge are 1,288 and 2,320 tpd, respectively (green vertical line in Figure 4.9a). The resulting standard deviation of the predicted sediment loads in the log domain at this discharge is 0.078. The distribution of the predicted sediment loads at the mean from the Monte Carlo simulation ranged from about 1,180 to 4,230 tpd (Figure 4.9b). The best-estimate of the exponent on the rating curve is 1.328, and the standard deviation of this estimate is 0.261. The resulting exponents from the Monte Carlo simulation ranged from 0.6 to 2.24 (Figure 4.9c). The coefficient (*a*) on the rating curve for each of the 1,000 estimates was back-calculated using the predicted sediment load (log) at the mean discharge and the exponent (*b*) for each step in the simulation. The annual suspended sediment loads at this site

Table 4.1. Summary of bed and suspended sand load regression equations and associated statistics.

Measurement Site	Mean Discharge ¹	a ²	b ²		Average Bias Correction Factor ³	Best-estimate Sand Load at log Mean Discharge (tons) ⁴			
			Mean	Standard Deviation		Mean	Lower 95% Confidence Limit	Upper 95% Confidence Limit	Standard Deviation (log)
Bed Load									
Darr	2,933	0.016	1.399	0.227	1.09	1,123	742	1,697	0.109
Overton	3,960	0.012	1.356	0.376	1.11	946	527	1,698	0.154
Kearney	3,967	0.161	1.077	0.341	1.20	1,212	719	2,044	0.138
Shelton	3,354	0.081	1.149	0.307	1.08	912	561	1,481	0.128
Grand Island	3,888	0.025	1.323	0.317	1.15	1,375	823	2,297	0.136
Suspended Sand Load									
Darr	2,516	0.133	1.271	0.231	1.11	2,791	1,941	4,014	0.096
Overton	3,600	0.111	1.209	0.223	1.12	2,213	1,635	2,994	0.080
Kearney	3,459	0.025	1.407	0.283	1.19	2,361	1,551	3,592	0.111
Shelton	2,892	0.003	1.607	0.195	1.08	1,253	921	1,705	0.081
Grand Island	3,609	0.027	1.412	0.251	1.15	2,817	1,971	4,025	0.094

¹ Discharge based on mean of logarithms of measured data set

² Coefficient and exponent of power function rating curve (Sediment Load=a*Discharge^b)

³ Average bias correction factor for mean daily discharges in the four-year data set

⁴ Best-estimate sediment load, confidence limits and standard deviation (log domain) of regression confidence bands at mean discharge of measured data set

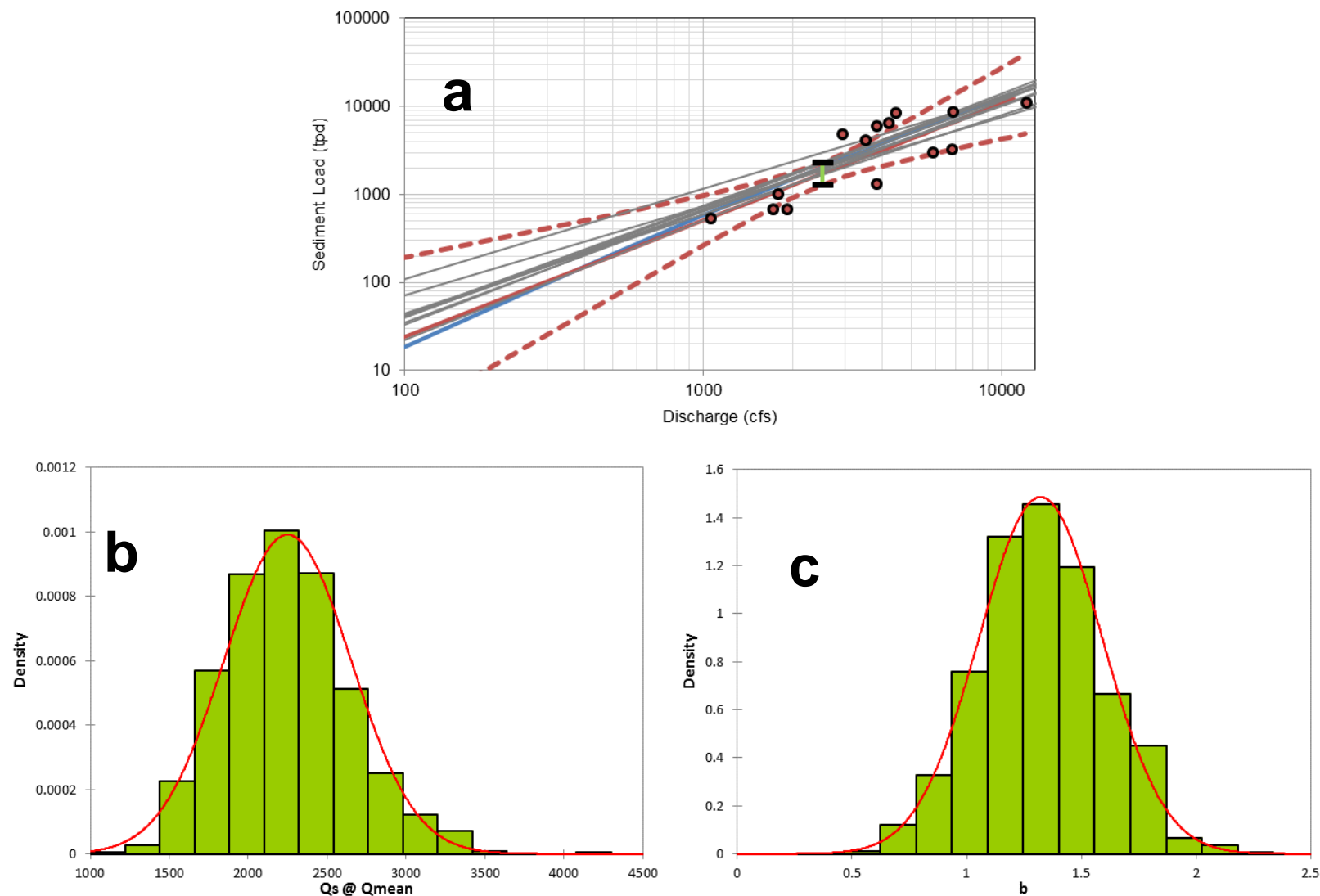


Figure 4.9. (a) Suspended sand rating curves at Overton. Light grey lines are sample curves from the Monte Carlo simulation; (b) Distribution of estimated sediment loads at the mean (log) discharge of the measured data set from Monte Carlo simulation; (c) Distribution of the exponents on the Overton suspended sand load rating curve from the Monte Carlo simulation.

from the Monte Carlo simulations had central tendency very close to the best-estimate values for each year that were presented in the previous section, but ranged from 204,000 tons to 743,000 tons in 2010, 499,000 tons to 1.73M tons in 2011, 342,000 tons to 1.15M tons in 2012, 55,000 tons to 367,000 tons in 2013, and from 206,000 tons to 694,000 tons in 2014 (**Figure 4.10**).

The statistical distribution of total sediment loads at each site was estimated by performing independent Monte Carlo simulations for the bed and suspended sand loads, and adding the corresponding bed and suspended loads for each step in the simulation. The resulting distribution of total sand transport balances, computed from the difference between the upstream inflow and downstream outflow in each segment of the reach for each step in the simulation (Figure 4.7) suggest the following with respect to the statistical significance ($\alpha=.05$, two-tailed) of the aggradation/degradation trends:

1. The median value of the sediment balance indicates degradation in the reaches from Darr to Overton, Overton to Kearney, and Shelton to Grand Island, and aggradation between Kearney and Shelton.
2. Darr to Overton:
 - a. The degradational trend is statistically significant only during SY2012.
 - b. The probability that the reach was degradational during the other years ranged from 71 percent (2011) to 92 percent (2010) (**Table 4.2**).
3. Overton to Kearney:
 - a. The degradational trends during 2010, 2011, 2012 and 2014 and the aggradational trend in 2013 are not statistically significant. Note that the aggradational trend in 2013 results from the input of 100,000 tons at Cottonwood Ranch during the Pilot Sediment Augmentation Study.
 - b. The probability that the reach was degradational during 2010, 2011, 2012 and 2014 ranged from 71 percent (2014) to 83 percent (2010) and the probability of aggradation in 2013 was 88 percent.
4. Kearney to Shelton:
 - a. The aggradational trends are not only statistically significant for any of the survey years.
 - b. The probability that the reach was degradational ranged from 78 percent (2011) to 89 percent (2014).
5. Shelton to Grand Island:
 - a. The degradation trends are statistically significant only for SY2010 and SY2012.
6. The probability that the reach was degradational during 2011, 2013 and 2014 ranged from 75 percent (2013) to 94 percent (2011).

Table 4.2. Probability of degradation when mean indicates degradation, or aggradation when mean indicates aggradation.

Survey Year	Darr-Overton (%)	Overton-Kearney (%)	Kearney-Shelton (%)	Shelton-Grand Island (%)
2010	92	83	82	97
2011	71	73	78	94
2012	98	76	86	95
2013	86	88	87	75
2014	87	71	89	89

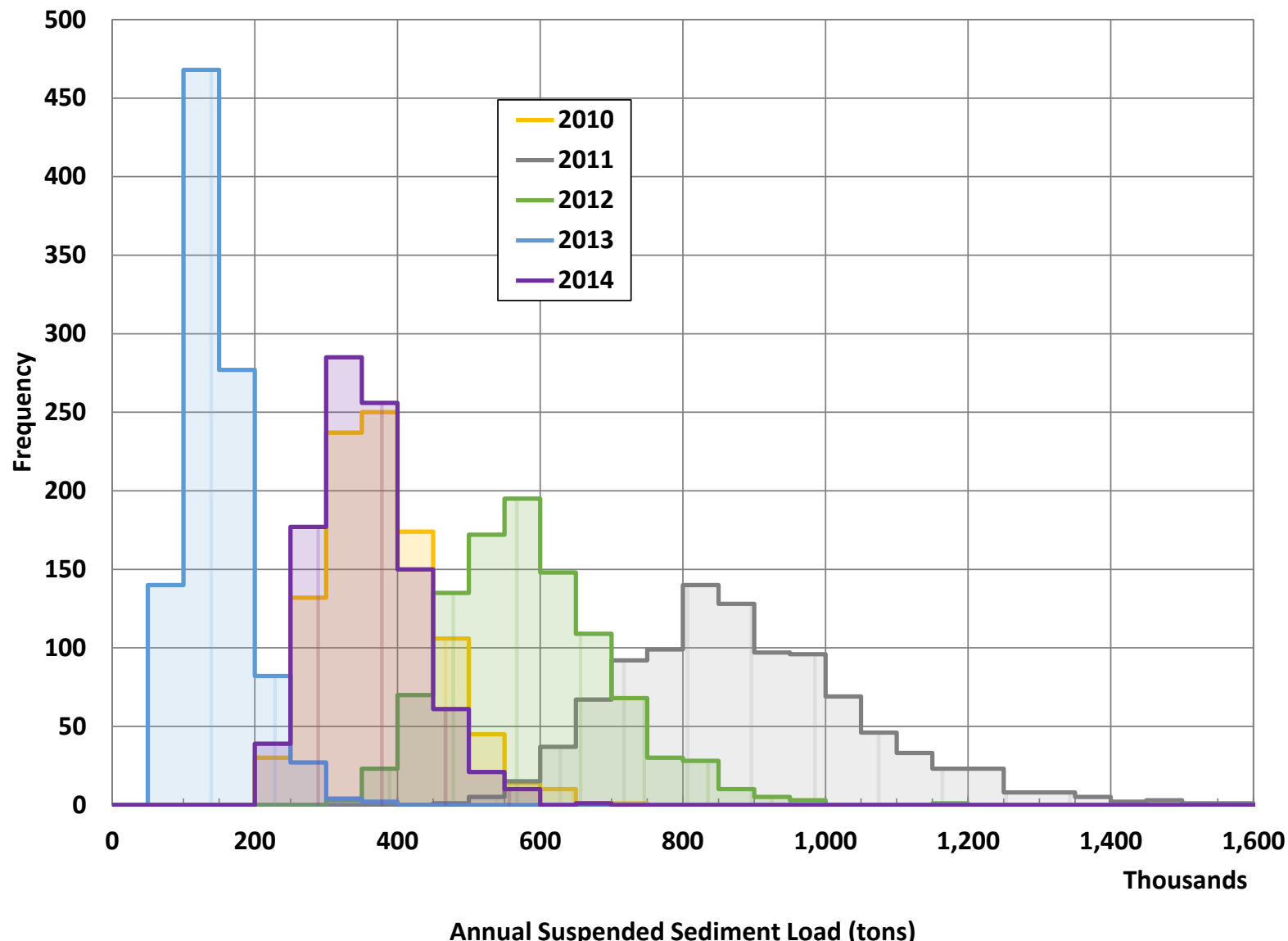


Figure 4.10. Distribution of estimated annual suspended sand loads at Overton based on the 1,000 Monte Carlo trials for each of the five years covered by the monitoring surveys.

Unfortunately, it is not possible to quantify the uncertainty in the survey-based estimates in the same manner as the rating curve-based estimates. Uncertainty associated with the elevations of individual survey points is quite small. Monte Carlo simulation for the 2013 annual report (Tetra Tech, 2013) using the reported error statistics from the GPS data logger showed that the potential error in the surveyed elevations at the individual points at the middle primary transect of AP29 would result in only about ± 0.13 percent variability in year-to-year change in cross-sectional area. The amount of uncertainty associated with how well the transects represent the area changes within each AP, as well as the overall, approximately 5-mile reach represented by the AP, cannot be quantified with the available data. A simple test using the 2012 and 2013 LiDAR surfaces for a bar in the south channel at Jeffreys Island that was regularly inundated by J-2 Return hydropower releases but was dry during both LiDAR surveys showed that the volume change estimated from three transects in the middle of the bar was within about 2 percent of the volume change estimated by overlaying the two LiDAR surfaces (**Figure 4.11**). The excellent agreement for this test is due to the relatively uniform distribution of aggradation/degradation zones through the sample area. Attempts to perform a similar test on a larger reach of the river channel were not successful because of the confounding effects of the water-surface at the time of the surveys and the fact that a significant part of the bed elevation changes occur in the inundated part of the channel. Further systematic testing of this issue may ultimately show that use of high-resolution LiDAR data, collected at low flows may provide improved estimates of the aggradation/ degradation status of the reach than the transect surveys. This is particularly true if tests using green LiDAR that can penetrate relatively clear, shallow water are successful.

The yearly aggradation/degradation volume estimated from the survey data for 2011 are within the 90 percent (two-tailed) confidence bands on the corresponding rating-curve based estimates (**Figure 4.12b**). For the other years, most of the survey-based estimates are outside the confidence bands on the rating curve-based estimates (**Figures 4.12a, c-e**). This suggests that the survey-based estimates that rely on data from a limited number of cross sections may not adequately represent conditions over the broader reaches in which they are located.

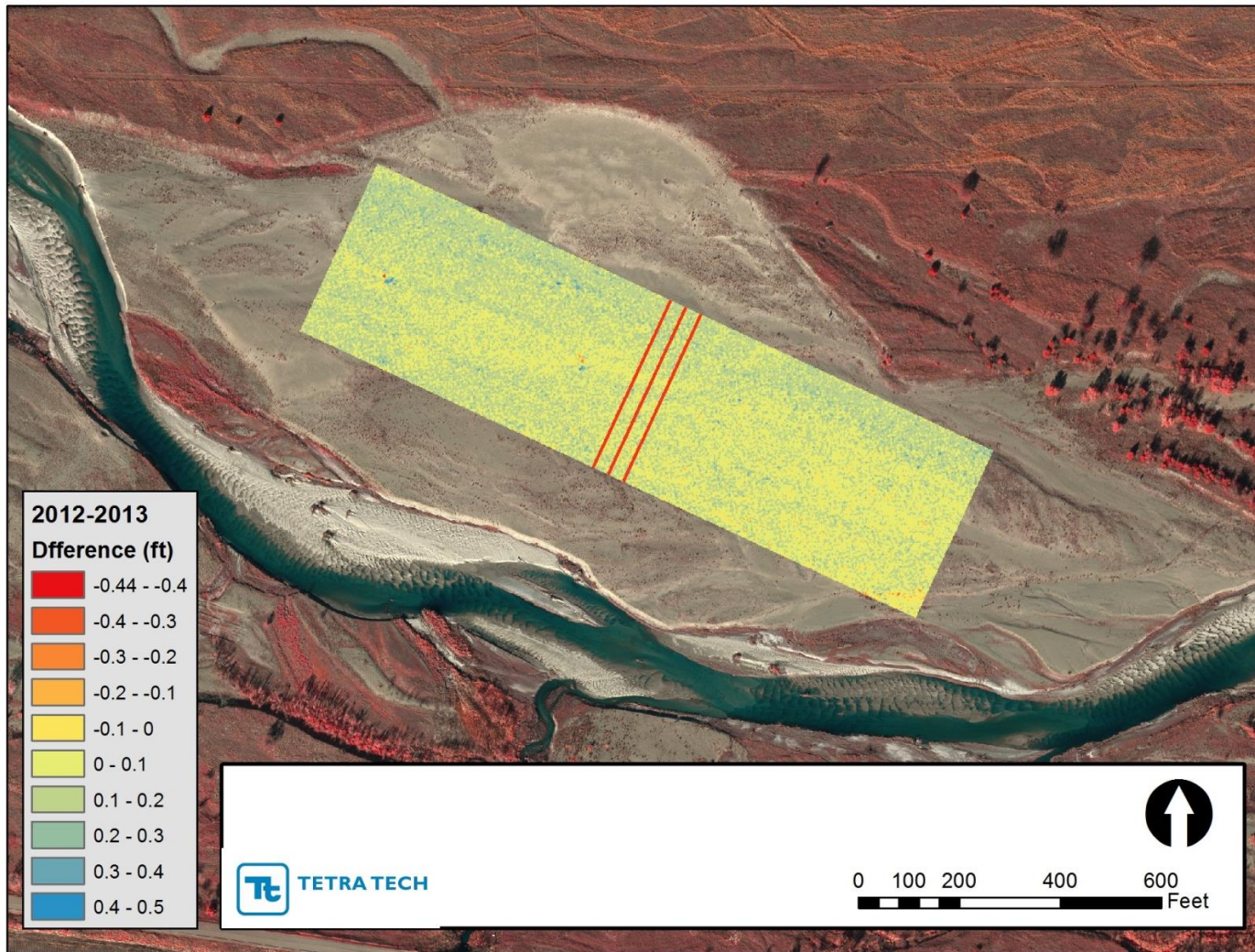


Figure 4.11. Area used to test agreement between cross section-based volume estimates and estimates based on the complete LiDAR surface (~RM245.5, south channel at Jeffreys Island approximately midway between AP36 and AP37).

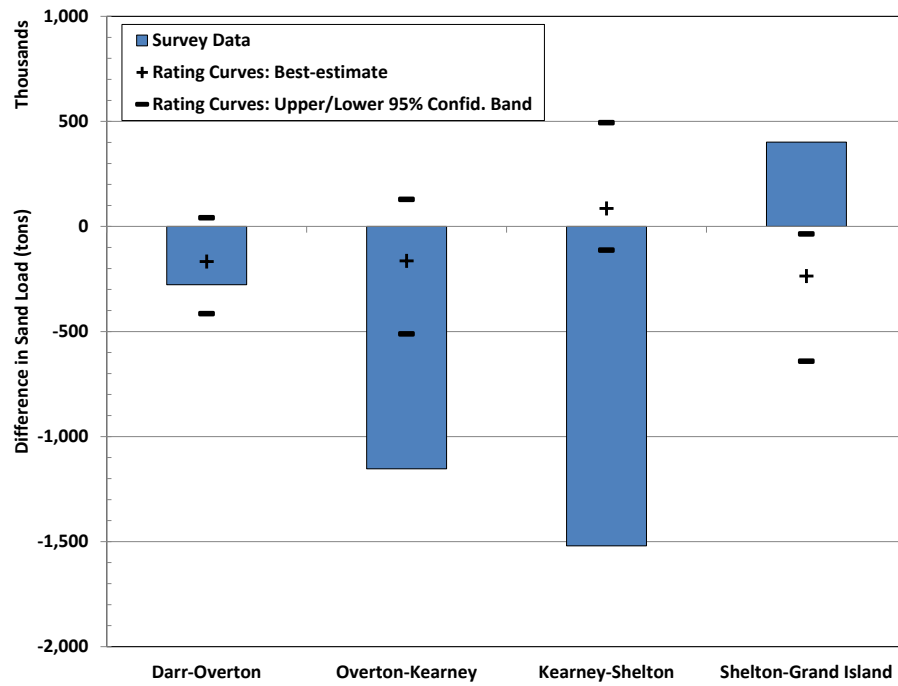


Figure 4.12a. Best-estimate of aggradation/degradation volumes based on the survey data (bars) and mean and upper and lower 95-percent confidence limits on the volumes predicted by the sediment rating curves (symbols) for 2010.

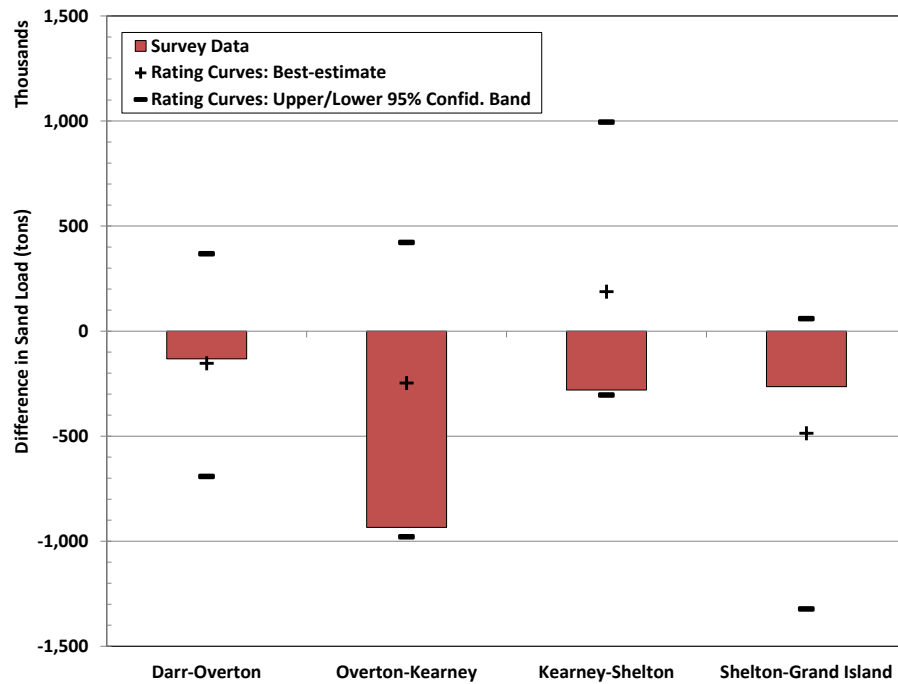


Figure 4.12b. Best-estimate of aggradation/degradation volumes based on the survey data (bars) and mean and upper and lower 95-percent confidence limits on the volumes predicted by the sediment rating curves (symbols) for 2011.

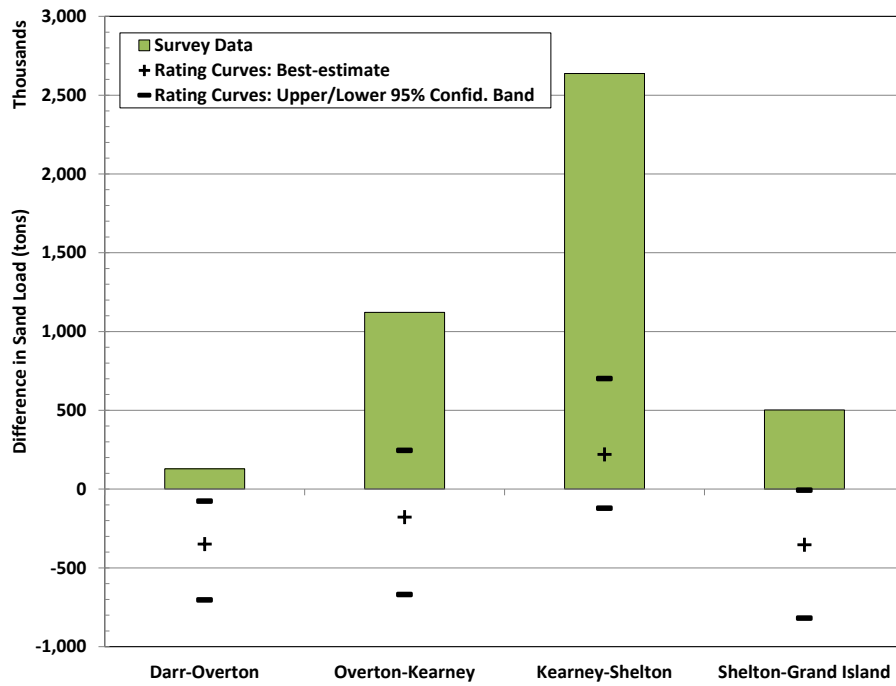


Figure 4.12c. Best-estimate of aggradation/degradation volumes based on the survey data (bars) and mean and upper and lower 95-percent confidence limits on the volumes predicted by the sediment rating curves (symbols) for 2012.

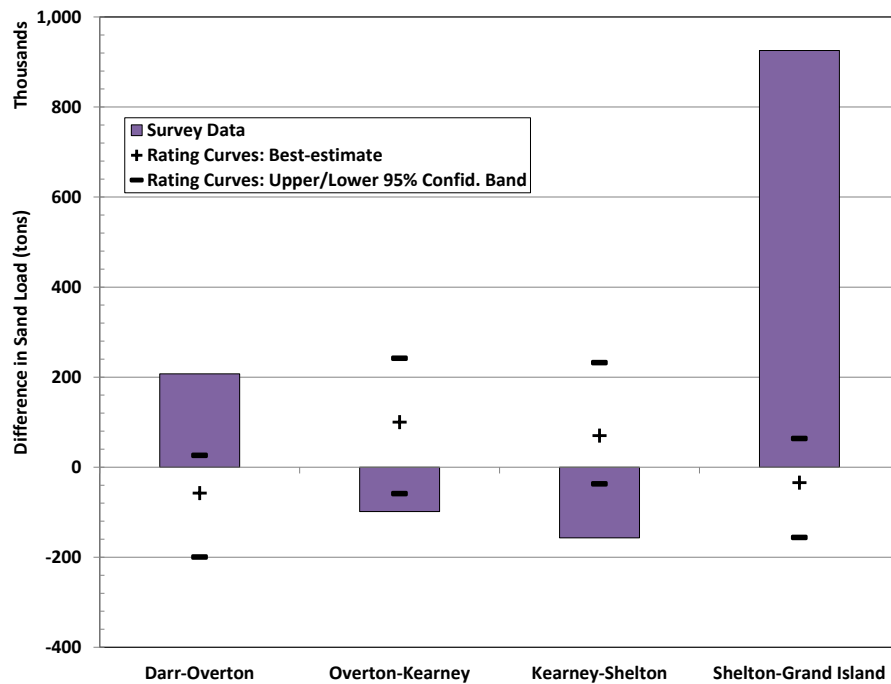


Figure 4.12d. Best-estimate of aggradation/degradation volumes based on the survey data (bars) and mean and upper and lower 95-percent confidence limits on the volumes predicted by the sediment rating curves (symbols) for 2013.

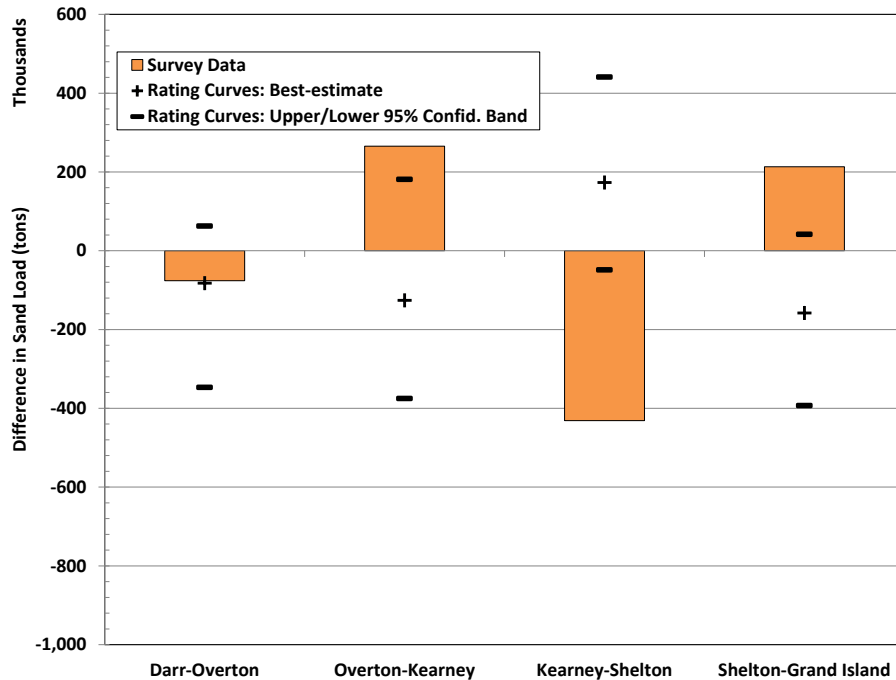


Figure 4.12e. Best-estimate of aggradation/degradation volumes based on the survey data (bars) and mean and upper and lower 95-percent confidence limits on the volumes predicted by the sediment rating curves (symbols) for 2014.

Using the SEDVEG Gen3 Model with a 48-year flow record (1947-1990) that was adjusted to represent current operations of the system, Reclamation estimated that the reach between the Overton and Elm Creek Bridges has a net sediment deficit of about 185,000 tons/year under the existing flow regime (DOI Reclamation and USFWS, 2006). They also estimated that the reach between Elm Creek and Chapman had net sediment excess of about 62,000 tons/year, with most of the excess occurring downstream from Chapman. HEC-6T modeling by Tetra Tech (2010) using observed hydrology for the 12.5-year period from October 1989 through April 2002 estimated that the annual sediment deficit between Overton and Elm Creek was about 150,000 tons. Although the results were not presented in terms of volumes, HEC-6T modeling of the overall monitoring reach by Tetra Tech (see HDR and Tetra Tech, 2011) was consistent with the Tetra Tech (2010) findings in the Overton to Elm Creek Reach and showed that the reach between Kearney and Shelton was slightly aggradational, the reach between Shelton and Grand Island was degradational, and the remainder of the reach was approximately in balance, with localized zones of both aggradation and degradation. Flows during the monitoring period have been much higher than the typical flows in the records used for both the DOI (2006) and Tetra Tech (2010) modeling (Figure 4.13).

The rating curves for Overton, Kearney and Grand Island were integrated over the published mean daily flows from the USGS records for the longest available overlapping record (WY1984 through WY2014) to provide longer-term estimates of the annual sediment loads and sediment balance¹³. The best-estimate annual sand load at Overton averaged about 580,000 tons over the 31-year period, and ranged from about 72,000 tons (WY2004) to 2.46M tons (WY1984) (Figures 4.14 and 4.15). The sand loads at Kearney during this period averaged about 722,000

¹³ Longer-term records are not available for the Lexington or the Shelton gages.

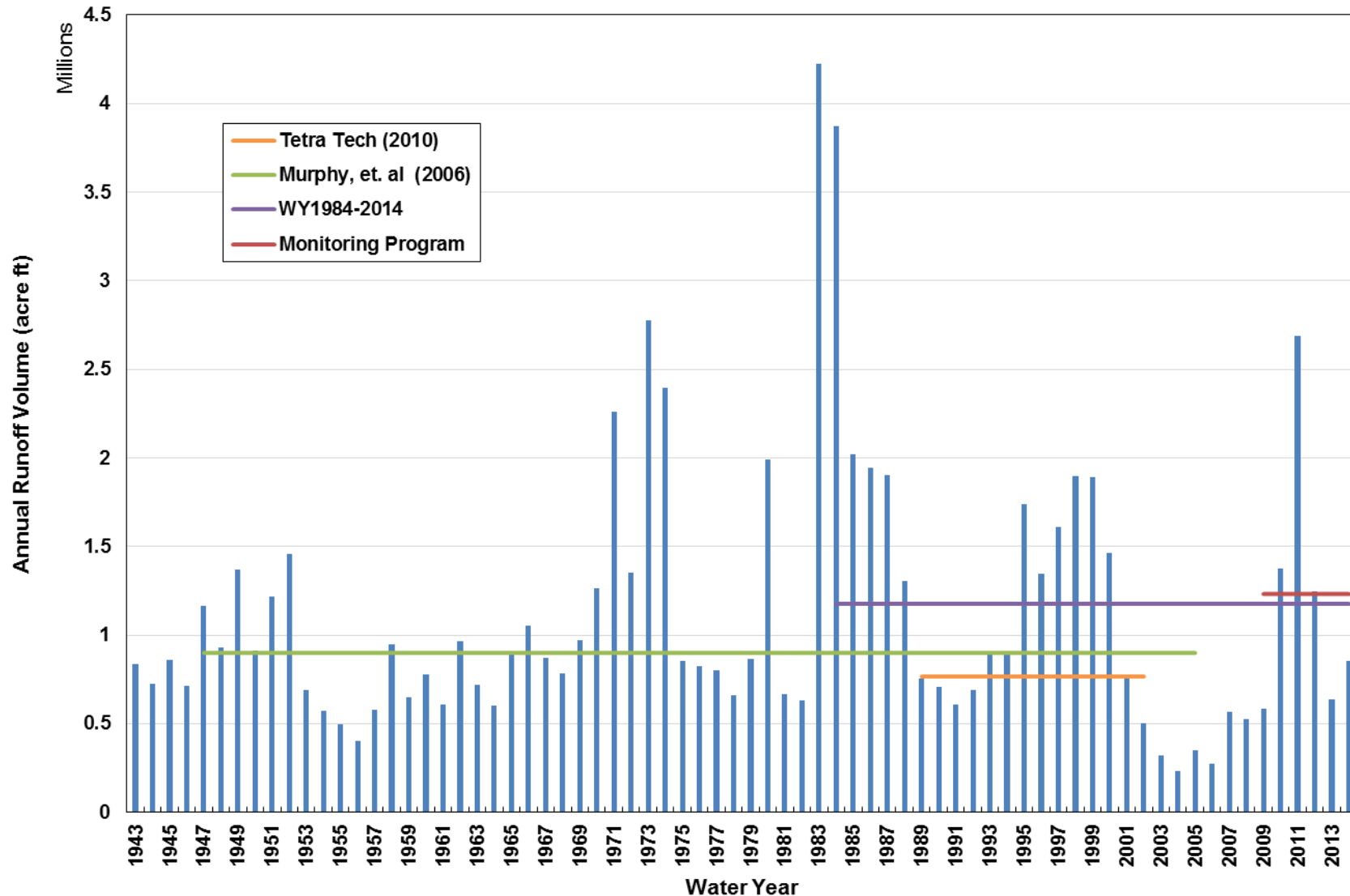


Figure 4.13. Annual total runoff volume at the USGS Overton gage between WY1943 and WY2014. Also shown are the mean flows for the 48-year record used for the DOI (2006) model, the Tetra Tech (2010) model and the 5-year monitoring period.

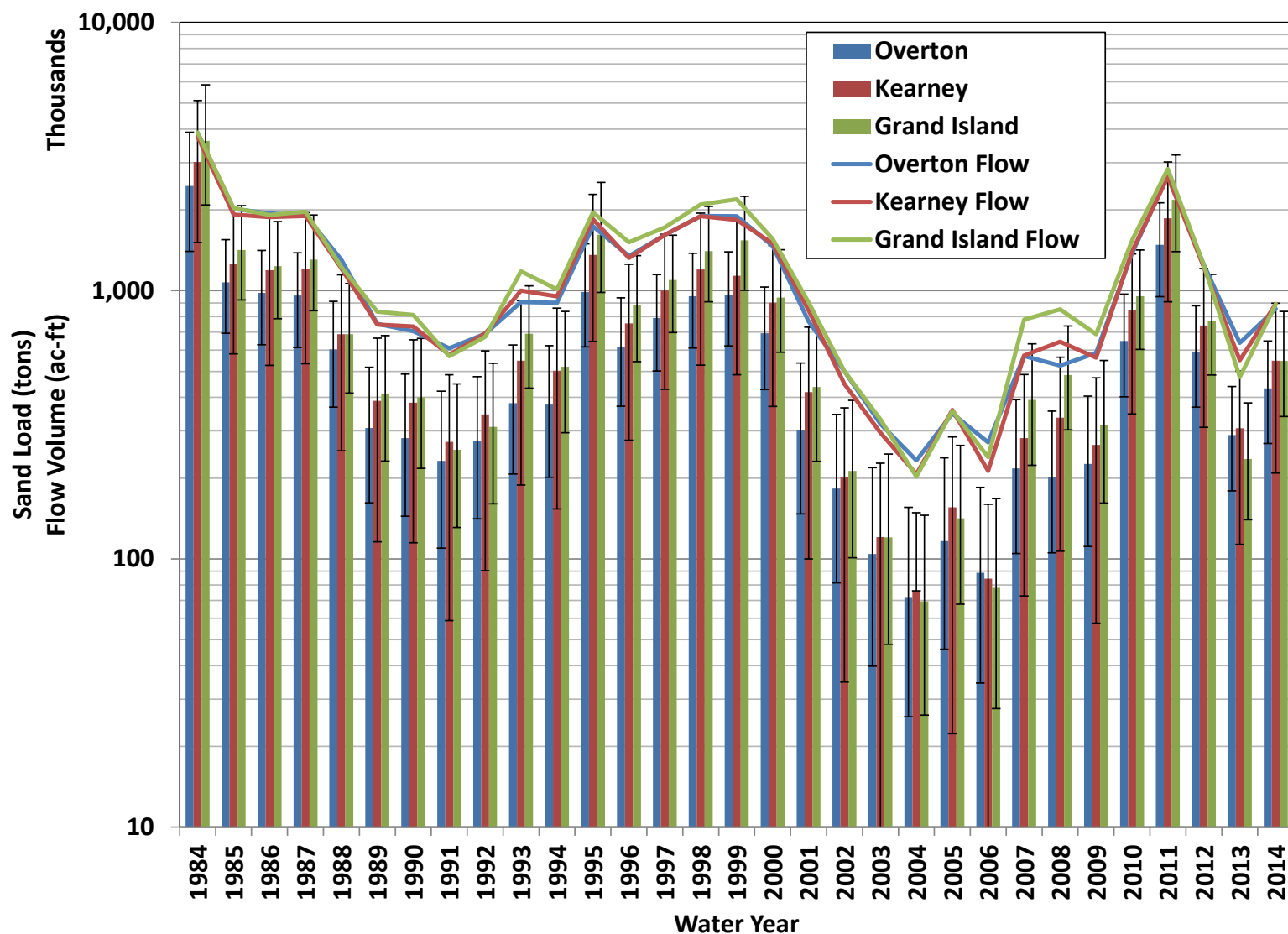


Figure 4.14. Estimated average annual total sand load passing the Overton, Kearney, and Grand Island gages during individual years from WY1984 through WY2014, based on integration of the respective rating curves over the USGS published mean daily flows. Also shown are the upper and lower 95-percent confidence limits from the Monte Carlo simulations.

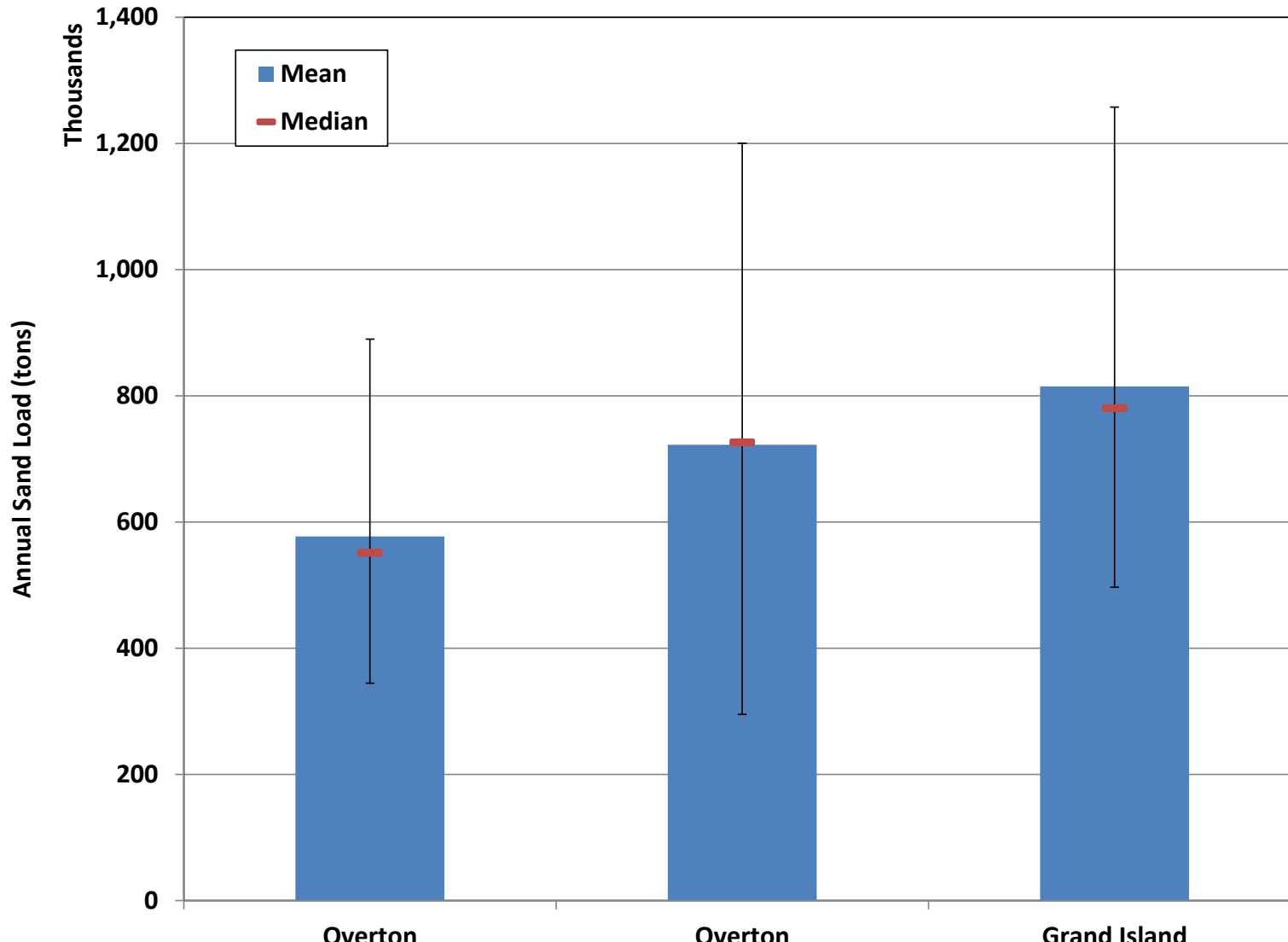


Figure 4.15. Average annual total sand load passing the Overton, Kearney, and Grand Island gages based on integration of the respective rating curves over the USGS published mean daily flows for the period from WY1984 through WY2014. Also shown are the median values and 5th and 95th percentiles from the Monte Carlo simulations.

tons, and ranged from 76,000 to 3.01M tons, and the loads at Grand Island averaged 815,000 tons, and ranged from 69,000 to 3.61M ton. Based on these loads, the best-estimate of the sediment deficit between Overton and Kearney averaged 145,000 tons over the period and deficit between Kearney and Grand Island averaged 93,000 tons (**Figures 4.16a** and **4.17**, respectively). Based on Monte Carlo simulations similar to those described above, the 95-percent (two-tailed) confidence bands on these estimates are, however, quite large, in all cases crossing zero (**Figure 4.16b**). This indicates that, even though nearly all of the annual estimates indicate degradation in both reaches, the values are not statistically significant.

To help put the confidence bands on these estimates into perspective, the mean value of the sediment balance from the Monte Carlo simulations for the Overton to Kearney reach was negative (i.e., degradational) in 30 of the 31 years, and the distributions for the individual years suggest an approximately 70-percent chance, on average, that the reach was, in fact, degradational. Similarly, the mean value of the sediment balance for the Kearney to Grand Island Reach was negative in 24 of the 31 years, with an average 63-percent chance that the reach was actually degradational. The mean values from this analysis also indicate that both reaches are more strongly degradational during high-flow years than during low-flow years (**Figure 4.18**).

All of the above evidence points to a general degradational tendency upstream from Kearney, with the best-estimate of the long-term average between Overton and Kearney in the range of about 145,000 tons per year. The available evidence for the reach between Kearney and Grand Island is less clear, with both the surveys and rating curves indicating aggradation between Kearney and Shelton, but the two methods indicating opposite trends (aggradation based on surveys, degradation based on rating curves) between Shelton and Grand Island. Because the various lines of evidence are not consistent, and because conditions in the portion of the reach downstream from Shelton are highly variable, it cannot be concluded with a reasonable degree of certainty that this reach is either aggradational or degradational.

4.2 Flow #3

Increasing $Q_{1.5}$ with Program flows will increase local boundary shear stress and frequency of inundation at the existing green line (elevation at which riparian vegetation can establish). These changes will increase riparian plant mortality along margins of the channel, raising the elevation of the green line, providing more exposed sandbar area and a wider, unvegetated main channel.

The extent to which the GLE and resulting unvegetated widths measured at the pure panel APs are responsive to flow was assessed by correlating these metrics with various discharge metrics. As specified in the DAP, the edges of unvegetated segments along each transect are identified by the GLE points. To remove the effects of river slope in the correlations, the GLE values were normalized to the 1,200-cfs water surface (i.e., the difference between the GLE and the local 1,200-cfs water surface was used rather than the actual elevation). In addition, the differences in the modeled water-surface elevations (subsequently referred to as stage for brevity) for the applicable discharge metrics were used in the analysis, rather than the actual discharge. The following specific correlations were evaluated:

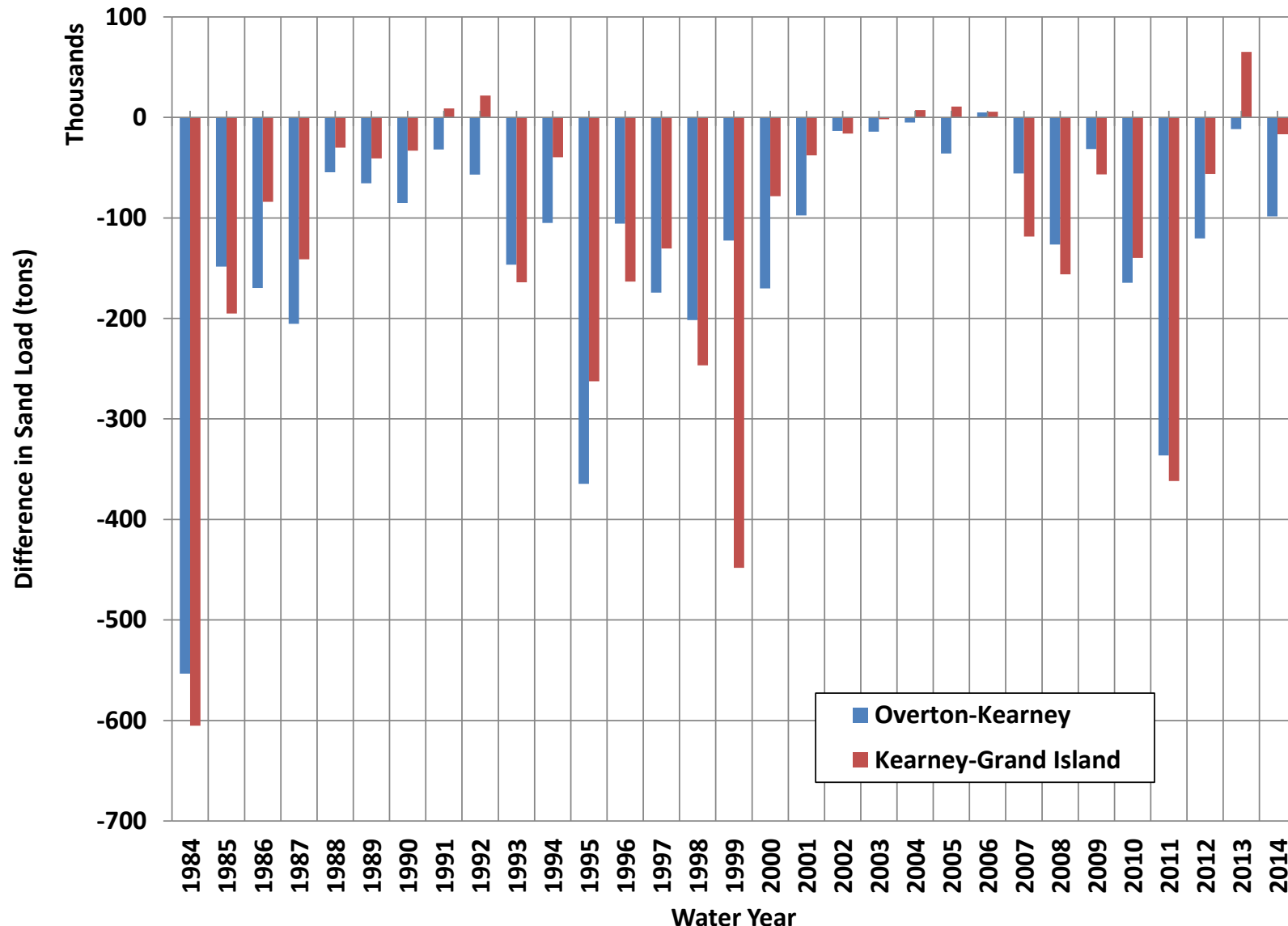


Figure 4.16a. Estimated annual sand transport balance between Overton, Kearney and Grand Island from WY1984 through WY2014.

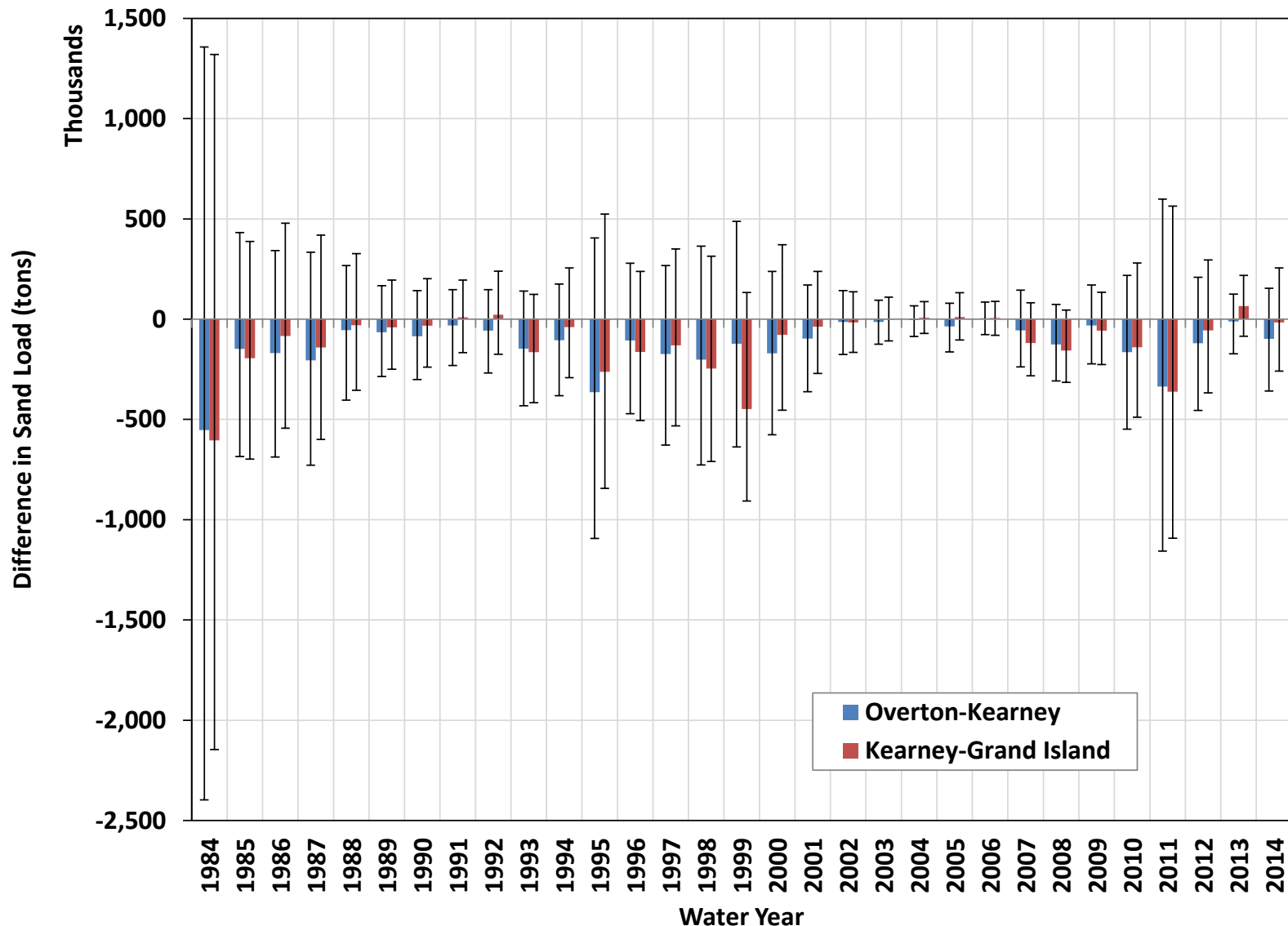


Figure 4.16b. Estimated annual sand transport balance between Overton, Kearney and Grand Island from WY1984 through WY2014. Same as Figure 4.16a with confidence limits from Monte Carlo simulations.

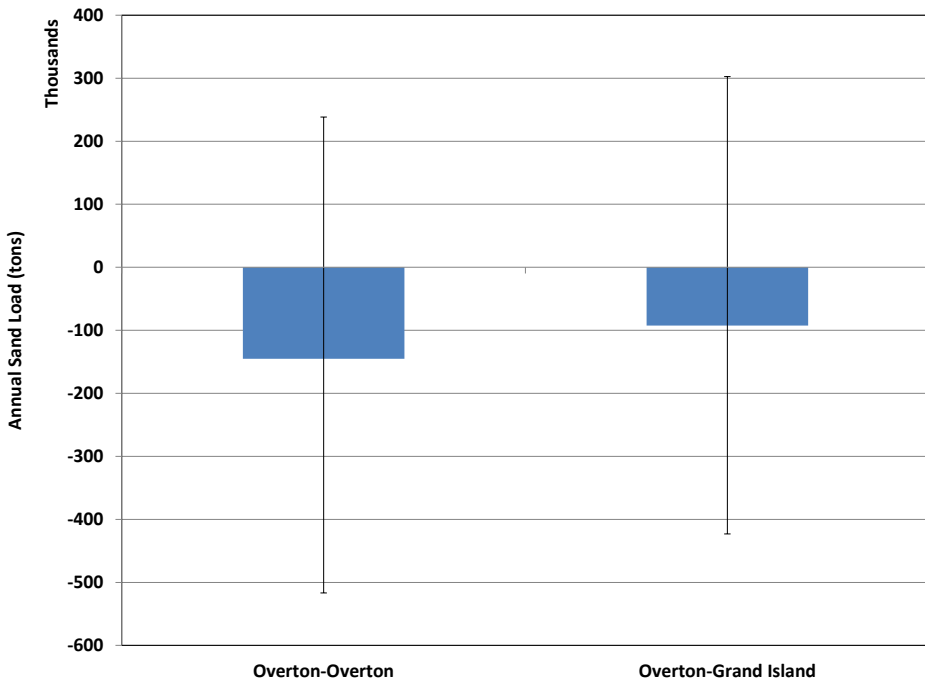


Figure 4.17. Mean and median annual sand transport balance between Overton, Kearney and Grand Island from WY1984 through WY2014. Also shown are the 5th and 95th percentile results from the Monte Carlo simulations.

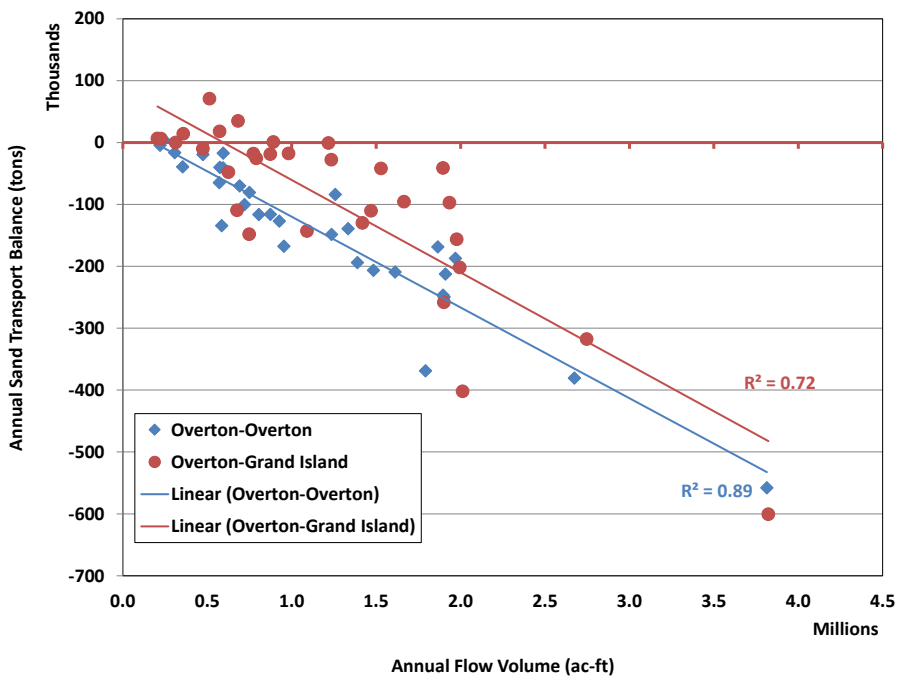


Figure 4.18. Relationship between estimated mean sand balance and total flow volume in the Overton to Kearney and Kearney to Grand Island reaches.

1. GLE versus stage at annual peak discharge (Q_p , Monitoring Plan Section 5.1.1), defined as the maximum mean daily discharge between January 1 and the date of the survey in each year.
2. GLE versus stage at germination season discharge (Q_{Ger} , Monitoring Plan Section 5.1.2), defined as the either the mean or median mean daily discharge between June 1 and July 15, the primary season for establishment of cottonwood seedlings. For this analysis, the correlations were performed using both the mean and median discharges.
3. Total unvegetated width (W_{unveg}) versus stage at annual peak discharge (Q_p).
4. Total unvegetated width (W_{unveg}) versus stage at germination season discharge (Q_{Ger}).
5. Total unvegetated width (W_{unveg}) versus GLE.

4.2.1. Height of Green Line above 1,200-cfs Water Surface

One of the benchmarks established by the Program is to maintain GLEs at least 1.5 feet above the 1,200-cfs water surface. As noted in Section 3.4.1, the green line elevation (GLE) (i.e., *the edge of vegetation on a sand bar or adjacent to a wetted channel, defined by at least 25 percent cover of vegetation*) tends to be responsive to the magnitude of flows. During 2011, when long-duration, high flows persisted throughout the reach, the average GLE at the primary geomorphic transects reached the 1.5-foot benchmark, with the average at 16 of the 20 pure panel APs at or above the benchmark (**Figures 4.19 and 4.20**). The average GLE was well below the benchmark during all other years at all of the APs. This result is not surprising since the vegetation that comprises the green line typically consists of annual species that germinate during the early part of the growing season when flows tend to be elevated.

4.2.2. Green Line Elevation versus Stage at Annual Peak Discharge

The year-to-year change in GLE is well-correlated to the difference in stage associated with the annual maximum discharges (**Figure 4.21**). Correlation using the Kendall test on the complete data set results in a Kendall's τ of 0.55, and p-value of less than 0.0001, indicating that the correlation is statistically significant.¹⁴

4.2.3. Green Line Elevation versus Stage at Germination Season Discharge

The year-to-year change in GLE is even more highly correlated with the stage at the mean discharge during the germination season than with the annual maximum discharge (**Figure 4.22**; Kendall's τ = 0.65, $p < 0.0001$). The germination season discharges were quite low and very similar in magnitude in 2012 and 2013, and the GLE had generally receded well into the low flow channel, eliminating the potential for contrast between the two data sets. As a result, the data points for the year-to-year changes from SY2012 to SY2013 cluster around the line of zero change in stage. An independent test of the median discharge during the germination season rather than the mean resulted in essentially the same correlation results. The correlation between the year-to-year change in GLE and the stage associated with the maximum discharge **during the germination season** is also statistically significant (Kendall's t = 0.60, $p < 0.0001$), only slightly weaker than the mean germination season discharge (**Figure 4.23**).

4.2.4. Total Unvegetated Channel Width

The Program has established a benchmark to maintain a target unvegetated channel width of 1,125 feet, with minimum width of at least 750 feet. As discussed in Section 3.4.2, the reach-wide average unvegetated channel width was substantially less than the minimum value in all years including 2011, the year with the largest unvegetated width (average~630 feet) (Figure 3.17b). With

¹⁴It should be noted that the difference between the GLE analysis presented here is based on year-to-year change selected metrics, rather than change vs. 2009, as was the case in Section 3.4.1.

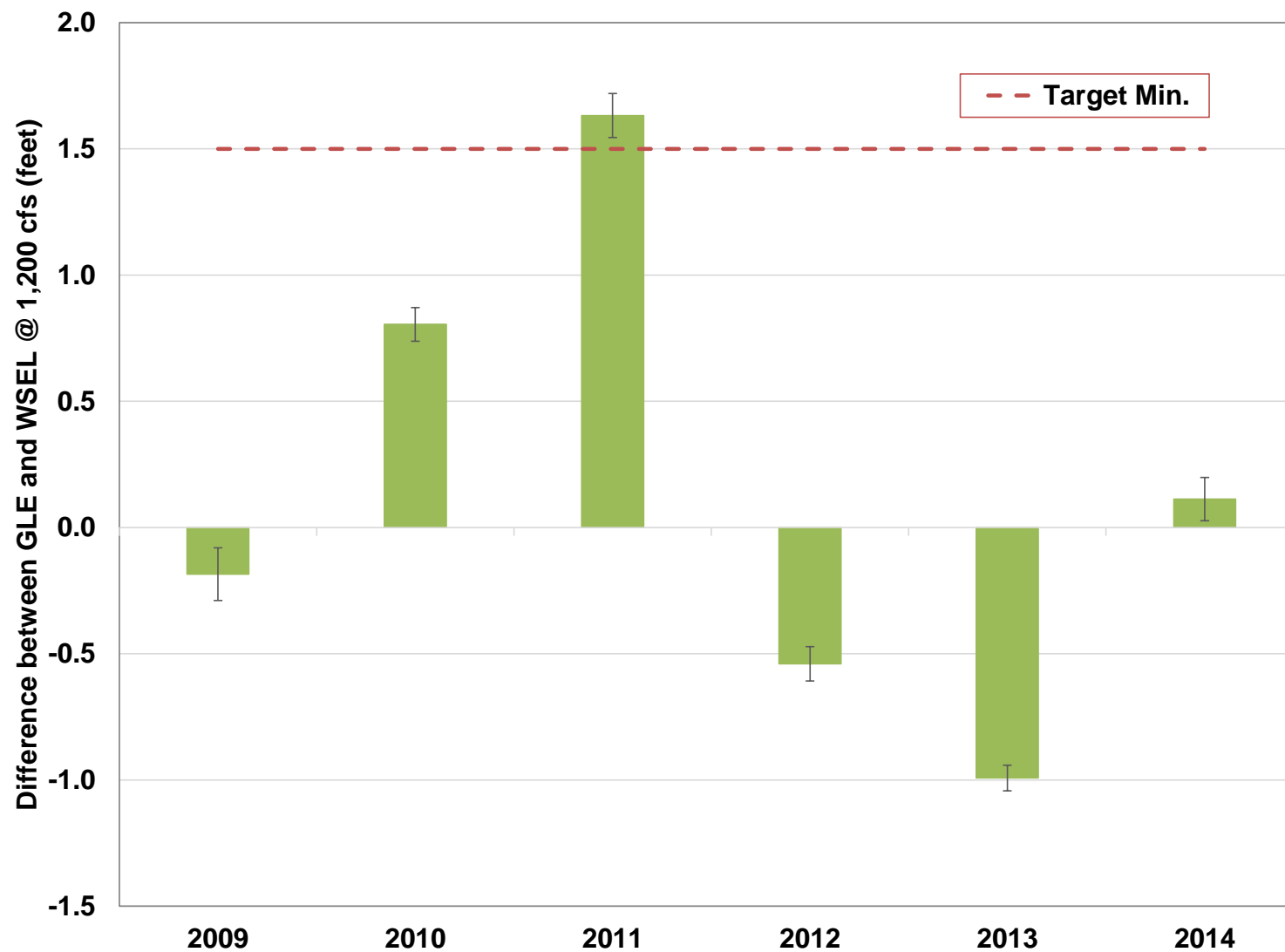


Figure 4.19. Reach-wide average height of the GLE points above the 1,200-cfs water surface at the pure panel APs from 2009 through 2014.

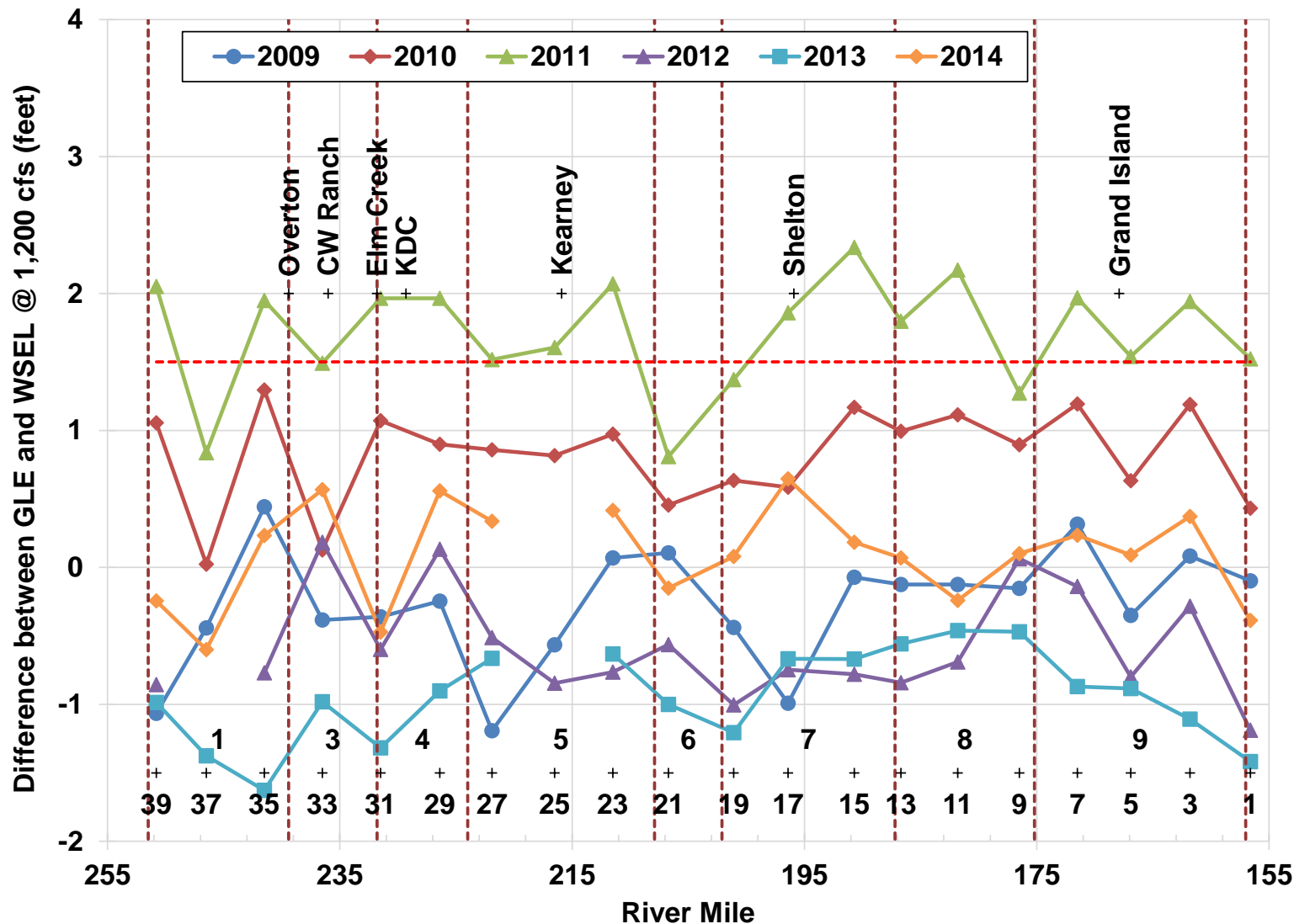


Figure 4.20. Average height of the GLE above the 1,200 cfs water surface at the each of the pure panel APs during 2009 through 2014, and performance benchmark of +1.5 feet.

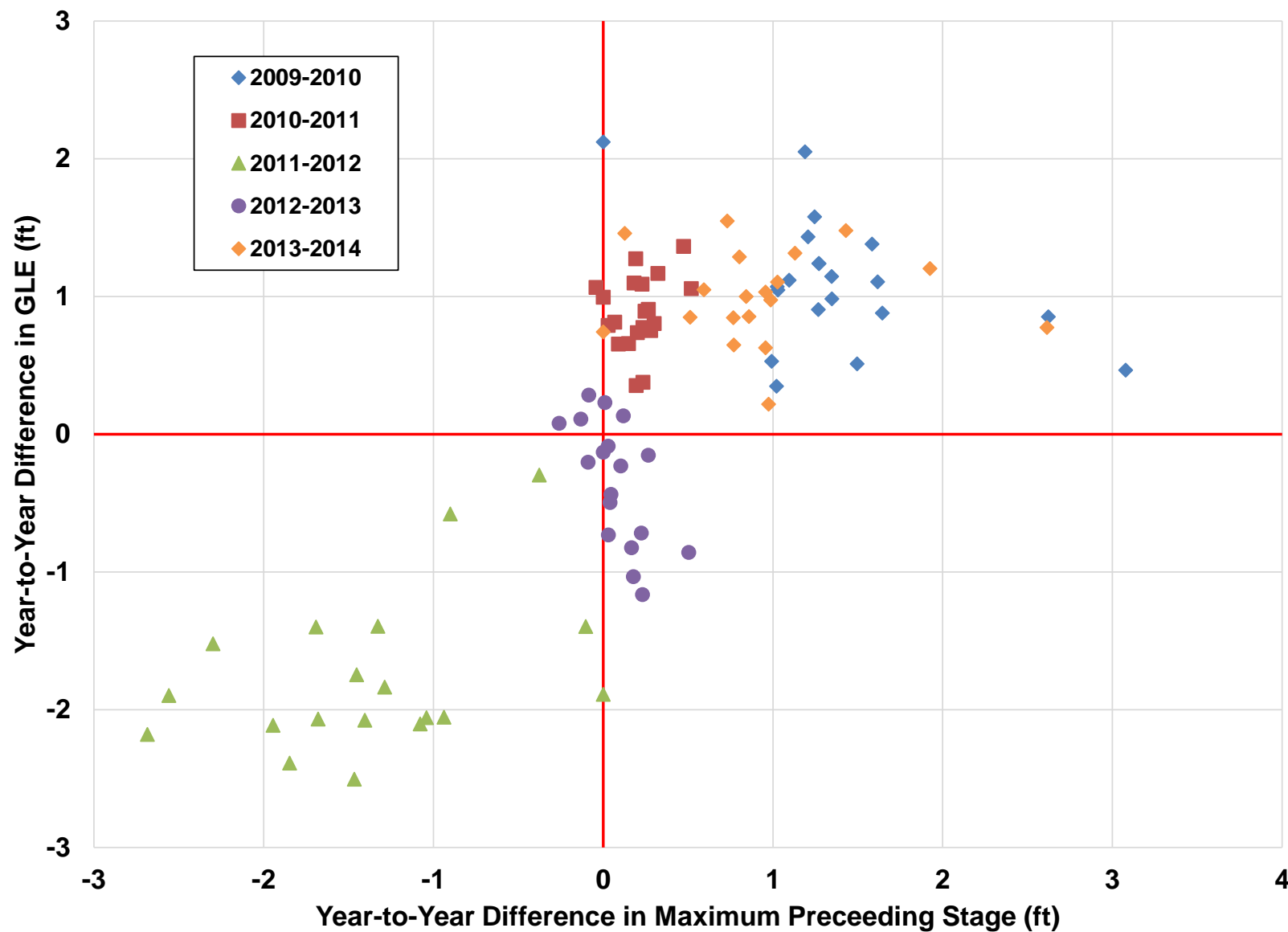


Figure 4.21. Yearly change in GLE versus year-to-year difference in stage at maximum mean daily flow preceding each survey at the pure panel APs (Kendall's $\tau = 0.55$, $p < 0.0001$).

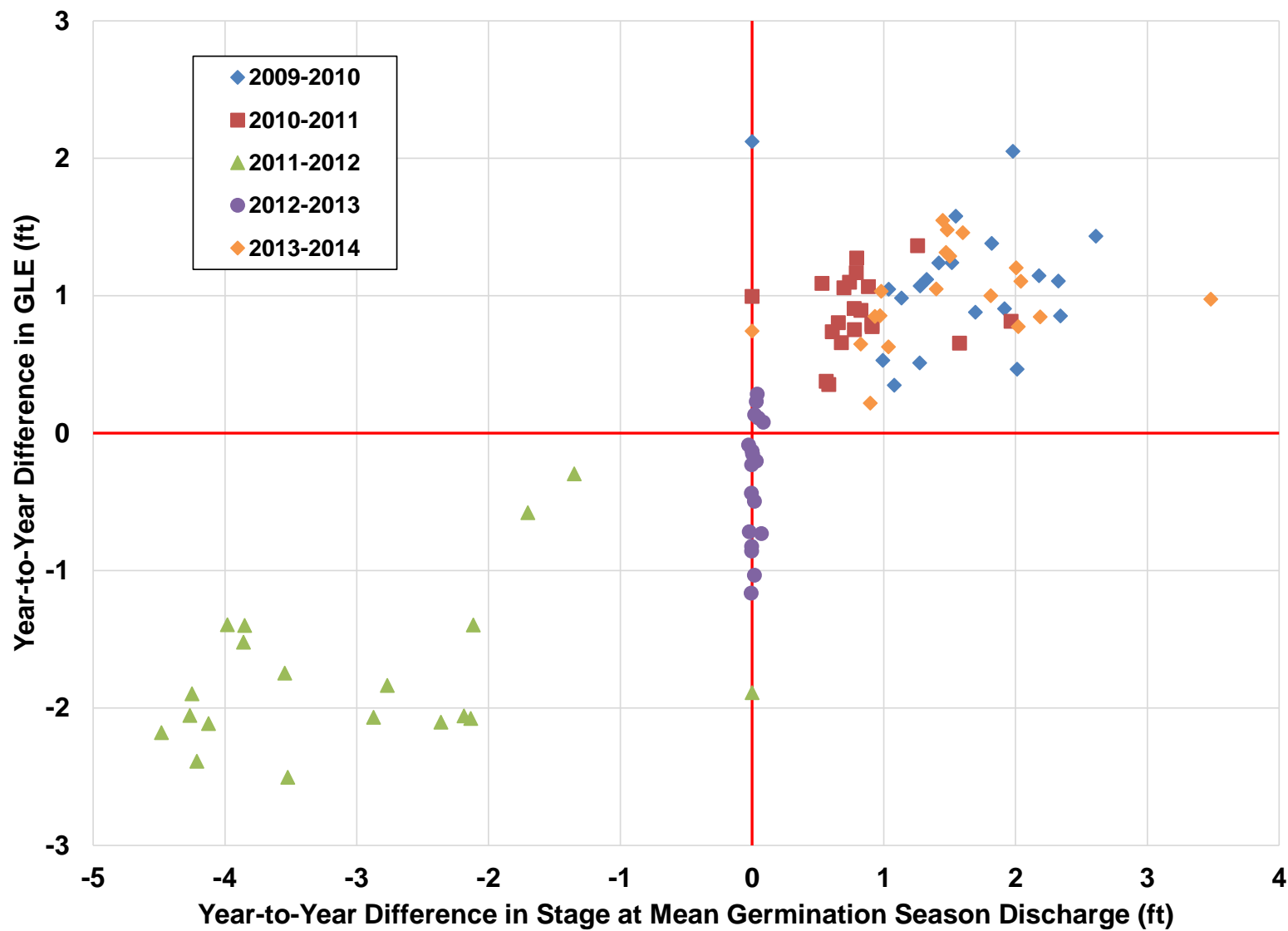


Figure 4.22. Yearly change in GLE versus year-to-year difference in stage at mean germination season discharge preceding each survey at the pure panel APs (Kendall's $\tau = 0.65$, $p < 0.0001$).

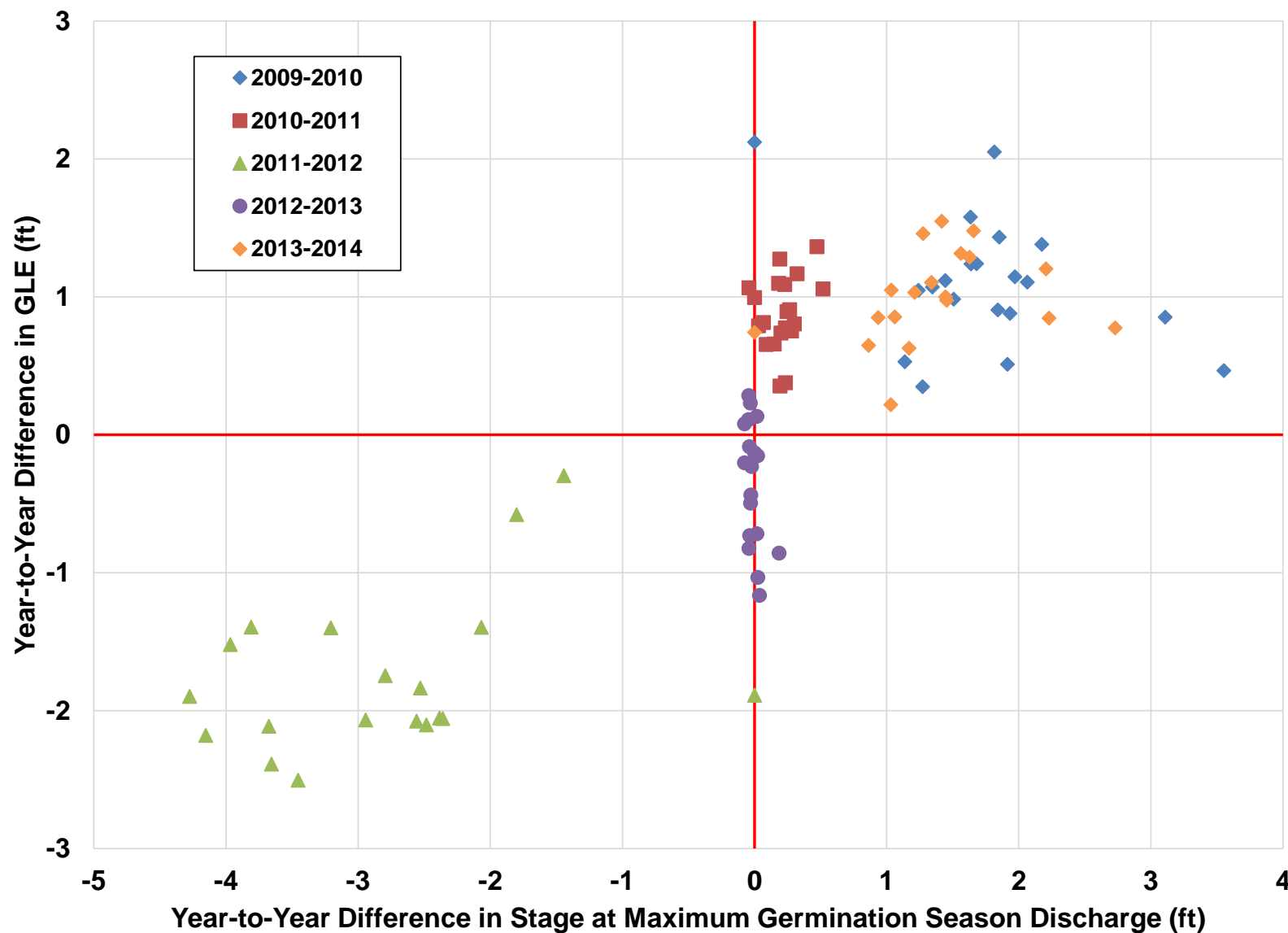


Figure 4.23. Yearly change in GLE versus year-to-year difference in stage at maximum germination season discharge preceding each survey at the pure panel APs (Kendall's $\tau = 0.60$, $p < 0.0001$).

the exception of Reach 6 in 2010 and 2014 and Reaches 4, 6, 7 and 9 in 2011, none of the geomorphic reaches had average unvegetated width exceeding the minimum threshold (Figure 3.17c).

4.2.5. Total Unvegetated Channel Width versus Stage at Annual Peak Discharge

Correlation between the year-to-year change in total unvegetated channel width and the difference in stage associated with the annual maximum discharge is statistically significant (**Figure 4.24**; Kendall's $t = 0.37$, $p < 0.0001$). The maximum discharges in 2010 and 2011 were both quite high; thus, the difference is relatively small, yet the total unvegetated width appears to have increased substantially at many locations between the two surveys, most likely due to the long duration of high flows in 2011 that prevented especially the annual species from growing on the sand bars and the low elevation areas along the channel banks. During SY2012, the GLE receded and the unvegetated width contracted due to the low-flow conditions, and the narrowing continued during the low flows in SY2013. The unvegetated width increased during SY2014, most likely due to the effects of the relatively high flows that occurred during June 2014.

4.2.6. Total Unvegetated Channel Width versus Stage at Mean Germination Season Discharge

Correlation between the year-to-year change in total unvegetated channel width and the difference in stage associated with the mean germination season discharge is also statistically significant (**Figure 4.25**; Kendall's $t = 0.39$, $p < 0.0001$). As with the GLE correlation analysis, the germination season discharges in 2012 and 2013 were very similar; thus, the changes in total unvegetated widths tend to cluster along the line of zero change in stage.

4.2.7. Total Unvegetated Channel Width versus Green Line Elevation

The year-to-year change in total unvegetated channel width is strongly correlated with the corresponding change in GLE (**Figure 4.26**; Kendall's $\tau = 0.49$, $p < 0.0001$).

Collectively, all of the results in this section show that both the GLE and unvegetated channel width are responsive to the magnitude of the preceding flows, with the strongest correlation between the GLE and the mean germination season discharge. This result suggests that inundation that prevents new vegetation and annual species from growing on the sand bars and low elevation areas along the margins of the channel are the key factor in maintaining the unvegetated channel width, as defined in the current version of the monitoring plan.

4.3 Flow #5

Increasing the magnitude and duration of the Q_{1.5} will increase riparian plant mortality along the margins of the river. There will be different relations for different species.

Priority Hypothesis Flow #5 postulates that increasing the magnitude and duration of the annual peak discharge will increase riparian plant mortality along the margins of the river, with potentially different relationships for different species. The following section specifically focuses on the relative influence of spraying versus peak flows on the distribution and frequency of common reed (*Phragmites australis*). The analysis was performed using the data from the pure panel APs, since only one data set is available for the majority of the rotating panel points¹⁵. Common reed was one of the most prevalent species in the reach during the initial (2009) monitoring survey, in terms of both frequency of occurrence (4th highest frequency of the sampled species behind ragweed,

¹⁵ The second set of rotating points was sampled for the second time in 2014. Two full datasets will be available for the rotating panels following the 2016 surveys.

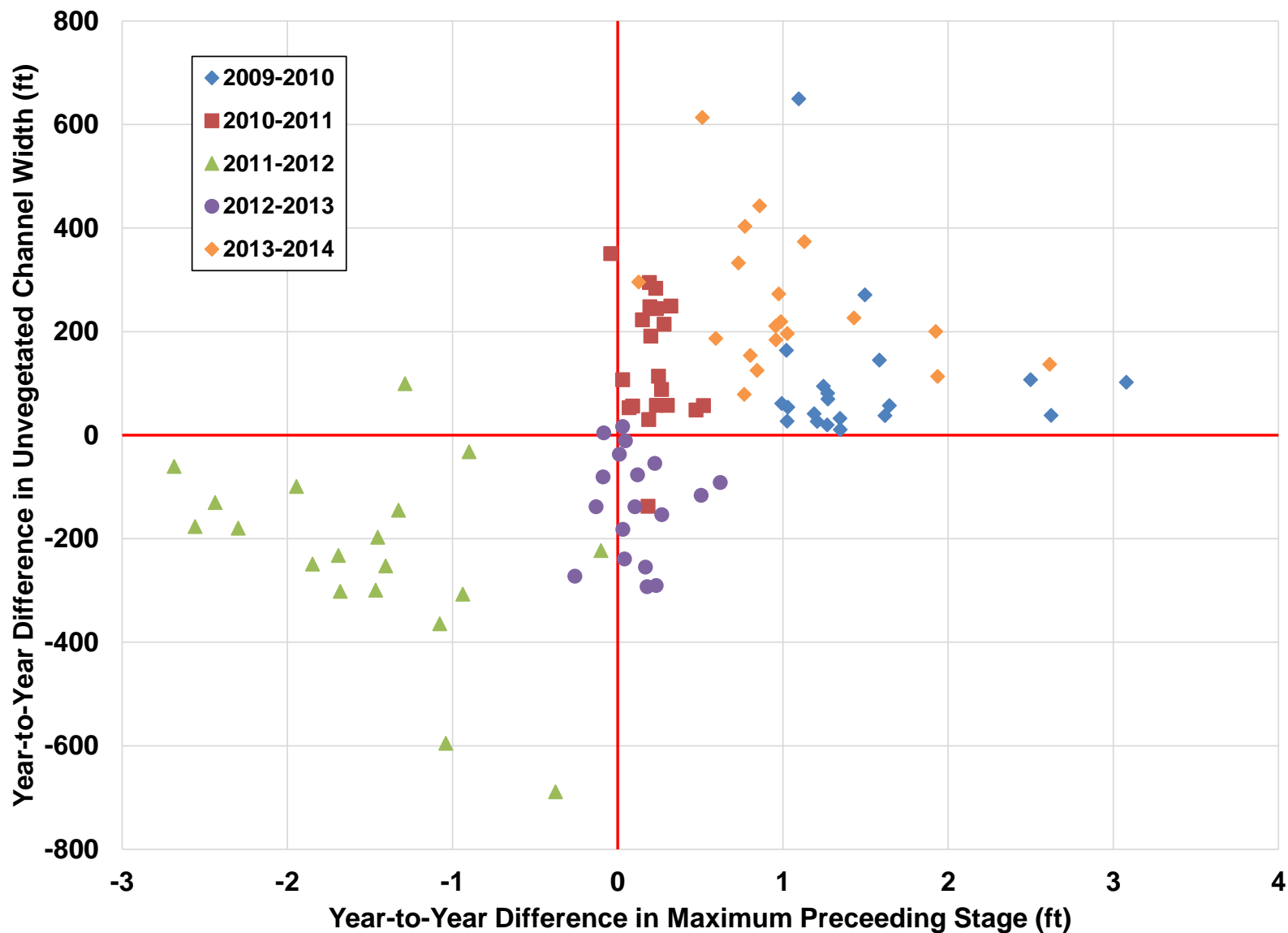


Figure 4.24. Yearly difference in total unvegetated channel width versus year-to-year difference in stage at maximum mean daily flow preceding each survey at the pure panel APs (Kendall's $\tau = 0.37$, $p < 0.0001$).

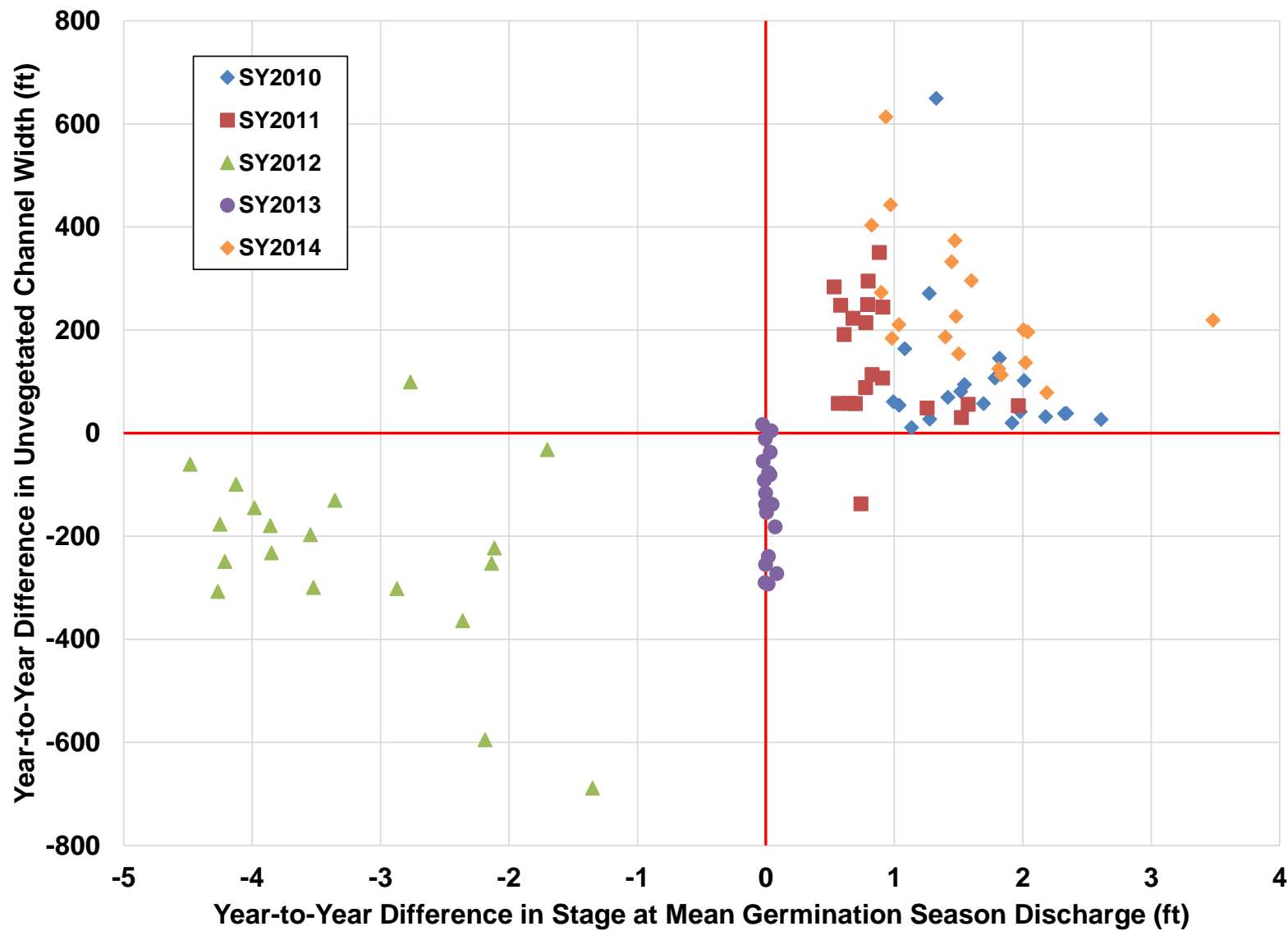


Figure 4.25. Yearly change in total unvegetated channel width versus year-to-year difference in stage at mean discharge during the germination season at the pure panel APs (Kendall's $\tau = 0.39$, $p = <0.0001$).

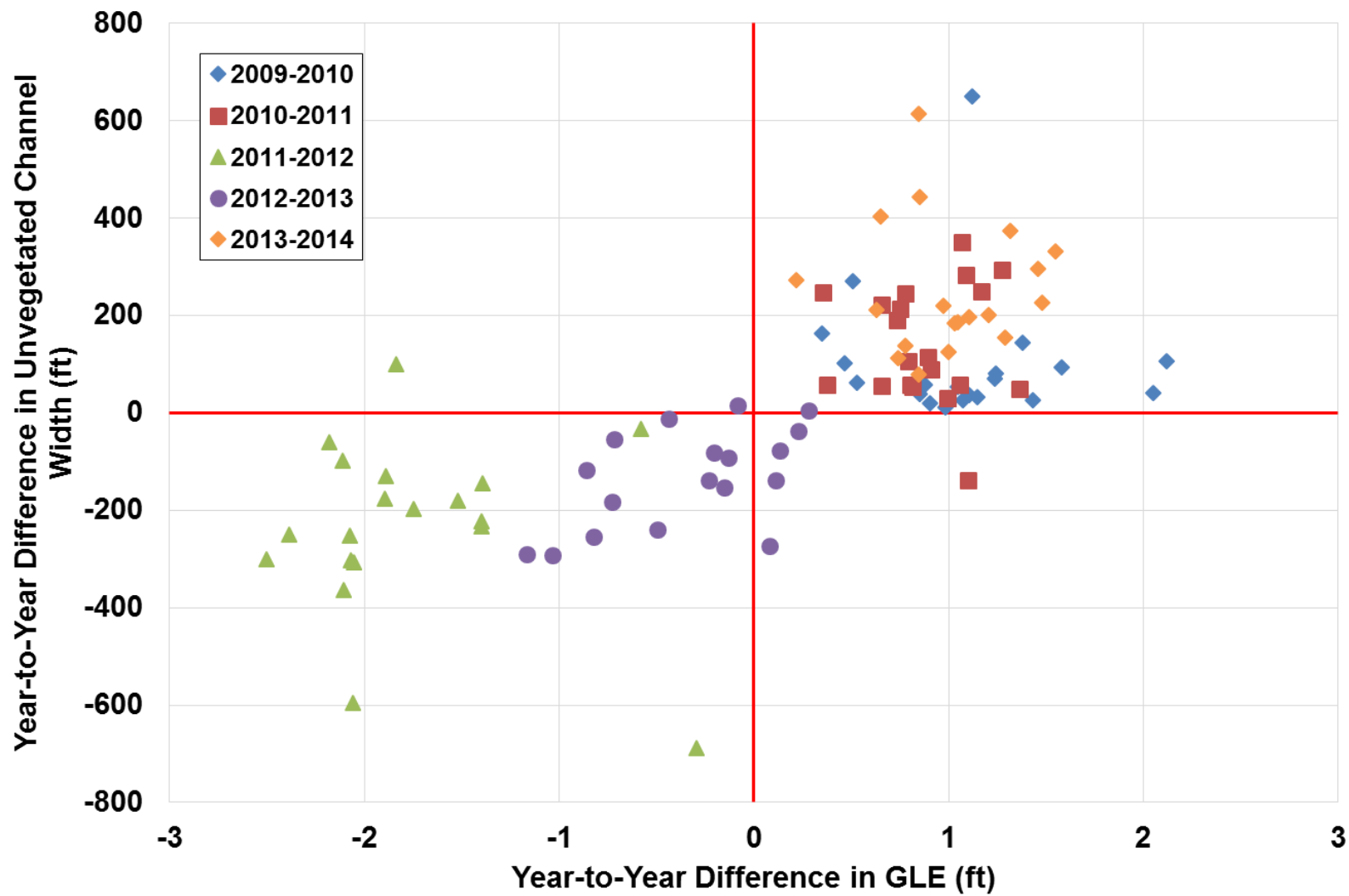


Figure 4.26. Yearly change in total unvegetated channel width versus year-to-year difference in GLE at the primary geomorphic transects of pure panel APs (Kendall's $\tau = 0.47$, $p < 0.0001$).

cocklebur and purple loosestrife) and percent cover (highest of sampled species) (Figures 3.18 and 4.5). The amount of common reed in the overall reach declined substantially between 2009 and 2010, remained relatively constant between 2010 and 2011, and declined substantially between 2011 and 2012. Common reed became slightly more prevalent between 2012 and 2013, and it continued to further increase between the 2013 and 2014 monitoring surveys, although the population remains significantly reduced compared to early monitoring levels (**Figure 4.27**). The variability in the averages among the individual APs was, however, quite high.

Based on the percent cover data, common reed was most prevalent in three specific portions of the overall study reach in 2009: AP23 through AP29 near and upstream from Kearney, AP17 and AP19 just upstream from Shelton, and AP1 and AP2 at the downstream end of the reach (**Figure 4.28**). A substantial amount of common reed was also present at AP3 near Grand Island, AP35 in the North Channel at Jeffreys Island and at AP39 just downstream from the Lexington Bridge. With the exception of AP17, the amount of common reed decreased at all of these anchor points in 2010 (Figure 4.29). At AP17, common reed increased from about 10-percent cover in 2009 to over 16 percent in 2011. The amount of common reed continued to decline at most of the anchor points from 2010 to 2011, however substantial increases occurred at AP19, AP23, AP27 and AP39. Generally low levels of common reed persisted through 2013 and 2014, with the most significant increases during this period occurring at AP3, AP23, and AP27.

A wide range of flows, weather conditions, and Program activities occurred during the five-year monitoring period that could potentially affect the quantity and distribution of common reed along the reach. Flow conditions could impact growth of common reed and other in-channel vegetation in at least three ways: (1) during low to moderate flows, the river provides an irrigation source, increasing growth potential, (2) high flows during the germination season can inundate the surfaces on which the plants grow, limiting germination potential and plant growth, and (3) during extremely high flows, plants can be removed due to scour around the base of the plants and uprooting due to direct shear or through lateral erosion and undercutting of the plant roots. Weather could also be a factor because growth of most species tends to be stronger during warm, wet periods than either cool, dry or hot, dry conditions. Program activities that affect common reed include disking, mowing and shredding, and herbicide spraying.

Total runoff volume during WY2009 at Overton was only about 52 percent of the long-term average, and this increased to about 120 percent of average in 2010 and nearly 240 percent of average in 2011 (**Figure 4.29**). WY2012 was slightly above normal in terms of total runoff (~110 percent of average); however, the bulk of that runoff occurred during Fall 2011. The runoff during the portion of the 2012 growing season preceding the monitoring surveys (April through July) was only about 55 percent of the long-term average. WY2013 was also a very dry year, with the total runoff only about 52 percent of average (including the late-September 2013 flood), but only about 41 percent of average during the portion of the 2013 growing season from April through August. Compared to the long-term average, WY2014 was normal to slightly dry, with total runoff about 87% of the long-term average.

Three specific variables were considered in evaluating the potential effects of flow on the prevalence of common reed:

1. Inundation depth at the maximum discharge (D_{max}),
2. Duration of inundation (Dur), and
3. Persistence of low flows during the growing season, quantified as the low flow that was equaled or exceeded 90 percent of the time (Q_{low}).

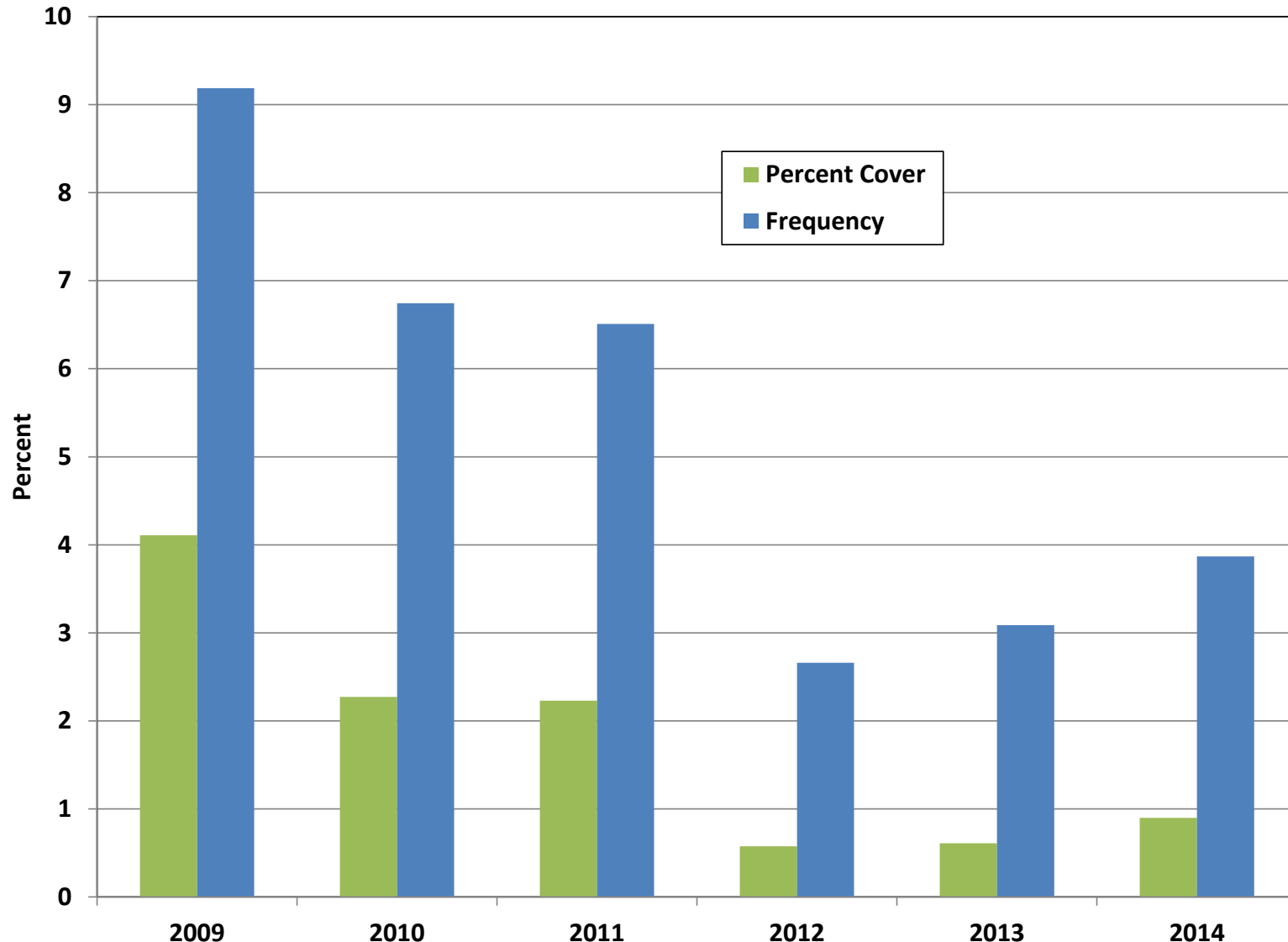


Figure 4.27. Average frequency of occurrence and percent cover for common reed (*Phragmites australis*) on a reach averaged basis observed during each of the six monitoring surveys.

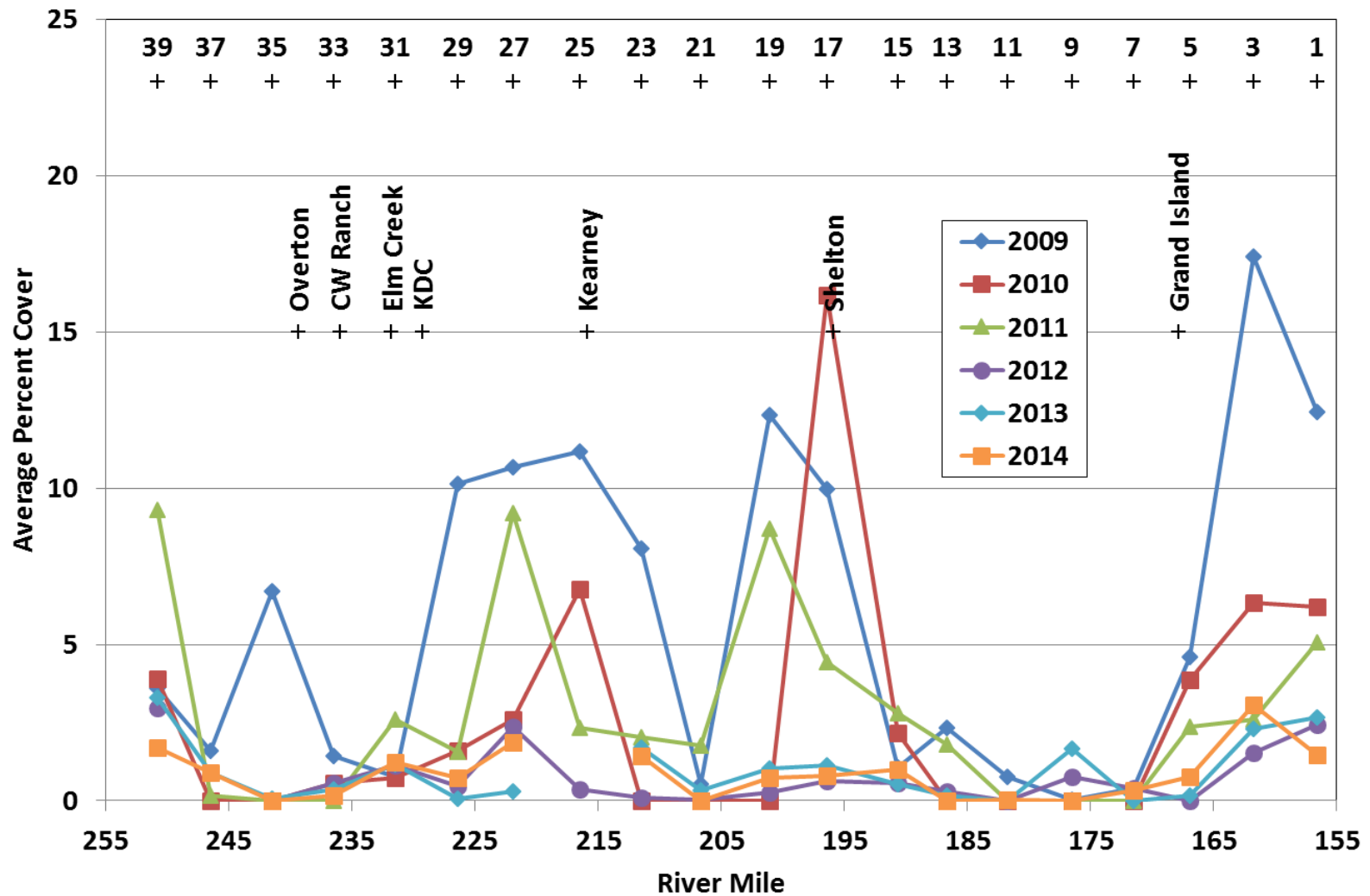


Figure 4.28. Average percent cover of common reed (*Phragmites australis*) at the pure panel anchor points during the six monitoring periods.

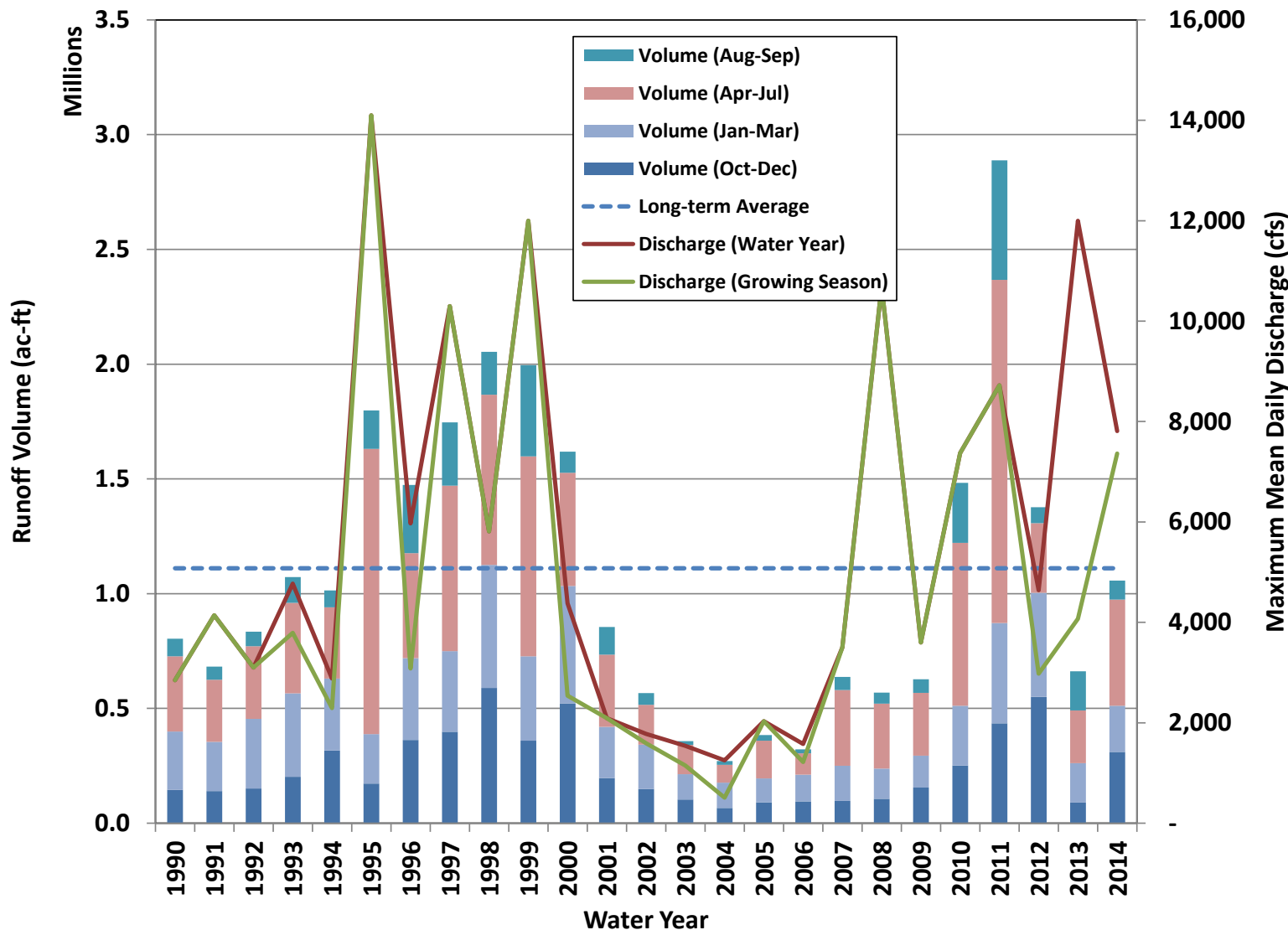


Figure 4.29. Total runoff volume at Overton during four periods of the water year and the maximum mean daily discharge during the entire water year and between April 1 and August 1 (~time of monitoring surveys) from WY1990 through WY2014. Long-term average volume based on gage data from WY1941 through WY2014.

The inundation depth at the maximum discharge (D_{max}) was selected as a surrogate for the effects of high flows, since the maximum velocities and shear stresses at the individual points are not available. A two-dimensional model has been developed for the Elm Creek Complex, however, that can provide an indication of the range of anticipated velocities for different flow depths. While the hydraulic characteristics of the APs will vary to some degree from those at the Elm Creek Complex, the range of variability in the relationship between depths and velocities is probably similar. Based on a comparison of the maximum water-surface elevation from the existing 1-dimensional HEC-RAS model with the elevations of the individual quadrats that contained common reed, about 45 percent of the quadrats were not inundated during the growing season in 2009; this decreased to only 3 percent in 2010 and 5.5 percent in 2011. In both 2012 and 2013, more than 90% of quadrats with common reed were not inundated due to the persistent low flows. In 2014, spring flows were much higher, and only about 13 percent of quadrats with common reed were not inundated (**Figure 4.30**). In 2009, about 10 percent of the quadrates with phragmites were inundated to a depth of at least 1 foot, and in 2010, 2011 and 2014, about ten percent were inundated to depths in the range of 3 feet or more. In 2012 and 2013, only about 2 percent of the quadrates were inundated to a depth of one foot or more.

Based on results from the Elm Creek 2D model, maximum velocities at locations with depths in the 1-foot to 3-feet range are about 6 fps, and most areas have velocities between 1.5 and 4 fps (**Figure 4.31**). Pollen-Bankhead et al. (2011) found that very high velocities, well above those that occur in the Platte River, are required to uproot established common reed plants (**Figure 4.32**); thus, it is unlikely that this process is responsible for the reduction in common reed during the monitoring period. If common reed is removed by the direct action of the water, this most likely occurs through lateral erosion and undercutting of the sandbars and banklines on which the plants are growing (**Figure 4.33**). While this does occur in the study reach, field observations indicate that it occurs only in limited areas, primarily on the heads, and to a lesser extent, along the margins, of sand bars. The thick, rhizomatous root structure appears to be very effective in binding the soil and limiting the rate and magnitude of lateral erosion and undercutting in areas where common reed is abundant.

Weather conditions during the monitoring period varied in a manner similar to the runoff. In 2009, the total precipitation during the portion of the growing season prior to the monitoring surveys (April 1 through July 31, for purposes of this analysis) varied from about 10 inches in the portion of the reach upstream from Elm Creek to about 15.6 inches downstream from Elm Creek (**Figure 4.34**). Precipitation during this period in 2010 ranged from about 12.8 inches at Cozad to more than 19 inches near Grand Island. A very similar volume of precipitation was observed in 2011, with the highest measurements occurring near Kearney. Precipitation during 2012 was very low, with a total rainfall of 9.4 inches at Kearney, and an average of 7.5 inches at all five gages. Precipitation in 2013 and 2014 were very similar to 2009, with approximately 10 inches of rain falling at Cozad, increasing downstream to 13.6 inches (2013) and 15.5 inches (2014) at Grand Island.

Based on data from the weather station at Grand Island Regional Airport [the only station in the Global Historical Climatology Network (GHCN) in close proximity to the study reach for which long-term temperature records are maintained], the mean daily temperature during April through July is 64.9°F. In 2009, this period was cooler than average, with mean temperature of 63.4°F. It was slightly warmer than normal in 2010 and 2011 (65.6°F and 65.2°F, respectively), very warm in 2012 (70.3°F), and then slightly cooler than normal (64.2°F) in 2013. In 2014, the average growing season temperature was 65.2°F (**Figure 4.35**). A better measure of the overall temperature regime that affects plant growth is growing degree days (GDD). GDD is computed based on the deviation of the minimum and maximum temperatures from a reference temperature chosen based on plant or animal species and life stage of interest. GDD values are

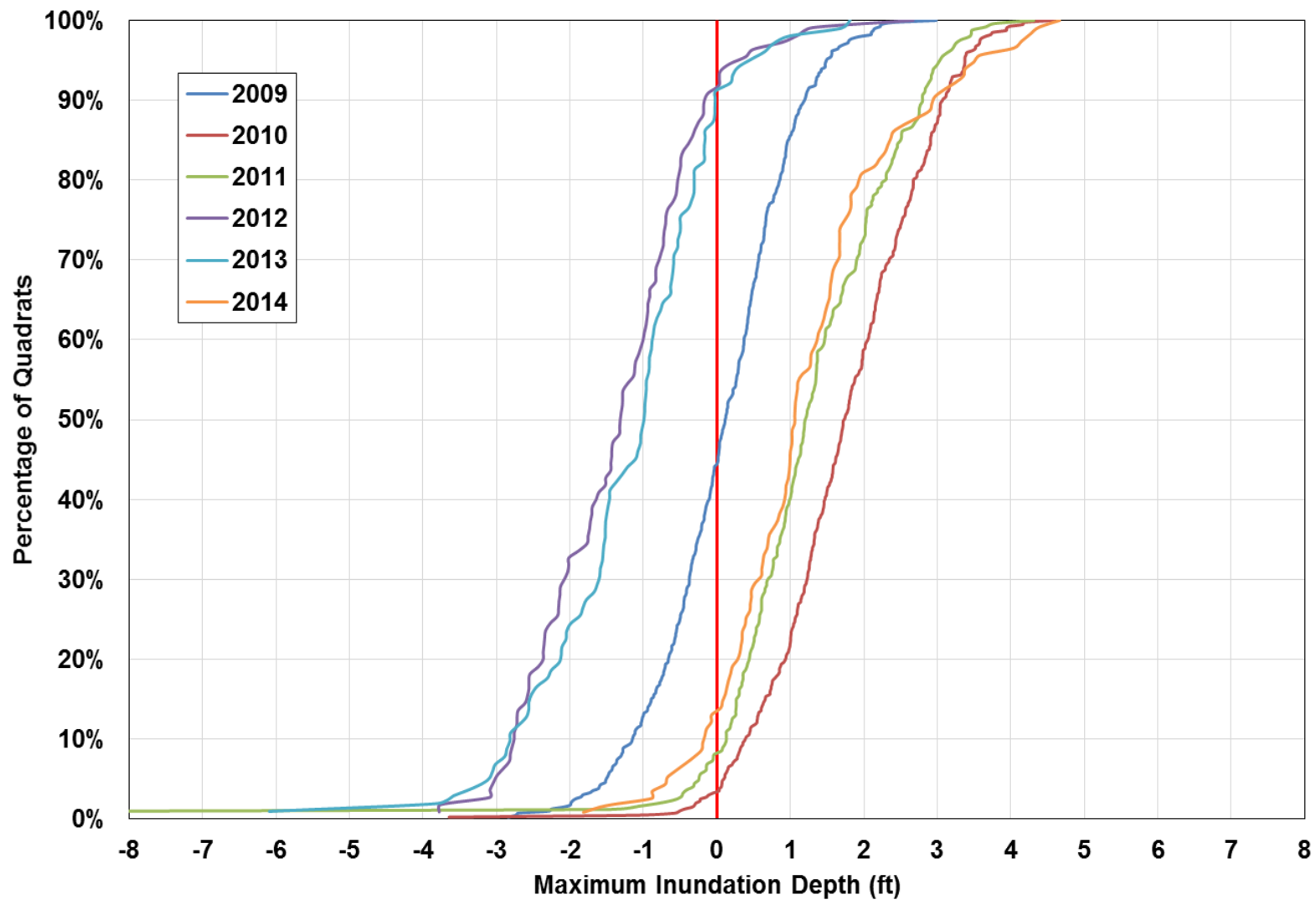


Figure 4.30. Cumulative distribution of inundation depths at the maximum discharge during the growing season for quadrats containing common reed during each of the five monitoring surveys.

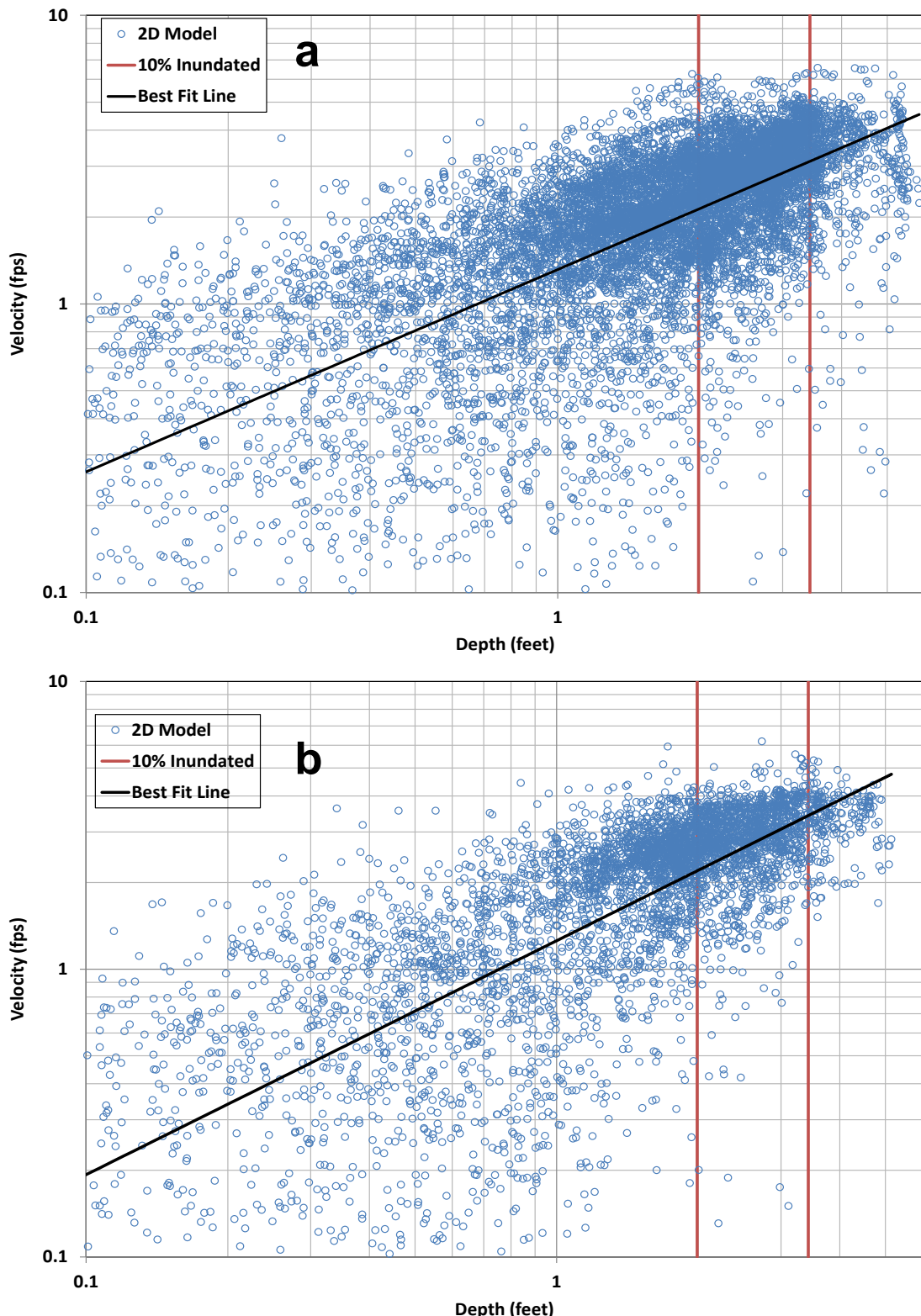


Figure 4.31. Depths and velocities from the Elm Creek 2-D model at a discharge of approximately 3,200 cfs: (a) Elm Creek Bridge to Kearney Diversion Structure, (b) downstream from Kearney Diversion Structure.

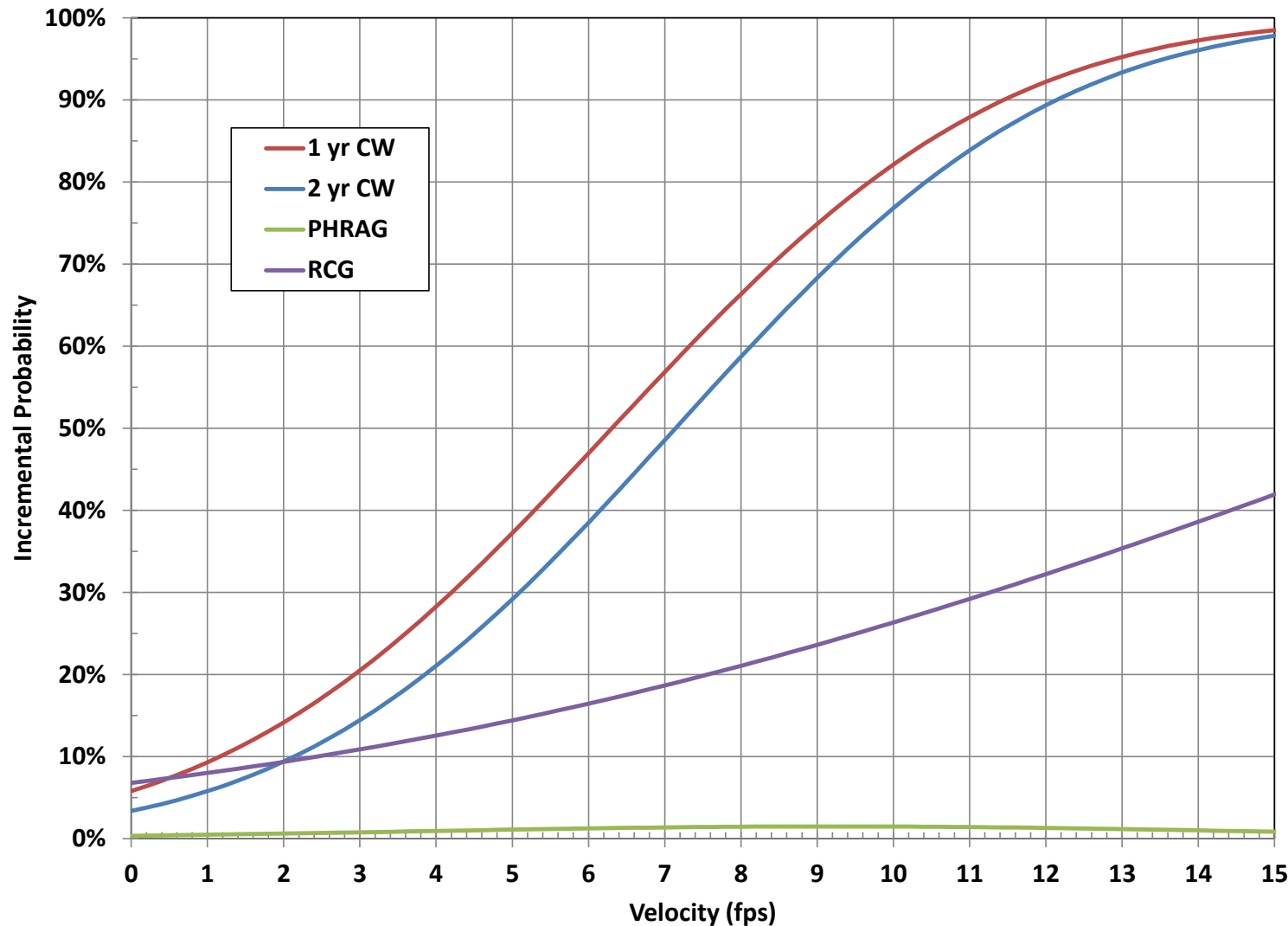


Figure 4.32. Incremental probability of plant removal for 1- and 2-year-old Cottonwood (1-year CW and 2-year CW), common reed (PHRAG) and reed canary grass (RCG) based on results from Pollen-Bankhead et al. (2011).



Figure 4.33. Typical lateral erosion and undercutting of the edge of a sand bar with common reed in the Elm Creek Complex.

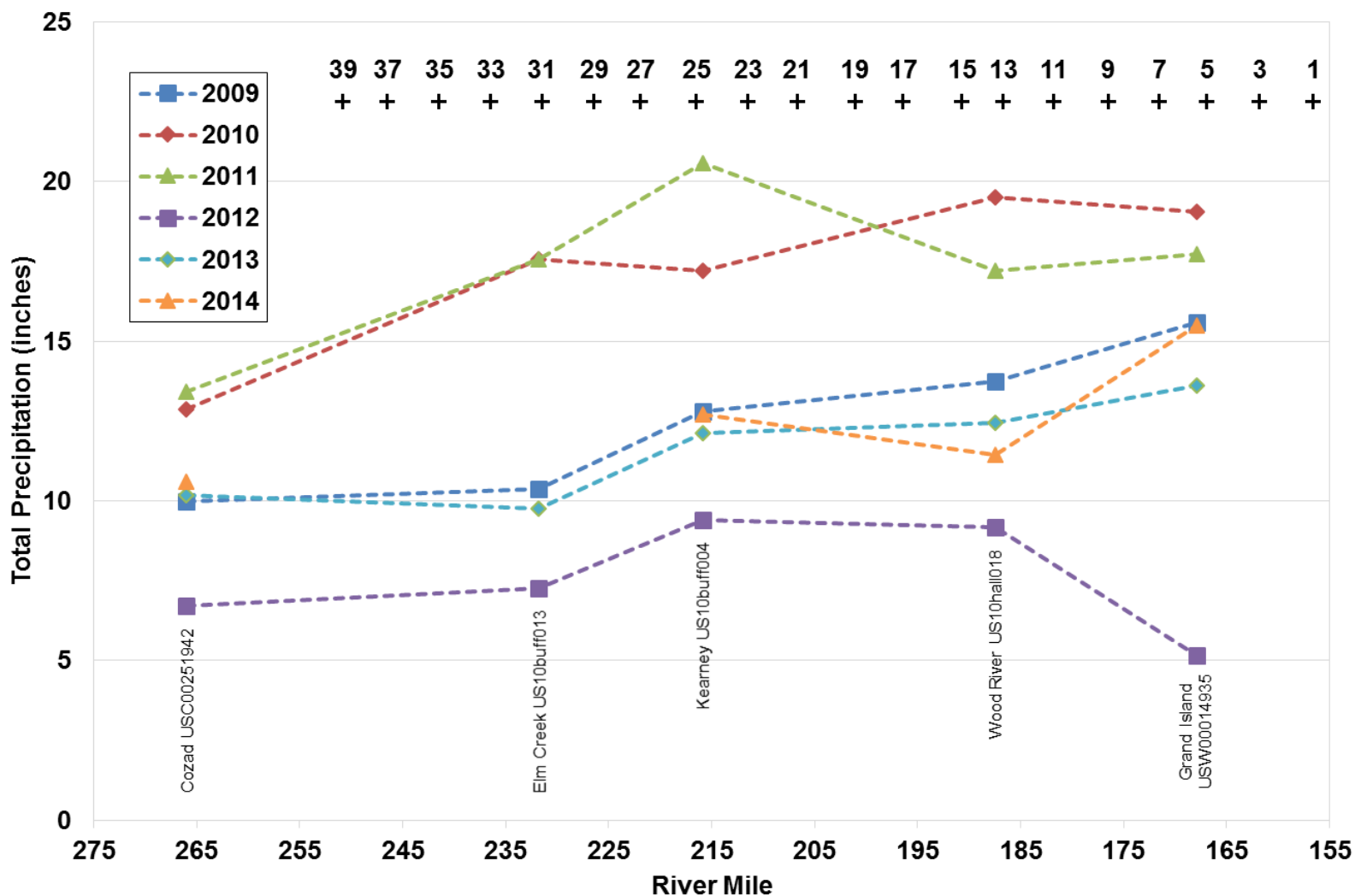


Figure 4.34. Total precipitation during the period from April through July in each of the five monitoring years at five weather stations along the project reach. [Global Historical Climatology Network (GHCN) station numbers used as the data source follow the names].

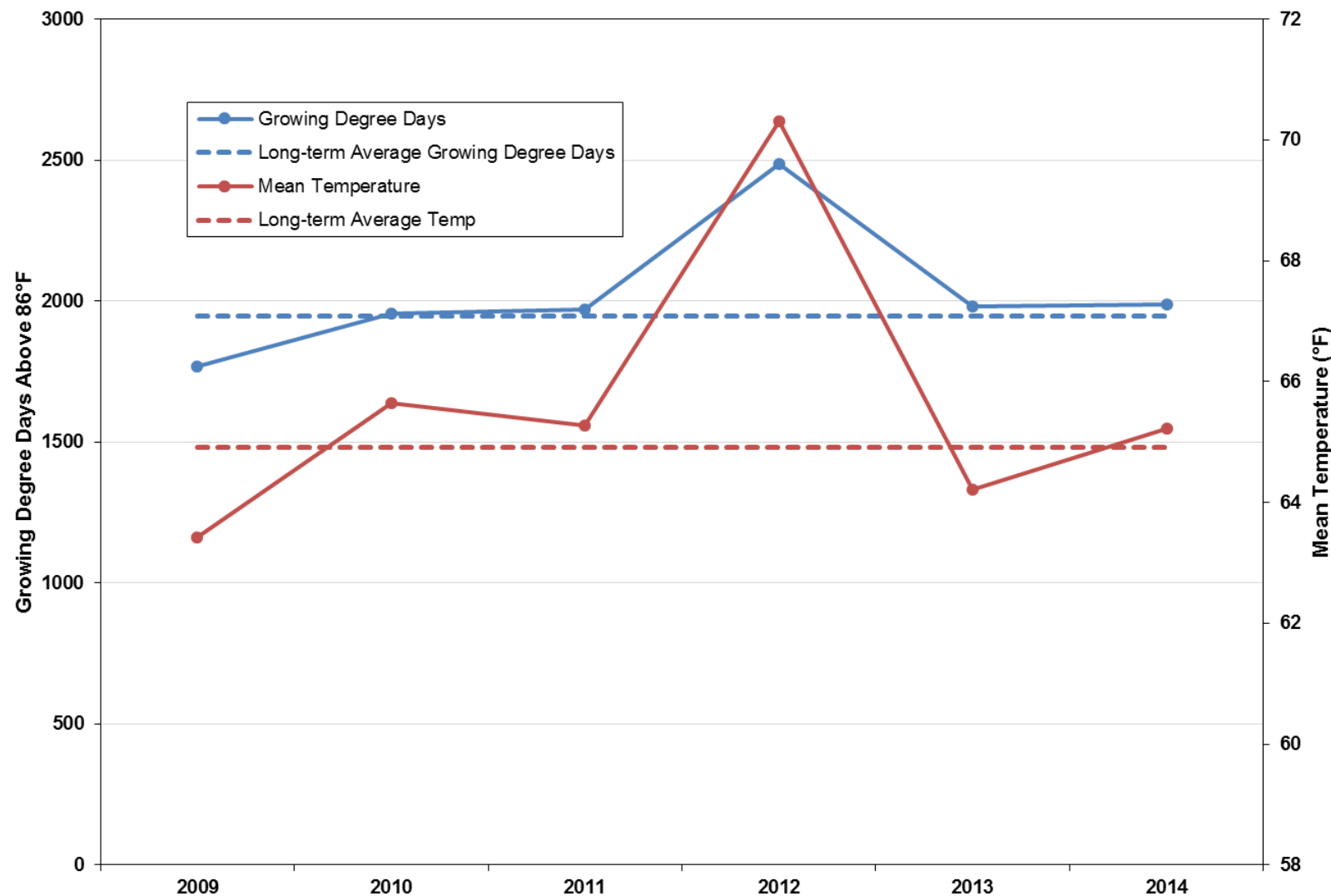


Figure 4.35. Growing degree days (GDD) above a baseline temperature of 86°F and average temperature at the Grand Island Station (GCHND Sta USW00014935) during the period from April through July during the monitoring period.

based on the deviation of the minimum and maximum temperatures from a reference temperature chosen based on plant or animal species and life stage of interest. GDD values are accumulative measures of heat, as plants will mature in a stepwise manner based on the ambient air temperature in the absence of atypical environmental stressors such as drought or disease. As a result, higher values of GDD indicate greater growth potential. Using a base temperature of 50°F¹⁶, the long-term average GDD (1938 to 2014) was 1,948 (Figure 4.35). The first year of the monitoring period was the only year with GDD below the long-term average (1,769), 2010, 2011, 2013 and 2014 were about average (1,955, 1969, 1,981, and 1987, respectively), and 2012 was well above average at 2,487.

Mechanical actions performed by the Program that can affect the presence and persistence of common reed include herbicide spraying, disk, mowing and shredding on the surface of the sand bars, and in some cases, direct grading to construct new islands. The Program maintains a GIS database documenting these actions that includes the specific limits of spraying. This database was used to identify the anchor points at which spraying occurred (**Table 4.3**) and to quantify the spraying intensity at each of the pure panel APs by identifying the individual quadrats that fall within the spraying limits, and calculating the percentage of the quadrats that were sprayed prior to each sampling period (**Figure 4.36**). Spraying typically occurs in September and October of each year, with the intensity varying along the reach, based at least in part, on the amount of common reed that is present. Spraying occurred at 7 of the 20 pure panel APs in Fall 2008, with about 9 percent of the approximately 4300 vegetation quadrats that were sampled in 2009 being sprayed. The spraying intensity increased significantly in fall 2009, with at least some spraying at 13 of the 20 pure panel APs, and about 26 percent of the approximately 5,900 quadrats being sprayed. In fall 2010 and 2011, approximately 10% of surveyed quadrats were sprayed, with spraying occurring at 9 pure panel APs in 2010 and 18 in 2011. Spraying decreased incrementally in the last two years of the monitoring period, with less than 6% of quadrats being sprayed in Fall 2012, and only 4% in Fall 2013 (**Figure 4.37**).

The database was also used to identify other mechanical actions at the anchor points that could potentially affect the amount of phragmites (**Table 4.44**). Based on this information, disk was conducted at four of the pure panel APs (AP9, AP11, AP15 and AP19) in 2008, no disk was conducted between 2009 and 2012, and only AP11 was disked in 2013. The amount of common reed that was present at AP9 and AP11 in 2009 when the monitoring program began was relatively low; however, AP19 had a relatively large amount, in spite of the disk. None of these APs was sprayed in 2008. Shredding and mowing was conducted at AP7 and AP29 in 2008. About 75 percent of the vegetation quadrats at AP7 were sprayed and no spraying occurred at AP29 in 2008. The monitoring data indicate that little or no common reed was present at AP7, and AP29 had among the largest amounts of common reed in 2009. Shredding and mowing occurred at four of the APs (AP9, AP13, AP37 and AP39), and large, mid-channel islands were mechanically removed at AP33 in Fall 2009. The amount of common reed at these APs was relatively low in 2010. Aside from spraying, the only mechanical actions documented in the Program database for Fall 2010 was shredding and mowing at AP29. With the exception of AP19, AP27 and AP39, the amount of common reed present at the pure panel APs was relatively low in 2011. Spraying was the only documented Program action at the pure panel APs potentially affecting the amount of common reed in Fall 2011, and documented actions other than spraying in Fall 2012 consisted of clearing and grubbing at AP23 and shredding and

¹⁶ As can be expected, the value of GDD is very sensitive to the chosen base temperature. In this case, 50°F was chosen based on the analysis of Gilmore *et al.* (2010), which correlates GDD and reflectance ratio for remote sensing of *Phragmites* sp. in coastal environments. The adequacy of 50°F is supported by Galinato (1986), considering the common temperatures required for germination of *Phragmites australis* seeds.

Table 4.3. Anchor points at which at least some aerial spraying occurred during the indicated year.

AP	Maintenance Year							AP	Maintenance Year						
	2008	2009	2010	2011	2012	2013	2014		2008	2009	2010	2011	2012	2013	2014
40								18							
39								17							
38								16							
37B								15							
37A								14							
36B								13B							
36A								13A							
35B								12B							
35A								12A							
34								11B							
33N								11A							
33								10C							
33S								10B							
32N								10A							
32								10							
32S								9C							
31								9B							
30								9A							
29								8D							
28								8C							
27								8B							
26								8A							
25								7C							
24								7B							
23B								7A							
23A								6B							
22B								6A							
22A								5							
21B								4							
21A								3							
20B								2							
20A								1							
19B															
19A															

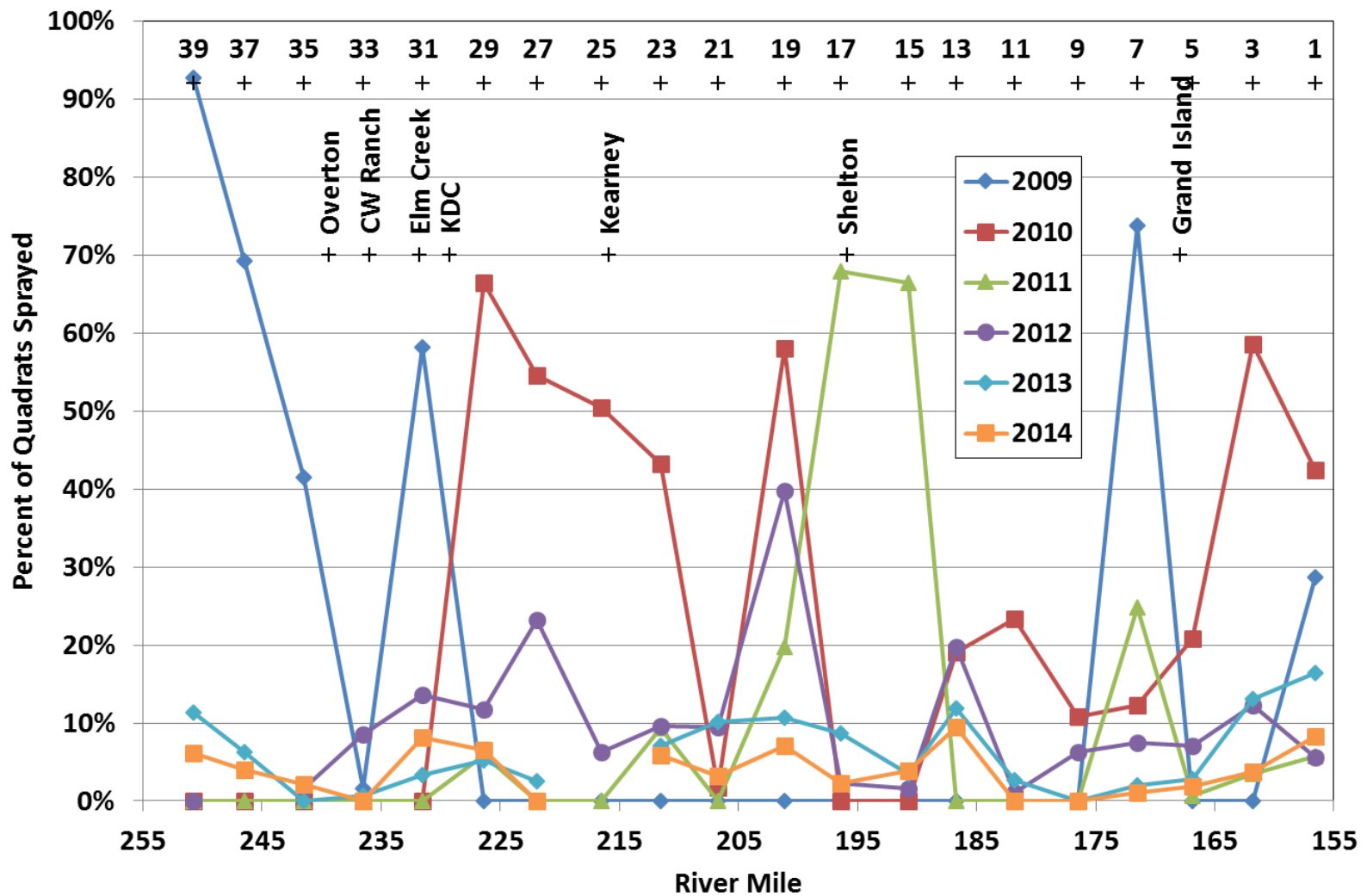


Figure 4.36. Percentage of individual vegetation sampling quadrats sprayed at each of the pure panel APs prior to each sampling period. Spraying typically occurs in early-fall; thus, the spraying indicated for each year occurred during fall of the previous year.

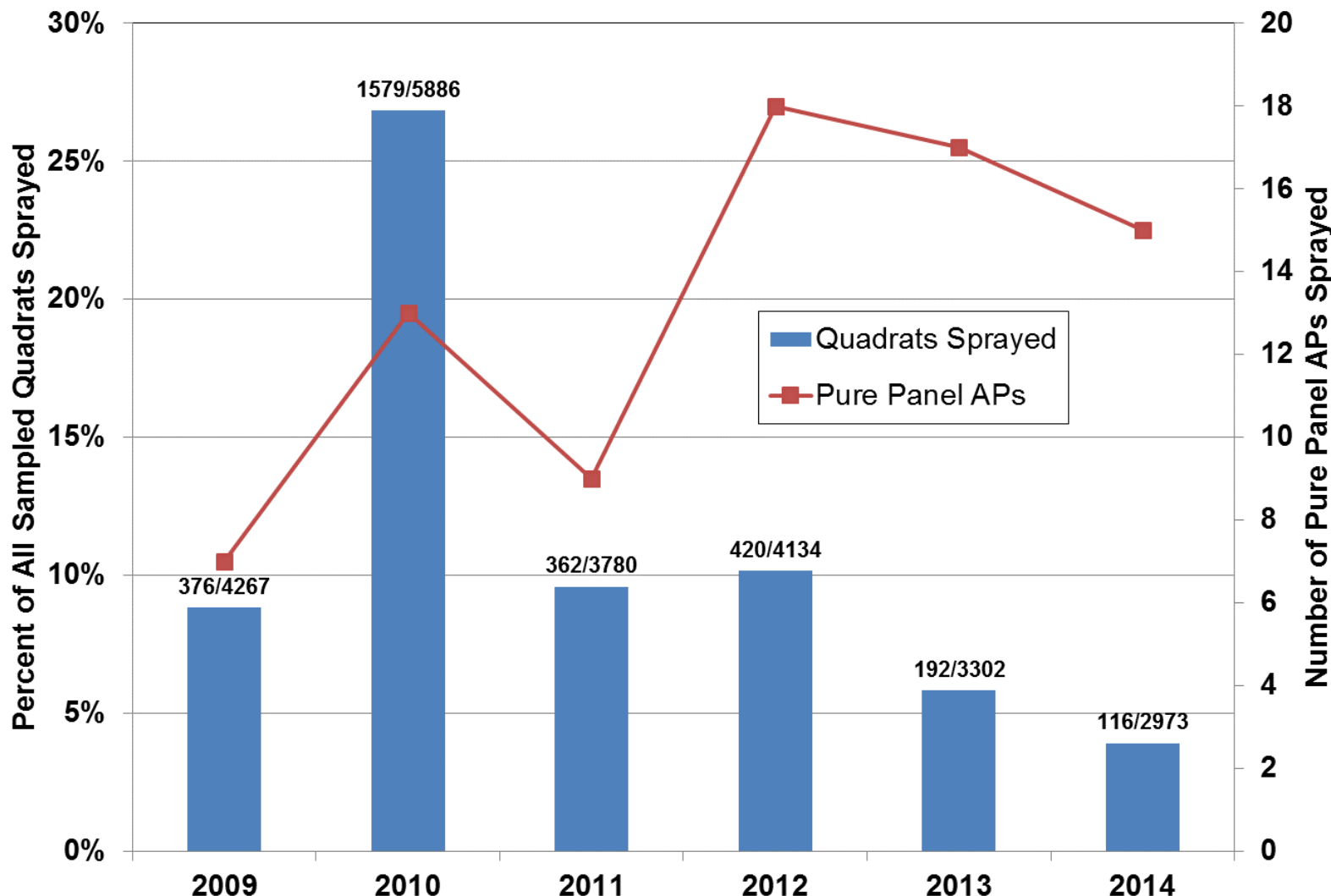


Figure 4.37. Percentage of all sampled quadrats sprayed at pure panel anchor points and number of pure panel APs receiving at least some spraying during the preceding fall of the indicated year. First number in each label is number of quadrats sprayed; second number is total number of sampled quadrats.

Table 4.4. Summary of PRRIP mechanical and other direct treatments at the APs for 2008 through 2013 other than aerial spraying.

Anchor Point	2008	2009	2010	2011	2012	2013
40	Shredding/Mowing	Shredding/Mowing, Chemical				
39	Chemical	Shredding/Mowing, Chemical				
38	Tree Clearing, Chemical	Shredding/Mowing				
37A	Tree Clearing	Shredding/Mowing				
35B						
34		Shredding/Mowing	Shredding/Mowing			
33		Island Construction, Tree Clearing/Removal,	Off Channel Habitat	Pre-emergent, Chemical	Prescribed Fire, Noxious Weed Control, Tree Clearing	
32			Shredding/Mowing, Chemical, Tree Clearing	Herbicide	Prescribed Fire, Noxious Weed Control, Shredding/Mowing	
31					Shredding/Mowing	
30	Disking	Disking, Chemical	Clear and Smooth, Tree clearing, disk	Grass Seeding, Herbicide, disk	Prescribed fire, tree clearing, Island Construction, disk, Pre-emergent, Noxious Weed Control	
29	Shredding/Mowing	Shredding/Mowing	Shredding/Mowing			
28	Shredding/Mowing	Shredding/Mowing				
24				Herbicide		
23	Spraying			Herbicide	Clear and Grub	
22	Spraying			Noxious Weed Control, Seedbed Prep, Grass Seeding, Herbicide		Disking
21	Spraying,					

Anchor Point	2008	2009	2010	2011	2012	2013
20	Spraying					
19	Disking					
18	Disking	Chemical				
16		Chemical	Shredding/Mowing			
15	Spraying					
14	Disking					Disking
13B		Shredding/Mowing			Tree Clearing, Seedbed Prep.	
13A				Herbicide		
12				Prescribed Fire, Herbicide, Tree/brush mulching	Disking, Pre- emergent, Shredding/Mowing	Disking
11B				Herbicide		Disking
11A	Disking			Herbicide		Disking
10						
10A	Disking	Shredding/Mowing, Chemical				
9C		Shredding/Mowing, Chemical				
9A	Disking					
8D	Shredding/Mowing	Shredding/Mowing, Chemical				
8A	Shredding/Mowing	Shredding/Mowing, Chemical				
7C		Shredding/Mowing, Chemical				
7A	Shredding/Mowing	Chemical				
6B	Shredding/Mowing	Shredding/Mowing, Chemical				
6A	Chemical	Chemical				
1	Chemical	Chemical				

mowing at AP31. Very little common reed was present at these APs in 2012. In 2013, disking and spraying were the only documented program maintenance actions.

Based on the available information related to the above factors, a multiple correlation analysis was conducted using the Spearman correlation coefficient (ρ) to assess whether there is a statistically-significant relationship between average percent cover and year-to-year change in percent cover of common reed at the pure panel APs and the following six variables:

1. Percent of quadrats at the AP sprayed (Percent Sprayed),
2. Maximum depth of inundation averaged over all quadrats (D_{avg}),
3. Average duration of inundation for all quadrats (Dur),
4. Discharge equaled or exceeded 90 percent of the time (Q_{low}),
5. Number of growing degree days during the growing season preceding the monitoring surveys (April through July) (GDD),
6. Total precipitation during the growing season preceding the monitoring surveys (April through July) (Precip).

The Spearman coefficient is based on the ranks of the observations and not their values; thus, it does not rely on assumptions of normality and linearity. The analysis was performed only on the pure panel APs that had more than 3.5-percent average cover during the initial monitoring survey (2009)¹⁷, since changes at those with lower amounts provide little contrast to assess the effects of the various parameters. As illustrated in Figure 4.28, the amount of common reed changed very little at the APs that were not included in the analysis. The analysis for percent cover indicates a statistically-significant positive correlation with the 90th percentile (low) flow ($\rho=0.423$, $p=0.001$), total precipitation ($\rho=0.407$, $p=0.001$), and a negative correlation with the number of growing degree days above 50°F ($\rho=-0.647$, $p<0.0001$) (**Table 4.5**). These results suggest that the availability of irrigation water is the primary factor in the amount of common reed in the reach. The results also indicate that the percent cover of common reed at any point in time is not strongly correlated with the intensity of spraying. This is a misleading result, because the spraying was focused on areas with significant amounts of common reed.

To overcome this issue, the correlation was also performed on the year-to-year change in percent cover versus the listed variables (**Table 4.6**). Because data on the amount of common reed prior to the 2009 surveys are not available, the data were reduced to only the last five years of the surveys¹⁸. Results of the analysis indicate that spraying is the only one of the variables for which the correlations with year-to-year change in common reed is statistically significant ($\rho=-0.416$, $p=0.002$). The negative value indicates that common reed decreased with increasing spraying intensity (**Figure 4.38**). The lack of correlation with the number of growing degree days, maximum inundation depth, duration of inundation, persistence of low flows during the growing season, or precipitation can be clearly seen in the data plots (**Figures 4.39a through 4.39e**). The lack of correlation with maximum inundation depths and duration of inundation, in particular, indicates that high flows are not effective in removing common reed.

¹⁷ This includes APs 1, 3, 5, 17, 19, 23, 25, 27, 29, 35A, and 39.

¹⁸ Removing the 2009 data also changes the correlation statistics for all other data. Thus, only the correlations with year-to-year change in common reed coverage are considered here.

Table 4.5. Correlation (Spearman) and p-values for percent cover of common reed versus possible influencing variables.

Correlation matrix (Spearman):								
Variables	%Site Sprayed	Max Inundation Depth (ft)	Duration of Inundation (days)	Q low (cfs)	Growing Degree Days	Total Precipitation (inches)	% Cover All Species	% Cover Common Reed
%Site Sprayed	1	0.007	0.086	0.020	0.064	0.001	0.051	-0.083
Max Inund Depth (ft)	0.007	1	0.746	0.610	-0.397	0.660	0.005	0.146
Duration of Inundation (days)	0.086	0.746	1	0.757	-0.405	0.750	-0.045	0.205
Q low (cfs)	0.020	0.610	0.757	1	-0.571	0.861	-0.005	0.423
Growing Degree Days	0.064	-0.397	-0.405	-0.571	1	-0.587	-0.169	-0.647
Total Precipitation (inches)	0.001	0.660	0.750	0.861	-0.587	1	0.120	0.407
% Cover All Species	0.051	0.005	-0.045	-0.005	-0.169	0.120	1	0.323
% Cover Common Reed	-0.083	0.146	0.205	0.423	-0.647	0.407	0.323	1
p-values:								
%Site Sprayed	0	0.958	0.499	0.878	0.616	0.993	0.686	0.513
Max Inund Depth (ft)	0.958	0	< 0.0001	< 0.0001	0.001	< 0.0001	0.968	0.248
Duration of Inundation (days)	0.499	< 0.0001	0	< 0.0001	0.001	< 0.0001	0.725	0.105
Q low (cfs)	0.878	< 0.0001	< 0.0001	0	< 0.0001	< 0.0001	0.968	0.001
Growing Degree Days	0.616	0.001	0.001	< 0.0001	0	< 0.0001	0.182	< 0.0001
Total Precipitation (inches)	0.993	< 0.0001	< 0.0001	< 0.0001	< 0.0001	0	0.343	0.001
% Cover All Species	0.686	0.968	0.725	0.968	0.182	0.343	0	0.009
% Cover Common Reed	0.513	0.248	0.105	0.001	< 0.0001	0.001	0.009	0

Values in bold are different from 0 at a significance level (α)=0.05

Table 4.6. Correlation (Spearman) and p-values for year-to-year change in percent cover of common reed versus possible influencing variables.

Correlation matrix (Spearman):								
Variables	%Site Sprayed	Max Inundation Depth (ft)	Duration of Inundation (days)	Q low (cfs)	Growing Degree Days	Total Precipitation (inches)	% Cover All Species	% Cover Common Reed
%Site Sprayed	1	-0.012	0.039	0.036	-0.177	0.029	-0.007	-0.416
Max Inund Depth (ft)	-0.012	1	0.769	0.527	-0.610	0.614	-0.231	-0.068
Duration of Inundation (days)	0.039	0.769	1	0.817	-0.741	0.816	-0.382	-0.046
Q low (cfs)	0.036	0.527	0.817	1	-0.724	0.852	-0.432	-0.054
Growing Degree Days	-0.177	-0.610	-0.741	-0.724	1	-0.848	0.113	0.055
Total Precipitation (inches)	0.029	0.614	0.816	0.852	-0.848	1	-0.315	0.130
% Cover All Species	-0.007	-0.231	-0.382	-0.432	0.113	-0.315	1	0.213
% Cover Common Reed	-0.416	-0.068	-0.046	-0.054	0.055	0.130	0.213	1
p-values:								
%Site Sprayed	0	0.929	0.783	0.797	0.205	0.837	0.959	0.002
Max Inund Depth (ft)	0.929	0	< 0.0001	0.0001	< 0.0001	< 0.0001	0.095	0.628
Duration of Inundation (days)	0.783	< 0.0001	0	0.0001	< 0.0001	< 0.0001	0.005	0.745
Q low (cfs)	0.797	< 0.0001	< 0.0001	0	< 0.0001	< 0.0001	0.001	0.700
Growing Degree Days	0.205	< 0.0001	< 0.0001	0.0001	< 0.0001	0	< 0.0001	0.419
Total Precipitation (inches)	0.837	< 0.0001	< 0.0001	0.0001	< 0.0001	0	0.022	0.352
% Cover All Species	0.959	0.095	0.005	0.001	0.419	0.022	0	0.125
% Cover Common Reed	0.002	0.628	0.745	0.700	0.693	0.352	0.125	0

Values in bold are different from 0 at a significance level (α)=0.05

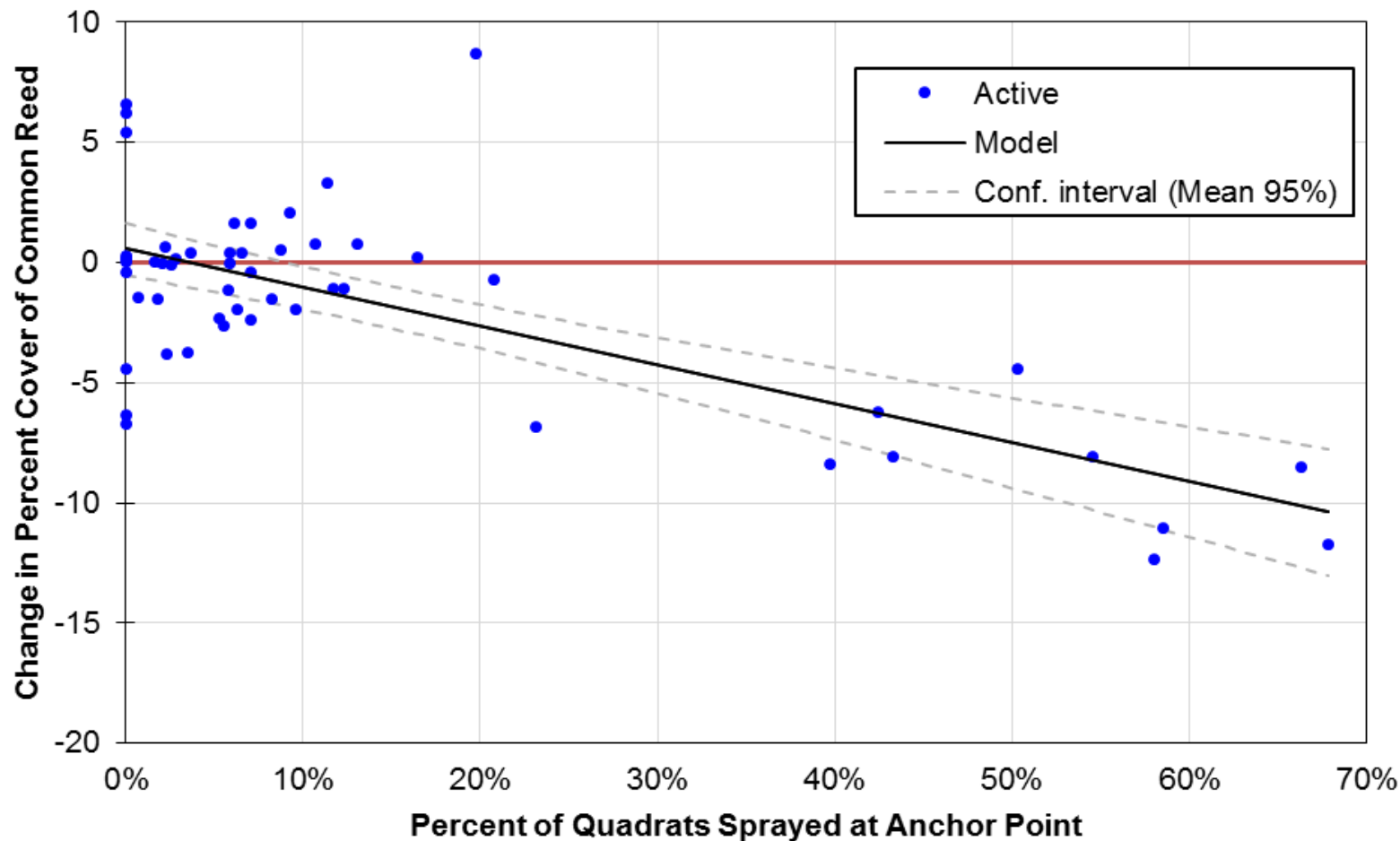


Figure 4.38. Change in percent cover of common reed versus percent of quadrats sprayed at pure panel APs with more than 3.5 percent average cover of common reed during the 2009 survey.

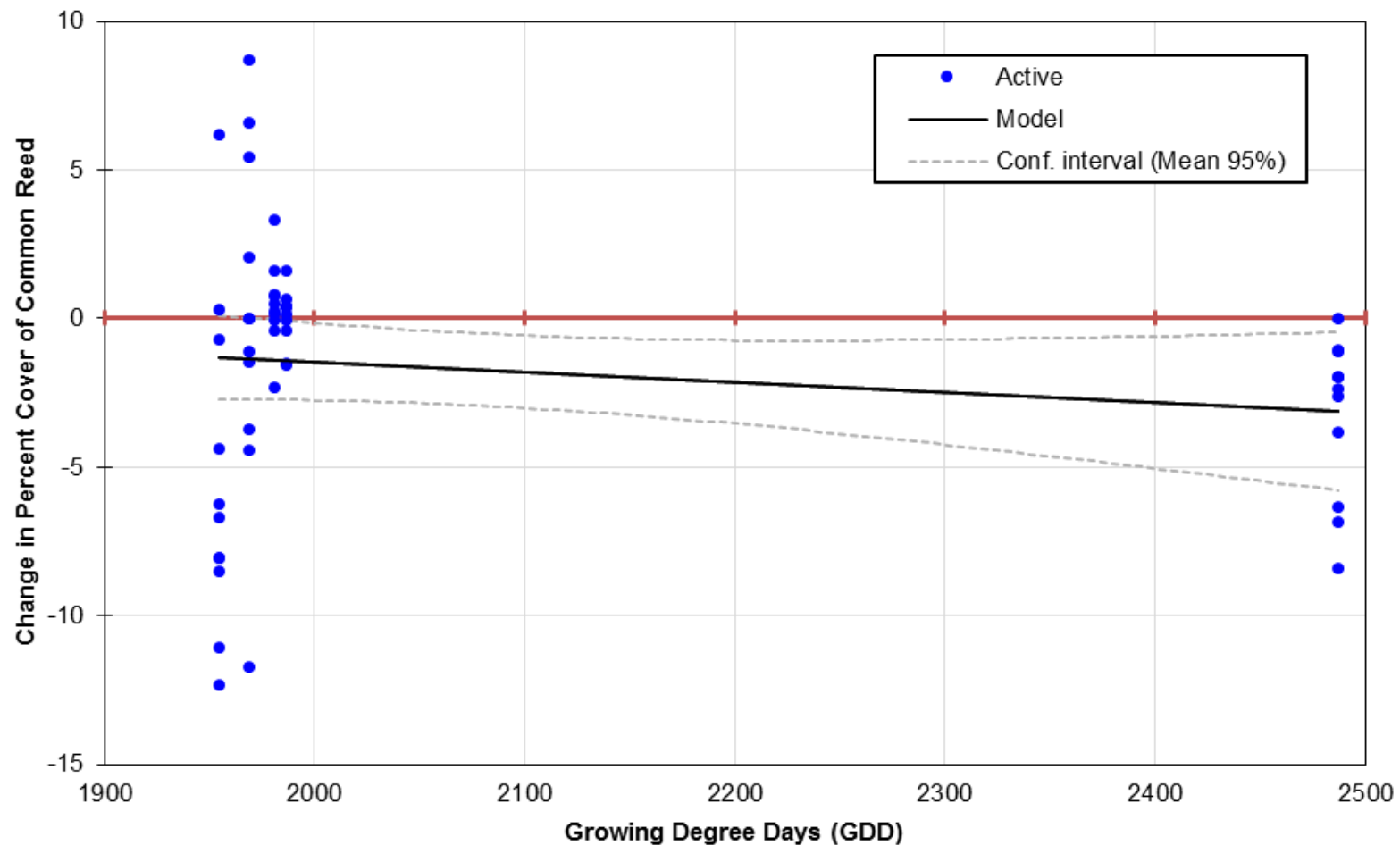


Figure 4.39a Change in percent cover of common reed versus growing degree days at pure panel APs with more than 3.5 percent average cover of common reed during the 2009 survey.

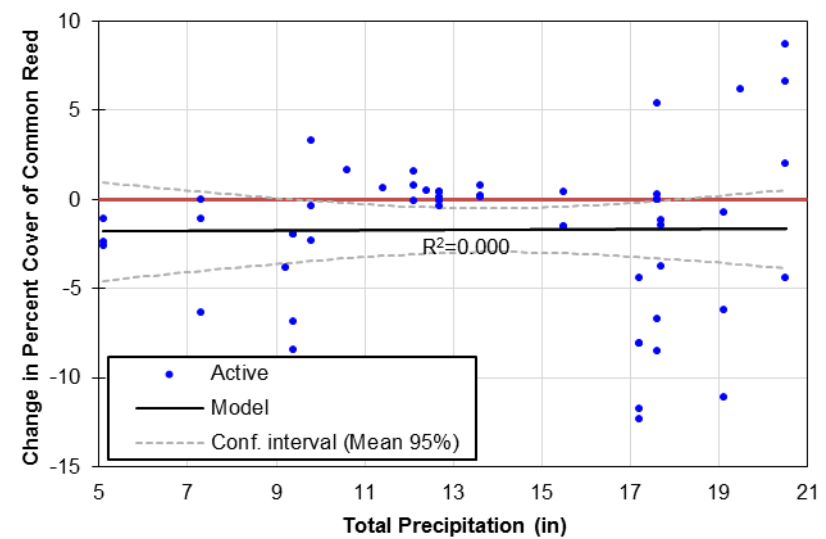
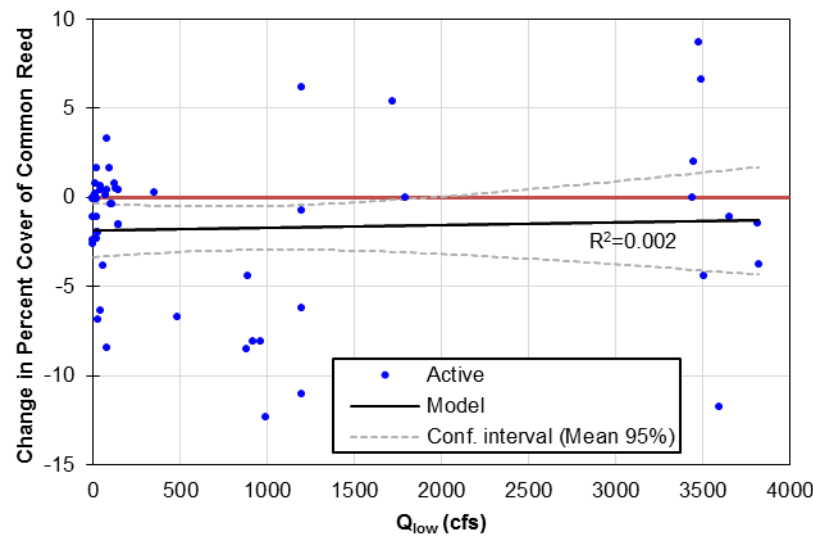
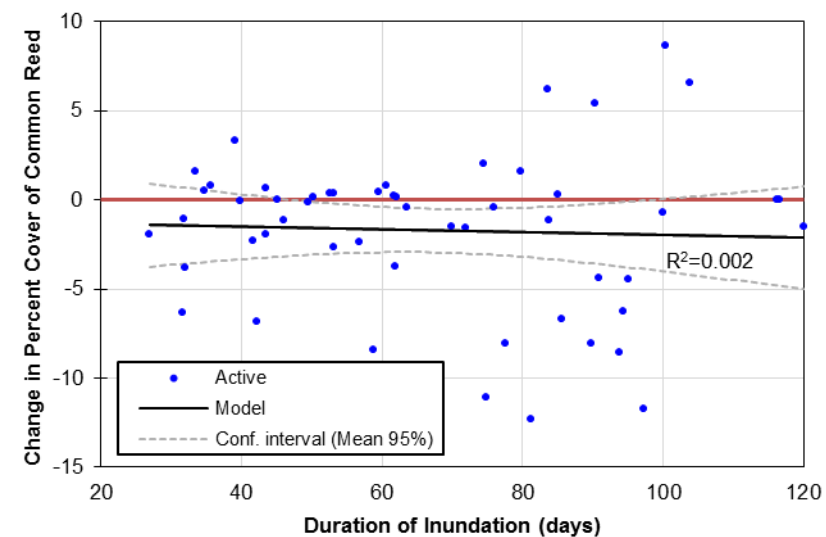
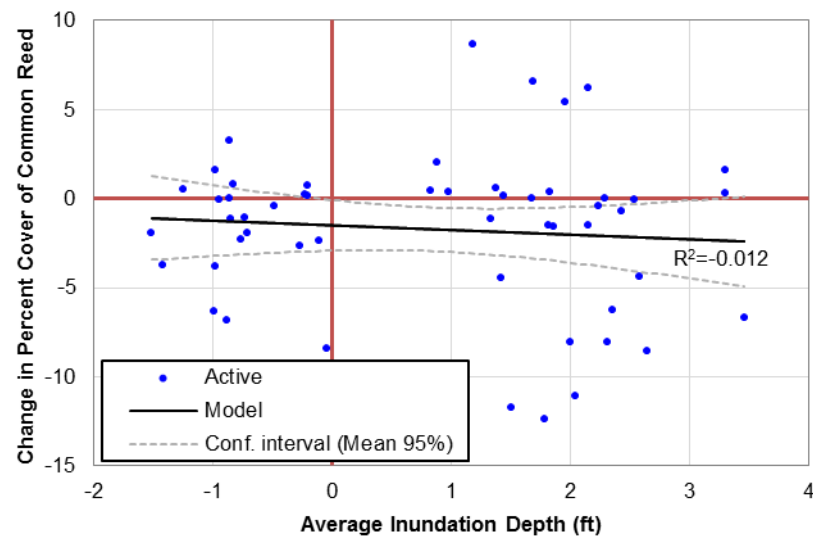


Figure 4.39b-e. Clockwise from top left, change in percent cover of common reed versus average inundation depth, duration of inundation, total precipitation during the growing season measured at Grand Island, and the 90th percentile low flow during the growing season.

4.4 Mechanical #2

Increasing the Q1.5 in the main channel by consolidating 85 percent of the flow, and aided by Program flow and a sediment balance, flows will exceed stream power thresholds that will convert main channel from meander morphology in anastomosed reaches to braided morphology with an average braiding index greater than 3.

The correlation between total unvegetated width (W_{unveg}), braiding index (BI) and percent consolidation at 8,000 cfs was determined to assess the extent to which the unvegetated width and amount of braiding are influenced by the relative amount of the total flow carried in the primary flow path. The amount of flow consolidation ranges from about 41 percent in the main branch at AP7, AP9, and AP23 to 100 percent at several locations that are spread throughout the reach and represent about 39 percent of the total reach length (**Figure 4.40**). The length-weighted, average percent consolidation in the areas with less than 100 percent consolidation is about 66 percent.

The correlation between these three metrics is relatively weak, but statistically significant at the 95-percent level (**Figure 4.41** through **Figure 4.44**; **Table 4.7**). As discussed in Section 3.4.2., the unvegetated widths were greatest during 2011, when long-duration, high flows occurred in the reach prior to the monitoring surveys (Figure 3.17b). The average braiding index changed very little over the 5-year period encompassed by the surveys, although changes did occur at some APs (Figure 3.6b). Based on a two-sample t-test, the total unvegetated width at locations with less than 85-percent flow consolidation is not significantly different from the widths at locations having greater than 85 percent consolidation ($t=1.36$, $p=0.191$). The difference in the mean braiding index between these two data set is also not statistically significant ($t=0.568$, $p=0.577$).

Management actions at AP 9 (Shoemaker Island), AP21 (Rowe Sanctuary) and AP33 (Cottonwood Ranch) have likely altered (or at minimum, masked) the relationships between flow, braiding index and channel width. To assess whether the correlation is different at the sites that have not been affected by these management actions, the data for these three APs were removed, and the statistical tests repeated for the censored data sets. The results indicate that braiding index and unvegetated width are still significantly correlated with flow consolidation, and the strength of the relationship increases when AP9, AP21, and AP33 are excluded from the data set (Table 4.7). This is particularly true for unvegetated width where the Pearson correlation coefficient increases from 0.27 to 0.49, and the R^2 value increases from 0.09 to 0.24. Based on these results, it appears that flow consolidation may result in a wider unvegetated channel and more braiding.

Table 4.7. Correlation matrix for percent flow consolidation, average braiding index and average unvegetated channel width at all of the pure panel APs, and all pure panel APs, except AP9, AP21 and AP33.

Variables	All Data			Excluding AP 9, 21 and 33*		
	Flow Consolidation at 8,000 cfs	Braiding Index	Unvegetated Width (feet)	Flow Consolidation at 8,000 cfs	Braiding Index	Unvegetated Width (feet)
Correlation matrix (Pearson):						
Flow Consolidation at 8,000 cfs	1	0.273	0.297	1	0.299	0.489
Braiding Index	0.273	1	0.297	0.299	1	0.325
Unvegetated Width (feet)	0.297	0.297	1	0.489	0.325	1
p-values:						
Flow Consolidation at 8,000 cfs	0	0.003	0.001	0	0.003	0.000
Braiding Index	0.003	0	0.001	0.003	0	0.001
Unvegetated Width (feet)	0.001	0.001	0	< 0.0001	0.001	0

Values in bold are different from 0 with a significance level alpha=0.05

*Management activities at AP9, 21 and 33 may have affected the relationship.

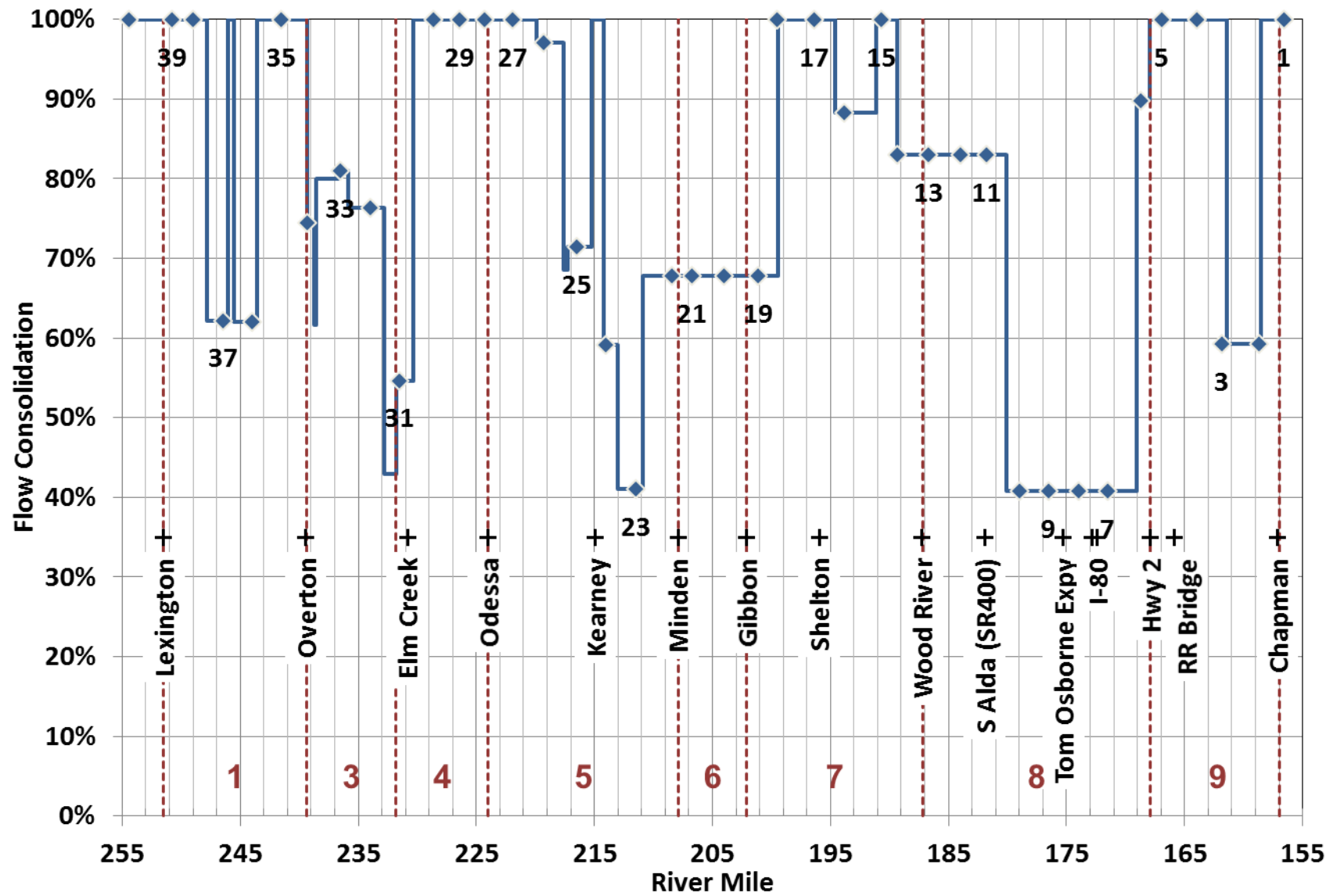


Figure 4.40. Percent flow consolidation (i.e., percent of flow in the main flow path) at 8,000 cfs.

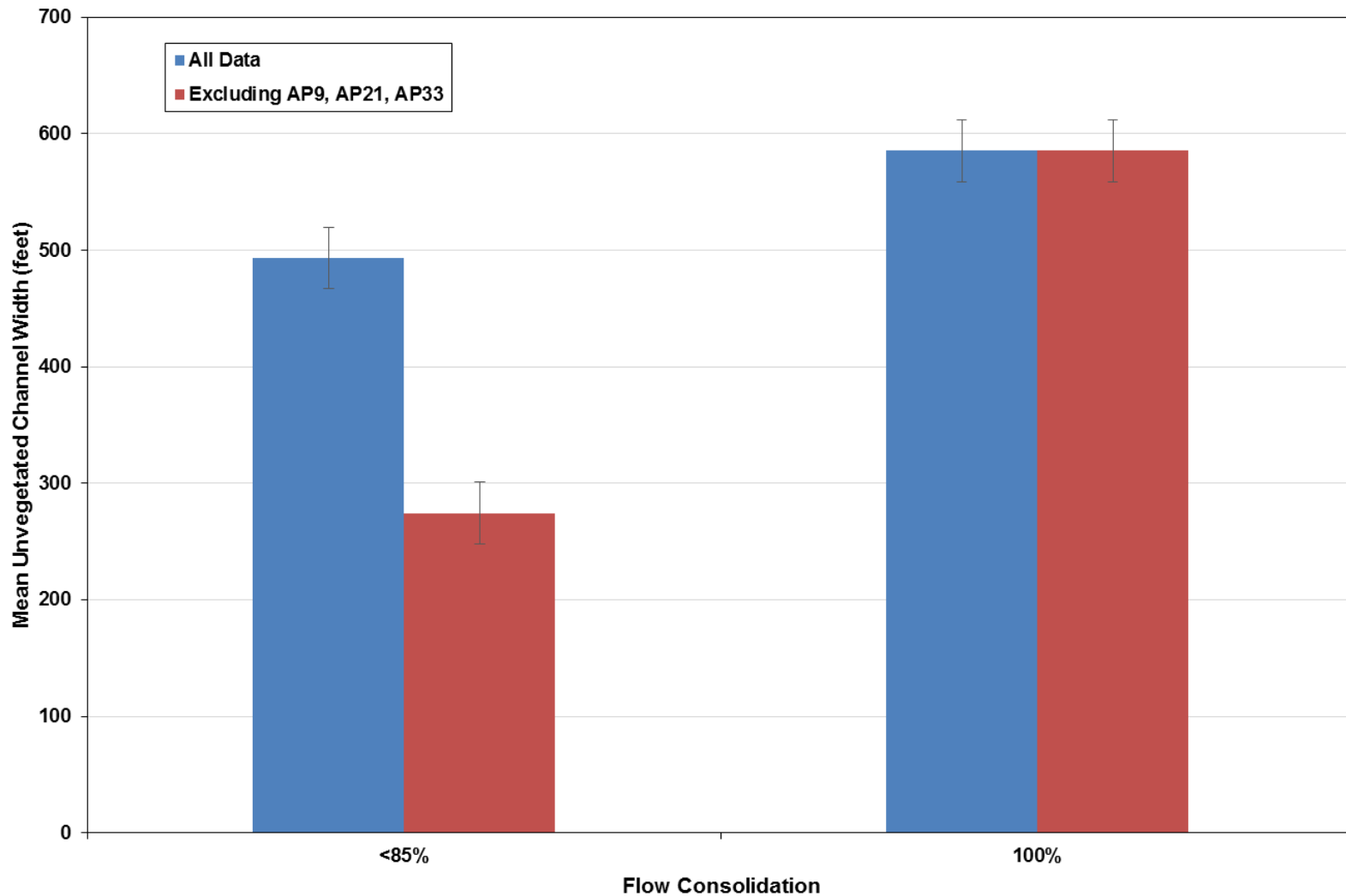


Figure 4.41a. Mean unvegetated channel width at sites with less than 85-percent flow consolidation and sites with 100-percent flow consolidation based on 2014 monitoring data.

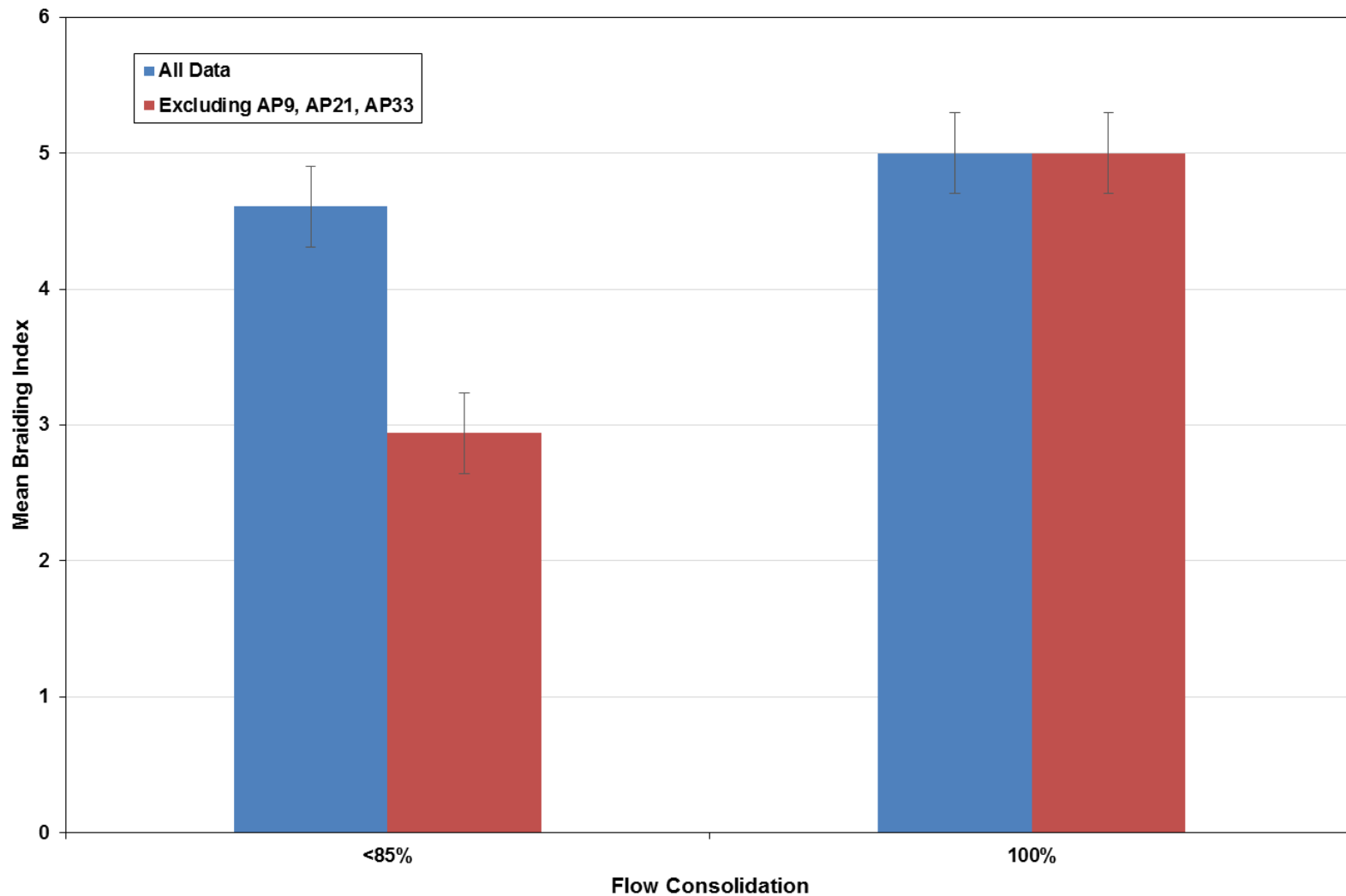


Figure 4.41b. Mean braiding index at sites with less than 85-percent flow consolidation and sites with 100-percent flow consolidation based on 2014 monitoring data.

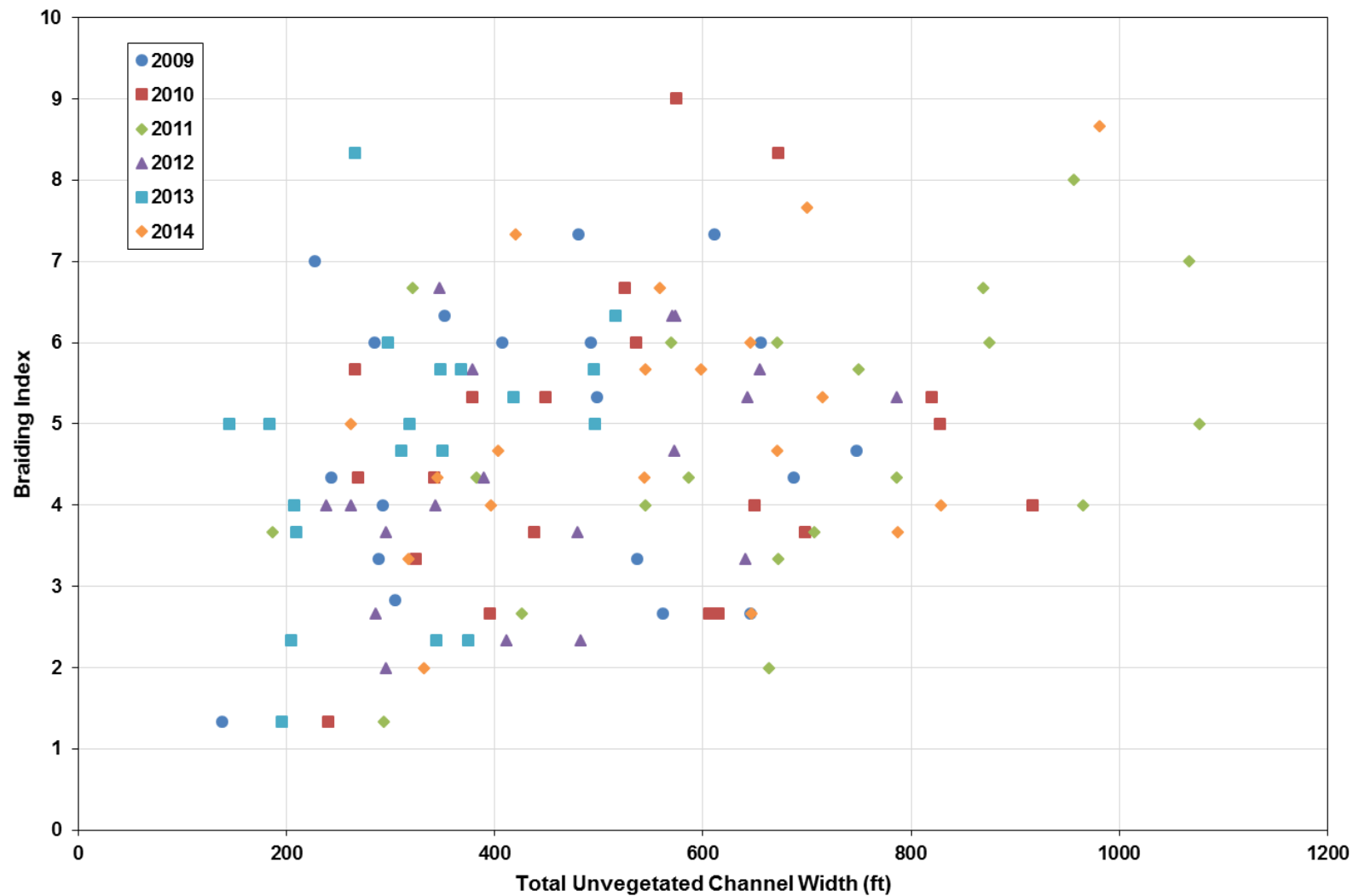


Figure 4.42. Total unvegetated channel width versus braiding index (Kendall's $t = 0.19$, $p=0.004$).

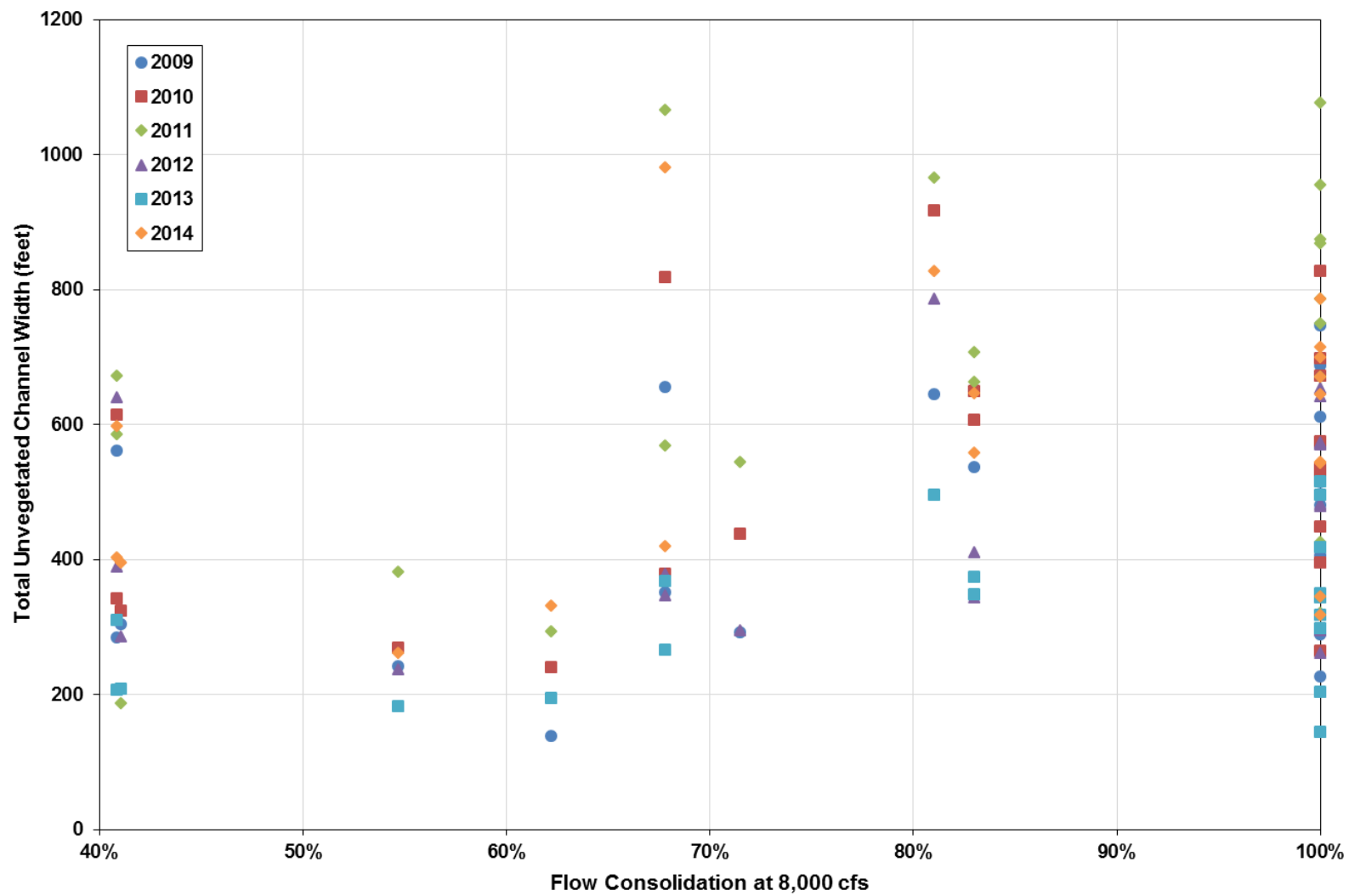


Figure 4.43. Total unvegetated channel width versus percent flow consolidation at 8,000 cfs (Kendall's $t = 0.18$, $p=0.012$).

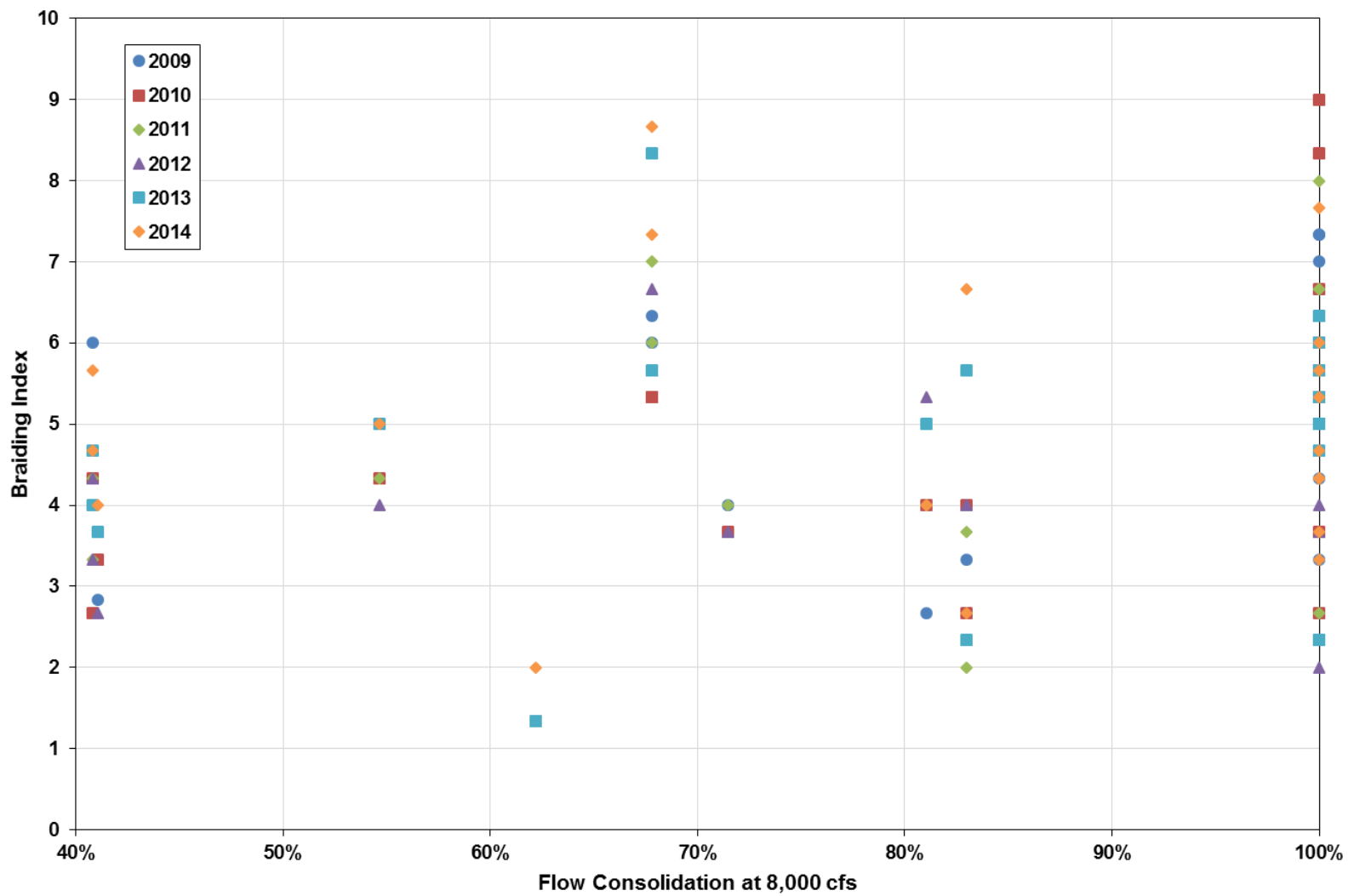


Figure 4.44. Braiding index versus percent flow consolidation at 8,000 cfs (Kendall's $t = 0.24$, $p=0.002$).

5 SUMMARY AND CONCLUSIONS

With the 2014 field season, the Platte River Geomorphic and Vegetation Monitoring Program has completed six years of detailed field monitoring, and the data have been used to quantify at least 35 individual performance metrics that fall into one of the following six general categories: Hydrologic, Hydraulic, Geomorphic, Vegetation, Sediment, and Whooping Crane (Table 2.3). This annual report presents a summary of all six years of data, including spatial and temporal trends in each of the metrics. To provide a focused and in-depth analysis of key issues of concern to the Program, this report also includes detailed analysis of specific aspects of the four hypotheses: Flow #1, Flow #3, Flow #5, Mechanical #2.

Hydrologic conditions during the monitoring period varied considerably, from relatively dry years in WY2009 and WY2013 to one of the wettest years on record (WY2011) (Figure 4.13), providing good contrast to assess the response of the monitoring reach to flow conditions. Although WY2012 ranked as a relatively wet year based on the flows for the entire year, most of the flow volume occurred during Fall 2011; flows during the growing season between April 1 and the monitoring surveys that were conducted in July and August were very low. In fact, the April through July runoff volumes in both 2012 and 2013 were in the lower 25th percentile of years since the early-1940s. The peak discharges in 2010 and 2011 were moderately high, as well, while the 2009, 2012 and 2013 peaks (prior to the September 2013 flood) were in the low to average range (Figure 5.1). The 2014 peak discharge was moderate. Based on the WY1942 through WY2014 data, the recurrence intervals of the 2009 and 2012 peaks were in the range of 1.5 to 2 years, and the 2010 and 2011 peaks were in the range of 3 to 5 years (Figure 5.2). The pre-September 2013 peak discharge shown in Figure 5.1 occurred during a short-duration, medium-flow release that was conducted by the Program in mid-April. These discharges also had a recurrence interval of about 1.5 years. The September 2013 flood peak had a recurrence interval of about 7 years at Overton and about 4 years at Grand Island, and the 2014 peak had a recurrence interval of about 4 years at Overton and between 3 and 3.5 years at Grand Island.

In addition to the wide range of flow conditions, flow-sediment-mechanical (FSM) actions were conducted during the monitoring period at specific locations along the reach that could potentially affect the channel characteristics at the APs where the monitoring data are being collected. These actions included the Elm Creek and Shoemaker Island Adaptive Management Experiments, the Pilot Sediment Augmentation Project at the Dyer and Cottonwood Ranch sites, additional overbank clearing and grading of sand into the channel at Cottonwood Ranch in 2009 and 2010, and spraying to control common reed (*Phragmites australis*) and other introduced species in several locations along the reach. Additional, related actions were also conducted at the Rowe Sanctuary that likely affect the characteristics of at least AP21.

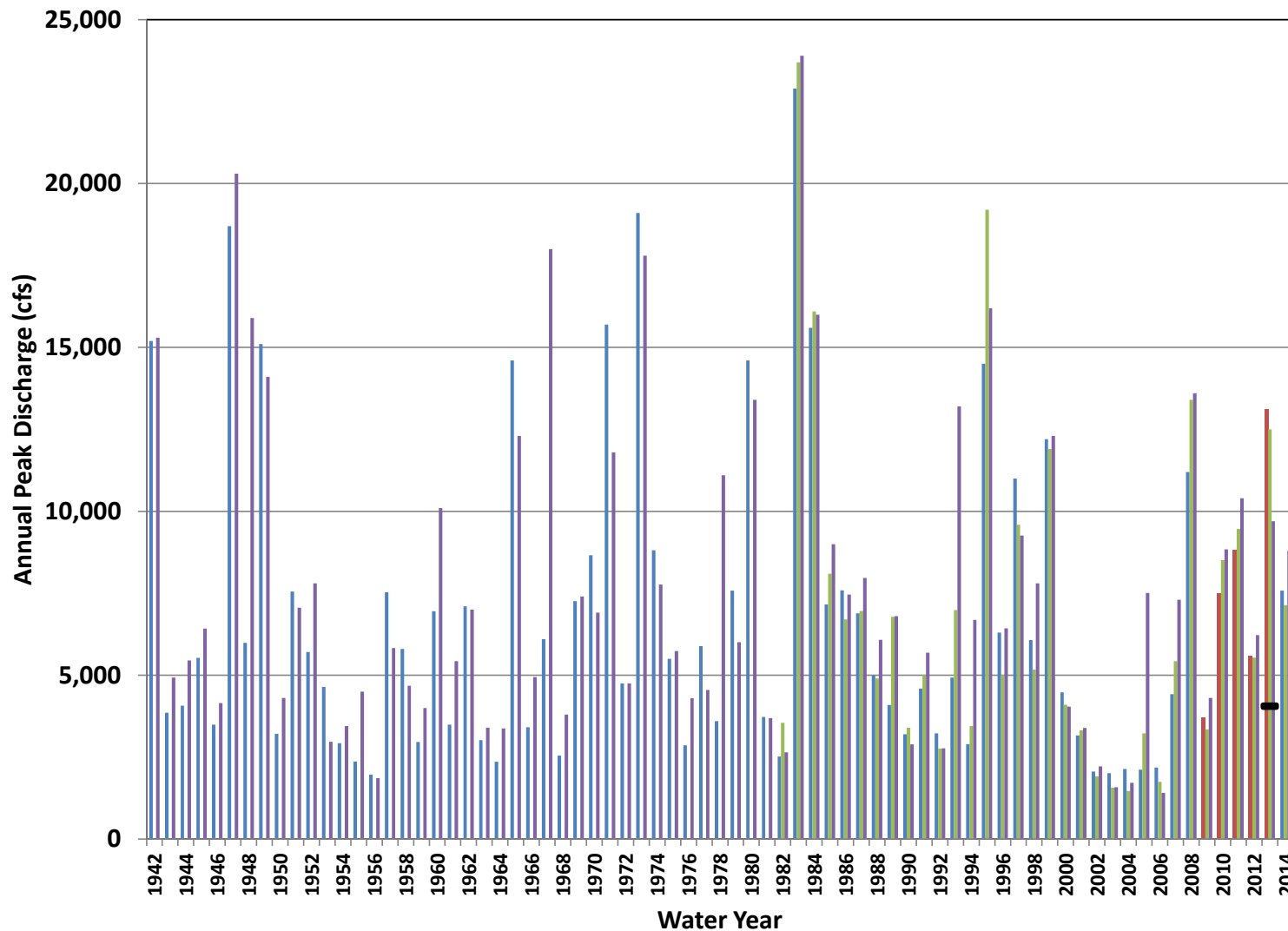


Figure 5.1. Annual peak discharges at the USGS Overton, Kearney, and Grand Island gages (note that Kearney record started in 1982). Also shown by the black mark is the approximate WY2013 peak discharges prior to the September flood at the three locations.

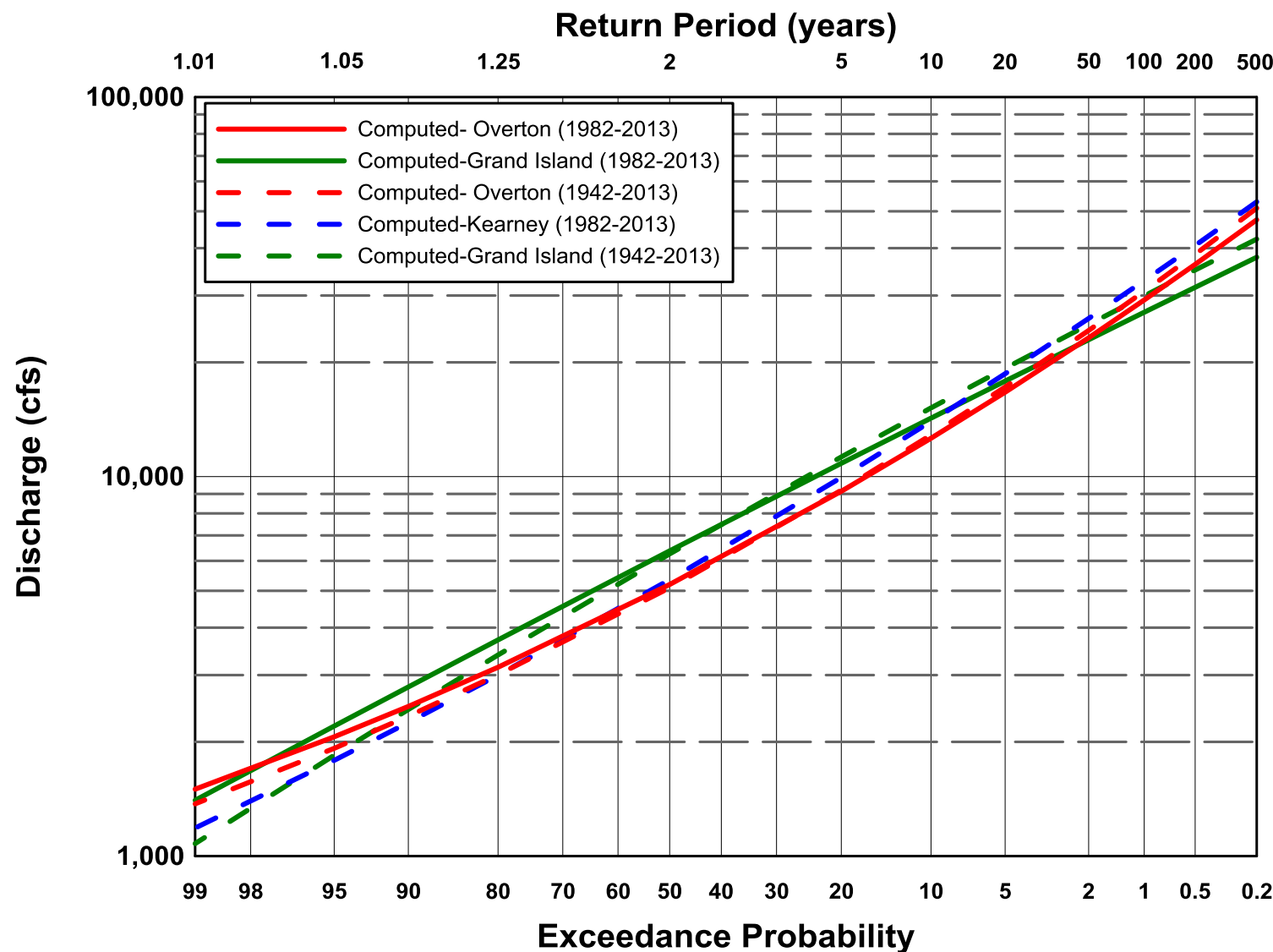


Figure 5.2. Flood-frequency curves for the annual peak flows from WY1942 through WY2013 at the USGS Overton, Kearney (WY1982-WY2013, only), and Grand Island gages.

Key observations from the spatial and temporal trend analysis of the geomorphic and vegetation data include the following:

1. The basic geomorphic and vegetation data provide a basis for evaluating a wide range of trends in the physical response of the reach to flows, Program actions and other factors.
 - 1.1. The reach-wide average braiding index changed very little during the period, although the index for 2012 was somewhat lower than the other years (Figure 3.6). Geomorphic Reaches 4 (Elm Creek to Odessa; Table 2.1) and 6 (Minden to Gibbon) typically had the highest braiding indices and Reaches 1 (Lexington to Overton), 2 (south channel at Jeffreys Island), 3 (Overton to Elm Creek), and 8 (Wood River to Grand Island) typically had the lowest indices. The braiding index in 2013 in Reach 6 was substantially higher than in previous years. The reason for the large increase in Reach 6 is not apparent, but it could be related to activities at the Row Sanctuary.
 - 1.2. The reach-wide average total channel width showed a modest (not statistically significant) increasing trend from 2009 through 2011, and has remained essentially the same since 2011 (Figure 3.7). In general, the changes in year-to-year width were very small. Geomorphic Reaches 4, 6, 7 (Gibbon to Wood River) and 9 (Grand Island to Chapman) have the largest total channel width (all exceeding 1,000 feet in all years), while Reaches 1 and 2 have the narrowest (in the range of 500 to 550 feet).
 - 1.3. The reach-wide average wetted channel width at 1,200 cfs was consistently in the range of 450 to 480 feet in 2009, 2010 and 2011, increased to about 505 feet in 2012, decreased back to about 485 feet in 2013, and then decreased even further to 440 feet in 2014 (Figure 3.8). The 2014 average width is the smallest during the 6-year monitoring period. Reaches with the largest wetted channel width generally correspond to the reaches with the largest braiding index and total channel width (i.e., Reaches 4, 6, 7 and 9).
 - 1.4. The reach-wide average width-to-mean depth ratio at the 1,200-cfs water surface declined from about 170 in 2009 to about 130 in 2011, increased to over 240 in 2012, and then declined back to about 215 in 2013 (Figure 3.11). In 2014, the average width-to-depth ratio decreased further to about 150, similar to 2010. The large decrease in 2014 appears to result from deepening of the channel thalweg (as indicated by the maximum channel depths) during the September 2013 flood and the high flows in June 2014.
 - 1.5. Based on the transect surveys at the pure panel APs, the overall monitoring reach appears to have degraded by about 3.6M tons between 2009 and 2011, aggraded by about 5.6M tons during 2012, and then continued to aggrade by about 1.6M tons in 2013 (Figure 3.12). The survey data indicate that the reach was approximately in-balance to slightly degradational (~0.5M tons of degradation) in 2014. The bulk of the degradation during the first two years occurred in the portion of the reach upstream from Minden, with Reach 5 showing the most degradation. The portion of the reach downstream from Minden appears to have been roughly in sediment-transport balance during this period. The data indicate that all of the reaches aggraded between the 2011 and 2013 surveys, with the bulk of the aggradation occurring in the portion of the reach downstream from Minden.
 - 1.6. The green line elevation (GLE) data indicate that the lower limit of vegetation is very responsive to flow; however, this appears to be primarily related to inundation levels that prevent annual vegetation from establishing rather than scour of the perennial

species. The reach-wide average GLE was about 1 foot higher in 2010 than during the initial survey in 2009, and this increased even further to about 1.9 feet by the 2011 surveys (Figure 3.14). The low flows in 2012 and 2013 allowed the vegetation to encroach back into the channel to levels that were similar to those in 2009, and the average GLE was about 0.9 feet above the 2009 level in 2014.

- 1.7. The reach-wide average total unvegetated channel width increased substantially from about 430 feet in 2009 to 630 feet in 2011 and then declined back to only about 310 feet by 2013 (Figure 3.17). Consistent with the changes in GLE, the unvegetated width increased back to about 525 feet in 2014.
- 1.8. Of the four species of primary interest, the frequency of purple loosestrife, common reed and willow declined substantially between 2009 and 2012, and then increased by a modest amount during 2013. The frequency of these species was similar in 2013 and 2014. In contrast, eastern cottonwood occurred relatively infrequently during the first three years, but increased substantially during 2012. The frequency of eastern cottonwood declined during 2013 and 2014, but still remains higher than during the initial survey in 2009.
- 1.9. Purple loosestrife is most common in the portion of the reach downstream from Minden, while common reed is most common in the reaches between Elm Creek and Minden (Reaches 4 and 5), Gibbon and Wood River (Reach 7) and Grand Island and Chapman (Reach 9) (Figure 3.19). Eastern cottonwood is more or less evenly distributed throughout the monitoring reach, although it occurred infrequently in Reaches 2, 6 and 7 during the early years of the monitoring program. It remains relatively infrequent in Reach 2 and 6, but increased substantially during 2012 in Reach 7. Willow was most common in Reaches 4 and 5 (Elm Creek to Minden) in 2009, but declined substantially in those reaches in later years.
- 1.10. Consistent with the trends in the GLE, the mean height of the four species of primary interest above the 1,200 cfs water-surface was generally greatest during the high-flow years in 2010 and 2011 (in the range of 1 to 1.8 feet), declined during the low flows in 2012 and 2013, and increased back to 0.5 to 1.0 feet in 2014 (Figure 3.37).
- 1.11. The bed and bar material tends to fine in the downstream direction, with median (D_{50}) sizes of 1 to 2 mm in the upstream part of the reach to less than 1 mm in the downstream part of the reach (Figures 3.53 and 3.55). The data also indicate that the reach-wide average D_{50} of the bed material became somewhat finer during the first 3 monitoring years (~1.2 mm to about 0.75 mm), but has increased back to about 1 mm in 2014 (Figure 3.54). Considering the variability of the underlying data, these trends may not be statistically significant.
- 1.12. With respect to the whooping crane-related metrics, unobstructed channel widths were generally greatest during the first three years (reach-wide average of 620 to 720 feet), and then declined substantially to only about 420 feet by 2012. The 2013 data showed a substantial increase to about 515 feet, and the average width continued to increase to about 570 feet in 2014 (Figure 3.56). The procedures used to estimate unobstructed channel width have evolved over the monitoring period; thus, some of the differences are likely due to uncertainty associated with the measurement/calculation techniques. Starting in 2013, these width are being measured directly with a laser rangefinder to eliminate as much of the uncertainty as possible.

2. An understanding of the relative sediment transport balance along the reach is a key factor in evaluating **Hypothesis Flow #1**. The following conclusions can be drawn from the analysis presented in this report.
 - 2.1. Integration of the bed and suspended sand-load rating curves over the applicable flow records and comparison of the resulting annual loads passing each of the bridges where the measurements were taken indicates that the segment between Darr and Overton was degradational throughout the monitoring period, and Overton to Kearney was degradational during SY2010, 2011, 2012 sand 2014 and aggradational during SY2013. The reach between Kearney and Shelton was aggradational throughout the period, and Shelton to Grand Island was degradational during all years, although the amount of degradation in SY2013 was relatively small (Figure 4.7).
 - 2.2. Based on the best-fit rating curves, the sand transport balance over the 5-year period included annual sediment deficits of 162,000 tons between Darr and Overton, 123,000 tons between Overton and Kearney, and 254,000 tons between Shelton and Grand Island, and an approximately 147,000 ton excess between Kearney and Shelton (Figure 4.7).
 - 2.3. Extrapolation of the aggradation/degradation volumes from the cross-section surveys at the pure panel APs to the overall length of the measurement-bridge segments results in estimates of the sand balance that, in many cases, are quite different from the rating curve-based estimates. For example, the surveys indicate that the segment between Darr and Overton was aggradational SY2012 and SY2013, resulting in an average annual degradation rate over the five-year period of about 30,000 tons compared to the rating curve-based estimate of about 162,000 tons (Figure 4.8). The survey-based estimates between Overton and Kearney indicate aggradation during SY2012 and SY2014, but the magnitude of degradation during the other years was greater than the rating-curve based estimates, resulting in average annual degradation of about 160,000 tons over the 5-year period, compared to about 123,000 tons based on the rating curves. The segment between Kearney and Shelton degraded during four of the five years, but the significant aggradation in SY2012 resulted in average annual aggradation of about 50,000 tons over the 5-year period, about one-third of the rating-curve based estimate of 147,000 tons/year. Finally, the segment between Shelton and Grand Island aggraded during four of the five years based on the survey data, resulting in average annual aggradation of about 356,000 tons over the five-year period. As noted above, the rating-curves indicate net degradation of about 254,000 tons per year in this segment.
 - 2.4. Monte Carlo simulations were performed for the sand load rating curves to quantify the uncertainty in the estimates. Based on the distribution of the estimated annual loads, the magnitude of the uncertainty exceeds the magnitude of the differences in annual sediment loads between the measurement sites in nearly all of the years and all of the reaches. The only results for which at least 95 percent of the degradation or aggradation estimates had the same sign is the degradation between Darr and Overton in SY2012, and the degradation between Shelton and Grand Island in SY2010 and SY2012. Using a one-tailed α -value of 0.05, these are the only three cases for which we can reject the alternative hypothesis that the indicated sediment deficit (or excess) is statistically significant. Nonetheless, the probability that the Darr to Kearney and Shelton to Grand Island reaches are, in fact, degradational and the Kearney to Shelton reach is aggradational is relatively high (Table 4.2)

- 2.5. Unfortunately, data are not available to directly assess the uncertainty in the survey-based estimates. Uncertainty in these estimates stems from at least three factors: (1) uncertainty in the horizontal position and elevation of the individual survey points, (2) uncertainty in how well the three surveyed transects represent the aggradation response of the channel within the individual AP, and (3) uncertainty in how well the response at the AP represents the overall response of the river in the approximately 5-mile segment of the river represented by the AP. Tests of the data using the reported accuracy of the individual points from the RTK-GPS datalogger indicate that the first of these sources of uncertainty is very small compared to the other two sources. Based on the available information about the river away from the transects, it is likely that the uncertainty associated with other two factors is relatively large.
- 2.6. In general, the above results strongly indicate that the portion of the reach upstream from Kearney is degradational, with an average annual sand deficit in the range of 100,000 tons between Darr and Overton and 140,000 tons between Overton and Kearney. Considering results from the surveys and the independent analysis done by both DOI Reclamation and USFWS (2006) and Tetra Tech (2010), the portion of the reach downstream from Kearney is most likely aggradational, with sediment excess in the range of 100,000 tons per year. There are, however, contradictory lines of evidence; thus, this conclusion is only weakly supported by the data. In considering these results, it is very important to recognize that the sediment loads along the reach vary significantly from year to year, based primarily on the magnitude and duration of the flows, and the overall sediment balance may change depending on the type of flow year. While long-term planning based on average annual estimates may provide a reasonable basis for certain long-term decisions, changes during extreme years may actually overwhelm the anticipated average annual difference.
3. The GLE and unvegetated channel width data provide a means of assessing the extent to which the unvegetated channel width responds to flow, as postulated by **Hypothesis Flow #3**:
 - 3.1. The reach-wide averaged greenline (GLE) data indicate that the Program's benchmark of 1.5 feet above the 1,200-cfs water surface was met only in SY2011, when long-duration, high flows persisted in the reach (Figure 4.19).
 - 3.2. GLE is well-correlated to the annual peak discharge (Figure 4.21), but is even more highly-correlated with the average discharge during germination season (Figure 4.22).
 - 3.3. The total unvegetated width is also positively correlated with both the annual peak discharge and the average germination season discharge (Figures 4.24 and 4.25).
 - 3.4. As expected from the above results, total unvegetated width is strongly correlated with GLE (Figure 4.26).
4. In relation to **Hypothesis Flow #5**, common reed has been identified as a potentially important factor in preventing the river from sustaining the wide, braided character that is important to good quality habitat for the target species. Both the frequency of occurrence and percent cover of common reed declined during the monitoring period. Several factors that could have contributed to the decline, including Program activities, were identified, quantified to the extent possible, and evaluated using multiple correlation analysis.
 - 4.1. Analysis of the year-to-year changes in percent cover of common reed versus a range of potential factors shows statistically-significant, negative correlation with spraying (Table 4.6; Figure 4.39).

- 4.2. Correlation of year-to-year changes in percent cover of common reed was not statistically significant for any of the other factors that were considered (i.e., maximum inundation depth, duration of inundation, 90th percentile (low) flow during growing season, growing degree days, and precipitation) (Table 4.6; Figure 4.40).
5. Flow consolidation is also postulated to be an important factor in maintaining the wide, braided character that is important to good quality habitat (**Hypothesis Mechanical #2**).
 - 5.1. Both the mean unvegetated channel width and mean braiding index at APs with more than 85-percent flow consolidation are larger than at the sites with than 85-percent flow consolidation (Figure 4.43). When all sites, including those where management activities that have substantially altered the channel, are considered, the difference in mean braiding index is statistically significant, but the difference in unvegetated channel width is not. When the three APs where the management actions have occurred (AP9, AP21 and AP33) are excluded from the data sets, the differences in both variables is statistically significant.
 - 5.2. These results suggest that flow consolidation may have a positive influence on both unvegetated channel width and the amount of braiding.

6 REFERENCES

Ayres Associates and Olsson Associates, 2010. Platte River Recovery Implementation Program, Year 1 (2009) Report, Channel Geomorphology and In-Channel Vegetation of the Central Platte River. Prepared for PRRIP, February, 52 p.

Ayres Associates and Olsson Associates, 2011. Platte River Recovery Implementation Program, Year 2 (2010) Report, Channel Geomorphology and In-Channel Vegetation of the Central Platte River. Prepared for PRRIP, March, 45 p.

Ayres Associates and Olsson Associates, 2012. Platte River Recovery Implementation Program, Year 2 (2010) Report, Channel Geomorphology and In-Channel Vegetation of the Central Platte River. Prepared for PRRIP, April, 46 p.

Cohn, T.A., and E.J. Gilroy. 1991. Estimating Loads from Periodic Records. U.S. Geological Survey Branch of Systems Analysis Technical Report 91.01. 81 p.

Daubenmire, R., 1959. A Canopy-Coverage Method of Vegetational Analysis. Northwest.

Duan, N., 1983. Smearing Estimate: A Nonparametric Retransformation Method. Jour. Amer. Stat. Assoc., v. 87, pp. 605-610.

Ferguson, R.I. 1986. River Loads Underestimated by Rating Curves. *Water Resources Research*, v 22(1), pp. 74–76.

Fotherby, L.M., 2008. Valley Confinement as a Factor of Braided River Pattern for the Platte River. *Geomorphology*. v. 103, Issue 4, pp. 562-576.

Friesen, B., Von Loh, J., Schrott, J., Butler, J., Crawford, D., and Pucherelli, M., 2000. Central Platte River 1998 Land Cover/Use Mapping Project, Nebraska, Technical Memorandum 8260-00-08, Bureau of Reclamation, U.S. Fish and Wildlife Service, Denver, Colorado.

Hirsch, R.M., Helsel, D.R., Coh, T.A., Gilroy, E.J., 1993. Statistical Analysis of Hydrologic Data. In Maidment, D.R. (ed), *Handbook of Hydrology*. McGraw Hill, Inc., pp. 17.1–17.55.

Kaul, B., Sutherland, D., and Rolfsmeier, S., 2011. The Flora of Nebraska; Second Edition. The School of Natural Resources, University of Nebraska–Lincoln, Lincoln Nebraska.

Lichvar, R. and Kartesz, J., 2012. North American Digital Flora: National Wetland Plant List, version 3.0. Accessed: 9 January 2013. Available: http://wetland_plants.usace.army.mil.

Murphy, P.J., Fotherby, L.M., Randle, T.J., and Simons, R., 2006. Platte River Sediment Transport and Riparian Vegetation Model. Prepared for the Bureau of Reclamation, March, 151 p.

Platte River Recovery Implementation Program, 2006. Attachment 3, Adaptive Management Plan, 254 p.

Platte River Recovery Implementation Program, 2010. PRRIP Channel Geomorphology and In-Channel Vegetation Monitoring, 24 p.

Platte River Recovery Implementation Program, 2012a. Draft Channel Geomorphology and In-Channel Vegetation Data Analysis Plan, 45 p.

Platte River Recovery Implementation Program, 2012b. Adaptive Management on the Platte River, Adaptive Management Plan, 2012 “State of the Platte” Report – Executive Summary, 68 p.

Pollen-Bankhead, Thomas, N.R., and Simon, A., 2011. DRAFT Platte River Recovery Implementation Program, Directed Vegetation Research Study, Can Short Duration High Flows be used to Remove Vegetation from Bars in the Central Platte River? 102 p.

Rolfsmeier, S. and Steinauer, G., 2010. Terrestrial Ecological Systems and Natural Communities of Nebraska (Version IV – March 9, 2010). Nebraska Natural Heritage Program, Nebraska Game and Parks Commission. Lincoln, Nebraska. Available: <http://outdoornebraska.ne.gov/wildlife/programs/legacy/pdfs/Terrestrial%20Ecological%20Systems.pdf>. Science 33:43-64. Department of Botany, State College of Washington, Pullman, Washington.

Runkel, R.L., Crawford, C.G., and Cohn, T.A., 2004. Load Estimator (LOADEST): A Fortran Program for Estimating Constituent Loads in Streams and Rivers. Techniques and Methods Book 4, Chapter A5, U.S. Geological Survey, Reston, Virginia.

Shen, H.W. and Julien, P.Y., 1993. Erosion and Sediment Transport. In Maidment, D.R. (ed), *Handbook of Hydrology*. McGraw Hill, Inc., pp. 12.1–12.6.

Tetra Tech, 2010. Hydraulic and Sediment-transport Modeling for the Platte River Sediment Augmentation Feasibility Study, Nebraska. Appendix B, Modeling Evaluation, Final Platte River from Lexington to Odessa Bridges, Sediment Augmentation Experiment Alternatives Screening Study Summary Report, prepared for Platte River Recovery Implementation Program, September 7, 92 p.

Tetra Tech, 2012. Elm Creek Two-dimensional Hydraulic and Sediment-transport Modeling Report, submitted to Platte River Recovery Implementation Program, October 26, 104 p.

Tetra Tech, 2013. Elm Creek FSM Annual Monitoring Report. Prepared for the Platte River Recovery Implementation Program, March, 73 p.

Tetra Tech, 2014. 2013 Elm Creek FSM Annual Monitoring Report. Prepared for the Platte River Recovery Implementation Program, April, 212 p.

The Flatwater Group, in association with Tetra Tech and HDR, 2014. Sediment Augmentation Final Pilot Study Report, prepared for the Platte River Recovery Implementation Program, April, 123 p.

U.S. Department of Agriculture-Natural Resources Conservation Service (USDA-NRCS), 2013. The PLANTS Database. National Plant Data Team, Greensboro, NC 27401-4901 USA. Accessed: 9 January. Available: <http://plants.usda.gov>.

U.S. Department of Interior, Bureau of Reclamation and U.S. Fish and Wildlife Service, 2006. Platte River Recovery Implementation Program, Final Environmental Impact Statement, River Geomorphology, pp. 5-57.

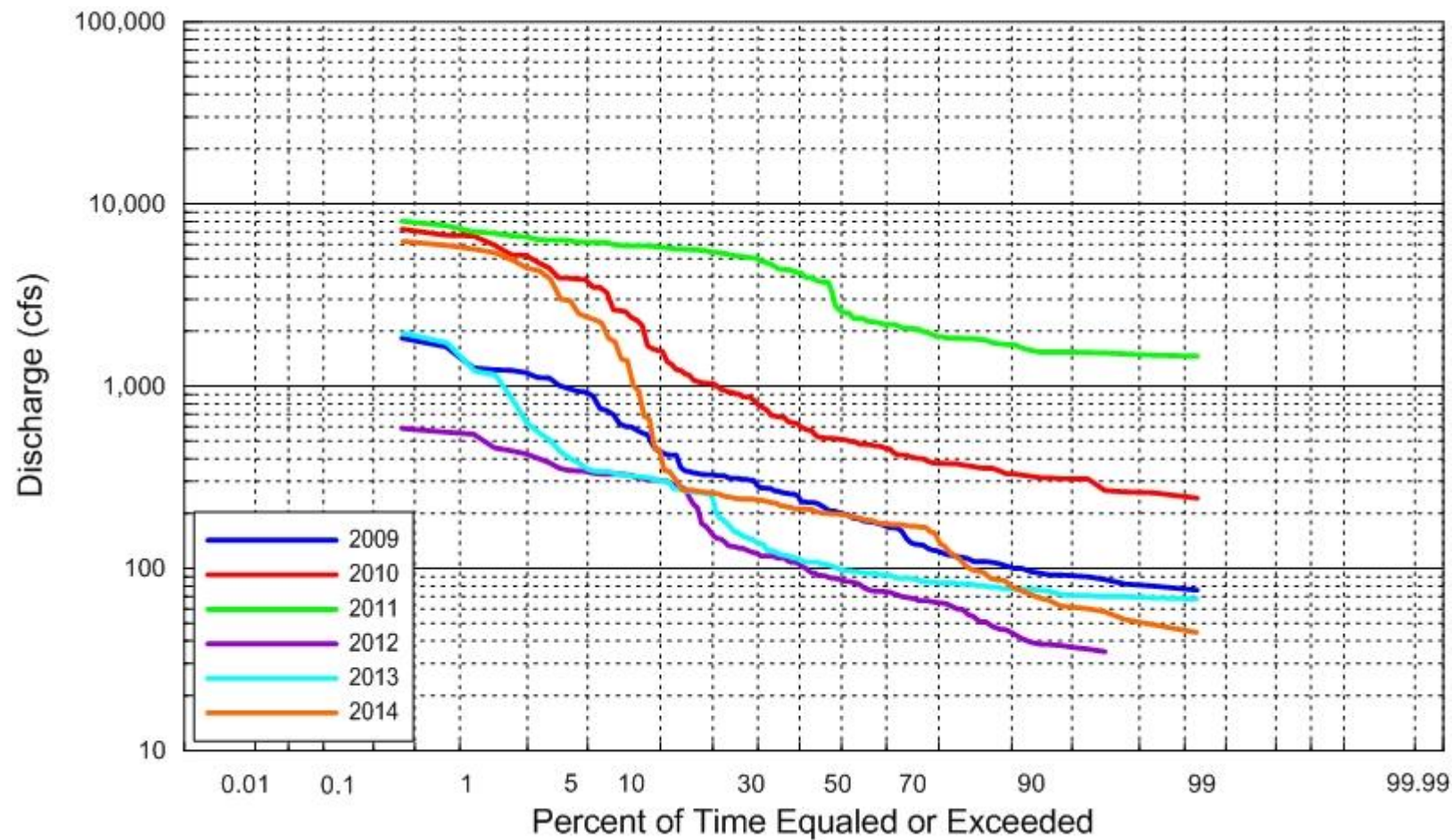
U.S. Geological Survey. 1992. Recommendations for Use of Retransformation Methods in Regression Models Used to Estimate Sediment Loads ["The Bias Correction Problem"]. *Office of Surface Water Technical Memorandum* No. 93.08. December 31.

Walling, D.E. 1977. Limitations of the Rating Curve technique for Estimating Suspended Sediment Loads, with Particular Reference to British Rivers. In: Erosion and Solid Matter Transport in Inland Waters, *Proceedings of Paris Symposium*. July. IAHS Publication No. 122, pp. 34–48.

APPENDIX A.1

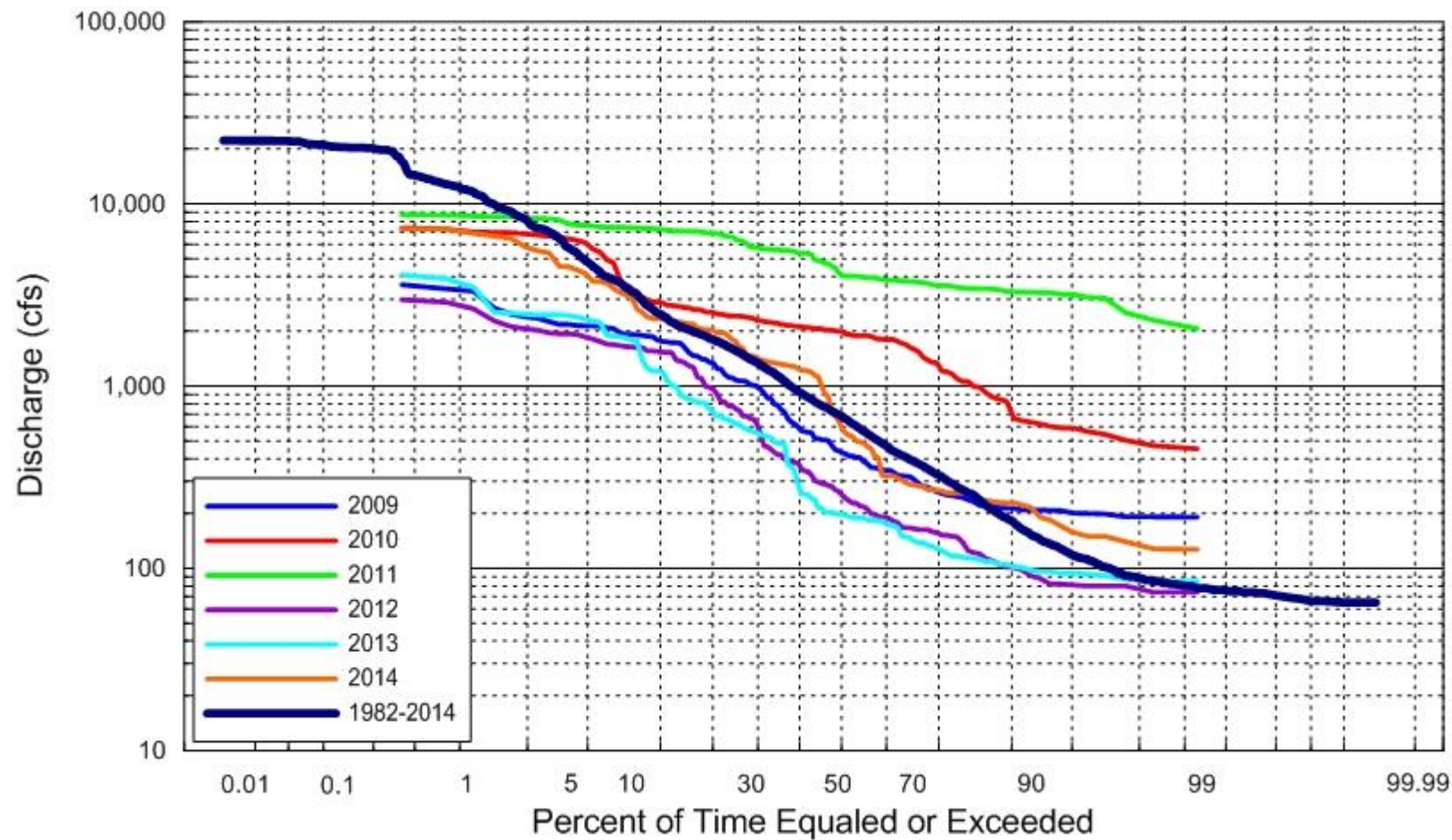
Mean Daily Flow-duration Curves for Germination Season

Germination Season (June 1 – July 10) for Lexington



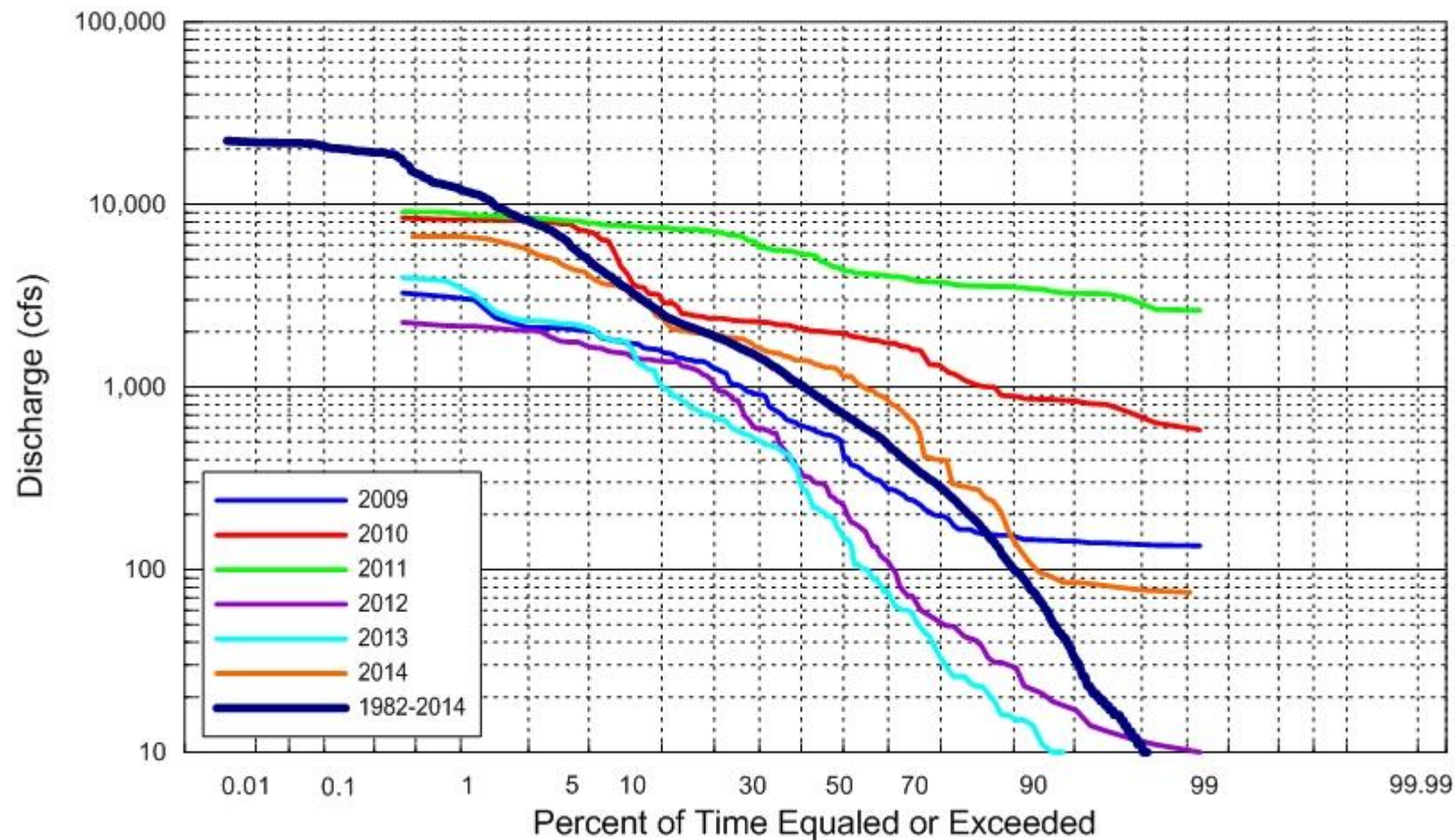
A.1.1

Germination Season (June 1 – July 10) for Overton



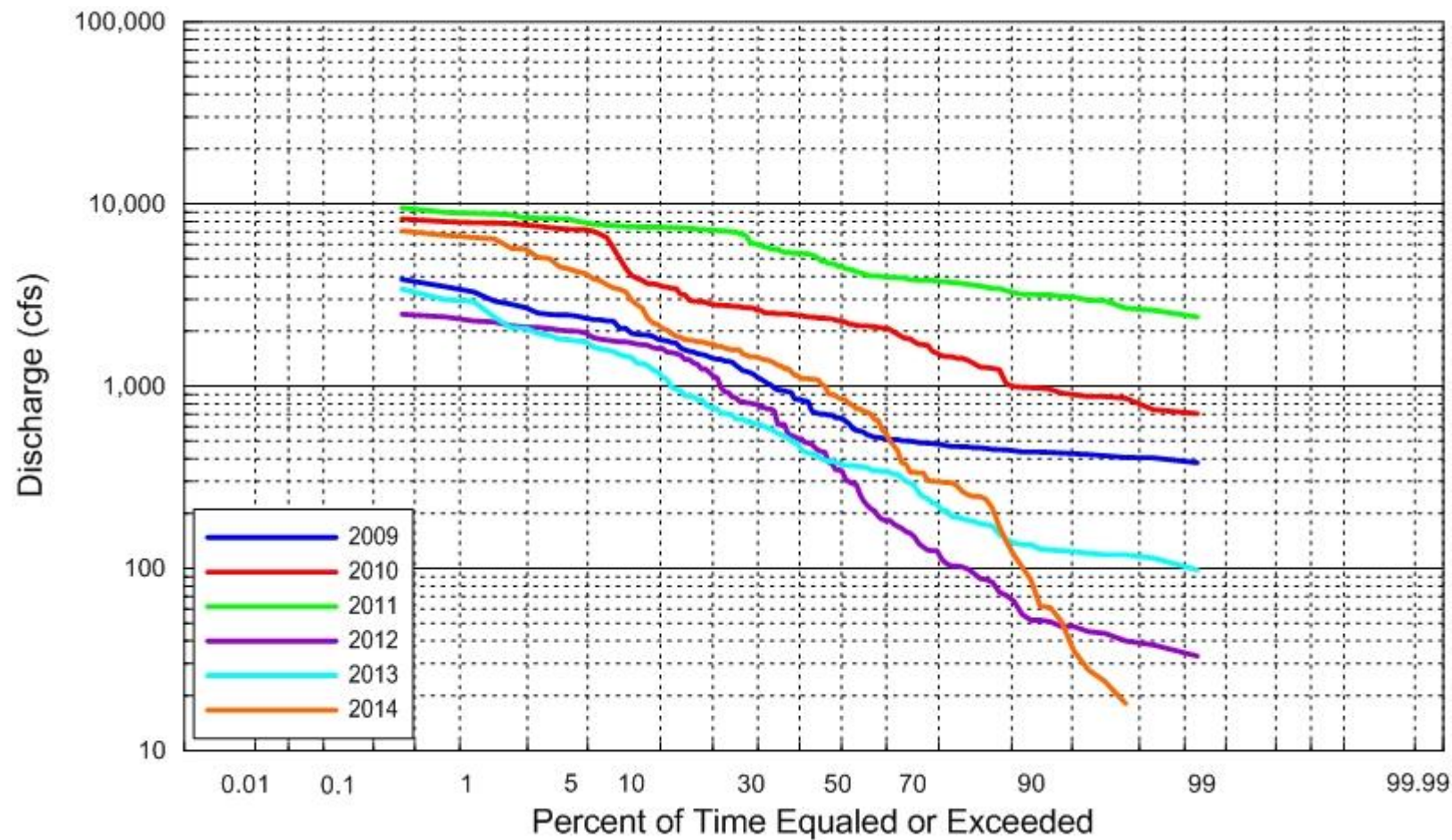
A.1.2

Germination Season (June 1 – July 10) for Kearney



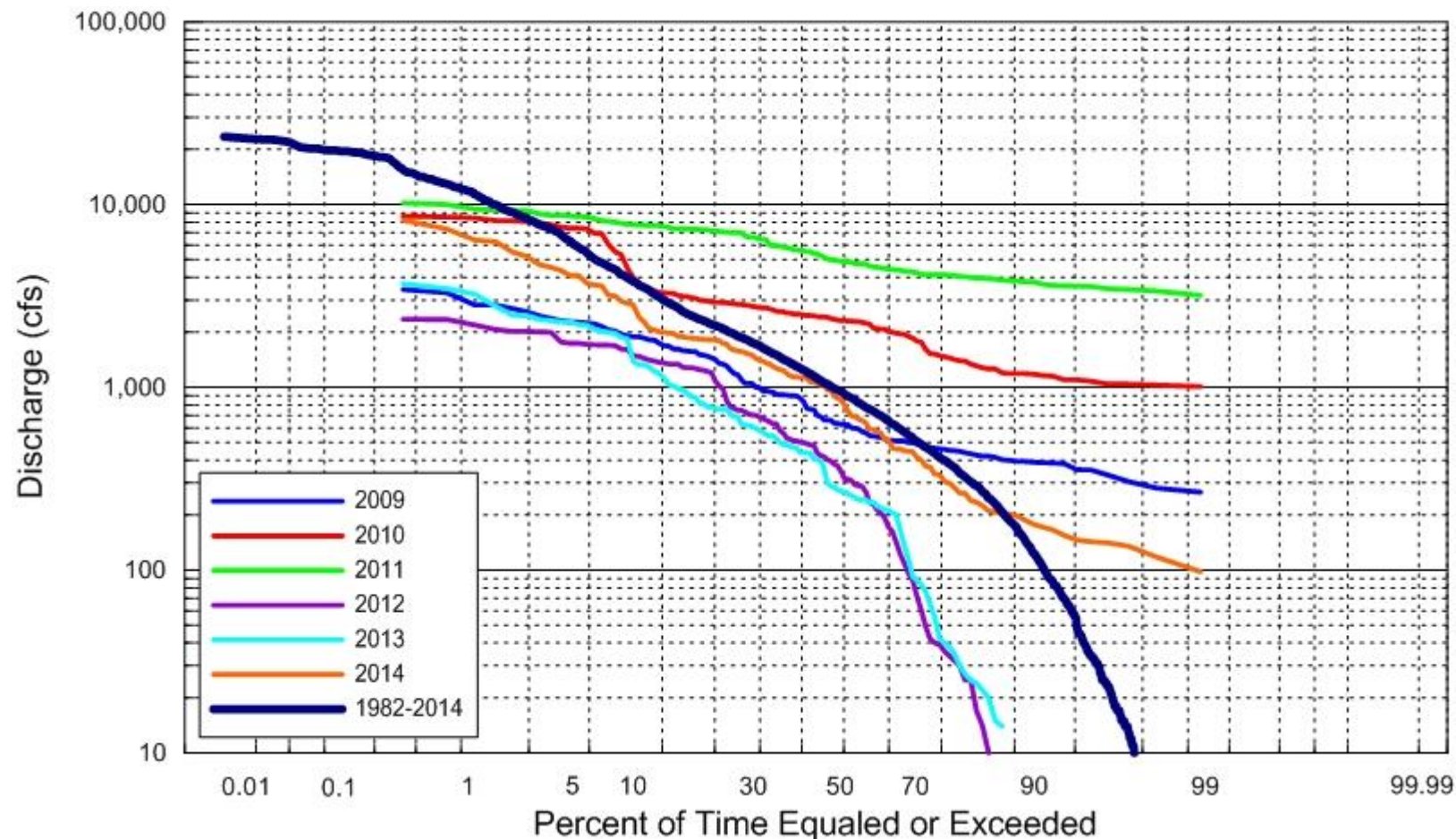
A.1.3

Germination Season (June 1 – July 10) for Shelton



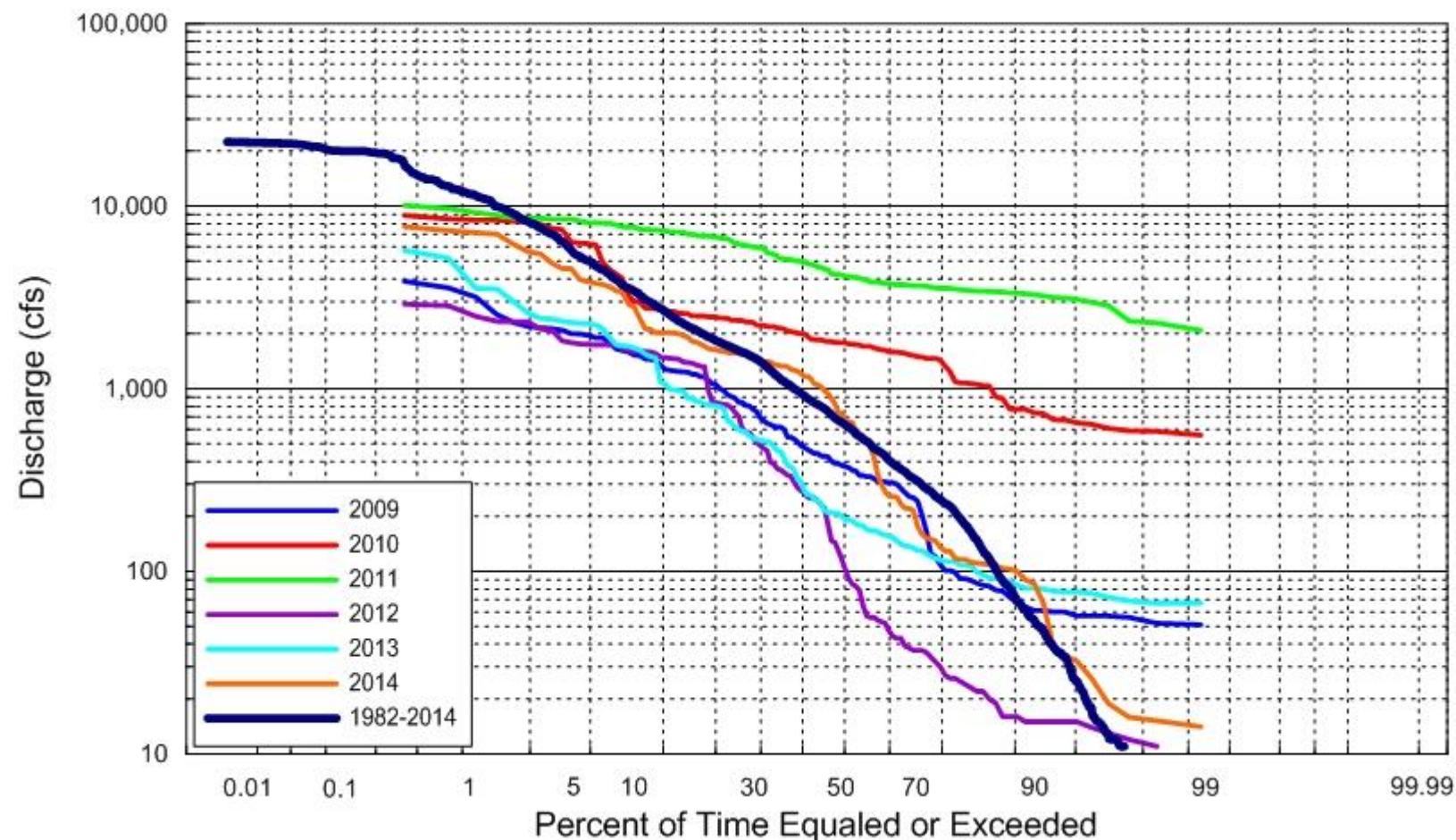
A.1.4

Germination Season (June 1 – July 10) for Grand Island



A.1.5

Germination Season (June 1 – July 10) for Odessa

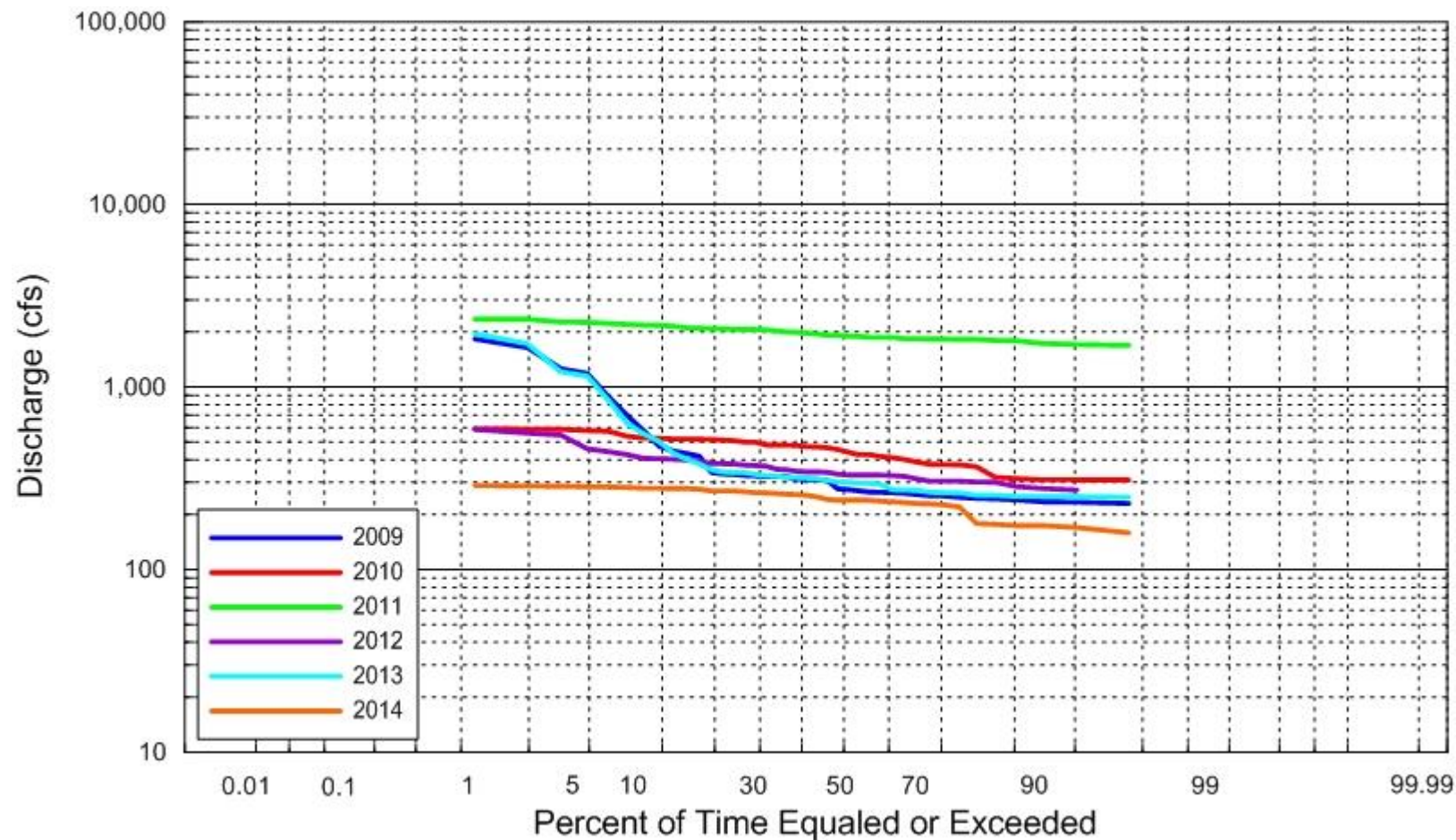


A.1.6

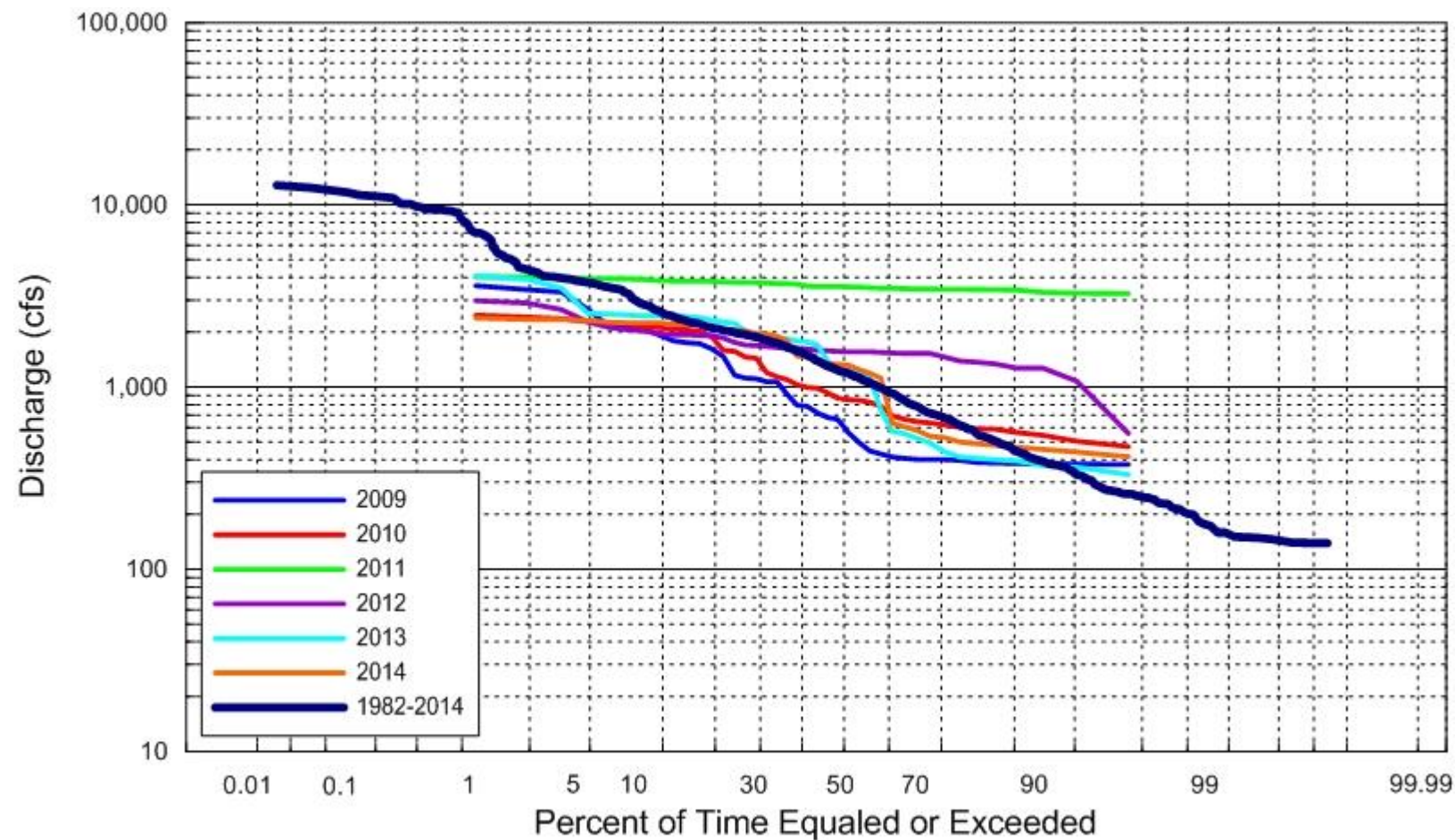
APPENDIX A.2

Mean Daily Flow-duration Curves for Spring Whooping Crane

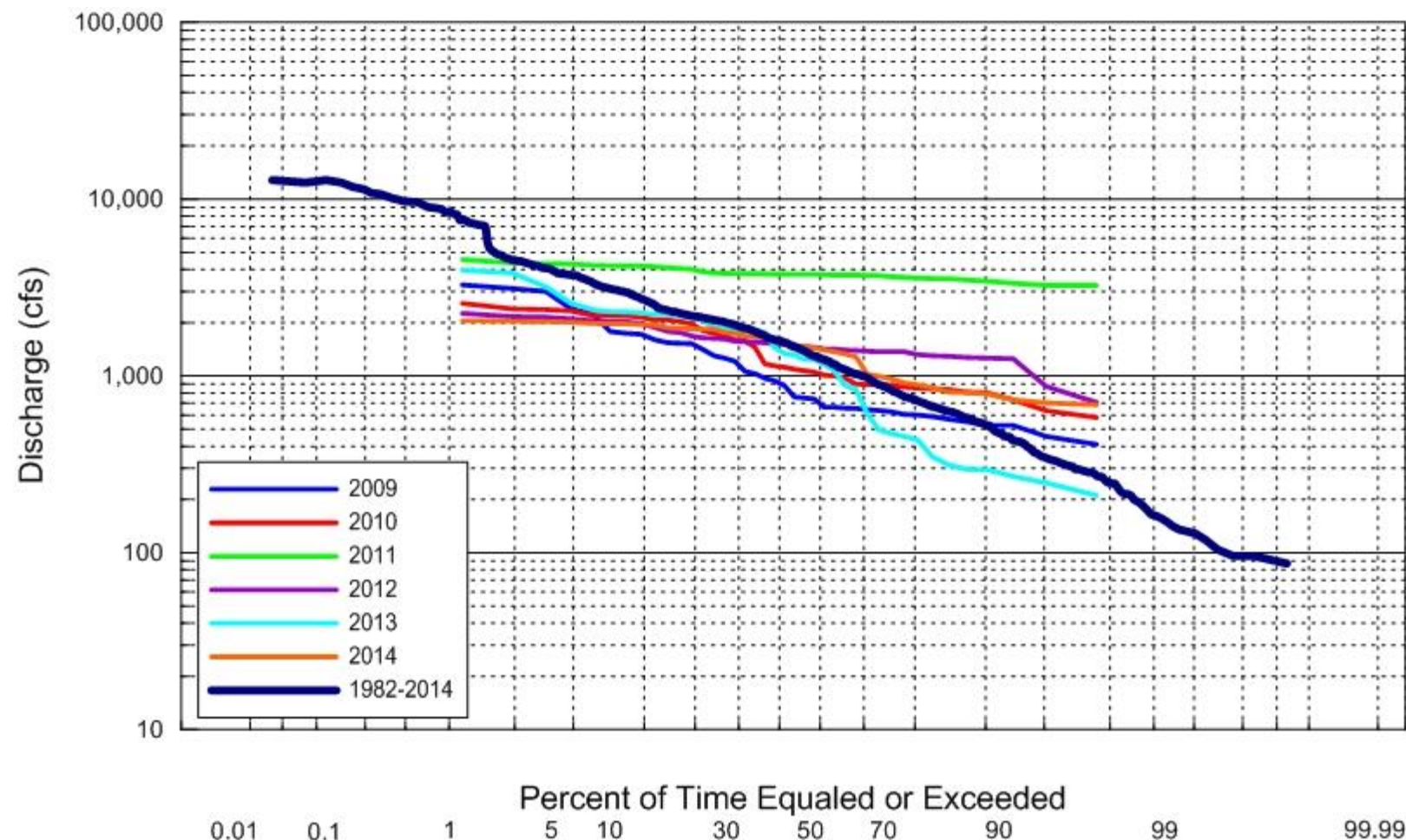
Spring Whooping Crane (June 1 – July 10) for Lexington



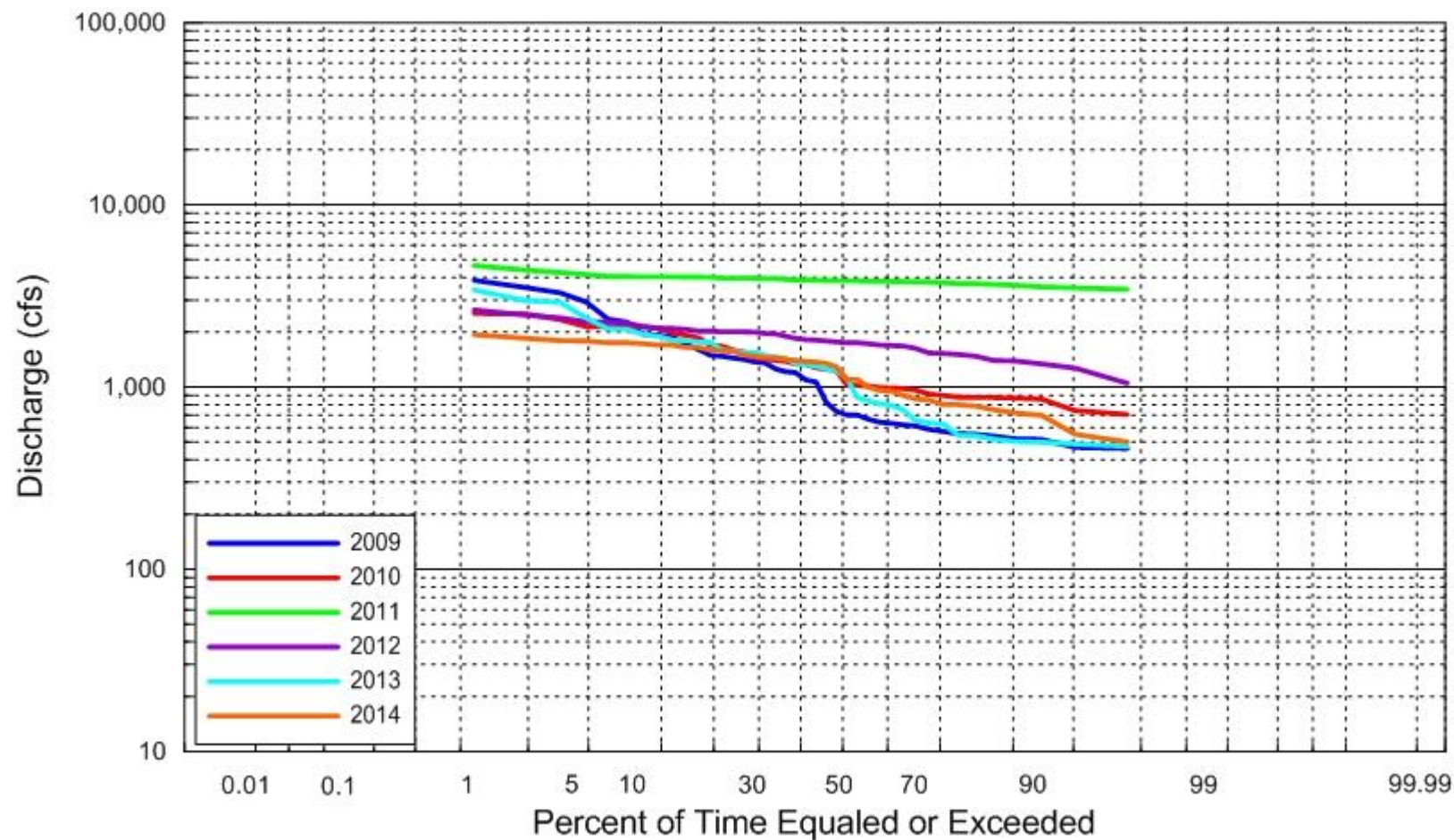
Spring Whooping Crane (June 1 – July 10) for Overton



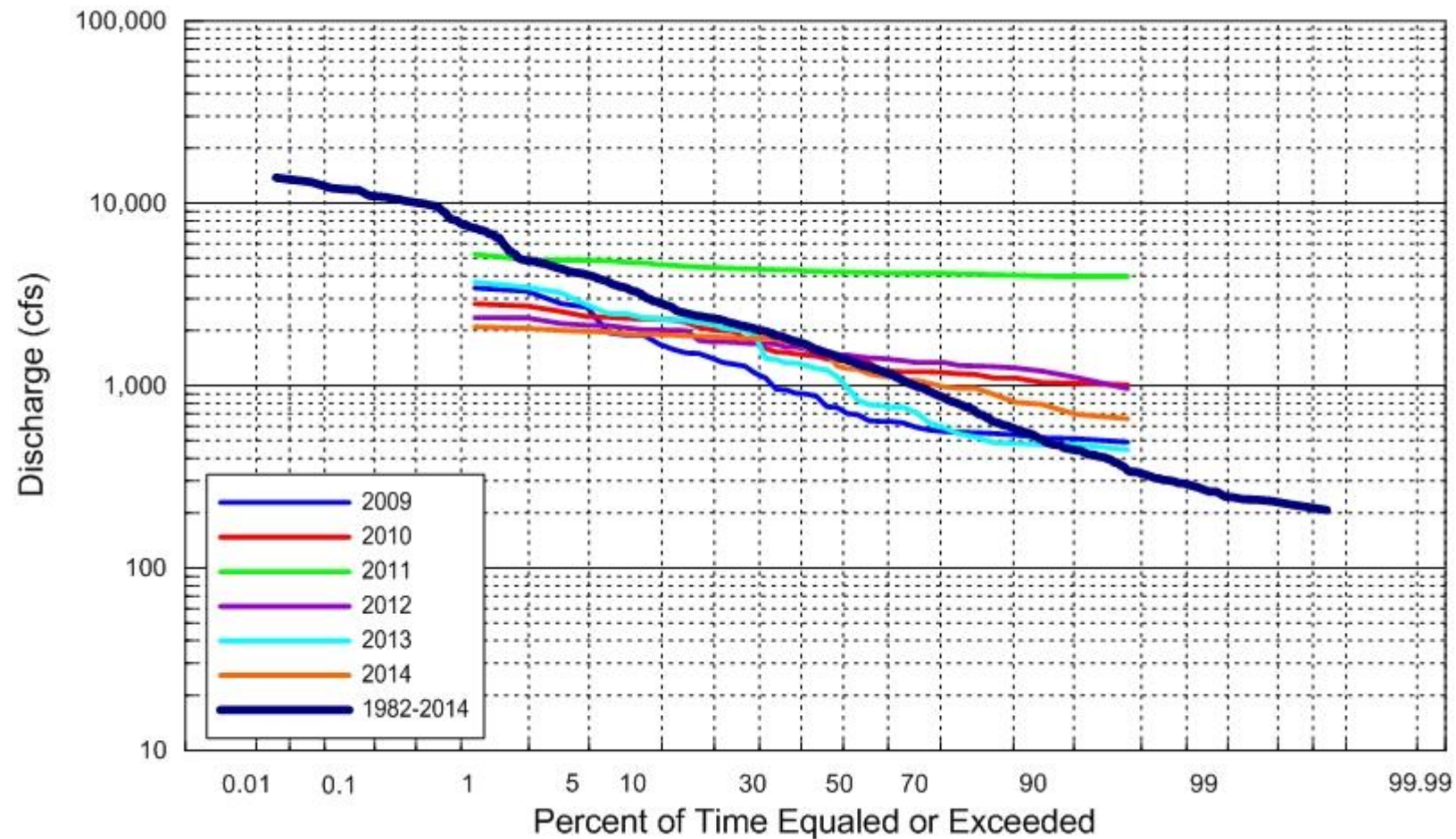
Spring Whooping Crane (June 1 – July 10) for Kearney



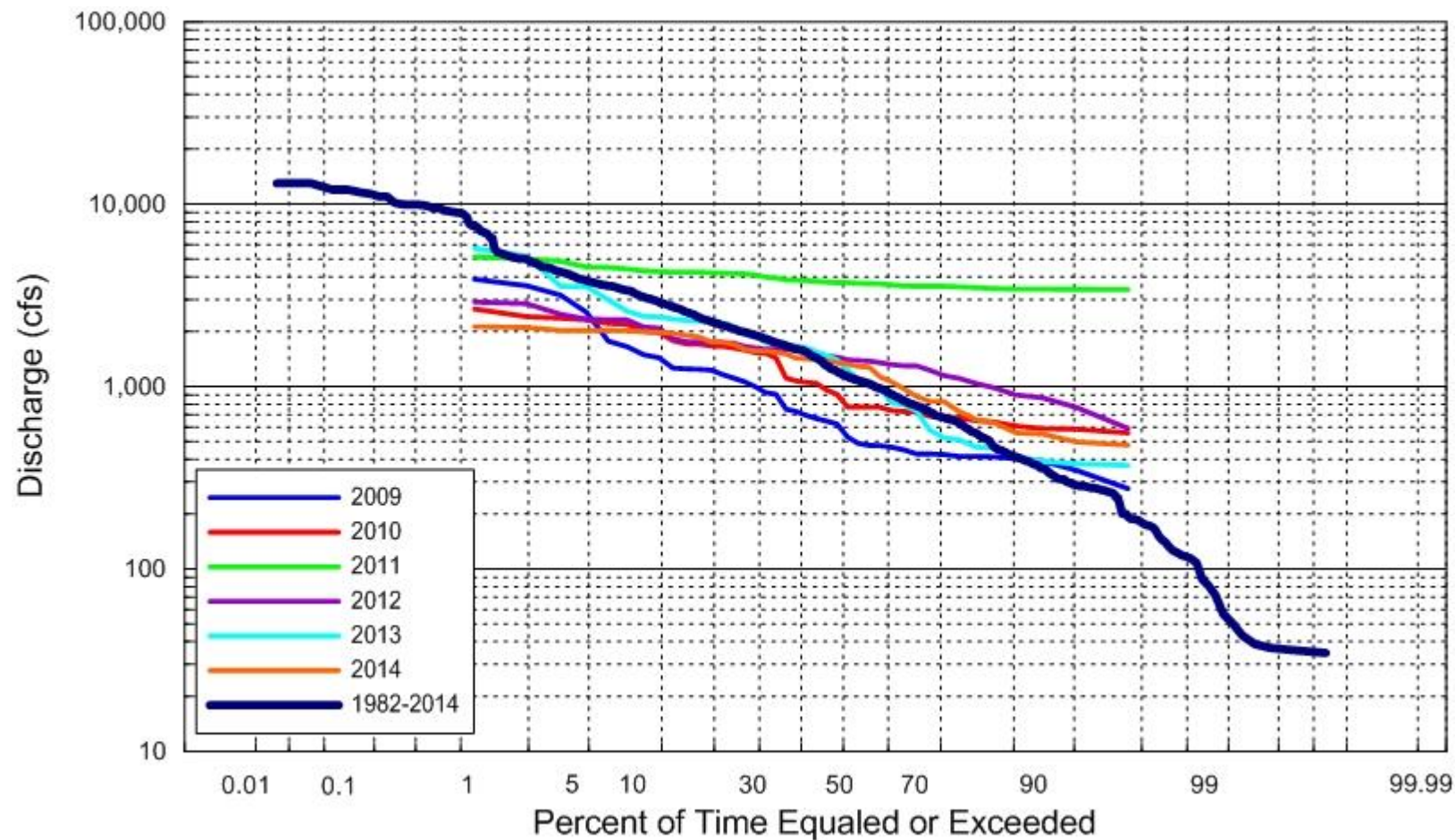
Spring Whooping Crane (June 1 – July 10) for Shelton



Spring Whooping Crane (June 1 – July 10) for Grand Island



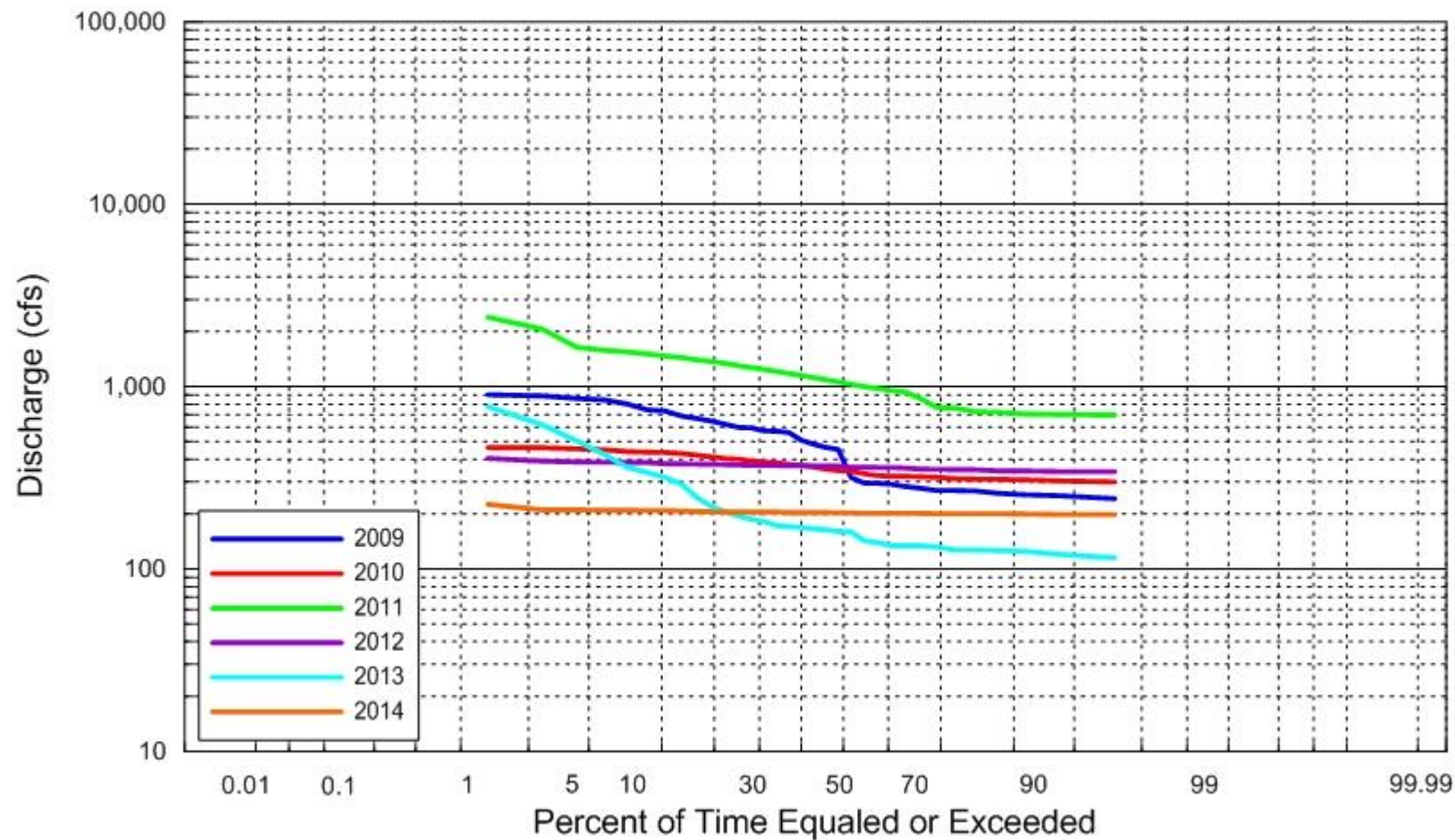
Spring Whooping Crane (June 1 – July 10) for Odessa



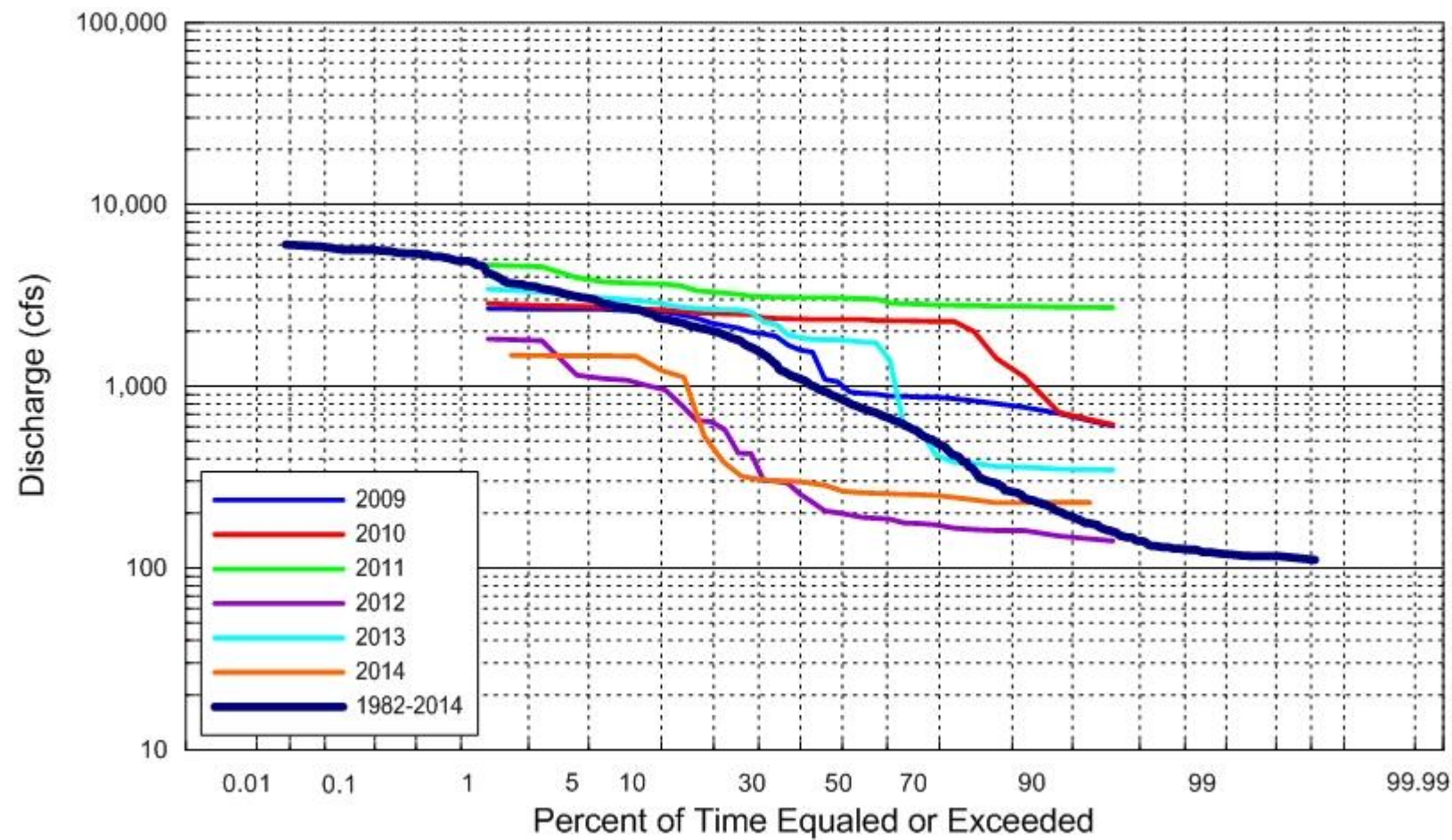
APPENDIX A.3

Mean Daily Flow-duration Curves for Fall Whooping Crane

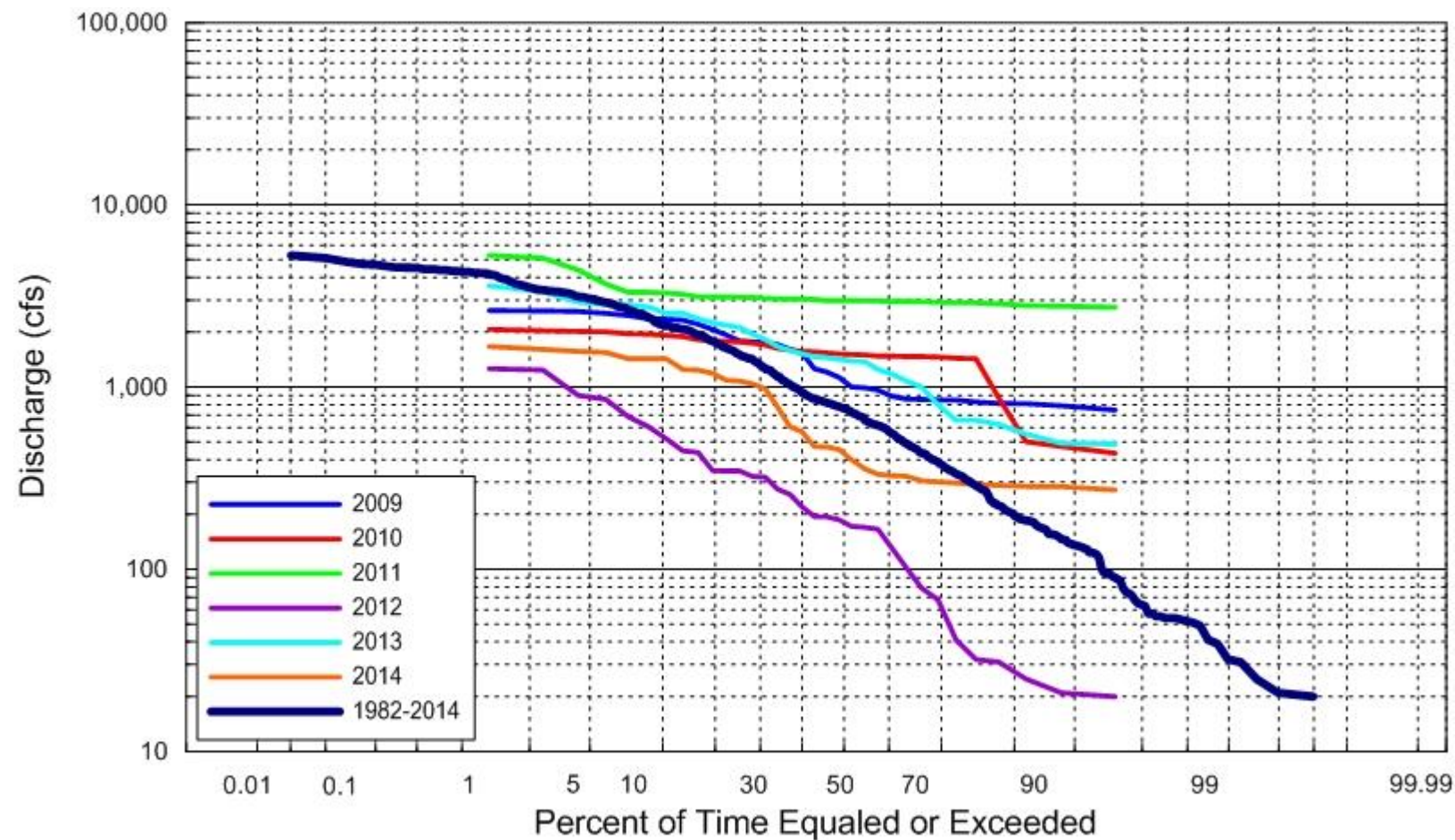
Fall Whooping Crane (June 1 – July 10) for Lexington



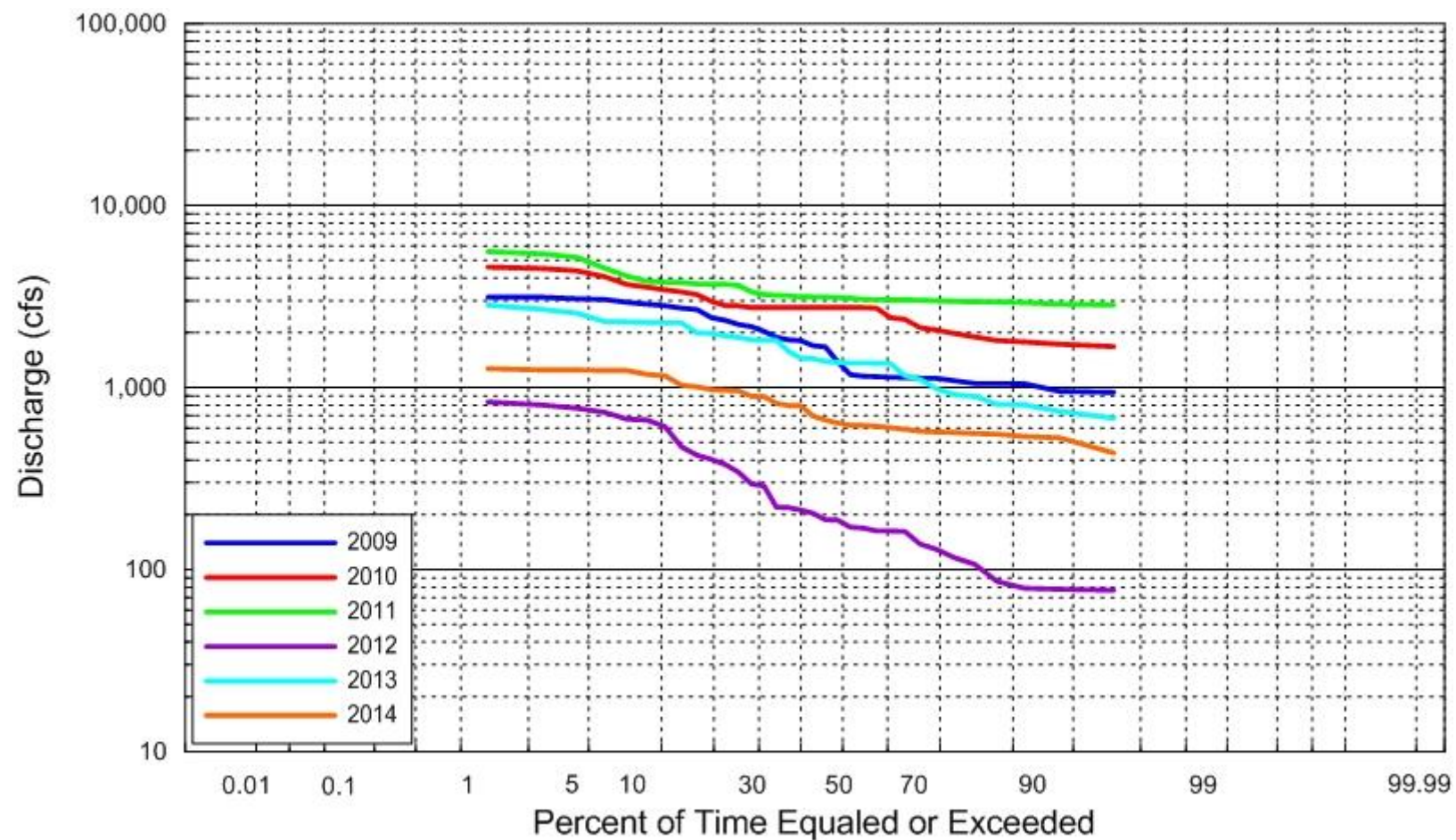
Fall Whooping Crane (June 1 – July 10) for Overton



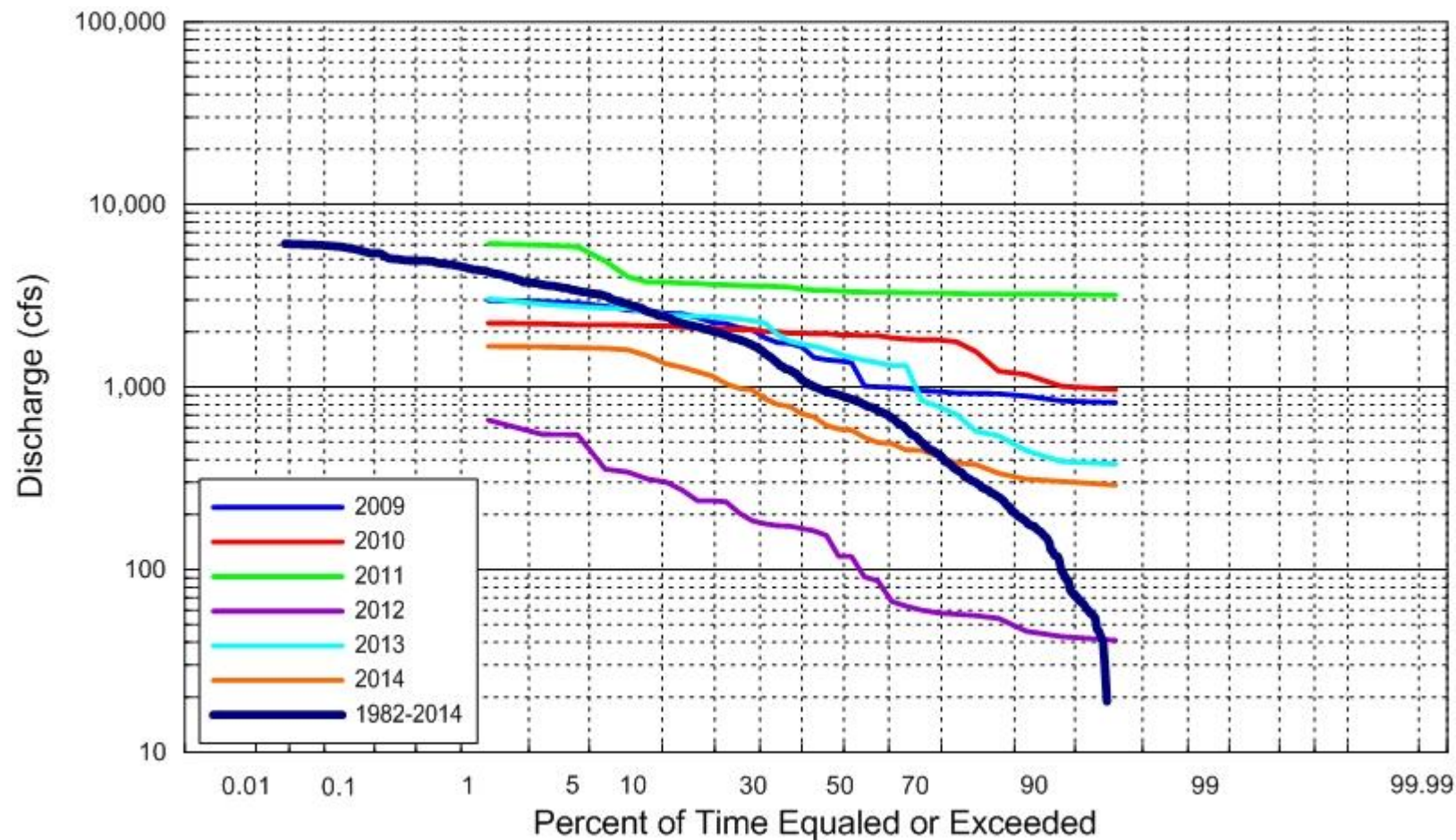
Fall Whooping Crane (June 1 – July 10) for Kearney



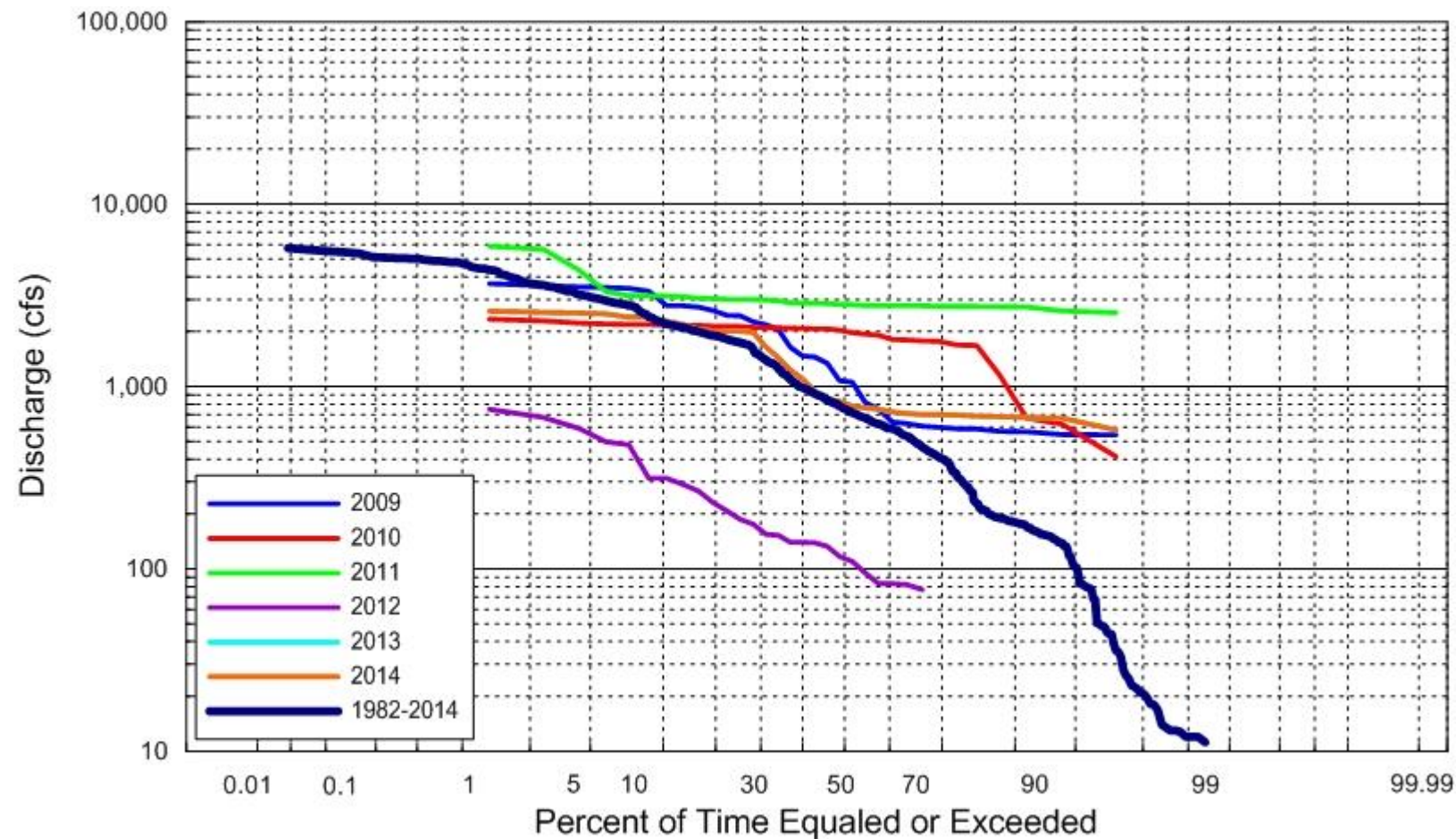
Fall Whooping Crane (June 1 – July 10) for Shelton



Fall Whooping Crane (June 1 – July 10) for Grand Island



Fall Whooping Crane (June 1 – July 10) for Odessa



APPENDICES B.1 through B.6

- Appendix B.1: Summary of Geomorphic and Selected Vegetation Metrics - 2009
- Appendix B.2: Summary of Geomorphic and Selected Vegetation Metrics - 2010
- Appendix B.3: Summary of Geomorphic and Selected Vegetation Metrics – 2011
- Appendix B.4: Summary of Geomorphic and Selected Vegetation Metrics - 2012
- Appendix B.5: Summary of Geomorphic and Selected Vegetation Metrics - 2013
- Appendix B.6: Summary of Geomorphic and Selected Vegetation Metrics - 2014

Appendix B.1-B.6.xlsb

APPENDIX C

Vegetation Data

Appendix C.xlsxm